Dissertation zur Erlangung des Doktorgrades

Fakultät für Chemie und Pharmazie

Ludwig-Maximilians-Universität München

Syntheses of nipecotic acid derivatives with new N-arylalkenyl and N-arylalkynyl substituents and with new photoswitchable residues as mGAT1 inhibitors

Toni Alexander Lutz

aus München

2017

Erklärung

Diese Dissertation wurde im Sinne von § 7 Abs. 1 bzw. 2 der Promotionsordnung vom 28. November 2011 von Herrn Prof. Dr. Klaus T. Wanner betreut.

Eidesstattliche Versicherung

Diese Dissertation wurde eigenständig und ohne unerlaubte Hilfe erarbeitet.

München, den 11.04.2017

.....

(Toni Lutz)

Dissertation eingereicht am	12.04.2017
1. Gutachter	Prof. Dr. Klaus T. Wanner
2. Gutachter	Prof. Dr. Franz Paintner
Mündliche Prüfung am	05.05.2017

Die vorliegende Arbeit entstand in der Zeit von August 2011 bis März 2017

am Department Pharmazie – Zentrum für Pharmaforschung –

der Ludwig-Maximilians-Universität München auf Anregung und unter Leitung von

Herrn Prof. Dr. Klaus T. Wanner

Für die engagierte, ausgezeichnete und sehr hilfreiche Betreuung und Förderung

meiner Arbeit sowie die hervorragenden Forschungsbedingungen danke ich

Herrn Prof. Dr. Klaus T. Wanner sehr herzlich.

Herrn Prof. Dr. Paintner danke ich herzlich

für die Übernahme des Korreferats.

Danksagung

Für die gute Zusammenarbeit und die schöne gemeinsame Zeit möchte ich mich bei allen aktuellen und ehemaligen Mitarbeiterinnen und Mitarbeitern des Arbeitskreises bedanken.

Besonderer Dank gilt meinen ehemaligen Laborkollegen Ludwig Angermeier, Tobias Hauke und Tim (Hölle) Hellenbrand für die super Zeit im und rund ums Labor, wie beispielsweise vieler Schafkopfrunden und gemeinsamer Treffen und Unternehmungen außerhalb der Uni.

Meinen Bachelor-Studenten Patrick Spanner und Thomas Ackermann sowie meinem Wahlpflichtpraktikanten Florian Schanzer danke ich für ihre Mithilfe im Labor und die durchgeführten Synthesen im Rahmen ihrer Arbeiten. Die Zusammenarbeit mit euch hat mir sehr Spaß gemacht und ich wünsche euch alles Gute für eure jeweilige Zukunft!

Dr. Georg Höfner sowie dem gesamten Team der biologischen Prüfabteilung, insbesondre Silke Duensing-Kropp und Ljiljana Galogaza, danke ich sehr für die Testung der von mir synthetisierten Verbindungen, v.a. für die aufwendige Testung meiner photoschaltbaren Verbindungen und die dabei jeweils erforderliche gute Abstimmung im zeitlichen Ablauf.

Dr. Lars Allmendinger und den Mitarbeiterinnen der analytischen Abteilung, insbesondere Claudia Glas und Ursula Groß gilt besonderer Dank für die Messung all meiner IR-, MS- und NMR-Spektren, v.a. aber für das Möglichmachen der Messung sehr vieler NMR-Kinetik-Experimente und die stets sehr gute zeitliche Koordination dafür.

Den Mitarbeitern des AK Trauners, v.a. Dr. Martin Sumser, danke ich für die andauernde Bereitstellung ihrer Messgeräte, v.a. des Monochromators und des UV-Spektrometers und für das Ermöglichen unzähliger (Kinetik)-Messungen an diesen Geräten.

Katharina Heimberger und Annerose Kärtner danke ich für die Unterstützung bei allen organisatorischen Aufgaben sowie die Versorgung mit Büro- und Labormaterialien.

Für die hervorragende Organisation der von mir betreuten Studentenpraktika möchte ich Herrn Dr. Jörg Pabel und Elisabeth Zoller herzlich danken. Dr. Jörg Pabel und Dr. Thejavathi Renukappa-Gutke danke ich außerdem für das Korrekturlesen meiner Publikationen.

Besonderer Dank gilt auch all meinen Münchener, Holzkirchner und Uni-Freunden für die zeitliche Begleitung durch meine Promotionszeit und die vielen gemeinsamen Erlebnisse.

Größter Dank geht an meine Familie, an meine Schwester, an meine Eltern und meine Tante, für die bedingungslose Unterstützung und den Rückhalt von zu Hause und vor allem dafür, dass ihr zu jedem Zeitpunkt an mich geglaubt habt und immer für mich da wart! Ihr habt mir diese Doktorarbeit erst möglich gemacht.

This cumulative thesis is based on the following original publications and manuscripts:

2013:

Miriam Sindelar, **Toni A. Lutz**, Marilena Petrera, Georg Höfner, and Klaus T. Wanner;

Journal of Medicinal Chemistry **2013**, *56*, 1323-1340.

"Focused Pseudostatic Hydrazone Libraries Screened by Mass Spectrometry Binding Assay – Optimizing Affinities towards γ-Aminobutyric Acid Transporter 1"

2015:

Toni A. Lutz, Patrick Spanner, and Klaus T. Wanner;

Tetrahedron **2016**, 72, 1579-1589.

“A general approach to substituted diphenyldiazenes”

2016:

Toni A. Lutz, Thomas Wein, Georg Höfner, and Klaus T. Wanner;

ChemMedChem **2017**, 12, 362-371.

“Development of highly potent GAT1 Inhibitors:
Synthesis of Nipecotic Acids Derivatives with *N*-arylalkinyl substituents”

2017:

Toni A. Lutz, Thomas Wein, Georg Höfner, and Klaus T. Wanner;

Manuscript to be submitted to *Journal of Medicinal Chemistry*.

“Development of new photoswitchable azobenzene bound GABA uptake inhibitors
with distinctly enhanced potency upon photoactivation”

Table of contents

1 Introduction

The investigation of the relationships between chemical structures and their biological effect is the principal aim of medicinal chemical research. Active compounds may be found in a library of various different chemical structures by means of high-throughput screening. Identified hits can then be used as lead structure for the design of further drugs. However, since this common method is time-consuming and expensive, nowadays the computer based design represents a wide spread and established method. In this context, drug development in pharmaceutical research mostly begins with the identification and characterization of a biological target which may be an enzyme or a membrane bound protein like receptors or transporters that mediate a physiological effect.

In general, two different strategies can be pursued: The “target based drug design” requires the knowledge of the exact 3D structure of the target in presence of the ligand that may be generated by X-ray crystallography. In this case detailed knowledge about the binding site of the substrate and kind of interactions of the substrate with the protein complex can be gained. By means of respective computer programs ligands can be fit into the binding pocket of the target (“docking”) and binding affinities can be calculated as docking scores dependent on the structure of the substrate. Based on these values potential new structures can be created that might have a similar or even better affinity to the corresponding target.

If the target structure is not known, the “ligand based drug design” can be pursued alternatively. Based on physiochemical features of known ligands it is intended to design new active compounds by means of a pharmacophore model that describes the interactions between ligand and target. By means of this model substance libraries can then be screened for additional potentially active substances.

The most active evaluated compounds can serve as basic structures for the development of more potent and/or more selective new ones by slight chemical modifications if they fulfill given requirements regarding physical and chemical features regarding molecular weight, lipophilicity, and solubility. Based on biological test results for related compounds, structure activity theories can be set up that might lead to a better understanding of the interactions between ligand and target, and thus may again support the further drug research.

1.1 CNS diseases and the physiologic significance of GABA

Diseases based on the central nervous system (CNS) are widely spread around the world. Various neurological disorders belong to this field, such as dementia, epilepsy, depression, multiple sclerosis, Parkinson's disease or neuropathic pain.[1] Among these, epilepsy affects over 50 million patients and is thus one of the most abundant diseases.[2] Though there are meanwhile over 15 different antiepileptic drugs approved, about a third of the patients continue to have seizures regularly, despite of a comprehensive treatment, and the half of them are suffering from complex psychiatric, behavioral, cognitive, and social problems.[3] In order to provide an appropriate medical supply for all affected patients, there is the continuous need for exploration of new antiepileptic drugs.

In physiological context, in particular γ-aminobutyric acid (GABA, **1**, Chart 1) represents a significant key substance since it is known to be the major inhibitory neurotransmitter in the CNS.[4] In the first section, the neurotransmission of this amino acid will be discussed briefly as well as the possibilities to increase this neurotransmission in order to treat CNS diseases.

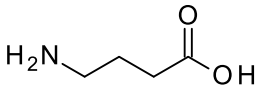

GABA (**1**)

Figure 1: Structure of γ-aminobutyric acid

1.1.1 GABA Neurotransmission

Synthesis of GABA occurs in the presynaptic neuron through enzymatic decarboxylation of the excitatory neurotransmitter glutamate by the glutamic acid decarboxylase (GAD). Formed GABA is packed into vesicles by a vesicular neurotransmitter transporter (VGAT) for storage.[5] Upon depolarization of the presynaptic neuron GABA is released into the synaptic cleft by exocytosis and can then bind to its corresponding pre- and post-synaptic receptors of which two types of GABA receptors are to differentiate: The ionotropic $GABA_A$ receptors are mainly located on the postsynaptic side and play as ligand controlled chloride channels the dominant role in mediating fast further signal transduction. The metabotropic $GABA_B$ receptors are G-protein coupled receptors (GPCR) and found on both pre- and post-synaptic neurons.[5]

Binding of GABA to the $GABA_A$ receptors causes a hyperpolarization of the postsynaptic neuron through the influx of chloride which is leading to a reduced excitability of this neuron. The presynaptic $GABA_B$ receptors adjust the further release of GABA by a negative feedback mechanism. Binding leads to an inhibition by suppressing calcium influx. Postsynaptic $GABA_B$ receptors convey hyperpolarization of its neuron through the elevated efflux of potassium.[5]

For the termination of GABAergic signaling, GABA must be removed from the synaptic cleft which is mediated by specific GABA transport proteins (GATs) being responsible for the reuptake of GABA into the presynaptic neuron or its transport into adjacent glia cells.[6] After the reuptake into the presynaptic neuron GABA can be recycled by the packing into vesicles again. The transport into glia cells mainly leads to enzymatic decomposition of the neurotransmitter to succinic semialdehyde by GABA transaminase (GABA-T).[7]

The described neurotransmission of GABA is displayed in Figure 2.

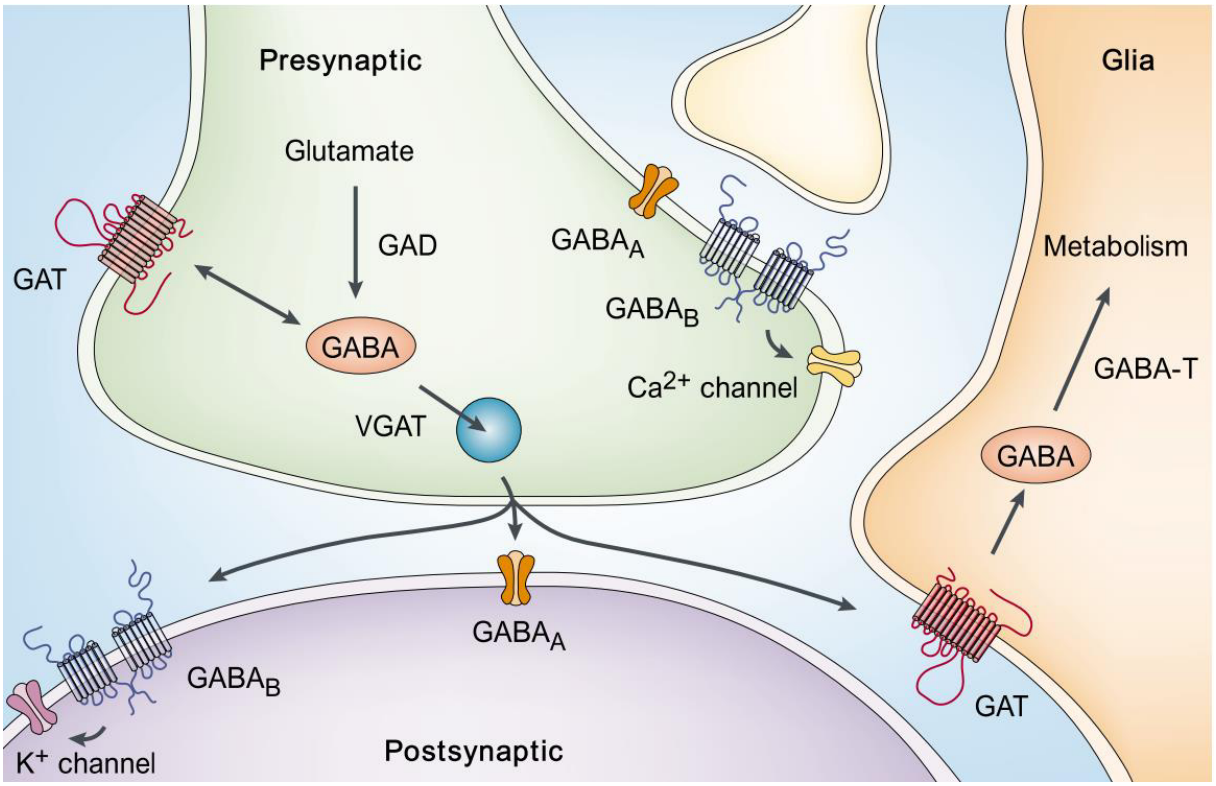

Figure 2*:* GABA neurotransmission according to Owens et al.:[5] *GABA is synthetized by GAD and stored in vesicles by VGAT. It is released into the synaptic cleft in response to an action potential. In the synaptic cleft it can interact with receptors ($GABA_A$ and $GABA_B$) for further signal transmission or in the sense of a negative feedback. Reuptake of GABA in the presynaptic neuron or glia cells occurs through the activity of GABA transporters (GATs).*

1.1.2 Pathology and Therapy

A reduced GABAergic signaling in the CNS leads to an imbalance between the excitatory and inhibitory neurotransmission[7] and is assumed to be associated with the pathogenesis of epilepsy and other CNS diseases mentioned above.[4] In case of a pathological diminished inhibitory activity of GABA, therapeutic active compounds, which aim for an increase of the GABAergic neurotransmission, can help to restore the balance between excitatory and inhibitory neurotransmitters. Thereby, the different GABA receptors, the GABA decomposing transaminase and the GATs represent suitable targets.

Positive allosteric modulators of the $GABA_A$ receptors are represented by the benzodiazepines which constitute ligands of a specific allosteric binding site. The occupation of these binding sites leads to a conformational change of the receptor upon which in presence of GABA an elevated opening frequency of the chloride channels occurs as consequence.[7] As an example of drugs that act via this mechanism, diazepam (**2**, figure 3) should be mentioned as one of the most spread benzodiazepines. Another option to increase the neurotransmission of GABA can be realized by the binding of an agonist, e.g. baclofen (**3**, figure 3) to the metabotropic $GABA_B$ receptor. By the irreversible inhibition of GABA transaminase by vigabatrin (**4**, figure 3) a similar goal can be pursued since the neurotransmitter will not be decomposed in this case. Finally, an increased GABA level also occurs when the GABA transporters are blocked since GABA will not be removed from the synaptic cleft as a consequence. Tiagabine (**5**, figure 3) is approved as antiepileptic drug and acts as inhibitor of the GABA transporter subtype 1 (GAT1).

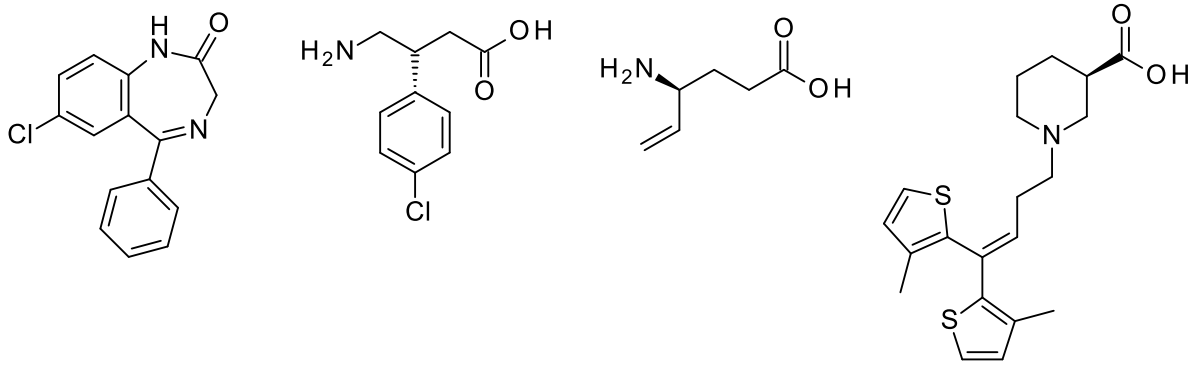

Diazepam (**2**) (*R*)-Baclofen (**3**) (*S*)-Vigabatrin (**4**) (*R*)-Tiagabine (**5**)

Figure 3: Current drugs with influence of the GABA neurotransmission (eutomers are depicted).

1.2 GABA Transporters

Transporters (solute carriers, SLCs) enable the exchange of ions, neurotransmitters or amino acids through cellular membranes. Since their inhibition can lead to an increased GABA level, GATs represent an interesting target for the development of new antiepileptic drugs. Different aspects of GATs have been investigated in the last years. The knowledge discovered in these studies concerning function and structure of these targets as well as the respective ligands addressing this target are discussed in the following part.

1.2.1 The SLC6 transporter family

The most important type of transporters are derived from the solute carrier 6 (SLC6) gene family of which 20 different transporters subtypes are known so far.[8] According to the amino acid sequence they can be divided up into 4 main subtypes (figure 4): monoamine transporters, GABA transporters, and two groups of amino acid transporters.

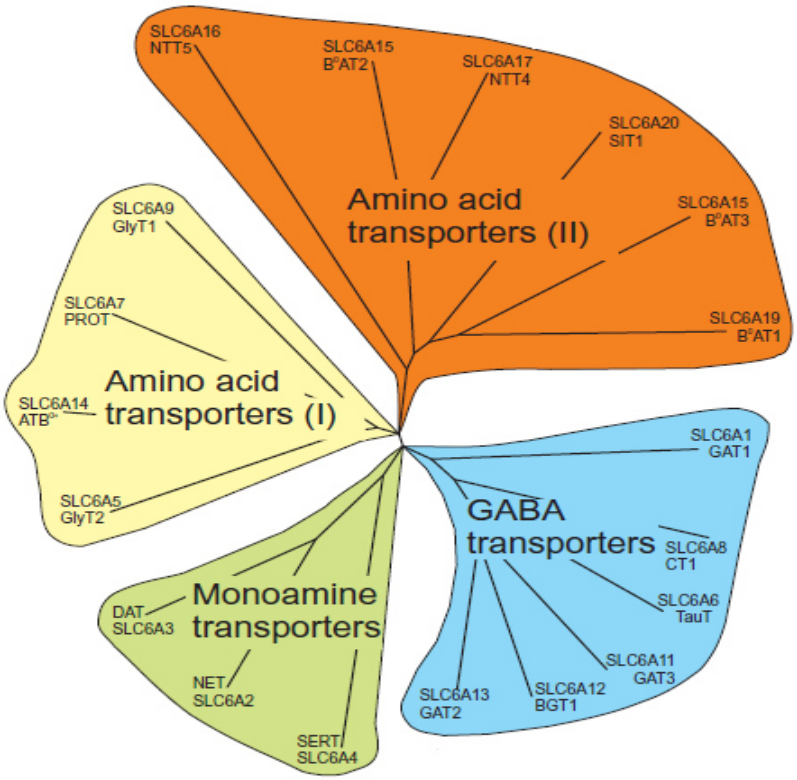

Figure 4: Transporters of the SLC6-family according to Bröer et al.[9]

The monoamine transporters include the transporters for the well-known neurotransmitters noradrenaline (NET), dopamine (DAT) and serotonin (SERT). The different GABA transporters GAT1, BGT1, GAT2, and GAT3 as well as the transporters for taurine (TauT) and creatine (CT1) belong to the group of GABA transporters. The first group of the amino acid transporters contains transporters for glycine (GlyT1 and GlyT2), proline (PROT) and one for neutral and cationic amino acids (ATB1). The second group of amino acid transporters is involved in epithelial and brain amino acid transport. Most members accept a variety of amino acids for transportation. The physiological role of the transporter members of this group is not completely understood so far.[9]

These neurotransmitter transporters are also called neurotransmitter-sodium-symporters (NSSs) or Na^+/Cl^- dependent transporters[10] since they entail the co-transport of Na^+ of which transportation goes along the concentration gradient into the inside of the cell, mediating the transport of the actual substrate against its concentration gradient into the same direction. Thereby, the Na^+/K^+-ATPase guarantees for this ongoing mechanism through the maintaining of the sodium gradient.[9] The stoichiometric ratio of substrate and the co-transported ions is varying within the different types of NSSs.

The elucidation of the molecular structure of these NSSs was subject to intensive research. The isolation of the first NSS was achieved for GAT1 from rat brain by Radian et al.[11] The analysis of the amino acid sequence led to the cloning and sequencing of this transporter by Gustella et al.[12] followed by the transporters for noradrenalin,[13] dopamine,[14] serotonin[15] and glycin.[16] Thereupon, it could already be claimed that the transporters were consisting of 12 transmembrane helices.[17] However, the final structure was elucidated by Yamashita et al.[18] within whose work the successful crystallization of the leucine transporter $LeuT_{Aa}$ from the bacteria *Aquifex aeolicus* in the presence of its substrate leucine and two sodium ions could be accomplished. Though the identity in the total sequence of $LeuT_{Aa}$ as compared to that of the eukaryotic SLC6-transporters is just 20-25%, the homology in sequence for areas in the region of the substrate binding site amounts to 55-67%.[19] For this reason the results of Yamashita et al. concerning $LeuT_{Aa}$ constitute a valid base for the understanding of the construction and function of neurotransmitter transporters in general.[20] The obtained structure of $LeuT_{Aa}$ is displayed in Figure 5.

Accordingly, the transporter consists of 12 transmembrane helices (TMs) that are connected by corresponding loops both intra- and extracellularly. Both the amino- and the carboxy-terminus are located in the inside. The authors compare the spatial structure of the transporter to a “shallow shot glass”. It consists of an inner ring which is formed by helices TM1, 3, 6 and 8 and an outer ring that is represented by TM2, 4, 5, 7, 9 and 10. The inner ring contains the binding site for leucine and two sodium ions within the region of TM1 and TM6 that are arranged antiparallel. Because of an interruption of the helical structure they are divided into two proportions (a+b) in the middle so that C=O- and NH-groups are exposed for the formation of hydrogen and ionic bonds. The first 10 TMs are characterized by a repeated structural element. TM1-5 and TM6-10 are interconvertible by rotation of 176.5° through a pseudo-two-fold axis of symmetry that proceeds parallel to the membrane.[18]

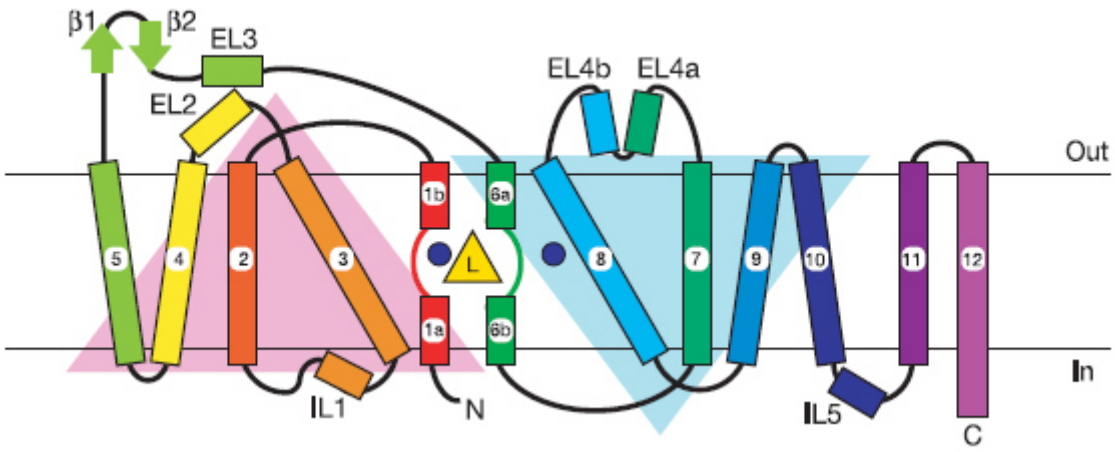

Figure 5: Structure of $LeuT_{Aa}$ according to Yamashita et al.[18]

This particular arrangement led to the assumption that the general transport mechanism of these NSSs follows the model of “alternate access”.[21, 22] In this case, the transporter consists of an intra- and extracellular border. Both gates can be alternately open or close to one side triggered by a conformational change which is induced by the binding of the substrate and leads to a directed transport. During the transport the transporter in general passes several conformations. In the initial state of the transport cycle the transporter exists in the “outward facing open” (OFo, Figure 6 left) conformation concerning the extracellular side, enabling the substrate and ions to get into the S1 binding site. Subsequently, a conformational change follows causing the close of the extracellular gate (“outward facing closed”, OFc, figure 6 middle). Thereafter, the transporter changes to the “inward facing close” (IFc, not depicted)

conformation upon which the intracellular gate opens immediately, and releases the substrate and ion to the cytoplasm ("inward facing open", IFo, figure 6 right).[23]

After the elucidation of the OFc state, Krishnamurty et al. were able to crystallize both the OFo and the IFo state and analyzing the same.[24] As a result, a more detailed understanding of the different conformations and molecular processes running during the transport was possible and mainly confirmed the postulated transport mechanism of Yamashita et al.

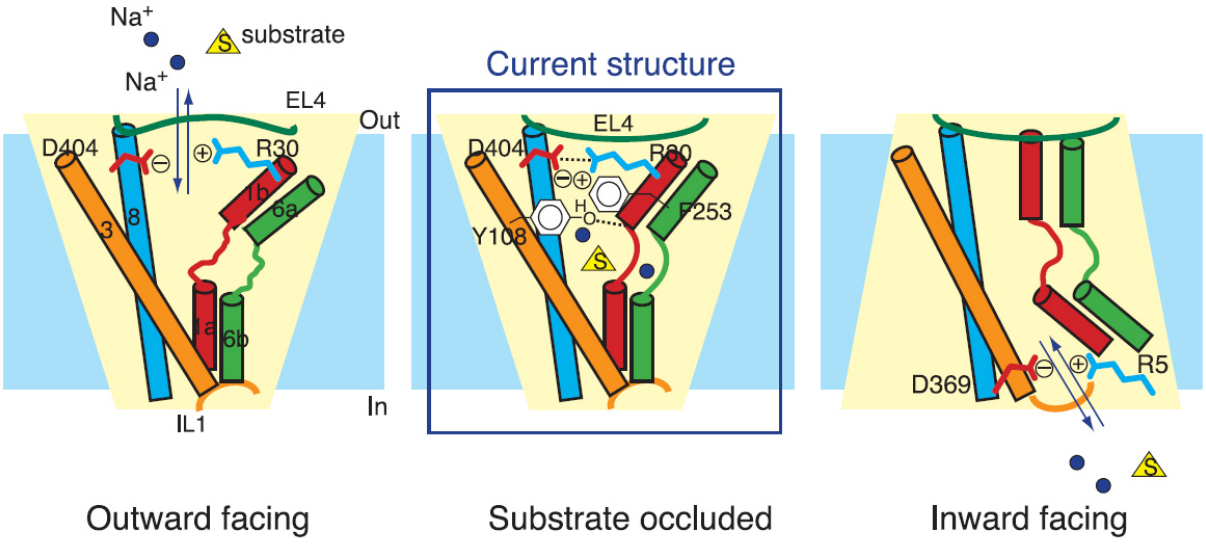

Figure 6: Postulated Transport mechanism of $LeuT_{Aa}$ according to Yamashita et al.[18]

These three states of $LeuT_{Aa}$ are displayed in figure 6. In the "outward facing" conformation the extracellular site is accessible for the substrates and ions. In this state the two amino acids arg30 and asp404, which are mainly responsible for the extracellular gate, do not interact. Closing the extracellular side is on the one hand facilitated by the formation of a salt bridge between both amino acids and on the other one by the two aromatic amino acids tyr108 and phe253 of which interaction leads to a hydrophobic cap ("substrate occluded"). Access to the intracellular site is blocked by a saltbridge of arg5 and asp369 (intracellular gate) and a dense network of the helicale segments TM1a, TM6b and TM8. This region is becoming vacant by the conformational change to the "inward facing" state. Thereby, opening and closing of the extra and intracellular gates might be enabled by the movement of the helicale segments TM1b-TM6a (extracellular) and TM1a-TM6b (intracellular) relatively to the TM3 and TM8 backbone and a slight rotation of the latter. In this context, binding and unbinding of substrate and ions may stabilize the helices in the different conformational states.[18]

Based on molecular-dynamic simulations and other experimental data Shi at al. reported a second binding site S2 which is located above the extracellular gate of LeuT.[25] They claim that the occupation of this binding site is necessary for the allosteric release of the substrate to the cytoplasm. The existence of S2 was also validated in other studies[26, 27] though its function is still discussed.[28, 29] S2 might be relevant as non-competitive binding site for LeuT inhibitors upon which binding prevents the transporter going through the conformational changes.[28]

Recently, Penmatsa et al. were able to crystalize the eukaryotic DAT that was gained from *Drosophila melanogaster* bound to the tricyclic antidepressant nortriptyline.[30] It was found that the crystal structure of this NSS is in excellent accordance with the previously published structure for prokaryotic LeuT. Lately, also X-ray crystallographic structures of the human SERT in complex with the antidepressant (S)-citalopram or paroxetine were described by Coleman et. al.[31] In this context likewise the location of an allosteric binding site in the extracellular vestibule could be identified. Accordingly, the occupation of this site sterically hinders the ligand unbinding from the central binding site.

These new transporter structures will serve as promising tool for future homology models for the mammalian NSS, as it is up to now commonly established for LeuT.

1.2.2 Classification of GABA transporters

GATs exist in four subtypes with different types of designations dependent from the species from which they are derived (Table 1). According to the human genome organization (HUGO) these four subtypes are generally named as GAT1, BGT1, GAT2, and GAT3.[32] However, there are also other nomenclatures in use, e.g. when derived from human the four transporters were explicitly designated as hGAT1, hBGT1, hGAT2 and hGAT3 and when cloned from mice as mGAT1, mGAT2, mGAT3 and mGAT4, respectively.[33] Within this thesis, modeling studies will refer to hGAT1, whilst biological data will be measured for mGAT1-4.

Table 1: Nomenclature of GATs

Species	GAT designation			
HUGO	GAT1	BGT1	GAT2	GAT3
human	hGAT-1	hBGT-1	hGAT-2	hGAT-3
mouse	mGAT1	mGAT2	mGAT3	mGAT4

All subtypes differ both in their expression pattern and their pharmacological significance: GAT1 is mainly located in the membranes of presynaptic neurons and represents the most abundant and the most important GABA transporter in the brain.[34] According to newer studies, BGT1 and GAT2 are mainly located in the liver and kidney instead of the CNS and do not have considerable affinity to GABA.[35] BGT1 is preferentially transporting betaine[36] and GAT2 particularly carries taurine.[37] Thus, these two subtypes do not play an important role in the termination of GABAergic neurotransmission. However, next to GAT1, subtype GAT3 has an important function in the CNS since it is especially located on the glia cells and therefore is also connected with decomposition or recycling of GABA.[38]

1.2.3 GABA transporters as pharmacolocical targets

Since the inhibition of GABA transporters can increase the residence time of GABA in the synaptic cleft and contribute to restore a physiological neurotransmitter balance the same represent an interesting target for the drug development. In this context, it is the aim to identify compounds that inhibit the GABA uptake effectively, but do not bind to the GABA receptors. For the first, acyclic analogue compounds of GABA were developed that were not found to be selective to one of the transporter subtypes and additionally turned out to act as ligands for the $GABA_A$ receptor.[39] In contrast to this, some cyclic amino acids like guvacin (**6**, Table 2) or nipecotic acid (**7**, Table 2) have proved to be a better starting point for the development of GAT inhibitors.[40] Except from mGAT2, the inhibitory potencies (pIC_{50} values) for **6** and **7** (Table 2) are of a similar order of magnitude concerning all subtypes mGAT1-4 and do not show pronounced selectivity. For nipecotic acid (**7**) it has to be recognized the (*R*)-enantiomer is significantly more potent than the (*S*)-enantiomer concerning inhibitory activity towards all GATs. The corresponding pIC_{50} values for **6** and (*R*)-**7** regarding mGAT1 are

located in the range of 5. For the other subtypes mGAT2-4 the values were found to reach from about 3 (mGAT2) up to almost 5 (mGAT3, mGAT4), respectively.

Table 2: pIC_{50}-values of small amino acids as GABA analogues

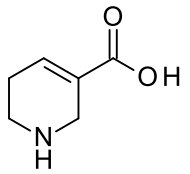

guvacin (**6**)

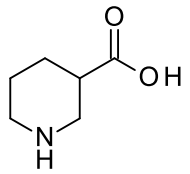

(*RS*)-nipecotic acid ((*RS*)-**7**)

Compound	GABA uptake inhibition (pIC_{50} ± SEM)[a]			
	mGAT1	mGAT2	mGAT3	mGAT4
6	4.87 ± 0.06	3.31 ± 0.03	4.59 ± 0.05	4.59 ± 0.05
(*R*)-**7**	5.12 ± 0.03	3.40 ± 0.05	4.76 ± 0.05	4.95 ± 0.05
(*S*)-**7**	4.24 ± 0.05	3.13 ± 0.14	3.83 ± 0.04	3.63 ± 0.06

a) For sake of comparability all listed functional inhibitory potencies (pIC_{50} values) derive from the biological test of our research group (GABA uptake assay based on HEK293 cells stably expressing the different mGATs).

However, the sole amino acids are highly polar and are moreover present as zwitterion under physiological conditions, a circumstance that prevents them to cross the blood brain barrier and thus to reach the CNS.[41] Furthermore they simultaneously serve as substrate of the GATs. To solve the problem of inefficient CNS penetration lipophilic side chains to the nitrogen of the cyclic amino acids were introduced in a next step. Thus constructed compounds were not only more lipophilic and able to reach the CNS, but even showed an enhanced subtype selectivity towards mGAT1. In this context, compounds like NO711 (**8**, Table 3),[42] SKF-89976 (**9**, Table 3)[43] or tiagabine (**10**, Table 3)[44] were introduced of which the latter was finally approved as antiepileptic drug in the adjunctive therapy. The pIC_{50}-values towards mGAT1 of these compounds were found to be increased by one to two decimal powers (values are in the range of 6-7) as compared to compounds **6** and **7** (Table 2) whereas the ones for mGAT2-4 hardly raised or even decreased (pIC_{50} values located between 3 and 4).

Table 3: Classical mGAT1-selective inhibitors and their pIC_{50}-values.

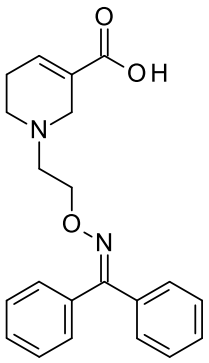

NO711 (**8**)

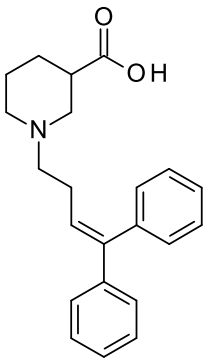

SKF-89976 (**9**)

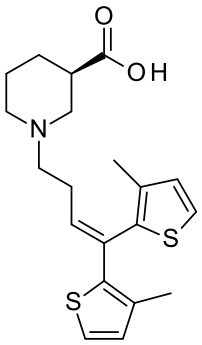

Tiagabine (**10**)

Compound	GABA uptake inhibition (pIC_{50} ± SEM)[a]			
	mGAT1	mGAT2	mGAT3	mGAT4
8	6.83 ± 0.06	3.20 ± 0.09	3.62 ± 0.04	3.07 ± 0.05
9	6.16 ± 0.05	3.43 ± 0.07	3.71 ± 0.04	3.56 ± 0.06
10	6.88 ± 0.12	50%[b]	64%[b]	73%[b]

a) For sake of comparability all listed functional inhibitory potencies (pIC_{50} values) derive from the biological test of our research group (GABA uptake assay based on HEK293 cells stably expressing the different mGATs).

b) A complete inhibition curve for determination of pIC_{50} was not measured if [^{3}H]GABA uptake remained 50% or above already at a concentration of 100 µM inhibitor in two experiments.

The residues of N-substituted nipecotic acid and other cyclic amino acids in general consist of a spacer of four or five atoms which partly also includes a hetero atom with an terminal attached aromatic moiety. SAR studies of Anderson et al. indicated the 2-biphenyl and the 2-benzylphenyl residue as aromatic component of the N-substituent for the first time to be advantageous concerning inhibitory potency towards mGAT1, as it is the case for compounds (*R*)-**11** and (*R*)-**12** (Figure 7).[45] The affinity of N-substituted nipecotic acid derivatives bearing the biphenyl type moiety could recently be validated in the study of M. Petrera, in whose target compounds the alkoxyalkyl spacer was exchanged through a but-3-en-1-yl linker, resulting in compound (*RS*)-**13** (Figure 7).[46] The racemic mixture of this parent compound already exhibited a similar inhibitory activity and can be viewed as starting point for the development of various further mGAT1 selective inhibitors. Exchanging the 2-biphenyl moiety in this structure by a 2-benzylphenyl residue, as it is the case for (*RS*)-**14** (Figure 7), inhibitory potencies towards mGAT1 decreased by about one decimal power in this case.

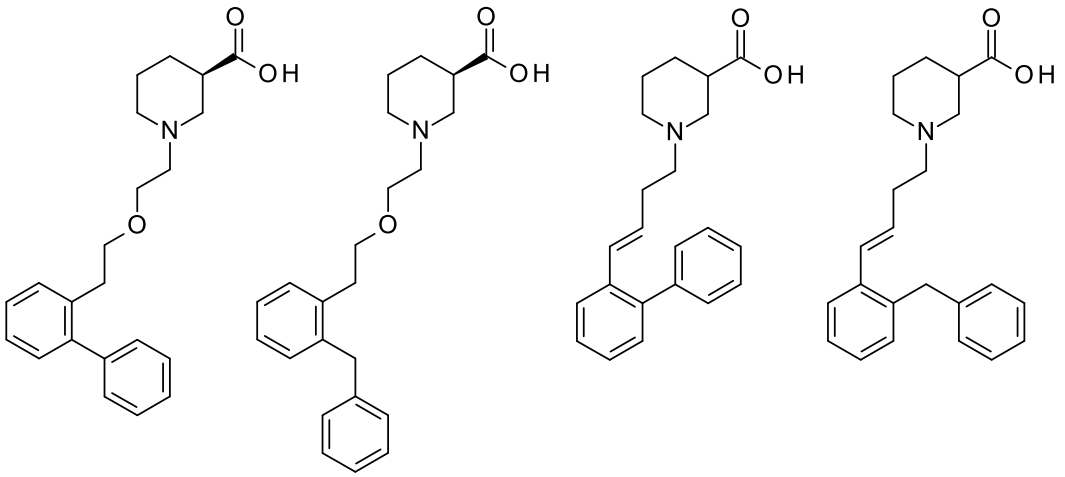

Figure 7: New generation of GAT1 selective inhibitors by a) Anderson et al.[45] and b) Petrera et al.[46]
a: pIC_{50} values calculated from Anderson et al.[45]; values measured in synaptosomal preparations from rat (comparable to mGAT1); b: pIC_{50} values from Petrera et al.[46]; values refer to mGAT1

Although it is the aim of this thesis to search for new GAT1 selective inhibitors, for sake of completeness it should be mentioned that also ligands have been developed that aim at the other transporter subtypes BGT1, GAT2 and GAT3, though there are almost none with a pronounced subtype selectivity that would allow to gain reliable data on the pharmacological profile of the individual transporter. To what extent these transporters can play a role for the treatment of epilepsy or other diseases is also topic of various parallel studies.[35-38]

1.2.4 Binding modes of GABA and GAT1 inhibitors

The findings about LeuT (see chapter 1.2.1) have served as valid base for the understanding of also human neurotransmitter transporters such as the GABA transporter, as there is the already mentioned similarity between both transporter types. Therefore, many molecular modeling studies deal with this transporter type and represent a useful tool for the study and development of new and highly potent GAT1 inhibitors. For this reason, two publications that resulted from my PhD studies also comprise structure target interactions and binding calculations, gained from molecular modeling results.

In our research group a three dimensional model for the human GABA transporter hGAT1 was developed and interactions between GABA and the substrate binding site were investigated by docking studies.[47] Thereby, the derived binding modes of GABA in hGAT1 and leucine in $LeuT_{Aa}$ are both highly similar (Figure 8). The carboxylic group of GABA in hGAT1 is bound to one of the sodium ions (Na1) as it is also true for leucine in LeuT and is additionally stabilized by hydrogen bonds addressing the hydroxyl function of Tyr140 and the amide of Leu64 and Gly65. The amino function is fixed by hydrogen bonds to the hydroxyl function of Thr400 and Ser396 and Tyr60 and to the carbonyl function Ser396 and Tyr60. The different substrate specificity is mainly the result of 3 amino acid exchanges in hGAT1 compared to LeuT, Ser256 to Gly297, Asn21 to Tyr60 and Ile359 to Thr400 which results in slightly modified interactions.

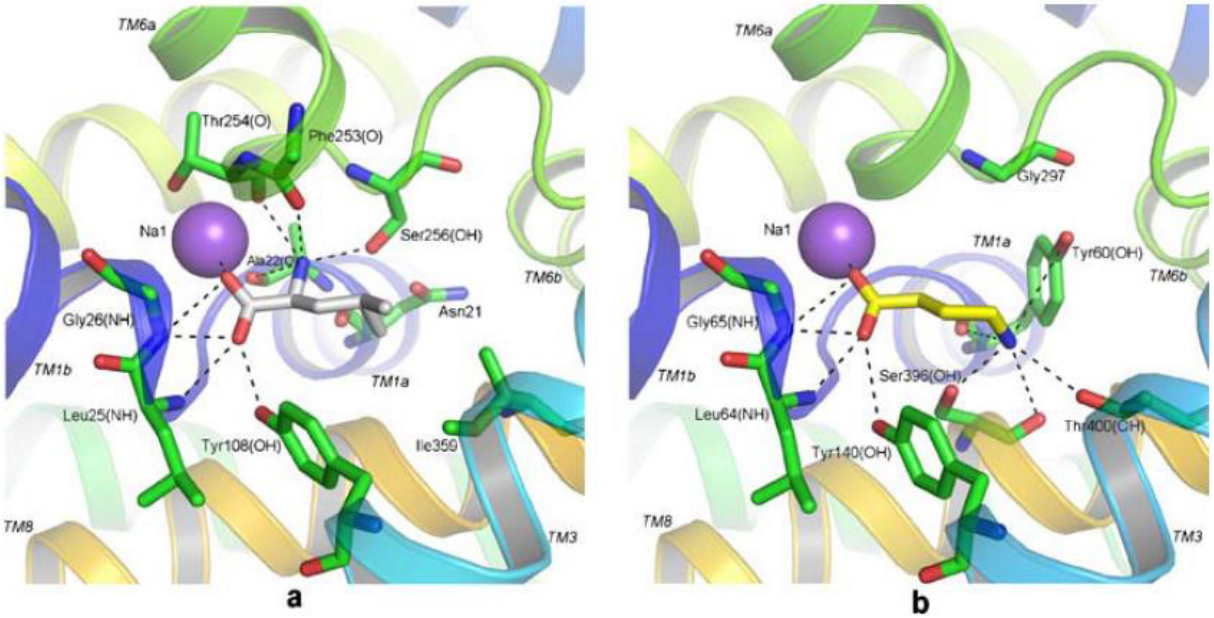

Figure 8: Binding mode of a) Leucin in LeuT and b) GABA in hGAT1 according to Wein et al.[47]

A further homology modelling study of hGAT1 was also based on the crystal structure of LeuT and investigated the binding modes of GABA, nipecotic acid and Tiagabine.[48] Accordingly, nipecotic acid can adopt two different binding poses. In the preferred one, the carboxyl function again participates in ionic interactions to the sodium Na1 and polar interactions to Tyr140 and Gly65, thus similar as compared to the interactions of GABA. The nitrogen is oriented to the intercellular side and exhibits similar hydrogen bonds to Tyr60 and Ser396.

Due to its huge lipophilic side chain Tiagabine is present in another binding pose as compared to the smaller ligands (Figure 9a). In this case, the nitrogen of the nipecotic acid subunit is directed to the extracellular side, shaping a hydrogen bond to Phe294. The hydrophobic side chain is outside of the binding site S1 and stabilized by aliphatic sidechains in this region. This binding mode requires "open-to-out conformation" with the extracellular gate between Phe294 and Tyr140 to be open.[48]

Recently, our work group published an overview dealing with the different binding modes of a variety of small and large ligands of hGAT1.[49] In this context, the new GAT1 inhibitor **13** (Figure 7) by M. Petrera was investigated in the same homology model[46] as well, indicating a similar binding mode like Tiagabine (Figure 9b). Though, due to the biphenyl moiety, further interactions could be observed, facilitated by the side chain of Phe294. This is rather rotated towards the terminal phenyl residue of **13** enabling access to the backbone atoms of Thr290 and Gln291 in the TM6 helix and thus additional interactions as compared to tiagabine. In this context, it was additionally demonstrated that substituents (e.g. halogens) of the terminal phenyl residue of the biphenyl moiety of compound **13** could lead to even more potent GAT1 inhibitors by addressing this area.

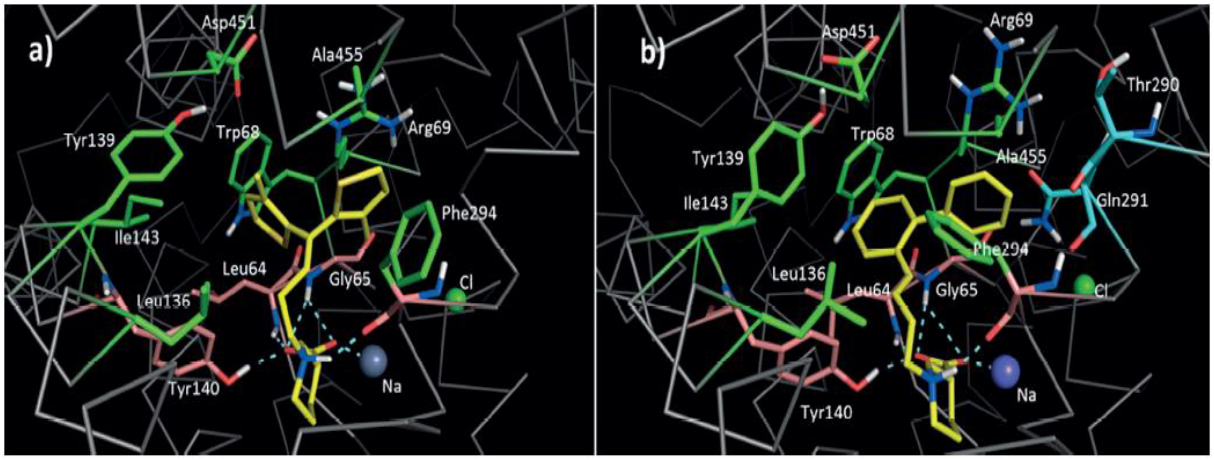

Figure 9: Binding mode of a) Tiagabine and b) compound **13** in hGAT1 according to Wein et al.[46]

1.3 Cross-coupling reactions as synthetic tool in medicinal chemistry

Cross-coupling reactions are the modern way of forming carbon-carbon bonds and thus also represent a powerful tool to the easy access of many stable ligands in medicinal chemistry. Within the publications of this thesis in particular the Suzuki and Sonogashira cross coupling reactions were applied as they can contribute to the construction of new GAT1 inhibitors that are based on *N*-arylalkenyl or *N*-arylalkynyl substituents.

Cross-coupling reactions are generally based on transition-metal catalysts.[50] Among them, the palladium-catalyzed ones are the most prominent. The generally accepted mechanism for these type of reactions is depicted in Scheme 1.

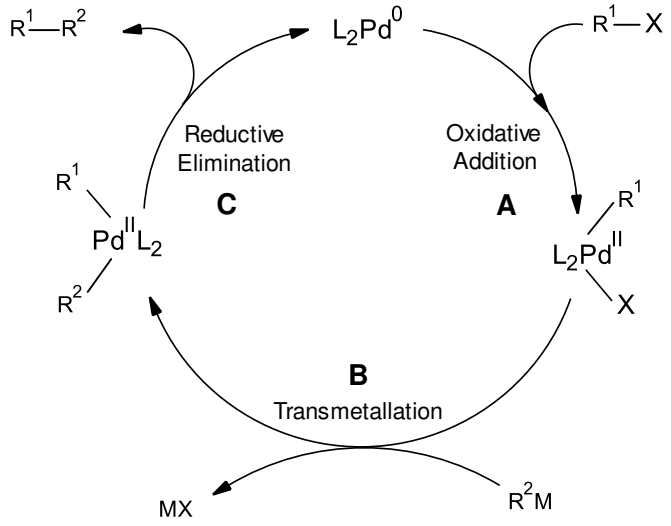

Scheme 1: General reaction cycle of palladium catalyzed cross-coupling reactions

The reaction mechanism generally begins with the oxidative addition (A) of mostly an organic halide (R^1-X) to the palladium(0)-catalyst, leading to an arylpalladium(II)-halide intermediate. Subsequently, the second reaction partner R^2M, an organometallic compound, undergoes transmetallation (B), whereby the organic residue is transferred to the palladium(II)-species by eliminating the functional groups as metal halide (MX). Subsequent reductive elimination (C) of the R^1-Pd^{II}-R^2 intermediate follows, forming the new C-C bond and thus delivering the respective organic product with simultaneous regeneration of the catalyst.[51]

Several factors determine the success of the reaction. The oxidative addition mostly is the rate determining step of the cross-coupling reactions. The ability for the palladium(0)-catalyst to insert into the R^1-X bond is facilitated when the binding energies of these bonds are reduced. Thus, the tendency to undergo oxidative addition can be stated with the reactivity order of the leaving group with I > OTf > Br >> Cl.[51] Additionally aryl halides with neighbored electron withdrawing groups are more reactive than those with electron pushing substituents.

The transmetallation is usually facilitated by a base. In case of the Suzuki reaction for example the addition of hydroxide to the metal of R^2M, here boron, leads to a fourfold coordinated boronate complex in this case and therefore a better nucleophilic species to attack the electrophile palladium(II).[52] It is also known the base HO^- to attack the R^1-Pd(II)-X complex and to displace the halide. The thus formed R_1-Pd(II)-OH intermediate can then react with the organometallic compound R^2M transferring the organic moiety from the metal M to the palladium(II).[52] The high reactivity of the R^1-Pd(II)-OH is owed to the basicity of the Pd-OH species and the high need of the boron center to form a bond to the oxygen. In case of the Sonogashira reaction the base should deprotonate a terminal alkine in order to equally increase the nucleophilicity. Since the usually used bases are not strong enough for that purpose copper is usually applied as co-catalyst. This Cu(I)-halide as Lewis acid can form a π-alkine-complex that mediates deprotonation, resulting in an copper acetylide as nucleophilic agent for the transmetallation.[53]

Also the solvents used and the nature of the bases have an impact on these reactions. Whereas Suzuki couplings are mostly performed in a two phase system that arises by adding an inorganic base to a homogeneous mixture of organic solvent and water,[52] Sonogashira couplings are usually established in amines as solvents that in this case simultaneously represent the base. Inorganic bases like carbonates or phosphates are usually combined with aqueous systems. These allow the dissolution of the base which may accelerate the reaction. Though side reactions like hydrolysis are more likely to appear under these conditions.

Finally diverse ligands (L) of the palladium have been established in order to stabilize the palladium(0) species and to mediate reactivity of the same towards all three steps of the catalytic cycle. The use of electron rich phosphines thereby was found to show enhanced rates oxidative addition and reductive elimination step.[54]

1.4 The use of light for the activity control of ligands

Since neurotransmission is based on the interaction of ligands with proteins such as transporters, there was the idea to modify ligands with a light controllable functional group as approach to study the structure and function of their targets in dependence on the different activity of those ligands. This chapter will deal with photoswitchable compounds and their establishment in medicinal chemistry.

1.4.1 Photochromism and photoswitchable compounds

A molecular switch is a chemical species that can be reversibly shifted between two or more stable states. The molecules may be switched between these states in response to an external environmental stimuli, such as changes in pH, light, temperature or an electric current.[55]

If this transformation is caused by using light of a set wavelength, this phenomenon is also known as photochromism. Thereby, different physicochemical properties of the molecule may change such as absorption spectra, refractive index, dielectric constant, oxidation/reduction potential, and geometrical structure.[56] These molecular changes have been used in various fields for example in photonic devices such as erasable optical memory media (Compact Disc), in nanotechnology for application in molecular computers or responsive drug delivery systems and also play an important role in molecular self-assembly and photo-controlled biological systems. In the latter case, photochromic compounds may also occur as ligands for proteins.

Photochromic reactions include isomerization reactions of C=C or N=N double bounds but also pericyclic reactions like rearrangements or ring opening and closing reactions. These are mostly unimolecular reactions upon which the thermodynamically stable form reversibly turns to a form of a higher energy level under illumination.[56] Back reactions can be caused by light of a different wavelength or by heating in the dark (thermal relaxation). For this reason, photochromic compounds are also called photoswitchable compounds. Ideal photoswitches undergo reversible photochemistry without any side reactions so that many rounds of active/inactive states can be produced.

Isomerization reactions are one of the most spread photochromic reactions and are based on this principle. Whereas E/Z-isomerization reactions of C=C double bonds like diarylethenes

mostly result in products that are stable under physiologic conditions and additionally may form phenanthrene-like side products during irradiation[57] the ones of N=N double bonds like azobenzenes rather tend to do back isomerize to the thermodynamically more stable form by itself within a characteristic time interval.[58] Furthermore, many isomerization cycles are possible without the occurrence of side or decomposition reactions. Therefore, photochromic E/Z-isomerization of azobenzenes has been used extensively in molecular switches, e.g. for the photo-control of biomolecules, often taking advantage of its geometrical change of shape upon isomerization to produce a supramolecular result.

The thermodynamically stable (*E*)-isomer of azobenzene can be isomerized to its (*Z*)-isomer by using light with a wavelength of 340 nm. The (*Z*)-isomer adopts a bent conformation with its phenyl rings twisted by about 55° out of the plane from the azo group (Figure 10). This is the reason that both isomers strongly differ in their absorption spectra. Whereas (*E*)-azobenzene shows a weak n–π* band near 440 nm and a strong π–π* transition near 320 nm (*Z*)-azobenzene has a stronger n–π* band also near 440 nm and shorter wavelength bands at 280 nm and 250 nm (Figure 8). Back isomerization can be induced by light with a wavelength of 450 nm or by thermal relaxation.[58] Since the absorption spectra of the (*E*)- and (*Z*)-isomer overlap substantially, isomerization never runs in a quantitative scale and irradiation produces a photostationary state with up to 95% of the (*E*)-isomer.[58] However, thermal relaxation of the (*Z*)-isomer leads to essentially 100% of the original (*E*)-isomer. Unmodified azobenzene undergoes thermal relaxation on a timescale of days at room temperature.[58]

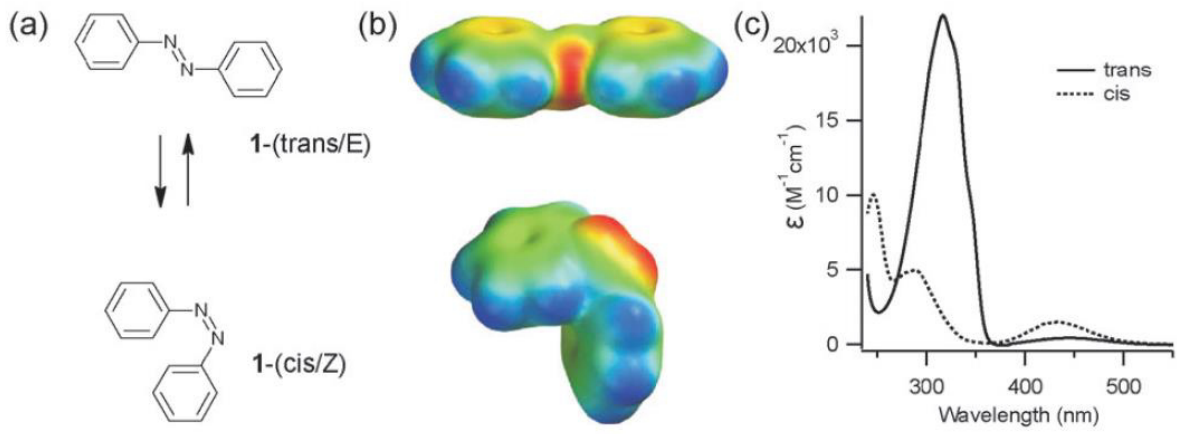

Figure 10: a) chemical and b) 3D structures of (*E*)- and (*Z*)-azobenzene; c) UV spectra of (*E*)- and (*Z*)-azobenzene[58]

1.4.2 Establishments of photoswitchable ligands

Provided a particular molecule can be made light sensitive by a simple modification, the light induced management of neuronal activity represents an elegant possibility to control a target since light can be regulated with high temporal and spatial precision. This can be achieved if some basic requirements are fulfilled. Accordingly, the modified molecule must absorb light effectively at a wavelength compatible with biological systems (λ = 340 nm up to 800nm). The modification must allow a photochemical reaction with high efficiency so that the light dosage required to trigger an effect is not too high, but it should simultaneously modify the ligand in a manner that leads to substantial change in biological activity. Finally, the modification should be inert towards biological conditions and non-toxic both before and after irradiation.

A variety of approaches have been taken to chemically modify a ligand in a manner aimed at endowing it with a light-controlled function. Among them, photoaffinity labeling is based on a photochemical reaction between a photo labile group of a ligand and a functional group of the protein, in order to interconnect ligand and target covalently.[59] In case of phototriggering ("caging") a substrate of a target is liberated by removing a photolabile protection group ("caging" group) from an appropriate precursor molecule by means of light and thus releasing a key functional group for its activation.[58] Finally, photoswitchable ligands are a class of compounds that, as aforementioned, make use of light in order to control activity of a biological target reversibly. Ideally, the structural change after irradiation will bring along a significant difference of affinity to the targeted biomolecule. In this way, photoswitches offer the possibility to introduce light sensitivity to various biological targets, thereby facilitating the mentioned precise control of neuronal activity with light.

In recent time, many studies appeared on this subject using in particular photoswitchable ligands based on azobenzene, because it inheres most of the criteria outlined above. Using azobenzenes as photoresponsive elements, it was already possible to develop photoswitches for targets like epithelial sodium channels,[60] insulin receptors,[61] the acetylcholinesterase,[62] μ-opioid receptors,[63] TRPV1-channels,[64] glutamate receptors,[65] NMDA receptors,[66] AMPA receptors,[67] local anesthetics[68] as well as cell division.[69] Our research group recently described the use of this method for the first time to control the activity of mGAT1 by means of a photoswitchable GABA uptake inhibitor.[70]

2 Aims and Scope

Even though a large number of different antiepileptic drugs (1.1.2 Pathology and Therapy) exists, not all epilepsy patients show a sufficient therapeutic response to medical treatment with antiepileptic drugs. In this context, GATs represent an interesting target for the drug development. The principle aim of this study was to find new ligands acting as highly potent and selective inhibitors for mGAT1 as well as new photoswitchable ligands for this target.

2.1 Nipecotic acid derivatives with *N*-arylalkenyl and *N*-arylalkynyl substituents

Recently, M. Sindelar from our group created a variety of GABA uptake inhibitors based on the hydrazone containing structure (*RS*)-**15** (Scheme 2).[71] Outgoing from these structures it was intended to exchange the hydrolytically sensitive hydrazone-type spacer through the hydrocarbon analogous pent-4-en-1yl-spacer in order to obtain the stable carba analogue structures (*RS*)-**16** (Scheme 2) for all identified hydrazone based hit compounds. The effects to the targeted mGAT1 should be comparably investigated for both types of compounds. Synthetic access to these carba analogue compounds may be inspired by the synthetic approaches of M. Petrera[46] that were already leading to the homologue compounds with but-3-in-1-yl spacer (see (*RS*)-**13**, Figure 7), but were intended to be optimized in scope of syntheses of the representatives with the longer spacer.

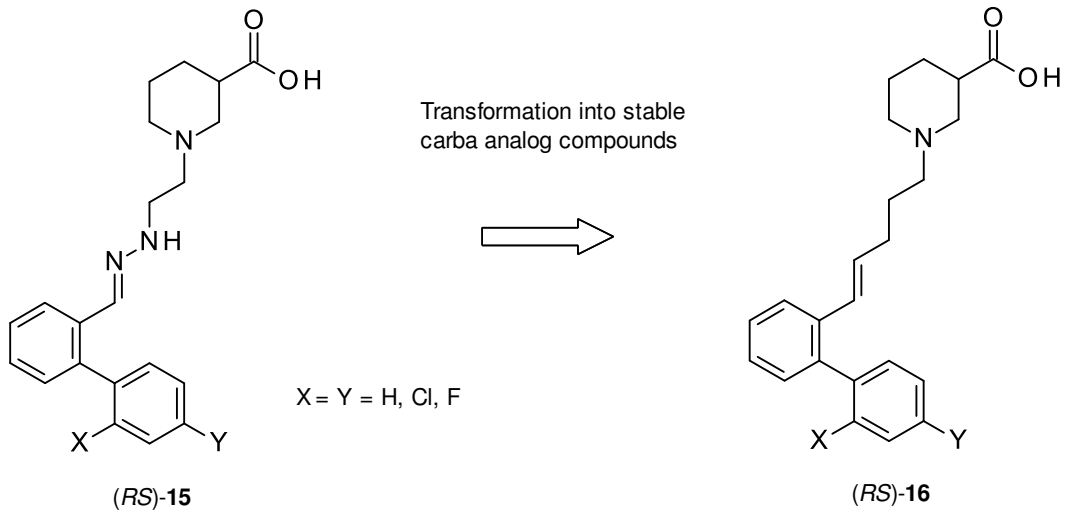

(*RS*)-**15** (*RS*)-**16**

Scheme 2: Potent GAT1 inhibitors by M. Sindelar[71] and stable carba analogue target compounds

Beyond, a new spacer type should be established as part of the N-substituent of nipecotic acid that typically links the amino acid with the aryl moiety. Since compounds containing a double bond in the spacer, linking an appropriate aromatic residue with nipecotic acid, in the past mostly delivered compounds with promising affinities to mGAT1, it was now intended to investigate analogue structures bearing a triple bond instead of the double bond in (apart from that) identical compounds, in order to explore the influence of the different geometry of ligands, resulting from a more linear spacer type, on the biological activity. Compounds may be represented by the basic structure (*RS*)-**17** (Scheme 3).

As shown in Scheme 3 target compounds were considered to be made by N-alkylation of nipecotic acid ester **18** (Scheme 3) with the but-3-ynyl or pent-4-ynyl halide **19**, followed by a Sonogashira cross-coupling reaction in order to introduce a first phenyl moiety as key step. Thereby, the electrophile that may be used for this purpose should also bear a second halogen function in order to link a second phenyl moiety to the thus gained coupling product in a next step. For this reason, 1-bromo-2-iodo benzene (**20**) could represent a suitable component for the Sonogashira reaction. By means of an ensuing Suzuki cross-coupling reaction, different phenyl moieties, that may exhibit different substituents in the 2´ or 4´ position, could be attached in a flexible manner. In this context, appropriate substituted phenylboronic acid derivatives (**21**) could be employed as building blocks for the terminal phenyl moiety.

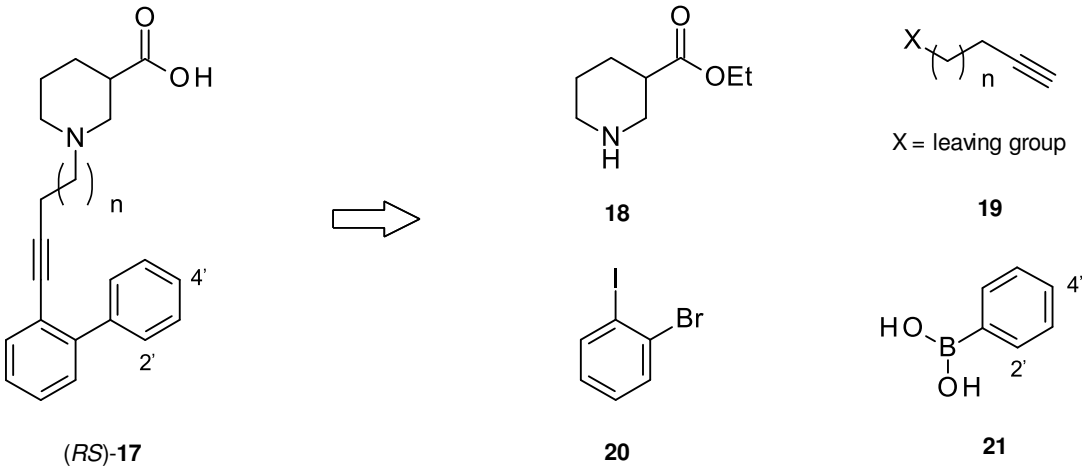

Scheme 3: Basic target structure for GABA uptake inhibitors with alkynyl spacer and retro synthesis plan

2.2 Nipecotic acid derivatives with photoswitchable N-substituents

Since photoswitchable GAT inhibitors may open up the possibility for the selective and precise control of the activity of GATs and may thus allow the further investigation of their structure and function, a series of new photoswitchable GAT1 inhibitors was intended to be developed.

As an progression towards the already existing photoswitchable GABA uptake inhibitors like (*R*)-**22** (Scheme 4),[70] which is characterized by an ethoxyethyl spacer, derivatives based on an unsaturated spacer type with four or five carbon atoms including either a double or triple bond were envisaged. In this context, the photosensitive subunit should be represented by a diphenyldiazene or a naphthylphenyldiazene with either *ortho*-, *meta*- or *para*-connection of both aromatic systems (see general Structure **23**, Scheme 4).

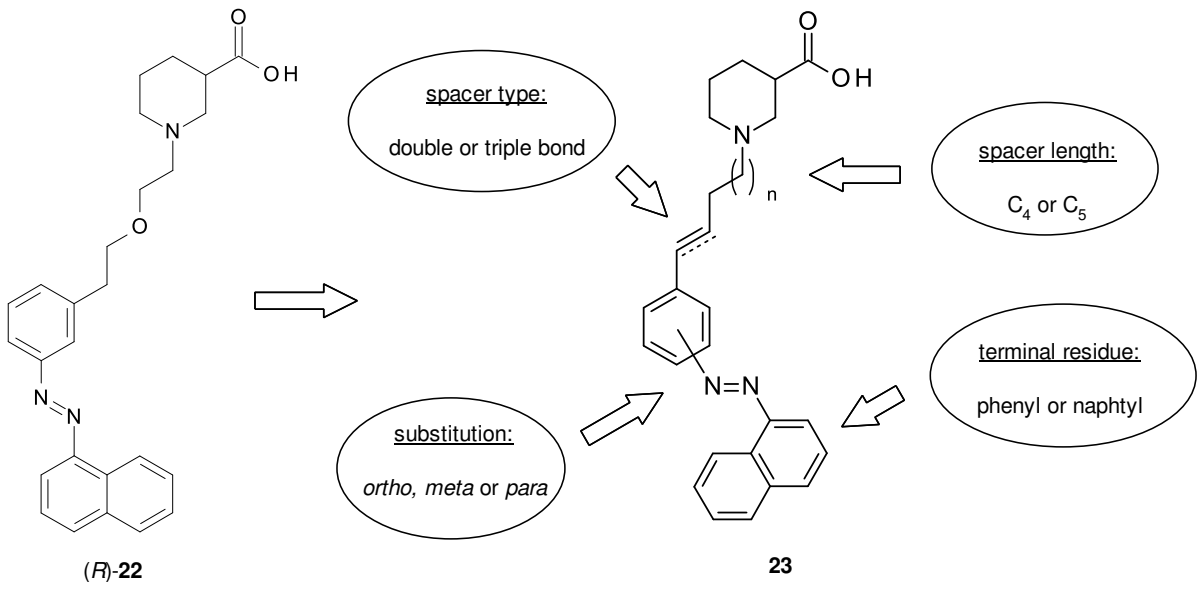

Scheme 4: Already existing most efficient phtotswitchable GAT1 inhibitor and design of the desired new ones

Among the already existing photoswitchable GAT1 inhibitors, the most effective compound (*R*)-**22** (Scheme 4) exhibited a pIC_{50} of 6.39±0.08 for its pure (*E*)-configuration. After irradiation with light, a decreased value of 5.78±0.03 could be observed in the biological test.[70] In order to get compounds whose activity can be increased by the use of light, new derivatives should exhibit a low inhibitory activity towards the transporter in their ground states and a preferably significant higher one in their photoirradiated ones.

Synthesis of these series of compounds was intended to be achieved either by a convergent synthesis route interconnecting the pre-built photosensitive subunit with the nipecotic acid derivative that already bears the spacer with a terminal alkyne or vinyl boronic acid ester. Alternatively, a linear synthesis route, starting from the diaryldiazene and establishing one cross coupling reaction in order to introduce the spacer first, followed by the connection of the thus gained final N-substituent with nipecotic acid, could be developed.

Besides the final photoswitchable ligands, it might be useful to have diaryldiazenes units that are characterized by a specific substitution pattern as it is shown for structure **24** in Scheme 5. Provided a given diphenyldiazene to bear substituents like halogens at one of the two phenyl moieties in the *ortho*- or *para*-position of the diazene function, the resulting photosensitive subunit might not only lead to enhanced interactions with the target as it was found in previous studies,[71] but may also allow to tune the isomerization kinetics of the photosensitive compounds as well as the wavelength of the necessary light used for that purpose. A halogen function on the other phenyl moiety would make it possible to assemble it to the final photosensitive target compounds by cross coupling reactions.

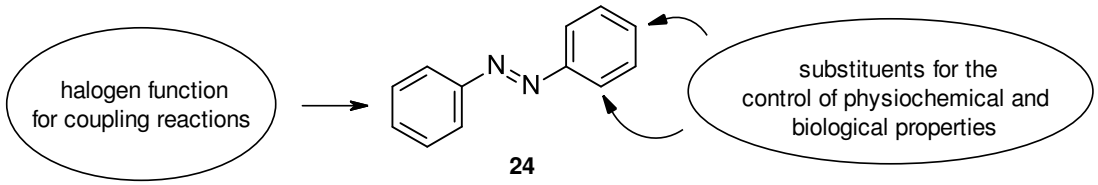

Scheme 5: General composition of substituted diphenyldiazenes

The synthetic access to these unsymmetrically substituted diphenyldiazenes may be possible by the establishment of an azo coupling reaction using diazotized aniline with leaving function and an N-protected aniline derivative, which might also bring along a further substituent, as coupling components. The N-protection group should enable a regio selective azo coupling, activate this building block for electrophilic aromatic substitution, and should be introduced before and cleaved after the azo coupling in an easy and selective manner, respectively. The resulting amine function may also be transformed into a further halogen at the end.

3 Summary of manuscripts and published results

3.1 Focused Pseudostatic Hydrazone Libraries Screened by MS Binding Assay – Optimizing Affinities towards γ-Aminobutyric Acid Transporter 1

Screening of compound libraries, generated by simple and most efficient reactions commonly used in dynamic combinatorial chemistry displays a valuable tool for the fast hit identification among a high amount of compounds differing in their kind of composition of the building blocks set in respectively.

This publication applies this method for the hit identification of potential mGAT1 inhibitors. The latter were generated as hydrazones from the in situ reaction of a nipecotic acid derived hydrazine as one fixed building block and a library of diverse aromatic aldehydes as variable second building blocks with complementary reactivity. Generation of the libraries was performed in presence of the target under conditions appropriate for a subsequent MS binding assay of the same sample. To facilitate hit detection, libraries were kept pseudostatic, meaning that the thus generated one-dimensional libraries staying almost constant in their composition but still dynamic in their natural entity. This was achieved by reacting sets of different aldehydes with an excess of the hydrazine derived nipecotic acid. After library generation was performed, addition of the native MS marker NO711 to the same sample directly enabled detection of active libraries by the MS binding assay.

In this manner a hydrazone generated from biphenyl-2-carbaldehyde was identified as one of two hits from a first screening round (pK_i = 6.186 ± 0.028). In this context, another aim was to further improve the affinities to mGAT1 by substitution of the biphenyl residue. Accordingly, hydrazone libraries comprising compounds with different substituted biphenyl moieties were generated and screened under the same conditions. In this way the screening of various focused pseudostatic hydrazone libraries revealed many hydrazone hits with even higher affinities than the original hit compound generated from the sole biphenyl-2-carbaldehyde. The most potent hit compounds exhibited halogen substituents in the *ortho*- and/or the *para*-position of the terminal phenyl moiety. For these compounds p*K*i values up to 8.094 ± 0.098 could be observed and thus almost 2 log units higher than that of the original lead compound.

A choice of the most potent hydrazone derivatives found in this way should serve as template for the synthesis of stable carba analogue compounds since the hydrazones tend to be sensitive towards hydrolysis. For this reason, the hydrazone containing spacer of overall 5 atoms, interconnecting the nitrogen of nipecotic acid with the biphenyl subunit, was exchanged by a hydrocarbon type pent-4-en-1-yl spacer that entails the most similarity to the hydrazone spacer concerning length and molecule geometry.

Synthetic access was realized similar to a method of M. Petrera[46] by the synthesis of an N-alkylated nipecotic acid derivative bearing a vinyl boronic acid ester at the ω-position of the spacer, which could be subjected to two consecutive Suzuki-Miyaura reactions. By means of the first one, 1-bromo-2-iodobenzene was attached that already exhibited a further halogen in order to tie on the second terminal phenyl moieties which were employed as substituted phenyl boronic acid derivatives, by means of a second Suzuki reaction.

The thus gained carba analogue compounds were tested under the described conditions by MS binding assay. Though all this compounds showed a slightly less affinity at the targeted mGAT1, the rank order of potency of these carba analogues in the binding studies was the same as the one of the corresponding hydrazone derivatives. Thus, it could be demonstrated that the hydrazone based hit compounds found by the screening can be successfully used as starting point for the development of almost equally potent stable lead structures.

Declaration of contributions:

The main intention of this study, the application of MS binding assay for the screening of compound libraries was introduced by Miriam Sindelar as well as the development and implementation of the described screening method leading to the hydrazone based hit compounds including synthesis and analytic of these derivatives. Synthesis and analytic of all carba analogue compounds and precursors was done by me.

3.2 Development of highly potent GAT1 Inhibitors: Synthesis of Nipecotic Acids Derivatives with N-arylalkynyl substituents

GABA uptake inhibitors based on an alkenyl spacer interconnecting the nitrogen of nipecotic acid with an appropriate aromatic residue, such as a 2-biphenyl moiety, were recently found to exhibit high affinity towards mGAT1.[46]

In this publication a further new stable spacer type for the assembly of potential GABA uptake inhibitors that was based on a triple bond was introduced and the affinities of the thus gained compounds towards mGAT1 were characterized by biological evaluation. New nipecotic acid derivatives were derived from the known highly potent GAT1 inhibitors based on an alkenyl type spacer by exchanging the but-3-en-1-yl or pent-4-en-1-yl linker by the more linear but-3-in-1-yl or pent-4-in-1-yl analogue one. The aromatic part of the N-substituent was again represented by diverse substituted biphenyl moieties since a homology modeling study with accompanied docking experiments, employed within this publication, revealed compounds bearing these types of aromatic residues as possibly highly potent.

In order to get access to these new type of ligands an appropriate synthesis route was developed. Accordingly, nipecotic acid derived terminal alkynes were established as suitable precursor molecules for the establishment of subsequent Sonogashira reactions in order to attach the aromatic residues. For this reason, three different aromatic electrophiles were used: 2-iododiphenylmethane, 2-iodobiphenyl and 2-bromoiodobenzene. Though the alkyne was used as starting material with just one equivalent – the nucleophile commonly needs to be used in excess for Sonogashira reactions[53] – yields for these cross couplings could be optimized to a high scale of up to 84%. The first two electrophiles delivered the finished preliminary parent compounds as GABA uptake inhibitors in just one key step. The third one was established in order to have a second halide for a subsequent Suzuki reaction upon which by reaction with diverse substituted phenylboronic acid derivatives as nucleophiles a variety of different terminal phenyl moieties could be introduced. For the construction of the biphenyl subunit a catalyst system established by the group of Buchwald[54] for the same purpose was successfully employed and adopted here since the former used Pd-catalyst (first publication) tended to form side reactions due to the neighbored triple bond of the spacer.

In accordance to the studies of M. Petrera,[46] among the basic structures, compounds bearing the biphenyl type residue as aromatic part were observed to exhibit higher binding affinities to mGAT1 than those with the 2-diphenylmethane subunit. Compounds with but-3-in-1-yl spacer turned out to contain the more appropriate spacer length for biologic activity than derivatives bearing the homologous longer one. As compared to the N-substituted nipecotic acid derivative with but-3-en-1-yl spacer and a terminal attached 2-biphenyl residue (*RS*)-**13** (Figure 7, pK_i = 7.15±0.07, pIC50 = 6.79±0.12), the biological test of the analogue parent compound (*RS*)-**17** (Scheme 3) with but-3-in-1-yl spacer exhibited an increased affinity and inhibitory activity towards mGAT1 (pK_i = 7.61±0.03, pIC_{50} = 7.00±0.06). Inspired by the homology modeling results and the intention of a further activity enhancement a series of related compounds of the lead structure (*RS*)-**17** (Scheme 3) with different substituents in the positions 2´ and 4´ of the terminal phenyl residue was synthesized and biologically characterized. This way binding affinities up to 8.33±0.01 (pK_i) and uptake inhibitory potencies up to 7.72±0.02 (pIC_{50}) of the enantiopure nipecotic acid derivatives could be observed. Thus, the new mGAT1 inhibitors are among the most potent ones known so far. All new compounds did not show considerable inhibitory activity towards the other GABA transporters which means the inhibitory effect to be selective towards mGAT1.

Declaration of contributions:

Thomas Wein did the hGAT1 homology modeling study this publication is based on for all GAT inhibitors including calculation of docking scores. Synthesis of all compounds and precursor molecules was done by myself including evaluation of all corresponding analytical data. The practical performance of the biological test of all compounds was carried out by the technical assistants of the group under supervision of Georg Höfner.

3.3 Development of new photoswitchable azobenzene bound GABA uptake inhibitors with distinctly enhanced potency upon photoactivation

The use of light as trigger to control the activity of GABA uptake inhibitors may be achieved by the establishment of ligands bearing a photoswitchable subunits with different inhibitory effects towards GAT1 dependent from the configurational states of this subunit.

Within this study a series of photosensitive nipecotic acid derivatives was synthesized and their inhibitory activity towards mGAT1 was characterized before and after photoirradiation. Thereby, the previous introduced alkenyl and alkinyl spacer types were used for construction of linkers with 4 or 5 carbon atoms. The biphenyl subunit was exchanged by a photosensitive one represented by either a diphenyldiazene or a naphthylphenyldiazene. Substitution of the internal phenyl unit was chosen to be *meta* or *para* in relation to the spacer because of the *ortho*-substitution from the outset did not seem to deliver potent GAT inhibitors according to a homology modeling study that was set in within this study in order to evaluate binding affinities to hGAT1 for both configurational states of the N-N-double bond in each case.

Synthesis of photoswitchable GAT1 inhibitors containing a double bond in the spacer was accomplished by a convergent synthesis route subjecting nipecotic acid derived vinylboronic acid esters to Suzuki cross-coupling reactions with the pre-built photosensitive subunits as electrophile, in order to generate the finished GAT1 inhibitors in just one key step. However, for compounds with alkyne spacer, a linear synthesis route turned out to be more efficient and was principally used for the construction of these type of GAT1 inhibitors. It started from the photoswitchable subunit and used but-3-in-1-ol or pent-4-in-1-ol as substrates for Sonogashira cross-coupling reactions, followed by the transformation of the alcohols into leaving groups and the final reaction of the gained electrophiles with nipecotic acid ester.

The appropriate wavelengths for the isomerization of the photosensitive subunits were found by UV spectroscopy and irradiation with light of different wavelength in the range of 350 nm or 375 nm. A stock solution in DMSO of all synthetized compounds was then irradiated immediately before the biological test until the photo stationary state was reached. The proportion of ($Z_{N=N}$)-isomer was determined by ^{1}H NMR-spectroscopy. Uptake inhibition experiments towards mGAT1 were performed subsequently for both photoirradiated and not photoirradiated samples of each compound.

Compounds containing an alkinyl- instead of an alkenyl-spacer turned out to exhibit higher differences in the biological activity at mGAT1 for their ground states as compared to their photoexcited ones, caused by irradiation. Thereby, the (*E*)-configured alkyne derivatives with C_4 spacer were found to display higher inhibitory potencies at mGAT1 than the homologues compounds with the C_5 linker. Commonly, mGAT1 inhibitors bearing photoswitchable subunits with a *meta*-substitution were observed to be less active for their (*E*)-configuration, but significantly more active for their photoequilibrium mixture after irradiation, whilst for the *para*-substituted ones the opposite was true. For mGAT1 inhibitors bearing diphenyldiazene subunits, potency differences before and after irradiation in general were found to be more distinctive than for those with naphthylphenyldiazene moieties.

The (*R*)-nipecotic acid derivative with but-3-in-1-yl spacer and an attached *meta*-substituted diphenyldiazene subunit was found to be the most efficient photoswitchable mGAT1 inhibitor. The functional inhibitory activity towards mGAT1 for its ground state was determined to be 4.65±0.05 (pIC_{50}). After irradiation, a distinctive higher one of 6.38±0.04 could be observed. Concerning this matter, it is the first GAT1 inhibitor that can be “switched on” effectively. Forward and back isomerization under physiological conditions (phosphate buffer, pH 7,4) was achieved by monochromatic light of 350 nm or 420 nm, resulting in a proportion of the more active (*Z*)-isomer of about 95% or 25%, respectively. The half-life of thermal relaxation was determined to be 15 days in DMSO or 22 days in phosphate buffer (pH 7,4) at 25 °C.

Declaration of contributions:

Thomas Wein did the modeling study for the photoswitchable GAT1 inhibitors. Synthesis of all compounds and precursor molecules was done by myself including evaluation of all corresponding analytical data. I also did all isomerization experiments and the measuring of kinetical data. The biological studies were carried out by the technical assistants of the group under supervision of Georg Höfner.

3.4 A general approach to substituted diphenyldiazenes

Azo compounds have found widespread chemical and pharmaceutical application e.g. as dyes and pigments, food additives, indicators for pH-measurements, initiators for radical reactions or as therapeutic agents. Meanwhile a major focus of diaryldiazenes is on their use as light sensitive molecular switches (see chapter 1.3.1).

Within this publication, a general approach to various specific substituted diphenyldiazenes as well as a method easily leading to different naphthylphenyldiazenes was introduced. According to Scheme 5 in chapter 2.2, diphenyldiazenes should bear a halogen function at one of the two phenyl moieties, allowing the assembly of the final photosensitive compounds by cross coupling reactions. Further substituents such as halogens or alkyl groups should be located preferentially in the *ortho*- and/or the *para*-position of the second phenyl moiety since substituents in these positions were on the one hand expected to improve binding affinities to mGAT1, and halogens in this position additionally might allow to adjust the isomerization kinetics and size of wavelength for photoisomerization.

However, the substitution pattern of aromatic azo compounds accessible by the classical reaction types or sequences is in general quite limited and leads to a mixture of symmetrically and unsymmetrically substituted diphenyldiazenes in the most cases and poor yields in consequence. In order to come to such specifically substituted diphenyldiazenes, within this study, the well-known azo coupling reaction method was used as key reaction step for the construction and two appropriate building blocks were established for this reaction type. This was realized by employing a phenyldiazonium derivative with an iodine substituent as first building block and an N-protected aniline derivative that might also bring along a further substituent, as second coupling component. Thereby, the N-protecting group was represented by a *N*,*N*-diallyl group and could as such fulfil two necessary requirements during synthesis: It prevents this coupling component to directly react by its primary aromatic amino function with the diazonium salt, leading to triazene formation and a lot of byproducts formed through rearrangements, and should nevertheless guarantee a sufficient electron density to undergo the desired electrophilic aromatic substitution.

The azo coupling reactions were found to run in useful to excellent yields dependent from the further substituent of the *N*-protected coupling component that might be present. Reaction conditions were optimized concerning pH, temperature and reaction time. Furthermore, after the azo coupling reaction, the *N*,*N*-diallyl protection group could be cleaved in an easy and selective way by establishing a method effecting C-C double bond isomerization, followed by hydrolysis of the resulting divinylamine. For this purpose, the use of the transition metal catalyst $RuClH(CO)(PPh_3)_3$ for the former and the ensuing application of hydroxylamine hydrochloride and triethylamine for the latter, under respectively adopted reaction conditions, delivered quantitative yields for both steps. The thus released primary aromatic amino function in the *para*-position provides the opportunity for a broad array of transformation reactions in a next step. This was exemplified on the one hand by its replacement by hydrogen in order to get a mono- (*ortho*-) substituted terminal phenyl moiety, and on the other one by employing adopted Sandmeyer or Schiemann type reactions in order to introduce chlorine or fluorine substituents for the construction of alternatively mono- (*para*-) or disubstituted (*ortho* and *para*) terminal phenyl moieties. All transformation reactions run with the common yields for these reaction types.

In context with this procedure also 1-naphthylamine was employed as coupling component and found to undergo the azo coupling without N-protection selectively and in quantitative scale to directly obtain the primary amine for possible further transformations.

Declaration of contributions:

Synthesis of substituted diphenyldiazenes and all precursor molecules was done by myself including evaluation of the analytical data of all compounds. Patrick Spanner did some preliminary experiments for the azo coupling reaction employing sole *N*,*N*-diallylaniline as basic coupling component within his bachelor thesis under my supervision.

4 Conclusions

As one of the most abundant CNS diseases, epilepsy is associated with a diminished GABAergic neurotransmission. Inhibition of GAT1, the most important GAT subtype in the brain leads to a higher GABA level and thus may help to alleviate symptoms resulting from that neurological disorder as it was already proved for the GAT1 selective inhibitor Tiagabine.

Within the first two studies of this thesis a series of nipecotic acid derivatives with new stable biphenyl alkenyl and biphenyl alkinyl residues as N-substituents were synthetized and characterized for their binding affinity and inhibitory potency at mGAT1. For the latter, a new synthesis route was developed giving flexible access to a wide range of aryl alkinyl substituents in general. Among the mentioned compounds, those bearing a pent-4-en-1-yl spacer could serve as hydrolytically stable carba analogues to the corresponding hydrazone derived nipecotic acid derivatives, though they exhibited a slightly lower binding affinity and functional inhibitory activity at mGAT1. However, compounds based on a but-3-in-1-yl spacer in both respects were found to be in a comparable scale potent as analogue nipecotic acid derivatives derived from a but-3-en-1-yl or an oxime spacer type which belong to the most potent mGAT1 inhibitors known so far. As compared to the latter the new alkinyl spacer types likewise are inert towards hydrolytic and oxidative influences. The new N-substituents may act as starting point for the development of further similar mGAT1 inhibitors. The N-substituted nipecotic acid derivative bearing the 2-biphenylbut-3-in-1-yl residue for example could already serve as starting material for the synthesis of the related derivative comprising a (*Z*)-but-3-en-1-yl spacer by stereo selective reduction of the triple bond of the spacer.[46] The optimized Sonogashira cross-coupling reaction conditions developed for the assembly of the biphenyl alkinyl residues as N-substituent could be equally used for the final construction of nipecotic acid derivatives with the same substituents but in 4 position.[72]

Within the next two studies, a series of new highly efficient photoswitchable GABA uptake inhibitors as well as a general synthesis route for new photosensitive subunits was introduced. For the design of nipecotic acid derivatives bearing a photosensitive subunit, N-substituents were varied regarding the length and saturation degree of the spacer as well as the types of diaryldiazenes and kind of their substitution. Among the 16 final photoswitches, a derivative bearing an *N*-but-3-in-1-yl linker with a terminal diphenyldiazene unit, revealed distinctly enhanced potency upon photoirradiation. In this manner, the highest inhibitory potency towards mGAT1 as well as the highest difference in inhibitory activity between its two configurational shapes could be observed for this compound. This property is described for the first time for the mentioned target and may be a valuable feature for biological studies. It may help to gain a more detailed knowledge about the structure and function of GAT1 by analyzing and comparing structure activity relationship for both isomeric compounds. Additionally, it may serve as template for the design of similar GAT1 inhibitors bearing various substituted photoswitchable diphenyl diazenes for the adjustment of isomerization kinetics. On this occasion, also a general method for the construction of different substituted diphenyldiazenes as well as naphthylphenyldiazens was developed. The final products of this approach can be used as building blocks for the assembly of a variety of photoswitchable target compounds in general. Thereby, the halogen substituents in the *ortho*- or *para*-position at one of the phenyl moieties may allow a faster isomerization kinetic without becoming considerable more polar as it is true for hydroxyl or amino functions. Among this choice of photoswitchable units, a naphthylphenyldiazene, that was gained this manner, was already used for the construction of the first photoswitchable GAT inhibitor.[70]

Overall, the new introduced compounds might represent a useful tool and intermediate step for the further progression in search of new mGAT1 selective inhibitors that one day possibly may serve as final active substances for the successful treatment of neurological diseases.

5 Further experiments

Besides the previous listed publications and manuscripts there were done further experiments that were not content of one of these studies. These are described in the following section.

5.1 Nipecotic acid derivatives with 2-thienylphenyl moiety

In context of the carba analogue compounds of the first publication two more nipecotic acid derivatives containing a 2-thienylphenyl moiety instead of the biphenyl subunit at the ω-position of the pent-4-en-1-yl-spacer (Scheme 6) were synthesized. Synthesis was achieved by a similar method as described in this publication (see Scheme 6).

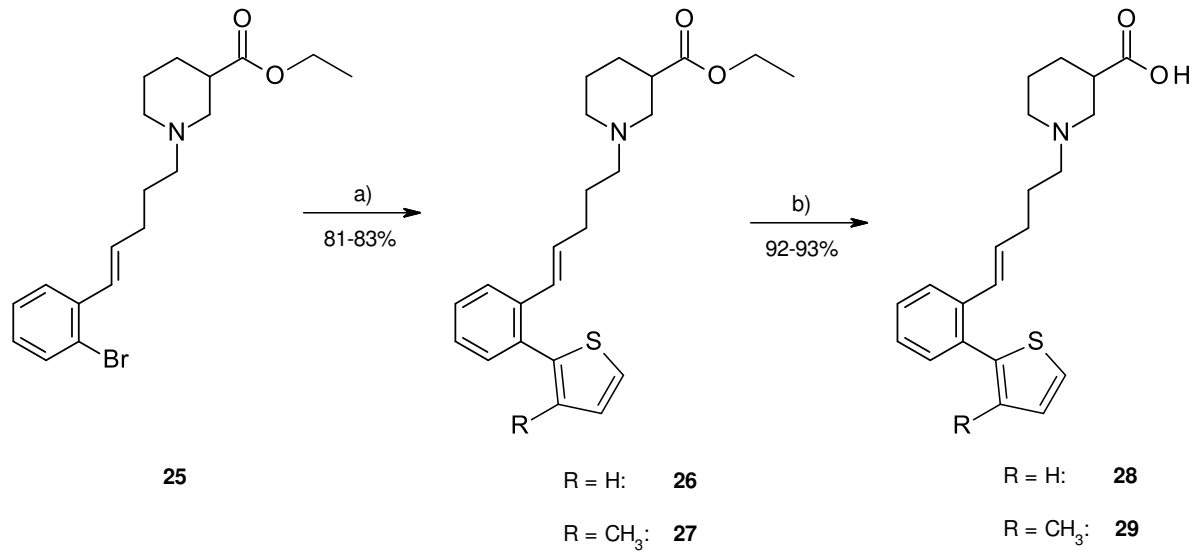

Scheme 6: Synthesis of nipecotic acid derivatives with 2-thienylphenyl moiety. Reagents and conditions: a) $PdOAc_2$ (2 mol%), SPhos (4 mol%), K_3PO_4 (5.0 equiv), 2-Thiopheneboronic acid MIDA ester (1.5 equiv) or 3-Methyl-2-thiopheneboronic acid MIDA ester (1.5 equiv), dioxane/water, 80 °C, 3 h; b) NaOH, EtOH, rt, 3 h.

For synthesis of this two target compounds, Ethyl 1-[(*E*)-5-(2-bromophenyl)pent-4-enyl]piperidine-3-carboxylate (**25**) was subjected to a Suzuki cross-coupling reaction with 2-Thiopheneboronic acid MIDA (= N-methyliminodiacetic acid) ester or 3-Methyl-2-thiopheneboronic acid MIDA ester to give the corresponding coupling products **26**-**27** as precursor molecules in good yields (81-83%). These could be cleaved into the final nipecotic acid derivatives **28**-**29** by basic hydrolysis (yield: 92-93%).

The free nipecotic acid derivatives **28** and **29** were equally characterized for their binding affinities at mGAT1 and inhibitory potencies towards mGAT1-4 (Table 4). Both characteristics were found to be in a similar scale as compared to the other carba analogue compounds described in this publication.

Table 4: binding affinities (pK_i) at mGAT1 and inhibitory potencies (pIC_{50}) towards mGAT1-4 of **27** and **28**

Compound	pK_i (± SEM)	pIC_{50} (± SEM)			
	mGAT1	mGAT1	mGAT2	mGAT3	mGAT4
28	6.04 ± 0.04	5.39 ± 0.09	67%[a]	73%[a]	55%[a]
29	5.89 ± 0.10	5.05 ± 0.10	52%[a]	69%[a]	36%[a]

[a] percentages represent remaining [^{3}H]GABA uptake in presence of 100 µM inhibitor

5.2 Sonogashira cross-coupling optimization reactions

The reaction conditions for the Sonogashira cross-coupling reactions of the second publication were extensively optimized (Table 5). This was done by the reaction of ethyl 1-but-3-yn-1-ylpiperidine-3-carboxylate (**30**) as alkyne component and 2-biphenylhalide (Ar-X, **31**) as electrophile in order to get the coupling product ethyl 1-[4-(2-biphenyl)but-3-yn-1-yl]piperidine-3-carboxylate (**32**, Scheme 7).

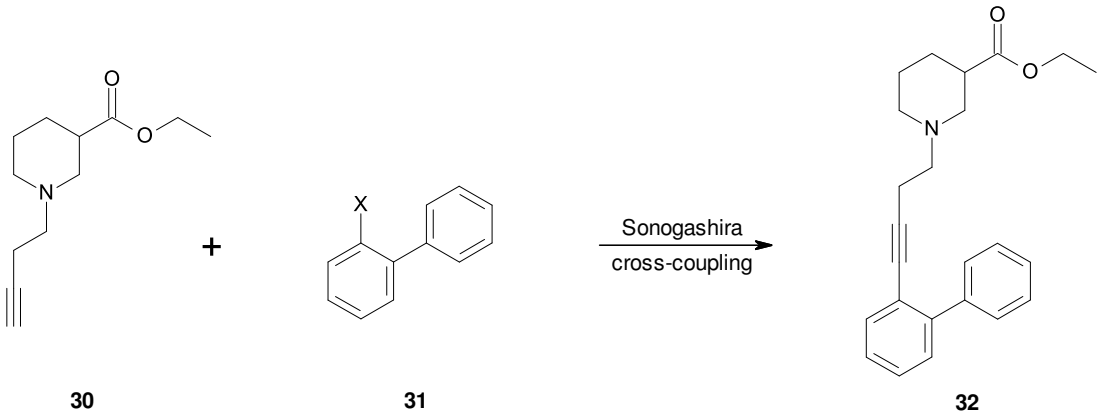

Scheme 7: Sonogashira cross-coupling model reaction. Reagents and conditions: see Table 5.

Starting from compounds **30** and **31** using standard conditions (10 mol% CuI, 5 mol% $Pd(PPh_3)_2Cl_2$, amine base pure or in a 1:1 mixture with THF, Table 1 entry 1-5) did not deliver the coupling product **32** in useful yields. For the first, Et_3N as base and dioxane as solvent were found to be most suitable. Changing the palladium catalyst to $Pd(dppf)_2Cl_2$ (Table 5, entry 6) did not significantly raise the yield but made the reaction rate faster. A higher temperature of 80° C instead of 60° C (Table 5, entry 7) turned out to form more side products instead of the desired one though at room temperature no reaction took place. However, by the exchange of the amine base through inorganic K_2CO_3 and the use a 5:1 mixture of dioxane and water, yields could be distinctly raised up to 45% dependent from the equivalents of the base used (Table 5 entry 8-12). A further clear improvement originated from the use of Ar-I as electrophile instead of Ar-Br (Table 5, entry 13) upon which the reaction time could be simultaneously lowered to 4 hours. In a next step the influence of the concentration of the copper catalyst was studied (Table 5, entry 14-18). The amount of 20 mol% was found to deliver the best yields whilst both a lower or higher concentration resulted in a distinct decrease of the same. Other established palladium catalysts (Table 5, entry 19-21) as well as a higher or lower concentration than 5 mol% of the $Pd(dppf)_2Cl_2$ (Table 5, entry 22-23) did not seem to be beneficial. Under the improved reaction conditions the organic base Et_3N (pure or in a 1:1 mixture with dioxane) likewise did not lead to useful results (Table 5, entry 19-20). Also the use of 3 equiv of Et_3N in combination with 3 equiv of

K_2CO_3 impaired the result noticeably (Table 5, entry 26) as compared to the sole use of K_2CO_3 in water under equal reaction conditions (Table 5, entry 16). The more polar solvent EtOH instead of dioxane (Table 5, entry 27) failed as well as the sole use of dioxane without water (Table 5, entry 28). A change of the proportion of dioxane/water from 5:1 to 4:2 (= 2:1) at the same total solvent amount and thus the same reaction concentration was done in order to enable the dissolution and usage of 6 equiv of K_2CO_3 but led to similar results (Table 5, entry 29) as compared to the original solvent proportion of 5:1 containing just 3 equiv of K_2CO_3 (Table 5, entry 16). In this context, the slightly stronger base K_3PO_4 delivered yields that were somewhat higher, independent from whether the 5:1 mixture of dioxane and water with 2 equiv of K_3PO_4 was used (Table 5, entry 30), or the 2:1 system in which 4 equiv could be dissolved (Table 5, entry 31). However, in the latter solvent proportion 3 equiv seemed to be sufficient (Table 5, entry 32) and delivered a more clearly aqueous phase. After the raise of the concentration of the total reaction mixture from 0.33 molar to 0.5 molar by halving the amount of organic solvent (ratio: 1:1), the reaction was finished within 3 hours (Table 5, entry 33). Since it is known that within a Sonogashira reaction the alkyne is mainly responsible for side reactions, this was reviewed by the use of 1.2 equiv of this component, resulting in an almost quantitative scale of the reaction (Table 5, entry 34). However, the alkyne **30** had to be synthesized first before the reaction with different commercially available electrophiles like **31** could be performed. Since the alkyne was completely consumed after all reactions and should for the mentioned reason not be used in excess, yields were intended to be referred to this building block. Finally, since the addition of any amine base was not tolerated and it might be possible that the piperidine derivative **30** – and thus the starting material – partially might be wasted for the initial reduction of the palladium catalyst, there was the attempt to cause this required reduction by sodium ascorbate. Though, its addition could not further improve the reaction yields (Table 5, entry 35+36). The found best results (Table 5, entry 33) were finally used for the synthesis of compounds within the second publication.

Table 4: Optimization studies of the Sonogashira cross-coupling reaction of Scheme 7

Entry	Ar-X	Cu (mol%)	Pd (mol%)	base	solvent	cond.	yield
1	X = Br	CuI (10%)	$Pd(PPh_3)_2Cl_2$ (5%)	Et_3N[1]	-	60°C, 72 h	11%
2	X = Br	CuI (10%)	$Pd(PPh_3)_2Cl_2$ (5%)	piperidine[1]	THF	60°C, 72 h	5%
3	X = Br	CuI (10%)	$Pd(PPh_3)_2Cl_2$ (5%)	iPr_2NH[1]	THF	60°C, 72 h	0%
4	X = Br	CuI (10%)	$Pd(PPh_3)_2Cl_2$ (5%)	Et_3N[1]	THF	60°C, 72 h	12%
5	X = Br	CuI (10%)	$Pd(PPh_3)_2Cl_2$ (5%)	Et_3N[1]	dioxane	60°C, 72 h	13%
6	X = Br	CuI (10%)	$Pd(dppf)_2Cl_2$ (5%)	Et_3N[1]	dioxane	60°C, 24 h	14%
7	X = Br	CuI (10%)	$Pd(dppf)_2Cl_2$ (5%)	Et_3N[1]	dioxane	80°C, 24 h	7%
8	X = Br	CuI (10%)	$Pd(dppf)_2Cl_2$ (5%)	-	diox/H_2O (5/1)	60°C, 24 h	0%
9	X = Br	CuI (10%)	$Pd(dppf)_2Cl_2$ (5%)	K_2CO_3, 1eq	diox/H_2O (5/1)	60°C, 24 h	30%
10	X = Br	CuI (10%)	$Pd(dppf)_2Cl_2$ (5%)	K_2CO_3, 2eq	diox/H_2O (5/1)	60°C, 24 h	36%
11	X = Br	CuI (10%)	$Pd(dppf)_2Cl_2$ (5%)	K_2CO_3, 3eq	diox/H_2O (5/1)	60°C, 24 h	45%
12	X = Br	CuI (10%)	$Pd(dppf)_2Cl_2$ (5%)	K_2CO_3, 4eq	diox/H_2O (5/1)	60°C, 24 h	44%
13	X = I	CuI (10%)	$Pd(dppf)_2Cl_2$ (5%)	K_2CO_3, 3eq	diox/H_2O (5/1)	60°C, 4h	61%
14	X = I	-	$Pd(dppf)_2Cl_2$ (5%)	K_2CO_3, 3eq	diox/H_2O (5/1)	60°C, 4h	0%
15	X = I	CuI (5%)	$Pd(dppf)_2Cl_2$ (5%)	K_2CO_3, 3eq	diox/H_2O (5/1)	60°C, 4h	53%
16	X = I	CuI (20%)	$Pd(dppf)_2Cl_2$ (5%)	K_2CO_3, 3eq	diox/H_2O (5/1)	60°C, 4h	72%
17	X = I	CuI (50%)	$Pd(dppf)_2Cl_2$ (5%)	K_2CO_3, 3eq	diox/H_2O (5/1)	60°C, 4h	57%
18	X = I	CuI (100%)	$Pd(dppf)_2Cl_2$ (5%)	K_2CO_3, 3eq	diox/H_2O (5/1)	60°C, 4h	48%
19	X = I	CuI (20%)	$Pd(PPh_3)_2Cl_2$ (5%)	K_2CO_3, 3eq	diox/H_2O (5/1)	60°C, 4h	40%
20	X = I	CuI (20%)	$Pd(PPh_3)_4$ (5%)	K_2CO_3, 3eq	diox/H_2O (5/1)	60°C, 4h	35%
21	X = I	CuI (20%)	$Pd(OAc)_2$ / S-Phos	K_2CO_3, 3eq	diox/H_2O (5/1)	60°C, 4h	38%
22	X = I	CuI (20%)	$Pd(dppf)_2Cl_2$ (10%)	K_2CO_3, 3eq	diox/H_2O (5/1)	60°C, 4h	58%
23	X = I	CuI (20%)	$Pd(dppf)_2Cl_2$ (2%)	K_2CO_3, 3eq	diox/H_2O (5/1)	60°C, 4h	66%
24	X = I	CuI (10%)	$Pd(dppf)_2Cl_2$ (5%)	Et_3N[1]	-	60°C, 4h	10%
25	X = I	CuI (20%)	$Pd(dppf)_2Cl_2$ (5%)	Et_3N[1]	dioxane	60°C, 4h	25%
26	X = I	CuI (20%)	$Pd(dppf)_2Cl_2$ (5%)	K_2CO_3/Et_3N[2]	diox/H_2O (5/1)	60°C, 4h	45%
27	X = I	CuI (20%)	$Pd(dppf)_2Cl_2$ (5%)	K_2CO_3, 3eq	EtOH/H_2O (2/1)	60°C, 4h	47%
28	X = I	CuI (20%)	$Pd(dppf)_2Cl_2$ (5%)	K_2CO_3, 3eq	dioxane	60°C, 4h	41%
29	X = I	CuI (20%)	$Pd(dppf)_2Cl_2$ (5%)	K_2CO_3, 6eq	diox/H_2O (2/1)	60°C, 4h	70%
30	X = I	CuI (20%)	$Pd(dppf)_2Cl_2$ (5%)	K_3PO_4, 2eq	diox/H_2O (5/1)	60°C, 4h	74%
31	X = I	CuI (20%)	$Pd(dppf)_2Cl_2$ (5%)	K_3PO_4, 4eq	diox/H_2O (2/1)	60°C, 4h	75%
32	X = I	CuI (20%)	$Pd(dppf)_2Cl_2$ (5%)	K_3PO_4, 3eq	diox/H_2O (2/1)	60°C, 4h	76%
33	X = I	CuI (20%)	$Pd(dppf)_2Cl_2$ (5%)	K_3PO_4, 3eq	diox/H_2O (1/1)	60°C, 3h	76%[3]
34	X = I	CuI (20%)	$Pd(dppf)_2Cl_2$ (5%)	K_2CO_3, 3eq	diox/H_2O (5/1)	60°C, 4h	96%[4]
35	X = I	CuI (20%)	$Pd(dppf)_2Cl_2$ (5%)	K_2CO_3, 3eq	diox/H_2O (2/1)	60°C, 4h	68%[5]
36	X = I	CuI (20%)	$Pd(dppf)_2Cl_2$ (5%)	K_3PO_4, 3eq	diox/H_2O (2/1)	60°C, 4h	71%[5]

[1] the base was used in excess (pure or in a 1:1 mixture with an additional solvent)

[2] 3 equiv of both K_2CO_3 and Et_3N were used

[3] the total concentration of the reaction mixture was raised from 0.33 molar to 0.5 molar

[4] 1.2 equiv of the alkyne component were used in this case

[5] 1.0 equiv sodium ascorbate was added to the reaction mixture

5.3 Alternative synthesis route for photoswitchable GABA uptake inhibitors

Originally, photoswitchable GABA uptake inhibitors containing an alkinyl spacer were intended to be synthesized by a linear synthesis route displayed in scheme **6**. Thereby, the terminal alkynes **33**-**34** should be reacted with *o-, m-* or *p*-iodoaniline (**35**) by Sonogashira cross-coupling reactions under the reaction conditions developed for the second publication in order to give the corresponding coupling products **36-37**. These primary aromatic amines should then be condensed with nitrosobenzene (**38**) to give the diphenyldiazene derivatives **39**-**40** as preliminary stages of the final photoswitches.

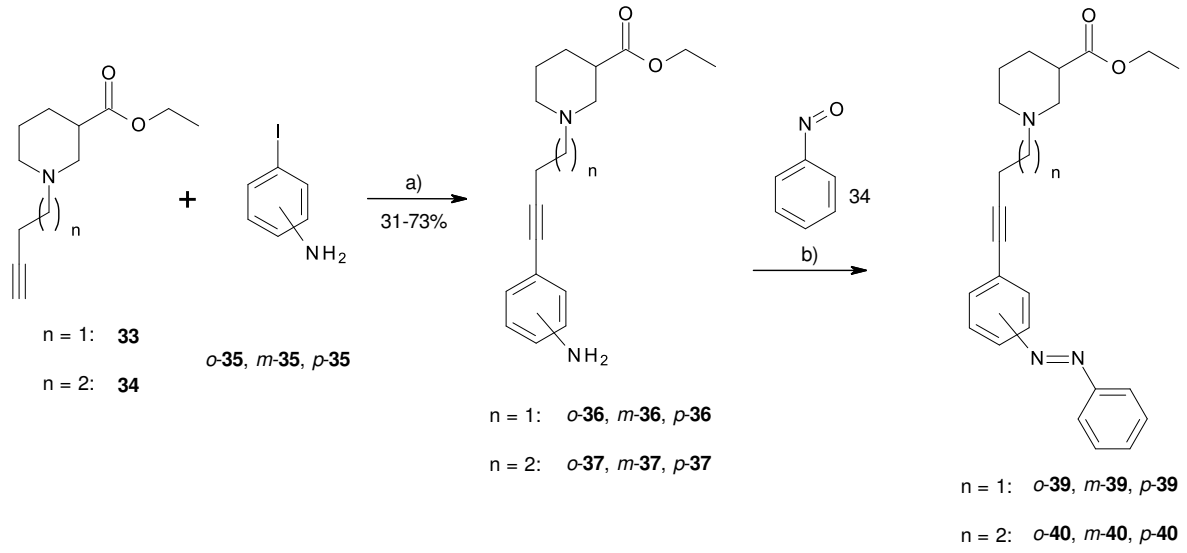

Scheme 6: Alternative synthesis route to photoswitchable GABA uptake inhibitors containing alkinyl spacers. Reagents and conditions: a) $Pd(dppf)_2Cl_2 \cdot CH_2Cl_2$ (5 mol%), CuI (20 mol%), K_3PO_4 (3 equiv), dioxane/water, 60 °C, 4 h; b) nitrosobenzene (1.2 or 1.5 equiv), HOAc, 60 °C, 3-4 h

It was found that by means of the Sonogashira reaction of **33**-**34** with **35**, the desired coupling products **36**-**37** could be obtained in moderate to useful yields (31-73%). However, the subsequent condensation with nitrosobenzene in order to build the final diphenyldiazenes **39**-**40** remained unsuccessfully as either no reaction occurred or a complex mixture of products was formed from which **35**-**36** were not able to be purified in a satisfactory way. For this reason a new way (see third publication) was developed and pursued for the synthesis of these and related compounds. Nevertheless, the intermediates **36**-**37** might be valuable synthetic building blocks and are characterized in the next chapter.

5.4 Syntheses and compound characterization data

All reactions of compounds listed in chapter 5.1-5.3 were carried out under nitrogen atmosphere in distilled and degassed solvents. For flash column chromatography (CC) silica gel (40−60 µm) was used. NMR spectra were measured with a Jeol Eclipse +400 (400 MHz) or a Jeol Eclipse +500 (500 MHz) spectrometer. ^{1}H NMR chemical shifts were referenced to TMS or CH_3OH, ^{13}C NMR chemical shifts to $CHCl_3$ or CH_3OH. The coupling constants were stated with an accuracy of 0.4 Hz. MestreNova software was used for further analysis of the spectra. IR spectra were recorded with a FT-IR spectrometer Paragon 1000 (PerkinElmer). Samples were measured either as KBr pellets or as films on NaCl plates. Mass spectra were measured with a mass spectrometer 59827A with 59980 particle beam LC/MS interface (Hewlett-Packard). High resolution mass spectrometry was carried out with a JMS GCmate II.

General Procedure for the Suzuki-Coupling using Phenylboronic acid MIDA esters (GP1):

$PdOAc_2$ (0.02 equiv), SPhos (0.04 equiv), K_3PO_4 (5.0 equiv), phenylboronic acid MIDA ester (1.5 equiv) and ethyl 1-[(*E*)-5-(2-bromophenyl)pent-4-enyl]piperidine-3-carboxylate (1.0 equiv) were dissolved in 1,4-dioxane (2.0 mL/mmol) and water (1.0 mL/mmol). The mixture was heated to 80° C and stirred for 3 h. After addition of water (10 mL/mmol) organic products was extracted with CH_2Cl_2 (10 mL/mmol). The combined organic layers were dried over Na_2SO_4 and the solvent was removed under reduced pressure. The crude product was purified by CC on silica gel (hexane/EtOAc = 8:2).

General Procedure for the hydrolysis of nipecotic acid ethyl ester derivatives (GP2):

The nipecotic acid ethyl ester derivatives (1.0 equiv) were dissolved in EtOH (5.0 mL/mmol). 2M NaOH (3.0 equiv) was added and the mixture was stirred for 4 h at rt. After the end of the reaction EtOH was removed under reduced pressure. The solid residue was dissolved in 25 mL/mmol of H_2O and the pH was adjusted to 6-7 (indicator paper) and the organic product was extracted with CH_2Cl_2. The combined organic layers were dried over Na_2SO_4 and the solvent was removed under reduced pressure.

General Procedure for the Sonogashira coupling of terminal alkynes and iodoanilines (GP3):

$Pd(dppf)_2Cl_2$ (0.05 equiv), CuI (0.2 equiv), K_3PO_4 (3.0 equiv), and the aryl iodide (1.0 equiv) were introduced in a Schlenk tube. The alkyne (1.0 equiv) in dioxane (2 mL/mmol) and degassed H_2O (1 mL/mmol) were added. The mixture was heated to 60 °C and stirred for 4 h. After cooling to rt, H_2O (10 mL/mmol) was added and the organic components were extracted with CH_2Cl_2 (10 mL/mmol). The organic layers were dried over Na_2SO_4 and the solvent was removed under reduced pressure. The crude product was purified by CC (hexane/ethyl acetate = 1:1) to give the pure coupling product.

Ethyl 1-{(*E*)-5-[2-(2-thienyl)phenyl]pent-4-enyl}piperidine-3-carboxylate (26):

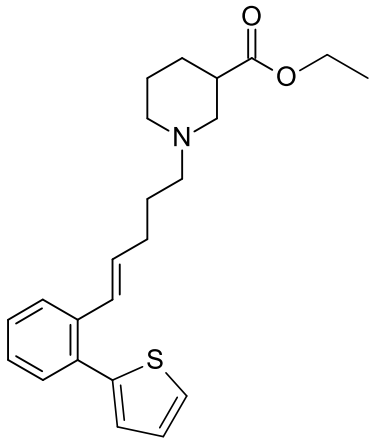

According to GP1 starting from $PdOAc_2$ (1.0 mg, 4.0 µmol), SPhos (3.5 mg, 8.0 µmol), K_3PO_4 (212 mg, 1.00 mmol), 2-Thiopheneboronic acid MIDA ester (73 mg, 0.30 mmol) and Ethyl 1-[(E)-5-(2-bromophenyl)pent-4-enyl]piperidine-3-carboxylate (76 mg, 0.20 mmol) **26** was obtained as slightly yellow oil (64 mg, 83%). R_f ≈ 0.2 (hexane/EtOAc = 8:2). IR (NaCl): $\tilde{\nu}$ = 3060, 2938, 2861, 2805, 2768, 1729, 1468, 1445, 1370, 1306, 1179, 1151, 1099, 1031, 967, 850, 757, 697 cm^{-1}. ^1H NMR (400 MHz, $CDCl_3$, TMS, 21 °C): δ = 1.24 (t, *J* = 7.1 Hz, 3 H, OCH_2CH_3), 1.43 (qd, *J* = 12.0/4.1 Hz, 1 H, $NCH_2CHCH_{ax}H_{eq}$), 1.51–1.76 (m, 4 H, $NCH_2CH_{ax}H_{eq}CH_2CH$, $NCH_2CH_2CH_2CHCH$, $NCH_2CH_{ax}H_{eq}CH_2CH$), 1.96 (m, 2 H, $NCH_2CHCH_{ax}H_{eq}$, $NCH_{ax}H_{eq}CH_2CH_2CH$), 2.13 (t, *J* = 10.7 Hz, 1 H, $NCH_{ax}H_{eq}CH$), 2.20 (qd, *J* = 7.3/1.3 Hz, 2 H, CH_2CHCHC), 2.38 (dd, *J* = 8.9/6.6 Hz, 2 H, $NCH_2CH_2CH_2CHCH$), 2.56 (tt, *J* = 10.6/3.8 Hz, 1 H, NCH_2CH_{ax}), 2.77 (d_{br}, *J* = 11.2 Hz, 1 H, $NCH_{ax}H_{eq}CH_2CH_2CH$), 2.99 (d_{br}, *J* = 9.7 Hz, 1 H, $NCH_{ax}H_{eq}CH$), 4.12 (q, *J* = 7.1 Hz, 2 H, OCH_2CH_3), 6.13 (dt, *J* = 15.7/6.9 Hz, 1 H, CH_2CHCHC), 6.62 (d, *J* = 15.7 Hz, 1 H, CH_2CHCHC), 7.06 (dd, *J* = 3.5/1.3 Hz, 1 H, SCC*H*), 7.09 (dd, *J* = 5.0/3.5 Hz, 1 H, SCHC*H*), 7.23 (td, *J* = 7.5/1.6 Hz, 1 H, $CH_2CHCHCCHCHCH$), 7.29 (td, *J* = 7.5/1.6 Hz, 1 H, $CH_2CHCHCCHCH$), 7.34 (dd, *J* = 5.1/1.3 Hz, 1 H, SCH), 7.39 (dd, *J* = 7.5/1.4 Hz, 1 H, $CH_2CHCHCCCH$), 7.52 (dd, *J* = 7.7/1.4 Hz, 1 H, $CH_2CHCHCCH$) ppm. ^{13}C NMR (101 MHz, $CDCl_3$, TMS, 21 °C): δ = 14.20 (q, 1 C, OCH_2CH_3), 24.62 (t, 1 C, $NCH_2CH_2CH_2CH$), 26.44 (t, 1 C, $NCH_2CH_2CH_2CHCH$), 27.03 (t, 1 C, NCH_2CHCH_2CH), 31.06 (t, 1 C, CH_2CHCHC), 41.90 (d, 1 C, NCH_2CH), 53.83 (t, 1 C, $NCH_2CH_2CH_2CH$), 55.50 (t, 1 C, NCH_2CH), 58.37 (t, 1 C, $NCH_2CH_2CH_2CHCH$), 60.24 (t, 1 C, OCH_2CH_3), 125.47 (d, 1 C, SCH), 126.52 (d, 1 C, $CH_2CHCHCCH$), 126.80 (d, 1 C, $CH_2CHCHCCHCHCH$), 127.08 (d, 1 C, SCCH), 127.20 (d, 1 C, SCHCH), 127.83 (d, 1 C, $CH_2CHCHCCHCH$), 129.17 (d, 1 C, CH_2CHCHC), 130.47 (d, 1 C, $CH_2CHCHCCCH$), 132.11 (d, 1 C, CH_2CHCHC), 132.55 (s, 1 C, SCC), 136.63 (s, 1 C, CH_2CHCHC), 142.50 (s, 1 C, SC), 174.23 (s, 1 C, C=O) ppm. MS (EI) *m/z*: 383.2 $[M]^+$. HRMS (EI): $[M]^+$ calcd for $C_{23}H_{29}NO_2S$: 383.1919; found: 383.1910.

Ethyl 1-{(*E*)-5-[2-(3-methyl-2-thienyl)phenyl]pent-4-enyl}piperidine-3-carboxylate (27):

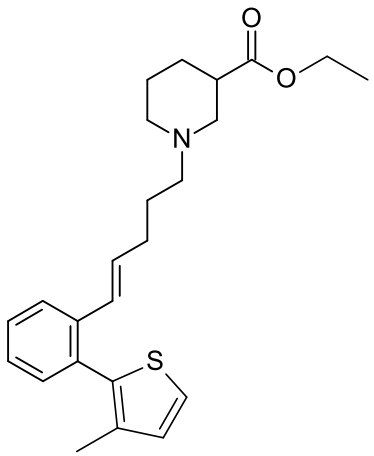

According to GP1 starting from $PdOAc_2$ (1.0 mg, 4.0 µmol), SPhos (3.5 mg, 8.0 µmol), K_3PO_4 (212 mg, 1.0 mmol), 3-Methyl-2-thiopheneboronic acid MIDA ester (76 mg, 0.30 mmol) and Ethyl 1-[(E)-5-(2-bromophenyl)pent-4-enyl]piperidine-3-carboxylate (76.1 mg, 0.20 mmol) **27** was obtained as slightly yellow oil (64 mg, 81%). R_f ≈ 0.2 (hexane/EtOAc = 8:2). IR (NaCl): $\tilde{\nu}$ = 3060, 2938, 2861, 2805, 1729, 1468, 1447, 1369, 1303, 1178, 1151, 1099, 1030, 966, 756 cm^{-1}. ^1H NMR (400 MHz, $CDCl_3$, TMS, 21 °C): δ = 1.25 (t, J = 7.1 Hz, 3 H, OCH_2CH_3), 1.42 (qd, J = 11.8/4.1 Hz, 1 H, $NCH_2CHCH_{ax}H_{eq}$), 1.50–1.65 (m, 3 H, $NCH_2CH_{ax}H_{eq}CH_2CH$, $NCH_2CH_2CH_2CHCH$), 1.71 (dp, J = 14.8/3.8 Hz, 1 H, $NCH_2CH_{ax}H_{eq}CH_2CH$), 1.89–1.99 (m, 2 H, $NCH_2CHCH_{ax}H_{eq}$, $NCH_{ax}H_{eq}CH_2CH_2CH$), 2.02 (s, 3 H, CCH_3), 2.07–2.18 (m, 3 H, $NCH_{ax}H_{eq}CH$, CH_2CHCHC), 2.29–2.37 (m, 2 H, $NCH_2CH_2CH_2CHCH$), 2.55 (tt, J = 10.6/3.8 Hz, 1 H, NCH_2CH_{ax}), 2.75 (d_{br}, J = 11.1 Hz, 1 H, $NCH_{ax}H_{eq}CH_2CH_2CH$), 2.97 (d_{br}, J = 10.5 Hz, 1 H, $NCH_{ax}H_{eq}CH$), 4.12 (q, J = 7.1 Hz, 2 H, OCH_2CH_3), 6.16 (dt, J = 15.8/6.7 Hz, 1 H, CH_2CHCHC), 6.27 (d, J = 15.9 Hz, 1 H, CH_2CHCHC), 6.91 (d, J = 5.1 Hz, 1 H, $SCHCH$), 7.19–7.28 (m, 3 H, SCH, $SCCCH$, $SCCCHCH$), 7.31 (td, J = 7.5/1.7 Hz, 1 H, $CH_2CHCHCCHCH$), 7.57 (d, J = 7.8 Hz, 1 H, $CH_2CHCHCCH$) ppm. ^{13}C NMR (101 MHz, $CDCl_3$, TMS, 21 °C): δ = 14.21 (q, 1 C, OCH_2CH_3), 14.40 (q, 1 C, CCH_3), 24.59 (t, 1 C, $NCH_2CH_2CH_2CH$), 26.51 (t, 1 C, $NCH_2CH_2CH_2CHCH$), 27.03 (t, 1 C, NCH_2CHCH_2CH), 31.08 (t, 1 C, CH_2CHCHC), 41.87 (d, 1 C, NCH_2CH), 53.80 (t, 1 C, $NCH_2CH_2CH_2CH$), 55.46 (t, 1 C, NCH_2CH), 58.31 (t, 1 C, $NCH_2CH_2CH_2CHCH$), 60.26 (t, 1 C, OCH_2CH_3), 123.86 (d, 1 C, SCH), 125.24 (d, 1 C, $CH_2CHCHCCH$), 126.38 (d, 1 C, $SCCCHCH$), 128.13 (d, 1 C, $CH_2CHCHCCHCH$), 128.44 (d, 1 C, CH_2CHCHC), 129.63 (d, 1 C, $SCHCH$), 131.55 (d, 1 C, CH_2CHCHC), 131.62 (d, 1 C, $SCCCH$), 132.33 (s, 1 C, SCC), 134.91 (s, 1 C, CCH_3), 136.13 (s, 1 C, SC), 137.64 (s, 1 C, CH_2CHCHC), 174.24 (s, 1 C, C=O) ppm. MS (EI) *m/z*: 397.2 $[M]^+$. HRMS (EI): $[M]^+$ calcd for $C_{24}H_{31}NO_2S$: 397.2075; found: 397.2070.

1-{(*E*)-5-[2-(2-thienyl)phenyl]pent-4-enyl}piperidine-3-carboxylic acid (28):

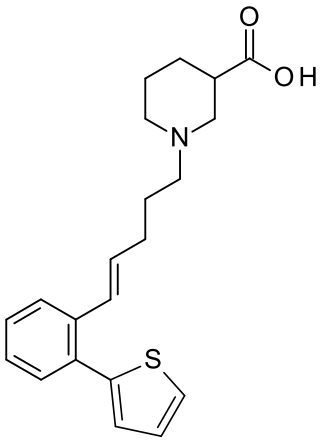

According to GP2 from **26** (38.4 mg, 0.100 mmol) and 2 N NaOH (0.15 ml, 0.30 mmol) **28** was obtained as colourless gum (33 mg, 93%). R_f ≈ 0.1 (CH_2Cl_2/CH_3OH = 9:1). IR (KBr): $\tilde{\nu}$ = 3415, 3062, 2951, 2864, 1712, 1597, 1475, 1446, 1385, 1247, 1216, 1081, 1041, 969, 850, 756, 700, 663 cm^{-1}. ^1H NMR (400 MHz, CD_3OD + 5 eq 1M NaOD, 21 °C): δ = 1.31 (qd, *J* = 12.6/4.0 Hz, 1 H, $NCH_2CHCH_{ax}H_{eq}$), 1.55 (qt, *J* = 13.0/3.8 Hz, 1 H, $NCH_2CH_{ax}H_{eq}CH_2CH$), 1.62–1.73 (m, 3 H, $NCH_2CH_{ax}H_{eq}CH_2CH$, $NCH_2CH_2CH_2CHCH$), 1.88 (td, *J* = 12.0/2.8 Hz, 1 H, $NCH_{ax}H_{eq}CH_2CH_2CH$), 1.92–2.02 (m, 2 H, $NCH_2CHCH_{ax}H_{eq}$, $NCH_{ax}H_{eq}CH$), 2.15 (q, *J* = 6.7 Hz, 2 H, CH_2CHCHC), 2.30–2.41 (m, 3 H, NCH_2CH_{ax}, $NCH_2CH_2CH_2CHCH$), 2.87 (d_{br}, *J* = 11.1 Hz, 1 H, $NCH_{ax}H_{eq}CH_2CH_2CH$), 3.09 (d_{br}, *J* = 11.2 Hz, 1 H, $NCH_{ax}H_{eq}CH$), 6.14 (dt, *J* = 15.7/6.9 Hz, 1 H, CH_2CHCHC), 6.54 (d, *J* = 15.8 Hz, 1 H, CH_2CHCHC), 7.01 (dd, *J* = 3.5/1.2 Hz, 1 H, SCCH), 7.10 (dd, *J* = 5.1/3.5 Hz, 1 H, SCHCH), 7.21–7.34 (m, 3 H, $CH_2CHCHCCHCHCH$, $CH_2CHCHCCHCH$, $CH_2CHCHCCCH$), 7.44 (dd, *J* = 5.2/1.2 Hz, 1 H, SCH), 7.51 (dd, *J* = 7.7/1.2 Hz, 1 H, $CH_2CHCHCCH$) ppm. ^{13}C NMR (101 MHz, CD_3OD + 5 eq 1M NaOD, 21 °C): δ = 25.63 (t, 1 C, $NCH_2CH_2CH_2CH$), 26.59 (t, 1 C, $NCH_2CH_2CH_2CHCH$), 29.25 (t, 1 C, NCH_2CHCH_2CH), 32.11 (t, 1 C CH_2CHCHC), 46.15 (d, 1 C, NCH_2CH), 54.65 (t, 1 C, $NCH_2CH_2CH_2CH$), 57.92 (t, 1 C, NCH_2CH), 59.59 (t, 1 C, $NCH_2CH_2CH_2CHCH$), 126.84 (d, 1 C, SCH), 127.52 (d, 1 C, $H_2CHCHCCH$), 128.05 (d, 1 C, SCCH), 128.23 (d, 1 C, SCHCH), 128.28 (d, 1 C, $CH_2CHCHCCHCHCH$), 129.12 (d, 1 C, $CH_2CHCHCCHCH$), 130.27 (d, 1 C, CH_2CHCHC), 131.32 (d, 1 C, SCCCH), 132.96 (d, 1 C, CH_2CHCHC), 133.71 (s, 1 C, SCC), 137.60 (s, 1 C, SCCC), 143.39 (s, 1 C, SC), 183.14 (s, 1 C, C=O) ppm. MS (EI) *m/z*: 355.2 $[M]^+$. HRMS (EI): $[M]^+$ calcd for $C_{21}H_{25}NO_2S$: 355.1606; found: 355.1600.

1-{(*E*)-5-[2-(3-methyl-2-thienyl)phenyl]pent-4-enyl}piperidine-3-carboxylic acid (29):

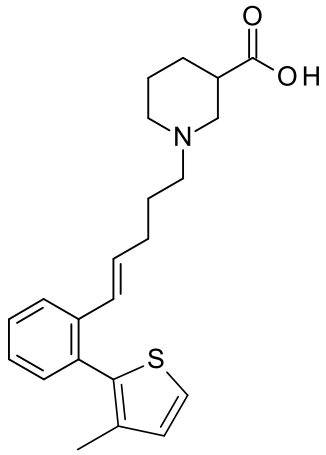

According to GP2 from **27** (39.8 mg, 0.100 mmol) and 2 N NaOH (0.15 ml, 0.30 mmol) **29** was obtained as colourless gum (34 mg, 92%). R_f ≈ 0.1 (CH_2Cl_2/CH_3OH = 9:1). IR (KBr): $\tilde{\nu}$ = 3406, 3059, 2942, 2861, 1710, 1596, 1477, 1448, 1383, 1217, 1009, 968, 832, 755, 711, 662 Cm^{-1}. ^1H NMR (400 MHz, CD_3OD + 5 eq 1M NaOD, 21 °C): δ = 1.30 (qd, J = 12.9/4.2 Hz, 1 H, $NCH_2CHCH_{ax}H_{eq}$), 1.48–1.71 (m, 4 H, $NCH_2CH_{ax}H_{eq}CH_2CH$, $NCH_2CH_2CH_2CHCH$, $NCH_2CH_{ax}H_{eq}CH_2CH$), 1.86 (td, J = 11.7/2.5 Hz, 1 H, $NCH_{ax}H_{eq}CH_2CH_2CH$), 1.92–2.0 (m, 5 H, $NCH_2CHCH_{ax}H_{eq}$, $NCH_{ax}H_{eq}CH$, CH_3), 2.06–2.13 (m, 2 H, CH_2CHCHC), 2.28–2.39 (m, 3 H, $NCH_2CH_2CH_2CHCH$, NCH_2CH_{ax}), 2.84 (d_{br}, J = 11.1 Hz, 1 H, $NCH_{ax}H_{eq}CH_2CH_2CH$), 3.06 (d_{br}, J = 11.1 Hz, 1 H, $NCH_{ax}H_{eq}CH$), 6.11–6.25 (m, 2 H, CH_2CHCHC, CH_2CHCHC), 6.93 (d, J = 5.1 Hz, 1 H, SCHCH), 7.17 (dd, J = 7.6/1.2 Hz, 1 H, SCCCH), 7.23 (td, J = 7.4/1.3 Hz, 1 H, SCCCHCH), 7.30–7.36 (m, 2 H, $CH_2CHCHCCHCH$, SCH), 7.59 (d, J = 7.1 Hz, 1 H, $CH_2CHCHCCH$) ppm. ^{13}C NMR (101 MHz, CD_3OD + 5 eq 1M NaOD, 21 °C): δ = 14.50 (q, 1 C, CH_3), 25.66 (t, 1 C, $NCH_2CH_2CH_2CH$), 26.66 (t, 1 C, $NCH_2CH_2CH_2CHCH$), 29.28 (t, 1 C, NCH_2CHCH_2CH), 32.16 (t, 1 C, CH_2CHCHC), 46.17 (d, 1 C, NCH_2CH), 54.67 (t, 1 C, $NCH_2CH_2CH_2CH$), 57.95 (t, 1 C, NCH_2CH), 59.53 (t, 1 C, $NCH_2CH_2CH_2CHCH$), 125.09 (d, 1 C, SCH), 126.35 (d, 1 C, $CH_2CHCHCCH$), 127.64 (d, 1 C, SCCCHCH), 129.46 (d, 1 C, CH_2CHCHC), 129.53 (d, 1 C, $CH_2CHCHCCHCH$), 130.75 (d, 1 C, SCHCH), 132.44 (d, 1 C, SCCCH), 132.46 (d, 1 C, CH_2CHCHC), 133.50 (s, 1 C, SCCCH), 136.02 (s, 1 C, CH_3C), 137.03 (s, 1 C, SC), 138.70 (s, 1 C, CH_2CHCHC), 183.09 (s, 1 C, C=O) ppm. MS (EI) *m/z*: 369.2 $[M]^+$. HRMS (EI): $[M]^+$ calcd for $C_{22}H_{27}NO_2S$: 369.1762; found: 369.1755.

Ethyl 1-[4-(2-aminophenyl)but-3-ynyl]piperidine-3-carboxylate (*o*-36):

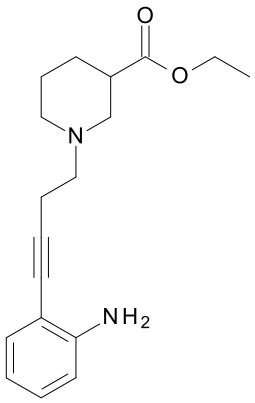

According to GP3 starting from ethyl 1-(but-3-yn-1-yl)piperidine-3-carboxylate (105 mg, 0.500 mmol), 3-iodoaniline (112 mg, 0.500 mmol), $Pd(dppf)_2Cl_2$ (20 mg, 25 µmol), CuI (40 mg, 0.10 mmol) and K_3PO_4 (328 mg, 1.50 mmol) *o*-**36** was obtained as colorless oil (76 mg, 51%). $R_f \approx 0.5$ (hexane/EtOAc = 1:1). IR (NaCl): $\tilde{\nu}$ = 3463, 3374, 3205, 3073, 3028, 2942, 2854, 2810, 2215, 1727, 1615, 1492, 1455, 1370, 1308, 1181, 1154, 1132, 1101, 1031, 747 cm^{-1}. ^1H NMR (400 MHz, $CDCl_3$, TMS, 21 °C): δ = 1.25 (t, *J* = 7.1 Hz, 3 H, OCH_2CH_3), 1.47 (qd, *J* = 11.5/3.5 Hz, 1 H, $NCH_2CHCH_{ax}H_{eq}$), 1.52–1.63 (m, 1 H, $NCH_2CH_{ax}H_{eq}CH_2CH$), 1.75 (dp, *J* = 13.2/3.6 Hz, 1 H, $NCH_2CH_{ax}H_{eq}CH_2CH$), 1.95 (dq, *J* = 13.0/4.0 Hz, 1 H, $NCH_2CHCH_{ax}H_{eq}$), 2.10 (td, *J* = 10.9/2.7 Hz, 1 H, $NCH_{ax}H_{eq}CH_2CH_2CH$), 2.27 (t, *J* = 10.6 Hz, 1 H, $NCH_{ax}H_{eq}CH$), 2.56 (tt, *J* = 10.4/3.8 Hz, 1 H, NCH_2CH_{ax}), 2.62–2.70 (m, 4 H, $NCH_2CH_2C{\equiv}C$, $NCH_2CH_2C{\equiv}C$), 2.81 (d_{br}, *J* = 11.1 Hz, 1 H, $NCH_{ax}H_{eq}CH_2CH_2CH$), 3.04 (d_{br}, *J* = 10.9/2.6 Hz, 1 H, $NCH_{ax}H_{eq}CH$), 4.12 (q, *J* = 7.1 Hz, 2 H, OCH_2CH_3), 4.35 (s, 2 H, H_2N), 6.61–6.69 (m, 2 H, H_2NCCH, $H_2NCCHCHCH$), 7.07 (td, *J* = 8.1/1.6 Hz, 1 H, $H_2NCCHCH$), 7.21 (dd, *J* = 7.6/1.5 Hz, 1 H, H_2NCCCH) ppm. ^{13}C NMR (101 MHz, $CDCl_3$, 21 °C, TMS): δ = 14.14 (t, 1 C, OCH_2CH_3), 17.88 (t, 1 C, $NCH_2CH_2C{\equiv}C$), 24.53 (t, 1 C, $NCH_2CH_2CH_2CH$), 26.81 (t, 1 C, NCH_2CHCH_2CH), 41.76 (d, 1 C, NCH_2CH), 53.35 (t, 1 C, $NCH_2CH_2CH_2CH$), 55.01 (t, 1 C, NCH_2CH), 57.43 (t, 1 C, $NCH_2CH_2C{\equiv}C$), 60.33 (t, 1 C, OCH_2CH_3), 78.11 (s, 1 C, $C{\equiv}CCH$), 93.78 (s, 1 C, $C{\equiv}CCH$), 108.38 (s, 1 C, H_2NCC), 113.92 (d, 1 C, H_2NCCH), 117.49 (d, 1 C, $H_2NCCHCHCH$), 128.91 (d, 1 C, $H_2NCCHCH$), 131.45 (d, 1 C, H_2NCCCH), 148.13 (s, 1 C, H_2NC) 174.06 (s, 1 C, C=O) ppm. MS (ESI^+) *m/z*: 301.8 ($[M+H]^+$). HRMS (EI): $[M]^+$ calcd for $C_{18}H_{24}N_2O_2$, 300.1838; found: 300.1837.

Ethyl 1-[4-(3-aminophenyl)but-3-ynyl]piperidine-3-carboxylate (*m*-36):

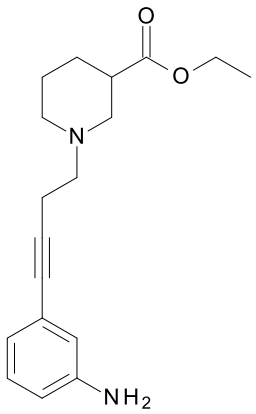

According to GP3 starting from ethyl 1-(but-3-yn-1-yl)piperidine-3-carboxylate (105 mg, 0.500 mmol), 3-iodoaniline (112 mg, 0.500 mmol), $Pd(dppf)_2Cl_2$ (20 mg, 25 µmol), CuI (40 mg, 0.10 mmol) and K_3PO_4 (328 mg, 1.50 mmol) *m*-**36** was obtained as colorless oil (98 mg, 33 %). $R_f \approx 0.4$ (hexane/EtOAc = 1:1). IR (NaCl): $\tilde{\nu}$ = 3455, 3374, 3219, 3046, 2977, 2943, 2854, 2811, 2234, 1724, 1622, 1599, 1580, 1491, 1468, 1447, 1371, 1313, 1183, 1153, 1101, 1031, 862, 781, 688 cm^{-1}. ^1H NMR (400 MHz, $CDCl_3$, TMS, 21 °C): δ = 1.25 (t, *J* = 7.1 Hz, 3 H, OCH_2CH_3), 1.44 (qd, *J* = 11.9/4.0 Hz, 1 H, $NCH_2CHCH_{ax}H_{eq}$), 1.52–1.64 (m, 1 H, $NCH_2CH_{ax}H_{eq}CH_2CH$), 1.74 (dp, *J* = 13.3/3.7 Hz, 1 H, $NCH_2CH_{ax}H_{eq}CH_2CH$), 1.95 (dq, *J* = 12.5/3.8 Hz, 1 H, $NCH_2CHCH_{ax}H_{eq}$), 2.11 (td, *J* = 11.0/2.8 Hz, 1 H, $NCH_{ax}H_{eq}CH_2CH_2CH$), 2.28 (t, *J* = 10.7 Hz, 1 H, $NCH_{ax}H_{eq}CH$), 2.52–2.61 (m, 3 H, NCH_2CH_{ax}, $NCH_2CH_2C{\equiv}C$), 2.65–2.72 (m, 2 H, $NCH_2CH_2C{\equiv}C$), 2.81 (d_{br}, *J* = 11.2 Hz, 1 H, $NCH_{ax}H_{eq}CH_2CH_2CH$), 3.04 (d_{br}, *J* = 11.1 Hz, 1 H, $NCH_{ax}H_{eq}CH$), 3.67 (s, 2 H, H_2N), 4.13 (q, *J* = 7.1 Hz, 2 H, OCH_2CH_3), 6.59 (ddd, *J* = 8.1/2.4/1.0 Hz, 1 H, $H_2NCCHCH$), 6.71 (t, *J* = 1.7 Hz, 1 H, H_2NCCHC), 6.79 (dt, *J* = 7.7/1.2 Hz, 1 H, $H_2NCCHCCH$), 7.06 (t, *J* = 7.8 Hz, 1 H, $H_2NCCHCH$) ppm. ^{13}C NMR (101 MHz, $CDCl_3$, 21 °C, TMS): δ = 14.13 (t, 1 C, OCH_2CH_3), 17.50 (t, 1 C, $NCH_2CH_2C{\equiv}C$), 24.49 (t, 1 C, $NCH_2CH_2CH_2CH$), 26.75 (t, 1 C, NCH_2CHCH_2CH), 41.75 (d, 1 C, NCH_2CH), 53.26 (t, 1 C, $NCH_2CH_2CH_2CH$), 55.00 (t, 1 C, NCH_2CH), 57.43 (t, 1 C, $NCH_2CH_2C{\equiv}C$), 60.28 (t, 1 C, OCH_2CH_3), 81.40 (s, 1 C, $C{\equiv}CCCH$), 87.61 (s, 1 C, $C{\equiv}CCCH$), 114.67 (d, 1 C, H_2NCCH), 117.78 (d, 1 C, H_2NCCHC, 121.81 (d, 1 C, $H_2NCCHCCH$), 124.30 (s, 1 C, $CH_2C{\equiv}CC$), 129.05 (d, 1 C, ($H_2NCCHCH$), 146.13 (s, 1 C, H_2NC) 174.08 (s, 1 C, C=O) ppm. MS (ESI^+) *m/z*: 302.0 ($[M+H]^+$). HRMS (EI): $[M]^+$ calcd for $C_{18}H_{24}N_2O_2$, 300.1838; found: 300.1831.

Ethyl 1-[4-(4-aminophenyl)but-3-ynyl]piperidine-3-carboxylate (*p*-36):

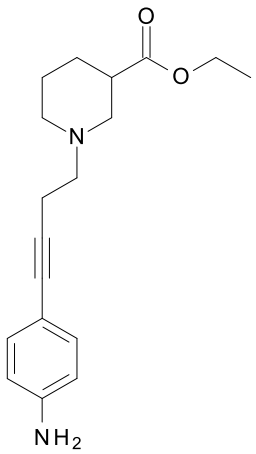

According to GP3 starting from ethyl 1-(but-3-yn-1-yl)piperidine-3-carboxylate (105 mg, 0.500 mmol), 4-iodoaniline (112 mg, 0.500 mmol), $Pd(dppf)_2Cl_2$ (20 mg, 25 µmol), CuI (40 mg, 0.10 mmol) and K_3PO_4 (328 mg, 1.50 mmol) *p*-**36** was obtained as colorless oil (110 mg, 73%). $R_f \approx 0.3$ (hexane/EtOAc = 1:1). IR (NaCl): $\tilde{\nu}$ = 3463, 3357, 3221, 3033, 2942, 2811, 2215, 1723, 1622, 1608, 1514, 1468, 1446, 1371, 1294, 1177, 1153, 1100, 1031, 828 cm^{-1}. ^1H NMR (400 MHz, $CDCl_3$, TMS, 21 °C): δ = 1.25 (t, *J* = 7.1 Hz, 3 H, OCH_2CH_3), 1.44 (qd, *J* = 12.1/4.0 Hz, 1 H, $NCH_2CHCH_{ax}H_{eq}$), 1.51–1.65 (m, 1 H, $NCH_2CH_{ax}H_{eq}CH_2CH$), 1.74 (dp, *J* = 13.3/3.7 Hz, 1 H, $NCH_2CH_{ax}H_{eq}CH_2CH$), 1.94 (dq, *J* = 13.0/4.0 Hz, 1 H, $NCH_2CHCH_{ax}H_{eq}$), 2.11 (td, *J* = 11.0/2.8 Hz, 1 H, $NCH_{ax}H_{eq}CH_2CH_2CH$), 2.27 (t, *J* = 10.7 Hz, 1 H, $NCH_{ax}H_{eq}CH$), 2.52–2.62 (m, 3 H, NCH_2CH_{ax}, $NCH_2CH_2CH_2C{\equiv}C$), 2.65–2.71 (m, 2 H, $NCH_2CH_2CH_2C{\equiv}C$), 2.81 (d_{br}, *J* = 11.1 Hz, 1 H, $NCH_{ax}H_{eq}CH_2CH_2CH$), 3.04 (d_{br}, *J* = 11.2/2.9 Hz, 1 H, $NCH_{ax}H_{eq}CH$), 3.75 (s, 2 H, H_2N), 4.13 (q, *J* = 7.1 Hz, 2 H, OCH_2CH_3), 6.54–6.61 (m, 2 H, H_2NCCH), 7.16–7.22 (m, 2 H, $H_2NCCHCH$) ppm. ^{13}C NMR (101 MHz, $CDCl_3$, 21 °C, TMS): δ = 14.16 (t, 1 C, OCH_2CH_3), 17.59 (t, 1 C, $NCH_2CH_2C{\equiv}C$), 24.53 (t, 1 C, $NCH_2CH_2CH_2CH$), 26.80 (t, 1 C, NCH_2CHCH_2CH), 41.82 (d, 1 C, NCH_2CH), 53.32 (t, 1 C, $NCH_2CH_2CH_2CH$), 55.08 (t, 1 C, NCH_2CH), 57.69 (t, 1 C, $NCH_2CH_2C{\equiv}C$), 60.28 (t, 1 C, OCH_2CH_3), 81.51 (s, 1 C, $C{\equiv}CCCH$), 85.65 (s, 1 C, $C{\equiv}CCCH$), 113.16 (s, 1 C, $CH_2C{\equiv}CC$), 114.64 (d, 2 C, H_2NCCH), 132.69 (d, 2 C, $H_2NCCHCH$), 146.02 (s, 1 C, H_2NC) 174.12 (s, 1 C, C=O) ppm. MS (ESI^+) *m/z*: 301.0 ($[M+H]^+$). HRMS (EI): $[M]^+$ calcd for $C_{18}H_{24}N_2O_2$, 300.1838; found: 300.1837.

Ethyl 1-[5-(2-aminophenyl)pent-4-ynyl]piperidine-3-carboxylate (*o*-37):

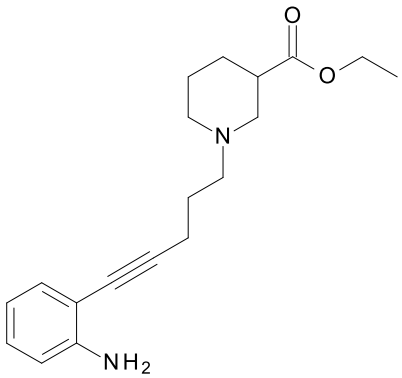

According to GP3 starting from ethyl 1-(pent-4-yn-1-yl)piperidine-3-carboxylate (112 mg, 0.500 mmol), 3-iodoaniline (112 mg, 0.500 mmol), $Pd(dppf)_2Cl_2$ (20 mg, 25 µmol), CuI (40 mg, 0.10 mmol) and K_3PO_4 (328 mg, 1.50 mmol) *o*-**37** was obtained as colorless oil (87 mg, 55 %). $R_f \approx 0.4$ (hexane/EtOAc = 1:1). IR (NaCl): $\tilde{\nu}$ = 3463, 3374, 3205, 3073, 3028, 2938, 2854, 2810, 2215, 1726, 1618, 1560, 1492, 1458, 1375, 1308, 1154, 1102, 1029, 749 cm^{-1}. ^1H NMR (400 MHz, $CDCl_3$, TMS, 21 °C): δ = 1.25 (t, *J* = 7.1 Hz, 3 H, OCH_2CH_3), 1.46 (qd, *J* = 12.0/3.8 Hz, 1 H, $NCH_2CHCH_{ax}H_{eq}$), 1.52–1.63 (m, 1 H, $NCH_2CH_{ax}H_{eq}CH_2CH$), 1.73 (dp, *J* = 13.5/3.7 Hz, 1 H, $NCH_2CH_{ax}H_{eq}CH_2CH$), 1.81 (p, *J* = 7.2 Hz, 2 H, $NCH_2CH_2CH_2C{\equiv}C$), 1.93 (dq, *J* = 13.2/3.8 Hz, 1 H, $NCH_2CHCH_{ax}H_{eq}$), 2.03 (td, *J* = 10.9/2.3 Hz, 1 H, $NCH_{ax}H_{eq}CH_2CH_2CH$), 2.20 (t, *J* = 10.4 Hz, 1 H, $NCH_{ax}H_{eq}CH$), 2.47–2.52 (m, 4 H, $NCH_2CH_2CH_2C{\equiv}C$, $NCH_2CH_2CH_2C{\equiv}C$), 2.57 (tt, *J* = 10.5/3.8 Hz, 1 H, NCH_2CH_{ax}), 2.76 (d_{br}, *J* = 10.9 Hz, 1 H, $NCH_{ax}H_{eq}CH_2CH_2CH$), 2.98 (d_{br}, *J* = 9.9 Hz, 1 H, $NCH_{ax}H_{eq}CH$), 4.13 (q, *J* = 7.1 Hz, 2 H, OCH_2CH_3), 4.18 (s, 2 H, H_2N), 6.63–6.69 (m, 2 H, H_2NCCH, $H_2NCCHCHCH$), 7.07 (td, *J* = 7.8/1.6 Hz, 1 H, $H_2NCCHCH$), 7.23 (dd, *J* = 7.6/1.5 Hz, 1 H, H_2NCCCH) ppm. ^{13}C NMR (101 MHz, $CDCl_3$, 21 °C, TMS): δ = 14.15 (t, 1 C, OCH_2CH_3), 17.54 (t, 1 C, $NCH_2CH_2CH_2C{\equiv}C$), 24.49 (t, 1 C, $NCH_2CH_2CH_2CH$), 26.16 (t, 1 C, $NCH_2CH_2CH_2C{\equiv}C$), 26.88 (t, 1 C, NCH_2CHCH_2CH), 41.79 (d, 1 C, NCH_2CH), 53.80 (t, 1 C, $NCH_2CH_2CH_2CH$), 55.42 (t, 1 C, NCH_2CH), 57.62 (t, 1 C, $NCH_2CH_2CH_2C{\equiv}C$), 60.25 (t, 1 C, OCH_2CH_3), 77.20 (s, 1 C, $C{\equiv}CCCH$), 95.10 (s, 1 C, $C{\equiv}CCCH$), 108.70 (s, 1 C, H_2NCC), 114.05 (d, 1 C, H_2NCCH), 117.71 (d, 1 C, $H_2NCCHCHCH$), 128.78 (d, 1 C, $H_2NCCHCH$), 131.92 (d, 1 C, H_2NCCCH), 147.60 (s, 1 C, H_2NC) 174.15 (s, 1 C, C=O) ppm. MS (ESI^+) *m/z*: 316.2 ($[M+H]^+$). HRMS (EI): $[M]^+$ calcd for $C_{19}H_{26}N_2O_2$, 314.1994; found 314.1997.

Ethyl 1-[5-(3-aminophenyl)pent-4-ynyl]piperidine-3-carboxylate (*m*-37):

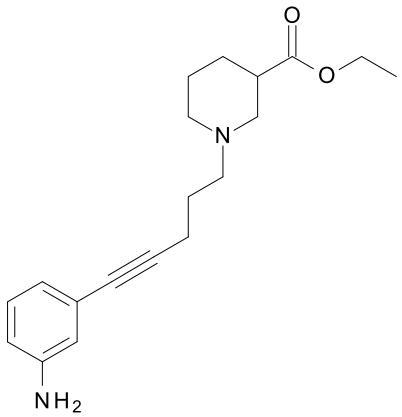

According to GP3 starting from ethyl 1-(pent-4-yn-1-yl)piperidine-3-carboxylate (112 mg, 0.500 mmol), 3-iodoaniline (112 mg, 0.500 mmol), $Pd(dppf)_2Cl_2$ (20 mg, 25 µmol), CuI (40 mg, 0.10 mmol) and K_3PO_4 (328 mg, 1.50 mmol) *m*-**37** was obtained as colorless oil (96 mg, 31%). $R_f \approx 0.3$ (hexane/EtOAc = 1:1). IR (NaCl): $\tilde{\nu}$ = 3461, 3375, 3218, 3046, 3028, 2942, 2808, 2771, 2233, 1724, 1621, 1599, 1580, 1491, 1468, 1447, 1372, 1306, 1203, 1180, 1152, 1104, 1029, 861, 780, 688 cm^{-1}. ^1H NMR (400 MHz, $CDCl_3$, TMS, 21 °C): δ = 1.26 (t, *J* = 7.1 Hz, 3 H, OCH_2CH_3), 1.45 (qd, *J* = 11.8/3.4 Hz, 1 H, $NCH_2CHCH_{ax}H_{eq}$), 1.52–1.64 (m, 1 H, $NCH_2CH_{ax}H_{eq}CH_2CH$), 1.69–1.82 (m, 3 H, $NCH_2CH_{ax}H_{eq}CH_2CH$, $NCH_2CH_2CH_2C{\equiv}C$), 1.94 (dq, *J* = 13.0/3.8 Hz, 1 H, $NCH_2CHCH_{ax}H_{eq}$), 2.02 (td, *J* = 10.9/2.3 Hz, 1 H, $NCH_{ax}H_{eq}CH_2CH_2CH$), 2.18 (t, *J* = 10.6 Hz, 1 H, $NCH_{ax}H_{eq}CH$), 2.42 (t, *J* = 7.1 Hz, 2 H, $NCH_2CH_2CH_2C{\equiv}C$), 2.45–2.51 (m, 2 H, $NCH_2CH_2CH_2C{\equiv}C$), 2.57 (tt, *J* = 10.4/3.8 Hz, 1 H, NCH_2CH_{ax}), 2.77 (d_{br}, *J* = 11.0 Hz, 1 H, $NCH_{ax}H_{eq}CH_2CH_2CH$), 2.99 (d_{br}, *J* = 11.1 Hz, 1 H, $NCH_{ax}H_{eq}CH$), 3.66 (s, 2 H, H_2N), 4.13 (q, *J* = 7.1 Hz, 2 H, OCH_2CH_3), 6.59 (ddd, *J* = 8.0/2.4/0.9 Hz, 1 H, $H_2NCCHCH$), 6.72 (t, *J* = 1.7 Hz, 1 H, H_2NCCHC), 6.79 (dt, *J* = 7.6/1.2 Hz, 1 H, $H_2NCCHCCH$), 7.06 (t, *J* = 7.8 Hz, 1 H, $H_2NCCHCH$) ppm. ^{13}C NMR (101 MHz, $CDCl_3$, 21 °C, TMS): δ = 14.16 (t, 1 C, OCH_2CH_3), 17.33 (t, 1 C, $NCH_2CH_2CH_2C{\equiv}C$), 24.53 (t, 1 C, $NCH_2CH_2CH_2CH$), 25.98 (t, 1 C, $NCH_2CH_2CH_2C{\equiv}C$), 26.92 (t, 1 C, NCH_2CHCH_2CH), 41.81 (d, 1 C, NCH_2CH), 53.80 (t, 1 C, $NCH_2CH_2CH_2CH$), 55.41 (t, 1 C, NCH_2CH), 57.69 (t, 1 C, $NCH_2CH_2CH_2C{\equiv}C$), 60.26 (t, 1 C, OCH_2CH_3), 80.88 (s, 1 C, $C{\equiv}CCCH$), 89.16 (s, 1 C, $C{\equiv}CCCH$), 114.57 (d, 1 C, H_2NCCH), 117.81 (d, 1 C, H_2NCCHC, 121.85 (d, 1 C, $H_2NCCHCCH$), 124.52 (s, 1 C, $CH_2C{\equiv}CC$), 129.06 (d, 1 C, ($H_2NCCHCH$), 146.13 (s, 1 C, H_2NC) 174.23 (s, 1 C, C=O) ppm. MS (ESI^+) *m/z*: 315.7 ($[M+H]^+$). HRMS (EI): $[M]^+$ calcd for $C_{19}H_{26}N_2O_2$, 314.1994; found 314.1991.

Ethyl 1-[5-(4-aminophenyl)pent-4-ynyl]piperidine-3-carboxylate (*p*-37):

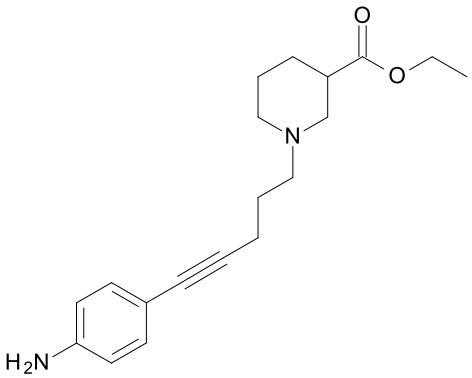

According to GP3 starting from ethyl 1-(pent-4-yn-1-yl)piperidine-3-carboxylate (112 mg, 0.500 mmol), 4-iodoaniline (112 mg, 0.500 mmol), $Pd(dppf)_2Cl_2$ (20 mg, 25 µmol), CuI (40 mg, 0.10 mmol) and K_3PO_4 (328 mg, 1.50 mmol) *p*-**37** was obtained as colorless oil (101 mg, 64%). $R_f \approx 0.2$ (hexane/EtOAc = 1:1). IR (NaCl): $\tilde{\nu}$ = 3454, 3374, 3220, 3033, 2940, 2808, 2772, 2218, 1719, 1624, 1608, 1514, 1467, 1449, 1371, 1296, 1176, 1152, 1103, 1028, 828 cm^{-1}. ^1H NMR (400 MHz, $CDCl_3$, TMS, 21 °C): δ = 1.25 (t, *J* = 7.1 Hz, 3 H, OCH_2CH_3), 1.45 (qd, *J* = 12.1/3.8 Hz, 1 H, $NCH_2CHCH_{ax}H_{eq}$), 1.51–1.64 (m, 1 H, $NCH_2CH_{ax}H_{eq}CH_2CH$), 1.68–1.82 (m, 3 H, $NCH_2CHCH_{ax}H_{eq}$, $NCH_2CH_2CH_2C{\equiv}C$), 1.90–2.04 (m, 2 H, $NCH_2CHCH_{ax}H_{eq}$, $NCH_{ax}H_{eq}CH_2CH_2CH$), 2.17 (t, *J* = 10.6 Hz, 1 H, $NCH_{ax}H_{eq}CH$), 2.41 (t, *J* = 7.1 Hz, 2 H, $NCH_2CH_2CH_2C{\equiv}C$), 2.45–2.51 (m, 2 H, $NCH_2CH_2CH_2C{\equiv}C$), 2.56 (tt, *J* = 10.6/3.8 Hz, 1 H, NCH_2CH_{ax}), 2.78 (d_{br}, *J* = 11.0 Hz, 1 H, $NCH_{ax}H_{eq}CH_2CH_2CH$), 2.99 (d_{br}, *J* = 10.8/2.1 Hz, 1 H, $NCH_{ax}H_{eq}CH$), 3.75 (s, 2 H, H_2N), 4.13 (q, *J* = 7.1 Hz, 2 H, OCH_2CH_3), 6.55–6.61 (m, 2 H, H_2NCCH), 7.17–7.21 (m, 2 H, $H_2NCCHCH$) ppm. ^{13}C NMR (101 MHz, $CDCl_3$, 21 °C, TMS): δ = 14.18 (t, 1 C, OCH_2CH_3), 17.41 (t, 1 C, $NCH_2CH_2CH_2C{\equiv}C$), 24.57 (t, 1 C, $NCH_2CH_2CH_2CH$), 26.20 (t, 1 C, $NCH_2CH_2CH_2C{\equiv}C$) 26.96 (t, 1 C, NCH_2CHCH_2CH), 41.87 (d, 1 C, NCH_2CH), 53.82 (t, 1 C, $NCH_2CH_2CH_2CH$), 55.47 (t, 1 C, NCH_2CH), 57.79 (t, 1 C, $NCH_2CH_2CH_2C{\equiv}C$), 60.26 (t, 1 C, OCH_2CH_3), 80.95 (s, 1 C, $C{\equiv}CCCH$), 87.20 (s, 1 C, $C{\equiv}CCCH$), 113.41 (s, 1 C, $CH_2C{\equiv}CC$), 114.67 (d, 2 C, H_2NCCH), 132.67 (d, 2 C, $H_2NCCHCH$), 145.91 (s, 1 C, H_2NC) 174.27 (s, 1 C, C=O) ppm. MS (ESI^+) *m/z*: 316.2 ($[M+H]^+$). HRMS (EI): $[M]^+$ calcd for $C_{19}H_{26}N_2O_2$, 314.1994; found 314.1996.

5.5 Thermal relaxation rates of photoswitchable compounds

For the third publication, the thermal relaxation rates of the ($Z_{N=N}$)-isomer of all photoswitchable compounds was determined by kinetic experiments using UV/vis or NMR spectroscopy at 25 °C. In the following section measurement data for all compounds, leading to the calculated half-life's of thermal relaxation within this publication, is given.

Experiments were performed as described in this publication (see appendix). For all photoswitches containing a C_4 spacer the thermal relaxation was measured both in DMSO by NMR spectroscopy and in aqueous media (phosphate buffer (PB), 10 mM, pH 7.4) by UV/Vis spectroscopy. In this case, UV/Vis measurements were done by a Cary50 spectrometer (Varian). Recording of full UV/Vis spectra within a kinetic experiment was possible. In case of long relaxation times, further measurements at 350 nm or 375 nm were done.

The half-life's of thermal relaxation of photoswitches with C_5 spacer were reviewed in aqueous media (phosphate buffer (PB), 10 mM, pH 7.4) by using a SpectraMax M2e UV/vis spectrometer. Within a kinetic experiment just one wavelength (350 nm or 375 nm) could be pursued. Half-life's of compounds with long relaxation times were determined by several singe point measurements within two weeks.

For sake of clarity in the following data tables the nomenclature of the photoswitchable compounds is derived from the corresponding publication (see appendix).

Half-life (*Z*)-*m*-**12a** in DMSO

time (h)	1H (E)*	1H (Z)*	total*	Z (%)	$t_{(1/2)}$
0	1.00	5.93	6.93	85.6	
1	1.03	4.58	5.61	81.6	14.5
2	1.02	3.51	4.53	77.5	13.9
3	1.03	2.95	3.98	74.1	14.4
5	1.03	2.18	3.21	67.8	14.8
7	1.04	1.64	2.68	61.2	14.5
10	1.01	1.00	2.01	50.2	13.0
14	1.03	0.74	1.77	41.8	13.5

*average integration for 1H (E) and 1H (Z) of isol. arom. signals

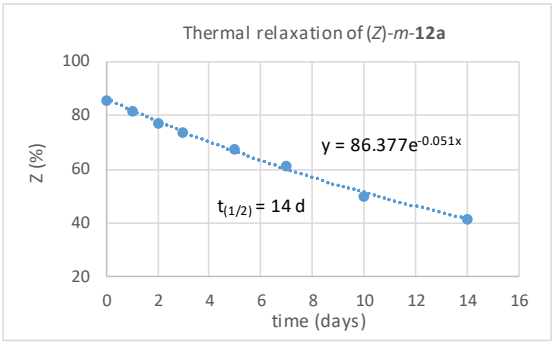

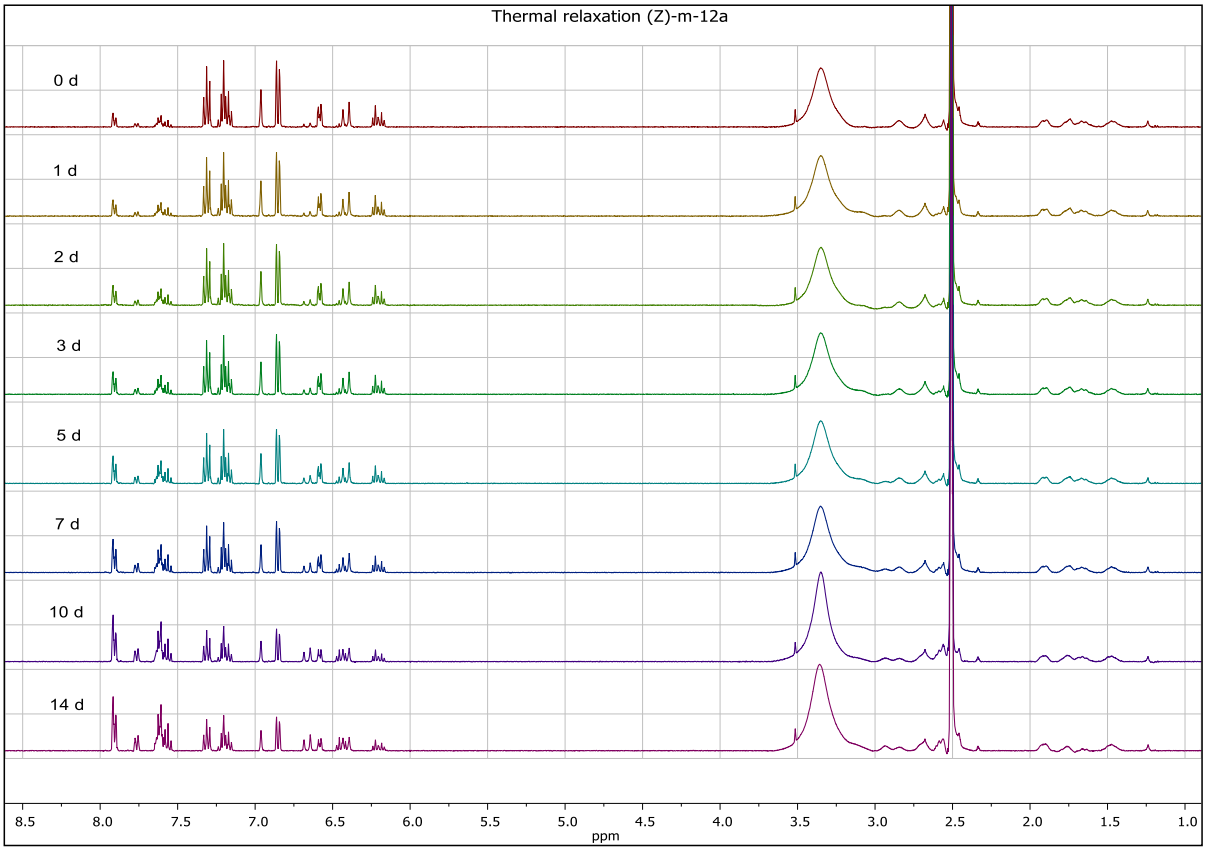

Half life of (*Z*)-*p*-**12a** in DMSO

time (h)	1H (E)*	1H (Z)*	total*	Z (%)	$t_{(1/2)}$
0	1.02	5.86	6.88	85.2	
4	1.02	2.87	3.89	73.8	19.3
8	1.00	1.83	2.83	64.7	20.1
12	1.00	1.34	2.34	57.3	21.0
20	1.03	0.99	2.02	49.2	25.2
28	1.02	0.74	1.76	42.0	27.4
36	1.02	0.54	1.56	34.6	27.7
48	1.02	0.43	1.45	29.6	31.4

*average integration for 1H (E) and 1H (Z) of isol. arom. signals

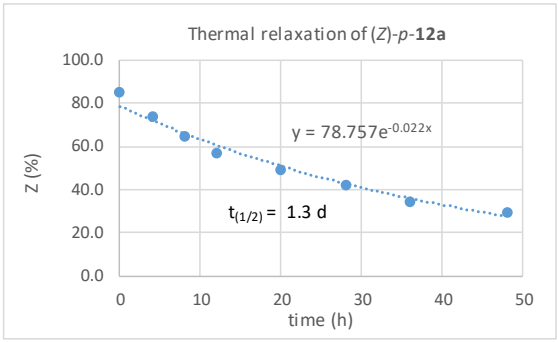

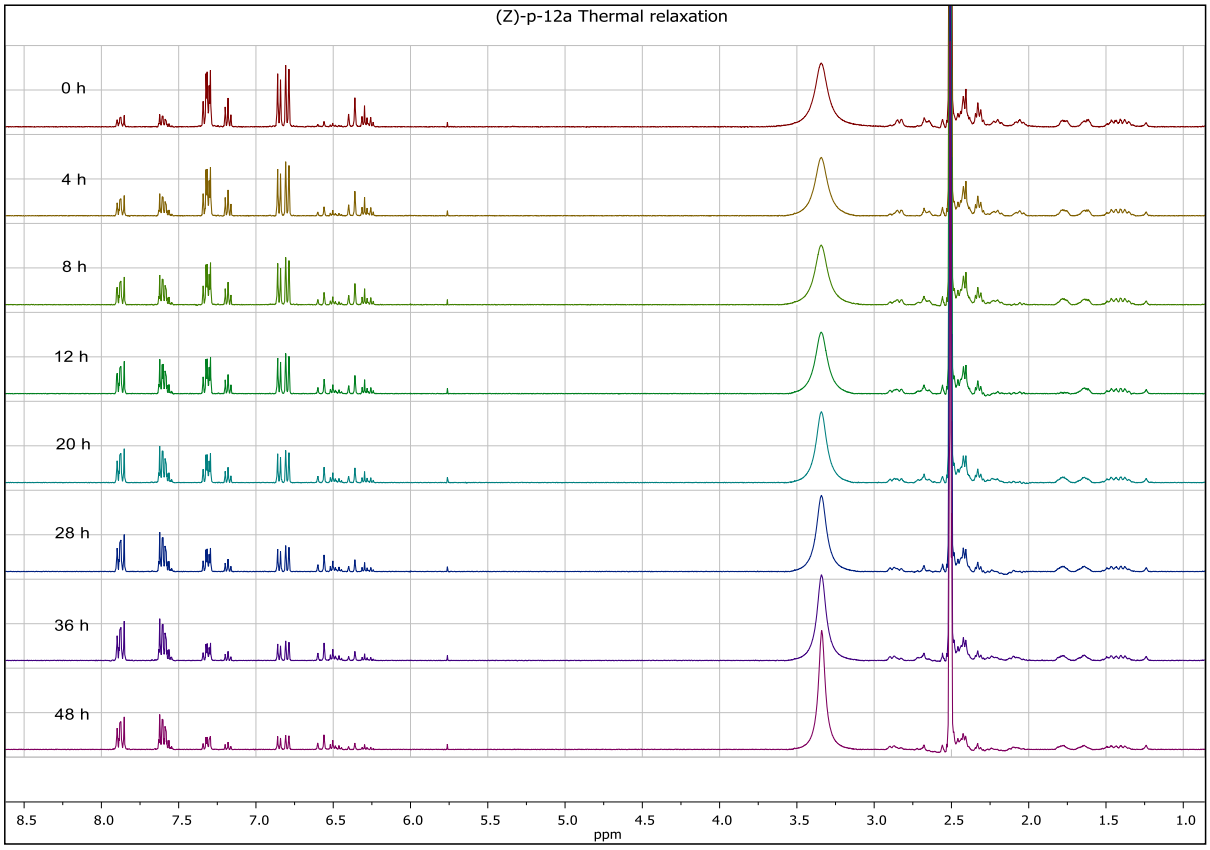

Half-life of (*Z*)-*m*-**12b** in DMSO

time (h)	1H (E)*	1H (Z)*	total*	Z (%)	$t_{(1/2)}$
0	1.02	3.66	4.68	78.2	
2	1.03	2.09	3.12	67.0	9.0
4	1.03	1.32	2.35	56.2	8.4
6	1.05	0.98	2.03	48.0	8.5
8	1.04	0.71	1.75	40.4	8.4
12	1.05	0.41	1.45	28.5	8.3
16	1.01	0.26	1.27	20.3	8.3
20	1.03	0.17	1.20	14.2	8.2
24	1.03	0.14	1.17	11.9	8.8

*average integration for 1H (E) and 1H (Z) of isol. arom. signals

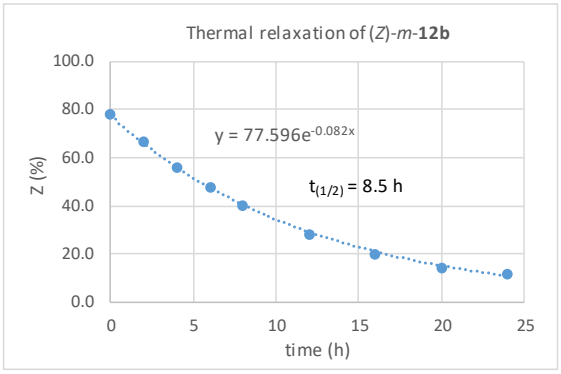

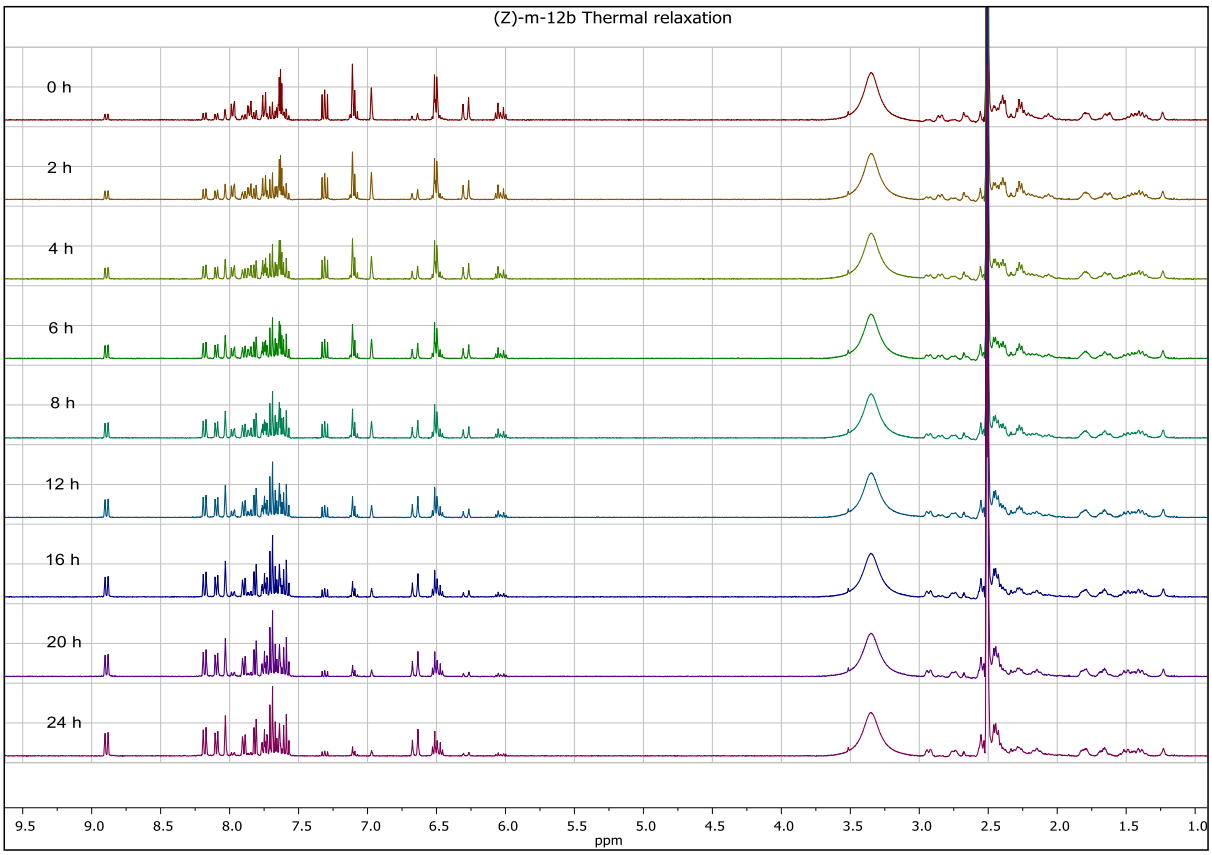

Half-life of (*Z*)-*p*-**12b** in DMSO

time (min)	1H (E)*	1H (Z)*	total*	Z (%)	$t_{(1/2)}$
0	1.02	1.54	2.56	60.2	
15	1.00	0.88	1.88	46.8	41.3
30	1.01	0.55	1.56	35.3	39.2
45	1.00	0.37	1.37	27.1	39.1
60	1.00	0.26	1.26	20.6	38.8
75	1.01	0.19	1.20	15.8	39.0
90	1.01	0.15	1.16	12.9	40.6

*average integration for 1H (E) and 1H (Z) of isol. arom. signals

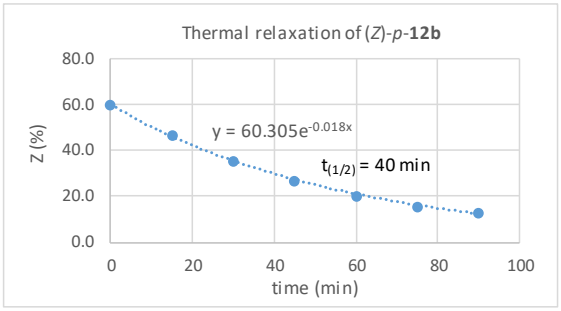

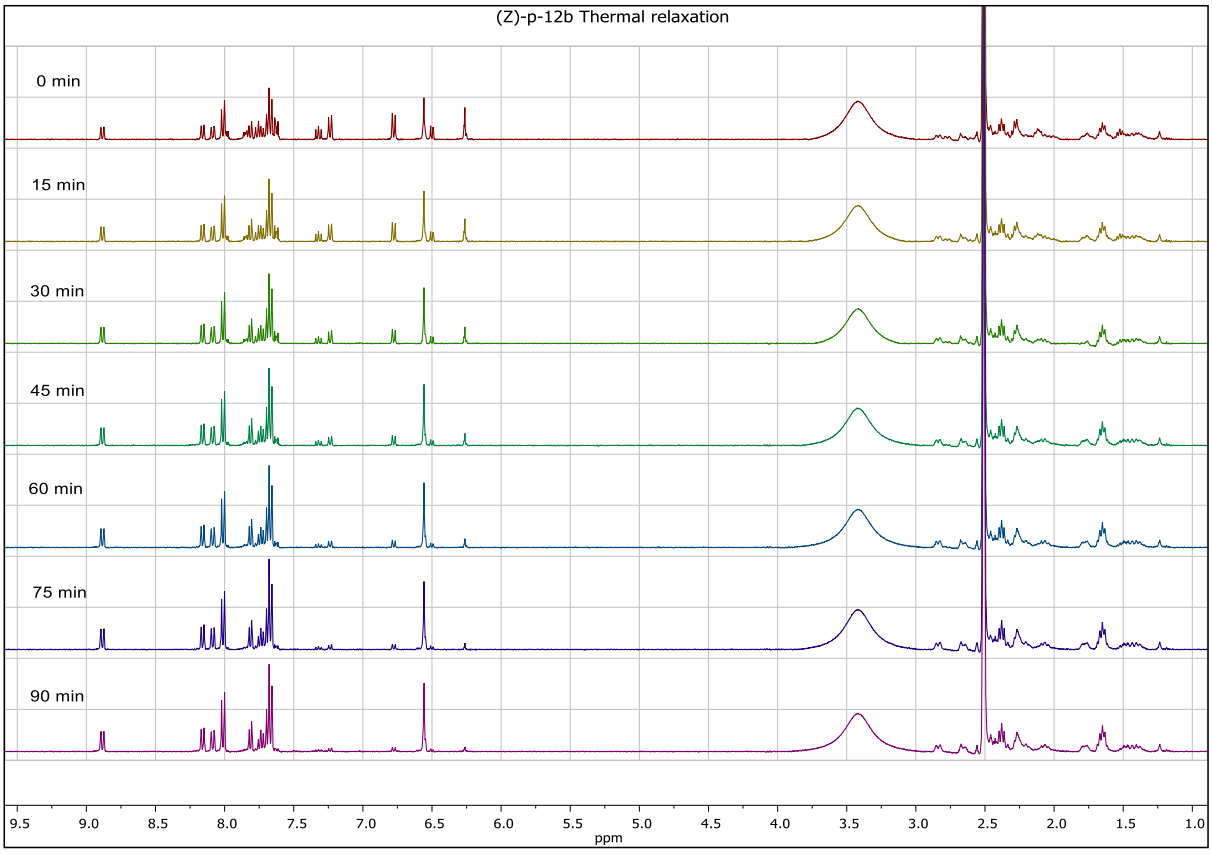

Half-life of (*Z*)-*m*-**20a** in DMSO

time (d)	1H (E)*	1H (Z)*	total*	Z (%)	$t_{(1/2)}$
0	1.01	4.23	5.24	80.7	
1	1.03	3.07	4.10	74.9	9.3
3	1.01	2.04	3.05	66.8	11.0
5	1.01	1.46	2.47	59.1	11.2
7	1.02	1.15	2.17	53.0	11.5
10	1.00	0.80	1.80	44.4	11.6
14	1.00	0.53	1.53	35.6	12.1
21	1.02	0.35	1.37	26.6	13.1

*average integration for 1H (E) and 1H (Z) of aromatic signals

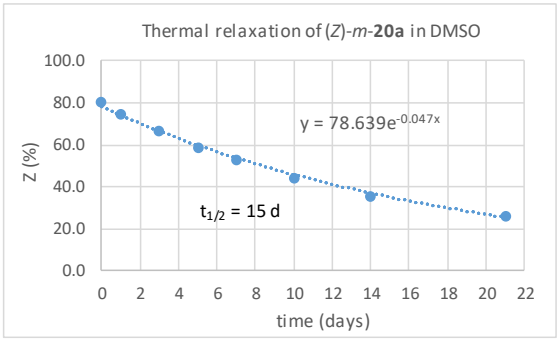

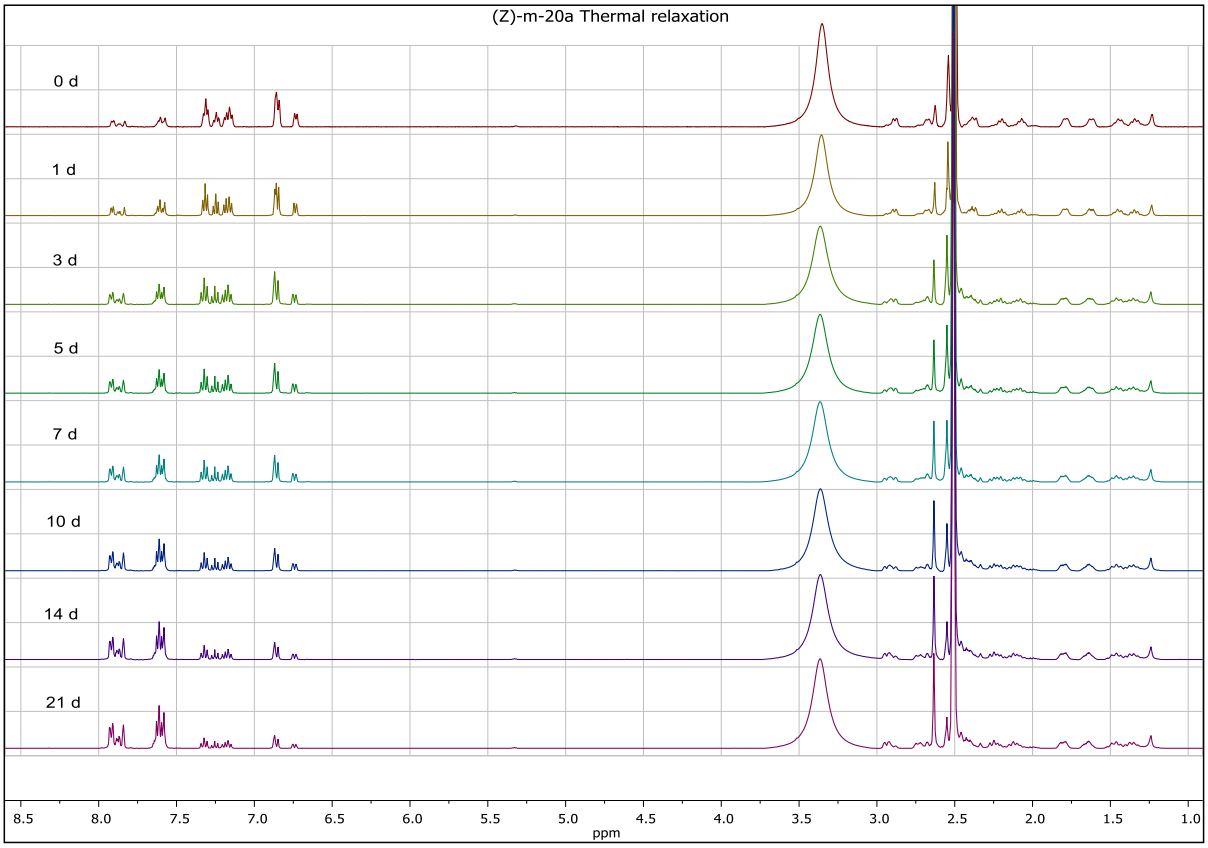

Half-life of (*Z*)-*p*-**20a** in DMSO

time (h)	1H (E)*	1H (Z)*	total*	Z (%)	$t_{(1/2)}$
0	1.03	4.27	5.30	80.6	
4	1.02	2.34	3.36	69.6	18.8
8	1.01	1.43	2.44	58.6	17.4
12	1.00	0.96	1.96	49.0	16.8
16	1.01	0.74	1.75	42.2	17.1
20	1.02	0.61	1.63	37.4	17.9
24	1.02	0.51	1.53	33.3	18.6

*average integration for 1H (E) and 1H (Z) of isol. arom. signals

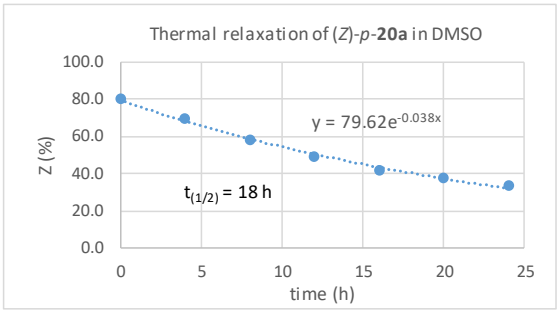

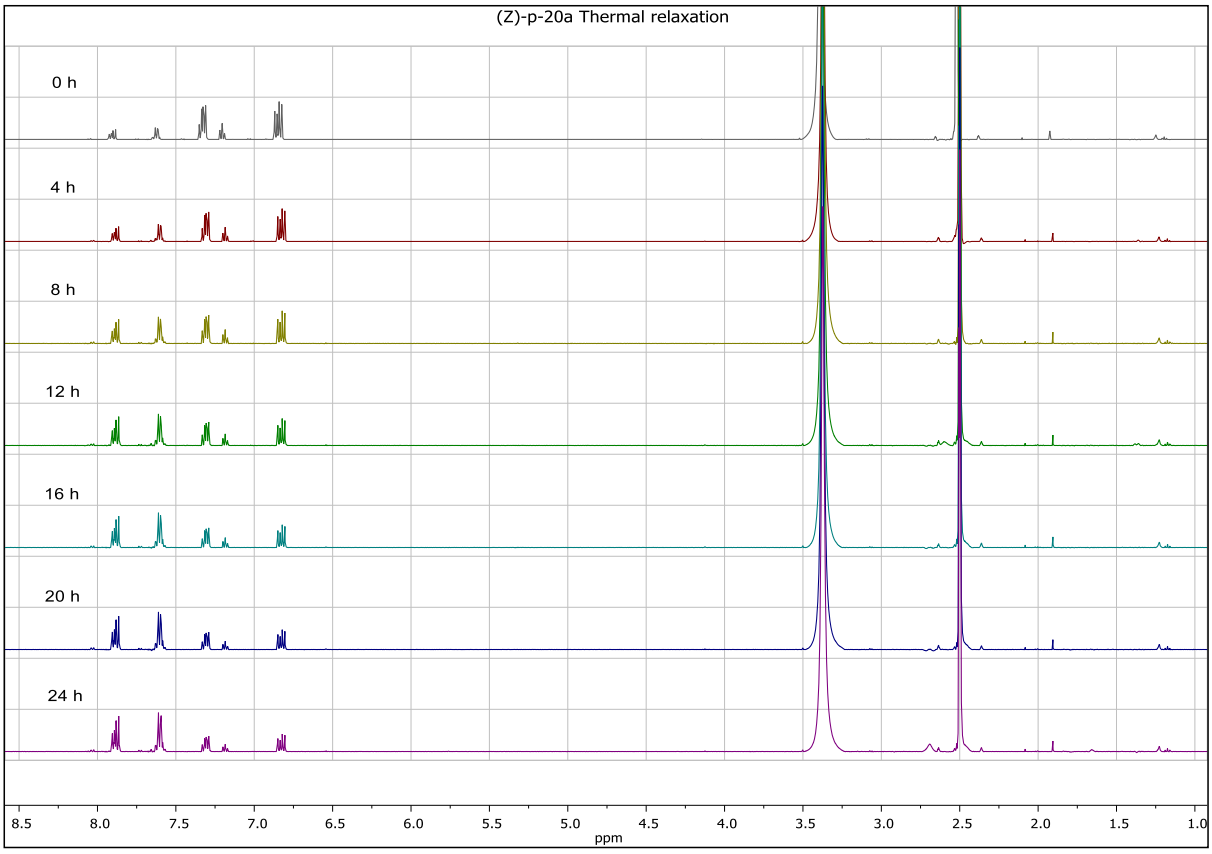

Half-life of (*Z*)-*m*-**20b** in DMSO

time (h)	1H (E)*	1H (Z)*	total*	Z (%)	$t_{(1/2)}$
0	1.01	4.84	5.84	82.8	
8	1.01	3.68	4.69	72.7	42.6
16	1.00	1.65	2.65	63.2	41.0
24	1.01	1.22	2.23	54.7	40.1
32	1.01	0.94	1.95	48.2	40.9
40	1.00	0.68	1.68	40.5	38.8
48	0.98	0.52	1.5	34.5	38.0
72	1.02	0.28	1.3	21.8	37.4

*average integration for 1H (E) and 1H (Z) of isol. arom. signals

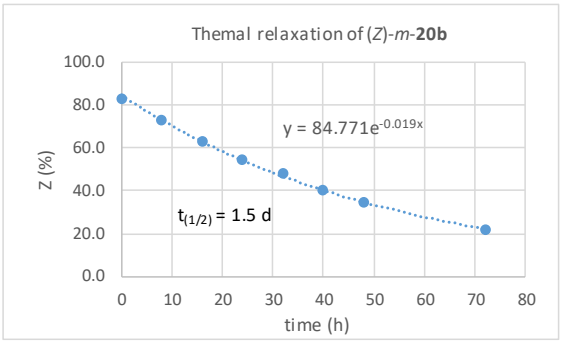

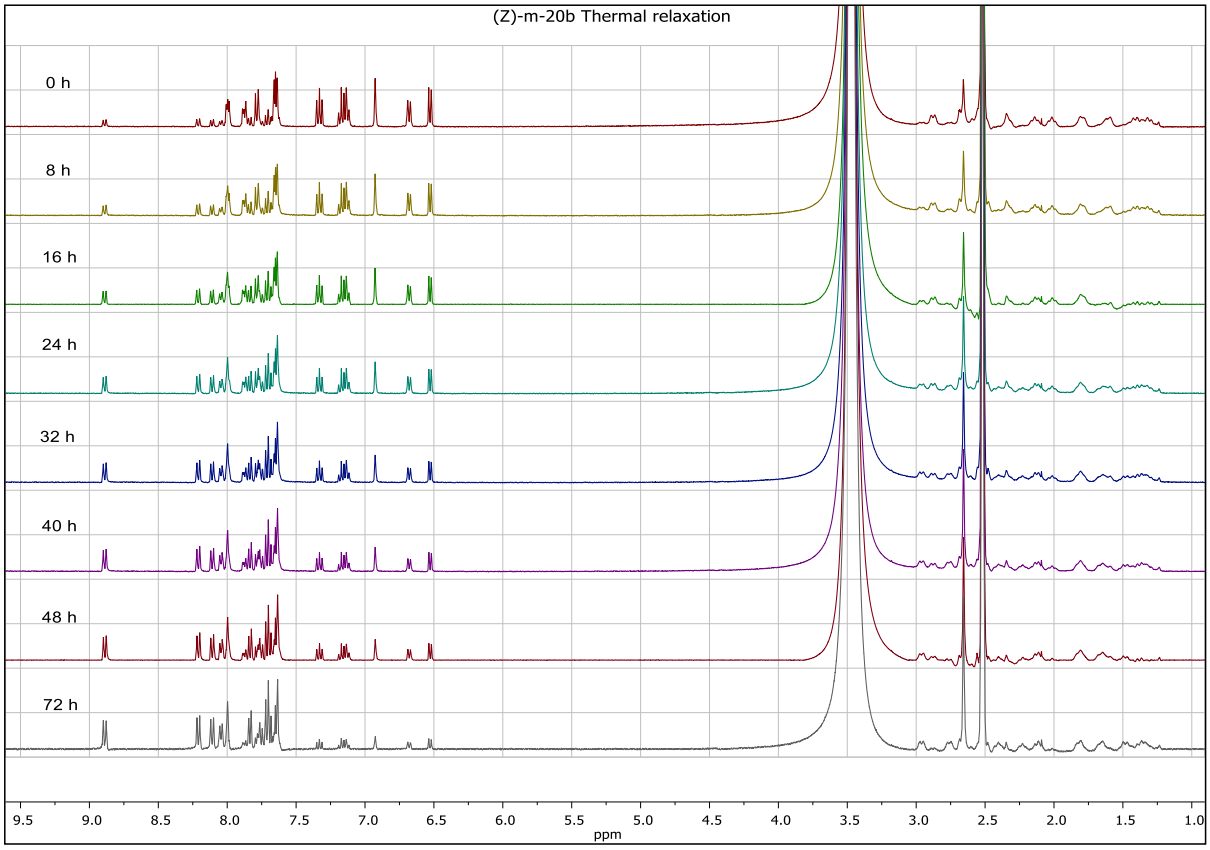

Half-life of (*Z*)-*p*-**20b** in DMSO

time (h)	1H (E)*	1H (Z)*	total*	Z (%)	$t_{(1/2)}$
0	1.04	1.94	2.98	65.1	
1	1.03	1.12	2.15	52.1	3.1
2	1.00	0.69	1.69	40.8	3.0
3	1.00	0.48	1.48	32.5	3.0
4	1.00	0.33	1.33	25.0	2.9
5	1.03	0.26	1.29	20.2	3.0
6	1.01	0.19	1.20	16.7	3.1
9	1.00	0.09	1.09	8.3	3.0
12	1.01	0.04	1.05	4.0	3.0

*average integration for 1H (E) and 1H (Z) of isol. arom. signals

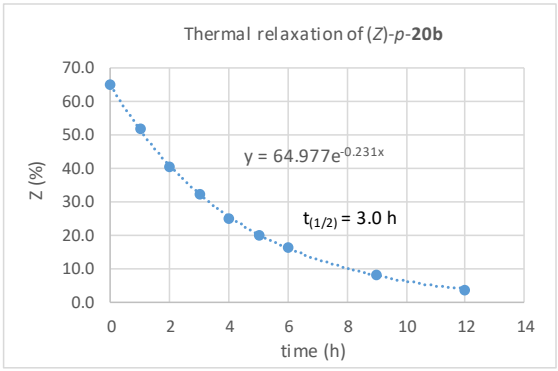

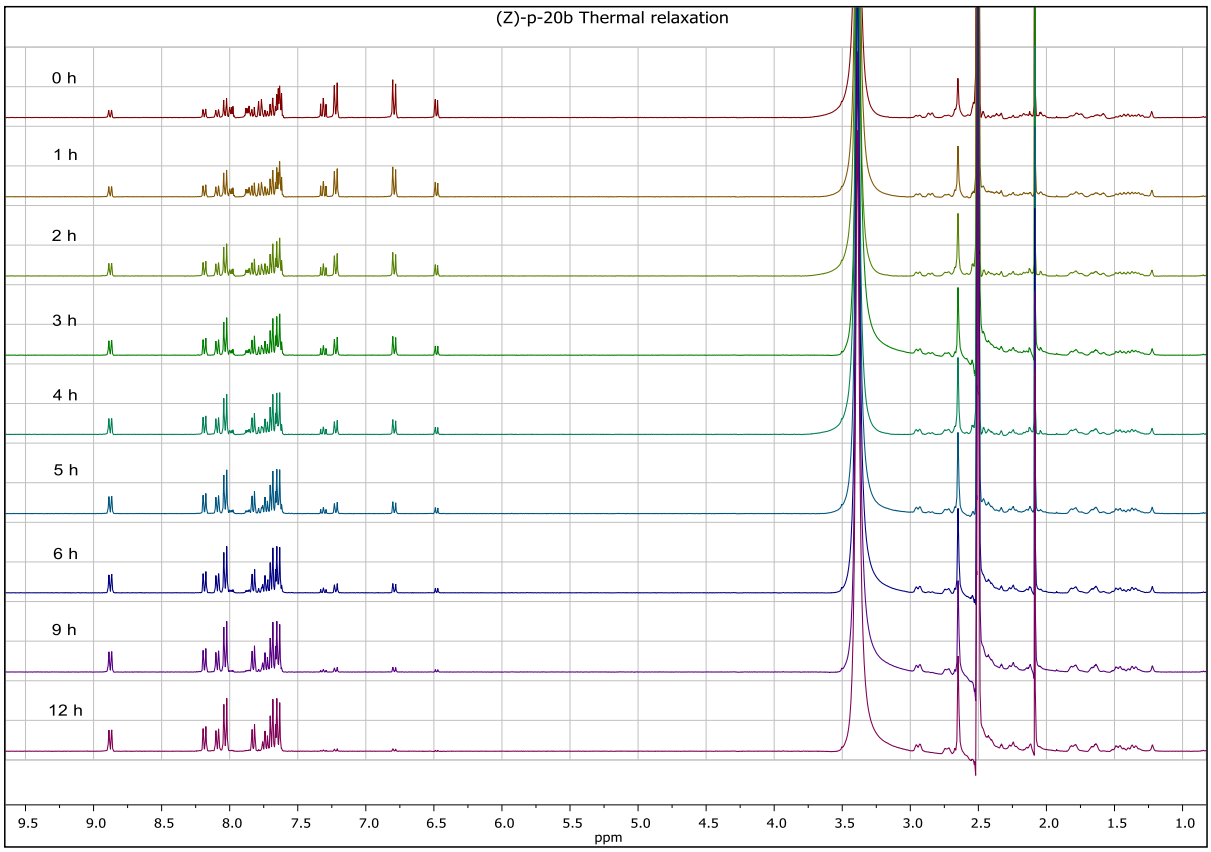

Half-life of (*Z*)-*m*-**12a** in PB (pH 7.4)

$A_{(t)}$ (350 nm)	time (d)	Z (%)	$t_{(1/2)}$
0.066	0	81.8	
0.090	1	72.0	5.3
0.102	2	66.9	6.9
0.110	3	63.6	8.7
0.118	4	60.2	9.9
0.125	5	57.2	10.3
0.138	7	51.7	10.6
0.155	10	44.5	11.4
0.166	14	39.8	13.4

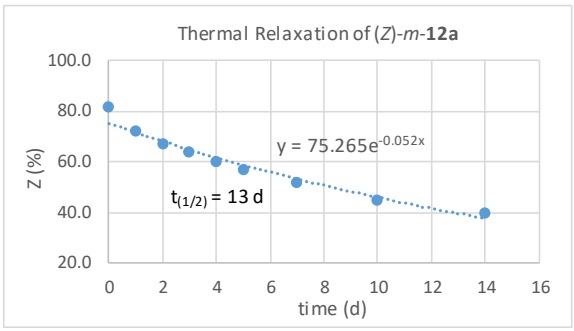

Calculations:

A (Z) = A (E) + (A (Z/E) - A (E)) / Z (%)

Z (%) = (A (Z/E) - A (E)) / (A (Z) - A (E))

A (Z/E) = 0.066 (measured) c = 25 µm

A (E) = 0.260 (measured) c = 25 µm

A (Z) = 0.024 (calculated) c = 25 µm

UV/Vis-spectra (kinetic tracking over the first 3 days):

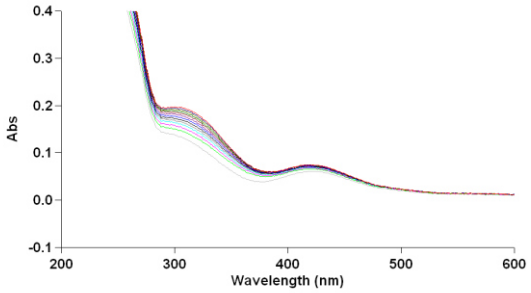

Half-life of (*Z*)-*p*-**12a** in PB (pH = 7,4)

$A_{(t)}$ 350 nm	time (h)	Z (%)	$t_{(1/2)}$
0.207	0	85.2	
0.319	8	68.7	25.8
0.395	16	57.5	28.2
0.462	24	47.7	28.7
0.528	32	38.0	27.5
0.600	40	27.5	24.5
0.654	48	19.5	22.6

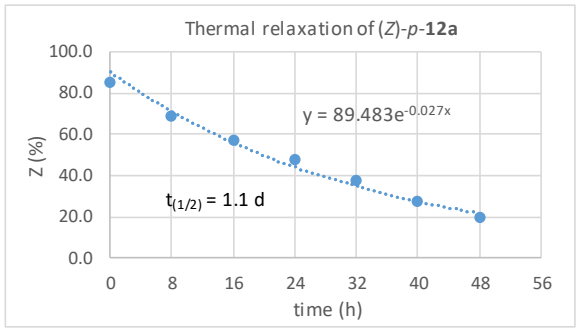

Calculations:

A (Z) = A (E) + (A (Z/E) - A (E)) / Z (%)

Z (%) = (A (Z/E) - A (E)) / (A (Z) - A (E))

A (Z/E) = 0.207 (measured) c = 50 µm

A (E) = 0.787 (measured) c = 50 µm

A (Z) = 0.137 (calculated) c = 50 µm

UV/Vis-spectra (kinetic tracking over 48 hours):

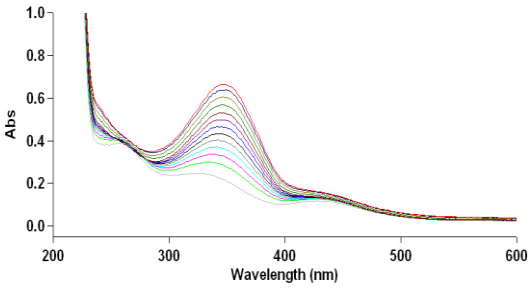

Half-life of (*Z*)-*m*-**12b** in PB (pH = 7,4)

$A_{(t)}$ 375 nm	time (h)	Z (%)	$t_{(1/2)}$
0.125	0	78.2	
0.130	2	72.8	19.4
0.134	4	68.9	21.9
0.137	6	65.0	22.5
0.141	8	61.2	22.6
0.149	12	54.4	22.9
0.155	16	48.5	23.2
0.161	20	42.7	22.9
0.166	24	37.8	22.8

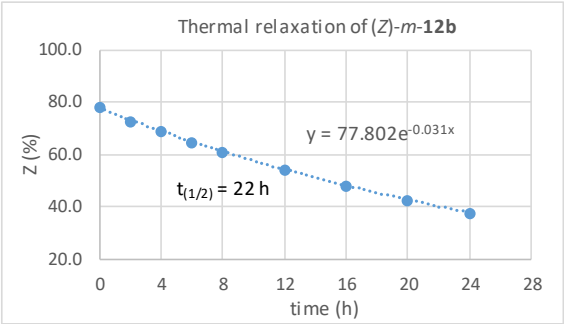

Calculations:

A (Z) = A (E) + (A (Z/E) - A (E)) / Z (%)

Z (%) = (A (Z/E) - A (E)) / (A (Z) - A (E))

A (Z/E) = 0.125 (measured) c = 20 µm

A (E) = 0.205 (measured) c = 20 µm

A (Z) = 0.102 (calculated) c = 20 µm

UV/Vis-spectra (kinetic tracking over 24 hours):

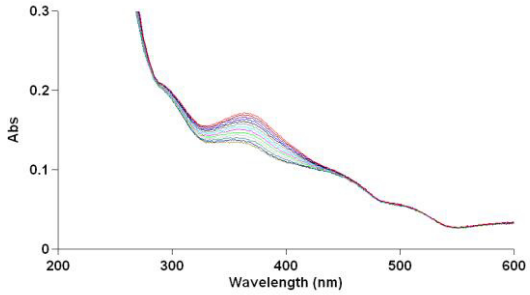

Half-life of (*Z*)-*p*-**12b** in PB (pH = 7.4)

$A_{(t)}$ 375 nm	time (h)	Z (%)	$t_{(1/2)}$
0.154	0.0	60.0	
0.166	0.5	42.8	1.0
0.175	1.0	30.0	1.0
0.180	1.5	22.8	1.1
0.184	2.0	17.1	1.1
0.187	2.5	12.8	1.1
0.189	3.0	10.0	1.2
0.190	3.5	8.6	1.2
0.191	4.0	7.1	1.3

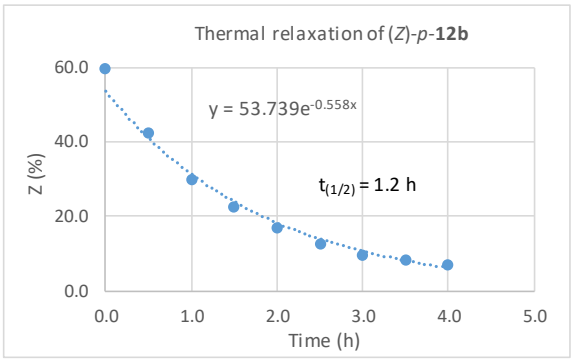

Calculations:

A (Z) = A (E) + (A (Z/E) - A (E)) / Z (%)

Z (%) = (A (Z/E) - A (E)) / (A (Z) - A (E))

A (Z/E) = 0.154 (measured) c = 10 µm

A (E) = 0.196 (measured) c = 10 µm

A (Z) = 0.126 (calculated) c = 10 µm

UV/Vis-spectra (kinetic tracking over 6 hours):

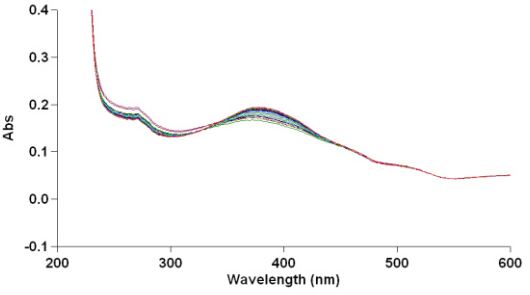

Half-life of (*Z*)-*m*-**20a** in PB (pH = 7.4)

$A_{(t)}$ 350 nm	time (d)	Z (%)	$t_{(1/2)}$
0.202	0	80.2	
0.212	1	78.1	26.2
0.223	2	75.7	24.0
0.234	3	73.3	23.1
0.256	5	68.6	22.2
0.285	7	62.8	19.8
0.307	10	57.6	20.9
0.339	14	50.8	21.3
0.378	21	42.4	22.8
0.411	28	35.3	23.6

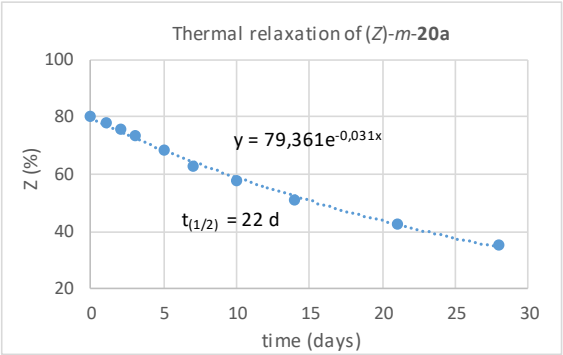

Calculations:

A (Z) = A (E) + (A (Z/E) - A (E)) / Z (%)

Z (%) = (A (Z/E) - A (E)) / (A (Z) - A (E))

A (Z/E) = 0.154 (measured) c = 50 µm

A (E) = 0.575 (measured) c = 50 µm

A (Z) = 0.110 (calculated) c = 50 µm

UV/Vis-spectra (kinetic tracking within the first 72 hours):

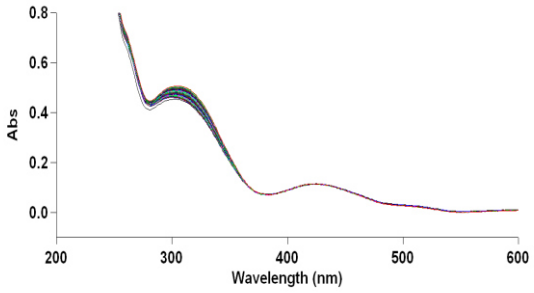

Half-life of (*Z*)-*p*-**20a** in PB (pH = 7,4)

$A_{(t)}$ 350 nm	time (d)	Z (%)	$t_{(1/2)}$
0.128	0.0	80.6	
0.158	0.5	75.0	4.8
0.186	1.0	69.8	4.8
0.211	1.5	65.2	4.8
0.235	2.0	60.7	4.9
0.279	3.0	52.7	4.9
0.316	4.0	45.7	4.9
0.348	5.0	39.8	4.9

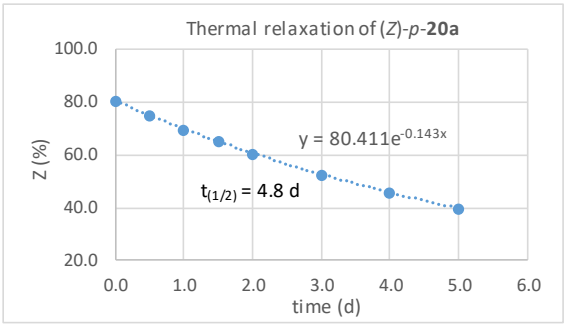

Calculations:

A (Z) = A (E) + (A (Z/E) - A (E)) / Z (%)

Z (%) = (A (Z/E) - A (E)) / (A (Z) - A (E))

A (Z/E) = 0.128 (measured) c = 25 µm

A (E) = 0.563 (measured) c = 25 µm

A (Z) = 0.023 (calculated) c = 25 µm

UV/Vis-spectra (kinetic tracking within the first 48 hours):

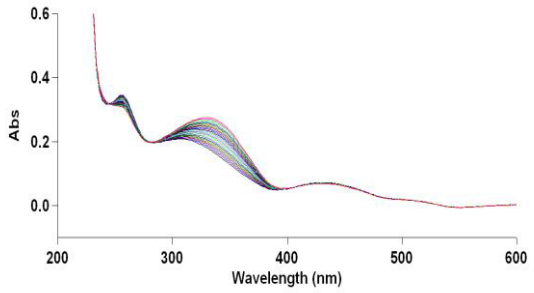

Half-life of (*Z*)-*m*-**20b** in PB (pH = 7,4)

$A_{(t)}$ 375 nm	time (h)	Z (%)	$t_{(1/2)}$
0.066	0	81.0	
0.086	4	70.7	20.4
0.106	8	60.5	19.0
0.123	12	51.8	18.6
0.138	16	44.1	18.2
0.151	20	37.4	17.9
0.163	24	31.2	17.4

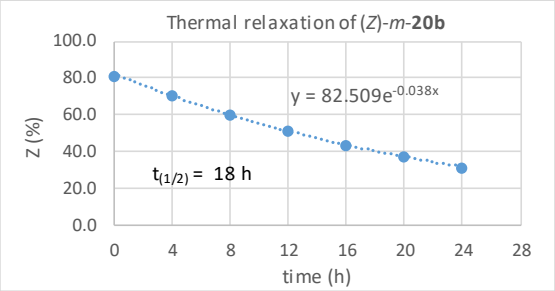

Calculations:

A (Z) = A (E) + (A (Z/E) - A (E)) / Z (%)

Z (%) = (A (Z/E) - A (E)) / (A (Z) - A (E))

A (Z/E) = 0.066 (measured) c = 20 µm

A (E) = 0.224 (measured) c = 20 µm

A (Z) = 0.029 (calculated) c = 20 µm

UV/Vis kinetic tracking over 24 hours:

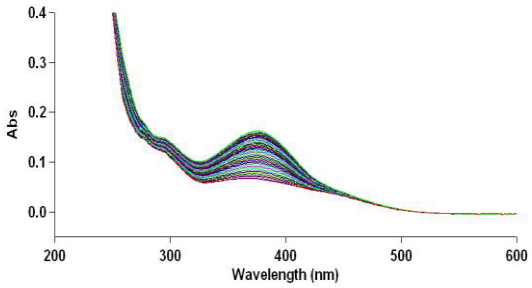

Half-life of (*Z*)-*p*-**20b** in PB (pH = 7.4)

$A_{(t)}$ 375 nm	time (h)	Z (%)	$t_{(1/2)}$
0.088	0	60.0	
0.103	1	49.2	3.5
0.117	2	39.1	3.2
0.128	3	31.1	3.2
0.137	4	24.6	3.1
0.143	5	20.3	3.2
0.149	6	15.9	3.1
0.158	9	9.4	3.3
0.163	12	5.7	3.4

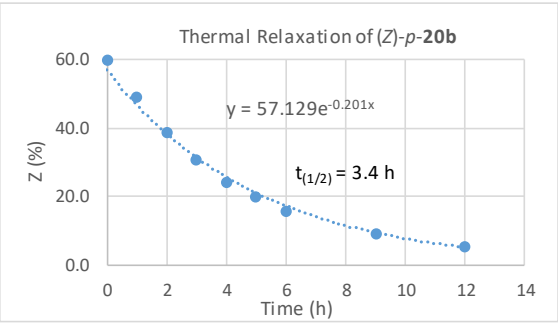

Calculations:

A (Z) = A (E) + (A (Z/E) - A (E)) / Z (%)

Z (%) = (A (Z/E) - A (E)) / (A (Z) - A (E))

A (Z/E) = 0.088 (measured) c = 10 µm

A (E) = 0.171 (measured) c = 10 µm

A (Z) = 0.033 (calculated) c = 10 µm

UV/Vis-spectra (kinetic tracking over 24 hours):

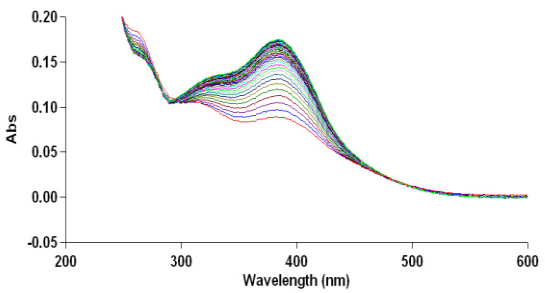

Half-life of (*Z*)-*m*-**13a** in PB (pH 7.4)

$A_{(t)}$ (350 nm)	time (d)	Z (%)	$t_{(1/2)}$
0.045	0	85.2	
0.077	3	67.7	9.1
0.098	7	56.3	11.7
0.118	10	45.3	11.0
0.131	14	38.3	12.1

A (E) = 0.201 A (Z) = 0.018 c = 20 µm

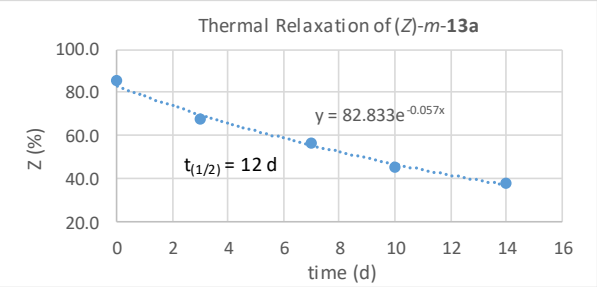

Half-life of (*Z*)-*p*-**13a** in PB (pH = 7,4)

$A_{(t)}$ 350 nm	time (h)	Z (%)	$t_{(1/2)}$
0.205	0	89.2	
0.290	8	75.4	33.0
0.329	16	69.0	43.2
0.375	24	61.5	44.7
0.411	32	55.6	46.9
0.452	40	48.9	46.1
0.486	48	43.4	46.2

A (E) = 0.752 A (Z) = 0.139 c = 50 µm

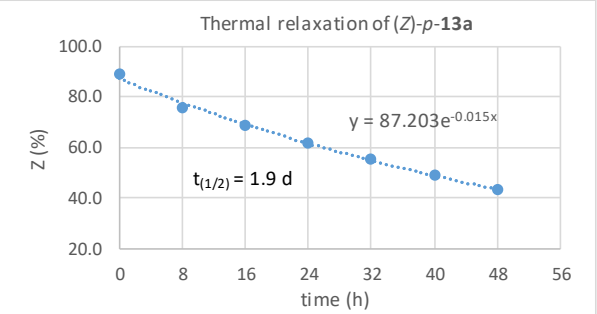

Half-life of (*Z*)-*m*-**13b** in PB (pH = 7,4)

$A_{(t)}$ 375 nm	time (h)	Z (%)	$t_{(1/2)}$
0.124	0	83.1	
0.156	4	57.6	8.6
0.170	8	46.4	9.5
0.180	12	38.4	10.8
0.189	16	31.2	11.3
0.197	20	24.8	11.5
0.204	24	19.2	11.4

A (E) = 0.228 A (Z) = 0.103 c = 20 µm

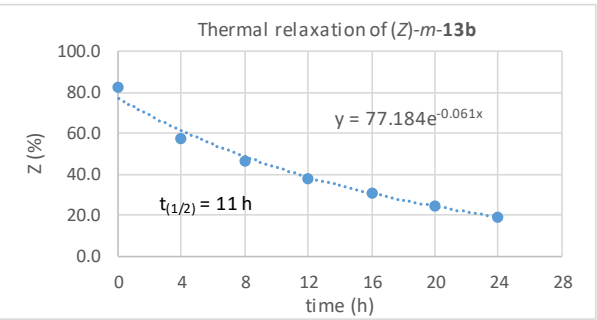

Half-life of (*Z*)-*p*-**13b** in PB (pH = 7.4)

$A_{(t)}$ 375 nm	time (h)	Z (%)	$t_{(1/2)}$
0.149	0.0	63.8	
0.157	0.5	50.8	1.5
0.164	1.0	39.3	1.4
0.170	1.5	29.5	1.3
0.175	2.0	21.3	1.3
0.179	3.0	14.8	1.4
0.181	4.0	11.4	1.6

A (E) = 0.188 A (Z) = 0.127 c = 10 µm

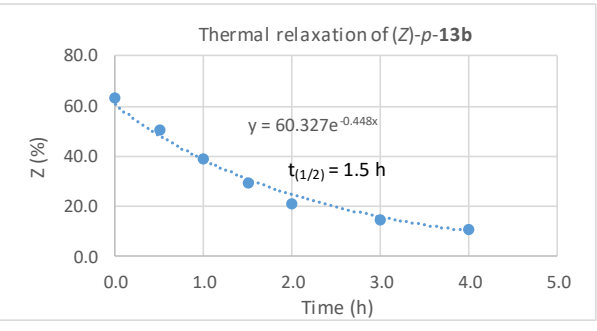

Half-life of (*Z*)-*m*-**21a** in PB (pH = 7.4)

$A_{(t)}$ 350 nm	time (d)	Z (%)	$t_{(1/2)}$
0.069	0	81.3	
0.084	3	71.3	15.8
0.118	7	55.1	14.5
0.134	10	46.5	15.2
0.145	14	40.6	16.0

A (E) = 0.221 A (Z) = 0.034 c = 20 µm

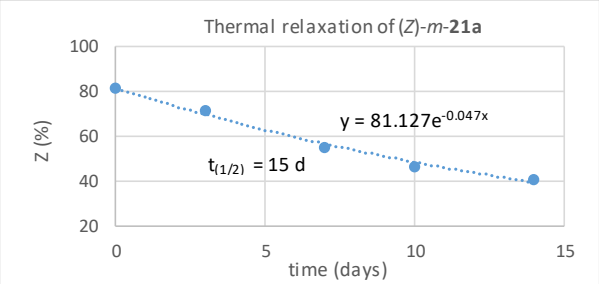

Half-life of (*Z*)-*p*-**21a** in PB (pH = 7,4)

$A_{(t)}$ 350 nm	time (d)	Z (%)	$t_{(1/2)}$
0.121	0	80.3	
0.162	1	70.1	5.1
0.187	2	63.8	6.0
0.207	3	58.9	6.7
0.230	4	53.3	6.8
0.246	5	49.4	7.1

A (E) = 0.448 A (Z) = 0.039 c = 20 µm

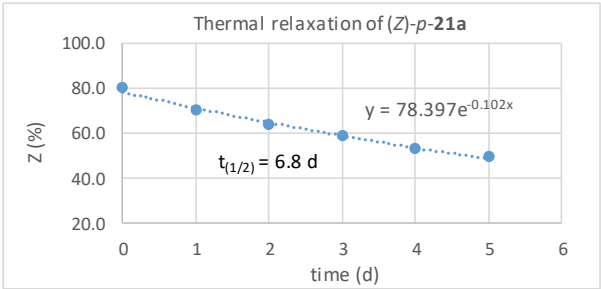

Half-life of (*Z*)-*m*-**21b** in PB (pH = 7,4)

$A_{(t)}$ 375 nm	time (h)	Z (%)	$t_{(1/2)}$
0.064	0	83.2	
0.076	4	76.2	31.5
0.083	8	72.3	39.5
0.089	12	68.9	44.1
0.108	24	58.2	46.5
0.137	48	41.8	48.3

A (E) = 0.211 A (Z) = 0.034 c = 20 µm

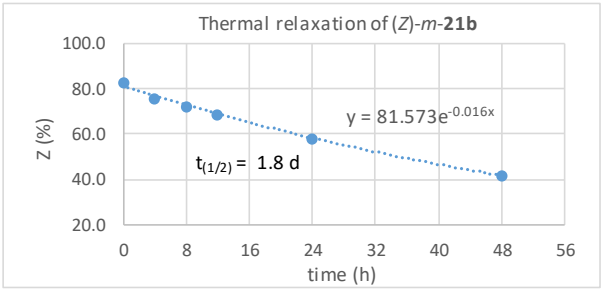

Half-life of (*Z*)-*p*-**21b** in PB (pH = 7.4)

$A_{(t)}$ 375 nm	time (h)	Z (%)	$t_{(1/2)}$
0.088	0	65.0	
0.095	0.5	58.9	3.5
0.100	1	54.7	4.0
0.105	1.5	50.4	4.1
0.109	2	47.0	4.3
0.116	3	41.0	4.5
0.122	4	35.8	4.6

A (E) = 0.164 A (Z) = 0.047 c = 10 µm

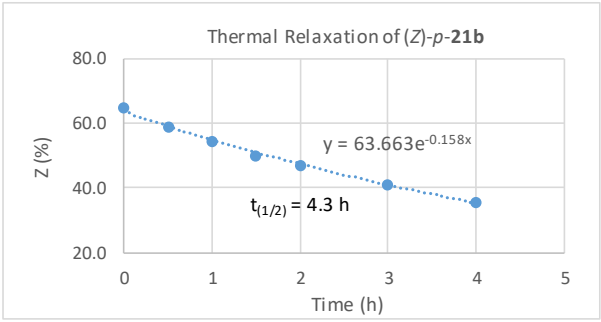

6 List of abbreviations

Aa	*Aquifex aeolicus* (bacterium)
CNS	central nervous system
DAT	dopamine transporter
EI	electron ionization
ESI	electrospray ionization
GABA	γ-aminobutyric acid
GABA-T	GABA transaminase
GAD	glutamic acid decarboxylase
GAT	GABA transporter
GlyT	glycine transporter
GPCR	G-protein coupled receptors
HRMS	high resolution mass spectrometry
HUGO	human genome organization
IC_{50}	half maximal inhibitory concentration
K_i	inhibition constant
L	ligand (for palladium catalyst)
LeuT	leucine transporter
mGAT1	murine γ-aminobutyric acid transporter subtype 1
MIDA	N-methyliminodiacetic acid
MS	mass spectrometry
NET	noradrenalin transporter
NMR	nuclear magnetic resonance
NSS	neurotransmitter-sodium-symporters
ProT	proline transporter
SERT	serotonin transporter
SLC	solute carrier
$t_{1/2}$	half-life
TM	transmembrane helix
VGAT	vesicular neurotransmitter transporter
WHO	world health organization

7 Literature

[1] Neurological disorders: Public health challenges, W. H. O. Europe, Geneva, **2006**. http://www.who.int/mental_health/neurology/neurodiso/en/

[2] Fact sheet epilepsy, W. H. O. Europe, Geneva, **2016**. http://www.who.int/mediacentre/factsheets/fs999/en/

[3] M. J. Brodie, F. Besag, J. B. Steinhoff, *Pharmacol. Rev.* **2016**, 68, 563-602.

[4] N. G. Bowery, T. G. Smart, *Br. J. Pharmacol.* **2006**, *147*, S109-S119.

[5] D. F. Owens, Arnold R. Kriegstein, *Nature Revi. Neurosc.* **2002**, 3, 715-727.

[6] L. A. Borden, *Neurochem. Internat.* **1996**, *29*, 335-356.

[7] A. C. Foster, J. A. Kemp, *Current Opinion in Pharmacol.* **2006**, *6*, 7-17.

[8] A. S. Kristensen, J. Andersen, T. N. Jorgensen, L. Sorensen, J. Eriksen, C. J. Loland, K. Stromgaard, U. Gether, *Pharmacol. Rev.* **2011**, *63*, 585-640.

[9] S. Bröer, U. Gether, *Br. J. Pharmacol.* **2012**, *167*, 256-278.

[10] N. Nelson, *J. Neurochem* **1998**, *71*, 1785-1803.

[11] R. Radian, A. Bendahan, B. I. Kanner, *J. Biol. Chem.* **1986**, *261*, 15437-15441.

[12] J. Guastella, N. Nelson, H. Nelson, L. Czyzyk, S. Keynan, M. C. Miedel, N. Davidson, H. A. Lester, B. I. Kanner, *Science (New York, N.Y.)* **1990**, *249*, 1303-1306.

[13] T. Pacholczyk, R. D. Blakely, S. G. Amara, *Nature* **1991**, *350*, 350-354.

[14] J. E. Kilty, D. Lorang, S. G. Amara, *Science (New York, N.Y.)* **1991**, *254*, 578-579.

[15] R. D. Blakely, H. E. Berson, R. T. Fremeau, M. G. Caron, M. M. Peek, H. K. Prince, C. C. Bradley, *Nature* **1991**, *354*, 66-70.

[16] J. Guastella, N. Brecha, C. Weigmann, H. A. Lester, N. Davidson, *Proc. Natl. Acad. Sci.* **1992**, *89*, 7189-7193.

[17] J. G. Chen, S. Liu-Chen, G. Rudnick, *J. Biol. Chem.* **1998**, *273*, 12675-12681.

[18] A. Yamashita, S. K. Singh, T. Kawate, Y. Jin, E. Gouaux, *Nature* **2005**, *437*, 215-223.

[19] T. Beuming, L. Shi, J. A. Javitch, H. Weinstein, *Mol. Pharm.* **2006**, 70, 1630-1642.

[20] A. Penmatsa, E. Gouaux, *J. Physiol.* **2014**, *592*, 863-869.

[21] O. Jardetzky, *Nature* **1966**, *211*, 969-970.

[22] E. Gouaux, Phil. Trans. R. Soc. B **2009**, 364, 149–154

[23] M. H. Cheng, I. Bahar, Biophys. J. **2013**, 105, 630-639

[24] H. Krishnamurthy, E. Gouaux, *Nature* **2012**, *481*, 469-474.

[25] L. Shi, M. Quick, Y. Zhao, H. Weinstein, J. A. Javitch, *Mol Cell* **2008**, *30*, 667-677.

[26] Y. Zhao, D. S. Terry, L. Shi, M. Quick, H. Weinstein, S. C. Blanchard, J. A. Javitch, *Nature* **2011**, *474*, 109-113.

[27] M. Quick, L. Shi, B. Zehnpfennig, H. Weinstein, J. A. Javitch, *Nat. Struct. Mol. Biol.* **2012**, *19*, 207-211.

[28] S. K. Singh, A. Yamashita, E. Gouaux, *Nature* **2007**, *448*, 952-956.

[29] C. L. Piscitelli, H. Krishnamurthy, E. Gouaux, *Nature* **2010**, *468*, 1129-1132.

[30] A. Penmatsa, K. H. Wang, E. Gouaux, *Nature* **2013**, *503*, 85-90

[31] J. A. Coleman, E. Green, E. Gouaux, *Nature* **2016**, *532*, 334-339

[32] K. K. Madsen, H. S. White, A. Schousboe, *Pharmacol. Ther.* **2010**, *125*, 394-401

[33] Q. R. Liu, B. López-Corcuera, S. Mandiyan, H. Nelson, N. Nelson, *J. Biol. Chem.* **1993**, *268*, 2106-2112.

[34] A. C. Lehre, N. M. Rowley, Y. Zhou, S. Holmseth, C. Guo, T. Holen, R. Hua, P. Laake, A. M. Olofsson, I. Poblete-Naredo, D. A. Rusakov, K. K. Madsen, R. P. Clausen, A. Schousboe, H. S. White, N. C. Danbolt, *Epilepsy research* **2011**, *95*, 70-81.

[35] S. A. Kempson, Y. Zhou, N. C. Danbolt, *Front. Physiol.* **2014**, *5*, 1-16.

[36] M. Palacin, R. Estevez, J. Bertran, A. Zorzano, *Physiol. Rev.* **1998**, *78*, 969-1054.

[37] Y. Zhou, S. Holmseth, C. Guo, B. Hassel, G. Höfner, H.S. Huitfeldt, K. T. Wanner, N. C. Danbolt, *J. Biol. Chem.* **2012**, *287*, 35733-35746.

[38] K. K. Madsen, R. P. Clausen, O. M. Larsson, P. Krogsgaard-Larsen, A. Schousboe, H. S. White, *J. Neurochem.* **2009**, *109*, 139-144

[39] A. Schousboe, P. Thorbek, P. Krogsgaard-Larsen, *J. Neurochem.* **1979**, *33*, 181-189

[40] P. Krogsgaard-Larsen, O. M. Larsson, A. Schousboe, *Epilepsy Research* **1987**, *1*, 77-93.

[41] K. E. Andersen, J. L. Sørensen, P. O. Huusfeldt, L. J. Knutsen, B. Lundt, H. Petersen, P. D. Suzdak, M. D. B. Swedberg, *J. Med. Chem.* **1999**, *42*, 4281-4291.

[42] P. D. Suzdak, K. Frederiksen, K. E. Andersen, P. O. Sorensen, L. J. S. Knutsen, E. B. Nielson, *Eur. J. Pharmacol*. **1992**, 223, 189-198.

[43] F. E. Ali, W. E. Bondinell, P. A. Dandridge, J. S. Frazee, E. Garvey, O. D. Stringer, J. W. Venslavsky, B. W. Volpe, L. M. Yunger, C. L. Zirkle, *J. Med. Chem.* **1985**, *28*, 653-660.

[44] E. B. Nielsen, P. D. Suzdak, K. E. Andersen, L. J.S. Knutsen, U. Sonnewald, C. Braestrup, *Eur. J. Pharmacol*. **1991**, 196, 257-260

[45] K. E. Andersen, J. Lau, B. F. Lundt, H. Petersen, P. O. Huusfeldt, P. D. Suzdak, M. D. B. Swedberg, *Bioorg. Med. Chem.* **2001**, *9*, 2773-2785.

[46] M. Petrera, T. Wein, L. Allmendinger, M. Sindelar, J. Pabel, G. Höfner, K. T. Wanner, *ChemMedChem* **2016**, *11*, 519-538.

[47] T. Wein, K. T. Wanner, *J. Mol. Model.* **2010**, 16, 155-161

[48] S. Skovstrup, O. Taboureau, H. Brauner-Osborne, F. S. Jorgensen, *ChemMedChem* **2010**, 5, 986-1000

[49] T. Wein, M. Petrera, L. Allmendinger, G. Höfner, K. T. Wanner, *ChemMedChem* **2016**, 11, 509-518

[50] C.C. Johansson Seechurn, M. O. Kitching, T. J. Colacot, V. Snieckus, *Angew. Chem. Int. Ed.* **2012**, 51, 5062–5085

[51] K. C. Nicolaou, P. G. Bulger, D. Sarlah, *Angew. Chem. Int. Ed.* **2005**, 44, 4442–4489

[52] A. J. J. Lennox and G. C. Lloyd-Jones, Chem. Soc. Rev., **2014**, 43, 412-443

[53] R. Chinchilla, C. Najera, *Chem. Rev.* **2007**, 107, 874-922

[54] R. Martin, S. Buchwald, *Acc. Chem. Res.* **2008**, 41, 1461-1473

[55] J. L. Zhang, J. Q. Zhong, J. D. Lin, W. P. Hu, K. Wu, G. Q. Xu, A. T. S. Wee, W. Chen, *Chem. Soc. Rev.*, **2015**, 44, 2998-3022

[56] M. Irie, *Chem. Rev.* **2000**, 100, 1683-1684

[57] M. Irie, T. Fukaminato, S. Kobatake, *Chem. Rev.* **2014**, 114, 12174-12277

[58] A. A. Beharry, G. A. Woolley, *Chem. Soc. Rev.* **2011**, 40, 4422-4437

[59] E. Smith, I. Collins, *Future Med. Chem.* **2015**, 7, 159–183

[60] M. Schönberger, M. Althaus, W. Clauss, D. Trauner, *Nat. Chem.* **2014,** 6, 712-719.

[61] J. Broichhagen, T. Podewin, H. Meyer-Berg, Y. von Ohlen, N. R. Johnston, B. J. Jones, S. R. Bloom, G. A. Rutter, A. Hoffmann-Röder, D. J. Hodson, D. Trauner, *Angew. Chemie Int. Ed.* **2015**, 54, 1-6.

[62] J. Broichhagen, I. Jurastow, K. Iwan, W. Kummer, D. Trauner, *Angew. Chemie Int. Ed.* **2014,** 53, 7657-7660.

[63] M. Schönberger, D. Trauner, *Angew. Chemie Int. Ed.* **2014,** 53, 3264-3267.

[64] J. A. Frank, M. Moroni, R. Moshourab, M. Sumser, G. R. Lewin, D. Trauner, *Nat. Commun.* **2015,** 6, 7188.

[65] A. Rullo, A. Reiner, A. Reiter, D. Trauner, E. Y. Isacoff, G. A. Woolley, *Chem. Commun.* **2014**, 50, 14613–14615.

[66] L. Laprell, E. Repak, V. Franckevicius, F. Hartrampf, J. Terhag, M. Hollmann, M. Sumser, N. Rebola, D. A. DiGregorio, D. Trauner, *Nat. Commun.* **2015,** 6, 8076.

[67] L. Laprell, K. Hüll, P. Stawski, C. Schön, S. Michalakis, M. Biel, M. Sumser, D. Trauner, *ACS Chem. Neurosc.* **2015**, 7, 15–20.

[68] M. Schoenberger, A. Damijonaitis, Z. Zhang, D. Nagel, D. Trauner, *ACS Chem. Neurosc.* **2014,** 5, 514-518.

[69] M. Borowiak, W. Nahaboo, M. Reynders, K. Nekolla, P. Jalinot, M. Rehberg, M. Delattre, S. Zahler, A. Vollmar, D. Trauner, O. Thorn-Seshold, *Cell* **2015,** 162, 403-411.

[70] G. Quandt, G. Höfner, J. Pabel, J. Dine, M. Eder, K. T. Wanner, *J. Med. Chem.* **2014,** 57, 6809-6821.

[71] M. Sindelar, T. A. Lutz, M. Petrera, K. T. Wanner, *J. Med. Chem.* **2013,** 56, 1323-1340.

[72] T. Hellenbrand, Dissertation, LMU Munich, July **2015**.

8 Publications and Manuscripts

1. *Focused Pseudostatic Hydrazone Libraries Screened by MS Binding Assay – Optimizing Affinities towards γ-Aminobutyric Acid Transporter 1*

2. *Development of highly potent GAT1 Inhibitors: Synthesis of Nipecotic Acids Derivatives with N-arylalkynyl substituents*

3. *Development of new photoswitchable azobenzene bound GABA uptake inhibitors with distinctly enhanced potency upon photoactivation*

4. *A general approach to substituted diphenyldiazenes*

Journal of Medicinal Chemistry

Article

pubs.acs.org/jmc

Focused Pseudostatic Hydrazone Libraries Screened by Mass Spectrometry Binding Assay: Optimizing Affinities toward γ-Aminobutyric Acid Transporter 1

Miriam Sindelar, Toni A. Lutz, Marilena Petrera,[†] and Klaus T. Wanner*

Center for Drug Research, Department of Pharmacy, Ludwig Maximilians University at Munich, Butenandtstrasse 9-13, D-81377 Munich, Germany

Supporting Information

ABSTRACT: Mass spectrometric (MS) binding assays, a powerful tool to determine affinities of single drug candidates toward chosen targets, were recently demonstrated to be suitable for the screening of compound libraries generated with reactions of dynamic combinatorial chemistry when rendering libraries pseudostatic. Screening of small hydrazone libraries targeting γ-aminobutyric acid transporter 1 (GAT1), the most abundant γ-aminobutyric acid (GABA) transporter in the central nervous system, revealed two nipecotic acid derived binders with submicromolar affinities. Starting from the biphenyl carrying hit as lead structure, the objective of the present study was to discover novel high affinity GAT1 binders by screening of biphenyl focused pseudostatic hydrazone libraries formed from hydrazine **10** and 36 biphenylcarbaldehydes **11c−al**. Hydrazone **12z** that carried a 2′,4′-dichlorobiphenyl residue was found to be the most potent binder with low nanomolar affinity (pK_i = 8.094 ± 0.098). When stable carba analogues of representative hydrazones were synthesized and evaluated, the best binder **13z** was again displaying the 2′,4′-dichlorobiphenyl moiety (pK_i = 6.930 ± 0.021).

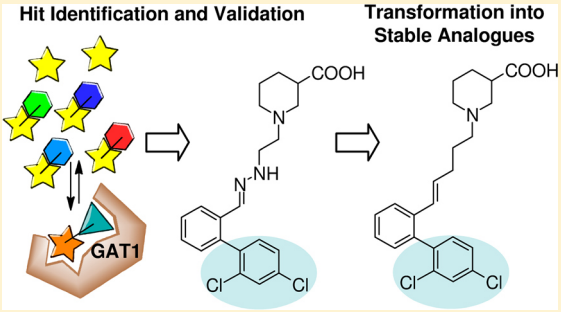

INTRODUCTION

γ-Aminobutyric acid (GABA, **1**, Chart 1) is the most abundant inhibitory neurotransmitter in the central nervous system (CNS).[1−3] A reduced GABAergic neurotransmission, in consequence an imbalance in the neurotransmitter equilibrium, is associated with neurological disorders, e.g., schizophrenia,[4] Parkinson's disease,[5] epilepsy,[6] Alzheimer's disease,[7] neuropathic pain,[8] Huntington's disease,[9] depression,[10−12] panic,[10,12] and mania.[10,12]

To restore the neurotransmitter equilibrium, GABAergic neurotransmission can be enhanced by CNS-active drugs targeting GABA receptors, metabolic enzymes, or GABA transport proteins (GATs). The last targets are membrane bound proteins encoded by genes assigned to the solute carrier 6 (SLC6) family[13] and mediate the transport of GABA across cell membranes utilizing a co-transport of sodium and chloride ions as energy supply.

Four different subtypes named mGAT1, mGAT2, mGAT3, and mGAT4 when cloned from murine brain cells are known. For other species, the nomenclature for GATs differs, e.g., for the human GATs, the declaration is given by the human genome organization (HUGO) resulting in GAT1, BGT1, GAT2, and GAT3 as corresponding transport proteins.[14] mGAT1 and mGAT4 are the most abundant GABA transporters in the CNS, from which mGAT1 is mainly responsible for the neuronal reuptake of GABA and mGAT4 is predominantly located in cell membranes of glial cells.[15] In contrast, the expression of mGAT2 and mGAT3 in the brain is very limited. That excludes a significant role in termination of GABA neurotransmission for these proteins for which high densities have been reported in liver and kidney.[16]

When GATs were defined as pharmacological CNS targets,[17] a first generation of inhibitors was disclosed including cyclic analogues of GABA (**1**). These small cyclic amino acids like nipecotic acid (**2**) and guvacine (**3**) (Chart 1) were in the 1970s found to be potent in vitro inhibitors.[18,19] Nevertheless, their potency was not confirmed in vivo because of their hydrophilic character preventing them from passing the blood−brain barrier in sufficient amount.[20] Consequently, a second generation of GAT inhibitors was born by substitution of the small amino acids with characteristic lipophilic side chains at the amino function that enabled them to cross the blood−brain barrier.[21] Examples of the affinity enhancing side chains are represented in SK&F-89976-A (**4**), tiagabine (**5**), and NO711 (**6**) that proved to have high affinity at and subtype selectivity for mGAT1 compared to the nonsubstituted amino acids (Chart 1).[22] In addition, **5** has successfully undergone clinical trials and is now in use as add-on medication for the treatment of epilepsy.[23]

On the basis of this success, further selective and potent inhibitors were developed in the style of these potent GAT1 inhibitors representing the third generation of mGAT1 inhibitory drugs. These were characterized by new side chains

Received: December 7, 2012
Published: January 21, 2013

dx.doi.org/10.1021/jm301800j | J. Med. Chem. 2013, 56, 1323−1340

Chart 1. Structures of GABA and GAT1 Inhibitors

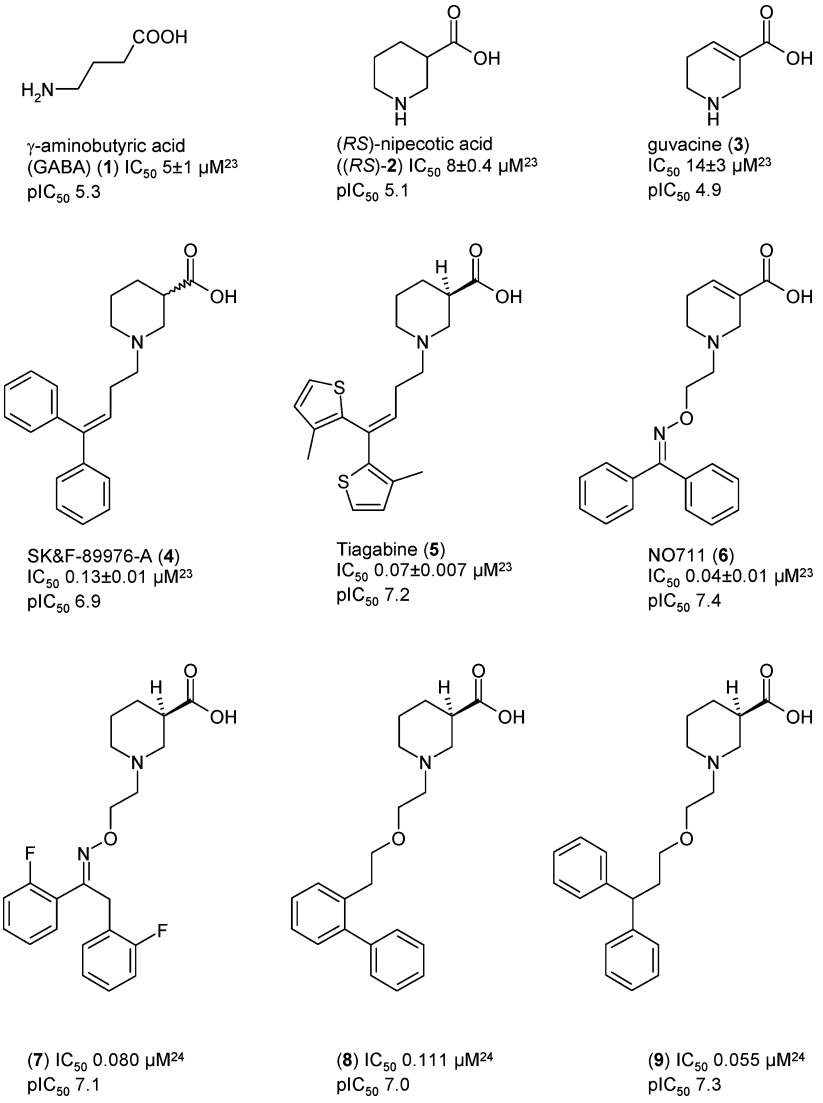

including the lipophilic aromatic domain attached to the amino group of the amino acid moiety (Chart 1). To this group belong a number of nipecotic acid based compounds in which the amino group of the hydrophilic amino acid moiety was connected via spacers differing in length and functionalities, like oxime and ether groups, to lipophilic aromatic residues. A selection of these third generation inhibitors, which had been developed by Andersen at al. in 1999 and 2001,[24] is displayed in Chart 1 (compounds **7**–**9**).

For GAT1, a screening method was developed several years ago that tested single drug candidates via a competitive MS binding assay, employing **6** as native MS marker.[25] This assay allowed the indirect determination of binding affinities toward GAT1 in analogy to radioligand binding studies, circumventing the necessity to apply radioactively labeled compounds.

Recently, we described a new method that applies MS binding assays,[26,27] which so far had been used for the characterization of the binding affinities of single test compounds toward a target only, to the screening of compound libraries generated by efficient and the most fundamental reactions known from dynamic combinatorial chemistry (DCC).[28] Both library generation and screening were performed in the presence of the protein target to improve assay performance. To facilitate hit detection, libraries were rendered pseudostatic. This was achieved by reacting sets of compounds with varying structure with a large excess of a single compound of complementary reactivity, the thus generated one-dimensional libraries being almost constant in composition but still dynamic in nature. After library generation was performed, addition of a native MS marker to the same sample directly enabled detection of active libraries by MS binding assays. The feasibility of this concept was demonstrated for mGAT1, a well established target for which, as mentioned above, a MS binding assay utilizing **6** as native marker was already known.[25] Screening of libraries, each of which consisted of four hydrazone compounds **12** (Scheme 1) and had been generated by reacting nipecotic acid derived hydrazine **10** with four different aldehydes **11**, revealed new GAT1 inhibitors resembling structures **8** and **9** (Chart 1).

In this study, a specific limit of maximum remaining marker binding caused by 10 μM hydrazones was chosen to define a library as active. As such, a 20% level (IC_{20} = 4 IC_{50}) was selected that attributed a minimum potency (IC_{50}) of 2.5 μM to a single hydrazone based on the assumption that all other library members were inactive. In deconvolution experiments testing the single aldehydes in combination with hydrazine **10**,

dx.doi.org/10.1021/jm301800j | J. Med. Chem. 2013, 56, 1323−1340

Scheme 1. Condensation of Hydrazine Derived Nipecotic Acid Building Block 10 with Diverse Aldehydes 11

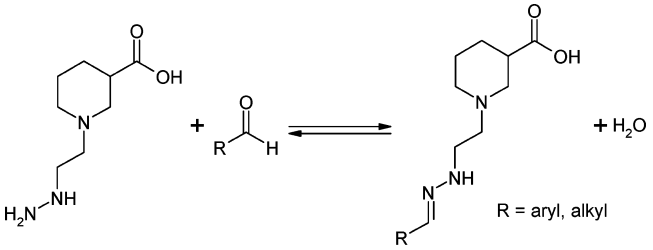

10 **11** **12**

out of each of the two libraries fulfilling this condition, a single hydrazone was identified to mostly represent the activity of the individual library. Thus, comparable to structure **8** (Chart 1) (*E*)-1-(2-{2-[1-(2′,4′-dichlorobiphenyl-2-yl)methylidene]-hydrazinyl}ethyl)piperidine-3-carboxylic acid (**12a**) (Chart 2) resulting from the reaction of hydazine **10** with biphenyl-2-carbaldehyde was found to reduce remaining marker binding in the deconvolution experiment to a value below the lower limit of quantification of the MS marker **6** (<5%), indicating an IC_{50} equal to or below 0.53 μM (IC_{05} = 19 IC_{50}). Resynthesis of **12a** and characterization in a full range competitive MS binding experiment finally revealed a pK_i of 6.186 ± 0.028 for this compound. The second hit, hydrazone **12b**, was derived from 2-thiophen-2-ylbenzaldehyde and gave rise to a remaining marker binding of 8.2 ± 0.4% in the deconvolution experiment and to a pK_i of 6.229 ± 0.039 in a full range competitive MS binding assay for the resynthesized compound.[28] That these mGAT1 binders are also functionally active was confirmed in [^{3}H]GABA uptake assays with mGAT1 expressing HEK293 cells, the pIC_{50} values amounting to 5.308 ± 0.096 (**12a**) and 5.542 ± 0.107 (**12b**), respectively (Chart 2).

Chart 2. Hydrazone Based GAT1 Inhibitors

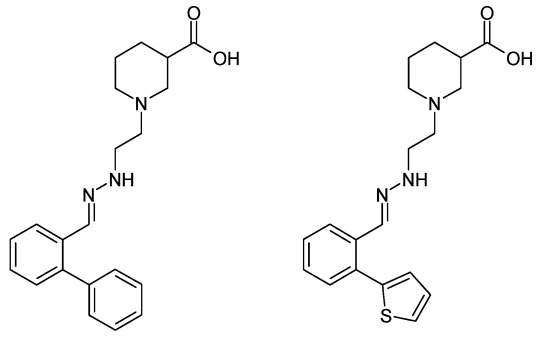

12a
pK_i 6.186±0.028
pIC_{50} 5.308±0.096[28]

12b
pK_i 6.229±0.039
pIC_{50} 5.542±0.107[28]

As we identified these two hits, **12a** and **12b**, with submicromolar potencies in the first library screening assays, the aim of the present study was to develop exemplarily for one of the two hits, compound **12a**, a focused library by introducing various substituents in the biaryl moiety to further optimize the affinity toward mGAT1 (Figure 1).

Biaryl focused pseudostatic hydrazone libraries (**12c−al**, Scheme 1) each derived from libraries of four biarylaldehydes (**11c−al**, Scheme 1) were therefore intended to be generated and subsequently screened by the MS binding assay, again employing **6** as native MS marker. As we aimed at improved affinities of desired hits compared to the hits searched in the first screening, the limit to define a library as active was further tightened by lowering it from 20% used in the original study[28] to 10%. In theory, this equals an IC_{50} of ∼1 μM for the compound, effecting reduction of marker binding to this limit when employed at 10 μM (IC_{10} = 9 IC_{50}). Hits contained in active libraries (<10% marker binding) were to be identified by applying the original deconvolution procedure and to be further evaluated after resynthesis.[28] As hydrazones are prone to hydrolysis,[29,28] liver-toxic,[30−32] and unstable against air,[33−35] they are not suitable as lead structures for drug discovery. But the results obtained from the screening of hydrazone libraries

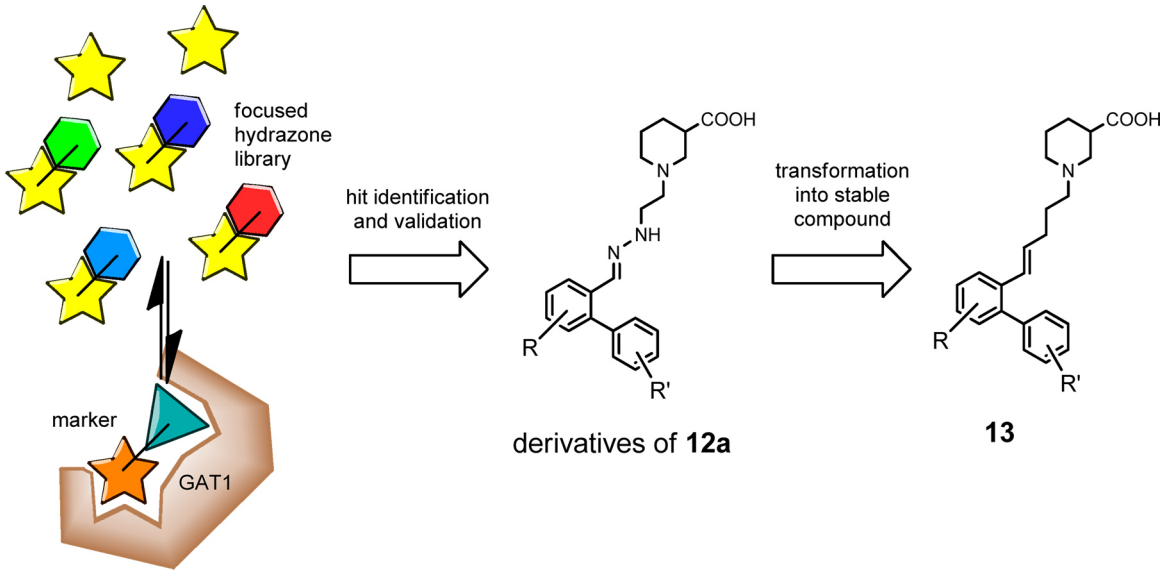

Figure 1. Focused hydrazone library generation and screening toward GAT1. After hit identification and validation of potent derivatives of hydrazone **12a**, corresponding carba analogues **13** were synthesized and evaluated.

dx.doi.org/10.1021/jm301800j | *J. Med. Chem.* 2013, 56, 1323−1340

Chart 3. Libraries Consisting of Biphenylcarbaldehydes 11c–al

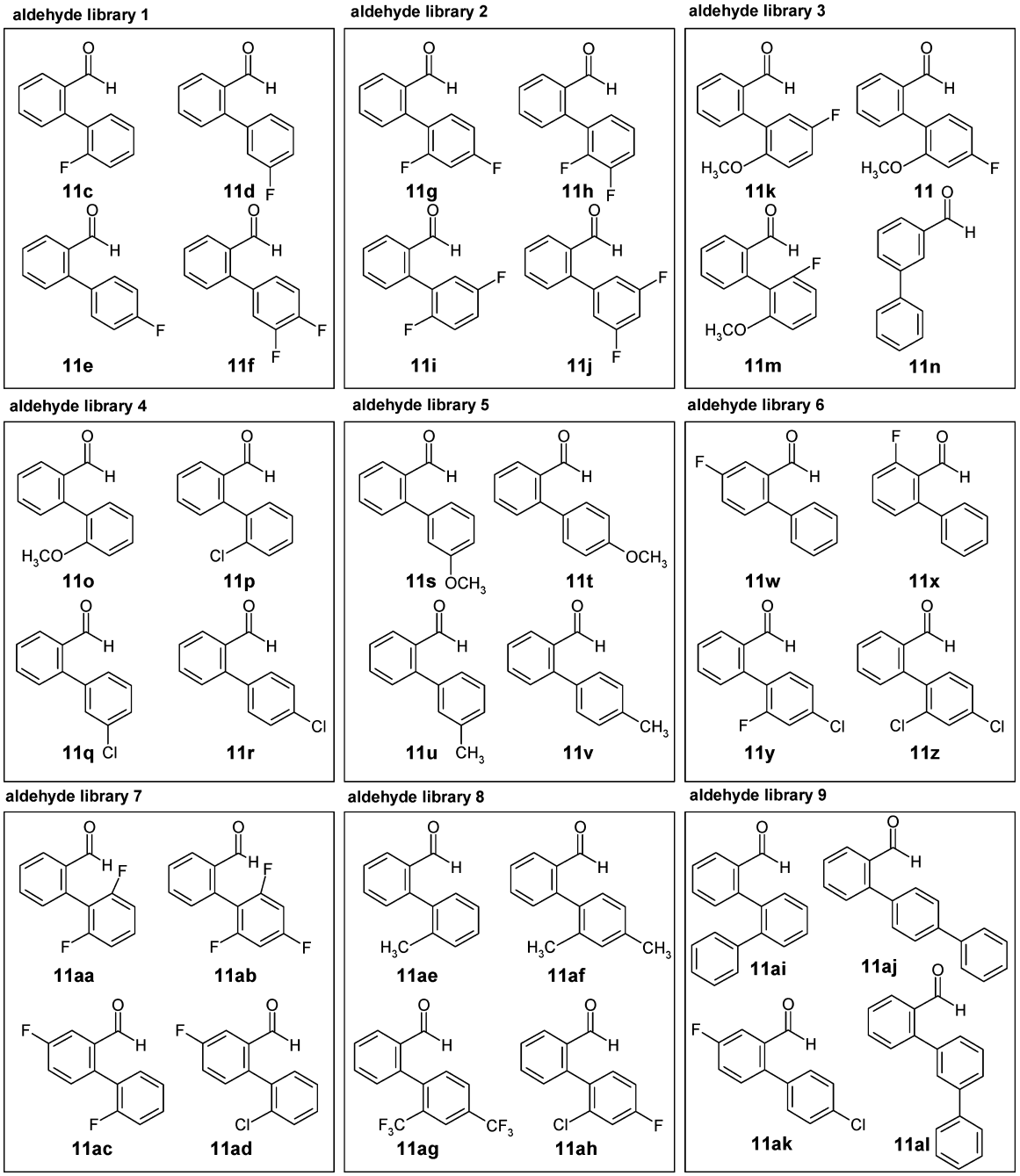

may nevertheless be of high value for drug discovery and support the development of stable analogues, which to demonstrate was a further aim of this study. Carba derivatives in which the hydrazone linker had been replaced by an all carbon chain with a double bond (CH=N–NH–CH_2–CH_2 → CH=CH–CH_2–CH_2–CH_2) were considered a good choice as stable substitutes of the hydrazone inhibitors. Thus, the synthesis and biological evaluation of carba analogues of a series of representative hydrazone inhibitors were also included in this study.

CHEMISTRY

Synthesis of Biarylcarbaldehydes. In general, biphenylcarbaldehydes **11c–11al** (Chart 3) required for library generation were synthesized via the Suzuki–Miyaura[36] reaction except for 4′-fluorobiphenyl-2-carbaldehyde (**11e**) and biphenyl-3-carbaldehyde (**11n**) that were purchased from Alfa Aesar and Sigma-Aldrich, respectively.

Thus, 2′-fluorobiphenyl-2-carbaldehyde (**11c**)[37,38] was obtained from 2-bromobenzaldehyde and 2-fluorophenylboronic acid, applying a literature method[39] that had been successfully employed in the synthesis of diversely substituted biphenyl-2-carbaldehydes (reaction conditions: 2-bromobenzaldehyde/substituted phenylboronic acid = 1:1, 5 mol % $Pd(OAc)_2$, DMF/H_2O = 2:1, 25 °C). For the preparation of the biphenyl-2-carbaldehydes **11d**, **11f**, **11h**, **11i**, **11j**, **11k**, **11m**, **11o**, **11p**, **11q**, **11r**, **11t**, **11u**, **11v**, **11w**, **11x**, **11ac**, **11ad**, and **11ae** this procedure had to be modified by adding common phosphine ligands (triphenylphosphine, dibenzylideneacetone, tri-*o*-tolyl-

dx.doi.org/10.1021/jm301800j | J. Med. Chem. 2013, 56, 1323–1340

Scheme 2. Synthesis of Nipecotic Acid Derived Carba Analogues 13[a]

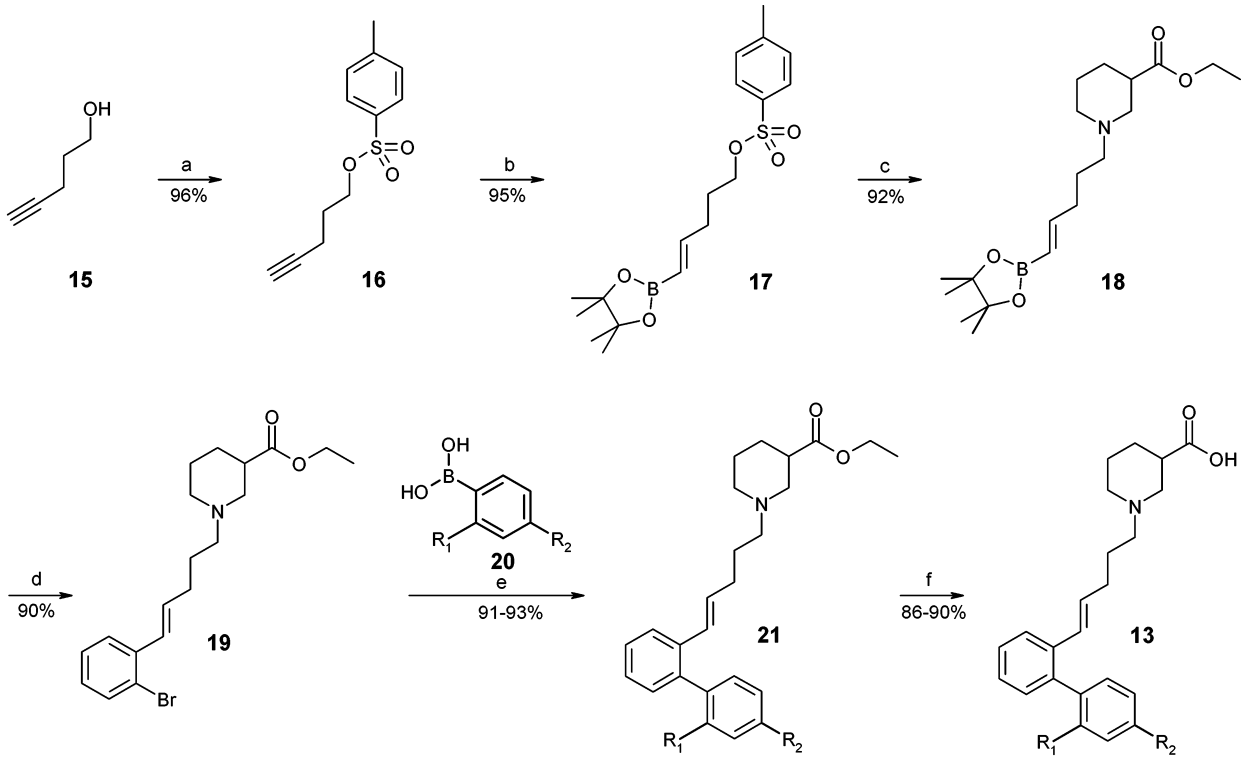

compd.	substitution	
13, 20, 21	R_1	R_2
c	F	H
g	F	F
p	Cl	H
ah	Cl	F
z	Cl	Cl

[a]Reagents and conditions: (a) TsCl, Et_3N, CH_2Cl_2, 0 °C to rt, 20 h; (b) pinacolborane, chloridobis(cyclopentadienyl)hydridozirconium no solvent, rt, 48 h; (c) ethyl nipecotate, no solvent, rt, 16 h; (d) Pd(dppf)Cl_2·CH_2Cl_2, 1-bromo-2-iodobenzene, K_2CO_3, 1,4-dioxane/H_2O 2:1, 72 h, rt; (e) Pd(dppf)Cl_2·CH_2Cl_2, RPhBO_2H, K_2CO_3, 1,4-dioxane/H_2O 2:1, 3 h, 60 °C; (f) NaOH, EtOH, 4 h, rt.

phosphine, or tri-*tert*-butylphosphine) and increasing the temperature from room temperature to 80 °C to improve the reaction rates and the yields (see Supporting Information).

The latter protocol could not be successfully applied to the synthesis of **11y** starting from 2-bromobenzaldehyde and 2-fluoro-4-chlorophenylboronic. But coupling of 2-bromobenzaldehyde and 2-fluoro-4-chlorophenylboronic acid to yield **11y** could be realized following a related literature method that had originally been used for coupling of pentafluorophenylboronic acid with halogenated benzene derivatives by means of CsF, Ag_2O, Pd$(dba)_3$·$CHCl_3$, and tri-*o*-tolylphosphine in pure DMF at 100 °C [40] (see Supporting Information).

In the case of other sterically demanding phenylboronic acid derivatives carrying electron withdrawing residues (2,4-difluorophenylboronic acid, 2,4-dichlorophenylboronic acid, 2,6-difluorophenylboronic acid, 2,4,6-trifluorophenylboronic acid, 2-chloro-4-fluorophenylboronic acid), the coupling with 2-bromobenzaldehyde gave poor yields or no coupling products at all under the applied conditions for the preparation of, for example, **11d**. However, an alternative approach starting from 2-formylphenylboronic acid, instead of 2-bromobenzaldehyde, and an appropriate halogenated benzene derivative instead of the corresponding phenylboronic acid gave access to the desired aldehydes. Thus, **11g**, **11z**, **11aa**, **11ab**, and **11ah** were obtained by reacting 2-formylphenylboronic acid with the appropriately halogen substituted benzene derivatives following a literature method that originally had been used for coupling of 1-bromo-2,3,4,5,6-pentafluorobenzene with 2-formylphenylboronic acid.[41]

The same reaction conditions that had been used for the coupling reactions of 2-formylphenylboronic acid with various aryl halides were finally also tested for the preparation of aldehydes **11s**, **11ab**, **11af**, **11ag**, **11ai**, **11aj**, **11ak**, and **11al** by coupling 2-bromobenzaldehyde again with the respective phenylboronic acid derivatives, leading to the desired compounds in yields of up to 90% (toluene/ethanol/2 M Na_2CO_3(aq) = 1:1:1, tetrakis(triphenylphosphine)-palladium(0)) (see Supporting Information).

Synthesis of the Hydrazones. Synthesis of individual hydrazones required for full scale competition experiments was carried out by combining 1 equiv of aldehyde with 1 equiv of hydrazine **10** according to Scheme 1, again following the

dx.doi.org/10.1021/jm301800j | *J. Med. Chem.* 2013, 56, 1323−1340

Scheme 3. Example for the Conversion of an Aldehyde Library into a Hydrazone Library (Aldehyde Library 1 → Hydrazone Library 1)

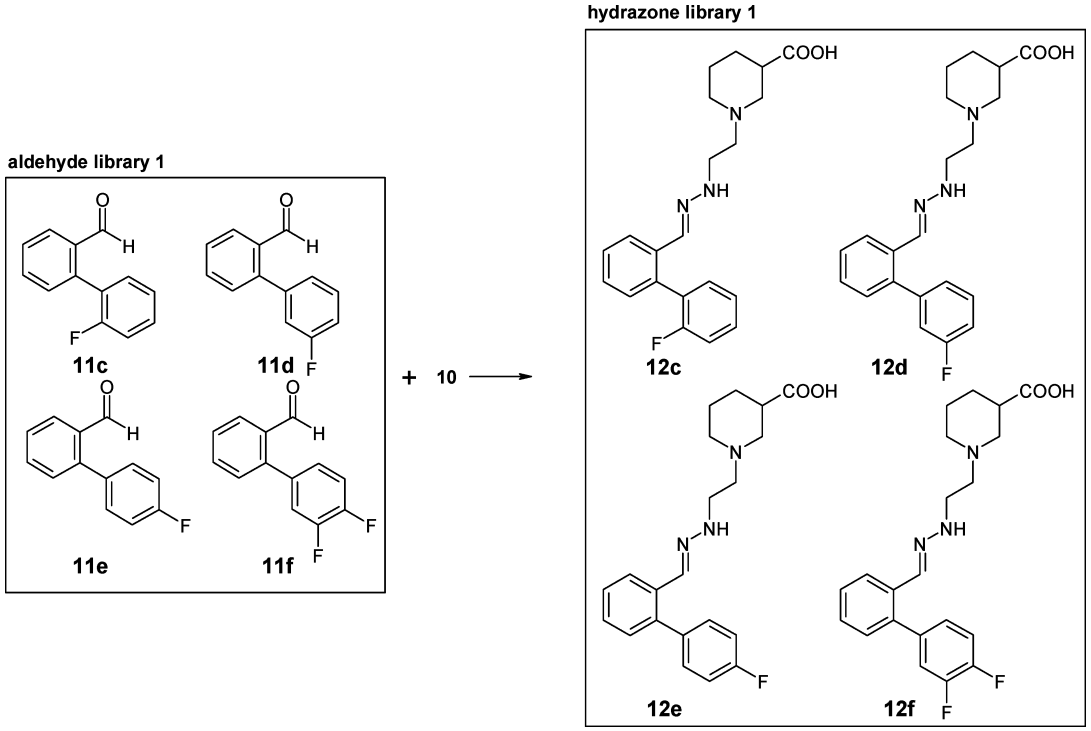

original protocol for hydrazone synthesis described previously.[28]

Synthesis of the Carba Analogues. For the synthesis of the carba analogues of the hydrazone derivatives the reaction sequence outlined in Scheme 2 has been developed. It features the vinylboronic acid derivative **18** as a key compound, which by two consecutive Suzuki−Miyaura reactions allows high flexibility with regard to construction and the substitution pattern of the biaryl moiety present in the target compounds **13**. For the synthesis of **18**, first pentynol **15** was transformed into the tosyl ester **16** by reaction with TsCl according to a literature method.[42] The resulting alkyne **16** was subsequently reacted with pinacolborane in the presence of Cp_2ZrHCl in analogy to a literature procedure,[43] to give the boronic acid ester **17**, which upon treatment with ethyl nipecotate provided **18** in 92% yield. Compound **18** allowed stepwise establishment of the biaryl moiety present in the final compounds **13**. Thus, a first Suzuki−Miyaura cross-coupling reaction between **18** and 1-bromo-2-iodobenzene yielded the monoaryl derivative **19**. Compound **19** was then subjected to a second Suzuki−Miyaura cross-coupling reaction with differently substituted phenylboronic acid derivatives [2-fluorophenylboronic acid (**20c**), 2,4-difluorophenylboronic acid (**20g**), 2-chlorophenylboronic acid (**20p**), 2-chloro-4-fluorophenylboronic acid (**20ah**), and 2,4-dichlorophenylboronic acid (**20z**)] to give the desired biaryl substituted nipecotic acid ester derivatives **21c**, **21g**, **21p**, **21ah**, and **21z** (yield 91−93%). These last compounds were finally converted to the free nipecotic acid derivatives **13c**, **13g**, **13p**, **13ah**, and **13z** by basic hydrolysis of the ethyl ester function (yield 86−90%).

RESULTS AND DISCUSSION

General Aspects of Library Generation and Screening. Libraries were generated and screened as described earlier.[28] Therefore, the respective experimental conditions are given here only in short form. To generate the hydrazone libraries, aldehyde libraries of four aldehydes each at 10 μM were reacted with a 2.5-fold excess of hydrazine **10** (100 μM initial concentration) at 37 °C for 4 h, in which the time span had turned out to be sufficient for complete conversion in the former[28] and in the present study. In addition, library generation was again performed in the presence of the target mGAT1 to improve assay performance. The activity of the libaries was finally analyzed by means of competitive MS binding experiments. To this end, following incubation of libraries with MS marker **6** (for 40 min), the amount of specifically protein-bound MS marker **6** was quantified by LC−ESI-MS/MS (after isolation of protein−ligand complexes and liberation of the bound ligands from the target), low amounts of remaining marker binding representing high library activity and vice versa. As for the original procedure, in addition to each screening experiment, control experiments employing aldehyde libraries (**11**) and hydrazine **10**[44] alone were perfomed to ensure that the building blocks in the concentrations used do not affect marker binding to a remarkable extent.

Screening and Deconvolution of Focused Biphenyl-2-carbaldehyde Derived Hydrazone Libraries. In our former study[28] that applied pseudostatic hydrazone libraries on mGAT1, **12a**, the hydrazone derived from biphenyl-2-carbaldehyde (**11a**), had been uncovered to display submicromolar affinity to mGAT1 (pK_i = 6.186 ± 0.028).[28] To further optimize the affinity of **12a** for mGAT1 in the present study, 36 aldehydes mainly delineated from biphenyl-2-carbaldehyde (**11a**) by additional small substituents in the phenyl rings (biphenylcarbaldehydes **11c**−**11al**) were selected for hydrazone generation and screening. These were grouped into nine libraries of four aldehydes (Chart 3), converted into hydrazone libraries (Scheme 3), and analyzed by competitive

MS binding assays as described above. Clearly, a higher number of aldehydes than four could be employed in library formation under otherwise identical conditions. But this would require reduction of the concentration of the individual aldehydes to further warrant the excess of hydrazine **10** over the aldehydes employed and thus the pseudostatic character of the libraries. However, with lowering hydrazone concentrations, the conditions for a library to be classified as active will also become more stringent (IC_{50} corresponds to the initial aldehyde concentration).

Table 1 summarizes the screening values of the aldehyde and hydrazone libraries 1−9. All hydrazone libraries were found to be highly active, reducing the remaining MS marker binding not only below 10%, the limit set for libraries to be considered as active, but even below the lower limit of quantitation (LLOQ) for the MS marker **6** of 5% (Table 1). Also library 5, which was the only exception, displayed a very low remaining marker binding of 6 ± 1%.

Table 1. Libary Screening Values of Aldehyde Libraries and Hydrazone Libraries

		library screening[a] (%)	
entry	library	aldehyde library	hydrazone library
1	library 1	82 ± 2	<5
2	library 2	81 ± 2	<5
3	library 3	88 ± 2	<5
4	library 4	79 ± 3	<5
5	library 5	91 ± 11	6 ± 1
6	library 6	85 ± 4	<5
7	library 7	35 ± 1	<5
8	library 8	81 ± 1	<5
9	library 9	81 ± 1	<5

[a]Percentage of remaining specific binding of NO711 (**6**) in the presence of pure aldehyde libraries and corresponding hydrazone libraries after an incubation time of 4 h for library generation and 40 min for marker binding to mGAT1, n = 4, ±SD, <5% = <50 pM derived from the LLOQ of NO711 (50 pM, as 1−2 nM of 20 nM applied NO711 is maximally bound to the membrane preparation). Control experiment for 100 μM hydrazine **10** was obtained comparable to published results. See ref 28.

In the deconvolution study of the hydrazone libraries, 21 of the 36 hydrazones were found to strongly influence MS marker binding, reducing it to 10% and below (Figure 2). Taking into account that a reduction of MS marker binding to 10% corresponds to an IC_{50} of ∼1 μM (IC_{10} = 9 IC_{50}), we considered it worthwhile to resynthesize most of the hydrazone derivatives that had reached this limit in the screening and to establish their pK_i values in MS competition experiments comprising complete competition curves. The data of these studies that had also been established to provide an improved insight on the influence of the substituent effects on the potency of the compounds are given in the section "Biphenyl-2-carbaldehyde Derived Hydrazone Hits".

Interestingly, one of the pure aldehyde libraries (tested in the absence of hydrazine **10**) had also given rise to a significant

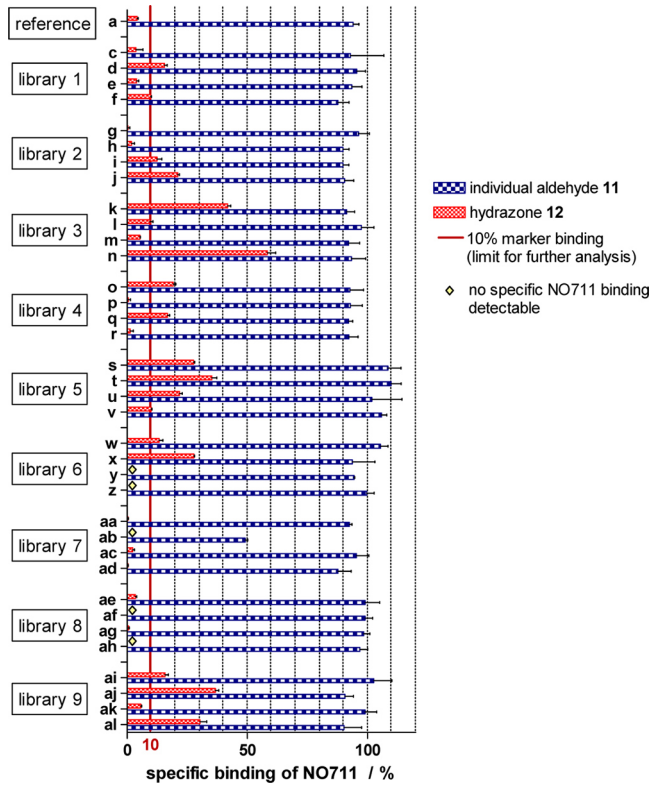

Figure 2. Deconvolution results of libraries 1−9. The limit for further analysis of a library was defined as 10% remaining marker binding.

reduction of MS marker binding. For aldehyde library 7 for which the screening value had amounted to 35 ± 1% (Table 1, entry 7), a deconvolution experiment (in the absence of hydrazine **10**) revealed aldehyde **11ab** to be by far the most potent binder of this group, reducing MS marker binding to 49 ± 1% (Figure 2). Accordingly, as a rough estimate, an IC_{50} of ∼10 μM can be attributed to this aldehyde.[28]

Biphenyl-2-carbaldehyde Derived Hydrazone Hits. Table 2 summarizes the pK_i values that had been found in full scale competitive MS binding assays for the separately resynthesized biphenyl-2-carbaldehyde derived hydrazones that had turned out as the most active ligands at mGAT1 in the deconvolution experiments (reduction of MS marker binding to ≤10%). Hydrazones **12d**, **12i**, **12j**, **12k**, **12n**, **12o**, **12q**, **12s**, **12t**, **12u**, **12w**, **12x**, **12ai**, **12aj**, and **12al** did not reach this limit and were excluded from further analysis.

The compounds that achieved the desired value below 10% are sorted according to the substitutents of the biaryl moiety starting with hydrazones exhibiting only F-substituents (Table 2, entries 2−9), F- and CH_3O-substituents (Table 2, entries 10 and 11), followed by those with either CH_3- (Table 2, entries 12−14), CF_3- (Table 2, entry 15), Cl- (Table 2, entries 16−18), or F- and Cl-substituents (Table 2, entries 19−22).

An F-substituent in the 2′-position increased the affinity by almost 1 order of magnitude, resulting in a pK_i of 6.914 ± 0.061 for **12c** (Table 2, entry 2) compared to the parent compound **12a** (6.186 ± 0.028, Chart 2, Table 2, entry 1), while a 4′-F-substituent (structure **12e**) caused a smaller increase, the affinity of **12e** amounting to a pK_i of 6.546 ± 0.067 (Table 2, entry 3). With F-substituents present in both the 2′- and 4′-position, a gain in binding energy (compared to **12a**) was observed that was roughly the sum of the increase of binding energies effected by the two F-substituents in **12c** and **12e**,

dx.doi.org/10.1021/jm301800j | J. Med. Chem. 2013, 56, 1323−1340

Table 2. Binding affinities (pK_i) of Resynthesized Biphenyl Derived Hydrazones Determined from Competitive MS Binding Assays and Inhibitory Potencies (pIC_{50}) at mGAT1 from [^{3}H]GABA Uptake Experiments

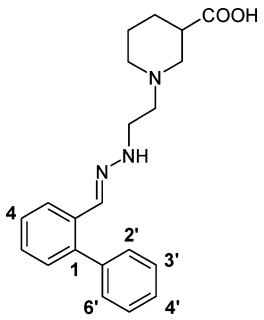

12a

		compd[a] (substitution pattern of the biphenyl moiety of **12a**)					biological testing	
entry	compd	4	2′	3′	4′	6′	binding affinity pK_i (n = 3 ± SEM)[b]	inhibitory potency pIC_{50}[c] (n = 3 ± SEM)[b]
1	**12a**	H	H	H	H	H	6.186 ± 0.028	5.308 ± 0.096
2	**12c**	H	F	H	H	H	6.914 ± 0.061	6.277 ± 0.061
3	**12e**	H	H	H	F	H	6.546 ± 0.067	5.746 ± 0.078
4	**12g**	H	F	H	F	H	7.449 ± 0.023	6.891 ± 0.078
5	**12h**	H	F	F	H	H	6.690 ± 0.036	5.824 ± 0.033
6	**12f**	H	H	F	F	H	6.204 ± 0.054	5.479 ± 0.095
7	**12aa**	H	F	H	H	F	6.883 ± 0.035	6.001 ± 0.014
8	**12ab**	H	F	H	F	F	7.514 ± 0.030	6.594 ± 0.046
9	**12ac**	F	F	H	H	H	6.578 ± 0.057	5.763 ± 0.037
10	**12m**	H	F	H	H	OCH_3	6.354 ± 0.062	5.648 ± 0.103
11	**12l**	H	OCH_3	H	F	H	6.119 ± 0.037	5.134 ± 0.094
12	**12ae**	H	CH_3	H	H	H	6.666 ± 0.044	5.806 ± 0.064
13	**12v**	H	H	H	CH_3	H	6.325 ± 0.065	5.468 ± 0.118
14	**12af**	H	CH_3	H	CH_3	H	7.135 ± 0.095	6.078 ± 0.020
15	**12ag**	H	CF_3	H	CF_3	H	6.769 ± 0.081	5.549 ± 0.047
16	**12p**	H	Cl	H	H	H	7.184 ± 0.063	6.320 ± 0.070
17	**12r**	H	H	H	Cl	H	6.762 ± 0.001	6.012 ± 0.121
18	**12z**	H	Cl	H	Cl	H	8.094 ± 0.098	7.213 ± 0.085
19	**12ad**	F	Cl	H	H	H	6.981 ± 0.060	5.909 ± 0.081
20	**12ak**	F	H	H	Cl	H	6.630 ± 0.040	5.708 ± 0.078
21	**12y**	H	F	H	Cl	H	7.607 ± 0.043	6.899 ± 0.147
22	**12ah**	H	Cl	H	F	H	7.835 ± 0.081	6.535 ± 0.082

[a]Individually resynthesized from appropriate biphenyl-2-carbaldehydes and evaluated hydrazones. [b]Data points for specific binding of NO711 (mean ± SD from triplicate values) in the presence of different concentrations of test compounds (M) resulted in binding curves for K_i determination by nonlinear regression. pK_i ± SEM obtained from three independent experiments,. [c]pIC_{50} values from [^{3}H]GABA uptake assays performed with mGAT1 expressing HEK293 cells. Value ± SEM obtained from three independent experiments.

hydrazone **12g** displaying a pK_i of 7.449 ± 0.023 (Table 2, entry 4). Comparing this effect with the difluoro substitution in **12h** (2′,3′-F_2, Table 2, entry 5), **12f** (3′,4′-F_2, Table 2, entry 6), and **12aa** (2′,6′-F_2, Table 2, entry 7), the pK_i values of the compounds amounting to 6.690 ± 0.036, 6.204 ± 0.054, and 6.883 ± 0.035, respectively, clearly reveals that the 2′,4′-F_2 substitution in **12g** represents the most favorable substitution pattern for the difluoro substituted compounds. In contrast to F-substituents in 2′- and 4′-position, a 3′-F-substituent decreases affinity compared to the parent compound **12a**, with hydrazone **12d** reducing MS marker binding in the deconvolution experiments far less (16 ± 1%, **12d**, Figure 2) than the reference compound **12a** (<5%). In line with that, upon transition from the 2′-F-substituted **12c** (pK_i = 6.914 ± 0.061, Table 2, entry 2) to the 2′,3′-F_2 hydrazone **12h**, a decrease in affinity occurs (pK_i = 6.690 ± 0.036, Table 2, entry 5). But the positive effect of the 2′-F-substituent clearly outweighs the negative effect of the 3′-F-substituent as the affinity of **12h** is still far higher than that of the parent compound **12a** (Table 2, entry 1). In addition, **12aa** (2′,6′-F_2, Table 2, entry 7) revealed that a second F-substituent in 6′-position is tolerated but does not improve the affinity toward mGAT1, expressed by a pK_i of 6.883 ± 0.035 very close to the pK_i of **12c** (2′-F_2 pK_i = 6.914 ± 0.061, Table 2, entry 2). Accordingly, the 2′,4′,6′-trifluoro substituted derivative **12ab** (2′,4′,6′-F_3, Table 2, entry 8), displayed a similar affinity, the pK_i being 7.514 ± 0.030, close to that of **12g** (2′,4′-F_2, pK_i = 7.449 ± 0.023, Table 2, entry 4), again indicating that a 6′-F-substituent does not significantly change affinity. Obviously a 4-F-substituent in the first ring does not lead to a beneficial effect, the affinity of the 4,2′-difluoro substituted hydrazone **12ac** (Table 2, entry 9) with a pK_i of 6.578 ± 0.057 being lower than that of the 2′-monofluoro substituted hydrazone **12c** (2′-F, 6.914 ± 0.061, Table 2, entry 2). Like the 4-fluoro substituent

dx.doi.org/10.1021/jm301800j | J. Med. Chem. 2013, 56, 1323−1340

in **12ac**, the 4-fluoro substituent in hydrazone **12w** also has a negative effect on the binding affinity, which in the latter case was even more pronounced reducing remaining MS marker binding to only 13 ± 2% in the deconvolution experiments, thus not reaching the limit of 10%, which is the condition hydrazones had to fulfill to be evaluated with regard to their pK_i values.

A methoxy function in 6′-position of the 2′-fluoro substituted system (2′-F,6′-OCH_3, **12m**, Table 2, entry 10) had an adverse effect on the affinity, as well, the pK_i value of **12m** (pK_i = 6.354 ± 0.062) ranging distinctly below that of the 2′-fluoro monosubstituted compound **12c** (pK_i = 6.914 ± 0.061, Table 2, entry 2) and close to that of the parent compound **12a** (pK_i = 6.186 ± 0.028, Table 2, entry 1). This was not unexpected as the 2′-OCH_3 substituted hydrazone **12o** had reduced MS marker binding in the deconvolution experiments no lower than 19 ± 1%. Anyway, the gain in binding affinity effected by the 2′-fluoro substituent in **12c** (2′-F) was nearly completely abolished by the additional 6′-OCH_3 substituent (in **12m**). A similar effect was observed for **12l**. The additional 2′-OCH_3-residue, by which this compound differs from **12e**, exhibiting a 4′-F-substituent, causes a pK_i reduction from 6.546 ± 0.067 (of **12e**, Table 2, entry 3) to 6.119 ± 0.037 (**12l**, Table 2, entry 11), **12l** thus being just as potent as the parent compound **12a** (pK_i = 6.186 ± 0.028, Table 2, entry 1).

Compared to a 2′-F substituent (**12c**, 2′-F, pK_i = 6.914 ± 0.061, Table 2, entry 2), the binding enhancing effect of a 2′-CH_3 is less pronounced (**12ae**, pK_i = 6.666 ± 0.044, Table 2, entry 12). The 4′-CH_3 substituted hydrazone **12v** (4′-CH_3) gave rise to a pK_i of 6.325 ± 0.065 (Table 2, entry 13), the 4′-CH_3 substituent thus having slightly improved the potency of the parent compound **12a** (pK_i = 6.186 ± 0.028, Table 2, entry 1) though the deconvolution value (percentage of remaining MS marker binding) of **12v** amounting to 10 ± 1% had been higher than that of **12a** (<5%), suggesting the opposite effect. This discrepancy is possibly attributed to the uncertainties of the experimental data that are commonly relatively large for biological systems. The positive effects of the 2′-methyl (as in **12ae**, 2′-CH_3) and the 4′-methyl group (as in **12v**, 4′-CH_3) were combined in the 2′,4′-disubstituted hydrazone **12af** (2′,4′-CH_3, Table 2, entry 14), reaching an affinity of pK_i = 7.135 ± 0.095. Among the 2′,4′-disubstituted derivatives, **12ag** (2′,4′-$(CF_3)_2$) exhibiting two CF_3 groups was also found to be more potent than the parent compound **12a** (pK_i = 6.186 ± 0.028, Table 2, entry 1) displaying a pK_i of 6.769 ± 0.081 (Table 2, entry 15) but less than the 2′,4′-dimethyl and 2′,4′-difluoro substituted hydrazones **12af** and **12g** (**12af**, 2′,4′-$(CH_3)_2$, pK_i = 7.135 ± 0.095, Table 2, entry 14; **12g**, 2′,4′-F_2, pK_i = 7.449 ± 0.023, Table 2, entry 4).

The largest increase in affinity by a single substituent was observed for a 2′-Cl residue, the respective compound **12p** (2′-Cl, Table 2, entry 16) achieving a pK_i of 7.184 ± 0.063 close to that of the 2′,4′-difluoro substituted derivative (**12g**, pK_i = 7.449 ± 0.023, Table 2, entry 4). An additional 4-F-substituent in the first ring again gave rise to a reduced affinity (**12ad**, 4-F,2′-Cl pK_i = 6.981 ± 0.060, Table 2, entry 19), in line with the results described above. The affinity of the 4′-Cl biphenylhydrazone **12r** (4′-Cl) with a pK_i of 6.762 ± 0.001 (Table 2, entry 17) was also higher than that of the 4′-F substituted analogue **12e** (pK_i = 6.546 ± 0.067, Table 2, entry 3). An additional 4-F substituent again led to a decrease in affinity, the pK_i of **12ak** (4-F,4′-Cl, pK_i = 6.630 ± 0.040, Table 2, entry 20) being lower than that of **12r** with a single 4′-Cl substituent (pK_i = 6.762 ± 0.001, Table 2, entry 17). But this decrease was less pronounced than that for the transition from **12p** (2′-Cl, Table 2, entry 16) to **12ad** (4-F,2′-Cl, Table 2, entry 19).

Combining the 2′- and the 4′-Cl-substitution in one compound led to the most potent biphenylhydrazone of this study, compound **12z** (2′,4′-Cl_2), with an affinity in the lower nanomolar range (pK_i = 8.094 ± 0.098, Table 2, entry 18), as the pK_i of this hydrazone derivative surpassed that of the parent compound **12a** (pK_i = 6.186 ± 0.028, Table 2, entry 1) by almost 2 log units.

Further high affinity ligands were obtained by mixed halogen substitution of the 2′,4′-position of the biphenyl moiety in **12a**. Compound **12ah**, the 2′-Cl,4′-F substituted compound, turned out to be the second most potent biphenylhydrazone derivative of this series (pK_i = 7.835 ± 0.081, Table 2, entry 22) followed by **12y** (2′-F,4′-Cl), exhibiting the reverse halogen substitution pattern, with a slightly diminished potency (pK_i = 7.607 ± 0.043, Table 2, entry 21).

In conclusion of these results, substitution in 2′,4′-position of the biphenyl moiety was most favorable to gain highly potent derivatives of the parent compound **12a**. Most of all, the presence of halogen substitutents such as F and even more Cl in these positions augmented binding affinities remarkably. This is best underlined by the high affinity displayed by the 2′,4′-Cl_2 biphenylhydrazone **12z** (2′,4′-Cl_2, pK_i = 8.094 ± 0.098, Table 2, entry 18). Besides, as demonstrated by these results, the screening data are in general in good accord with the results of the MS binding assays and can thus already be considered a good estimate for the potency of the studied compounds.

In addition to their binding affinities (pK_i values) all compounds were also characterized with respect to their inhibitory potencies (IC_{50}) in functional [^{3}H]GABA uptake assays performed with mGAT1 expressing HEK293 cells. As already stated in previous papers,[28] the pIC_{50} values of the uptake assay are generally lower than the pK_i values describing the binding affinity. This may be ascribed to the different assay conditions used for the [^{3}H]GABA uptake and for the MS binding assays. Most importantly MS binding assays are performed in a buffer system containing 1 M NaCl whereas for [^{3}H]GABA uptake assays a physiological buffer with 120 mM NaCl is used.[45] The high NaCl concentration in the MS binding assays is needed to improve ligand affinity of the MS marker **6**, which is otherwise, when NaCl is present in physiological concentration (like in the buffer for the [^{3}H]GABA uptake assay), about 1 log unit lower[25,49] under which conditions these assays were more difficult to perform (to avoid uncontrolled loss of specifically bound MS marker **6** during the separation of the protein−ligand complex from the rest of the incubation system).

As the high NaCl concentration (1 M) affects the affinity of every test compound in a manner similar to the affinity of the MS marker **6**, their pK_i values being a half to 1 log unit higher than those measured in the presence of physiological NaCl concentration, the differences observed between the pK_i values from MS binding assays (in the presence of 1 M NaCl) and the pIC_{50} values from [^{3}H]GABA uptake assays (in the presence of physiological NaCl concentration) can be largely ascribed to this phenomenon. Regardless of that, the rank order of potency that results from the pIC_{50} values of the [^{3}H]GABA uptake assays is in good accord with that resulting from the pK_i values of the MS binding assays. Thus, in line with that, hydrazone **12z**, which displays the highest binding affinity (pK_i) for mGAT1 of the compounds studied, turned out to also be the

dx.doi.org/10.1021/jm301800j | J. Med. Chem. 2013, 56, 1323−1340

Table 3. Comparison of hydrazones 12c, 12p, 12g, 12z, 12ah with Carba Analogues 13c, 13p, 13g, 13z, 13ah

12	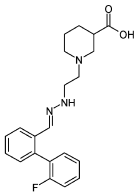 **12c**	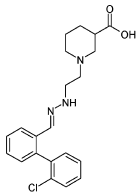 **12p**	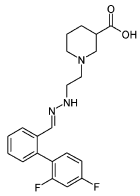 **12g**	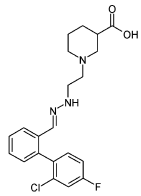 **12ah**	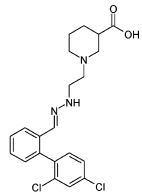 **12z**
pK_i[a]	6.914±0.061	7.184±0.063	7.449±0.023	7.834±0.081	8.094±0.098
pIC_{50}[b]	6.277±0.061	6.320±0.070	6.861±0.078	6.535±0.082	7.231±0.085
13	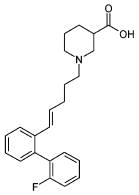 **13c**	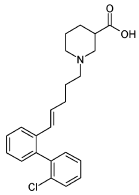 **13p**	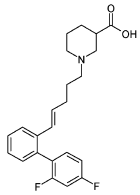 **13g**	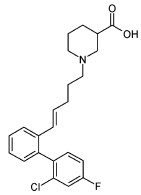 **13ah**	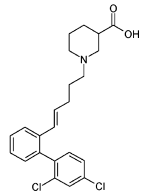 **13z**
pK_i[a]	6.189±0.020	6.079±0.037	6.228±0.014	6.505±0.039	6.930±0.021
pIC_{50}[b]	5.477±0.095	5.448±0.105	5.547±0.032	5.399±0.052	6.114±0.107

[a]Data points for specific binding of NO711 (mean ± SD from triplicate values) in the presence of different concentrations of test compounds (M) resulted in binding curves for K_i determination by nonlinear regression. pK_i ± SEM obtained from three independent experiments. [b]pIC_{50} values from [^{3}H]GABA uptake assays performed with mGAT1 expressing HEK293 cells. Value ± SEM obtained from three independent experiments.

most potent inhibitor in the [^{3}H]GABA uptake assay of mGAT1 expressing HEK293 cells, its pIC_{50} amounting to 7.213 ± 0.085 (Table 2, entry 18).

Carba Analogues for Biphenyl Derived Hydrazones. The final step of this study was aimed at the development of stable analogues of the hydrazone derivatives that can substitute the latter as lead structure for drug development, a purpose hydrazones are in general not suitable for because of their instability[28,33−35] and various harmful effects.[30−32]

A carba moiety in which the two nitrogen atoms of the hydrazone function (CH═N−NH) are replaced by carbon atoms transforming said function into an allyl group (CH═CH−CH_2) was considered to be a suitable substitute that at least with respect to the overall geometry should be able to mimic the original functional group. For this transformation a set of hydrazone derivatives was selected covering diverse activities ranging from medium to highly potent. Thus, for the hydrazones **12c**, **12p**, **12g**, **12ah**, and **12z** the corresponding carba analogues **13c**, **13p**, **13g**, **13ah**, and **13z** were synthesized (Table 3) and evaluated.

As shown in Table 3, the potencies of the hydrazone derivatives **12c**, **12p**, **12g**, **12ah**, and **12z** ranging from pK_i of 6.914 ± 0.061 (**12c**) to 8.094 ± 0.098 (**12z**) were not fully reached by the carba analogues **13c**, **13p**, **13g**, **13ah**, and **13z**, the pK_i values of the latter compounds being roughly 1 log unit lower than those of the corresponding hydrazone derivatives. But the rank order of potency remained mostly unchanged. Thus, also for the carba analogues, the 2′,4′-dichloro substituted derivative **13z** appeared to be the most potent compound in this series with a pK_i of 6.930 ± 0.021 followed by the 2′-chloro-4′-fluorocarba derivative **13ah** (pK_i of 6.505 ± 0.039) and the 2′,4′-difluorocarba derivative **13g** (pK_i of 6.228 ± 0.014). The rank order of potency for the carba analogues was in line with the respective rank order of potency for the hydrazones. Only the 2′-fluoro (**13c**, pK_i = 6.189 ± 0.020) and the 2′-chloro substituted carba analogue (**13p**, pK_i = 6.079 ± 0.037) deviated from the rank order of potency observed for the hydrazone derivatives, this time the 2′-fluoro derivative **13c** being more potent than the 2′-chloro derivative **13p**. But similar to the hydrazone derivatives **12c** and **12p**, the differences in potencies were also very small for the carba analogues **13c** and **13p**, rendering this change in the rank order of potency less meaningful.

The carba analogues were finally also characterized with respect to their potencies in [^{3}H]GABA uptake assays (Table 3). Again the pIC_{50} values for the [^{3}H]GABA uptake assays were somewhat lower than the corresponding pK_i values resulting from the MS binding assays, the reasons for this phenomenon being most likely those given in the section "Biphenyl-2-carbaldehyde Derived Hydrazone Hits". The sequence of potencies (pIC_{50}) was roughly in line with that of the affinities (pK_i) found for these compounds, **13c**, **13p**, and **13g** being nearly equally potent (**13c**, pIC_{50} = 5.477 ± 0.095; **13p**, pIC_{50} = 5.448 ± 0.105, **13g**, pIC_{50} = 5.547 ± 0.032), whereas **13z** showed an increased potency (**13z**, pIC_{50} = 6.114 ± 0.107). Only **13ah** (pIC_{50} = 5.399 ± 0.052) was slightly less potent than expected and equipotent to **13c**, **13p**, and **13g**.

According to the results described above, structure−activity data obtained from screening of hydrazone libraries represent valuable information regarding drug target binding which can be used for the construction of stable analogues as lead structures but should also be useful in guiding the optimization of these compounds. The reduced potency of the carba analogues versus the parent screening hits is attributed to the lower polarity of the all-carbon spacer and possibly also to its inability to participate in hydrogen bonds in contrast to the hydrazone function.

CONCLUSION

Recently, competitive MS binding assays have been shown to be applicable as a readout for the screening of compound

dx.doi.org/10.1021/jm301800j | J. Med. Chem. 2013, 56, 1323−1340

libraries, generated by simple and most efficient reactions commonly used in dynamic combinatorial chemistry. A key feature of this method is to take special means to render the libraries pseudostatic in order to obtain well-defined library compositions with almost equal concentrations of test compounds. Furthermore, by generation of the libraries in the presence of the target under conditions appropriate for the MS binding assay, library generation and screening are performed in the same sample, thus enhancing the assay performance. When this concept was applied to mGAT1 as target employing pseudostatic hydrazone libraries, two hits, hydrazones **12a** and **12b**, were identified as moderate (submicromolar) binders of mGAT1. Both hits displayed a biaryl system representing the lipophilic part that was attached via a spacer to a more polar residue, in the present case a nipecotic acid moiety that is characteristic of most mGAT1 inhibitors. The aim of the current study was to further improve the affinities for mGAT1 by optimizing the biphenyl system of **12a**, one of the two hits that had been identified in the first screening round. Accordingly, focused hydrazone libraries comprising compounds with differently substituted biphenyl moieties were generated under pseudostatic conditions and screened by the aforementioned method developed for mGAT1 which is based on competitive MS binding experiments utilizing NO711 (**6**) as native MS marker. The screening of 9 biaryl focused pseudostatic hydrazone libraries comprising 36 hydrazones revealed 21 hydrazone hits with higher affinities than the original lead system **12a** (pK_i = 6.186 ± 0.028). The most potent hit, **12z**, displaying a 2′,4′-dichloro substituted biphenyl moiety, exhibited an affinity in the lower nanomolar range, the pK_i = 8.094 ± 0.098 being almost 2 log units higher than of the original compound **12a**. Actually, 2′,4′-disubstituted biphenyl units appeared to be most favorable for increased binding affinities toward mGAT1 with Cl and F substituents being most rewarding. A set of representative metastable hydrazone derivatives was chosen to explore the suitability of these compounds as models for the construction of stable analogues as lead structures for further drug development. Of five representative biphenylhydrazones the corresponding stable carba analogues were synthesized and tested in competitive MS binding experiments and [^{3}H]GABA uptake assays. Again, a 2′,4′-dichloro substituted compound, i.e., **13z**, was found to be the most potent mGAT1 binder (pK_i = 6.930 ± 0.021), though the pK_i value of **13z** was 1 log unit lower than that of the hydrazone derivative **12z**. This is possibly a result of the reduced polarity of the carba analogue compared to the corresponding hydrazone derivative. But pleasingly, the rank order of potency of the five carba analogues in the binding studies was the same as that of the corresponding hydrazone derivatives. Thus, this study clearly demonstrated that screening of focused hydrazone libraries under pseudostatic conditions is a powerful tool to detect hits and that these can be successfully used as a starting point for the development of almost equally potent lead structures.

EXPERIMENTAL SECTION

Chemistry. Solvents used were of analytical grade and freshly destilled before use except for DMSO. Ethyl nipecotate was purchased from Sigma-Aldrich and freshly destilled before use. Other purchased reagents and reactants were used without further purification. TLC was carried out on precoated silica gel F_{254} glass plates (Merck). Flash column chromatography (CC) was performed on Merck silica gel 60 (mesh 0.040−0.063 mm). Solvents used for elution are reported in parentheses. ^{1}H NMR spectra were recorded on a JNMR-GX (JEOL, 400 or 500 MHz) at room temperature unless otherwise described. DMSO-d_6 was applied for at least 5 min to ultrasonic degassing before use. ^{1}H chemical shifts were internally referenced to TMS or MeOH for samples solved in D_2O or CD_3OD. The spectra were processed with the NMR software MestReNova (version 5.1.1-3092, 2007, Mestrelab Research S. L., Santiago de Compostela, Spain). Broadened signals in ^{1}H NMR spectra were supplemented by the index "br" (s_{br}, d_{br}, t_{br}). IR spectroscopy was performed with an FTIR spectrometer 410 (Jasco). Samples were measured either as KBr pellets or as films on NaCl plates. A Hewlett-Packard 5989 A with 59.980 B particle beam LC−MS interface was used for mass spectrometry (ionization: chemical (CH_5^+) or electron impact (70 eV)). High resolution mass spectrometry was carried out with a LTQ FT (ThermoFinnigan), FAB (Xenon, 6 kV, MBA, reference PEG), or a JMS GCmate II (Jeol). Purity testing was done by means of analytical HPLC on an Agilent 1100 instrument (G1329A ALS autosampler, G1316A column compartment, G1315B DAD detector, G1312A binary pump, G1322A degasser), equipped with a Lichrospher 100 RP-18 (5 μm) in a LiChroCART 125-4 column, with elution at 1 mL/min with phosphate buffer (5 mM $NaH_2PO_4 \cdot H_2O$, 5 mM $Na_2HPO_4 \cdot 2H_2O$, pH 7.0) to CH_3CN 40:60. Carba analogues **13c**, **13g**, **13p**, **13z**, **13ah** were ≥95% pure. Because of the tendency of hydrazones to hydrolyze, necessitating specific means to render compound libraries pseudostatic, HPLC analysis did not appear to be reasonable. Because of autoxidation of hydrazones and hydrazines, starting material and products were stored under Ar.

General Procedure for the Preparation of Hydrazones (GP1). According to the published procedure,[28] 1 equiv of the corresponding aldehyde in DMSO-d_6 (c = 0.1 M) was added to hydrazine **10**. For practical reasons NMR spectra were directly measured from this solution after at least five min. When all NMR measurements were finished, DMSO-d_6 was evaporated to give the desired hydrazone.[46] According to ^{1}H NMR spectra, hydrazones existed to ≥98% as *E*-isomers.

General Procedure for the Suzuki Coupling of 19 and Phenylboronic Acid Derivatives (GP2). Under nitrogen atmosphere Pd(dppf)$Cl_2 \cdot CH_2Cl_2$ (0.015 mmol, 5 mol %), the appropriate phenylboronic acid derivative (0.33 mmol), and compound **19** (114 mg, 0.300 mmol) were dissolved in 1,4-dioxane (0.6 mL), K_2CO_3 (124 mg, 0.90 mmol), and 0.3 mL of water. The resulting mixture was heated to 60 °C and stirred for 3 h. After addition of water (5 mL) the mixture was extracted three times with CH_2Cl_2 (5 mL). The combined organic layers were dried over Na_2SO_4, and the solvent was evaporated in vacuo. The crude product was purified by flash column chromatography on silica gel (*n*-pentane/CH_2Cl_2/EtOAc = 8/1/1 + 2% Et_3N).

General Procedure for the Hydrolysis of N-Substituted Piperidine-3-carboxylic Acid Ethyl Ester Derivatives 21 (GP3). The chosen piperidine-3-carboxylic acid ethyl ester derivative (0.2 mmol) was dissolved in EtOH (0.8 mL) followed by addition of NaOH (24.0 mg, 0.60 mmol, 0.050 mL, 12 M aqueous) (TLC monitoring). Upon completion of the reaction (approximately 4 h) water (5 mL) was added and the basic solution was washed with Et_2O (5 mL). Afterward the pH of the aqueous phase was adjusted to pH 6 with 1 M HCl and phosphate buffer solution (1 M, pH 7) and the product was extracted several times with CH_2Cl_2. The combined organic layers were dried over Na_2SO_4, and the solvent was removed in vacuo to give the appropriate product.

(*E*)-1-(2-{2-[1-(2′-Fluorobiphenyl-2-yl)methylidene]-hydrazinyl}ethyl)piperidine-3-carboxylic Acid (12c). According to GP1 from hydrazine **10** (8.71 mg, 46.5 μmol) and **11c** (9.31 mg, 46.5 μmol), **12c** was obtained as colorless, amorphous solid (17.2 mg, yield 100%). ^{1}H NMR (500 MHz, DMSO-d_6): δ 1.26−1.38 (m, 1H), 1.37−1.49 (m, 1H), 1.53−1.65 (m, 1H), 1.70−1.83 (m, 1H), 1.99 (t_{br}, J = 9.5 Hz, 1H), 2.12 (t_{br}, J = 9.8 Hz, 1H), 2.38 (tt, J = 9.9/3.9 Hz, 1H), 2.42 (t, J = 6.8 Hz, 2H), 2.56−2.67 (m, 1H), 2.81 (d_{br}, J = 10.6 Hz, 1H), 3.11 (t, J = 6.6 Hz, 2H), 7.14−7.25 (s_{br}, 1H), 7.20 (dd, J = 7.6/1.2 Hz, 1H), 7.25−7.35 (m, 5H), 7.35−7.40 (m, 1H), 7.43−7.52 (m, 1H), 7.87 (dd, J = 7.9/1.2 Hz, 1H) ppm. ^{13}C NMR (101 MHz,

dx.doi.org/10.1021/jm301800j | J. Med. Chem. 2013, 56, 1323−1340

DMSO-d_6): δ 23.9, 26.4, 41.0, 45.4, 53.2, 55.3, 56.3, 115.5 (d, $^2J_{CF}$ = 22.1 Hz), 123.7, 124.5 (d, $^{3/4}J_{CF}$ = 3.6 Hz), 126.8, 127.2 (d, $^2J_{CF}$ = 16.3 Hz), 127.9, 129.7 (d, $^3J_{CF}$ = 8.1 Hz), 130.4, 131.5, 131.8 (d, $^{3/4}J_{CF}$ = 3.3 Hz), 132.8, 134.4, 158.9 (d, $^1J_{CF}$ = 244.3 Hz), 175.0 ppm. ^{19}F NMR (471 MHz, DMSO-d_6): δ −115.00 ppm. MS (ESI+) m/z: 370 [M + H]$^+$. HRMS (ESI+): [M + H]$^+$ calcd for $C_{21}H_{25}O_2N_3F$, 370.1931; found, 370.1923.

(*E*)-1-(2-{2-[1-(4′-Fluorobiphenyl-2-yl)methylidene]-hydrazinyl}ethyl)piperidine-3-carboxylic Acid (12e). According to GP1 from hydrazine **10** (8.55 mg, 45.6 mmol) and **11e** (9.13 mg, 45.6 μmol), **12e** was obtained as slightly yellow, amorphous solid (16.9 mg, yield 100%). ^{1}H NMR (400 MHz, DMSO-d_6): δ 1.26−1.40 (m, 1H), 1.38−1.50 (m, 1H), 1.54−1.66 (m, 1H), 1.71−1.83 (m, 1H), 2.02 (t_{br}, J = 10.0 Hz, 1H), 2.15 (t_{br}, J = 10.2 Hz, 1H), 2.39 (tt, J = 8.9/3.9 Hz, 1H), 2.45 (t, J = 6.7 Hz, 2H), 2.56−2.69 (m, 1H), 2.82 (d_{br}, J = 10.3 Hz, 1H), 3.13 (t, J = 6.6 Hz, 2H), 7.01−7.18 (s_{br}, 1H), 7.17−7.23 (m, 1H), 7.24−7.31 (m, 3H), 7.31−7.39 (m, 3H), 7.43 (s, 1H), 7.85 (dd, J = 7.7/1.3 Hz, 1H) ppm. ^{13}C NMR (101 MHz, DMSO-d_6): δ 23.9, 26.4, 41.0, 45.5, 53.2, 55.3, 56.4, 115.1 (d, $^2J_{CF}$ = 21.0 Hz, 2C), 124.2, 126.9, 127.4, 130.0, 131.3 (d, $^3J_{CF}$ = 8.0 Hz, 2C), 132.0, 133.6, 136.2 (d, $^4J_{CF}$ = 3.3 Hz), 138.2, 161.4 (s, $^1J_{CF}$ = 240.7 Hz), 175.0 ppm. ^{19}F NMR (471 MHz, DMSO-d_6): δ −115.42 ppm. MS (ESI+) m/z: 370 [M + H]$^+$. HRMS (ESI+): [M + H]$^+$ calcd for $C_{21}H_{25}O_2N_3F$, 370.1931; found, 370.1923.

(*E*)-1-(2-{2-[1-(3′,4′-Difluorobiphenyl-2-yl)methylidene]-hydrazinyl}ethyl)piperidine-3-carboxylic Acid (12f). According to GP1 from hydrazine **10** (10.2 mg, 54.5 μmol) and **11f** (11.9 mg, 54.5 μmol), **12f** was obtained as a yellow, amorphous solid (21.1 mg, yield 100%). ^{1}H NMR (500 MHz, DMSO-d_6): δ 1.26−1.39 (m, 1H), 1.38−1.50 (m, 1H), 1.55−1.65 (m, 1H), 1.71−1.83 (m, 1H), 2.01 (t_{br}, J = 9.5 Hz, 1H), 2.14 (t_{br}, J = 9.9 Hz, 1H), 2.39 (tt, J = 9.9/3.9 Hz, 1H), 2.45 (t, J = 6.7 Hz, 2H), 2.58−2.68 (m, 1H), 2.84 (d_{br}, J = 9.7 Hz, 1H), 3.15 (t, J = 6.6 Hz, 2H), 7.13−7.18 (m, 1H), 7.19−7.26 (s_{br}, 1H), 7.23 (dd, J = 7.6/1.3 Hz, 1H), 7.29 (td, J = 7.4/1.4 Hz, 1H), 7.35 (td, J = 7.7/1.1 Hz, 1H), 7.39−7.46 (m, 1H), 7.44 (s, 1H), 7.52 (dt, J = 10.8/8.5 Hz, 1H), 7.85 (dd, J = 7.8/1.0 Hz, 1H) ppm. ^{13}C NMR (101 MHz, DMSO-d_6): δ 23.9, 26.5, 40.9, 45.4, 53.2, 55.3, 56.4, 117.3 (d, $^2J_{CF}$ = 16.9 Hz), 118.4 (d, $^2J_{CF}$ = 16.9 Hz), 124.2, 126.4 (d, J_{CF} = 6.4/3.4 Hz), 126.9, 127.8, 130.0, 131.5, 133.6, 137.1 (d, J_{CF} = 1.4 Hz), 137.4 (dd, J_{CF} = 6.1/3.8 Hz), 148.9 (d, $^{1/2}J_{CF}$ = 245.7/12.8 Hz), 149.0 (d, $^{1/2}J_{CF}$ = 245.7/12.8 Hz), 175.1 ppm. ^{19}F NMR (471 MHz, DMSO-d_6): δ −140.87 (m, 1 F), −138.46 (m, 1 F) ppm. MS (ESI+) m/z: 388 [M + H]$^+$. HRMS (ESI+): [M + H]$^+$ calcd for $C_{21}H_{24}O_2N_3F_2$, 388.1837; found, 388.1828.

(*E*)-1-(2-{2-[1-(2′,4′-Difluorobiphenyl-2-yl)methylidene]-hydrazinyl}ethyl)piperidine-3-carboxylic Acid (12g). According to GP1 from hydrazine **10** (10.8 mg, 57.9 μmol) and **11g** (12.6 mg, 57.9 μmol), **12g** was obtained as a yellow, amorphous solid (22.6 mg, yield 100%). ^{1}H NMR (400 MHz, DMSO-d_6): δ 1.25−1.51 (m, 2H), 1.53−1.66 (m, 1H), 1.70−1.83 (m, 1H), 1.99 (t_{br}, J = 10.4 Hz, 1H), 2.12 (t_{br}, J = 10.6 Hz, 1H), 2.30−2.48 (m, 3H), 2.62 (d_{br}, J = 11.8 Hz, 1H), 2.82 (d_{br}, J = 9.7 Hz, 1H), 3.12 (t, J = 6.4 Hz, 2H), 7.12−7.25 (m, 3H), 7.25−7.33 (m, 2H), 7.33−7.45 (m, 3H), 7.86 (d, J = 7.9 Hz, 1H) ppm. ^{13}C NMR (126 MHz, DMSO-d_6): δ 23.9, 26.4, 40.9, 45.4, 53.2, 55.3, 56.3, 103.9 (t, $^2J_{CF}$ = 26.2 Hz), 111.6 (dd, $^{2/4}J_{CF}$ = 21.3/3.4 Hz), 123.8, (dd, $^{2/4}J_{CF}$ = 15.6/3.5 Hz) 123.8, 126.8, 128.1, 130.5, 131.2, 131.9, 132.8 (dd, $^{3/3}J_{CF}$ = 9.6/4.8 Hz), 134.5, 159.0 (dd, $^{1/3}J_{CF}$ = 246.6/12.4 Hz), 161.8 (dd, $^{1/3}J_{CF}$ = 246.6/11.9 Hz), 175.1 ppm. ^{19}F NMR (471 MHz, DMSO-d_6): δ −110.87 (dt, J = 16.0/8.2 Hz), −110.40 (q, J = 8.0 Hz) ppm. MS (ESI+) m/z: 388.2 [M + H]$^+$. HRMS (ESI+): [M + H]$^+$ calcd for $C_{21}H_{24}F_2N_3O_2$, 388.1837; found, 388.1829.

(*E*)-1-(2-{2-[1-(2′,3′-Difluorobiphenyl-2-yl)methylidene]-hydrazinyl}ethyl)piperidine-3-carboxylic Acid (12h). According to GP1 from hydrazine **10** (8.78 mg, 46.9 μmol) and **11h** (10.2 mg, 46.9 μmol), **12h** was obtained as a yellow, amorphous solid (18.0 mg, yield 99%). ^{1}H NMR (500 MHz, DMSO-d_6): δ 1.25−1.38 (m, 1H), 1.38−1.50 (m, 1H), 1.54−1.65 (m, 1H), 1.71−1.83 (m, 1H), 1.99 (t_{br}, J = 9.6 Hz, 1H), 2.12 (t_{br}, J = 9.7 Hz, 1H), 2.38 (tt, J = 9.8/3.7 Hz, 1H), 2.42 (t, J = 6.7 Hz, 2H), 2.57−2.67 (m, 1H), 2.81 (d_{br}, J = 10.4 Hz, 1H), 3.12 (t, J = 6.6 Hz, 2H), 7.10−7.18 (m, 1H), 7.19−7.27 (m, 2H), 7.27−7.34 (m, 3H), 7.37−7.44 (m, 1H), 7.44−7.52 (m, 1H), 7.84−7.89 (m, 1H) ppm. ^{13}C NMR (126 MHz, DMSO-d_6): δ 23.9, 26.4, 40.9, 45.5, 53.2, 55.3, 56.4, 116.7 (d, $^2J_{CF}$ = 17.1 Hz), 123.9, 124.8 (dd, $^{3/4}J_{CF}$ = 7.5/4.6 Hz), 126.8, 127.0 (m_{CF}), 128.4, 129.7 (d, $^2J_{CF}$ = 12.8 Hz), 130.3, 131.0, 131.3 (s, $^3J_{CF}$ = 2.5 Hz), 134.4, 146.8 (dd, $^{1/2}J_{CF}$ = 246.4/12.7 Hz,), 149.7 (dd, $^{1/2}J_{CF}$ = 246.3/13.1 Hz), 175.0 ppm. ^{19}F NMR (471 MHz, DMSO-d_6): δ −140.82 (d, J = 23.21 Hz), −138.54 (d, J = 27.07 Hz) ppm. MS (ESI+) m/z: 388.7 [M + H]$^+$. HRMS (ESI+): [M + H]$^+$ calcd for $C_{21}H_{24}F_2N_3O_2$, 388.1837; found, 388.1828.

(*E*)-1-(2-{2-[1-(4′-Fluoro-2′-methoxybiphenyl-2-yl)-methylidene]hydrazinyl}ethyl)piperidine-3-carboxylic Acid (12l). According to GP1 from hydrazine **10** (13.2 mg, 70.3 μmol) and **11l** (16.2 mg, 70.3 μmol), **12l** was obtained as colorless, amorphous solid (28.1 mg, yield 99%). ^{1}H NMR (500 MHz, DMSO-d_6): δ 1.27−1.38 (m, 1H), 1.38−1.50 (m, 1H), 1.53−1.65 (m, 1H), 1.69−1.83 (m, 1H), 2.00 (t_{br}, J = 10.4 Hz, 1H), 2.14 (t_{br}, J = 9.8 Hz, 1H), 2.38 (tt, J = 9.7/3.9 Hz, 1H), 2.42 (t, J = 7.0 Hz, 2H), 2.56−2.67 (m, 1H), 2.81 (d_{br}, J = 11.3 Hz, 1H), 3.09 (t, J = 6.7 Hz, 2H), 3.71 (s, 3H), 6.84 (td, J = 8.4/2.5 Hz, 1H), 7.01 (dd, J = 11.5/2.4 Hz, 1H), 7.08 (dd, J = 7.6/1.3 Hz, 1H), 7.13 (dd, J = 8.3/7.0 Hz, 1H), 7.19 (s, 1H), 7.23 (td, J = 7.4/1.5 Hz, 1H), 7.26−7.33 (m, 1H), 7.81 (dd, J = 7.9/1.2 Hz, 1H) ppm. ^{13}C NMR (126 MHz, DMSO-d_6): δ 23.9, 26.4, 40.9, 45.5, 53.2, 55.3, 55.7, 56.4, 99.5 (d, $^2J_{CF}$ = 25.7 Hz), 106.6 (d, $^2J_{CF}$ = 21.0 Hz), 123.3, 124.8 (d, $^4J_{CF}$ = 2.8 Hz), 126.6, 127.2, 130.5, 131.8 (d, $^3J_{CF}$ = 10.0 Hz), 132.7, 134.4, 135.3, 157.5 (d, $^3J_{CF}$ = 10.2 Hz), 162.6 (d, $^1J_{CF}$ = 243.5 Hz), 175.1 ppm. ^{19}F NMR (471 MHz, DMSO-d_6): δ 111.80 (ddd, J = 11.4/8.4/7.2 Hz) ppm. MS (CI, CH_5^+) m/z: 400 [M + H]$^+$. HRMS (ESI+): [M + H]$^+$ calcd for $C_{22}H_{27}N_3O_3F$, 400.2036; found, 400.2029.

(*E*)-1-(2-{2-[1-(2′-Fluoro-6′-methoxybiphenyl-2-yl)-methylidene]hydrazinyl}ethyl)piperidine-3-carboxylic Acid (12m). According to GP1 from hydrazine **10** (4.72 mg, 25.5 μmol) and **11m** (5.80 mg, 25.2 μmol), **12m** was obtained as a yellow, amorphous solid (10.8 mg, yield 100%). ^{1}H NMR (500 MHz, DMSO-d_6): δ 1.25−1.36 (m, 1H), 1.35−1.48 (m, 1H), 1.52−1.64 (m, 1H), 1.70−1.81 (m, 1H), 1.96 (t_{br}, J = 9.9 Hz, 1H), 2.09 (t_{br}, J = 9.1 Hz, 1H), 2.32−2.39 (m, 1H), 2.39 (t, J = 6.7 Hz, 2H), 2.55−2.65 (m, 1H), 2.79 (d_{br}, J = 9.7 Hz, 1H), 3.07 (t, J = 6.6 Hz, 2H), 3.70 (s, 3H), 6.90 (t, J = 8.6 Hz, 1H), 6.97 (d, J = 8.5 Hz, 1H), 7.06−7.14 (s_{br}, 1H), 7.09 (dd, J = 7.6/1.0 Hz, 1H), 7.15 (s, 1H), 7.24 (td, J = 7.5/1.4 Hz, 1H), 7.31 (td, J = 7.7/1.0 Hz, 1H), 7.41 (td, J = 8.4/7.1 Hz, 1H), 7.83 (d, J = 7.9 Hz, 1H) ppm. ^{13}C NMR (101 MHz, DMSO-d_6): δ 23.9, 26.4, 40.9, 45.4, 53.2, 55.3, 55.9, 56.3, 107.3, 107.6 (d, 1 C, $^2J_{CF}$ = 22.9 Hz), 116.0 (d, $^2J_{CF}$ = 19.41 Hz), 123.4, 126.5, 127.7, 128.9, 129.8 (d, 1 C, $^3J_{CF}$ = 19.4 Hz), 131.0, 131.9, 134.9, 157.7 (d, $^3J_{CF}$ = 7.3 Hz), 159.5 (d, $^1J_{CF}$ = 241.6 Hz), 175.0 ppm. ^{19}F NMR (471 MHz, DMSO-d_6): δ −113.70 (t, J = 7.8 Hz) ppm. MS (ESI+) m/z: 400 [M + H]$^+$. HRMS (ESI+): [M + H]$^+$ calcd for $C_{22}H_{27}O_3N_3F$, 400.2036; found, 400.2028.

(*E*)-1-(2-{2-[1-(2′-Chlorobiphenyl-2-yl)methylidene]-hydrazinyl}ethyl)piperidine-3-carboxylic Acid (12p). According to GP1 from hydrazine **10** (12.7 mg, 68.1 μmol) and **11p** (14.8 mg, 68.4 μmol), **12p** was obtained as a yellow, amorphous solid (26.3 mg, yield 100%). ^{1}H NMR (500 MHz, DMSO-d_6): δ 1.26−1.37 (m, 1H), 1.37−1.48 (m, 1H), 1.54−1.63 (m, 1H), 1.69−1.82 (m, 1H), 1.97 (t_{br}, J = 9.9 Hz, 1H), 2.04−2.19 (m, 1H), 2.32−2.44 (m, 3H), 2.60 (d_{br}, J = 10.5 Hz, 1H), 2.80 (d_{br}, J = 10.8 Hz, 1H), 3.08 (t, J = 6.6 Hz, 2H), 7.09−7.13 (m, 1H), 7.12 (s, 1H), 7.18 (s_{br}, 1H), 7.25−7.33 (m, 2H), 7.33−7.39 (m, 1H), 7.40−7.47 (m, 2H), 7.53−7.61 (m, 1H), 7.86 (dd, J = 8.0/0.7 Hz, 1H) ppm. ^{13}C NMR (126 MHz, DMSO-d_6): δ 23.9, 26.4, 40.9, 45.3, 53.2, 55.3, 56.2, 123.5, 126.6, 127.2, 127.9, 129.2, 129.3, 129.8, 131.1, 131.7, 132.4, 134.1, 136.5, 138.6, 175.0 ppm. MS (ESI+) m/z: 386 [M + H]$^+$. HRMS (ESI+): [M + H]$^+$ calcd for $C_{21}H_{25}ClN_3O_2$, 386.1635; found, 368.1629.

(*E*)-1-(2-{2-[1-(4′-Chlorobiphenyl-2-yl)methylidene]-hydrazinyl}ethyl)piperidine-3-carboxylic Acid (12r). According to GP1 from hydrazine **10** (9.65 mg, 51.6 μmol) and **11r** (11.1 mg, 51.6 μmol), **12r** was obtained as a yellow, amorphous solid (20.0 mg, yield 100%). ^{1}H NMR (500 MHz, DMSO-d_6): δ 1.28−1.39 (m, 1H),

1.39−1.50 (m, 1H), 1.55−1.66 (m, 1H), 1.69−1.84 (m, 1H), 2.02 (t_{br}, J = 9.6 Hz, 1H), 2.15 (t_{br}, J = 10.0 Hz, 1H), 2.39 (tt, J = 9.9/3.8 Hz, 1H), 2.45 (t, J = 6.7 Hz, 2H), 2.58−2.67 (m, 1H), 2.83 (d_{br}, J = 11.6 Hz, 1H), 3.14 (t, J = 6.6 Hz, 2H), 7.20 (s_{br}, 1H), 7.21 (dd, J = 7.6/1.3 Hz, 1H), 7.29 (td, J = 7.4/1.5 Hz, 1H), 7.31−7.37 (m, 3H), 7.43 (s, 1H), 7.49−7.54 (m, 2H), 7.85 (dd, J = 7.8/1.3 Hz, 1H) ppm. ^{13}C NMR (126 MHz, DMSO-d_6): δ 23.9, 26.4, 40.9, 45.5, 53.2, 55.3, 56.4, 124.3, 126.9, 127.6, 128.2 (2C), 129.8, 131.2 (2C), 131.8, 132.0, 133.5, 137.9, 138.7, 175.0 ppm. MS (ESI+) m/z: 386.1 $[M + H]^+$. HRMS (ESI+): $[M + H]^+$ calcd for $C_{21}H_{25}ClN_3O_2$, 386.1635; found, 386.1629.

(*E*)-1-(2-{2-[1-(4′-Methylbiphenyl-2-yl)methylidene]-hydrazinyl}ethyl)piperidine-3-carboxylic Acid (12v). According to GP1 from hydrazine **10** (11.1 mg, 59.5 μmol) and **11v** (11.7, 59.5 μmol), **12v** was obtained as colorless, amorphous solid (21.6 mg, yield 100%). ^{1}H NMR (500 MHz, DMSO-d_6): δ 1.26−1.39 (m, 1H), 1.39−1.51 (m, 1H), 1.53−1.66 (m, 1H), 1.69−1.84 (m, 1H), 2.01 (t_{br}, J = 10.2 Hz, 1H), 2.15 (t_{br}, J = 10.3 Hz, 1H), 2.36 (s, 3H), 2.39 (tt, J = 9.9/2.8 Hz, 1H), 2.45 (t, J = 6.5 Hz, 2H), 2.58−2.67 (m, 1H), 2.82 (d_{br}, J = 9.5 Hz, 1H), 3.13 (t, J = 6.7 Hz, 2H), 7.08 (s, 1H), 7.15−7.23 (m, 3H), 7.23−7.34 (m, 4H), 7.47 (s, 1H), 7.78−7.87 (m, 1H) ppm. ^{13}C NMR (126 MHz, DMSO-d_6): δ 20.6, 23.9, 26.4, 40.9, 45.5, 53.2, 55.3, 56.4, 124.2, 126.9, 127.1, 128.8 (2C), 129.2 (2C), 129.9, 132.5, 133.4, 136.2, 136.9, 139.3, 175.0 ppm. MS (ESI+) m/z: 366.2 $[M + H]^+$. HRMS (ESI+): $[M + H]^+$ calcd for $C_{22}H_{28}N_3O_2$, 366.2182; found, 366.2174.

(*E*)-1-(2-{2-[1-(4′-Chloro-2′-fluorobiphenyl-2-yl)-methylidene]hydrazinyl}ethyl)piperidine-3-carboxylic Acid (12y). According to GP1 from hydrazine **10** (9.40 mg, 50.2 μmol) and **11y** (11.8 mg, 50.3 μmol), **12y** was obtained as a yellow, amorphous solid (20.3 mg, yield 100%). ^{1}H NMR (500 MHz, DMSO-d_6): δ 1.28−1.39 (m, 1H), 1.38−1.50 (m, 1H), 1.54−1.66 (m, 1H), 1.71−1.84 (m, 1H), 2.00 (t_{br}, J = 9.9 Hz, 1H), 2.14 (t_{br}, J = 10.1 Hz, 1H), 2.39 (tt, J = 9.8/3.8 Hz, 1H), 2.43 (t, J = 6.8 Hz, 2H), 2.57−2.68 (m, 1H), 2.82 (d_{br}, J = 9.2 Hz, 1H), 3.12 (t, J = 6.6 Hz, 2H), 7.14−7.25 (s_{br}, 1H), 7.19 (dd, J = 7.7/1.1 Hz, 1H), 7.27−7.29 (m, 1H), 7.30 (dd, J = 7.4/1.3 Hz, 1H), 7.33−7.43 (m, 3H), 7.53 (dd, J = 9.7/1.9 Hz, 1H), 7.85 (dd, J = 8.0/1.0 Hz, 1H) ppm. ^{13}C NMR (126 MHz, DMSO-d_6): δ 23.9, 26.4, 40.9, 45.5, 53.2, 55.3, 56.3, 116.1 (d, $^2J_{CF}$ = 26.3 Hz), 123.9, 124.8 (d, $^4J_{CF}$ = 3.7 Hz), 126.4 (d, $^2J_{CF}$ = 16.4 Hz), 126.8, 128.3, 130.3, 131.2, 131.6, 133.0 (d, $^3J_{CF}$ = 4.0 Hz), 133.1 (d, $^3J_{CF}$ = 10.4 Hz), 134.4, 158.9 (d, $^1J_{CF}$ = 248.0 Hz), 175.0 ppm. ^{19}F NMR (471 MHz, DMSO-d_6): δ −111.84 (m) ppm. MS (ESI+) m/z: 404.2 $[M + H]^+$. HRMS (ESI+): $[M + H]^+$ calcd for $C_{21}H_{24}ClFN_3O_2$, 404.1541; found, 404.1534.

(*E*)-1-(2-{2-[1-(2′,4′-Dichlorobiphenyl-2-yl)methylidene]-hydrazinyl}ethyl)piperidine-3-carboxylic Acid (12z). According to GP1 from hydrazine **10** (18.2 mg, 97.0 μmol) and **11z** (24.4 mg, 97.0 μmol), **12z** was obtained as a yellow, amorphous solid (40.6 mg, yield 99%). ^{1}H NMR (500 MHz, DMSO-d_6, 60 °C): δ 1.28−1.50 (m, 2H), 1.56−1.66 (m, 1H), 1.72−1.83 (m, 1H), 2.02 (t, J = 9.1 Hz, 1H), 2.16 (t, J = 10.3 Hz, 1H), 2.34−2.46 (m, 3H), 2.55−2.64 (m, 1H), 2.80 (dd, J = 11.1/3.3 Hz, 1H), 3.10 (t, J = 6.7 Hz, 2H), 7.10 (dd, J = 7.6/1.0 Hz, 1H), 7.16 (s, 1H), 7.28 (td, J = 7.5/1.4 Hz, 1H), 7.32 (d, J = 8.2 Hz, 1H), 7.34−7.39 (m, 1H), 7.48 (dd, J = 8.2/2.1 Hz, 1H), 7.68 (d, J = 2.1 Hz, 1H), 7.83 (dd, J = 8.0/1.2 Hz, 1H) ppm. ^{13}C NMR (126 MHz, DMSO-d_6, 60 °C): δ 23.9, 26.5, 41.1, 45.7, 53.2, 55.4, 56.4, 124.0, 126.6, 127.3, 128.1, 128.7, 129.7, 131.3, 132.9, 133.0, 133.6, 134.4, 135.4, 138.0, 174.9 ppm. ^{19}F NMR (471 MHz, DMSO-d_6): δ −111.84 (m) ppm. MS (ESI+) m/z: 420 $[M + H]^+$. HRMS (ESI+): $[M + H]^+$ calcd for $C_{21}H_{24}N_3O_2Cl_2$, 420.1246; found, 420.1210.

(*E*)-1-(2-{2-[1-(2′,6′-Difluorobiphenyl-2-yl)methylidene]-hydrazinyl}ethyl)piperidine-3-carboxylic Acid (12aa). According to GP1 from hydrazine **10** (6.51 mg, 34.7 μmol) and **11aa** (7.57 mg, 34.7 μmol), **12aa** was obtained as a yellow, amorphous solid (13.3 mg, yield 99%). ^{1}H NMR (500 MHz, DMSO-d_6): δ 1.26−1.50 (m, 2H), 1.53−1.65 (m, 1H), 1.70−1.83 (m, 1H), 1.99 (t_{br}, J = 9.4 Hz, 1H), 2.13 (t_{br}, J = 10.1 Hz, 1H), 2.33−2.45 (m, 3H), 2.56−2.66 (m, 1H), 2.81 (d_{br}, J = 9.7 Hz, 1H), 3.10 (t, J = 6.7 Hz, 2H), 7.14−7.27 (m, 5H), 7.31 (td, J = 7.5/1.3 Hz, 1H), 7.41 (td, J = 7.7/1.0 Hz, 1H), 7.52 (tt, J = 8.4/6.6 Hz, 1H), 7.87 (dd, J = 8.0/1.0 Hz, 1H) ppm. ^{13}C NMR (126 MHz, DMSO-d_6): δ 23.9, 26.4, 40.9, 45.4, 53.2, 55.3, 56.3, 111.7 (d, $^2J_{CF}$ = 25.8 Hz, 2C), 116.3 (t, $^2J_{CF}$ = 21.8 Hz), 124.1, 125.8, 126.7, 128.6, 130.3 (t, $^3J_{CF}$ = 10.4 Hz), 130.8, 130.9, 135.1, 159.4 (d, $^1J_{CF}$ = 245.4 Hz, 2C), 175.0 ppm. ^{19}F NMR (471 MHz, DMSO-d_6): δ −112.40 (t, J = 6.5 Hz) ppm. MS (ESI+) m/z: 388.3 $[M + H]^+$. HRMS (ESI+): $[M + H]^+$ calcd for $C_{21}H_{24}N_3O_2F_2$, 388.1837; found, 388.1834.

(*E*)-1-(2-{2-[1-(2′,4′,6′-Trifluorobiphenyl-2-yl)methylidene]-hydrazinyl}ethyl)piperidine-3-carboxylic Acid (12ab). According to GP1 from hydrazine **10** (10.9 mg, 58.4 μmol) and **11ab** (13.8 mg, 58.4 μmol), **12ab** was obtained as a yellow, amorphous solid (24.5 mg, yield 100%). ^{1}H NMR (500 MHz, DMSO-d_6): δ 1.27−1.39 (m, 1H), 1.38−1.50 (m, 1H), 1.53−1.66 (m, 1H), 1.68−1.85 (m, 1H), 1.99 (t_{br}, J = 9.8 Hz, 1H), 2.13 (t_{br}, J = 10.2 Hz, 1H), 2.34−2.45 (m, 3H), 2.55−2.69 (m, 1H), 2.82 (d_{br}, J = 10.7 Hz, 1H,), 3.11 (t, J = 6.4 Hz, 2H), 7.22 (dd, J = 7.6/0.9 Hz, 1H), 7.19−7.28 (s_{br}, 1H), 7.27 (s, 1H), 7.29−7.36 (m, 3H), 7.38−7.46 (m, 1H), 7.81−7.87 (m, 1H) ppm. ^{13}C NMR (126 MHz, DMSO-d_6): δ 23.9, 26.4, 40.9, 45.5, 53.2, 55.3, 56.3, 100.7 (t, $^2J_{CF}$ = 28.0 Hz, 2C), 113.2 (td, $^{2/4}J_{CF}$ = 22.2/4.8 Hz), 124.4, 124.9, 126.8, 128.8, 130.9, 131.0, 135.2, 159.6 (ddd, J_{CF} = 246.1/15.5/10.1 Hz, 2C), 161.7 (dt, J_{CF} = 246.1/15.9 Hz), 175.0 ppm. ^{19}F NMR (471 MHz, DMSO-d_6): δ −109.39 (t, J = 6.8 Hz), −108.58 (tt, J = 9.3/6.4 Hz) ppm. MS (ESI+) m/z: 406.0 $[M + H]^+$. HRMS (ESI+): $[M + H]^+$ calcd for $C_{21}H_{23}F_3N_3O_2$, 406.1742; found, 406.1735.

(*E*)-1-(2-{2-[1-(4,2′-Difluorobiphenyl-2-yl)methylidene]-hydrazinyl}ethyl)piperidine-3-carboxylic Acid (12ac). According to GP1 from hydrazine **10** (9.55 mg, 51.0 μmol) and **11ac** (11.1 mg, 51.0 μmol), **12ac** was obtained as a yellow, amorphous solid (21.0 mg, yield 100%). ^{1}H NMR (500 MHz, DMSO-d_6): δ 1.26−1.38 (m, 1H), 1.38−1.49 (m, 1H), 1.53−1.65 (m, 1H), 1.70−1.84 (m, 1H), 1.99 (t_{br}, J = 9.5 Hz, 1H), 2.12 (t_{br}, J = 10.0 Hz, 1H), 2.38 (tt, J = 9.9/3.8 Hz, 1H), 2.43 (t, J = 6.7 Hz, 2H), 2.58−2.66 (m, 1H), 2.81 (d, J = 9.8 Hz, 1H), 3.13 (t_{br}, J = 6.2 Hz, 2H), 7.11 (td, J = 8.4/2.8 Hz, 1H), 7.20 (t, J = 2.3 Hz, 1H), 7.25 (dd, J = 8.5/5.9 Hz, 1H), 7.28−7.35 (m, 3H), 7.43−7.51 (m, 2H), 7.56 (dd, J = 10.8/2.8 Hz, 1H) ppm. ^{13}C NMR (126 MHz, DMSO-d_6): δ 23.9, 26.4, 40.9, 45.3, 53.2, 55.3, 56.2, 109.2 (d, $^2J_{CF}$ = 22.9 Hz), 113.6 (d, $^2J_{CF}$ = 22.1 Hz), 115.5 (d, $^2J_{CF}$ = 22.1 Hz), 124.6 (d, $^4J_{CF}$ = 3.5 Hz), 126.3 (d, $^2J_{CF}$ = 16.1 Hz), 128.8 (d, $^4J_{CF}$ = 2.7 Hz), 129.4 (m_{CF}), 129.9 (d, $^3J_{CF}$ = 8.1 Hz), 132.0 (d, $^4J_{CF}$ = 3.2 Hz), 132.6 (d, $^3J_{CF}$ = 8.5 Hz), 137.0 (d, $^3J_{CF}$ = 9.0 Hz), 159.0 (s-d, $^1J_{CF}$ = 244.2 Hz), 162.0 (s-d, $^1J_{CF}$ = 244.0 Hz), 175.0 ppm. ^{19}F NMR (471 MHz, DMSO-d_6): δ −115.08 to −114.96 (td, J = 7.1/3.5 Hz), −114.06 to −113.90 (m) ppm. MS (ESI+) m/z: 388.3 $[M + H]^+$. HRMS (ESI$^+$): $[M + H]^+$ calcd for $C_{21}H_{24}N_3O_2F_2$, 388.1837; found, 388.1833.

(*E*)-1-(2-{2-[1-(2′-Chloro-4-fluorobiphenyl-2-yl)methylidene]-hydrazinyl}ethyl)piperidine-3-carboxylic Acid (12ad). According to GP1 from hydrazine **10** (7.17 mg, 38.3 μmol) and **11ad** (8.99 mg, 38.3 μmol), **12ad** was obtained as a yellow, amorphous solid (16.2 mg, yield 100%). ^{1}H NMR (500 MHz, DMSO-d_6): δ 1.26−1.37 (m, 1H), 1.37−1.47 (m, 1H), 1.54−1.63 (m, 1H), 1.70−1.82 (m, 1H), 1.97 (t_{br}, J = 10.2 Hz, 1H), 2.10 (t_{br}, J = 10.1 Hz, 1H), 2.32−2.44 (m, 3H), 2.56−2.63 (m, 1H), 2.79 (d_{br}, J = 9.2 Hz, 1H), 3.05−3.13 (m, 2H), 7.03 (d, J = 2.0 Hz, 1H), 7.10 (td, J = 8.4/2.8 Hz, 1H), 7.13−7.19 (m, 1H), 7.28−7.34 (m, 1H), 7.40−7.49 (m, 3H), 7.54 (dd, J = 10.8/2.7 Hz, 1H), 7.56−7.59 (m, 1H) ppm. ^{13}C NMR (126 MHz, DMSO-d_6): δ 23.9, 26.4, 40.9, 45.2, 53.1, 55.3, 56.1, 108.9 (d, $^2J_{CF}$ = 23.1 Hz), 113.3 (d, $^2J_{CF}$ = 22.3 Hz), 127.2, 129.2 (m_{CF}), 129.3 (d, $^4J_{CF}$ = 2.4 Hz), 129.5, 131.8, 132.0 (d, $^3J_{CF}$ = 8.50 Hz), 132.5 (d, $^4J_{CF}$ = 3.0 Hz), 132.6, 136.9 (d, 1 C, $^3J_{CF}$ = 8.2 Hz), 137.7, 161.8 (d, $^1J_{CF}$ = 243.3 Hz), 175.0 ppm. ^{19}F NMR (471 MHz, DMSO-d_6): δ −114.03 ppm. MS (ESI+) m/z: 404.3 $[M + H]^+$. HRMS (ESI$^+$): $[M + H]^+$ calcd for $C_{21}H_{24}N_3O_2F_2$, 404.1541; found, 404.1538.

(*E*)-1-(2-{2-[1-(2′-Methylbiphenyl-2-yl)methylidene]-hydrazinyl}ethyl)piperidine-3-carboxylic Acid (12ae). According to GP1 from hydrazine **10** (10.3 mg, 58.4 μmol) and **11ae** (11.5 mg, 58.4 μmol), **12ae** was obtained as a yellow, amorphous solid (21.3 mg, yield 100%). ^{1}H NMR (500 MHz, DMSO-d_6): δ 1.26−1.37 (m, 1H), 1.36−1.47 (m, 1H), 1.53−1.63 (m, 1H), 1.71−1.81 (m, 1H), 1.93−

dx.doi.org/10.1021/jm301800j | J. Med. Chem. 2013, 56, 1323−1340

2.02 (m, 1H), 2.00 (s, 3H), 2.06−2.18 (m, 1H), 2.33−2.40 (m, 1H), 2.40 (t, J = 6.7 Hz, 2H), 2.55−2.63 (m, 1H), 2.74−2.84 (m, 1H), 3.07 (t, J = 6.7 Hz, 2H), 7.03−7.15 (m, 3H), 7.10 (s, 1H), 7.22−7.35 (m, 5H), 7.85 (dd, J = 7.8/1.0 Hz, 1H) ppm. ^{13}C NMR (126 MHz, DMSO-d_6): δ 19.7, 23.8, 26.4, 40.9, 45.4, 53.2, 55.3, 56.3, 123.4, 125.7, 126.7, 127.2, 127.4, 129.5, 129.7, 131.7, 133.8, 135.4, 138.9, 139.6, 175.0 ppm. MS (ESI+) m/z: 366.2 $[M + H]^+$. HRMS (ESI+): $[M + H]^+$ calcd for $C_{22}H_{28}N_3O_2$, 366.2182; found, 366.2175.

(*E*)-1-(2-{2-[1-(2′,4′-Dimethylbiphenyl-2-yl)methylidene]-hydrazinyl}ethyl)piperidine-3-carboxylic Acid (12af). According to GP1 from hydrazine **10** (17.6 mg, 94.1 μmol) and **11af** (19.7 mg, 94.1 μmol), **12af** was obtained as a yellow, amorphous solid (38.5 mg, yield 100%). ^{1}H NMR (500 MHz, DMSO-d_6, 60 °C): δ 1.29−1.40 (m, 1H), 1.38−1.49 (m, 1H), 1.53−1.65 (m, 1H), 1.69−1.82 (m, 1H), 1.96 (s, 3H), 1.98−2.05 (m, 1H), 2.12−2.20 (m, 1H), 2.32 (s, 3H), 2.33−2.44 (m, 3H), 2.54−2.62 (m, 1H), 2.74−2.82 (m, 1H), 3.08 (t, J = 6.7 Hz, 2H), 6.96 (d, J = 7.6 Hz, 1H), 7.01−7.08 (m, 2H), 7.10 (s, 1H), 7.13 (s, 1H), 7.24 (td, J = 7.4/1.4 Hz, 1H), 7.29 (td, J = 7.4/0.9 Hz, 1H), 7.83 (dd, J = 7.8/1.1 Hz, 1H) ppm. ^{13}C NMR (126 MHz, DMSO-d_6, 60 °C): δ 19.6, 20.6, 23.9, 26.5, 41.0, 45.7, 53.2, 55.3, 56.4, 123.6, 126.2, 126.7, 127.0, 129.5, 129.7, 130.4, 132.4, 134.2, 135.2, 136.4, 136.8, 139.1, 174.8 ppm. MS (ESI+) m/z: 380.5 $[M + H]^+$. HRMS (ESI+): $[M + H]^+$ calcd for $C_{23}H_{30}N_3O_2$, 379.2260; found, 380.2334.

(*E*)-1-(2-{2-[1-(2′,4′-Bistrifluoromethylbiphenyl-2-yl)-methylidene]hydrazinyl}ethyl)piperidine-3-carboxylic Acid (12ag). According to GP1 from hydrazine **10** (14.4 mg, 77.1 μmol) and **11ag** (24.5 mg, 77.1 μmol), **12ag** was obtained as a yellow, amorphous solid (35.1 mg, yield 93%). ^{1}H NMR (500 MHz, DMSO-d_6): δ 1.25−1.47 (m, 2H), 1.52−1.63 (m, 1H), 1.71−1.81 (m, 1H), 1.94 (t, J = 10.5 Hz, 1H), 2.02−2.15 (m, 1H), 2.25−2.41 (m, 3H), 2.53−2.60 (m, 1H), 2.71−2.84 (m, 1H), 3.03 (t, J = 6.7 Hz, 2H), 7.05 (s, 1H), 7.13 (d, J = 7.6 Hz, 1H), 7.13−7.23 (s_{br}, 1H), 7.22−7.31 (m, 1H), 7.37−7.44 (m, 1H), 7.56−7.63 (m, 1H), 7.81 (d, J = 7.7 Hz, 1H), 8.11 (d, J = 8.1 Hz, 1H), 8.15 (s, 1H) ppm. ^{13}C NMR (126 MHz, DMSO-d_6): δ 23.8, 26.4, 40.9, 45.5, 53.1, 55.3, 56.4, 122.9 (m_{CF}), 123.1 (q, $^1J_{CF}$ = 274.8 Hz), 123.4 (q, $^1J_{CF}$ = 272.8 Hz), 124.0, 126.0, 128.5, 128.7 (q, $^2J_{CF}$ = 32.8 Hz), 128.8 (q, $^2J_{CF}$ = 32.2 Hz), 128.9 (m_{CF}), 129.3, 131.1, 133.7, 134.1, 134.5, 143.8, 175.0 ppm. ^{19}F NMR (471 MHz, DMSO-d_6): δ −61.12 (m), −57.61 (d, J = 2.5 Hz) ppm. MS (ESI+) m/z: 488.3 $[M + H]^+$. HRMS (ESI+): $[M + H]^+$ calcd for $C_{23}H_{24}F_6N_3O_2$, 487.1694; found, 488.1768.

(*E*)-1-(2-{2-[1-(2′-Chloro-4′-fluorobiphenyl-2-yl)-methylidene]hydrazinyl}ethyl)piperidine-3-carboxylic Acid (12ah). According to GP1 from hydrazine **10** (9.93 mg, 53.0 μmol) and **11ah** (12.4 mg, 53.0 μmol), **12ah** was obtained as a yellow, amorphous solid (21.3 mg, yield 100%). ^{1}H NMR (400 MHz, DMSO-d_6): δ 1.26−1.50 (m, 2H), 1.53−1.65 (m, 1H), 1.70−1.84 (m, 1H), 1.98 (t, J = 10.2 Hz, 1H), 2.12 (t, J = 10.0 Hz, 1H), 2.30−2.47 (m, 3H), 2.55−2.65 (m, 1H), 2.80 (d, J = 10.6 Hz, 1H), 3.09 (t, J = 6.7 Hz, 2H), 7.03−7.22 (m, 3H), 7.22−7.43 (m, 4H), 7.56 (dt, J = 8.9/2.3 Hz, 1H), 7.84 (d, J = 7.9 Hz, 1H) ppm. ^{13}C NMR (126 MHz, DMSO-d_6): δ 24.0, 26.5, 41.0, 45.5, 53.3, 55.4, 56.4, 114.5 (d, $^2J_{CF}$ = 21.3 Hz), 116.5 (d, $^2J_{CF}$ = 24.7 Hz), 123.7, 126.7, 128.1, 130.0, 131.2, 133.0 (d, $^3J_{CF}$ = 8.7 Hz), 133.4 (d, $^3J_{CF}$ = 10.5 Hz), 134.4, 135.3 (d, $^4J_{CF}$ = 3.6 Hz), 135.6, 161.4 (d, $^1J_{CF}$ = 247.8 Hz), 175.1 ppm. ^{19}F NMR (471 MHz, DMSO-d_6): δ −112.61 (tdd, J = 8.8/6.3/2.4 Hz) ppm. MS (ESI +) m/z: 404.3 $[M + H]^+$. HRMS (ESI+): $[M + H]^+$ calcd for $C_{21}H_{24}ClFN_3O_2$, 404.1541; found, 404.1537.

(*E*)-1-(2-{2-[1-(4′-Chloro-4-fluorobiphenyl-2-yl)methylidene]-hydrazinyl}ethyl)piperidine-3-carboxylic Acid (12ak). According to GP1 from hydrazine **10** (8.91 mg, 47.6 μmol) and **11ak** (11.2 mg, 47.6 μmol), **12ak** was obtained as a yellow, amorphous solid (19.3 mg, yield 100%). ^{1}H NMR (400 MHz, DMSO-d_6): δ 1.24−1.42 (m, 1H), 1.37−1.51 (m, 1H), 1.53−1.67 (m, 1H), 1.70−1.84 (m, 1H), 2.00 (t, J = 10.3 Hz, 1H), 2.13 (t_{br}, J = 10.3 Hz, 1H), 2.38 (tt, J = 9.8/3.7 Hz, 1H), 2.44 (t, J = 6.6 Hz, 2H), 2.56−2.67 (m, 1H), 2.82 (d_{br}, J = 10.7 Hz, 1H), 3.15 (t, J = 6.5 Hz, 2H), 7.10 (td, J = 8.4/2.8 Hz, 1H), 7.25 (dd, J = 8.5/5.9 Hz, 1H), 7.29−7.37 (m, 3H), 7.38−7.48 (m, 1H), 7.48−7.54 (m, 2H), 7.52−7.56 (m, 1H) ppm. ^{13}C NMR (101 MHz, DMSO-d_6): δ 23.9, 26.4, 41.0, 45.3, 53.2, 55.3, 56.3, 109.5 (d, $^2J_{CF}$ = 22.7 Hz) 113.7 (d, $^2J_{CF}$ = 22.1 Hz), 128.3 (2C), 129.7 (d, $^4J_{CF}$ = 2.7 Hz), 131.3 (2C), 132.1 (d, $^3J_{CF}$ = 8.7 Hz), 132.1, 134.1 (d, $^4J_{CF}$ = 2.5 Hz), 136.2, 137.8, 161.7 (d, $^1J_{CF}$ = 244.3 Hz), 175.0 ppm. ^{19}F NMR (471 MHz, DMSO-d_6): δ −114.45 (m) ppm. MS (ESI+) m/z: 404.2 $[M + H]^+$. HRMS (ESI+): $[M + H]^+$ calcd for $C_{21}H_{24}ClFN_3O_2$, 404.1541; found, 404.1539.

[(*E*)-5-(4,4,5,5-Tetramethyl-1,3,2-dioxaborolan-2-yl)pent-1-enyl]-4-methylbenzene Sulfonate (17). Chlorobis-(cyclopentadienyl)hydridozirconium (258 mg, 1.00 mmol) was added to a mixture of pent-4-ynyl-4-methylbenzenesulfonate[43] (2.38 g, 10.0 mmol) and 4,4,5,5-tetramethyl-1,3,2-dioxaborolane (1.41 g, 11.0 mmol). The mixture was stirred at room temperature for 48 h and afterward diluted with CH_2Cl_2. The solution was filtered through a short pad of silica gel (2 cm) and washed with CH_2Cl_2. The filtrate was concentrated and dried in vacuo to give **17** as a colorless, high viscous liquid (3.48 g, 95%). ^{1}H NMR (400 MHz, $CDCl_3$): δ 1.24 (s, 12H), 1.75 (p, J = 6.9 Hz, 2H), 2.15 (q, J = 6.9 Hz, 2H), 2.44 (s, 3H), 4.01 (t, J = 6.4 Hz, 2H), 5.33 (dt, J = 17.9/1.4 Hz, 1H), 6.47 (dt, J = 18.0/6.4 Hz, 1H), 7.33 (dd, J = 8.0/0.6 Hz, 2H), 7.77 (d, J = 8.4 Hz, 2H) ppm. ^{13}C NMR (101 MHz, $CDCl_3$): δ 21.6, 24.7 (4C), 27.3, 31.3, 69.8, 83.1 (2C), 120.0,[47] 127.9 (2C), 129.8 (2C), 133.0, 144.7, 151.7 ppm. MS (ESI+) m/z: 367.1 $[M + H]^+$. HRMS (EI, 70 eV): M^+ calcd for $C_{18}H_{27}BO_5S$, 366.1672; found, 366.1670.

Ethyl 1-[(*E*)-5-(4,4,5,5-Tetramethyl-1,3,2-dioxaborolan-2-yl)-pent-1-enyl]piperidine-3-carboxylate (18). Ethyl nipecotate (1.96 g, 12.5 mmol) was added to [(*E*)-5-(4,4,5,5-tetramethyl-1,3,2-dioxaborolan-2-yl)pent-4-enyl]-4-methylbenzene sulfonate (1.83 g, 5.00 mmol), and the mixture was stirred at room temperature for 16 h. Then water was added, and the aqueous phase was extracted with CH_2Cl_2. The organic phase was washed with water and concentrated under reduced pressure. The residue was dissolved in Et_2O and filtered through a short pad of silica gel (3 cm). The filtrate was concentrated and dried in high vacuum to give **18** as a pale yellow liquid (1.62 g, 4.6 mmol, 92%). The product was used without further purification. ^{1}H NMR (400 MHz, $CDCl_3$): δ 1.19−1.26 (m, 15H), 1.33−1.45 (m, 1H), 1.46−1.64 (m, 3H), 1.68 (dp, J = 10.4/3.5 Hz, 1H), 1.84−1.97 (m, 2H), 2.01−2.17 (m, 3H), 2.23−2.34 (m, 2H), 2.51 (tt, J = 10.6/3.7 Hz, 1H), 2.72 (d, J = 11.1 Hz, 1H), 2.94 (d, J = 10.1 Hz, 1H), 4.09 (q, J = 7.2 Hz, 2H), 5.40 (d, J = 18.0 Hz, 1H), 6.60 (dt, J = 17.9/6.4 Hz, 1H) ppm. ^{13}C NMR (101 MHz, $CDCl_3$): δ 14.14, 24.53, 24.7 (4C), 25.3, 27.0, 33.6, 41.8, 53.7, 55.4, 58.2, 60.2, 82.9 (2C), 154.0, 174.2 ppm. MS (ESI+) m/z: 352 $[M + H]^+$. HRMS (EI, 70 eV): M^+ calcd for $C_{19}H_{34}BNO_4$, 351.2580; found, 351.2572.

Ethyl 1-[(*E*)-5-(2-Bromophenyl)pent-1-enyl]piperidine-3-carboxylate (19). Under nitrogen atmosphere Pd(dppf)Cl_2·CH_2Cl_2 (41 mg, 0.025 mmol), 1-bromo-2-iodobenzene (312 mg, 1.10 mmol), and compound **18** (351 mg, 1.00 mmol) were dissolved in a mixture of 1,4-dioxane/water 2:1 (1.5 mL) and K_2CO_3 (414 mg, 3.00 mmol). The resulting mixture was stirred at room temperature for 72 h. After addition of water (5 mL) the mixture was extracted three times with CH_2Cl_2 (10 mL). The combined organic layers were dried over Na_2SO_4, and the solvent was removed in vacuo. The residue was purified by flash column chromatography on silica gel (*n*-pentane/CH_2Cl_2/EtOAc = 8/1/1 + 2% Et_3N, R_f = 0.3) to give the **19** as a colorless oil (342 mg, 90%). ^{1}H NMR (400 MHz, $CDCl_3$): δ 1.25 (t, J = 7.1 Hz, 3H), 1.44 (qd, J = 12.2/4.0 Hz, 1H), 1.52−1.65 (m, 1H), 1.65−1.77 (m, 3H), 1.90−2.03 (m, 2H), 2.15 (t, J = 10.6 Hz, 1H,), 2.27 (q, J = 6.9 Hz, 2H), 2.37−2.43 (m, 2H), 2.57 (tt, J = 10.6/3.8 Hz, 1H), 2.79 (d, J = 11.0 Hz, 1H), 3.01 (d, J = 10.4 Hz, 1H), 4.13 (q, J = 7.1 Hz, 2H), 6.16 (dt, J = 15.6/6.9 Hz, 1H), 6.71 (d, J = 15.7 Hz, 1H), 7.05 (td, J = 7.9/1.5 Hz, 1H), 7.24 (td, J = 7.5/0.7 Hz, 1H), 7.48 (dd, J = 7.8/1.4 Hz, 1H), 7.52 (dd, J = 8.0/0.7 Hz, 1H) ppm. ^{13}C NMR (101 MHz, $CDCl_3$): δ 14.2, 24.6, 26.3, 27.0, 30.9, 41.9, 53.8, 55.4, 58.2, 60.2, 123.1, 126.7, 127.3, 128.1, 128.9, 132.7, 133.5, 137.5, 174.2 ppm. MS (CI, CH_5^+) m/z: 381 $[M + H]^+$. HRMS (EI, 70 eV): M^+ calcd for $C_{19}H_{26}BrNO_2$, 379.1147; found, 379.1128.

Ethyl 1-[(*E*)-5-(2′-Fluorobiphenyl-2-yl)pent-4-en-1-yl]-piperidine-3-carboxylate (21c). According to the GP2 from **19** (114 mg, 0.300 mmol) and **20c** (46 mg, 0.33 mmol), **21c** was obtained

as a slightly yellow oil (110 mg, 93%). ^{1}H NMR (500 MHz, $CDCl_3$): δ 1.24 (t, J = 7.1 Hz, 3H), 1.42 (qd, J = 11.9/3.6 Hz, 1H), 1.50−1.61 (m, 3H), 1.70 (dp, J = 13.0/3.7 Hz, 1H), 1.89−1.97 (m, 2H), 2.06−2.14 (m, 3H), 2.28−2.33 (m, 2H), 2.53 (tt, J = 10.7/3.8 Hz, 1H), 2.73 (d, J = 11.1 Hz, 1H), 2.95 (d, J = 10.0 Hz, 1H), 4.12 (q, J = 7.1 Hz, 2H), 6.13 (dt, J = 15.7/6.7 Hz, 1H), 6.21 (d, J = 16.0 Hz, 1H), 7.13 (ddd, J = 9.8/8.2/1.1 Hz, 1H), 7.18 (td, J = 7.4/1.1 Hz, 1H), 7.21−7.28 (m, 3H), 7.31−7.37 (m, 2H), 7.59 (d, J = 7.7 Hz, 1H) ppm. ^{13}C NMR (126 MHz, $CDCl_3$): δ 14.2, 24.6, 26.4, 27.0, 31.0, 41.9, 53.8, 55.4, 58.2, 60.2, 115.5 (d, $^2J_{CF}$ = 22.4 Hz), 123.8 (d, $^4J_{CF}$ = 3.7 Hz), 125.3, 126.6, 128.0, 128.2, 128.5 (d, $^2J_{CF}$ = 16.3 Hz), 129.1 (d, $^3J_{CF}$ = 7.9 Hz), 130.5, 131.8, 132.1 (d, $^3J_{CF}$ = 3.5 Hz), 134.0, 136.5, 159.6 (d, $^1J_{CF}$ = 246.6 Hz), 174.3 ppm. MS (CI, CH_5^+) m/z: 396 [M + H]$^+$. HRMS (EI, 70 eV): M$^+$ calcd for $C_{25}H_{30}FNO_2$, 395.2261; found, 395.2265.

Ethyl 1-[(*E*)-5-(2′,4′-Difluorobiphenyl-2-yl)pent-4-en-1-yl]-piperidine-3-carboxylate (21g). According to GP2 from **19** (114 mg, 0.300 mmol) and **20g** (52 mg, 0.33 mmol), **21g** was obtained as a slightly yellow oil (113 mg, 91%). ^{1}H NMR (500 MHz, $CDCl_3$): δ 1.25 (t, J = 7.1 Hz, 3H), 1.42 (qd, J = 11.9/3.8 Hz, 1H), 1.49−1.64 (m, 3H), 1.71 (dp, J = 13.0/3.6 Hz, 1H), 1.89−1.97 (m, 2H), 2.05−2.16 (m, 3H), 2.28−2.35 (m, 2H), 2.54 (tt, J = 10.6/3.8 Hz, 1H), 2.74 (d, J = 10.6 Hz, 1H), 2.97 (d, J = 10.5 Hz, 1H), 4.12 (q, J = 7.1 Hz, 2H), 6.08−6.22 (m, 2H), 6.87−6.97 (m, 2H), 7.17−7.23 (m, 2H), 7.27 (td, J = 7.6/1.3 Hz, 1H), 7.35 (td, J = 7.6/1.2 Hz, 1H), 7.59 (d, J = 7.8 Hz, 1H) ppm. ^{13}C NMR (126 MHz, $CDCl_3$): δ 14.2, 24.6, 26.4, 27.0, 31.0, 41.9, 53.8, 55.5, 58.2, 60.3, 103.9 (dd, $^{2/2}J_{CF}$ = 26.4/25.2 Hz), 111.0 (dd, $^{2/4}J_{CF}$ = 21.0/3.8 Hz), 124.61 (dd, $^{2/4}J_{CF}$ = 16.6/3.8 Hz), 125.5, 126.7, 128.0, 128.2, 130.6, 132.1, 132.7 (dd, $^{3/3}J_{CF}$ = 9.5/5.0 Hz), 133.0, 136.7, 159.6 (dd, $^{1/3}J_{CF}$ = 249.2/11.9 Hz), 162.4 (dd, $^{1/3}J_{CF}$ = 248.4/11.5 Hz), 174.3 ppm. MS (CI, CH_5^+) m/z: 414 [M + H]$^+$. HRMS (EI, 70 eV): M$^+$ calcd for $C_{25}H_{29}F_2NO_2$, 413.2166; found, 413.2164.

Ethyl 1-[(*E*)-5-(2′-Chlorobiphenyl-2-yl)pent-4-en-1-yl]-piperidine-3-carboxylate (21p). According to the GP2 from **19** (114 mg, 0.300 mmol) and **20p** (52 mg, 0.33 mmol), **21p** was obtained as a slightly yellow oil (115 mg, 93%). ^{1}H NMR (500 MHz, $CDCl_3$): δ 1.24 (t, J = 7.1 Hz, 3H), 1.40 (qd, J = 11.7/3.7 Hz, 1H), 1.48−1.59 (m, 3H), 1.70 (dp, J = 13.1/3.6 Hz, 1H), 1.90 (m, 2H), 2.02−2.11 (m, 3H), 2.25−2.31 (m, 2H), 2.52 (tt, J = 10.6/3.8 Hz, 1H), 2.72 (d, J = 11.1 Hz, 1H), 2.94 (d, J = 10.4 Hz, 1H), 4.11 (q, J = 7.1 Hz, 2H), 6.02−6.15 (m, 2H), 7.15 (d, J = 7.5 Hz, 1H), 7.21−7.31 (m, 4H), 7.34 (t, J = 7.6 Hz, 1H), 7.43−7.47 (m, 1H), 7.59 (d, J = 7.8 Hz, 1H) ppm. ^{13}C NMR (101 MHz, $CDCl_3$): δ 14.2, 24.6, 26.4, 27.0, 31.0, 41.9, 53.8, 55.4, 58.2, 60.3, 125.0, 126.4 (2C), 128.0 (2C), 128.6, 129.4, 130.0, 131.6, 131.8, 133.5, 136.2, 137.6, 139.8, 174.3 ppm. MS (CI, CH_5^+) m/z: 412 [M + H]$^+$. HRMS (EI, 70 eV): M$^+$ calcd for $C_{25}H_{30}ClNO_2$, 411.1965; found, 411.1966.

Ethyl 1-[(*E*)-5-(2′,4′-Dichlorobiphenyl-2-yl)pent-4-en-1-yl]-piperidine-3-carboxylate (21z). According to the GP2 from **19** (114 mg, 0.300 mmol) and **20z** (63 mg, 0.33 mmol), **21z** was obtained as a slightly yellow oil (123 mg, 92%). ^{1}H NMR (400 MHz, $CDCl_3$, 21 °C, TMS): δ 1.25 (t, J = 7.1 Hz, 3H), 1.42 (qd, J = 12.0/3.7 Hz, 1H), 1.49−1.62 (m, 3H), 1.71 (dp, J = 13.2/3.6 Hz, 1H), 1.89−1.97 (m, 2H), 2.05−2.13 (m, 3H), 2.27−2.32 (m, 2H), 2.53 (td, J = 10.6/5.3 Hz, 1H), 2.73 (d, J = 11.0 Hz, 1H), 2.96 (d, J = 10.6 Hz, 1H), 4.12 (q, J = 7.1 Hz, 2H), 6.03 (d, J = 15.8 Hz, 1H), 6.13 (dt, J = 15.7/6.7 Hz, 1H), 7.12 (dd, J = 7.5/1.0 Hz, 1H), 7.17 (d, J = 8.2 Hz, 1H), 7.24−7.31 (m, 2H), 7.36 (td, J = 7.7/1.0 Hz, 1H), 7.49 (t, J = 1.7 Hz, 1H), 7.59 (d, J = 7.8 Hz, 1H) ppm. ^{13}C NMR (101 MHz, $CDCl_3$): δ 14.2, 24.6, 26.4, 27.0, 31.0, 41.9, 53.8, 55.4, 58.2, 60.3, 125.2, 126.6, 126.8, 127.6, 128.3, 129.2, 129.9, 132.2, 132.4, 133.7, 134.4, 136.3, 136.4, 138.5, 174.3 ppm. MS (CI, CH_5^+) m/z: 446 [M + H]$^+$. HRMS (EI, 70 eV): M$^+$ calcd for $C_{25}H_{29}Cl_2NO_2$, 445.1575; found, 445.1549.

Ethyl 1-[(*E*)-5-(2′-Chloro-4′-fluorobiphenyl-2-yl)pent-4-en-1-yl]piperidine-3-carboxylate (21ah). According to the GP2 from **19** (114 mg, 0.300 mmol) and **20ah** (58 mg, 0.33 mmol), **21ah** was obtained as slightly yellow oil (117 mg, 91%). ^{1}H NMR (500 MHz, $CDCl_3$): δ 1.25 (t, J = 7.1 Hz, 3H), 1.42 (qd, J = 12.3/3.9 Hz, 1H), 1.51−1.61 (m, 3H), 1.71 (dp, J = 13.4/3.6 Hz, 1H), 1.89−1.97 (m, 2H), 2.04−2.14 (m, 3H), 2.25−2.33 (m, 2H), 2.53 (tt, J = 10.6/3.8 Hz, 1H), 2.72 (d, J = 10.8 Hz, 1H), 2.96 (d, J = 10.1 Hz, 1H), 4.12 (q, J = 7.1 Hz, 2H), 6.03 (d, J = 15.8 Hz, 1H), 6.12 (dt, J = 15.6/6.7 Hz, 1H), 7.03 (td, J = 8.3/2.6 Hz, 1H), 7.12 (dd, J = 7.6/1.2 Hz, 1H), 7.18−7.28 (m, 3H), 7.35 (td, J = 7.7/1.1 Hz, 1H), 7.58 (d, J = 7.5 Hz, 1H) ppm. ^{13}C NMR (126 MHz, $CDCl_3$): δ 14.2, 24.6, 26.3, 27.0, 31.0, 41.8, 53.8, 55.4, 58.1, 60.2, 113.8 (d, $^2J_{CF}$ = 20.9 Hz), 116.6 (d, $^2J_{CF}$ = 24.5 Hz), 125.1, 126.5, 127.7, 128.2, 130.1, 132.0, 132.5 (d, $^3J_{CF}$ = 8.6 Hz), 134.2 (d, $^3J_{CF}$ = 10.3 Hz), 136.0 (d, $^4J_{CF}$ = 3.4 Hz), 136.4, 136.6, 161.7 (d, $^1J_{CF}$ = 249.3 Hz), 174.2 ppm. MS (ESI+) m/z: 430 [M + H]$^+$. HRMS (EI, 70 eV): M$^+$ calcd for $C_{25}H_{29}ClFNO_2$, 429.1871; found, 429.1875.

1-[(*E*)-5-(2′-Fluorobiphenyl-2-yl)pent-4-en-1-yl]piperidine-3-carboxylic Acid (13c). According to GP3 from **21c** (79 mg, 0.20 mmol), **13c** was obtained as a slightly yellow solid (63 mg, 86%). ^{1}H NMR (400 MHz, 0.1 M NaOD/CD_3OD = 1/2, 60 °C): δ 1.37 (qd, J = 12.7/4.1 Hz, 1H), 1.52−1.75 (m, 4H), 1.91 (td, J = 11.6/2.5 Hz, 1H), 2.02 (m, 2H), 2.11 (q, J = 7.1 Hz, 2H), 2.29−2.45 (m, 3H), 2.86 (d, J = 10.6 Hz, 1H), 3.11 (d, J = 9.8 Hz, 1H), 6.09−6.26 (m, 2H), 7.16−7.23 (m, 2H), 7.23−7.33 (m, 3H), 7.37 (t, J = 7.6 Hz, 1H), 7.40−7.48 (m, 1H), 7.61 (d, J = 7.9 Hz, 1H) ppm. ^{13}C NMR (101 MHz, NaOD/CD_3OD = 1/2, 60 °C): δ 25.8 26.8, 29.4, 32.0, 46.3, 54.8, 58.2, 59.5, 116.4 (d, $^2J_{CF}$ = 22.5 Hz), 125.1 (d, $^4J_{CF}$ = 3.8 Hz), 126.6, 127.7, 129.1, 129.7, 130.0 (s, $^2J_{CF}$ = 16.7 Hz), 130.5 (d, $^3J_{CF}$ = 7.9 Hz), 131.3, 132.8, 133.0 (d, $^3J_{CF}$ = 3.4 Hz), 135.5, 138.0, 161.0 (d, $^1J_{CF}$ = 244.7 Hz), 182.9 ppm. MS (CI, CH_5^+) m/z: 368 [M + H]$^+$. HRMS (EI, 70 eV): M$^+$ calcd for $C_{23}H_{26}FNO_2$, 367.1948; found, 367.1949. Purity: 98.5% (HPLC).

1-[(*E*)-5-(2′,4′-Difluorobiphenyl-2-yl)pent-4-en-1-yl]-piperidine-3-carboxylic Acid (13g). According to the GP3, starting from **21g** (83 mg, 0.20 mmol), **13g** was obtained as a slightly yellow solid (68 mg, 88%). ^{1}H NMR (400 MHz, 0.1 M NaOD/CD_3OD = 1/1, 60 °C): δ 1.25 (qd, J = 12.7/4.2 Hz, 1H), 1.35−1.52 (m, 3H), 1.58 (d, J = 13.5 Hz, 1H), 1.68 (td, J = 11.7/2.3 Hz, 1H), 1.80−1.98 (m, 4H), 2.04−2.14 (m, 1H), 2.14−2.26 (m, 1H), 2.33 (tt, J = 12.0/3.8 Hz, 1H), 2.63 (d, J = 10.1 Hz, 1H), 2.96 (d, J = 11.1 Hz, 1H), 5.90−6.07 (m, 2H), 6.65−6.75 (m, 2H), 6.85−6.95 (m, 2H), 6.99 (t, J = 7.5 Hz, 1H), 7.12 (t, J = 7.4 Hz, 1H), 7.41 (d, J = 7.9 Hz, 1H) ppm. ^{13}C NMR (101 MHz, 0.1 M NaOD/CD_3OD = 1/1, 60 °C): δ 25.1, 25.9, 28.7, 31.5, 45.6, 53.6, 57.4, 58.7, 104.4 (d, $^2J_{CF}$ = 26.5 Hz), 111.8 (d, $^2J_{CF}$ = 21.2, $^3J_{CF}$ = 3.5 Hz), 125.4 (dd, $^{2/4}J_{CF}$ = 16.6/3.1 Hz), 126.4, 127.4, 128.6, 129.1, 131.1, 133.1, 133.28 (dd, $^{3/3}J_{CF}$ = 9.5/5.0 Hz), 133.6, 137.3, 160.2 (dd, $^{1/3}J_{CF}$ = 247.2/11.3 Hz), 163.0 (dd, $^{1/3}J_{CF}$ = 247.7/11.4 Hz), 183.4 ppm. MS (CI, CH_5^+) m/z: 386 [M + H]$^+$. HRMS (EI, 70 eV): M$^+$ calcd for $C_{23}H_{25}F_2NO_2$, 385.1853; found, 385.1853. Purity: 100% (HPLC).

1-[(*E*)-5-(2′-Chlorobiphenyl-2-yl)pent-4-en-1-yl]piperidine-3-carboxylic Acid (13p). According to the GP3, starting from **21p** (82 mg, 0.20 mmol), **13p** was obtained as a slightly yellow solid (67 mg, 87%). ^{1}H NMR (400 MHz, 0.1 M NaOD/CD_3OD = 2/1, 60 °C, MeOH): δ 1.24 (qd, J = 12.8/4.2 Hz, 1H), 1.32−1.51 (m, 3H), 1.57 (d, J = 13.2 Hz, 1H), 1.66 (td, J = 11.5/2.1 Hz, 1H), 1.74−1.98 (m, 4H), 2.00−2.11 (m, 1H), 2.11−2.23 (m, 1H), 2.32 (tt, J = 11.5/3.4 Hz, 1H), 2.61 (d, J = 10.8 Hz, 1H), 2.94 (d, J = 9.6 Hz, 1H), 5.88−5.99 (m, 2H), 6.83 (d, J = 7.4 Hz, 1H), 6.89−6.97 (m, 2H), 6.99−7.11 (m, 3H), 7.23 (d, J = 7.1 Hz, 1H), 7.39 (d, J = 8.2 Hz, 1H) ppm. ^{13}C NMR (101 MHz, 0.1 M NaOD/CD_3OD = 2/1, 60 °C, MeOH): δ 25.1, 26.0, 28.7, 31.6, 45.5, 53.6, 57.5, 58.7, 126.1, 127.3, 127.5, 128.7, 128.9, 129.7, 130.1, 130.6, 132.3, 132.7, 133.9, 136.8, 138.3, 140.5, 183.4 ppm. MS (CI, CH_5^+) m/z: 384 [M + H]$^+$. HRMS (EI, 70 eV): M$^+$ calcd for $C_{23}H_{26}ClNO_2$, 383.1652; found, 383.1635. Purity: 100% (HPLC)

1-[(*E*)-5-(2′,4′-Dichlorobiphenyl-2-yl)pent-4-en-1-yl]-piperidine-3-carboxylic Acid (13z). According to GP3 from **21z** (89 mg, 0.20 mmol), **13z** was obtained as a slightly yellow solid (75 mg, 90%). ^{1}H NMR (400 MHz, 0.1 M NaOD/CD_3OD = 2/1, 60 °C): δ 1.28 (qd, J = 12.4/3.8 Hz, 1H), 1.40−1.54 (m, 3H), 1.60 (d, J = 12.8 Hz, 1H), 1.71 (t, J = 11.3 Hz, 1H), 1.80−2.01 (m, 4H), 2.04−2.16 (m, 1H), 2.22 (m, 1H), 2.34 (tt, J = 11.6/3.6 Hz, 1H), 2.66 (d, J = 10.4 Hz, 1H), 2.99 (d, J = 10.9 Hz, 1H), 5.88−6.03 (m, 2H), 6.81 (d, J = 7.4 Hz, 1H), 6.86 (d, J = 8.0 Hz, 1H), 6.93−7.04 (m, 2H), 7.13 (t, J =

7.4 Hz, 1H), 7.24 (s, 1H), 7.42 (d, J = 7.7 Hz, 1H). ^{13}C NMR (101 MHz, 0.1 M NaOD/CD_3OD = 2/1, 60 °C): δ 25.4, 26.3, 28.9, 31.8, 45.7, 54.1, 57.9, 59.0, 126.4, 127.4, 127. 7, 128.6, 129.2, 129.8, 130.5, 133.2, 133.3, 134.4, 135.0, 137.1, 137.2, 139.5, 183.1 ppm. MS (CI, CH_5^+) m/z: 418 $[M + H]^+$. HRMS (EI, 70 eV): M^+ calcd for $C_{23}H_{25}Cl_2NO_2$, 417.1262; found, 417.1257. Purity: 99.2% (HPLC).

1-[(*E*)-5-(2′-Chloro-4′-fluorobiphenyl-2-yl)pent-4-en-1-yl]-piperidine-3-carboxylic Acid (13ah). According to GP3 from **21ah** (86 mg, 0.20 mmol), **13ah** was obtained as a slightly yellow solid (75 mg, 90%). ^{1}H NMR (400 MHz, NaOD/CD_3OD = 1/2, 60 °C): δ 1.36 (qd, J = 12.6/4.1 Hz, 1H), 1.51−1.65 (m, 3H), 1.71 (dp, J = 13.5/3.3 Hz, 1H), 1.89−2.00 (m, 2H), 2.01−2.13 (m, 3H), 2.27−2.44 (m, 3H), 2.84 (d, J = 11.0 Hz, 1H), 3.06 (d, J = 11.3 Hz, 1H), 6.00−6.17 (m, 2H), 7.11 (dd, J = 7.6/1.0 Hz, 1H), 7.18 (td, J = 8.4/2.5 Hz, 1H), 7.21−7.27 (m, 1H), 7.28−7.36 (m, 2H), 7.40 (td, J = 7.4/1.0 Hz, 1H), 7.61 (d, J = 7.3 Hz, 1H) ppm. ^{13}C NMR (101 MHz, NaOD/CD_3OD = 1/2, 60 °C): δ 25.2, 26.0, 28.8, 31.7, 45.7, 54.3, 57.5, 58.9, 115.0 (d, $^2J_{CF}$ = 21.3 Hz), 117.3 (d, $^2J_{CF}$ = 25.2 Hz), 126.4, 127.7, 128.9, 129.3, 130.8, 133.1, 133.6 (d, $^3J_{CF}$ = 8.8 Hz), 134.9 (s, $^3J_{CF}$ = 10.2 Hz), 137.3, 137.5, 137.8, 163.0 (s, $^1J_{CF}$ = 248.2 Hz), 182.9 ppm. MS (ESI+) m/z: 402 $[M + H]^+$. HRMS (EI, 70 eV): M^+ calcd for $C_{23}H_{25}ClFNO_2$, 401.1558; found, 401.1558. Purity: 98.0% (HPLC).

Aldehydes. Detailed synthesis protocols for aldehydes are found in the Supporting Information.

MS Binding Experiments. mGAT1 Membrane Preparation. Membrane preparations of HEK293 cells stably expressing mGAT1[48] were prepared as described previously and stored at −80 °C.[25,49] On the day of the assay, an aliquot was rapidly thawed and diluted in a 20-fold volume of cold aqueous 0.9% NaCl (m/v). After centrifugation at 15 000 rpm and 4 °C for 20 min (CP56GII, P70AT, Hitachi Ltd., Tokyo, Japan), the pellet was resuspended in ice-cold assay buffer (see below) to a protein concentration of approximately 0.1 mg/mL[49] as previously described.[28]

Library Screening. Library screening experiments were performed as reported.[28] In short, quadruplicate samples in a total volume of 250 μL were employed. Phosphate buffer, pH 7.1 (12.5 mM $Na_2HPO_4{\cdot}2H_2O$, 12.5 mM $NaH_2PO_4{\cdot}H_2O$, 1 M NaCl adjusted with 2 M NaOH), was used as incubation buffer. Each sample contained 1% DMSO as final concentration. All solutions were added as 10-fold concentrated stock solutions. Aldehydes were present at 10 μM in the sample, hydrazine **10** at 100 μM. By addition of the mGAT1 membrane preparation, directly after combining hydrazine and aldehydes, a first incubation period of 4 h (for library generation) at 37 °C in a shaking water bath was started. The second incubation period of 40 min was started by addition of the MS marker **6** (20 nM final concentration in the sample). The binding experiment was stopped by a vacuum filtration step (96-well filter plate, Acroprep, glass fiber, 1.0 μm, 350 μL, Pall, Dreieich, Germany, 12-channel pipet). After multiple washing steps with ice-cold aqueous 1 M NaCl, the filter was dried (60 min, 50 °C) and cooled to room temperature. Subsequently the marker was liberated by elution of the filter plate with MeOH into a 96-deep-well plate. Each sample was supplemented with 200 μL of 1 nM $[^2H_{10}]$NO711 (in MeOH) as internal standard. For calibration, matrix blank samples (produced analogously in absence of NO711) were supplemented with 200 μL of methanolic calibration standards, 50 pM, 100 pM, 500 pM, or 1 nM NO711, and 200 μL of 1 nM $[^2H_{10}]$NO711 (in MeOH). All samples were dried to completeness (50 °C). For quantification by LC−ESI-MS/MS, samples were reconstituted in 200 μL of 10 mM ammonium formate buffer (pH 7.0)/MeOH (95:5, v/v).

As stated before, each library screening experiment included samples characterizing the pure aldehyde libraries and the pure hydrazine **10**, as well as matrix blanks and zero samples. Total binding and nonspecific binding of NO711 were determined as previously described.[28] If the nonspecific binding of the 20 nM NO711 concentration employed was less than 50 pM, the value was extrapolated by linear regression of the nonspecific binding of NO711 concentrations, >20 nM.

By employment of the results obtained for the calibration samples, calibration curves for marker quantitation were generated.

Deconvolution Experiments. The deconvolution experiments were carried out in the same way[28] as described for library screening except that the single aldehyde (10 μM per sample) was applied instead of the mixture of four aldehydes.

Competition Experiments Applying Pure Hydrazones. These experiments were performed as recently described,[25,49] applying the incubation buffer as described for "Library Screening".

LC−ESI-MS/MS. The methanolic eluates were dried and reconstituted with 10 mM ammonium formate buffer (pH 7.0)/methanol (95:5, v/v). Quantitation by LC−ESI-MS/MS was performed as described utilizing a API 3200 triple-quadrupole mass spectrometer.[25,49]

Analysis of Binding Experiments. Marker depletion was negligible (<10%) in all binding experiments. Specific binding was defined as the difference between total and nonspecific binding. A nonspecific binding less than 50 pM was not determined experimentally but extrapolated by linear regression for nonspecifically bound NO711 concentrations of ≥50 pM. The concentration of a competitor that inhibits 50% of specific binding (IC_{50}) was calculated from competition curves, plotting specifically bound NO711 concentrations vs log competitor concentration (eight different concentrations per competitor) with Prism 4.02 (GraphPad Software, San Diego, CA, U.S.) using the equation for one-site competition and nonlinear curve fitting. Specific binding determined for control samples in the absence of any competitor was set to 100%, whereas the bottom level was set to 0% (corresponds to the nonspecific binding of the employed NO711 concentration). K_i values were calculated according to Cheng and Prussoff[50] and were expressed as pK_i values. All results are expressed as the mean ± SEM (unless stated otherwise). pK_i values were determined in at least three separate experiments.

GABA Uptake Assays. [^{3}H]GABA uptake assays were performed as previously described.[48]

■ ASSOCIATED CONTENT

Ⓢ Supporting Information

General procedures for the synthesis of aldehydes and references and detailed analytic data of aldehydes. This material is available free of charge via the Internet at http://pubs.acs.org.

■ AUTHOR INFORMATION

Corresponding Author

*Phone: +49 2180 77249. Fax: +49 2180 77247. E-mail: Klaus.Wanner@cup.uni-muenchen.de.

Present Address

†Clinical Trial Oncology, Ente Ospedaliero Ospedali Galliera, Mura delle Cappuccine 14, 16128 Genova, Italy.

Notes

The authors declare no competing financial interest.

■ ACKNOWLEDGMENTS

Special thanks go to Silke Duensing-Kropp and Ljiljana Galogaza for excellent technical support.

■ DEDICATION

Dedicated to Professor H. Zipse with warm wishes on the occasion of his 50th birthday.

■ ABBREVIATIONS USED

BGT, betain γ-aminobutyric acid transporter; CC, column chromatography; DAD, diode array detector; DCC, dynamic combinatorial chemistry; GAT, γ-aminobutyric acid transporter; GP, general procedure; HUGO, human genome organization; IC_{10}, inhibitor concentration that reduces signal to 10%; IC_{20}, inhibitor concentration that reduces signal to

20%; LLOQ, lower limit of quantification; SLC6, solute carrier 6

REFERENCES

(1) Bowery, N. G.; Smart, T. G. GABA and glycine as neurotransmitters: a brief history. *Br. J. Pharmacol.* **2006**, *147*, S109−S119.

(2) Beleboni, R. O.; Carolino, R. O. G.; Pizzo, A. B.; Castellan-Baldan, L.; Coutinho-Netto, J.; dos Santos, W. F.; Coimbra, N. C. Pharmacological and biochemical aspects of GABAergic neurotransmission: pathological and neuropsychobiological relationships. *Cell. Mol. Neurobiol.* **2004**, *24*, 707−728.

(3) Owens, D. F.; Kriegstein, A. R. Is there more to GABA than synaptic inhibition? *Nat. Rev. Neurosci.* **2002**, *3*, 715−727.

(4) Geffen, Y.; Nudelman, A.; Gil-Ad, I.; Raphaeli, A.; Huang, M.; Savitsky, K.; Klapper, L.; Winkler, I.; Meltzer, H. Y.; Weizman, A. BL-1020: A novel antipsychotic drug with GABAergic activity and low catalepsy is efficacious in a rat model of schizophrenia. *Eur. Neuropsychopharmacol.* **2009**, *19*, 1−13.

(5) Ishiwari, K.; Mingot, S.; Correa, M.; Trevitt, J. T.; Carlson, B. B.; Salamone, J. D. The GABA uptake inhibitor β-alanine reduces pilocarpine-induced tremor and increases extracellular GABA in substantia nigra pars reticulata as measured by microdialysis. *J. Neurosci. Methods* **2004**, *140*, 39−46.

(6) Treiman, D. M. GABAergic mechanisms in epilepsy. *Epilepsia* **2001**, *42* (Suppl. 3), 8.

(7) Aoyagi, T.; Wada, T.; Nagai, M.; Kojima, F.; Harada, S.; Takeuchi, T.; Takahashi, H.; Hirokawa, K.; Tsumita, T. Increased γ-aminobutyrate aminotransferase activity in brain of patients with Alzheimer's disease. *Chem. Pharm. Bull.* **1990**, *38*, 1748−1749.

(8) Daemen, M. A. R. C.; Hoogland, G.; Cijintje, J.-M.; Spincemaille, G. H. Upregulation of the GABA-transporter GAT-1 in the spinal cord contributes to pain behaviour in experimental neuropathy. *Neurosci. Lett.* **2008**, *444*, 112−115.

(9) Zádori, D.; Geisz, A.; Vámos, E.; Vécsei, P. K. Valproate ameliorates the survival and the motor performance in a transgenic mouse model of Huntington's disease. *Pharmacol., Biochem. Behav.* **2009**, *94*, 148−153.

(10) Gajcy, K.; Lochynski, S.; Librowski, T. A role of GABA analogues in the treatment of neurological diseases. *Curr. Med. Chem.* **2010**, *17*, 2338−2347.

(11) Pilc, A.; Nowak, G. GABAergic hypotheses of anxiety and depression: focus on $GABA_B$ receptors. *Drugs Today* **2005**, *41*, 755−766.

(12) Krystal, J. H.; Sanacora, G.; Blumberg, H.; Anand, A.; Charney, D. S.; Marek, G.; Epperson, C. N.; Goddard, A.; Mason, G. F. Glutamate and GABA systems as targets for novel antidepressant and mood-stabilizing treatments. *Mol. Psychiatry* **2002**, *7*, S71−S80.

(13) Kirstensen, A. S.; Andersen, J.; Jørgensen, T. N.; Sørensen, J. E.; Loland, C. J.; Strømgaard, K.; Gether, U. SLC6 neurotransmitter transporters: structure, function, and regulation. *Pharmacol. Rev.* **2011**, *63*, 585−640.

(14) Madsen, K. K.; Rasmus, P. C.; Larsson, O. M.; Krogsgaard-Larsen, P.; Schousboe, A.; White, H. S. Synaptic and extrasynaptic GABA transporters as targets for anti-epileptic drugs. *J. Neurochem.* **2009**, *109*, 139−144.

(15) Palacín, M.; Estévez, R.; Bertran, J.; Zorzano, A. Molecular biology of mammalian plasma membrane amino acid transporters. *Physiol. Rev.* **1998**, *78*, 969−1054.

(16) (a) Zhou, Y.; Holmseth, S.; Guo, C.; Hassel, B.; Höfner, G.; Hitfeldt, H. S.; Wanner, K. T.; Danbolt, N. C. Deletion of the γ-aminobutyric acid transporter 2 (GAT2 and SLC6A13) gene in mice leads to changes in liver and brain taurine contents. *J. Biol. Chem.* **2012**, *287*, 35733−35746. (b) Zhou, Y.; Holmseth, S.; Hua, R.; Lehre, A. C.; Olofsson, A. M.; Poblete-Naredo, I.; Kempson, A. A.; Danbolt, N. C. The betaine-GABA transporter (BGT1, slc6a12) is predominantly expressed in the liver and at lower levels in the kidneys and at the brain surface. *Am. J. Physiol.: Renal Physiol.* **2012**, *304*, F316−F328. (c) Lehre, A. C.; Rowley, N. M.; Zhou, Y.; Homseth, S.; Guo, C.; Holen, T.; Hua, R.; Laake, P.; Olfsson, A. M.; Poblete-Naredo, I.; Rusakov, D. A.; Madsen, K. K.; Clausen, R. P.; Schousboe, A.; White, H. S.; Danbolt, N. C. Deletion of the betaine-GABA transporter (BGT1; slc6a12) gene does not affect seizure threshold of adult mice. *Epilepsy Res.* **2011**, *95*, 75−81.

(17) (a) Iversen, L. L.; Neal, M. J. The uptake of [^{3}H]GABA by slices of rat cerebral cortex. *J. Neurochem.* **1968**, *15*, 1141−1149. (b) Iversen, L. L.; Johnston, G. A. R. GABA uptake in rat central nervous system: comparison of uptake in slices and homogenates and the effects of some inhibitors. *J. Neurochem.* **1971**, *18*, 1939−1950.

(18) Krogsgaard-Larsen, P.; Johnston, G. A. R. Inhibition of GABA uptake in rat brain slices by nipecotic acid, various isoxazoles and related compounds. *J. Neurochem.* **1975**, *25*, 797−802.

(19) Krogsgaard-Larsen, P.; Falch, E.; Larsson, O. M.; Schousboe, A. GABA uptake inhibitors: relevance to antiepileptic drug research. *Epilepsy Res.* **1987**, *1*, 77−93.

(20) Frey, H.-H.; Popp, C.; Loescher, W. Influence of the inhibitors of high affinity GABA uptake on seizure threshold in mice. *Neuropharmacology* **1979**, *18*, 581−590.

(21) Ali, F. E.; Bondinell, W. E.; Dandridge, P. A.; Frazee, J. S.; Garvey, E.; Girard, G. R.; Kaiser, C.; Ku, T. W.; Lafferty, J. J.; Moonsammy, G. I.; Oh, H.-J.; Rush, J. A.; Setler, P. E.; Stringer, O. D.; Venslavsky, J. W.; Volpe, B. W.; Yunger, L. M.; Zirkle, C. L. Orally active and potent inhibitors of γ-aminobutyric acid uptake. *J. Med. Chem.* **1985**, *28*, 653−660.

(22) Dalby, N. O. GABA-level increasing and anticonvulsant effects of three different GABA uptake inhibitors. *Neuropharmacology* **2000**, *39*, 2399−2407.

(23) Borden, L. A.; Dhar, T. G. M.; Smith, K. E.; Weinshank, R. L.; Branchek, T. A.; Gluchowski, C. Tiagabine, SK& F 89976-A, CI-966, and NNC-711 are selective for the cloned GABA transporter GAT-1. *Eur. J. Pharmacol.* **1994**, *269*, 219−224.

(24) (a) Andersen, K. E.; Sørensen, J. L.; Huusfeldt, P. O.; Knutsen, L. J. S.; Lau, J.; Lundt, B. F.; Petersen, H.; Suzdak, P. D.; Swedberg, D. B. Synthesis of novel GABA uptake inhibitors. 4.1 Bioisosteric transformation and successive optimization of known GABA uptake inhibitors leading to a series of potent anticonvulsant drug candidates. *J. Med. Chem.* **1999**, *42*, 4281−4291. (b) Andersen, K. E.; Lau, J.; Lundt, B. F.; Petersen, H.; Huusfeldt, P. O.; Suzdak, P. D.; Swedberg, D. B. Synthesis of novel GABA uptake inhibitors. Part 6: Preparation and evaluation of N-Ω asymmetrically substituted nipecotic acid derivatives. *Bioorg. Med. Chem.* **2001**, *9*, 2773−2785.

(25) Zepperitz, C.; Höfner, G.; Wanner, K. T. MS-binding assays: kinetic, saturation, and competitive experiments based on quantitation of bound marker as exemplified by the GABA transporter mGAT1. *ChemMedChem* **2006**, *1*, 208−217.

(26) Höfner, G.; Wanner, K. T. Competitive binding assays made easy with a native marker and mass spectrometric quantification. *Angew. Chem., Int. Ed.* **2003**, *42*, 5235−5237.

(27) Höfner, G.; Zepperitz, C.; Wanner, K. T. MS Binding Assays. An Alternative to Radioligand Binding. In *Mass Spectrometry in Medicinal Chemistry*, 1st ed.; Wanner, K. T., Höfner, G., Eds.; Wiley, VCH: Weinheim, Germany, 2007; pp 247−283.

(28) (a) Sindelar, M.; Wanner, K. T. Library screening by means of mass spectrometry (MS) binding assays—exemplarily demonstrated for a pseudostatic library addressing γ-aminobutyric acid (GABA) transporter 1 (GAT1). *ChemMedChem* **2012**, *7*, 1678−1690. (b) Bucci, M. Methods: how to get GAT. *Nat. Chem. Biol.* **2012**, *8*, 678.

(29) Kalia, J.; Raines, R. T. Hydrolytic stability of hydrazones and oximes. *Angew. Chem.* **2008**, *47*, 7523−7526.

(30) Scharer, L.; Smith, J. P. Serum transaminase elevations and other hepatic abnormalities in patients receiving isoniazid. *Ann. Intern. Med.* **1969**, 1113−1120.

(31) Huq, F. Molecular modeling analysis of the metabolism of isoniazid. *J. Pharmacol. Toxicol.* **2006**, *1*, 447−455.

(32) Tafazoli, S.; Mashregi, M.; O'Brien, P. The role of hydrazine in isoniazid-induced hepatotoxicity in a hepatocyte inflammation model. *J. Toxicol. Appl. Pharmacol.* **2008**, *229*, 94−101.

(33) Busch, M.; Dietz, W. Autoxydation der hydrazone. *Ber. Dtsch.. Chem. Ges.* **1914**, *47*, 3277−3291.
(34) Harej, M.; Dolec, D. Autoxidation of hydrazones. Some new insights. *J. Org. Chem.* **2007**, *72*, 7214−7221.
(35) Yao, H. C.; Resnick, P. Azo-hydrazone conversion: the autoxydation of benzaldehyde phenylhydrazones. *J. Org. Chem.* **1965**, *30*, 2832−2834.
(36) Miyaura, N.; Yanagi, T.; Suzuki, A. The palladium-catalyzed cross-coupling reaction of phenylboronic acid with haloarenes in the presence of bases. *Chem. Commun.* **1981**, *11*, 513−519.
(37) Andrews, M. D.; Brown, A. D.; Fish, P. V.; Fray, M. J.; Lansdell, M. I.; Ryckmans, T.; Stobie, A.; Vakenhut, F.; Gray, D.; La, F. Preparation of *N*-(Pyrrolidin-3-yl) Carboxamide Derivatives as Serotonin and Noradrenalin Re-Uptake Inhibitors. PCT Int. Appl. WO 2006064351 A2 20060622, 2006.
(38) Kistensen, J.; Lysén, M.; Vedsø, P.; Begrup, M. Synthesis of ortho substituted arylboronic esters by in situ trapping of unstable lithio intermediates. *Org. Lett.* **2001**, *3*, 1435−1437.
(39) Zhao, J.; Yue, D.; Campo, M. A.; Larock, R. C. An aryl to imidoyl palladium migration process involving intramolecular C-H activation. *J. Am. Chem. Soc.* **2007**, *129*, 5288−5295.
(40) Korenaga, T.; Kosaki, T.; Fukumura, R.; Ema, T.; Sakai, T. Suzuki−Miyaura coupling reaction using pentafluorophenylboronic acid. *Org. Lett.* **2005**, *7*, 4915−4917.
(41) Irngartinger, H.; Escher, T. Strong electron acceptor properties of 3′-(pentafluorophenyl)isoxazolol[4′,5′:1,2][60]fullerene derivatives. *Tetrahedron* **1999**, *55*, 10753−10760.
(42) Zammit, S. C.; Cox, A. J.; Gow, R. M.; Zhang, Y.; Gilbert, R. E.; Krum, H.; Kelly, D. J; Williams, S. J. Evaluation and optimization of antifibrotic activity of cinnamoyl anthranilates. *Bioorg. Med. Chem. Lett.* **2009**, *19*, 7003−7006.
(43) Wang, Y. D.; Kimball, G.; Prashad, A. S.; Wang, Y. Zr-mediated hydroboration: stereoselective synthesis of vinyl boronic esters. *Tetrahedron Lett.* **2005**, *46*, 8777−8780.
(44) Obtained marker binding of samples of **10** (100 μM) was in good accordance with published data.
(45) Braestrup, C.; Nielsen, E. B.; Sonnewald, U.; Knutsen, L. J. S.; Andersen, K. E.; Jansen, J. A.; Frederiksen, P. H. A.; Mortensen, A.; Suzdak, P. D. (*R*)-*N*-[4,4-Bis(3-methyl-2-thienyl)but-3-en-1-yl]-nipecotic acid binds with high affinity to the brain γ-aminobutyric acid uptake carrier. *J. Neurochem.* **1990**, 639−647.
(46) Control experiments confirmed that NMR spectra of the isolated hydrazones before evaporation of the solvent and after resolvation with DMSO-d_6 were identical.
(47) ^{13}C-signal of B−CH was strongly broadened in ^{13}C NMR spectrum. Chemical shift was determined from cross-peaks of HMQC and HMBC spectra.
(48) Kragler, A.; Höfner, G.; Wanner, K. T. Synthesis and biological evaluation of aminomethylphenol derivatives as inhibitors of the murine GABA transporters mGAT1−GAT4. *Eur. J. Med. Chem.* **2008**, *43*, 2404−2411.
(49) Zepperitz, C.; Höfner, G.; Wanner, K. T. Expanding the scope of MS binding assays to low-affinity markers as exemplified for mGAT1. *Anal. Bioanal. Chem.* **2008**, *391*, 309−316.
(50) Cheng, Y. C.; Prussoff, W. H. Relationship between the inhibition constant (K_i) and the concentration of inhibitor which causes 50 per cent inhibition (IC_{50}) of an enzymatic reaction. *Biochem. Pharmacol.* **1973**, *22*, 3099−3108.

- Second publication -
DOI: 10.1002/cmdc.201600599
CHEMMEDCHEM Full Papers

Development of Highly Potent GAT1 Inhibitors: Synthesis of Nipecotic Acid Derivatives with *N*-Arylalkynyl Substituents

Toni Lutz, Thomas Wein, Georg Höfner, and Klaus T. Wanner*[a]

A new scaffold of highly potent and mGAT1-selective inhibitors has been developed. Compounds in this class are characterized by an alkyne-type spacer connecting nipecotic acid with an aromatic moiety. Preliminary evaluations made it apparent that a nipecotic acid derivative with an *N*-butynyl linker and a terminal 2-biphenyl residue exhibiting a binding affinity (pK_i) of 7.61 ± 0.03 to mGAT1 and uptake inhibition (pIC_{50}) of 7.00 ± 0.06 selective for mGAT1 could serve as a hit compound. Docking calculations for compounds based on this structure in an hGAT1 homology modeling study indicated binding affinities similar to or even higher than that of the well-known mGAT1 inhibitor tiagabine. Synthesis of the designed compounds was readily carried out by two consecutive cross-coupling reactions, giving flexible access to variously substituted biphenyl subunits. With an appropriate substitution pattern of the biphenyl moiety, the binding affinity of enantiopure (*R*)-nipecotic acid derivatives to mGAT1 increased to $pK_i = 8.33 \pm 0.01$, and the uptake inhibitory potency up to $pIC_{50} = 7.72 \pm 0.02$.

Introduction

Epilepsy is a major chronic disease of the central nervous system (CNS) that affects 50 million people worldwide regardless of age and socioeconomic status.[1] Besides current seizures, affected individuals are often exposed to stigma and discrimination. More than 15 different approved antiepileptic drugs available to date are still inadequate, as more than half of treated patients either suffer from adverse side effects or continue to have seizures.[2] To provide an appropriate medical supply for all affected patients, there is an ongoing need for additional exploration of new antiepileptic drugs.

γ-Aminobutyric acid (GABA, **1**, Figure 1) is the major inhibitory neurotransmitter in the CNS.[3] An imbalance between the excitatory neurotransmission mediated by glutamate and the inhibitory neurotransmission effected by GABA due to decreased GABAergic signaling[4] is thought to be a major factor in the pathogenesis of epilepsy.[1,5] Various pharmacological mechanisms have been successfully followed to enhance GABA neurotransmission for the treatment of epilepsy. As GABAergic neurotransmission is terminated by specific GABA transport proteins responsible for the reuptake of GABA into the presynaptic neuron or its transport into glia cells,[6] the inhibition of GABA transporters (GATs) is a viable strategy for improving GABA signaling,[7] besides drugs that target GABA receptors or metabolic enzymes responsible for the degradation of GABA.[4]

GABA transporters are membrane-bound proteins that belong to the solute carrier family 6 (SLC-6),[8] which are present in four different subtypes termed mGAT1, mGAT2, mGAT3, and mGAT4 when cloned from mice. Different nomenclature is used for other species. The human GATs are designated GAT1, BGT1, GAT2, and GAT3 by the human genome organization (HUGO); these correspond to mGAT1, mGAT2, mGAT3, and mGAT4, respectively.[7] Of these, GAT1 (GAT1 ≡ mGAT1) is located mainly on presynaptic neurons and is the most abundant GABA transporter in the brain.[9]

The first generation of GAT inhibitors reported includes cyclic analogues of GABA such as (*R*)-nipecotic acid (**2**, Figure 1).[10] Although they exhibit reasonable affinity for and in vitro potency toward mGAT1 ($pK_i = 4.50 \pm 0.05$),[11] these compounds were of limited utility for pharmacological treatment owing to their inability to cross the blood–brain barrier (BBB).[12] However, providing nipecotic acid and related compounds with a lipophilic side chain resulted in compounds such as tiagabine (**3**, Figure 1) and SKF-88976A (**4**, Figure 1),[13,14] which are able to cross the BBB; moreover, they were found to have substantially improved potency at and subtype selectivity for GAT1.[11]

We recently introduced compounds **5** and **6** (Figure 1) and related derivatives, the lipophilic part of which is characterized by a biphenylvinyl or a benzylphenylvinyl unit. For the parent compounds **5** and **6**, high binding affinities for GAT1 were observed (**5**: $pK_i = 7.15 \pm 0.07$; **6**: $pK_i = 6.16 \pm 0.07$).[15] For the biphenyl derivative **5**, docking studies indicated that halogen substitution of the terminal phenyl group might provide compounds with enhanced binding affinities for hGAT1; this was indeed verified, as halogen-substituted derivatives of **5** were found to exhibit binding affinities of $pK_i \geq 8$. As an extension of the aforementioned studies, we intended to explore the binding affinities of compounds clearly related to **5** and its derivatives, but which have an alkynyl instead of an alkenyl spacer,

[a] T. Lutz, Dr. T. Wein, Dr. G. Höfner, Prof. Dr. K. T. Wanner
Department for Pharmacy, Center for Drug Research, Ludwig-Maximilians-Universität München, Butenandtstr. 7–13, 81377 Munich (Germany)
E-mail: klaus.wanner@cup.uni-muenchen.de

Supporting information for this article can be found under: http://dx.doi.org/10.1002/cmdc.201600599.

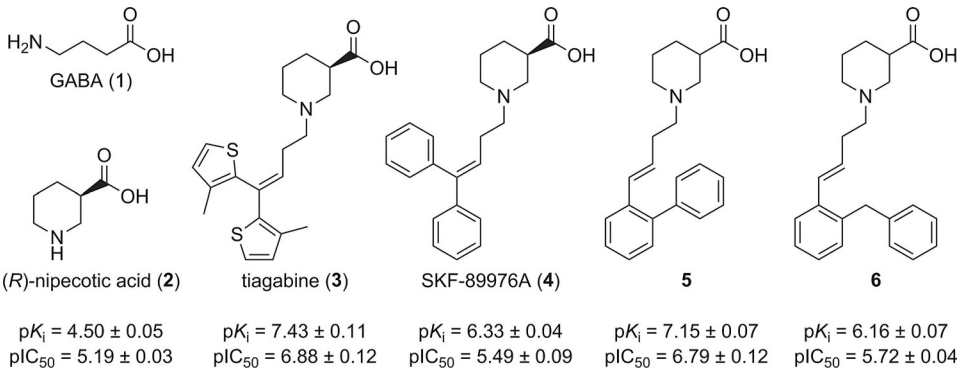

Figure 1. Structure of GABA and known GAT1 inhibitors derived from nipecotic acid (values refer to mGAT1[11]).

that is, *N*-substituted nipecotic acid exhibiting various *N*-arylalkynyl residues. A preliminary evaluation revealed the present compound **17a**, with a 2-biphenylbut-3-ynyl moiety (Table 2, entry 1) to possess a binding affinity for mGAT1 of $pK_i = 7.61 \pm 0.03$ and a functional inhibitory activity of $pIC_{50} = 7.00 \pm 0.06$, thus surpassing analogous biphenyl derivative **5** (Figure 1) in affinity and potency. Docking studies with homology models for hGAT1 performed with **17a** and derivatives substituted at the terminal aromatic residue revealed a possible increase in affinity for these compounds over analogous derivatives of compound **5**.

For the efficient preparation of these compounds, we designed a linear synthetic route that makes use of two successive cross-coupling reactions as key steps. This also preserves a high degree of flexibility with regard to the substitution pattern of the terminal phenyl residue. The new ligands of nipecotic acid as a whole should then also be inert toward hydrolysis and oxidation, advantageous features absent from many similar potent GAT1 inhibitors.[16,17]

Results and Discussion

Homology modeling

Previous studies by Wein et al.[11] and Petrera et al.[15] have shown that docking into an hGAT1 model generated by homology modeling from the X-ray crystallographic structure of the leucine transporter from *Aquifex aeolicus*[18] (LeuT, PDB ID: 2A65) featuring a "closed" protein conformation provides a solid base for interpretation of various binding modes and biological binding data. This structure of LeuT includes a substrate molecule leucine trapped in the active site, called the S1 site. This S1 site is closed to the outside by a lipophilic pair of amino acids, phenylalanine and tyrosine, and a salt bridge between aspartate and arginine and is therefore not accessible directly from the extracellular medium. Another LeuT X-ray structure includes two tryptophan molecules which are located in the S2 above the S1 site oriented toward the extracellular medium, thus keeping the S1 site open to the outside (PDB ID: 3F3A).[19] This "open-to-out" structure has been used as starting point for homology calculations as well, but did not yield hGAT1 models with significant prediction potential.

To investigate the binding affinities of nipecotic acid derivatives with an *N*-alkynyl residue with a terminal triple bond and a biphenyl residue attached to the amino nitrogen atom, we performed docking calculations with our hGAT1 homology model described previously[11] and with compounds (*R*)-**17a–l** (Table 2, entries 1–11) characterized by an *N*-but-3-ynyl spacer, and (*R*)-**18a–l** (Table 2, entries 12–22) by an *N*-pent-4-ynyl spacer as ligands. The obtained docking scores for compounds (*R*)-**17a** (-11.82 kcal mol^{-1}) and (*R*)-**18a** (-11.58 kcal mol^{-1}), representing the parent structures as well as for the respective substituted analogues (*R*)-**17b–l** (in the range of -11.27 to -12.53 kcal mol^{-1}) and (*R*)-**18b–l** (-11.30 to -12.30 kcal mol^{-1}) were mostly comparable to the scoring value of tiagabine (**3**, Figure 1; -11.96 kcal mol^{-1}). However, depending on the substitution pattern of the biphenyl residue, partly higher and lower docking values were found. According to the scoring values, nipecotic acid derivatives (*R*)-**17a–l** with a but-3-ynyl spacer should generally possess higher binding affinities than the homologous compounds (*R*)-**18a–l**, exhibiting a pent-4-ynyl spacer.

Compound (*R*)-**17f** (Table 2, entry 6a) containing a but-3-ynyl spacer with a terminal dichloro-substituted biphenyl moiety (2′=4′=Cl) appears to possess the highest docking score (-12.53 kcal mol^{-1}), which is higher than that of tiagabine (**3**, -11.96 kcal mol^{-1}) and also higher than the corresponding compound (*R*)-**18f** (-12.30 kcal mol^{-1}) with a longer linker. Visual inspection of the docking poses of tiagabine (**3**), (*R*)-**17f**, and (*R*)-**18f** reveal almost identical interactions of the compounds with the hGAT1 protein (Figure 2): the carboxyl group interacts mainly with the sodium atom Na1 and forms additional hydrogen bonds with the backbone NH groups of Leu64 and Gly65. The lipophilic portions interact with Leu64, Trp68, Arg69, Leu136, Tyr140, Thr290, Gln291, Phe294, and Ala455, where the dichloro-substituted biphenyl moieties of (*R*)-**17f** and (*R*)-**18f** are both in the same orientation and position. The side chain of Arg69 forms a cation–π interaction with one of the lipophilic rings of tiagabine or with the terminal phenyl group of the compounds (*R*)-**17f** and (*R*)-**18f**. The obtained hydrogen bonds between the NH group of the nipecotic acid moiety and the main chain oxygen atom of Phe294 are significantly different. For tiagabine and (*R*)-**17f**, the distance of the NH to the oxygen atom is 1.7 and 1.9 Å, respectively. In

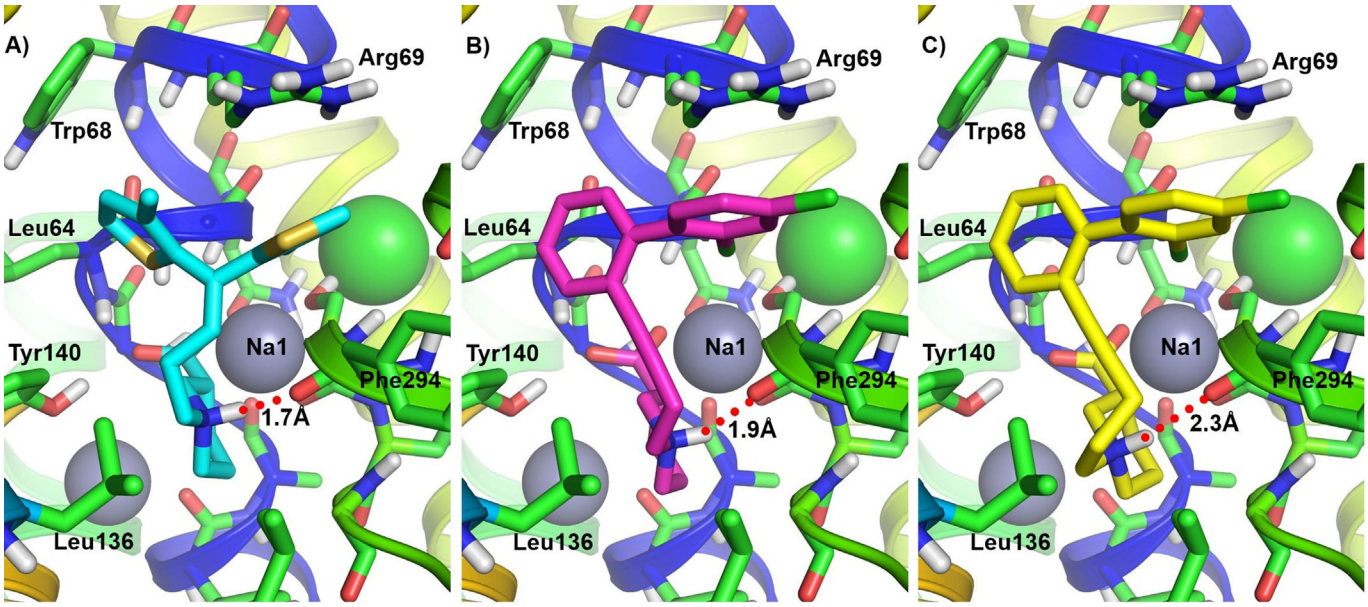

Figure 2. Best docking pose of A) tiagabine, B) **17 f** and C) **18 f** in the "closed" site of hGAT1: tiagabine in cyan, **17 f** in magenta, and **18 f** in yellow. TM10–TM12, Thr290, Gln291, and Ala455 are not displayed for clarity. The hydrogen bond from NH to Phe294 C=O is shown with a red dotted line, and the NH–O distance is given in Å.

the case of compound (*R*)-**18 f** the NH–O distance is increased to 2.3 Å, and is therefore slightly too long for a perfect hydrogen bond; this is a possible reason for the lower docking score of (*R*)-**18 f** than that of (*R*)-**17 f**. This unfavorable docking pose of (*R*)-**18 f** is likely to be a result of the strong interactions of the carboxyl group of (*R*)-**18 f** which is trapped in the strong hydrogen bond network with Na1, Leu64, and Gly65, and the multiple interactions of the lipophilic regions, forcing it to adopt a similar position as the lipophilic portions in tiagabine and (*R*)-**17 f**. However, the 5-biphenylpent-4-ynyl linker is then apparently too long to allow a pose necessary for a reasonable hydrogen bond between the NH group and the carbonyl oxygen atom of Phe294.

Chemistry

For the synthesis of the desired nipecotic acid derivatives **17 a–l** and **18 a–l** with an *N*-but-3-ynyl and an *N*-pent-4-ynyl residue with a terminal 2-benzylphenyl or 2-biphenyl moiety, we intended to start from the *N*-alkynyl-substituted compounds **7** and **8** (Scheme 1). A Sonogashira reaction of these compounds with the respective aryl halides was expected to give access to the esters **9**, **10**, **15**, and **16** (Scheme 1), respectively, with a lipophilic aryl subunit attached to the alkyne terminus. In addition, a more flexible approach with regard to the variation of the substitution pattern of the terminal phenyl group of the biphenyl moiety of **15 a** and **16 a** should be established. This was thought to be best achieved by a stepwise construction of the biphenyl subunit of a biphenyl residue carrying nipecotic acid derivatives **15 b–l** and **16 b–l**. In other words, first the monoaryl derivatives **13** and **14** (Scheme 1) should be synthesized, which upon a Suzuki–Miyaura reaction with phenyl boronic acids, the structures of which could be freely chosen, would give the biphenyl-substituted nipecotic acid derivatives **15 b–l** and **16 b–l**. Upon subsequent hydrolysis of the ester function of the benzylphenyl and biphenyl residues containing nipecotic acid esters, the free nipecotic acid

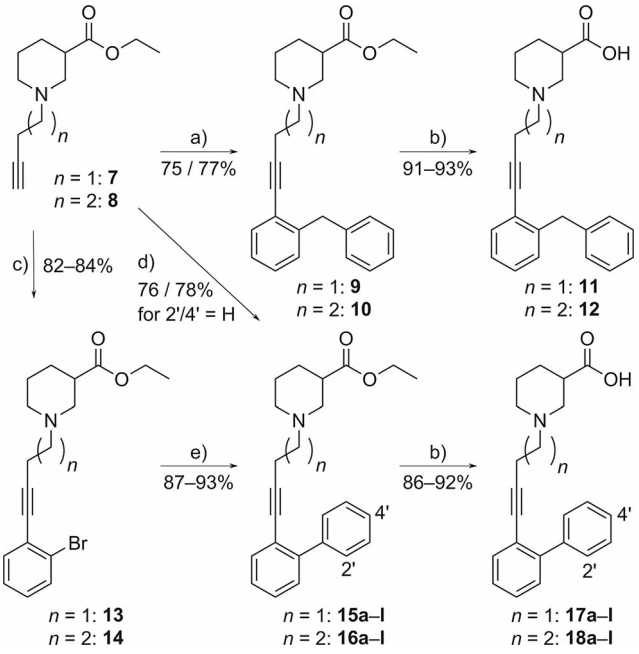

Scheme 1. Synthesis of GAT inhibitors with *N*-arylalkynyl residues. *Reagents and conditions*: a) 2-iododiphenylmethane (1.0 equiv), $Pd(dppf)_2Cl_2 \cdot CH_2Cl_2$ (5 mol%), CuI (20 mol%), K_3PO_4, dioxane/H_2O (1:1), 60 °C, 3 h; b) NaOH (2 M), EtOH, RT, 6 h; c) 2-bromoiodobenzene (1.0 equiv), $Pd(dppf)_2Cl_2 \cdot CH_2Cl_2$ (5 mol%), CuI (20 mol%), K_2CO_3, dioxane/H_2O, 60 °C, 3 h; d) 2-iodobiphenyl (1.0 equiv), $Pd(dppf)_2Cl_2 \cdot CH_2Cl_2$ (5 mol%), CuI (20 mol%), K_3PO_4, dioxane/H_2O (2:1), 60 °C, 3 h; e) phenylboronic acid derivative (1.5 equiv), $Pd_2(dba)_3 \cdot CHCl_3$ (1 mol%), S-Phos (4 mol%), K_3PO_4, dioxane/H_2O (1:1), 60 °C, 6 h.

derivatives **11**, **12**, **17a–l**, and **18a–l** should finally be accessible.

When subjected to Sonogashira reaction, the two *N*-alkynyl-substituted nipecotic acid derivatives **7** and **8** underwent the coupling reactions as expected. These coupling reactions were performed by heating the starting material, i.e., **7** and **8** together with 20 mol% CuI, 5 mol% $Pd(dppf)Cl_2{\cdot}CH_2Cl_2$, and K_2CO_3 or K_3PO_4 with 1.0 equiv of the respective aryl halide in dioxane/water for 3 h at 60 °C. That way with all three aryl halides used, i.e., with 2-iododiphenylmethane, 2-iodobiphenyl, and 2-bromoiodobenzene, the corresponding coupling products **9** and **10**, **13**, and **14**, as well as **15a** and **16a**, respectively, could be obtained in good yields (75–84%; Scheme 1). The building blocks **13** and **14** designed for subsequent Suzuki–Miyaura reactions, via the aryl bromide function present in these molecules, for the construction of the terminal biphenyl residue, were found to be well suited for this purpose. Coupling reactions were performed with a set of phenylboronic acids carrying one to two additional substituents which were either chlorine, fluorine, or methyl, by which a substitution pattern has been gained similar to that studied for analogous systems previously, such as compound **5** (Figure 1).[15] $Pd_2(dba)_3{\cdot}CHCl_3$ (1 mol%) and S-Phos (4 mol%) as catalyst systems were found to be well suited to effect the desired coupling reactions, providing coupling products **15b–l** and **16b–l** after heating for 6 h at 60 °C in dioxane/water in the presence of K_3PO_2 in good yields (87–93%). The free nipecotic acid derivatives **11**–**12**, **17a–l**, and **18a–l** were finally obtained by basic hydrolysis of the carboxylic acid ester functions of the precursors **9**–**10**, **15a–l**, and **16a–l**, with yields ranging from 86 to 93% (Scheme 1).

Biological evaluations

For all free nipecotic acid derivatives synthesized in the context of this study, binding affinities for mGAT1 were determined in MS Binding Assays with NO711 as MS marker.[20] In addition, their functional activity was established in uptake assays at the four GABA transporter subtypes mGAT1–mGAT4 with an assay system based on HEK293 cells stably expressing the individual mouse GABA transporters.[21] When NO711 binding or GABA uptake was decreased by at least by 50% at a concentration of 100 μM, affinity in binding assays (pK_i values) or inhibitory potencies in uptake assays (pIC_{50} values) were assessed, otherwise only the percentage of decrease in binding or uptake was noted.

At first, the influence of the structure of the diaryl moiety attached to the *N*-alkynyl linker of the test compounds on the biological activity was analyzed. As can be seen from a comparison of the parent compounds **11** and **17a**, both possessing a C_4 linker, the former, however, a terminal 2-benzylphenyl, and the latter, a 2-biphenyl moiety, the 2-biphenyl moiety gives rise to a distinctly higher binding affinity, of more than one log unit, at mGAT1 (Table 1, entry 1, **11**, $pK_i = 6.49 \pm 0.03$; Table 2, entry 1, **17a**, $pK_i = 7.61 \pm 0.03$). A similar situation was found for the homologous compounds **12** and **18a** with a C_5 instead of C_4 spacer. Again, the biphenyl derivative **18a** showed a higher affinity for mGAT1 (Table 2, entry 12, $pK_i = 6.16 \pm 0.02$) than compound **12** with a 2-benzylphenyl residue (Table 1, entry 2, $pK_i = 5.66 \pm 0.04$), although in this case, the difference was less pronounced. In addition, it was apparent that the shorter C_4 linker is more favorable than the longer C_5 for high binding affinity (pK_i) at mGAT1.

Table 1. GAT inhibitors with a diphenylmethane moiety and their inhibitory potencies at mGAT1–4 and binding affinities for mGAT1.

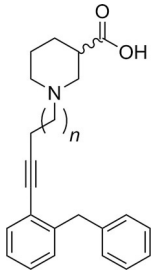

Entry	Compd	*n*	pK_i[a] mGAT1	pIC_{50}[b] mGAT1	mGAT2	mGAT3	mGAT4
1	**11**	1	6.49 ± 0.03	5.87 ± 0.06	70%	66%	57%
2	**12**	2	5.66 ± 0.04	5.13 ± 0.08	4.11	4.50	4.44

[a] Data are the mean ± SEM of three independent experiments, each performed in triplicate. [b] Values are the mean ± SEM of three (mGAT1) or one (mGAT2–4) independent experiment, each performed in triplicate; percentages are the remaining [^{3}H]GABA uptake in the presence of 100 μM inhibitor.

With regard to the influence of the diaryl moiety on the binding affinity, these results are in good agreement with those reported for the analogous system with a C=C double bond instead of a C≡C triple bond in the C_4 linker. Also, in that case with a pK_i value of 7.15 ± 0.07, the affinity for mGAT1 of the biphenyl derivative **5** (Figure 1) was distinctly higher than that of the corresponding derivative **6** (Figure 1), the pK_i of which amounted to 6.16 ± 0.07. Finally, the inhibitory potencies (pIC_{50} values) of **11**, **12**, **17a**, and **18a** at mGAT1 were found to be in good agreement with the binding affinities (pK_i values) determined for this transporter. Moreover, the determination of inhibitory potencies of these compounds at mGAT2–mGAT4 revealed that they all exhibit high subtype selectivity in favor of mGAT1, pIC_{50} values for mGAT1, pIC_{50} values for mGAT3–mGAT4 being only around 4.50 and below.

Because of the lower biological activities of the 2-benzylphenyl-residue-carrying compounds **11** and **12** as compared with the analogous 2-biphenyl derivatives **17a** and **18a**, only derivatives of the latter were studied next. Because of the results obtained in a study of the structure–activity relationship of **5**,[15] substitution was limited to the *ortho* (2′) and *para* (4′) positions of the terminal phenyl residue. In the case of the nipecotic acid derivative **18a** having the C_5 spacer, substitution of the terminal phenyl residue had only minor effects on the already relatively low mGAT1 affinity ($pK_i = 6.16 \pm 0.02$, Table 2, entry 12). When **18a** was substituted with chlorine, fluorine, or a methyl group at the *ortho* position, only a slight tendency toward higher pK_i values (≈6.3, Table 2, entries 13–15) could be observed. In contrast, substitution of **18a** with a chlorine at

Table 2. GAT inhibitors with biphenyl moieties and their inhibitory potencies toward mGAT1–4 and binding affinities toward mGAT1.

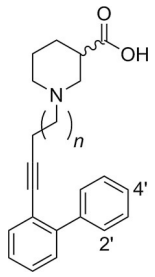

Entry	Compd	*n*	2′	4′	pK_i[a] mGAT1	pIC_{50}[b] mGAT1	mGAT2	mGAT3	mGAT4
1	**17a**	1	H	H	7.61 ± 0.03	7.00 ± 0.06	70%	66%	57%
2	**17b**	1	Cl	H	7.91 ± 0.03	7.29 ± 0.12	62%	47%	43%
3	**17c**	1	F	H	7.77 ± 0.05	7.12 ± 0.10	45%	74%	52%
4	**17d**	1	CH_3	H	8.13 ± 0.05	7.22 ± 0.06	75%	60%	52%
4a	(*R*)-**17d**	1	CH_3	H	**8.32 ± 0.03**	7.60 ± 0.12	78%	59%	4.29
5	**17e**	1	H	Cl	7.37 ± 0.07	6.73 ± 0.08	4.11	4.50	4.44
6	**17f**	1	Cl	Cl	8.16 ± 0.04	7.26 ± 0.08	70%	4.65	4.59
6a	(*R*)-**17f**	1	Cl	Cl	**8.31 ± 0.07**	7.72 ± 0.02	71%	4.79	4.38
7	**17g**	1	F	F	8.02 ± 0.09	7.31 ± 0.12	54%	62%	41%
7a	(*R*)-**17g**	1	F	F	**8.21 ± 0.06**	7.56 ± 0.10	87%	69%	4.32
8	**17h**	1	CH_3	CH_3	7.68 ± 0.07	6.68 ± 0.13	57%	49%	4.04
9	**17i**	1	Cl	F	8.13 ± 0.08	7.35 ± 0.03	4.39	48%	4.33
9a	(*R*)-**17i**	1	Cl	F	**8.33 ± 0.01**	7.68 ± 0.10	55%	4.56	4.29
10	**17k**	1	CH_3	Cl	7.78 ± 0.03	6.80 ± 0.08	4.54	4.40	4.49
11	**17l**	1	CH_3	F	7.90 ± 0.03	7.11 ± 0.10	4.39	47%	55%
12	**18a**	2	H	H	6.16 ± 0.02	5.42 ± 0.10	86%	64%	61%
13	**18b**	2	Cl	H	6.29 ± 0.01	5.80 ± 0.11	54%	82%	48%
14	**18c**	2	F	H	6.29 ± 0.07	5.56 ± 0.13	42%	82%	56%
15	**18d**	2	CH_3	H	6.27 ± 0.06	5.89 ± 0.05	67%	66%	4.26
16	**18e**	2	H	Cl	6.07 ± 0.01	5.47 ± 0.06	45%	4.71	47%
17	**18f**	2	Cl	Cl	6.55 ± 0.01	6.03 ± 0.06	4.18	4.50	4.44
18	**18g**	2	F	F	6.42 ± 0.09	5.70 ± 0.13	68%	53%	53%
19	**18h**	2	CH_3	CH_3	6.09 ± 0.12	5.46 ± 0.12	47%	54%	4.05
20	**18i**	2	Cl	F	6.46 ± 0.04	5.77 ± 0.08	4.39	46%	4.33
21	**18k**	2	CH_3	Cl	6.40 ± 0.05	6.01 ± 0.06	4.54	4.60	4.63
22	**18l**	2	CH_3	F	6.18 ± 0.09	5.88 ± 0.05	4.28	4.31	4.43

[a] Data are the mean ± SEM of three independent experiments, each performed in triplicate. [b] Values are the mean ± SEM of three (mGAT1) or one (mGAT2–4) independent experiment, each performed in triplicate; percentages are the remaining [^{3}H]GABA uptake in the presence of 100 μM inhibitor.

the *para* position, exhibited a slight tendency toward lower mGAT1 binding affinities ($pK_i = 6.07 \pm 0.01$, Table 2 entry 16). Upon substitution of the distal phenyl residue in the 2′- and 4′-positions with two halogens (2′-Cl, 4′-Cl; 2′-F, 4′-F; 2′-Cl, 4′-F) or with a 2′-methyl group and a 4′-chloro, mGAT1 affinity increased slightly further ($pK_i \approx 6.4$–6.5, Table 2, entries 17, 18, 20, 21), but remained almost the same as for the parent compound **18a** with two methyl groups or one methyl and one fluorine substituent at the 2′- and 4′-positions ($pK_i \approx 6.1$–6.2, Table 2, entries 19 and 22).

Substitution of the terminal phenyl ring of nipecotic acid derivative **17a** possessing only a C_4 instead of C_5 spacer, but also a distinctly higher mGAT1 affinity relative to its homologue **18a** gave rise to trends quite similar to those observed for the latter, **18a**. Upon introduction of a chlorine, fluorine, or methyl substituent at the 2′-position of the distal phenyl group, a distinct increase in mGAT1 affinity occurs, the methyl derivative **17d** exhibiting in this series the highest pK_i value ($pK_i = 8.13 \pm 0.05$; Table 2, entry 4). In contrast, a chlorine substituent at the 4′-position leads to a decrease in mGAT1 binding affinity below the level of the parent compound **17a** (**17e**, pK_i 7.37 ± 0.07, Table 2, entry 5). With two chlorine or two fluorine or one chlorine at the 2′-position and one fluorine at the 4′-position, again good binding affinities are obtained (**17f**, $pK_i = 8.16 \pm 0.04$; **17g**, $pK_i = 8.02 \pm 0.09$; **17i**, $pK_i = 8.13 \pm 0.08$; Table 2, entries 6, 7, and 9). But although a first methyl group at the 2′-position (see **17d**, Table 2, entry 4) led to a substantial improvement in mGAT1 binding affinity, for a second methyl group or a chlorine or a fluorine substituent (Table 2, entries 8, 10, and 11) the opposite is true; the pK_i values relative to the monomethyl derivative **17d** ($pK_i = 8.13 \pm 0.05$, Table 2, entry 4) are lowered by about 0.2 to 0.4 log units.

In general, the results obtained in the biological evaluations confirm the results of the molecular modeling described above regarding the influence of the length of the alkynyl spacer on GAT1 affinity. Thus, compounds **17a–l** with a but-3-ynyl spacer were found to be more affine for GAT1 than compounds **18a–l** with a pent-4-ynyl spacer. However, the homology model cannot explain the 1–2 log units the pK_i values for compounds with a C_5 spacer are lower than those with a C_4 linker. But the calculated binding affinities for nipecotic acid derivatives with the but-3-ynyl spacer were in line with the results of the biological studies, delivering pK_i values close to that of tiagabine or even better. Regarding these compounds, our homology modeling study indicated the 2′,4′-dichloro-substituted derivative **17f** (Table 2, entry 6) to possess a particularly high binding affinity for GAT1 as it had yielded the highest docking scores. This proved true, as the pK_i value of **17f** for mGAT1 ranged among the highest found in this study. However, also the three test compounds **17g** (2′-F, 4′-F, Table 2, entry 7), **17i** (2′-Cl, 4′-F, Table 2, entry 9), and **17d** (2′-CH_3, Table 2, entry 4) reached comparably high binding affinities for mGAT1 (pK_i), although their docking scores in molecular modeling had been lower.

The inhibitory potencies of all studied analogues **17a–l** and **18a–l** at mGAT1 (pIC_{50}) were about a half log unit lower than the corresponding pK_i values. The difference between pIC_{50} and pK_i values is a common phenomenon constantly observed for mGAT1 inhibitors when characterized in the test systems used,[20] but apart from this difference the data for binding affinity (pK_i) and inhibitory potency (pIC_{50}) are still in good agreement with each other. From the inhibitory potencies found at mGAT2–mGAT4, it also became apparent that all compounds possess a clear preference for mGAT1.

For mGAT1 inhibitors delineated from nipecotic acid, it is well known that the biological activity resides mainly in the *R* enantiomer. Therefore, of the nipecotic acid derivatives with the highest mGAT1 binding affinities, that is, **17d**, **17f**, **17g**,

and **17 i**, the corresponding enantiopure *R* isomers were also synthesized and characterized in mGAT1 binding and uptake assays. As expected, each of these *R* enantiomers shows a higher mGAT binding affinity than the racemic compound, the increase amounting to about 0.2 log units. With mGAT1 binding affinities being in the range of 8.2–8.3 (pK_i), enantiomers (*R*)-**17 d**, (*R*)-**17 f**, (*R*)-**17 g**, and (*R*)-**17 i**, (Table 2, entries 4a, 6a, 7a, and 9a) are among the best binders known so far for this target. As compared with the 2′,4′-dichloro-substituted derivative of (*R*)-**4** ($pK_i = 8.33 \pm 0.06$, $pIC_{50} = 7.43 \pm 0.10$),[15] which is one of the most active mGAT1 inhibitors, the binding affinity of the most active mGAT1 inhibitors of this study was found to be in the same range, and their inhibitory potencies even somewhat higher. Relative to *N*-substituted derivatives of guvacine with an oxime spacer that are known to be among the most potent mGAT1 inhibitors to date,[17] the best of the nipecotic acid derivatives with an alkyne spacer described in this study generally show inhibitory potencies (pIC_{50}) and binding affinities (pK_i) in a similar range. In contrast to the former, the *N*-arylalkynyl substituents have the advantage of being devoid of a potentially labile oxime function.

Conclusions

In summary, a new series of GABA uptake inhibitors with an alkyne-type spacer connecting nipecotic acid via the amino nitrogen atom as polar substructure with an aromatic subunit have been synthesized and characterized for their biological activity at the GABA transporter subtype 1. At the ω-position of the alkynyl linker, the biphenyl-type residue was found to be more suitable than the 2-benzylphenyl moiety with regard to biological activity. Moreover, compounds with the shorter but-3-ynyl spacer linking the nitrogen of nipecotic acid with the biphenyl subunit turned out to possess higher affinity for and potency at mGAT1 than those with a C_5 linker.

This way compound **17 a** (Table 2) containing a biphenylbut-3-ynyl ligand was identified as a parent compound with a distinctly improved binding affinity of 7.61 ± 0.03 (pK_i) and inhibitory potency of 7.00 ± 0.06 (pIC_{50}) as compared to the analogue **5** (Figure 1) with an alkenyl spacer ($pK_i = 7.15 \pm 0.07$, $pIC_{50} = 6.79 \pm 0.12$). Guided by the results of a homology modeling study, a series of related compounds with different substituents at the 2′- and 4′-positions of the terminal ring of the biphenyl residue were synthesized and characterized for their binding affinity for and inhibitory potency at mGAT1. Synthesis of these compounds was accomplished by two efficient cross-coupling reactions. Among the synthesized compounds, the 2′-methyl and 2′,4′-dihalogen-substituted derivatives **17 d**, **17 f**, **17 g**, and **17 i** (Table 2, entries 4, 6, 7, and 9) were found to be the most potent derivatives with binding affinities up to 8.33 ± 0.01 (pK_i) and uptake inhibitory potencies up to 7.72 ± 0.02 (pIC_{50}) for the more potent *R* enantiomers. According to the inhibitory potencies found for the GABA transporter subtypes mGAT2–4, this series of compounds appears to be highly subtype selective toward mGAT1.

Overall within this study a new type of nipecotic acid derivative exhibiting a spacer with a triple bond linking the aforementioned polar unit with a 2-biphenyl residue was identified, possessing outstanding binding affinities and potencies and clear subtype selectivity toward mGAT1. Because of the stability inherent to the *N*-biphenylalkynyl substituent, these nipecotic acid derivatives are a valuable starting point for further optimization studies.

Experimental Section

Computational studies

For homology modeling of a "closed" GAT1 conformation the 3D structure (PDB ID: 2A65)[18] was taken from the RCSB Protein Data Bank.[22] The only available 3D structure of an "open-to-out" conformation (PDB ID: 3F3A)[19] was chosen as a template for an "open" GAT1 conformation. The human GAT1 sequence (Swiss-Prot[23] accession number P30531) was aligned to the LeuT sequence using the alignment from Skovstrup et al.[24] The Modeller software package version 9v8[25] was used to generate 30 structures of each conformer. The two sodium atoms (Na1 and Na2) located close to the S1 binding site were copied into the hGAT1 structures. A chloride ion was placed into the putative chloride binding site proposed by Zomot et al.[26] and Forrest et al.[27] However, the chloride ion has no direct contact to the active site and its presence has no impact for the docking calculations. The models with the lowest Modeller objective function were checked with PROCHECK[28] for structural consistency and further used for docking calculations.

The molecules for docking were exported from our in-house Instant JChem 5.4 database[29] as 2D MDL mol files. Protonation at pH 7.4 and the 2D to 3D conversion was done using ChemAxon Marvin 5.4.0.1[30] "cxcalc" and "molconvert". The command line tool "prepare_dpf42.py" was used for conversion into AutoDock4 pdbqt input files. Appropriate protein input files were prepared with the AutoDock tools.[31] Docking grids were calculated with "autogrid4" and docking was performed with AutoDock4 version 4.2.3.[32] The binding region was defined by a 18 Å × 18 Å × 18 Å box centered between the two gatekeeping residues Tyr139 and Phe294. The side chains of the four gatekeeping residues (Tyr139, Phe294, Arg69, Asp451) were treated as flexible during docking. Ten poses for each molecule were generated and scored with the AutoDock4 scoring function.[32]

Chemistry

All reactions were carried out under nitrogen atmosphere in distilled solvents. Dioxane was dried over sodium and distilled under nitrogen. Commercial available reagents were used without further purification. Flash column chromatography (CC) was performed using silica gel (40–60 μm). NMR spectra were measured with a Jeol Eclipse +400 (400 MHz) and a Jeol Eclipse +500 (500 MHz) spectrometer or an Avance III HD 400 MHz Bruker BioSpin and an Avance III HD 500 MHz Bruker BioSpin spectrometer. ^1H NMR chemical shifts were referenced to TMS and ^{13}C NMR chemical shifts were referenced to $CHCl_3$. The coupling constants were stated with an accuracy of 0.5 Hz. MestreNova software was used for further analysis of the spectra. IR spectra were recorded with a FT-IR spectrometer Paragon 1000 (PerkinElmer). Samples were measured either as KBr pellets or as films on NaCl plates. Spectrum v2.00 software (PerkinElmer) was used for analysis. Mass spectra were measured with a mass spectrometer 59827A with 59980 particle beam LC–MS interface (Hewlett–Packard). High resolution mass spectrometry was carried out with a LTQ FT (ThermoFinnigan), FAB

(Xenon, 6 kV, MBA, reference PEG), or a JMS GCmate II (Jeol). Optical rotations were determined by a 241 MC Polarimeter ADP440+ at $\lambda = 589$ cm^{-1}. Purity testing of the enantiopure test compounds (*R*)-**17 d**, (*R*)-**17 f**, (*R*)-**17 g**, and (*R*)-**17 i** was done by means of analytical HPLC on a Merck-Hitachi HPLC system (L7400 intelligent pump and L7400 UV Detector) using elution from a 250 mm×4 mm LiChrospher 100RP-8 column (5 μm particle size), the UV absorbance detection set at 254 nm, using a flow rate of 1.0 mL min^{-1} and as solvent: phosphate buffer (10 mM)/MeCN = 4:6. The purity of all tested compounds was >95 %. See the Supporting Information for characterization data for the described compounds.

General procedure for the Sonogashira cross-coupling reactions (GP 1): Under nitrogen atmosphere $Pd(dppf)_2Cl_2$ (0.05 equiv), CuI (0.2 equiv), K_3PO_4 (3.0 equiv), and the aryl iodide (1.0 equiv) were introduced in a Schlenk tube. Subsequently the alkyne (1.0 equiv) in dioxane (1 mL mmol^{-1}) and H_2O (1 mL mmol^{-1}) were added. The mixture was heated at 60 °C and stirred for 3 h. After cooling to room temperature, CH_2Cl_2 (10 mL mmol^{-1}) and H_2O (10 mL mmol^{-1}) were added and the organic components were extracted with CH_2Cl_2. The combined organic layers were dried over Na_2SO_4 and the solvent was removed under reduced pressure. The crude product was purified by CC (eluting with hexane/EtOAc 8:2) to give the corresponding coupling product.

General procedure for the Suzuki cross-coupling reactions (GP 2): Under nitrogen atmosphere $Pd_2(dba)_3{\cdot}CHCl_3$ (0.01 equiv), S-Phos (0.04 equiv), K_3PO_4 (2.0 equiv) and the corresponding phenylboronic acid derivative (1.5 equiv) were introduced in a Schlenk tube. Subsequently the aryl bromide (1.0 equiv) in dioxane (1 mL mmol^{-1}) and H_2O (1 mL mmol^{-1}) were added. The mixture was heated at 60 °C and stirred for 6 h. After cooling to room temperature, CH_2Cl_2 (10 mL mmol^{-1}) and H_2O (10 mL mmol^{-1}) were added and the organic components were extracted with CH_2Cl_2. The combined organic layers were dried over Na_2SO_4 and the solvent was removed under reduced pressure. The crude product was purified by CC (eluting with hexane/EtOAc 8:2) to give the corresponding coupling product.

General procedure for the hydrolysis of nipecotic acid ethyl esters (GP 3): The corresponding ester was dissolved in EtOH (5 mL mmol^{-1}) and 2 M NaOH (1.5 mL mmol^{-1}, 3.0 equiv) was added. The mixture was stirred for about 4 h at room temperature (checked by TLC). After complete conversion, the solvent was removed under reduced pressure. The resulting solid residue was dissolved in 25 mL mmol^{-1} of H_2O and the pH was adjusted to 6–7 (indicator paper). The amino acid was then extracted several times with CH_2Cl_2. The combined organic layers were dried over Na_2SO_4 and the solvent was removed under reduced pressure. The resulting residue was dissolved in MeOH (5 mL mmol^{-1}) followed by the addition of H_2O (50 mL mmol^{-1}) and was then freeze dried to give the corresponding amino acid as amorphous solid.

Syntheses

Ethyl 1-but-3-yn-1-ylpiperidine-3-carboxylate (7): Ethyl nipecotate (25 mmol, 4.0 g, 2.5 equiv) was added to but-3-yn-1-yl-4-methylbenzenesulfonate (10 mmol, 2.2 g, 1.0 equiv) and the mixture was stirred for 24 h at room temperature. Then CH_2Cl_2 (100 mL) and H_2O (100 mL) were added and the product was extracted with CH_2Cl_2. The combined organic layers were dried over Na_2SO_4 and the solvent was removed under reduced pressure. After purification by CC (eluting with hexane/EtOAc 1:1) **7** was obtained as colorless oil (2.02 g, 96 %).

Ethyl 1-pent-4-yn-1-ylpiperidine-3-carboxylate (8): Ethyl nipecotate (25 mmol, 4.0 g, 2.5 equiv) was added to pent-4-yn-1-yl-4-methylbenzenesulfonate (10 mmol, 2.4 g, 1.0 equiv) and the mixture was stirred for 24 h at room temperature. Then CH_2Cl_2 (100 mL) and H_2O (100 mL) were added and the product was extracted with CH_2Cl_2. The combined organic layers were dried over Na_2SO_4 and the solvent was removed under reduced pressure. After purification by CC (eluting with hexane/EtOAc 1:1) **8** was obtained as colorless oil (2.10 g, 94 %).

Ethyl 1-[4-(2-benzylphenyl)but-3-yn-1-yl]piperidine-3-carboxylate (9): According to GP 1 starting from **7** (105 mg, 0.50 mmol) and 1-benzyl-2-iodo-benzene (147 mg, 0.500 mmol) **9** was obtained as colorless oil (145 mg, 77 %).

Ethyl 1-[5-(2-benzylphenyl)pent-4-yn-1-yl]piperidine-3-carboxylate (10): According to GP 1 starting from **8** (112 mg, 0.500 mmol) and 1-benzyl-2-iodo-benzene (147 mg, 0.500 mmol) **10** was obtained as colorless oil (146 mg, 75 %).

1-[4-(2-Benzylphenyl)but-3-yn-1-yl]piperidine-3-carboxylic acid (11): According to GP 3 starting from **9** (113 mg, 0.300 mmol) and 2 N NaOH (0.450 mL, 0.900 mmol) **11** was obtained as colorless amorphous solid (95 mg, 91 %).

1-[5-(2-Benzylphenyl)pent-4-yn-1-yl]piperidine-3-carboxylic acid (12): According to GP 3 starting from **10** (117 mg, 0.300 mmol) and 2 N NaOH (0.450 mL, 0.900 mmol) **12** was obtained as colorless amorphous solid (101 mg, 93 %).

Ethyl 1-[4-(2-bromophenyl)but-3-yn-1-yl]piperidine-3-carboxylate (13): According to GP 1 starting from **7** (2.10 g, 10.0 mmol) and 1-bromo-2-iodo-benzene (2.82 g, 10.0 mmol) **13** was obtained as colorless oil (3.01 g, 82 %).

Ethyl 1-[5-(2-bromophenyl)pent-4-yn-1-yl]piperidine-3-carboxylate (14): According to GP 1 starting from **8** (2.24 g, 10.0 mmol) and 1-bromo-2-iodo-benzene (2.82 g, 10.0 mmol) **14** was obtained as colorless oil (3.16 g, 84 %).

Ethyl 1-[4-(2-phenylphenyl)but-3-yn-1-yl]piperidine-3-carboxylate (15 a): Method 1: According to GP 1 starting from **7** (105 mg, 0.500 mmol) and 1-iodo-2-phenyl-benzene (140 mg, 0.500 mmol) **15 a** was obtained as colorless oil (137 mg, 76 %); Method 2: According to GP 2 starting from **13** (110 mg, 0.300 mmol), $Pd_2(dba)_3{\cdot}x\,CHCl_3$ (3.2 mg, 3.0 μmol), S-Phos (5.0 mg, 12 μmol), K_3PO_4 (131 mg, 0.600 mmol) and phenylboronic acid (55 mg, 0.45 mmol) **15 a** was obtained as colorless oil (100 mg, 93 %). The analytical data is in accordance with the one described in method 1.

Ethyl 1-[5-(2-phenylphenyl)pent-4-yn-1-yl]piperidine-3-carboxylate (16 a): Method 1: According to GP 1 starting from **8** (112 mg, 0.500 mmol) and 1-iodo-2-phenyl-benzene (140 mg, 0.500 mmol) **16 a** was obtained as colorless oil (145 mg, 78 %); Method 2: According to GP2 starting from **14** (114 mg, 0.300 mmol), $Pd_2(dba)_3{\cdot}x\,CHCl_3$ (3.2 mg, 3.0 μmol), S-Phos (5.0 mg, 12 μmol), K_3PO_4 (131 mg, 0.600 mmol), and phenylboronic acid (55 mg, 0.45 mmol) **16 b** was obtained as colorless oil (105 mg, 94 %). The analytical data is in accordance with the one described in method 1.

Ethyl 1-{4-[2-(2-chlorophenyl)phenyl]but-3-yn-1-yl}piperidine-3-carboxylate (15 b): According to GP2 starting from **13** (110 mg, 0.300 mmol), $Pd_2(dba)_3{\cdot}x\,CHCl_3$ (3.2 mg, 3.0 μmol), S-Phos (5.0 mg, 12 μmol), K_3PO_4 (131 mg, 0.600 mmol), and 2-chlorophenylboronic acid (70 mg, 0.45 mmol) **15 b** was obtained as colorless oil (106 mg, 90 %).

Ethyl 1-{5-[2-(2-chlorophenyl)phenyl]pent-4-yn-1-yl}piperidine-3-carboxylate (16b): According to GP2 starting from **14** (114 mg, 0.300 mmol), $Pd_2(dba)_3{\cdot}x\,CHCl_3$ (3.2 mg, 3.0 μmol), S-Phos (5.0 mg, 12 μmol), K_3PO_4 (131 mg, 0.600 mmol), and 2-chlorophenylboronic acid (70 mg, 0.45 mmol) **16b** was obtained as colorless oil (112 mg, 91%).

Ethyl 1-{4-[2-(2-fluorophenyl)phenyl]but-3-yn-1-yl}piperidine-3-carboxylate (15c): According to GP2 starting from **13** (110 mg, 0.300 mmol), $Pd_2(dba)_3{\cdot}x\,CHCl_3$ (3.2 mg, 3.0 μmol), S-Phos (5.0 mg, 12 μmol), K_3PO_4 (131 mg, 0.600 mmol), and 2-fluorophenylboronic acid (63 mg, 0.45 mmol) **15c** was obtained as colorless oil (101 mg, 89%).

Ethyl 1-{5-[2-(2-fluorophenyl)phenyl]pent-4-yn-1-yl}piperidine-3-carboxylate (16c): According to GP2 starting from **14** (114 mg, 0.300 mmol), $Pd_2(dba)_3{\cdot}x\,CHCl_3$ (3.2 mg, 3.0 μmol), S-Phos (5.0 mg, 12 μmol), K_3PO_4 (131 mg, 0.600 mmol), and 2-fluorophenylboronic acid (63 mg, 0.45 mmol) **16c** was obtained as colorless oil (107 mg, 91%).

Ethyl 1-{4-[2-(2-methylphenyl)phenyl]but-3-yn-1-yl}piperidine-3-carboxylate (15d): According to GP2 starting from **13** (110 mg, 0.300 mmol), $Pd_2(dba)_3{\cdot}x\,CHCl_3$ (3.2 mg, 3.0 μmol), S-Phos (5.0 mg, 12 μmol), K_3PO_4 (131 mg, 0.600 mmol), and 2-methylphenylboronic acid (61 mg, 0.45 mmol) **15d** was obtained as colorless oil (103 mg, 92%).

Ethyl 1-{5-[2-(2-methylphenyl)phenyl]pent-4-yn-1-yl}piperidine-3-carboxylate (16d): According to GP2 starting from **14** (114 mg, 0.300 mmol), $Pd_2(dba)_3{\cdot}x\,CHCl_3$ (3.2 mg, 3.0 μmol), S-Phos (5.0 mg, 12 μmol), K_3PO_4 (131 mg, 0.600 mmol), and 2-methylphenylboronic acid (61 mg, 0.45 mmol) **16d** was obtained as colorless oil (108 mg, 93%).

Ethyl 1-{4-[2-(4-chlorophenyl)phenyl]but-3-yn-1-yl}piperidine-3-carboxylate (15e): According to GP2 starting from **13** (110 mg, 0.300 mmol), $Pd_2(dba)_3{\cdot}x\,CHCl_3$ (3.2 mg, 3.0 μmol), S-Phos (5.0 mg, 12 μmol), K_3PO_4 (131 mg, 0.600 mmol), and 4-chlorophenylboronic acid (70 mg, 0.45 mmol) **15e** was obtained as colorless oil (108 mg, 91%).

Ethyl 1-{5-[2-(4-chlorophenyl)phenyl]pent-4-yn-1-yl}piperidine-3-carboxylate (16e): According to GP2 starting from **14** (114 mg, 0.300 mmol), $Pd_2(dba)_3{\cdot}x\,CHCl_3$ (3.2 mg, 3.0 μmol), S-Phos (5.0 mg, 12 μmol), K_3PO_4 (131 mg, 0.600 mmol), and 4-chlorophenylboronic acid (70 mg, 0.45 mmol) **16e** was obtained as colorless oil (112 mg, 91%).

Ethyl 1-{4-[2-(2,4-dichlorophenyl)phenyl]but-3-yn-1-yl}piperidine-3-carboxylate (15f): According to GP2 starting from **13** (110 mg, 0.300 mmol), $Pd_2(dba)_3{\cdot}x\,CHCl_3$ (3.2 mg, 3.0 μmol), S-Phos (5.0 mg, 12 μmol), K_3PO_4 (131 mg, 0.600 mmol), and 2,4-dichlorophenylboronic acid (86 mg, 0.45 mmol) **15f** was obtained as colorless oil (112 mg, 87%).

Ethyl 1-{5-[2-(2,4-dichlorophenyl)phenyl]pent-4-yn-1-yl}piperidine-3-carboxylate (16f): According to GP2 starting from **14** (114 mg, 0.300 mmol), $Pd_2(dba)_3{\cdot}x\,CHCl_3$ (3.2 mg, 3.0 μmol), S-Phos (5.0 mg, 12 μmol), K_3PO_4 (131 mg, 0.600 mmol), and 2,4-dichlorophenylboronic acid (86 mg, 0.45 mmol) **16f** was obtained as colorless oil (117 mg, 88%).

Ethyl 1-{4-[2-(2,4-difluorophenyl)phenyl]but-3-yn-1-yl}piperidine-3-carboxylate (15g): According to GP2 starting from **13** (110 mg, 0.300 mmol), $Pd_2(dba)_3{\cdot}x\,CHCl_3$ (3.2 mg, 3.0 μmol), S-Phos (5.0 mg, 12 μmol), K_3PO_4 (131 mg, 0.600 mmol), and 2,4-difluorophenylboronic acid (71 mg, 0.45 mmol) **15g** was obtained as colorless oil (103 mg, 87%).

Ethyl 1-{5-[2-(2,4-difluorophenyl)phenyl]pent-4-yn-1-yl}piperidine-3-carboxylate (16g): According to GP2 starting from **14** (114 mg, 0.300 mmol), $Pd_2(dba)_3{\cdot}x\,CHCl_3$ (3.2 mg, 3.0 μmol), S-Phos (5.0 mg, 12 μmol), K_3PO_4 (131 mg, 0.600 mmol), and 2,4-difluorophenylboronic acid (71 mg, 0.45 mmol) **16g** was obtained as colorless oil (106 mg, 86%).

Ethyl 1-{4-[2-(2,4-dimethylphenyl)phenyl]but-3-yn-1-yl}piperidine-3-carboxylate (15h): According to GP2 starting from **13** (110 mg, 0.300 mmol), $Pd_2(dba)_3{\cdot}x\,CHCl_3$ (3.2 mg, 3.0 μmol), S-Phos (5.0 mg, 12 μmol), K_3PO_4 (131 mg, 0.600 mmol), and 2,4-dimethylphenylboronic acid (68 mg, 0.45 mmol) **15h** was obtained as colorless oil (107 mg, 92%).

Ethyl 1-{5-[2-(2,4-dimethylphenyl)phenyl]pent-4-yn-1-yl}piperidine-3-carboxylate (16h): According to GP2 starting from **14** (114 mg, 0.300 mmol), $Pd_2(dba)_3{\cdot}x\,CHCl_3$ (3.2 mg, 3.0 μmol), S-Phos (5.0 mg, 12 μmol), K_3PO_4 (131 mg, 0.600 mmol), and 2,4-dimethylphenylboronic acid (68 mg, 0.45 mmol) **16h** was obtained as colorless oil (110 mg, 91%).

Ethyl 1-{4-[2-(2-chloro-4-fluorophenyl)phenyl]but-3-yn-1-yl}piperidine-3-carboxylate (15i): According to GP2 starting from **13** (110 mg, 0.300 mmol), $Pd_2(dba)_3{\cdot}x\,CHCl_3$ (3.2 mg, 3.0 μmol), S-Phos (5.0 mg, 12 μmol), K_3PO_4 (131 mg, 0.600 mmol), and 2-chloro-4-fluorophenylboronic acid (80 mg, 0.45 mmol) **15i** was obtained as colorless oil (108 mg, 87%).

Ethyl 1-{5-[2-(2-chloro-4-fluorophenyl)phenyl]pent-4-yn-1-yl}piperidine-3-carboxylate (16i): According to GP2 starting from **14** (114 mg, 0.300 mmol), $Pd_2(dba)_3{\cdot}x\,CHCl_3$ (3.2 mg, 3.0 μmol), S-Phos (5.0 mg, 12 μmol), K_3PO_4 (131 mg, 0.600 mmol), and 2-chloro-4-fluorophenylboronic acid (80 mg, 0.45 mmol) **16i** was obtained as colorless oil (114 mg, 89%).

Ethyl 1-{4-[2-(4-chloro-2-methylphenyl)phenyl]but-3-yn-1-yl}piperidine-3-carboxylate (15k): According to GP2 starting from **13** (110 mg, 0.300 mmol), $Pd_2(dba)_3{\cdot}x\,CHCl_3$ (3.2 mg, 3.0 μmol), S-Phos (5.0 mg, 12 μmol), K_3PO_4 (131 mg, 0.600 mmol), and 4-chloro-2-methylphenylboronic acid (77 mg, 0.45 mmol, 1.5 equiv) **15k** was obtained as colorless oil (110 mg, 90%).

Ethyl 1-{5-[2-(4-chloro-2-methylphenyl)phenyl]pent-4-yn-1-yl}piperidine-3-carboxylate (16k): According to GP2 starting from **14** (114 mg, 0.300 mmol), $Pd_2(dba)_3{\cdot}x\,CHCl_3$ (3.2 mg, 3.0 μmol), S-Phos (5.0 mg, 12 μmol), K_3PO_4 (131 mg, 0.600 mmol), and 4-chloro-2-methylphenylboronic acid (77 mg, 0.45 mmol) **16k** was obtained as colorless oil (115 mg, 91%).

Ethyl 1-{4-[2-(4-fluoro-2-methylphenyl)phenyl]but-3-yn-1-yl}piperidine-3-carboxylate (15l): According to GP2 starting from **13** (110 mg, 0.300 mmol), $Pd_2(dba)_3{\cdot}x\,CHCl_3$ (3.2 mg, 3.0 μmol), S-Phos (5.0 mg, 12 μmol), K_3PO_4 (131 mg, 0.600 mmol), and 4-fluoro-2-methylphenylboronic acid (70 mg, 0.45 mmol) **15l** was obtained as colorless oil (105 mg, 89%).

Ethyl 1-{5-[2-(4-fluoro-2-methylphenyl)phenyl]pent-4-yn-1-yl}piperidine-3-carboxylate (16l): According to GP2 starting from **14** (114 mg, 0.300 mmol), $Pd_2(dba)_3{\cdot}x\,CHCl_3$ (3.2 mg, 3.0 μmol), S-Phos (5.0 mg, 12 μmol), K_3PO_4 (131 mg, 0.600 mmol), and 4-fluoro-2-methylphenylboronic acid (70 mg, 0.45 mmol) **16l** was obtained as colorless oil (108 mg, 88%).

1-[4-(2-Phenylphenyl)but-3-yn-1-yl]piperidine-3-carboxylic acid (17a): According to GP3 starting from **15a** (108 mg, 0.300 mmol)

and 2 N NaOH (0.45 mL, 0.90 mmol) **17a** was obtained as colorless amorphous solid (90 mg, 90%).

1-[5-(2-Phenylphenyl)pent-4-yn-1-yl]piperidine-3-carboxylic acid (18a): According to GP3 starting from **16a** (112 mg, 0.300 mmol) and 2 N NaOH (0.45 mL, 0.90 mmol) **18a** was obtained as colorless amorphous solid (92 mg, 88%).

1-{4-[2-(2-Chlorophenyl)phenyl]but-3-yn-1-yl}piperidine-3-carboxylic acid (17b): According to GP3 starting from **15b** (79 mg, 0.20 mmol) and 2 N NaOH (0.30 mL, 0.60 mmol) **17b** was obtained as colorless amorphous solid (65 mg, 88%).

1-{5-[2-(2-Chlorophenyl)phenyl]pent-4-yn-1-yl}piperidine-3-carboxylic acid (18b): According to GP3 starting from **16b** (82 mg, 0.20 mmol) and 2 N NaOH (0.30 mL, 0.60 mmol) **18b** was obtained as colorless amorphous solid (68 mg, 89%).

1-{4-[2-(2-Fluorophenyl)phenyl]but-3-yn-1-yl}piperidine-3-carboxylic acid (17c): According to GP3 starting from **15c** (76 mg, 0.20 mmol) and 2 N NaOH (0.30 mL, 0.60 mmol) **17c** was obtained as colorless amorphous solid (64 mg, 88%).

1-{5-[2-(2-Fluorophenyl)phenyl]pent-4-yn-1-yl}piperidine-3-carboxylic acid (18c): According to GP3 starting from **16c** (79 mg, 0.20 mmol) and 2 N NaOH (0.30 mL, 0.60 mmol) **18c** was obtained as colorless amorphous solid (66 mg, 90%).

1-{4-[2-(2-Methylphenyl)phenyl]but-3-yn-1-yl}piperidine-3-carboxylic acid (17d): According to GP3 starting from **15d** (75 mg, 0.20 mmol) and 2 N NaOH (0.30 mL, 0.60 mmol) **17d** was obtained as colorless amorphous solid (63 mg, 91%).

1-{5-[2-(2-Methylphenyl)phenyl]pent-4-yn-1-yl}piperidine-3-carboxylic acid (18d): According to GP3 starting from **16d** (78 mg, 0.20 mmol) and 2 N NaOH (0.30 mL, 0.60 mmol) **18d** was obtained as colorless amorphous solid (66 mg, 91%).

1-{4-[2-(4-Chlorophenyl)phenyl]but-3-yn-1-yl}piperidine-3-carboxylic acid (17e): According to GP3 starting from **15e** (79 mg, 0.20 mmol) and 2 N NaOH (0.30 mL, 0.60 mmol) **17e** was obtained as colorless amorphous solid (66 mg, 90%): $R_f \approx 0.1$ (CH_2Cl_2/CH_3OH 9:1).

1-{5-[2-(4-Chlorophenyl)phenyl]pent-4-yn-1-yl}piperidine-3-carboxylic acid (18e): According to GP3 starting from **16e** (82 mg, 0.20 mmol) and 2 N NaOH (0.30 mL, 0.60 mmol) **18e** was obtained as colorless amorphous solid (68 mg, 89%).

1-{4-[2-(2,4-Dichlorophenyl)phenyl]but-3-yn-1-yl}piperidine-3-carboxylic acid (17f): According to GP3 starting from **15f** (86 mg, 0.20 mmol) and 2 N NaOH (0.30 mL, 0.60 mmol) **17f** was obtained as colorless amorphous solid (70 mg, 87%).

1-{5-[2-(2,4-Dichlorophenyl)phenyl]pent-4-yn-1-yl}piperidine-3-carboxylic acid (18f): According to GP3 starting from **16f** (89 mg, 0.20 mmol) and 2 N NaOH (0.30 mL, 0.60 mmol) **18f** was obtained as colorless amorphous solid (71 mg, 86%).

1-{4-[2-(2,4-Difluorophenyl)phenyl]but-3-yn-1-yl}piperidine-3-carboxylic acid (17g): According to GP3 starting from **15g** (79 mg, 0.20 mmol) and 2 N NaOH (0.30 mL, 0.60 mmol) **17g** was obtained as colorless amorphous solid (66 mg, 89%).

1-{5-[2-(2,4-Difluorophenyl)phenyl]pent-4-yn-1-yl}piperidine-3-carboxylic acid (18g): According to GP3 starting from **16g** (82 mg, 0.20 mmol) and 2 N NaOH (0.30 mL, 0.60 mmol) **18g** was obtained as colorless amorphous solid (68 mg, 89%).

1-{4-[2-(2,4-Dimethylphenyl)phenyl]but-3-yn-1-yl}piperidine-3-carboxylic acid (17h): According to GP3 starting from **15h** (78 mg, 0.20 mmol) and 2 N NaOH (0.30 mL, 0.60 mmol) **17h** was obtained as colorless amorphous solid (65 mg, 90%).

1-{5-[2-(2,4-Dimethylphenyl)phenyl]pent-4-yn-1-yl}piperidine-3-carboxylic acid (18h): According to GP3 starting from **16h** (81 mg, 0.20 mmol) and 2 N NaOH (0.30 mL, 0.60 mmol) **18h** was obtained as colorless amorphous solid (68 mg, 91%).

1-{4-[2-(2-Chloro-4-fluorophenyl)phenyl]but-3-yn-1-yl}piperidine-3-carboxylic acid (17i): According to GP3 starting from **15i** (83 mg, 0.20 mmol) and 2 N NaOH (0.30 mL, 0.60 mmol) **17i** was obtained as colorless amorphous solid (67 mg, 87%).

1-{5-[2-(2-Chloro-4-fluorophenyl)phenyl]pent-4-yn-1-yl}piperidine-3-carboxylic acid (18i): According to GP3 starting from **16i** (86 mg, 0.20 mmol) and 2 N NaOH (0.30 mL, 0.60 mmol) **18i** was obtained as colorless amorphous solid (71 mg, 89%).

1-{4-[2-(4-Chloro-2-methylphenyl)phenyl]but-3-yn-1-yl}piperidine-3-carboxylic acid (17k): According to GP3 starting from **15k** (82 mg, 0.20 mmol) and 2 N NaOH (0.30 mL, 0.60 mmol) **17k** was obtained as colorless amorphous solid (68 mg, 89%).

1-{5-[2-(4-Chloro-2-methylphenyl)phenyl]pent-4-yn-1-yl}piperidine-3-carboxylic acid (18k): According to GP3 starting from **16k** (85 mg, 0.20 mmol) and 2 N NaOH (0.30 mL, 0.60 mmol) **18k** was obtained as colorless amorphous solid (73 mg, 92%).

1-{4-[2-(4-Fluoro-2-methylphenyl)phenyl]but-3-yn-1-yl}piperidine-3-carboxylic acid (17l): According to GP3 starting from **15l** (79 mg, 0.20 mmol) and 2 N NaOH (0.30 mL, 0.60 mmol) **17l** was obtained as colorless amorphous solid (66 mg, 90%).

1-{5-[2-(4-Fluoro-2-methylphenyl)phenyl]pent-4-yn-1-yl}piperidine-3-carboxylic acid (18l): According to GP3 starting from **16l** (82 mg, 0.20 mmol) and 2 N NaOH (0.30 mL, 0.60 mmol) **18l** was obtained as colorless amorphous solid (69 mg, 91%).

(*R*)-Ethyl 1-but-3-yn-1-ylpiperidine-3-carboxylate ((*R*)-7): To but-3-yn-1-yl-4-methylbenzenesulfonate (5.0 mmol, 1.1 g, 1.0 equiv) was added (*R*)-ethyl nipecotate (12.5 mmol, 1.6 g, 3.0 equiv) and the mixture was stirred for 24 h at room temperature. Then CH_2Cl_2 (100 mL) and H_2O (100 mL) were added and the product was extracted with CH_2Cl_2. The combined organic layers were dried over Na_2SO_4 and the solvent was removed under reduced pressure. After purification by CC (eluting with hexane/EtOAc = 1:1) (*R*)-**7** was obtained as colorless oil (1.0 g, 95%).

(*R*)-Ethyl 1-[4-(2-bromophenyl)but-3-yn-1-yl]piperidine-3-carboxylate ((*R*)-13): According to GP1 starting from (*R*)-**7** (1.1 g, 5.0 mmol, 1.0 equiv) and 1-bromo-2-iodo-benzene (1.4 g, 5.0 mmol, 1.0 equiv) (*R*)-**13** was obtained as colorless oil (1.5 g, 83%).

(*R*)-Ethyl 1-{4-[2-(2-methylphenyl)phenyl]but-3-yn-1-yl}piperidine-3-carboxylate ((*R*)-15d): According to GP2 starting from (*R*)-**13** (110 mg, 0.300 mmol), $Pd_2(dba)_3 \cdot x CHCl_3$ (3.2 mg, 3.0 μmol), S-Phos (5.0 mg, 12 μmol), K_3PO_4 (131 mg, 0.600 mmol) and 2-methylphenylboronic acid (61 mg, 0.45 mmol) (*R*)-**15d** was obtained as colorless oil (101 mg, 91%).

(*R*)-Ethyl 1-{4-[2-(2,4-dichlorophenyl)phenyl]but-3-yn-1-yl}piperidine-3-carboxylate ((*R*)-15f): According to GP2 starting from (*R*)-**13** (110 mg, 0.300 mmol), $Pd_2(dba)_3 \cdot x CHCl_3$ (3.2 mg, 3.0 μmol), S-Phos (5.0 mg, 12 μmol), K_3PO_4 (131 mg, 0.600 mmol), and 2,4-dichlorophenylboronic acid (86 mg, 0.45 mmol) (*R*)-**15f** was obtained as colorless oil (110 mg, 86%).

(*R*)-Ethyl 1-{4-[2-(2,4-difluorophenyl)phenyl]but-3-yn-1-yl}piperidine-3-carboxylate ((*R*)-15 g): According to GP2 starting from (*R*)-**13** (110 mg, 0.300 mmol), $Pd_2(dba)_3{\cdot}x CHCl_3$ (3.2 mg, 3.0 μmol), S-Phos (5.0 mg, 12 μmol), K_3PO_4 (131 mg, 0.600 mmol), and 2,4-difluorophenylboronic acid (71 mg, 0.45 mmol) (*R*)-**15 g** was obtained as colorless oil (104 mg, 88%).

(*R*)-Ethyl 1-{4-[2-(2-chloro-4-fluorophenyl)phenyl]but-3-yn-1-yl}-piperidine-3-carboxylate ((*R*)-15 i): According to GP2 starting from (*R*)-**13** (110 mg, 0.300 mmol), $Pd_2(dba)_3{\cdot}x CHCl_3$ (3.2 mg, 3.0 μmol), S-Phos (5.0 mg, 12 μmol), K_3PO_4 (131 mg, 0.600 mmol), and 2-chloro-4-fluorophenylboronic acid (80 mg, 0.45 mmol) (*R*)-**15 i** was obtained as colorless oil (110 mg, 89%).

(*R*)-1-{4-[2-(2-Methylphenyl)phenyl]but-3-yn-1-yl}piperidine-3-carboxylic acid ((*R*)-17 d): According to GP3 starting from (*R*)-**15 d** (75 mg, 0.20 mmol, 1.0 equiv) and 2N NaOH (0.30 mL, 0.60 mmol) (*R*)-**17 d** was obtained as colorless amorphous solid (64 mg, 92%).

(*R*)-1-{4-[2-(2,4-Dichlorophenyl)phenyl]but-3-yn-1-yl}piperidine-3-carboxylic acid ((*R*)-17 f): According to GP3 starting from (*R*)-**15 f** (86 mg, 0.20 mmol) and 2N NaOH (0.30 mL, 0.60 mmol) (*R*)-**17 f** was obtained as colorless amorphous solid (71 mg, 88%).

(*R*)-1-{4-[2-(2,4-Difluorophenyl)phenyl]but-3-yn-1-yl}piperidine-3-carboxylic acid ((*R*)-17 g): According to GP3 starting from (*R*)-**15 g** (79 mg, 0.20 mmol, 1.0 equiv) and 2N NaOH (0.30 mL, 0.60 mmol) (*R*)-**17 g** was obtained as colorless amorphous solid (66 mg, 89%).

(*R*)-1-{4-[2-(2-Chloro-4-fluoro-phenyl)phenyl]but-3-yn-1-yl}piperidine-3-carboxylic acid ((*R*)-17 i): According to GP3 starting from (*R*)-**15 i** (83 mg, 0.20 mmol, 1.0 equiv) and 2N NaOH (0.30 mL, 0.60 mmol) (*R*)-**17 i** was obtained as colorless amorphous solid (70 mg, 91%).

Keywords: cross-coupling reactions · GABA uptake inhibitors · molecular modeling · nipecotic acid · structure–activity relationships

[1] Epilepsy Fact Sheet (updated February 2016), World Health Organization: http://www.who.int/mediacentre/factsheets/fs999/en/ (accessed February 3, 2017).
[2] M. J. Brodie, F. Besag, A. B. Ettinger, M. Mula, G. Gobbi, S. Comai, A. P. Aldenkamp, J. B. Steinhoff, *Pharmacol. Rev.* **2016**, *68*, 563 – 602.
[3] N. G. Bowery, T. G. Smart, *Br. J. Pharmacol.* **2006**, *147*, S109 – S119.
[4] A. C. Foster, J. A. Kemp, *Curr. Opin. Pharmacol.* **2006**, *6*, 7 – 17.
[5] H. S. White, A. Schousboe, *Encyclopedia of Basic Epilepsy Research, Vol. 1*, Elsevier, Amsterdam, **2009**.
[6] L. A. Borden, *Neurochem. Int.* **1996**, *29*, 335 – 356.
[7] K. K. Madsen, R. P. Clausen, O. M. Larsson, P. Krogsgaard-Larsen, A. Schousboe, H. S. White, *J. Neurochem.* **2009**, *109*, 139 – 144.
[8] S. Bröer, U. Gether, *Br. J. Pharmacol.* **2012**, *167*, 256 – 278.
[9] A. C. Lehre, N. M. Rowley, Y. Zhou, S. Holmseth, C. Guo, T. Holen, R. Hua, P. Laake, A. M. Olofsson, I. Poblete-Naredo, D. A. Rusakov, K. K. Madsen, R. P. Clausen, A. Schousboe, H. S. White, N. C. Danbolt, *Epilepsy Res.* **2011**, *95*, 70 – 81.
[10] P. Krogsgaard-Larsen, E. Falch, O. M. Larsson, A. Schousboe, *Epilepsy Res.* **1987**, *1*, 77 – 93.
[11] T. Wein, M. Petrera, L. Allmendinger, G. Höfner, J. Pabel, K. T. Wanner, *ChemMedChem* **2016**, *11*, 509 – 518.
[12] K. E. Andersen, J. L. Sørensen, P. O. Huusfeldt, L. J. S. Knutsen, J. Lau, B. F. Lundt, H. Petersen, P. D. Suzdak, M. D. B. Swedberg, *J. Med. Chem.* **1999**, *42*, 4281 – 4291.
[13] F. E. Ali, W. E. Bondinell, P. A. Dandridge, J. S. Frazee, E. Garvey, G. R. Girard, C. Kaiser, T. W. Ku, J. J. Lafferty, G. I. Moonsammy, H.-J. Oh, J. A. Rush, P. E. Setler, O. D. Stringer, J. W. Venslavsky, B. W. Volpe, L. M. Yunger, C. L. Zirkle, *J. Med. Chem.* **1985**, *28*, 653 – 660.
[14] N. O. Dalby, *Neuropharmacology* **2000**, *39*, 2399 – 2407.
[15] M. Petrera, T. Wein, L. Allmendinger, M. Sindelar, J. Pabel, G. Höfner, K. T. Wanner, *ChemMedChem* **2016**, *11*, 519 – 538.
[16] M. Sindelar, T. A. Lutz, M. Petrera, K. T. Wanner, *J. Med. Chem.* **2013**, *56*, 1323 – 1340.
[17] F. Kern, K. T. Wanner, *ChemMedChem* **2015**, *10*, 396 – 410.
[18] A. Yamashita, S. K. Singh, T. Kawate, Y. Jin, E. Gouaux, *Nature* **2005**, *437*, 215 – 223.
[19] S. K. Singh, C. L. Piscitelli, A. Yamashita, E. Gouaux, *Science* **2008**, *322*, 1655 – 1661.
[20] C. Zepperitz, G. Höfner, K. T. Wanner, *ChemMedChem* **2006**, *1*, 208 – 217.
[21] A. Kragler, G. Höfner, K. T. Wanner, *Eur. J. Med. Chem.* **2008**, *43*, 2404 – 2411.
[22] H. M. Berman, J. Westbrook, Z. Feng, G. Gilliland, T. N. Bhat, H. Weissig, I. N. Shindyalov, P. E. Bourne, *Nucleic Acids Res.* **2000**, *28*, 235 – 242.
[23] B. Boeckmann, A. Bairoch, R. Apweiler, M.-C. Blatter, A. Estreicher, E. Gasteiger, M. J. Martin, K. Michoud, C. O'Donovan, I. Phan, S. Pilbout, M. Schneider, *Nucleic Acids Res.* **2003**, *31*, 365 – 370.
[24] S. Skovstrup, O. Taboureau, H. Bräuner-Osborne, F. S. Jørgensen, *ChemMedChem* **2010**, *5*, 986 – 1000.
[25] M.-y. Shen, A. Sali, *Protein Sci.* **2006**, *15*, 2507 – 2524.
[26] E. Zomot, A. Bendahan, M. Quick, Y. Zhao, J. A. Javitch, B. I. Kanner, *Nature* **2007**, *449*, 726 – 730.
[27] L. R. Forrest, S. Tavoulari, Y.-W. Zhang, G. Rudnick, B. Honig, *Proc. Natl. Acad. Sci. USA* **2007**, *104*, 12761 – 12766.
[28] R. A. Laskowski, M. W. MacArthur, D. S. Moss, J. M. Thornton, *J. Appl. Crystallogr.* **1993**, *26*, 283 – 291.
[29] Instant JChem (version 14.9.1.0), ChemAxon, **2010**, www.chemaxon.com/.
[30] Marvin (version 15.11.9.0), ChemAxon, **2010**, www.chemaxon.com/.
[31] M. F. Sanner, *J. Mol. Graphics Modell.* **1999**, *17*, 55 – 84.
[32] R. Huey, G. M. Morris, A. J. Olson, D. S. Goodsell, *J. Comput. Chem.* **2007**, *28*, 1145 – 1152.

Manuscript received: November 30, 2016
Revised: January 20, 2017
Accepted Article published: January 26, 2017
Final Article published: February 10, 2017

CHEMMEDCHEM
Chemistry & Drug Discovery

Supporting Information

Development of highly potent GAT1 Inhibitors: Synthesis of Nipecotic Acids Derivatives with *N*-arylalkinyl Substituents

Toni Lutz, Dr. Thomas Wein, Dr. Georg Höfner, and Prof. Dr. Klaus T. Wanner

Spectral and physical data for compounds **7-14, 15a-l, 16a-l, 17a-l, and 18a-l**

Ethyl 1-but-3-yn-1-ylpiperidine-3-carboxylate (7):

R_f≈0.5 (hexane/ethyl acetate 1:1). ^{1}H NMR (500 MHz, $CDCl_3$): δ=1.22 (t, J=7.1 Hz, 3H, OCH_2CH_3), 1.40 (qd, J=11.8, 3.9 Hz, 1H, $NCH_2CHCH_{ax}H_{eq}$), 1.48–1.60 (m, 1H, $NCH_2CH_{ax}H_{eq}CH_2CH$), 1.70 (dp, J=10.9, 3.8 Hz, 1H, $NCH_2CH_{ax}H_{eq}CH_2CH$), 1.87–1.94 (m, 1H, $NCH_2CHCH_{ax}H_{eq}$), 1.95 (t, J=2.7 Hz, 1H, C≡CH), 2.04 (td, J=11.0, 2.8 Hz, 1H, $NCH_{ax}H_{eq}CH_2CH_2CH$), 2.19 (t, J=10.6 Hz, 1H, $NCH_{ax}H_{eq}CH$), 2.32–2.38 (m, 2H, NCH_2CH_2C≡CH), 2.52 (tt, J=10.8, 3.8 Hz, 1H, NCH_2CH_{ax}), 2.58 (t, J=7.9 Hz, 2H, NCH_2CH_2C≡C), 2.75 (d, J=11.1 Hz, 1H, $NCH_{ax}H_{eq}CH_2CH_2CH$), 2.95 (d, J=11.1 Hz, 1H, $NCH_{ax}H_{eq}CH$), 4.10 (q, J=7.1 Hz, 2H, OCH_2CH_3) ppm; ^{13}C NMR (126 MHz, $CDCl_3$): δ = 14.30 (OCH_2CH_3), 16.74 (NCH_2CH_2C≡C), 24.60 ($NCH_2CH_2CH_2CH$), 26.92 (NCH_2CHCH_2), 41.86 (NCH_2CH), 53.43 ($NCH_2CH_2CH_2CH$), 55.12 (NCH_2CH), 57.34 (NCH_2CH_2C≡CH), 60.45 (OCH_2CH_3), 69.10 (C≡CH), 82.85 (C≡CH), 174.20 (C=O) ppm; IR (KBr): $\tilde{\nu}$=3298, 2944, 2812, 2118, 1731, 1371, 1310, 1180, 1153, 1032 cm^{-1}; M ($C_{12}H_{19}NO_2$) = 209.28. MS (CI, CH_5^+) *m/z*: 210 $[M+H]^+$; HRMS-EI$^+$ *m/z* $[M]^+$ calcd for $C_{12}H_{19}NO_2$: 209.1416, found: 209.1430.

Ethyl 1-pent-4-yn-1-ylpiperidine-3-carboxylate (8):

R_f≈0.4 (hexane/ethyl acetate 1:1). ^{1}H NMR (400 MHz, $CDCl_3$): δ=1.23 (t, J=7.1 Hz, 3H, OCH_2CH_3), 1.42 (qd, J=11.8, 3.5 Hz, 1H, $NCH_2CHCH_{ax}H_{eq}$), 1.48–1.59 (m, 1H, $NCH_2CH_{ax}H_{eq}CH_2CH$), 1.63–1.74 (m, 3H, $NCH_2CH_2CH_2C$≡CH, $NCH_2CH_{ax}H_{eq}CH_2CH$), 1.84–1.93 (m, 2H, $NCH_2CHCH_{ax}H_{eq}$, C≡CH), 1.98 (td, J=11.0, 2.6 Hz, 1H, $NCH_{ax}H_{eq}CH_2CH_2CH$), 2.10–2.22 (m, 3H, $NCH_{ax}H_{eq}CH$, $NCH_2CH_2CH_2C$≡C), 2.37–2.43 (m, 2H, $NCH_2CH_2CH_2C$≡C), 2.51 (tt, J=10.3, 3.8 Hz, 1H, NCH_2CH_{ax}), 2.70 (d, J=11.1 Hz, 1H, $NCH_{ax}H_{eq}CH_2CH_2CH$), 2.91 (d, J=10.2 Hz, 1H, $NCH_{ax}H_{eq}CH$), 4.10 (q, J=7.1 Hz, 2H, OCH_2CH_3) ppm; ^{13}C NMR (101 MHz, $CDCl_3$): δ=14.17 (OCH_2CH_3), 16.31 ($NCH_2CH_2CH_2C$≡CH), 24.54 ($NCH_2CH_2CH_2CH$), 25.77 ($NCH_2CH_2CH_2C$≡C), 26.91 (NCH_2CHCH_2), 41.84 (NCH_2CH), 53.79 ($NCH_2CH_2CH_2CH$), 55.42 (NCH_2CH), 57.44 ($NCH_2CH_2CH_2C$≡CH), 60.23 (OCH_2CH_3), 68.30 (C≡CH), 84.23 (C≡CH), 174.18 (C=O) ppm; IR (KBr): $\tilde{\nu}$=3298, 2943, 2808, 2771, 2117, 1732, 1469, 1371, 1308, 1179, 1152, 1030 cm^{-1}; MS (CI, CH_5^+) *m/z*: 224 $[M+H]^+$; HRMS-EI$^+$ *m/z* $[M]^+$ calcd for $C_{13}H_{21}NO_2$: 223.1572, found: 223.1572.

Ethyl 1-[4-(2-benzylphenyl)but-3-yn-1-yl]piperidine-3-carboxylate (9):

R_f≈0.3 (hexane/ethyl acetate 8:2). ^{1}H NMR (400 MHz, $CDCl_3$): δ=1.24 (t, J = 7.1 Hz, 3H, OCH_2CH_3), 1.43 (qd, J=12.0, 4.0 Hz, 1H, $NCH_2CHCH_{ax}H_{eq}$), 1.50–1.65 (m, 1H, $NCH_2CH_{ax}H_{eq}CH_2CH$), 1.71 (dp, J=13.5/, 3.7 Hz, 1H, $NCH_2CH_{ax}H_{eq}CH_2CH$), 1.92 (dq, J=13.0, 3.8 Hz, 1H, $NCH_2CHCH_{ax}H_{eq}$), 2.02 (td, J=11.0, 2.7 Hz, 1H, $NCH_{ax}H_{eq}CH_2CH_2CH$), 2.24 (t, J=10.6 Hz, 1H, $NCH_{ax}H_{eq}CH$), 2.50–2.72 (m, 5H, $NCH_2CH_2C{\equiv}C$, $NCH_2CH_2C{\equiv}C$, NCH_2CH_{ax}), 2.80 (d_{br}, J=11.1 Hz, 1H, $NCH_{ax}H_{eq}CH_2CH_2CH$), 3.02 (d_{br}, J=10.5 Hz, 1H, $NCH_{ax}H_{eq}CH$), 4.08–4.16 (m, 4H, OCH_2CH_3, CCH_2C), 7.07–7.23 (m, 6H, $C{\equiv}CCCCH$, $C{\equiv}CCCHCH$, $H_2CCCHCHCH$, $C{\equiv}CCCCHCH$, $H_2CCCHCH$), 7.23–7.30 (m, 2H, $H_2CCCHCH$), 7.40 (dd, J=7.5, 1.3 Hz, 1H, $C{\equiv}CCCH$) ppm; ^{13}C NMR (101 MHz, $CDCl_3$): δ=14.16 (OCH_2CH_3), 17.86 ($NCH_2CH_2C{\equiv}C$), 24.51 ($NCH_2CH_2CH_2CH$), 26.79 (NCH_2CHCH_2), 40.12 (CCH_2C), 41.75 (NCH_2CH), 53.38 ($NCH_2CH_2CH_2CH$), 55.09 (NCH_2CH), 57.50 ($NCH_2CH_2C{\equiv}C$), 60.28 (OCH_2CH_3), 80.33 ($C{\equiv}CCCH$), 92.38 ($C{\equiv}CCCH$), 123.36 ($CH_2C{\equiv}CC$), 125.90 ($CH_2C{\equiv}CCCHCH$), 125.96 ($H_2CCCHCHCH$), 127.85 ($CH_2C{\equiv}CCCHCHCH$), 128.27 (2C, $H_2CCCHCH$), 128.87 (2C, H_2CCCH), 129.23 ($CH_2C{\equiv}CCCCH$), 132.12 ($CH_2C{\equiv}CCCH$), 140.72 ($CCCH_2C$), 142.82 ($CCCH_2C$), 174.05 (C=O) ppm; IR (KBr): $\tilde{\nu}$=3388, 3062, 3026, 2941, 2854, 2808, 2224, 1730, 1599, 1483, 1448, 1369, 1308, 1213, 1180, 1153, 1134, 1101, 1032, 758 cm^{-1}; MS (CI, CH_5^+) *m/z*: 376 $[M+H]^+$; HRMS-EI$^+$ *m/z* $[M]^+$ calcd for $C_{25}H_{29}NO_2$: 375.2198, found: 375.2194.

Ethyl 1-[5-(2-benzylphenyl)pent-4-yn-1-yl]piperidine-3-carboxylate (10):

R_f≈0.25 (hexane/ethyl acetate 8:2). ^{1}H NMR (400 MHz, $CDCl_3$): δ=1.25 (t, J = 7.1 Hz, 3H, OCH_2CH_3), 1.44 (qd, J=11.8, 4.4 Hz, 1H, $NCH_2CHCH_{ax}H_{eq}$), 1.50–1.62 (m, 1H, $NCH_2CH_{ax}H_{eq}CH_2CH$), 1.66–1.81 (m, 3H, $NCH_2CH_{ax}H_{eq}CH_2CH$, $NCH_2CH_2CH_2C{\equiv}C$), 1.87–2.01 (m, 2H, $NCH_2CHCH_{ax}H_{eq}$, $NCH_{ax}H_{eq}CH_2CH_2CH$), 2.15 (t, J=10.0 Hz, 1H, $NCH_{ax}H_{eq}CH$), 2.41–2.49 (m, 4H, $NCH_2CH_2CH_2C{\equiv}C$, $NCH_2CH_2CH_2C{\equiv}C$) 2.56 (tt, J=10.5, 3.8 Hz, 1H, NCH_2CH_{ax}), 2.72 (d_{br}, J=11.1 Hz, 1H, $NCH_{ax}H_{eq}CH_2CH_2CH$), 2.95 (d_{br}, J=10.8 Hz, 1H, $NCH_{ax}H_{eq}CH$), 4.08–4.17 (m, 4H, OCH_2CH_3, CCH_2C), 7.08–7.22 (m, 6H, $C{\equiv}CCCCH$, $C{\equiv}CCCHCH$, $H_2CCCHCHCH$, $C{\equiv}CCCCHCH$, H_2CCCH), 7.23–7.29 (m, 2H, $H_2CCCHCH$), 7.40 (dd, J=7.5, 1.4 Hz, 1H, $C{\equiv}CCCH$) ppm; ^{13}C NMR (101 MHz, $CDCl_3$): δ=14.18 (OCH_2CH_3), 17.50 ($NCH_2CH_2CH_2C{\equiv}C$), 24.51 ($NCH_2CH_2CH_2CH$), 26.00 ($NCH_2CH_2CH_2C{\equiv}C$) 26.91 (NCH_2CHCH_2), 40.10 (CCH_2C), 41.80 (NCH_2CH), 53.78 ($NCH_2CH_2CH_2CH$), 55.39 (NCH_2CH), 57.68 ($NCH_2CH_2CH_2C{\equiv}C$), 60.26 (OCH_2CH_3), 79.73 ($C{\equiv}CCCH$), 93.84 ($C{\equiv}CCCH$), 123.58 ($CH_2C{\equiv}CC$), 125.90 ($CH_2C{\equiv}CCCHCH$), 125.96 ($H_2CCCHCHCH$), 127.73 ($CH_2C{\equiv}CCCHCHCH$), 128.28 (2C, $H_2CCCHCH$), 128.86 (2C, H_2CCCH), 129.21 ($CH_2C{\equiv}CCCCH$), 132.13 ($CH_2C{\equiv}CCCH$), 140.72 ($sCCCH_2C$), 142.69 ($CCCH_2C$), 174.18 (C=O) ppm; IR (KBr): $\tilde{\nu}$=3438, 3060, 3026, 2941, 2854, 2806, 2771, 2224, 1730, 1599, 1483, 1450, 1371, 1308, 1178, 1151, 1105, 1030, 758 cm^{-1}; MS (CI, CH_5^+) *m/z*: 390 $[M+H]^+$; HRMS-EI$^+$ *m/z* $[M]^+$ calcd for $C_{26}H_{31}NO_2$: 389.2355, found: 389.2354.

1-[4-(2-Benzylphenyl)but-3-yn-1-yl]piperidine-3-carboxylic acid (11):

R_f≈0.1 (CH_2Cl_2/CH_3OH 9:1). ^{1}H NMR (400 MHz, 1N NaOD/CH_3OD 1:2, 60 °C): δ=1.33 (qd, J=12.2, 3.8 Hz, 1H, $NCH_2CHCH_{ax}H_{eq}$), 1.53 (qt, J=12.4, 3.6 Hz, 1H, $NCH_2CH_{ax}H_{eq}CH_2CH$), 1.67 (dp, J=13.2, 3.3 Hz, 1H, $NCH_2CH_{ax}H_{eq}CH_2CH$), 1.92 (dq, J=12.4, 3.0 Hz, 1H, $NCH_2CHCH_{ax}H_{eq}$), 2.08 (t_{br}, J=10.9 Hz, 1H, $NCH_{ax}H_{eq}CH_2CH_2CH$), 2.20 (t, J=10.6 Hz, 1H, $NCH_{ax}H_{eq}CH$), 2.36 (tt, J=11.1, 3.7 Hz, 1H, NCH_2CH_{ax}), 2.56–2.71 (m, 4H, $NCH_2CH_2C{\equiv}C$, $NCH_2CH_2C{\equiv}C$), 2.88 (d_{br}, J=11.6 Hz, 1H, $NCH_{ax}H_{eq}CH_2CH_2CH$), 3.05 (d_{br}, J=10.1 Hz, 1H, $NCH_{ax}H_{eq}CH$), 4.12 (s, 2H, CCH_2C), 7.17–7.25 (m, 5H, $C{\equiv}CCCCH$, $C{\equiv}CCCHCH$, $H_2CCCHCHCH$, H_2CCCH), 7.25–7.32 (m, 3H, $C{\equiv}CCCCHCH$, $H_2CCCHCH$), 7.41 (d, J=7.6 Hz, 1H, $C{\equiv}CCCH$) ppm; ^{13}C NMR (101 MHz, 1N NaOD/CH_3OD 1:2, 60 °C): δ=17.40 ($NCH_2CH_2C{\equiv}C$), 25.04 ($NCH_2CH_2CH_2CH$), 28.58 (NCH_2CHCH_2), 40.80 (CCH_2C), 45.59 (NCH_2CH), 53.94 ($NCH_2CH_2CH_2CH$), 57.20 (NCH_2CH), 57.87 ($NCH_2CH_2C{\equiv}C$), 81.48 ($C{\equiv}CCCH$), 93.05 ($C{\equiv}CCCH$), 124.09 ($CH_2C{\equiv}CC$), 126.92 ($H_2CCCHCHCH$), 127.23 ($CH_2C{\equiv}CCCHCH$), 129.15 ($CH_2C{\equiv}CCCHCHCH$), 129.24 (2C, $H_2CCCHCH$), 129.52 (2C, H_2CCCH), 130.50 ($CH_2C{\equiv}CCCCH$), 133.10 ($CH_2C{\equiv}CCCH$), 141.94 ($CCCH_2C$), 143.82 ($CCCH_2C$), 182.61 (C=O) ppm. IR (KBr): $\tilde{\nu}$=3384, 3061, 3025, 2942, 2860, 2224, 1713, 1596, 1494, 1484, 1450, 1392, 1305, 1217, 1155, 1100, 1073, 1041, 1030, 757 cm^{-1}; MS (ESI$^+$) *m/z*: 348 $[M+H]^+$; HRMS-EI$^+$ *m/z* $[M]^+$ calcd for $C_{23}H_{25}NO_2$: 347.1885, found 347.1886.

1-[5-(2-Benzylphenyl)pent-4-yn-1-yl]piperidine-3-carboxylic acid (12):

R_f≈0.1 (CH_2Cl_2/CH_3OH 9:1). ^{1}H NMR (400 MHz, 1N NaOD/CH_3OD 1:2, 60 °C): δ=1.38–1.52 (m, 1H, $NCH_2CHCH_{ax}H_{eq}$), 1.53–1.65 (m, 1H, $NCH_2CH_{ax}H_{eq}CH_2CH$), 1.66–1.75 (m, 1H, $NCH_2CH_{ax}H_{eq}CH_2CH$), 1.75–1.85 (m, 2H, $NCH_2CH_2CH_2C{\equiv}C$), 1.91 (dq, J=13.3, 4.2 Hz, 1H, $NCH_2CHCH_{ax}H_{eq}$), 2.24 (t_{br}, J=10.7 Hz, 1H, $NCH_{ax}H_{eq}CH_2CH_2CH$), 2.33–2.49 (m, 4H, $NCH_{ax}H_{eq}CH$, NCH_2CH_{ax}, $NCH_2CH_2CH_2C{\equiv}C$), 2.59–2.69 (m, 2H, $NCH_2CH_2CH_2C{\equiv}C$), 2.86 (dt, J=11.8, 4.1 Hz, 1H, $NCH_{ax}H_{eq}CH_2CH_2CH$), 3.05 (d_{br}, J=9.0 Hz, 1H, $NCH_{ax}H_{eq}CH$), 4.13 (s, 2H, CCH_2C), 7.16–7.25 (m, 5H, $C{\equiv}CCCCH$, $C{\equiv}CCCHCH$, $H_2CCCHCHCH$, H_2CCCH), 7.25–7.33 (m, 3H, $C{\equiv}CCCCHCH$, $H_2CCCHCH$), 7.42 (dd, J=6.7, 2.6 Hz, 1H, $C{\equiv}CCCH$) ppm; ^{13}C NMR (101 MHz, 1N NaOD/CH_3OD 1:2, 60 °C): δ=17.85 ($NCH_2CH_2CH_2C{\equiv}C$), 24.32 ($NCH_2CH_2CH_2CH$), 25.30 ($NCH_2CH_2CH_2C{\equiv}C$), 28.02 (NCH_2CHCH_2), 40.76 (CCH_2C), 44.65 (NCH_2CH), 54.32 ($NCH_2CH_2CH_2CH$), 57.08 (NCH_2CH), 58.23 ($NCH_2CH_2CH_2C{\equiv}C$), 81.20 ($C{\equiv}CCCH$), 94.07 ($C{\equiv}CCCH$), 124.23 ($CH_2C{\equiv}CC$), 126.98 ($H_2CCCHCHCH$), 127.25 ($CH_2C{\equiv}CCCHCH$), 129.15 ($CH_2C{\equiv}CCCHCHCH$), 129.30 (2C, $H_2CCCHCH$), 129.48 (2C, H_2CCCH), 130.53 ($CH_2C{\equiv}CCCCH$), 133.08 ($CH_2C{\equiv}CCCH$), 141.96 ($CCCH_2C$), 143.70 ($CCCH_2C$), 181.87 (C=O) ppm; IR (KBr): $\tilde{\nu}$=3386, 3060, 3025, 2925, 2860, 2224, 1718, 1597, 1493, 1483, 1449, 1388, 1305, 1217, 1153, 1073, 1029, 758 cm^{-1}; MS (ESI$^+$) *m/z*: 362 $[M+H]^+$; HRMS-EI$^+$ *m/z* $[M]^+$ calcd for $C_{24}H_{27}NO_2$: 361.2042, found: 361.2047.

Ethyl 1-[4-(2-bromophenyl)but-3-yn-1-yl]piperidine-3-carboxylate (13):

R_f≈0.3 (hexane/ethyl acetate 8:2). ^{1}H NMR (500 MHz, $CDCl_3$): δ=1.25 (t, J=7.1 Hz, 3H, OCH_2CH_3), 1.45 (qd, J=11.5, 3.5 Hz, 1H, $NCH_2CHCH_{ax}H_{eq}$), 1.52–1.65 (m, 1H, $NCH_2CH_{ax}H_{eq}CH_2CH$), 1.75 (dp, J=10.8, 3.6 Hz, 1H, $NCH_2CH_{ax}H_{eq}CH_2CH$), 1.90–2.00 (m, 1H, $NCH_2CHCH_{ax}H_{eq}$), 2.14 (td, J=11.0, 2.7 Hz, 1H, $NCH_{ax}H_{eq}CH_2CH_2CH$), 2.30 (t, J=10.6 Hz, 1H, $NCH_{ax}H_{eq}CH$), 2.57 (tt, J=10.7/3.8 Hz, 1H, NCH_2CH_{ax}), 2.62–2.69 (m, 2H, $NCH_2CH_2C{\equiv}C$), 2.71–2.78 (m, 2H, $NCH_2CH_2C{\equiv}C$), 2.83 (d_{br}, J=11.1 Hz, 1H, $NCH_{ax}H_{eq}CH_2CH_2CH$), 3.06 (d_{br}, J=10.7 Hz, 1H, $NCH_{ax}H_{eq}CH$), 4.13 (q, J=7.1 Hz, 2H, OCH_2CH_3), 7.12 (td, J=8.0, 1.6 Hz, 1 H, $BrCCHCH$), 7.22 (td, J=7.6, 1.1 Hz, 1H, $BrCCCHCH$), 7.42 (dd, J = 7.7, 1.5 Hz, 1H, $C{\equiv}CCCH$), 7.55 (dd, J=8.0, 0.8 Hz, 1H, $BrCCH$) ppm; ^{13}C NMR (125 MHz, $CDCl_3$): δ=14.17 (OCH_2CH_3), 17.85 ($NCH_2CH_2C{\equiv}C$), 24.57 ($NCH_2CH_2CH_2CH$), 26.78 (NCH_2CHCH_2), 41.84 (NCH_2CH), 53.33 ($NCH_2CH_2CH_2CH$), 55.05 (NCH_2CH), 57.20 ($NCH_2CH_2C{\equiv}C$), 60.29 (OCH_2CH_3), 79.98 ($C{\equiv}CCCH$), 93.47 ($C{\equiv}CCCH$), 125.36 (CBr), 125.71 ($BrCC$), 126.84 ($BrCCCHCH$), 128.76 ($BrCCHCH$), 132.20 ($BrCCH$), 133.26 ($BrCCCH$), 174.08 (C=O) ppm; IR (KBr): $\tilde{\nu}$=3436, 3064, 2943, 2854, 2810, 2231, 1730, 1587, 1557, 1469, 1434, 1370, 1308, 1180, 1153, 1101, 1052, 1026, 862, 754 cm^{-1}; MS (CI, CH_5^+) *m/z*: 364 $[M+H]^+$; HRMS-EI$^+$ *m/z* $[M]^+$ calcd for $C_{18}H_{22}BrNO_2$: 363.0834, found: 363.0835.

Ethyl 1-[5-(2-bromophenyl)pent-4-yn-1-yl]piperidine-3-carboxylate (14):

R_f≈0.25 (hexane/ethyl acetate 8:2). ^{1}H NMR (500 MHz, $CDCl_3$): δ=1.25 (t, J=7.1 Hz, 3H, OCH_2CH_3), 1.46 (qd, J=12.0, 3.9 Hz, 1H, $NCH_2CHCH_{ax}H_{eq}$), 1.52–1.62 (m, 1H, $NCH_2CH_{ax}H_{eq}CH_2CH$), 1.73 (dp, J=13.0 Hz, 1H, $NCH_2CH_{ax}H_{eq}CH_2CH$), 1.82 (p, J=7.1 Hz, 2H, $NCH_2CH_2CH_2C{\equiv}C$), 1.89–1.95 (m, 1H, $NCH_2CHCH_{ax}H_{eq}$), 2.04 (td, J=10.9, 2.4 Hz, 1H, $NCH_{ax}H_{eq}CH_2CH_2CH$), 2.21 (t, J=10.4 Hz, 1H, $NCH_{ax}H_{eq}CH$), 2.49–2.59 (m, 5H, $NCH_2CH_2CH_2C{\equiv}C$, $NCH_2CH_2CH_2C{\equiv}C$, NCH_2CH_{ax}), 2.77 (d_{br}, J=11.0 Hz, 1H, $NCH_{ax}H_{eq}CH_2CH_2CH$), 2.99 (d_{br}, J=9.9 Hz, 1 H, $NCH_{ax}H_{eq}CH$), 4.13 (q, J=7.1 Hz, 2H, OCH_2CH_3), 7.11 (td, J=7.8, 1.7 Hz, 1H, $BrCCHCH$), 7.22 (td, J=7.6, 1.2 Hz, 1H, $BrCCCHCH$), 7.41 (dd, J=7.7, 1.7 Hz, 1H, $BrCCCH$), 7.55 (dd, J=8.1, 1.2 Hz, 1H, $BrCCH$) ppm; ^{13}C NMR (125 MHz, $CDCl_3$): δ=14.18 (OCH_2CH_3), 17.50 ($NCH_2CH_2CH_2C{\equiv}C$), 24.56 ($NCH_2CH_2CH_2CH$), 25.78 ($NCH_2CH_2CH_2C{\equiv}C$), 26.92 (NCH_2CHCH_2), 41.85 (NCH_2CH), 53.83 ($NCH_2CH_2CH_2CH$), 55.47 (NCH_2CH), 57.57 ($NCH_2CH_2CH_2C{\equiv}C$), 60.24 (OCH_2CH_3), 79.52 ($CH_2C{\equiv}C$), 94.98 ($CH_2C{\equiv}C$), 125.40 (CBr), 125.86 ($BrCC$), 126.84 ($BrCCCHCH$), 128.64 ($BrCCHCH$), 132.19 ($BrCCH$), 133.20 ($BrCCCH$), 174.23 (C=O) ppm; IR (KBr): $\tilde{\nu}$=3376, 3065, 2942, 2807, 2770, 2231, 1730, 1587, 1556, 1469, 1434, 1371, 1306, 1178, 1151, 1026, 754 cm^{-1}; MS (CI, CH_5^+) *m/z*: 378 $[M+H]^+$; HRMS-EI$^+$ *m/z* $[M]^+$ calcd for $C_{19}H_{24}BrNO_2$: 377.0990, found: 377.1000.

Ethyl 1-[4-(2-phenylphenyl)but-3-yn-1-yl]piperidine-3-carboxylate (15a):

R_f≈0.3 (hexane/ethyl acetate 8:2). ^{1}H NMR (400 MHz, $CDCl_3$): δ=1.24 (t, J=7.1 Hz, 3H, OCH_2CH_3), 1.41 (qd, J=12.1, 3.2 Hz, 1H, $NCH_2CHCH_{ax}H_{eq}$), 1.53 (qt, J=12.1, 3.8 Hz, 1H, $NCH_2CH_{ax}H_{eq}CH_2CH$), 1.69 (dp, J=13.2, 3.4 Hz, 1H, $NCH_2CH_{ax}H_{eq}CH_2CH$), 1.92 (dq, J=12.2, 3.8 Hz, 1H, $NCH_2CHCH_{ax}H_{eq}$), 2.02 (td, J=11.0, 2.6 Hz, 1H, $NCH_{ax}H_{eq}CH_2CH_2CH$), 2.20 (t, J=10.6 Hz, 1H, $NCH_{ax}H_{eq}CH$), 2.44–2.58 (m, 5H, $NCH_2CH_2C{\equiv}C$, $NCH_2CH_2C{\equiv}C$, NCH_2CH_{ax}), 2.72 (d_{br}, J=11.3 Hz, 1H, $NCH_{ax}H_{eq}CH_2CH_2CH$), 2.95 (d_{br}, J=10.8 Hz, 1H, $NCH_{ax}H_{eq}CH$), 4.12 (q, J=7.1 Hz, 2H, OCH_2CH_3), 7.25 (td, J=7.6, 1.5 Hz, 1H, C≡CCCHCH), 7.30–7.37 (m, 3H, C≡CCCCCHCHCH, C≡CCCCHCH, C≡CCCCH), 7.40 (td, J=7.6, 1.2 Hz, 2H, C≡CCCCCHCH), 7.50 (d, J=7.4 Hz, 1H, C≡CCCH), 7.58 (dd, J=8.2, 1.3 Hz, 2H, C≡CCCCCH) ppm; ^{13}C NMR (101 MHz, $CDCl_3$): δ = 14.15 (OCH_2CH_3), 17.61 ($NCH_2CH_2C{\equiv}C$), 24.53 ($NCH_2CH_2CH_2CH$), 26.77 (NCH_2CHCH_2), 41.79 (NCH_2CH), 53.12 ($NCH_2CH_2CH_2CH$), 54.92 (NCH_2CH), 57.05 ($NCH_2CH_2C{\equiv}C$), 60.26 (OCH_2CH_3), 80.82 (C≡CCCH), 91.29 (C≡CCCH), 121.96 ($CH_2C{\equiv}CC$), 126.85 ($CH_2C{\equiv}CCCHCH$), 127.20 (C≡CCCCCHCHCH), 127.74 (2C, C≡CCCCCHCH), 127.81 ($CH_2C{\equiv}CCCHCHCH$), 129.20 (2C, C≡CCCCCH), 129.33 ($CH_2C{\equiv}CCCCH$), 132.91 ($CH_2C{\equiv}CCCH$), 140.61 (C≡CCCC), 143.56 (C≡CCC), 174.06 (C=O) ppm; IR (KBr): $\tilde{\nu}$=3438, 3060, 3022, 2978, 2943, 2854, 2810, 2227, 1730, 1475, 1448, 1433, 1371, 1308, 1180, 1153, 1101, 1032, 758, 737, 700 cm^{-1}; MS (CI, CH_5^+) *m/z*: 362 $[M+H]^+$; HRMS-EI$^+$ *m/z* $[M]^+$ calcd for $C_{24}H_{27}NO_2$: 361.2042, found: 361.2041.

Ethyl 1-[5-(2-phenylphenyl)pent-4-yn-1-yl]piperidine-3-carboxylate (16a):

R_f≈0.25 (hexane/ethyl acetate 8:2). ^{1}H NMR (400 MHz, $CDCl_3$): δ=1.25 (t, J=7.1 Hz, 3H, OCH_2CH_3), 1.43 (qd, J=11.7, 3.7 Hz, 1H, $NCH_2CHCH_{ax}H_{eq}$), 1.49–1.60 (m, 1H, $NCH_2CH_{ax}H_{eq}CH_2CH$), 1.60–1.74 (m, 3H, $NCH_2CH_2CH_2C{\equiv}C$, $NCH_2CH_{ax}H_{eq}CH_2CH$), 1.87–1.96 (m, 2H, $NCH_2CHCH_{ax}H_{eq}$, $NCH_{ax}H_{eq}CH_2CH_2CH$), 2.10 (t, J=10.5 Hz, 1H, $NCH_{ax}H_{eq}CH$), 2.28–2.35 (m, 4H, $NCH_2CH_2CH_2C{\equiv}C$, $NCH_2CH_2CH_2C{\equiv}C$), 2.53 (tt, J=10.4, 3.8 Hz, 1 H, NCH_2CH_{ax}), 2.67 (d_{br}, J=11.0 Hz, 1H, $NCH_{ax}H_{eq}CH_2CH_2CH$), 2.90 (d_{br}, J=9.9 Hz, 1H, $NCH_{ax}H_{eq}CH$), 4.13 (q, J=7.1 Hz, 2H, OCH_2CH_3), 7.26 (td, J=7.0, 2.1 Hz, 1H, C≡CCCHCH), 7.29–7.37 (m, 3H, C≡CCCCCHCHCH, C≡CCCCH, C≡CCCCHCH), 7.38–7.44 (m, 2H, C≡CCCCCHCH), 7.50 (d, J=8.2 Hz, 1H, $CH_2CHCHCCH$), 7.56–7.60 (m, 2H, C≡CCCCCH) ppm; ^{13}C NMR (101 MHz, $CDCl_3$): δ=14.18 (OCH_2CH_3), 17.45 ($NCH_2CH_2CH_2C{\equiv}C$), 24.54 ($NCH_2CH_2CH_2CH$), 25.68 ($NCH_2CH_2CH_2C{\equiv}C$), 26.93 (NCH_2CHCH_2), 41.83 (NCH_2CH), 53.73 ($NCH_2CH_2CH_2CH$), 55.42 (NCH_2CH), 57.55 ($NCH_2CH_2CH_2C{\equiv}C$), 60.23 (OCH_2CH_3), 80.25 ($CH_2C{\equiv}C$), 92.79 ($CH_2C{\equiv}C$), 122.15 ($CH_2C{\equiv}CC$), 126.85 ($CH_2C{\equiv}CCCHCH$), 127.17 (C≡CCCCCHCHCH), 127.70 ($CH_2C{\equiv}CCCHCHCH$), 127.76 (2C, C≡CCCCCHCH), 129.20 (2C, C≡CCCCCH), 129.35 ($CH_2C{\equiv}CCCCH$), 132.94 ($CH_2C{\equiv}CCCH$), 140.73 (C≡CCCC), 143.54 (C≡CCC), 174.22 (C=O) ppm; IR (KBr): $\tilde{\nu}$=3385, 3060, 2941, 2806, 2770, 2226, 1730, 1476, 1449, 1432, 1370, 1306, 1178, 1151, 1104, 1030, 757, 736, 699 cm^{-1}; MS (CI, CH_5^+) *m/z*: 376 $[M+H]^+$; HRMS-EI$^+$ *m/z* $[M]^+$ calcd for $C_{25}H_{29}NO_2$: 375.2198, found: 375.2192.

Ethyl 1-{4-[2-(2-chlorophenyl)phenyl]but-3-yn-1-yl}piperidine-3-carboxylate (15b):

R_f≈0.3 (hexane/ethyl acetate 8:2). ^{1}H NMR (400 MHz, $CDCl_3$): δ=1.24 (t, J=7.1 Hz, 3H, OCH_2CH_3), 1.39 (qd, J=11.9, 3.7 Hz, 1H, $NCH_2CHCH_{ax}H_{eq}$), 1.45–1.57 (m, 1H, $NCH_2CH_{ax}H_{eq}CH_2CH$), 1.68 (dp, J=13.1, 3.3 Hz, 1H, $NCH_2CH_{ax}H_{eq}CH_2CH$), 1.86–2.00 (m, 2H, $NCH_2CHCH_{ax}H_{eq}$, $NCH_{ax}H_{eq}CH_2CH_2CH$), 2.15 (t, J=10.7 Hz, 1H, $NCH_{ax}H_{eq}CH$), 2.33–2.44 (m, 4H, $NCH_2CH_2C{\equiv}C$, $NCH_2CH_2C{\equiv}C$), 2.50 (tt, J=10.4, 3.8 Hz, 1H, NCH_2CH_{ax}), 2.65 (d_{br}, J=11.2 Hz, 1H, $NCH_{ax}H_{eq}CH_2CH_2CH$), 2.88 (d_{br}, J=11.0 Hz, 1H, $NCH_{ax}H_{eq}CH$), 4.12 (q, J=7.1 Hz, 2H, OCH_2CH_3), 7.24–7.36 (m, 6H, C≡CCCCH, ClCCCH, ClCCCHCH, ClCCHCH, C≡CCCHCH, C≡CCCCHCH), 7.43–7.51 (m, 2H, ClCCH, C≡CCCH,) ppm; ^{13}C NMR (101 MHz, $CDCl_3$): δ=14.16 (OCH_2CH_3), 17.42 ($NCH_2CH_2C{\equiv}C$), 24.51 ($NCH_2CH_2CH_2CH$), 26.77 (NCH_2CHCH_2), 41.78 (NCH_2CH), 53.03 ($NCH_2CH_2CH_2CH$), 54.86 (NCH_2CH), 57.08 ($NCH_2CH_2C{\equiv}C$), 60.27 (OCH_2CH_3), 80.04 (C≡CCCH), 91.80 (C≡CCCH), 123.38 ($CH_2C{\equiv}CC$), 126.13 (ClCCCHCH), 127.28 ($CH_2C{\equiv}CCCHCHCH$), 127.54 ($CH_2C{\equiv}CCCHCH$), 128.65 (ClCCCH), 129.22 (ClCCH), 129.53 ($CH_2C{\equiv}CCCCH$), 131.46 (ClCCHCH), 131.83 ($CH_2C{\equiv}CCCH$), 133.28 (ClC), 139.79 (ClCC), 141.80 (ClCCC), 174.08 (C=O) ppm; IR (KBr): $\tilde{\nu}$=3360, 3059, 2977, 2941, 2810, 2229, 1728, 1586, 1490, 1466, 1444, 1366, 1252, 1177, 1153, 1100, 1071, 1033, 757 cm^{-1}; MS (CI, CH_5^+) *m/z*: 396 $[M+H]^+$; HRMS-EI$^+$ *m/z* $[M]^+$ calcd for $C_{24}H_{26}ClNO_2$: 395.1652, found: 395.1653.

Ethyl 1-{5-[2-(2-chlorophenyl)phenyl]pent-4-yn-1-yl}piperidine-3-carboxylate (16b):

R_f≈0.25 (hexane/ethyl acetate 8:2). ^{1}H NMR (400 MHz, $CDCl_3$): δ=1.24 (t, J=7.1 Hz, 3H, OCH_2CH_3), 1.44 (qd, J=12.1, 3.7 Hz, 1H, $NCH_2CHCH_{ax}H_{eq}$), 1.50–1.60 (m, 1H, $NCH_2CH_{ax}H_{eq}CH_2CH$), 1.64 (p, J=7.2 Hz, 2H, $NCH_2CH_2CH_2C{\equiv}C$), 1.71 (dp, J=13.2, 3.6 Hz, 1H, $NCH_2CH_{ax}H_{eq}CH_2CH$), 1.88–1.97 (m, 2H, $NCH_2CHCH_{ax}H_{eq}$, $NCH_{ax}H_{eq}CH_2CH_2CH$), 2.11 (t, J=10.5 Hz, 1H, $NCH_{ax}H_{eq}CH$), 2.27–2.35 (m, 4H, $NCH_2CH_2CH_2C{\equiv}C$, $NCH_2CH_2CH_2C{\equiv}C$), 2.53 (tt, J=10.4, 3.8 Hz, 1H, NCH_2CH_{ax}), 2.66 (d_{br}, J=11.1 Hz, 1H, $NCH_{ax}H_{eq}CH_2CH_2CH$), 2.90 (d_{br}, J=10.2 Hz, 1H, $NCH_{ax}H_{eq}CH$), 4.12 (q, J=7.1 Hz, 2H, OCH_2CH_3), 7.24–7.34 (m, 3H, $C{\equiv}CCCHCH$, $C{\equiv}CCCCH$, $C{\equiv}CCCCHCH$), 7.37 (d, J=8.5 Hz, 2H, $ClCCCH$), 7.47–7.52 (m, 3H, $ClCCHCH$, $C{\equiv}CCCH$) ppm; ^{13}C NMR (101 MHz, $CDCl_3$): δ=14.34 (OCH_2CH_3), 17.60 ($NCH_2CH_2CH_2C{\equiv}C$), 24.72 ($NCH_2CH_2CH_2CH$), 25.86 ($NCH_2CH_2CH_2C{\equiv}C$), 27.07 (NCH_2CHCH_2), 42.00 (NCH_2CH), 53.96 ($NCH_2CH_2CH_2CH$), 55.54 (NCH_2CH), 57.75 ($NCH_2CH_2CH_2C{\equiv}C$), 60.41 (OCH_2CH_3), 80.14 ($CH_2C{\equiv}C$), 93.38 ($CH_2C{\equiv}C$), 122.28 ($CH_2C{\equiv}CC$), 126.00 ($ClCCCHCH$), 127.37 ($CH_2C{\equiv}CCCHCH$), 127.96 ($CH_2C{\equiv}CCCHCHCH$), 128.13 ($ClCCCH$), 128.75 ($ClCCH$), 129.30 ($CH_2C{\equiv}CCCCH$), 130.72 ($CH_2C{\equiv}CCCH$), 133.18 ($ClCCHCH$), 133.35 (ClC), 139.34 ($ClCC$), 142.43 ($ClCCC$), 174.37 (C=O) ppm; IR (KBr): $\tilde{\nu}$=3435, 3059, 2941, 2806, 2771, 2229, 1730, 1466, 1441, 1428, 1371, 1306, 1178, 1151, 1104, 1072, 1032, 1005, 756 cm^{-1}; MS (CI, CH_5^+) *m/z*: 410 $[M+H]^+$; HRMS-EI$^+$ *m/z* $[M]^+$ calcd for $C_{25}H_{28}ClNO_2$: 409.1809, found: 409.1811.

Ethyl 1-{4-[2-(2-fluorophenyl)phenyl]but-3-yn-1-yl}piperidine-3-carboxylate (15c):

R_f≈0.3 (hexane/ethyl acetate 8:2). ^{1}H NMR (500 MHz, $CDCl_3$): δ=1.24 (t, J=7.1 Hz, 3H, OCH_2CH_3), 1.40 (qd, J=12.0, 3.8 Hz, 1H, $NCH_2CHCH_{ax}H_{eq}$), 1.46–1.58 (m, 1H, $NCH_2CH_{ax}H_{eq}CH_2CH$), 1.69 (dp, J=13.4, 3.6 Hz, 1H, $NCH_2CH_{ax}H_{eq}CH_2CH$), 1.87–1.95 (m, 1H, $NCH_2CHCH_{ax}H_{eq}$), 1.99 (td, J=11.0/2.8 Hz, 1H, $NCH_{ax}H_{eq}CH_2CH_2CH$), 2.17 (t, J=10.7 Hz, 1H, $NCH_{ax}H_{eq}CH$), 2.39–2.55 (m, 5H, $NCH_2CH_2C{\equiv}C$, $NCH_2CH_2C{\equiv}C$, NCH_2CH_{ax}), 2.68 (d_{br}, J=11.3 Hz, 1H, $NCH_{ax}H_{eq}CH_2CH_2CH$), 2.91 (dd, J=11.1, 3.1 Hz, 1H, $NCH_{ax}H_{eq}CH$), 4.12 (q, J=7.1 Hz, 2H, OCH_2CH_3), 7.10–7.20 (m, 2H, $FCCH$, $FCCCHCH$), 7.27–7.37 (m, 4H, $FCCHCH$, $C{\equiv}CCCCH$, $C{\equiv}CCCCHCH$, $C{\equiv}CCCHCH$), 7.41 (td, J=7.5, 1.8 Hz, 1H, $FCCCH$), 7.50 (dt, J=7.0, 1.3 Hz, 1H, $C{\equiv}CCCH$) ppm; ^{13}C NMR (101 MHz, $CDCl_3$): δ=14.15 (OCH_2CH_3), 17.47 ($NCH_2CH_2C{\equiv}C$), 24.52 ($NCH_2CH_2CH_2CH$), 26.77 (NCH_2CHCH_2), 41.78 (NCH_2CH), 53.07 ($NCH_2CH_2CH_2CH$), 54.88 (NCH_2CH), 57.10 ($NCH_2CH_2C{\equiv}C$), 60.28 (OCH_2CH_3), 80.21 ($C{\equiv}CCCH$), 91.39 ($C{\equiv}CCCH$), 115.43 (d, $^2J_{CF}$=22.4 Hz, $FCCH$), 123.40 ($CH_2C{\equiv}CC$), 123.45 (d, $^4J_{CF}$=3.5 Hz, $FCCCHCH$), 127.46 ($CH_2C{\equiv}CCCHCH$), 127.54 ($CH_2C{\equiv}CCCHCHCH$), 128.42 (d, $^2J_{CF}$=15.3 Hz, FCC), 129.22 (d, $^3J_{CF}$=8.1 Hz, $FCCHCH$), 129.96 ($CH_2C{\equiv}CCCCH$), 131.83 (d, $^3J_{CF}$=2.8 Hz, $FCCCH$), 132.24 ($CH_2C{\equiv}CCCH$), 138.09 ($CH_2C{\equiv}CCC$), 159.67 (s, $^1J_{CF}$=247.4 Hz, FC), 174.08 (C=O) ppm; IR (KBr): $\tilde{\nu}$=3437, 3061, 2978, 2943, 2854, 2810, 2228, 1730, 1500, 1472, 1440, 1370, 1305, 1213, 1180, 1153, 1100, 1033, 824, 757 cm^{-1}; MS (CI, CH_5^+) *m/z*: 380 $[M+H]^+$; HRMS-EI$^+$ *m/z* $[M]^+$ calcd for $C_{24}H_{26}FNO_2$: 379.1948, found: 379.1947.

Ethyl 1-{5-[2-(2-fluorophenyl)phenyl]pent-4-yn-1-yl}piperidine-3-carboxylate (16c):

R_f≈0.25 (hexane/ethyl acetate 8:2). ^{1}H NMR (400 MHz, $CDCl_3$): δ=1.25 (t, J=7.1 Hz, 3H, OCH_2CH_3), 1.43 (qd, J=12.3, 3.7 Hz, 1H, $NCH_2CHCH_{ax}H_{eq}$), 1.48–1.63 (m, 3H, $NCH_2CH_{ax}H_{eq}CH_2CH$, $NCH_2CH_2CH_2C{\equiv}C$), 1.70 (dp, J=13.1, 3.7 Hz, 1H, $NCH_2CH_{ax}H_{eq}CH_2CH$), 1.86–1.96 (m, 2H, $NCH_2CHCH_{ax}H_{eq}$, $NCH_{ax}H_{eq}CH_2CH_2CH$), 2.09 (t, J=10.5 Hz, 1H, $NCH_{ax}H_{eq}CH$), 2.22–2.32 (m, J=8.4, 6.8 Hz, 4H, $NCH_2CH_2CH_2C{\equiv}C$, $NCH_2CH_2CH_2C{\equiv}C$), 2.52 (tt, J=10.4, 3.8 Hz, 1H, NCH_2CH_{ax}), 2.65 (d_{br}, J=11.3 Hz, 1H, $NCH_{ax}H_{eq}CH_2CH_2CH$), 2.88 (d_{br}, J=10.4 Hz, 1H, $NCH_{ax}H_{eq}CH$), 4.13 (q, J=7.1 Hz, 2H, OCH_2CH_3), 7.10–7.21 (m, 2H, $FCCH$, $FCCCHCH$), 7.27–7.37 (m, 4H, $C{\equiv}CCCCH$, $C{\equiv}CCCCHCH$, $C{\equiv}CCCHCH$, $FCCHCH$), 7.41 (td, J=7.5, 1.8 Hz, 1H, $FCCCH$), 7.51 (dt, J=6.5, 1.5 Hz, 1 H, $C{\equiv}CCCH$); ^{13}C NMR (101 MHz, $CDCl_3$): δ=14.18 (OCH_2CH_3), 17.34 ($NCH_2CH_2CH_2C{\equiv}C$), 24.54 ($NCH_2CH_2CH_2C{\equiv}C$), 25.68 ($NCH_2CH_2CH_2CH$), 26.94 (NCH_2CHCH_2), 41.84 (NCH_2CH), 53.71 ($NCH_2CH_2CH_2CH$), 55.41 (NCH_2CH), 57.40 ($NCH_2CH_2CH_2C{\equiv}C$), 60.24 (OCH_2CH_3), 79.64 ($CH_2C{\equiv}C$), 92.88 ($CH_2C{\equiv}C$), 115.45 (d, $^2J_{CF}$=22.4 Hz, $FCCH$), 123.49 (d, $^4J_{CF}$=3.5 Hz, $FCCCHCH$), 123.60 ($CH_2C{\equiv}CC$), 127.35 ($CH_2C{\equiv}CCCHCH$), 127.54 ($CH_2C{\equiv}CCCHCHCH$), 128.53 (s, $^2J_{CF}$=15.4 Hz, FCC), 129.21 (d, $^3J_{CF}$=8.0 Hz, $FCCHCH$), 129.96 ($CH_2C{\equiv}CCCCH$), 131.81 (d, $^3J_{CF}$=3.2 Hz, $FCCCH$), 132.30 ($CH_2C{\equiv}CCCH$), 138.01 ($CH_2C{\equiv}CCC$), 159.69 (d, $^1J_{CF}$=247.3 Hz, FC), 174.24 (C=O) ppm; IR (KBr): $\tilde{\nu}$=3434, 3061, 2942, 2865, 2807, 2771, 2229, 1730, 1500, 1472, 1439, 1371, 1306, 1212, 1179,

1152, 1106, 1031, 824, 757 cm^{-1} ; MS (CI, CH_5^+) *m/z*: 394 $[M+H]^+$; HRMS-EI$^+$ *m/z* $[M]^+$ calcd for $C_{25}H_{28}FNO_2$: 393.2104, found: 393.2105.

Ethyl 1-{4-[2-(2-methylphenyl)phenyl]but-3-yn-1-yl}piperidine-3-carboxylate (15d):

R_f≈0.3 (hexane/ethyl acetate 8:2). ^{1}H NMR (400 MHz, $CDCl_3$): δ=1.24 (t, *J*=7.1 Hz, 3H, OCH_2CH_3), 1.39 (qd, *J*=11.9, 3.8 Hz, 1H, $NCH_2CHCH_{ax}H_{eq}$), 1.44–1.56 (m, 1H, $NCH_2CH_{ax}H_{eq}CH_2CH$), 1.67 (dp, *J*=13.1, 3.6 Hz, 1H, $NCH_2CH_{ax}H_{eq}CH_2CH$), 1.87–2.00 (m, 2H, $NCH_2CHCH_{ax}H_{eq}$, $NCH_{ax}H_{eq}CH_2CH_2CH$), 2.10–2.19 (m, 4H, $NCH_{ax}H_{eq}CH$, H_3CC), 2.31–2.39 (m, 4H, $NCH_2CH_2C{\equiv}C$, $NCH_2CH_2C{\equiv}C$), 2.49 (tt, *J*=10.4, 3.8 Hz, 1H, NCH_2CH_{ax}), 2.64 (d_{br}, *J*=11.1 Hz, 1H, $NCH_{ax}H_{eq}CH_2CH_2CH$), 2.87 (d_{br}, *J*=9.8 Hz, 1H, $NCH_{ax}H_{eq}CH$), 4.12 (q, *J*=7.1 Hz, 2H, OCH_2CH_3), 7.14–7.34 (m, 7H, H_{Ar}), 7.46 (dd, *J*=7.6, 1.4 Hz, 1H, C≡CCCH) ppm; ^{13}C NMR (101 MHz, $CDCl_3$): δ=14.18 (OCH_2CH_3), 17.45 ($NCH_2CH_2C{\equiv}C$), 19.96 (H_3CC), 24.54 ($NCH_2CH_2CH_2CH$), 26.79 (NCH_2CHCH_2), 41.81 (NCH_2CH), 53.05 ($NCH_2CH_2CH_2CH$), 54.88 (NCH_2CH), 57.13 ($NCH_2CH_2C{\equiv}C$), 60.28 (OCH_2CH_3), 80.45 (C≡CCCH), 91.27 (C≡CCCH), 123.26 ($CH_2C{\equiv}CC$), 125.17 ($CH_2C{\equiv}CCCCH$), 126.81 ($CH_2C{\equiv}CCCHCH$), 127.31 ($H_3CCCHCH$), 127.42 ($CH_2C{\equiv}CCCHCHCH$), 129.35 ($H_3CCCCHCH$), 129.56 (2C, H_3CCCCH, H_3CCCH), 131.78 ($CH_2C{\equiv}CCCH$), 136.13 (H_3CC), 140.95 (H_3CCC), 144.40 ($CH_2C{\equiv}CCC$), 174.12 (C=O) ppm; IR (KBr): $\tilde{\nu}$=3363, 3059, 2940, 2853, 2808, 2228, 1731, 1561, 1473, 1442, 1370, 1310, 1179, 1152, 1133, 1101, 1033, 757 cm^{-1} ; MS (CI, CH_5^+) *m/z*: 376 $[M+H]^+$; HRMS-EI$^+$ *m/z* $[M]^+$ calcd for $C_{25}H_{29}NO_2$: 375.2198, found: 375.2197.

Ethyl 1-{5-[2-(2-methylphenyl)phenyl]pent-4-yn-1-yl}piperidine-3-carboxylate (16d):

R_f≈0.25 (hexane/ethyl acetate 8:2). ^{1}H NMR (500 MHz, $CDCl_3$): δ=1.26 (t, *J*=7.1 Hz, 3H, OCH_2CH_3), 1.37–1.59 (m, 4H, $NCH_2CHCH_{ax}H_{eq}$, $NCH_2CH_2CH_2C{\equiv}C$, $NCH_2CH_{ax}H_{eq}CH_2CH$), 1.69 (dp, *J*=13.0, 3.5 Hz, 1H, $NCH_2CH_{ax}H_{eq}CH_2CH$), 1.84–1.95 (m, 2H, $NCH_2CHCH_{ax}H_{eq}$, $NCH_{ax}H_{eq}CH_2CH_2CH$), 2.06 (t, *J*=10.7 Hz, 1H, $NCH_{ax}H_{eq}CH$), 2.12–2.18 (m, 5H, $NCH_2CH_2CH_2C{\equiv}C$, H_3CC), 2.22 (t, *J*=6.9 Hz, 2H, $NCH_2CH_2CH_2C{\equiv}C$), 2.51 (tt, *J*=10.4, 3.8 Hz, 1H, NCH_2CH_{ax}), 2.63 (d_{br}, *J*=11.4 Hz, 1H, $NCH_{ax}H_{eq}CH_2CH_2CH$), 2.85 (d_{br}, *J*=10.3 Hz, 1H, $NCH_{ax}H_{eq}CH$), 4.13 (q, *J*=7.1 Hz, 2H, OCH_2CH_3), 7.15–7.34 (m, 7H, H_{Ar}), 7.47 (dd, *J*=7.2,1.9 Hz, 1H, C≡CCCH) ppm; ^{13}C NMR (101 MHz, $CDCl_3$): δ=14.21 (OCH_2CH_3), 17.27 ($NCH_2CH_2CH_2C{\equiv}C$), 19.97 (H_3CC), 24.56 ($NCH_2CH_2CH_2CH$), 25.69 ($NCH_2CH_2CH_2C{\equiv}C$), 26.97 (NCH_2CHCH_2), 41.87 (NCH_2CH), 53.68 ($NCH_2CH_2CH_2CH$), 55.41 (NCH_2CH), 57.24 ($NCH_2CH_2CH_2C{\equiv}C$), 60.23 (OCH_2CH_3), 79.88 (C≡CCCH), 92.65 (C≡CCCH), 123.42 ($CH_2C{\equiv}CC$), 125.22 ($CH_2C{\equiv}CCCCH$), 126.80 ($CH_2C{\equiv}CCCHCH$), 127.31 (2 C, $H_3CCCHCH$, $CH_2C{\equiv}CCCHCHCH$), 129.36 ($H_3CCCCHCH$), 129.58 (2 C, H_3CCCCH, H_3CCCH), 131.88 ($CH_2C{\equiv}CCCH$), 136.09 (H_3CC), 141.04 (H_3CCC), 144.27 ($CH_2C{\equiv}CCC$), 174.27 (C=O) ppm; IR (KBr): $\tilde{\nu}$=3357, 3059, 2940, 2807, 2771, 2228, 1731, 1560, 1474, 1442, 1372, 1306, 1178, 1151, 1132, 1104, 1031, 758 cm^{-1} ; MS (CI, CH_5^+) *m/z*: 390 $[M+H]^+$; HRMS-EI$^+$ *m/z* $[M]^+$ calcd for $C_{26}H_{31}NO_2$: 389.2355, found: 389.2354.

Ethyl 1-{4-[2-(4-chlorophenyl)phenyl]but-3-yn-1-yl}piperidine-3-carboxylate (15e):

R_f≈0.3 (hexane/ethyl acetate 8:2). ^{1}H NMR (400 MHz, $CDCl_3$): δ=1.24 (t, *J*=7.1 Hz, 3H, OCH_2CH_3), 1.42 (qd, *J*=11.8, 3.7 Hz, 1H, $NCH_2CHCH_{ax}H_{eq}$), 1.48–1.59 (m, 1H, $NCH_2CH_{ax}H_{eq}CH_2CH$), 1.70 (dp, *J*=13.2, 3.6 Hz, 1H, $NCH_2CH_{ax}H_{eq}CH_2CH$), 1.88–1.96 (m, 1H, $NCH_2CHCH_{ax}H_{eq}$), 2.03 (td, *J*=10.9, 2.6 Hz, 1H, $NCH_{ax}H_{eq}CH_2CH_2CH$), 2.20 (t, *J*=10.6 Hz, 1H, $NCH_{ax}H_{eq}CH$), 2.45–2.58 (m, 5H, NCH_2CH_{ax}, $NCH_2CH_2C{\equiv}C$, $NCH_2CH_2C{\equiv}C$), 2.72 (d_{br}, *J*=11.1 Hz, 1H, $NCH_{ax}H_{eq}CH_2CH_2CH$), 2.95 (d_{br}, *J*=10.9 Hz, 1H, $NCH_{ax}H_{eq}CH$), 4.12 (q, *J*=7.1 Hz, 2H, OCH_2CH_3), 7.24–7.33 (m, 3H, C≡CCCHCH, C≡CCCCH, C≡CCCCHCH), 7.37 (d, *J*=8.4 Hz, 2H, CClCH), 7.47–7.52 (m, 3H, CClCHCH, C≡CCCH) ppm; ^{13}C NMR (101 MHz, $CDCl_3$): δ=14.31 (OCH_2CH_3), 17.79 ($NCH_2CH_2C{\equiv}C$), 24.68 ($NCH_2CH_2CH_2CH$), 26.92 (NCH_2CHCH_2), 41.95 (NCH_2CH), 53.34 ($NCH_2CH_2CH_2CH$), 55.09 (NCH_2CH), 57.19 ($NCH_2CH_2C{\equiv}C$), 60.45 (OCH_2CH_3), 80.67 ($CH_2C{\equiv}C$), 91.91 ($CH_2C{\equiv}C$), 122.10 ($CH_2C{\equiv}CC$), 127.35 ($CH_2C{\equiv}CCCHCH$), 128.08 (3 C, $CH_2C{\equiv}CCCHCHCH$, ClCCH), 129.29 ($CH_2C{\equiv}CCCCH$), 130.71 ($CH_2C{\equiv}CCCH$), 133.19 (2 C, ClCCHCH), 133.39 (CCl), 139.22 (ClCCHCHC), 142.44 ($CH_2C{\equiv}CCC$), 174.22 (C=O) ppm; IR (KBr): $\tilde{\nu}$=3435, 3059, 2943, 2854, 2810, 2227, 1730, 1597, 1497, 1475, 1442, 1397, 1370, 1305, 1180, 1153, 1091, 1032, 1005 758 cm^{-1}; MS (CI, CH_5^+) *m/z*: 396 $[M+H]^+$; HRMS-EI$^+$ *m/z* $[M]^+$ calcd for $C_{24}H_{26}ClNO_2$: 395.1652, found: 395.1652.

Ethyl 1-{5-[2-(4-chlorophenyl)phenyl]pent-4-yn-1-yl}piperidine-3-carboxylate (16e):

R_f≈0.25 (hexane/ethyl acetate 8:2). ^{1}H NMR (400 MHz, $CDCl_3$): δ=1.24 (t, J=7.1 Hz, 3H, OCH_2CH_3), 1.44 (qd, J=12.1, 3.7 Hz, 1H, $NCH_2CHCH_{ax}H_{eq}$), 1.50–1.60 (m, 1H, $NCH_2CH_{ax}H_{eq}CH_2CH$), 1.64 (p, J=7.2 Hz, 2H, $NCH_2CH_2CH_2C{\equiv}C$), 1.71 (dp, J=13.2, 3.6 Hz, 1H, $NCH_2CH_{ax}H_{eq}CH_2CH$), 1.88–1.97 (m, 2H, $NCH_2CHCH_{ax}H_{eq}$, $NCH_{ax}H_{eq}CH_2CH_2CH$), 2.11 (t, J=10.5 Hz, 1H, $NCH_{ax}H_{eq}CH$), 2.27–2.35 (m, 4H, $NCH_2CH_2CH_2C{\equiv}C$, $NCH_2CH_2CH_2C{\equiv}C$), 2.53 (tt, J=10.4, 3.8 Hz, 1H, NCH_2CH_{ax}), 2.66 (d_{br}, J=11.1 Hz, 1H, $NCH_{ax}H_{eq}CH_2CH_2CH$), 2.90 (d_{br}, J=10.2 Hz, 1H, $NCH_{ax}H_{eq}CH$), 4.12 (q, J=7.1 Hz, 2H, OCH_2CH_3), 7.24–7.34 (m, 3H, $C{\equiv}CCCHCH$, $C{\equiv}CCCCH$, $C{\equiv}CCCCHCH$), 7.37 (d, J=8.5 Hz, 2H, $ClCCH$), 7.47–7.52 (m, 3H, $ClCCHCH$, $C{\equiv}CCCH$) ppm; ^{13}C NMR (101 MHz, $CDCl_3$): δ=14.34 (OCH_2CH_3), 17.60 ($NCH_2CH_2CH_2C{\equiv}C$), 24.72 ($NCH_2CH_2CH_2CH$), 25.86 ($NCH_2CH_2CH_2C{\equiv}C$), 27.07 (NCH_2CHCH_2), 42.00 (NCH_2CH), 53.96 ($NCH_2CH_2CH_2CH$), 55.54 (NCH_2CH), 57.75 ($NCH_2CH_2CH_2C{\equiv}C$), 60.41 (OCH_2CH_3), 80.14 ($CH_2C{\equiv}C$), 93.38 ($CH_2C{\equiv}C$), 122.28 ($CH_2C{\equiv}CC$), 127.37 ($CH_2C{\equiv}CCCHCH$), 127.96 ($CH_2C{\equiv}CCCHCHCH$), 128.13 (2 C, $ClCCH$), 129.30 ($ClCCHCHCH$), 130.72 ($CH_2C{\equiv}CCCH$), 133.18 (2C, $ClCCHCH$), 133.35 (ClC), 139.34 ($ClCCHCHCC$), 142.43 ($CH_2C{\equiv}CCC$), 174.37 (C=O) ppm; IR (KBr): $\tilde{\nu}$ = 3435, 3059, 2942, 2865, 2807, 2771, 2227, 1730, 1593, 1497, 1475, 1441, 1371, 1306, 1178, 1151, 1091, 1030, 1004, 831, 759 cm^{-1}; MS (CI, CH_5^+) *m/z*: 410 $[M+H]^+$; HRMS-EI$^+$ *m/z* $[M]^+$ calcd for $C_{25}H_{28}ClNO_2$: 409.1809, found: 409.1811.

Ethyl 1-{4-[2-(2,4-dichlorophenyl)phenyl]but-3-yn-1-yl}piperidine-3-carboxylate (15f):

R_f≈0.3 (hexane/ethyl acetate 8:2). ^{1}H NMR (500 MHz, $CDCl_3$): δ=1.24 (t, J=7.1 Hz, 3H, OCH_2CH_3), 1.36–1.57 (m, 2H, $NCH_2CHCH_{ax}H_{eq}$, $NCH_2CH_{ax}H_{eq}CH_2CH$), 1.70 (dp, J=10.8, 3.8 Hz, 1H, $NCH_2CH_{ax}H_{eq}CH_2CH$), 1.88–2.02 (m, 2H, $NCH_2CHCH_{ax}H_{eq}$, $NCH_{ax}H_{eq}CH_2CH_2CH$), 2.17 (t, J=10.6 Hz, 1H, $NCH_{ax}H_{eq}CH$), 2.36–2.45 (m, 4H, $NCH_2CH_2C{\equiv}C$, $NCH_2CH_2C{\equiv}C$), 2.51 (tt, J=10.5, 3.8 Hz, 1H, NCH_2CH_{ax}), 2.67 (d_{br}, J=11.1 Hz, 1H, $NCH_{ax}H_{eq}CH_2CH_2CH$), 2.90 (d_{br}, J=11.0 Hz, 1H, $NCH_{ax}H_{eq}CH$), 4.12 (q, J=7.1 Hz, 2H, OCH_2CH_3), 7.21–7.36 (m, 5H, $C{\equiv}CCCCH$, $ClCCHCH$, $ClCCHCH$, $C{\equiv}CCCHCH$, $C{\equiv}CCCCHCH$), 7.46–7.50 (m, 2H, $ClCCHCCCl$, $C{\equiv}CCCH$) ppm; ^{13}C NMR (101 MHz, $CDCl_3$): δ=14.16 (OCH_2CH_3), 17.55 ($NCH_2CH_2C{\equiv}C$), 24.51 ($NCH_2CH_2CH_2CH$), 26.76 (NCH_2CHCH_2), 41.77 (NCH_2CH), 53.15 ($NCH_2CH_2CH_2CH$), 54.90 (NCH_2CH), 57.09 ($NCH_2CH_2C{\equiv}C$), 60.28 (OCH_2CH_3), 79.81 ($C{\equiv}CCH$), 92.21 ($C{\equiv}CCH$), 123.39 ($CH_2C{\equiv}CC$), 126.49 ($ClCCHCH$), 127.37 ($ClCCCCHCH$), 127.85 ($CH_2C{\equiv}CCCHCH$), 129.06 ($ClCCHCCl$), 129.47 ($ClCCCCH$), 131.98 ($CH_2C{\equiv}CCCH$), 132.31 ($ClCCHCH$), 133.71 (CCl), 134.14 (CCl), 138.36 ($ClCCHCHC$), 140.59 ($ClCCC$), 174.05 (C=O) ppm; IR (KBr): $\tilde{\nu}$=3376, 3061, 2941, 2852, 2809, 2229, 1730, 1586, 1466, 1440, 1372, 1305, 1179, 1152, 1101, 1032, 1004, 863, 812, 760 cm^{-1}; MS (CI, CH_5^+) *m/z*: 430 $[M+H]^+$; HRMS-EI$^+$ *m/z* $[M]^+$ calcd for $C_{24}H_{25}Cl_2NO_2$: 429.1262, found: 429.1236.

Ethyl 1-{5-[2-(2,4-dichlorophenyl)phenyl]pent-4-yn-1-yl}piperidine-3-carboxylate (16f):

R_f≈0.25 (hexane/ethyl acetate 8:2). ^{1}H NMR (500 MHz, $CDCl_3$): δ=1.24 (t, J=7.1 Hz, 3H, OCH_2CH_3), 1.38–1.59 (m, 4H, $NCH_2CHCH_{ax}H_{eq}$, $NCH_2CH_{ax}H_{eq}CH_2CH$, $NCH_2CH_2CH_2C{\equiv}C$), 1.71 (dp, J=13.0, 3.6 Hz, 1H, $NCH_2CH_{ax}H_{eq}CH_2CH$), 1.86–1.97 (m, 2H, $NCH_2CHCH_{ax}H_{eq}$, $NCH_{ax}H_{eq}CH_2CH_2CH$), 2.09 (t, J=10.5 Hz, 1H, $NCH_{ax}H_{eq}CH$), 2.17–2.22 (m, 2H, $NCH_2CH_2CH_2C{\equiv}C$), 2.25 (t, J=6.9 Hz, 2H, $NCH_2CH_2CH_2C{\equiv}C$), 2.52 (tt, J=10.3, 3.7 Hz, 1H, NCH_2CH_{ax}), 2.64 (d_{br}, J=11.3 Hz, 1H, $NCH_{ax}H_{eq}CH_2CH_2CH$), 2.87 (d_{br}, J=10.5 Hz, 1H, $NCH_{ax}H_{eq}CH$), 4.12 (q, J=7.1 Hz, 2H, OCH_2CH_3), 7.19–7.34 (m, 5H, $ClCCCCH$, $ClCCCH$, $ClCCHCH$, $ClCCCCHCH$, $C{\equiv}CCCHCH$), 7.45–7.51 (m, 2H, $ClCCHCCl$, $C{\equiv}CCCH$) ppm; ^{13}C NMR (101 MHz, $CDCl_3$): δ=14.19 (OCH_2CH_3), 17.29 ($NCH_2CH_2CH_2C{\equiv}C$), 24.56 ($NCH_2CH_2CH_2CH$), 25.68 ($NCH_2CH_2CH_2C{\equiv}C$), 26.91 (NCH_2CHCH_2), 41.84 (NCH_2CH), 53.74 ($NCH_2CH_2CH_2CH$), 55.37 (NCH_2CH), 57.33 ($NCH_2CH_2CH_2C{\equiv}C$), 60.23 (OCH_2CH_3), 79.25 ($CH_2C{\equiv}C$), 93.61 ($CH_2C{\equiv}C$), 123.56 ($CH_2C{\equiv}CC$), 126.53 ($ClCCCH$), 127.26 ($ClCCCCHCH$), 127.85 ($CH_2C{\equiv}CCCHCH$), 129.10 ($ClCCHCCl$), 129.46 ($ClCCCCH$), 132.05 ($CH_2C{\equiv}CCCH$), 132.29 ($ClCCHCH$), 133.69 (CCl), 134.15 (CCl), 138.48 ($ClCCC$), 140.48 ($ClCCC$), 174.20 (C=O) ppm; IR (KBr): $\tilde{\nu}$=3380, 3061, 2941, 2806, 2771, 2229, 1730, 1586, 1466, 1439, 1373, 1306, 1178, 1151, 1101, 1071, 1029, 864, 813, 760 cm^{-1}; MS (CI, CH_5^+) *m/z*: 444 $[M+H]^+$; HRMS-EI$^+$ *m/z* $[M]^+$ calcd for $C_{25}H_{27}Cl_2NO_2$: 443.1419, found: 443.1438.

Ethyl 1-{4-[2-(2,4-difluorophenyl)phenyl]but-3-yn-1-yl}piperidine-3-carboxylate (15g):

R_f≈0.3 (hexane/ethyl acetate 8:2). ^{1}H NMR (500 MHz, $CDCl_3$): δ=1.24 (t, J=7.1 Hz, 3H, OCH_2CH_3), 1.42 (qd, J=12.0, 3.8, 1H, $NCH_2CHCH_{ax}H_{eq}$), 1.47–1.59 (m, 1H, $NCH_2CH_{ax}H_{eq}CH_2CH$), 1.70 (dp, J=13.0, 3.7 Hz, 1H, $NCH_2CH_{ax}H_{eq}CH_2CH$), 1.92 (dq, J=12.6, 3.8, 1H, $NCH_2CHCH_{ax}H_{eq}$), 2.02 (td, J=10.9, 2.8 Hz, 1H, $NCH_{ax}H_{eq}CH_2CH_2CH$), 2.19 (t, J=10.6 Hz, 1H, $NCH_{ax}H_{eq}CH$), 2.40–2.55 (m, 5H, $NCH_2CH_2C{\equiv}C$, $NCH_2CH_2C{\equiv}C$, NCH_2CH_{ax}), 2.70 (dt, J=11.2, 3.8 Hz, 1H, $NCH_{ax}H_{eq}CH_2CH_2CH$), 2.93 (dd, J=11.0, 3.2 Hz, 1H, $NCH_{ax}H_{eq}CH$), 4.12 (q, J=7.2 Hz, 2H, OCH_2CH_3), 6.85–6.97 (m, 2H, FCCHCF, FCCHCH), 7.27–7.42 (m, 4H, C≡CCCCH, C≡CCCCHCH, C≡CCCHCH, FCCCH), 7.48–7.53 (m, 1H, C≡CCCH) ppm; ^{13}C NMR (101 MHz, $CDCl_3$): δ=14.15 (OCH_2CH_3), 17.51 ($NCH_2CH_2C{\equiv}C$), 24.52 ($NCH_2CH_2CH_2CH$), 26.76 (NCH_2CHCH_2), 41.79 (NCH_2CH), 53.16 ($NCH_2CH_2CH_2CH$), 54.90 (NCH_2CH), 57.14 ($NCH_2CH_2C{\equiv}C$), 60.30 (OCH_2CH_3), 80.03 (C≡CCCH), 91.61 (C≡CCCH), 103.39 (d, $^2J_{CF}$=25.8 Hz, FCCHCF), 110.65 (dd, $^2J_{CF}$=21.0 Hz, $^4J_{CF}$=3.7 Hz, FCCHCH), 123.50 ($CH_2C{\equiv}CC$), 124.57 (dd, $^2J_{CF}$=15.6 Hz, $^4J_{CF}$=3.8 Hz, FCC), 127.54 ($CH_2C{\equiv}CCCHCH$), 127.71 ($CH_2C{\equiv}CCCHCHCH$), 129.99 ($CH_2C{\equiv}CCCCH$), 132.38 ($CH_2C{\equiv}CCCH$), 132.55 (dd, $^3J_{CF}$=9.5, $^3J_{CF}$=4.9 Hz, FCCCH), 137.11 ($CH_2C{\equiv}CCC$), 159.76 (dd, $^1J_{CF}$=249.9, $^3J_{CF}$=11.9 Hz, CF), 162.41 (dd, $^1J_{CF}$=248.5, $^3J_{CF}$=11.6 Hz, CF), 174.05 (C=O) ppm; IR (KBr): $\tilde{\nu}$=3423, 3061, 2941, 2854, 2811, 2228, 1729, 1618, 1593, 1510, 1478, 1420, 1370, 1265, 1179, 1152, 1139, 1099, 1032, 963, 849, 761 cm^{-1}; MS (CI, CH_5^+) *m/z*: 398 $[M+H]^+$; HRMS-EI$^+$ *m/z* $[M]^+$ calcd for $C_{24}H_{25}F_2NO_2$: 397.1853, found: 397.1848.

Ethyl 1-{5-[2-(2,4-difluorophenyl)phenyl]pent-4-yn-1-yl}piperidine-3-carboxylate (16g):

R_f≈0.25 (hexane/ethyl acetate 8:2). ^{1}H NMR (500 MHz, $CDCl_3$): δ=1.25 (t, J=7.1 Hz, 3H, OCH_2CH_3), 1.44 (qd, J=11.8, 3.6 Hz, 1H, $NCH_2CHCH_{ax}H_{eq}$), 1.49 – 1.65 (m, 3H, $NCH_2CH_{ax}H_{eq}CH_2CH$, $NCH_2CH_2CH_2C{\equiv}C$), 1.71 (dp, J=13.1, 3.7 Hz, 1H, $NCH_2CH_{ax}H_{eq}CH_2CH$), 1.86–1.98 (m, 2H, $NCH_2CHCH_{ax}H_{eq}$, $NCH_{ax}H_{eq}CH_2CH_2CH$), 2.11 (t, J=10.5 Hz, 1H, $NCH_{ax}H_{eq}CH$), 2.24–2.32 (m, 4H, $NCH_2CH_2CH_2C{\equiv}C$, $NCH_2CH_2CH_2C{\equiv}C$), 2.53 (tt, J=10.4, 3.8 Hz, 1H, NCH_2CH_{ax}), 2.66 (d_{br}, J=11.1 Hz, 1H, $NCH_{ax}H_{eq}CH_2CH_2CH$), 2.89 (d_{br}, J=10.3 Hz, 1H, $NCH_{ax}H_{eq}CH$), 4.13 (q, J=7.1 Hz, 2H, OCH_2CH_3), 6.86–6.96 (m, 2H, FCCHCF, FCCHCH), 7.26–7.42 (m, 4H, C≡CCCCH, C≡CCCCHCH, C≡CCCHCH, FCCCH), 7.47–7.53 (m, 1H, C≡CCCH) ppm; ^{13}C NMR (101 MHz, $CDCl_3$): δ=14.17 (OCH_2CH_3), 17.33 ($NCH_2CH_2CH_2C{\equiv}C$), 24.56 ($NCH_2CH_2CH_2CH$), 25.76 ($NCH_2CH_2CH_2C{\equiv}C$), 26.93 (NCH_2CHCH_2), 41.85 (NCH_2CH), 53.78 ($NCH_2CH_2CH_2CH$), 55.41 (NCH_2CH), 57.45 ($NCH_2CH_2CH_2C{\equiv}C$), 60.25 (OCH_2CH_3), 79.47 ($CH_2C{\equiv}C$), 93.12 ($CH_2C{\equiv}C$), 103.79 (d, $^2J_{CF}$=25.8 Hz, 1C, FCCHCF), 110.68 (dd, $^2J_{CF}$=21.1 Hz, $^4J_{CF}$=3.7 Hz, FCCHCH), 123.70 ($CH_2C{\equiv}CC$), 124.68 (dd, $^2J_{CF}$=15.6 Hz, $^4J_{CF}$=3.6 Hz, FCCCH), 127.43 ($CH_2C{\equiv}CCCHCH$), 127.72 ($CH_2C{\equiv}CCCHCHCH$), 129.97 ($CH_2C{\equiv}CCCCH$), 132.40 ($CH_2C{\equiv}CCCH$), 132.52 (dd, $^3J_{CF}$=9.4 Hz, $^3J_{CF}$=4.9 Hz, FCCCH), 137.06 ($CH_2C{\equiv}CCC$), 158.41–161.12 (dd, $^1J_{CF}$ = 250.2 Hz, $^3J_{CF}$ = 12.1 Hz, CF), 162.38 (dd, $^1J_{CF}$ = 248.7 Hz, $^3J_{CF}$ = 11.7 Hz, CF), 174.21 (C=O) ppm; IR (KBr): $\tilde{\nu}$=3347, 3061, 2941, 2865, 2806, 2771, 2230, 1730, 1618, 1593, 1511, 1479, 1420, 1266, 1178, 1140, 1099, 1030, 964, 849, 761 cm^{-1}; MS (CI, CH_5^+) *m/z*: 412 $[M+H]^+$; HRMS-EI$^+$ *m/z* $[M]^+$ calcd for $C_{25}H_{27}F_2NO_2$: 411.2010, found: 411.2008.

Ethyl 1-{4-[2-(2,4-dimethylphenyl)phenyl]but-3-yn-1-yl}piperidine-3-carboxylate (15h):

R_f≈0.3 (hexane/ethyl acetate 8:2). ^{1}H NMR (400 MHz, $CDCl_3$): δ=1.24 (t, J=7.1 Hz, 3H, OCH_2CH_3), 1.40 (qd, J=12.0, 3.9 Hz, 1H, $NCH_2CHCH_{ax}H_{eq}$), 1.45–1.55 (m, 1H, $NCH_2CH_{ax}H_{eq}CH_2CH$), 1.68 (dp, J=13.2, 3.6 Hz, 1H, $NCH_2CH_{ax}H_{eq}CH_2CH$), 1.86–1.98 (m, 2H, $NCH_2CHCH_{ax}H_{eq}$, $NCH_{ax}H_{eq}CH_2CH_2CH$), 2.09–2.18 (m, 4H, $H_3CCCHCC$, $NCH_{ax}H_{eq}CH$), 2.32–2.42 (m, 7H, H_3CCC, $NCH_2CH_2C{\equiv}C$, $NCH_2CH_2C{\equiv}C$), 2.50 (tt, J=10.5, 3.8 Hz, 1H, NCH_2CH_{ax}), 2.64 (d_{br}, J=11.1 Hz, 1H, $NCH_{ax}H_{eq}CH_2CH_2CH$), 2.88 (d_{br}, J=9.5 Hz, 1H, $NCH_{ax}H_{eq}CH$), 4.12 (q, J=7.1 Hz, 2H, OCH_2CH_3), 7.01 (d, J=8.2 Hz, 1H, $H_3CCCHCH$), 7.04–7.08 (m, 2H, $H_3CCCHCH$, H_3CCCHC), 7.18 (dd, J=7.5, 1.2 Hz, 1H, C≡CCCCH), 7.25 (td, J=7.5, 1.6 Hz, 1H, C≡CCCHCH), 7.29 (td, J=7.5, 1.5 Hz, 1H, C≡CCCCHCH), 7.45 (dd, J=7.6, 1.3 Hz, 1H, C≡CCCH) ppm; ^{13}C NMR (101 MHz, $CDCl_3$): δ=14.16 (OCH_2CH_3), 17.56 ($NCH_2CH_2C{\equiv}C$), 19.87 (H_3CCC), 21.11 ($H_3CCCHCC$), 24.52 ($NCH_2CH_2CH_2CH$), 26.80 (NCH_2CHCH_2), 41.79 (NCH_2CH), 53.06 ($NCH_2CH_2CH_2CH$), 54.94 (NCH_2CH), 57.17 ($NCH_2CH_2C{\equiv}C$), 60.25 (OCH_2CH_3), 80.61 (C≡CCCH), 91.15 (C≡CCCH), 123.39 ($CH_2C{\equiv}CC$), 125.87 ($H_3CCCHCH$), 126.64 ($CH_2C{\equiv}CCCHCH$), 127.36 ($CH_2C{\equiv}CCCHCHCH$), 129.53 (2 C, $H_3CCCHCH$, $CH_2C{\equiv}CCCCH$), 130.35 ($H_3CCCHCC$), 131.78 ($CH_2C{\equiv}CCCH$), 135.89 (H_3CCC), 136.72 ($H_3CCCHCC$), 138.09 (H_3CCC), 144.39 ($CH_2C{\equiv}CCCH$), 174.06 (C=O) ppm; IR (KBr): $\tilde{\nu}$=3387, 3057, 2941, 2856, 2810, 2228, 1730, 1615, 1476,

1441, 1371, 1305, 1217, 1180, 1153, 1133, 1101, 1032, 755 cm^{-1}; MS (CI, CH_5^+) *m/z*: 390 $[M+H]^+$; HRMS-EI$^+$ *m/z* $[M]^+$ calcd for $C_{26}H_{31}NO_2$: 389.2355, found: 389.2360.

Ethyl 1-{5-[2-(2,4-dimethylphenyl)phenyl]pent-4-yn-1-yl}piperidine-3-carboxylate (16h):

R_f≈0.25 (hexane/ethyl acetate 8:2). ^{1}H NMR (400 MHz, $CDCl_3$): δ=1.25 (t, *J*=7.1 Hz, 3H, OCH_2CH_3), 1.39–1.57 (m, 4H, $NCH_2CHCH_{ax}H_{eq}$, $NCH_2CH_{ax}H_{eq}CH_2CH$, $NCH_2CH_2CH_2C{\equiv}C$), 1.69 (dp, *J*=13.1, 3.7 Hz, 1H, $NCH_2CH_{ax}H_{eq}CH_2CH$), 1.85–1.95 (m, 2H, $NCH_2CHCH_{ax}H_{eq}$, $NCH_{ax}H_{eq}CH_2CH_2CH$), 2.07 (t, *J*=10.5 Hz, 1H, $NCH_{ax}H_{eq}CH$), 2.12–2.17 (m, 5H, $H_3CCCHCC$, $NCH_2CH_2CH_2C{\equiv}C$), 2.24 (t, *J*=6.9 Hz, 2H, $NCH_2CH_2CH_2C{\equiv}C$), 2.35 (s, 3H, H_3CC), 2.51 (tt, *J*=10.5, 3.8 Hz, 1H, NCH_2CH_{ax}), 2.62 (d_{br}, *J*=11.1 Hz, 1H, $NCH_{ax}H_{eq}CH_2CH_2CH$), 2.86 (d_{br}, *J*=9.5 Hz, 1H, $NCH_{ax}H_{eq}CH$), 4.13 (q, *J*=7.1 Hz, 2H, OCH_2CH_3), 7.02 (d, *J*=8.2 Hz, 1H, $H_3CCCHCH$), 7.05–7.08 (m, 2H, $H_3CCCHCH$, $H_3CCCHCH$), 7.15–7.19 (m, 1H, $C{\equiv}CCCCH$), 7.25 (td, *J*=7.5, 1.6 Hz, 1H, $C{\equiv}CCCHCH$), 7.29 (td, *J*=7.5, 1.5 Hz, 1H, $C{\equiv}CCCCHCH$), 7.46 (dd, *J*=7.6, 1.3 Hz, 1H, $C{\equiv}CCCH$) ppm; ^{13}C NMR (101 MHz, $CDCl_3$): δ=14.21 (OCH_2CH_3), 17.32 ($NCH_2CH_2CH_2C{\equiv}C$), 19.91 (H_3CCC), 21.14 ($H_3CCCHCC$), 24.60 ($NCH_2CH_2CH_2CH$), 25.72 ($NCH_2CH_2CH_2C{\equiv}C$) 26.99 (NCH_2CHCH_2), 41.90 (NCH_2CH), 53.68 ($NCH_2CH_2CH_2CH$), 55.41 (NCH_2CH), 57.26 ($NCH_2CH_2CH_2C{\equiv}C$), 60.24 (OCH_2CH_3), 80.07 ($C{\equiv}CCCH$), 92.48 ($C{\equiv}CCCH$), 123.56 ($CH_2C{\equiv}CC$), 125.94 ($H_3CCCHCH$), 126.66 ($CH_2C{\equiv}CCCHCH$), 127.27 ($CH_2C{\equiv}CCCHCHCH$), 129.53 ($H_3CCCHCH$ or $CH_2C{\equiv}CCCCH$), 129.62 ($H_3CCCHCH$ or $CH_2C{\equiv}CCCCH$), 130.43 ($H_3CCCHCC$), 131.92 ($CH_2C{\equiv}CCCH$), 135.88 (H_3CCC), 136.69 ($H_3CCCHCC$), 138.19 (H_3CCC), 144.25 ($CH_2C{\equiv}CCCH$), 174.25 (C=O) ppm; IR (KBr): $\tilde{\nu}$=3358, 3057, 2941, 2865, 2806, 2227, 1731, 1615, 1476, 1440, 1372, 1306, 1178, 1151, 1132, 1104, 1030, 760 cm^{-1}; MS (CI, CH_5^+) *m/z*: 404 $[M+H]^+$; HRMS-EI$^+$ *m/z* $[M]^+$ calcd for $C_{27}H_{33}NO_2$: 403.2511, found: 403.2520.

Ethyl 1-{4-[2-(2-chloro-4-fluorophenyl)phenyl]but-3-yn-1-yl}piperidine-3-carboxylate (15i):

R_f≈0.3 (hexane/ethyl acetate 8:2). ^{1}H NMR (500 MHz, $CDCl_3$): δ=1.24 (t, *J*=7.1 Hz, 3H, OCH_2CH_3), 1.41 (qd, *J*=11.8, 3.9 Hz, 1H, $NCH_2CHCH_{ax}H_{eq}$), 1.47–1.59 (m, 1H, $NCH_2CH_{ax}H_{eq}CH_2CH$), 1.69 (dp, *J*=10.8, 3.8 Hz, 1H, $NCH_2CH_{ax}H_{eq}CH_2CH$), 1.92 (dq, *J*=13.0, 4.0 Hz, 1H, $NCH_2CHCH_{ax}H_{eq}$), 2.00 (td, *J*=11.1, 3.1 Hz, 1H, $NCH_{ax}H_{eq}CH_2CH_2CH$), 2.18 (t, *J*=10.6 Hz, 1H, $NCH_{ax}H_{eq}CH$), 2.35–2.46 (m, 4H, $NCH_2CH_2C{\equiv}C$, $NCH_2CH_2C{\equiv}C$), 2.51 (tt, *J*=10.5, 3.9 Hz, 1H, NCH_2CH_{ax}), 2.68 (d_{br}, *J*=11.1 Hz, 1H, $NCH_{ax}H_{eq}CH_2CH_2CH$), 2.91 (d_{br}, *J*=10.7 Hz, 1H, $NCH_{ax}H_{eq}CH$), 4.12 (q, *J*=7.2 Hz, 2H, OCH_2CH_3), 7.02 (td, *J*=8.3, 2.6 Hz, 1H, $FCCHCH$), 7.20–7.25 (m, 2H, $FCCHCCl$, $C{\equiv}CCCCH$), 7.27–7.30 (m, 1H, $FCCHCH$), 7.30–7.36 (m, 2H, $C{\equiv}CCCHCH$, $C{\equiv}CCCCHCH$), 7.47–7.50 (m, 1H, $C{\equiv}CCCH$) ppm; ^{13}C NMR (126 MHz, $CDCl_3$, 25 °C, TMS): δ=14.18 (OCH_2CH_3), 17.50 ($NCH_2CH_2CH_2C{\equiv}C$), 24.51 ($NCH_2CH_2CH_2CH$), 26.78 (NCH_2CHCH_2), 41.78 (NCH_2CH), 53.16 ($NCH_2CH_2CH_2CH$), 54.91 (NCH_2CH), 57.15 ($NCH_2CH_2C{\equiv}C$), 60.33 (OCH_2CH_3), 79.95 ($C{\equiv}CCCH$), 92.01 ($C{\equiv}CCCH$), 113.44 (d, $^2J_{CF}$=20.9 Hz, $FCCHCH$), 116.53 (d, $^2J_{CF}$=24.5 Hz, $FCCHCCl$), 123.62 ($CH_2C{\equiv}CC$), 127.37 ($CH_2C{\equiv}CCCHCHCH$), 127.76 ($CH_2C{\equiv}CCCHCH$), 129.72 ($CH_2C{\equiv}CCCCH$), 132.00 ($CH_2C{\equiv}CCCH$), 132.46 (d, $^3J_{CF}$=8.6 Hz, $FCCHCH$), 134.13 (d, $^3J_{CF}$=10.4 Hz, ClC), 135.99 (d, $^4J_{CF}$ = 4.1 Hz, $ClCC$), 140.79 (d, $CH_2C{\equiv}CCC$), 161.81 (d, $^1J_{CF}$ = 249.3 Hz, FC), 174.04 (C=O) ppm; IR (KBr): $\tilde{\nu}$=3062, 2941, 2855, 2807, 2228, 1730, 1604, 1503, 1473, 1442, 1370, 1257, 1201, 1181, 1153, 1100, 1033, 897, 858, 761 cm^{-1}; MS (EI, 70 eV) *m/z*: 413 $[M]^+$; HRMS-EI$^+$ *m/z* $[M]^+$ calcd for $C_{24}H_{25}ClFNO_2$: 413.1558, found: 413.1570.

Ethyl 1-{5-[2-(2-chloro-4-fluorophenyl)phenyl]pent-4-yn-1-yl}piperidine-3-carboxylate (16i):

R_f≈0.25 (hexane/ethyl acetate 8:2). ^{1}H NMR (500 MHz, $CDCl_3$): δ=1.26 (t, *J*=7.2 Hz, 3H, OCH_2CH_3), 1.44 (qd, *J*=11.8, 4.1 Hz, 1H, $NCH_2CHCH_{ax}H_{eq}$), 1.51–1.62 (m, 3H, $NCH_2CH_{ax}H_{eq}CH_2CH$, $NCH_2CH_2CH_2C{\equiv}C$), 1.71 (dp, *J*=13.3, 3.6 Hz, 1H, $NCH_2CH_{ax}H_{eq}CH_2CH$), 1.89–1.98 (m, 2H, $NCH_2CHCH_{ax}H_{eq}$,), 2.11 (t, *J*=10.8 Hz, 1H, $NCH_{ax}H_{eq}CH_2CH_2CH$), 2.21–2.29 (m, 4H, $NCH_2CH_2CH_2C{\equiv}C$, $NCH_2CH_2CH_2C{\equiv}C$), 2.55 (tt, *J*=10.7, 3.8 Hz, 1H, NCH_2CH_{ax}), 2.67 (d_{br}, *J*=10.4 Hz, 1H, $NCH_{ax}H_{eq}CH_2CH_2CH$), 2.90 (d_{br}, *J*=10.2 Hz, 1H, $NCH_{ax}H_{eq}CH$), 4.13 (q, *J*=7.1 Hz, 2H, OCH_2CH_3), 7.03 (td, *J*=8.3, 2.6 Hz, 1H, $FCCHCH$), 7.20–7.25 (m, 2H, $FCCHCCl$, $C{\equiv}CCCCH$), 7.28–7.31 (m, 1H, $FCCHCH$), 7.31–7.35 (m, 2H, $C{\equiv}CCCHCH$, $C{\equiv}CCCCHCH$), 7.46–7.52 (m, 1H, $C{\equiv}CCCH$) ppm; ^{13}C NMR (126 MHz, $CDCl_3$): δ=14.20 (OCH_2CH_3), 17.32 ($NCH_2CH_2CH_2C{\equiv}C$), 24.49 ($NCH_2CH_2CH_2CH$), 25.65 ($NCH_2CH_2CH_2C{\equiv}C$), 26.93 (NCH_2CHCH_2), 41.77

(NCH$_2$*C*H), 53.74 (N*C*H$_2$CH$_2$CH$_2$CH), 55.37 (N*C*H$_2$CH), 57.36 (N*C*H$_2$CH$_2$CH$_2$C≡C), 60.31 (O*C*H$_2$CH$_3$), 79.44 (CH$_2$C≡*C*), 93.40 (CH$_2$*C*≡C), 113.51 (d, $^2J_{CF}$=20.9 Hz, FC*C*HCH), 116.57 (d, $^2J_{CF}$=24.5 Hz, FC*C*HCCl), 123.78 (CH$_2$C≡C*C*), 127.28 (CH$_2$C≡CCCHCH*C*H), 127.77 (CH$_2$C≡CCCH*C*H), 129.70 (CH$_2$C≡CCC*C*H), 132.06 (CH$_2$C≡CC*C*H), 132.44 (d, $^3J_{CF}$=8.6 Hz, FCCH*C*H), 134.15 (d, $^3J_{CF}$=10.4 Hz, Cl*C*), 136.12 (d, $^4J_{CF}$=3.6 Hz, ClC*C*), 140.72 (CH$_2$C≡CC*C*), 161.78 (d, $^1J_{CF}$=249.3 Hz, F*C*), 174.14 (*C*=O) ppm; IR (KBr): $\tilde{\nu}$=3062, 2940, 2807, 2228, 1729, 1604, 1503, 1473, 1442, 1371, 1256, 1201, 1178, 1151, 1029, 897, 857, 760 cm^{-1}; MS (EI, 70 eV) *m/z*: 427 [M]$^+$; HRMS-EI$^+$ *m/z* [M]$^+$ calcd for $C_{25}H_{27}ClFNO_2$: 427.1714, found: 427.1714.

Ethyl 1-{4-[2-(4-chloro-2-methylphenyl)phenyl]but-3-yn-1-yl}piperidine-3-carboxylate (15k):

R_f≈0.3 (hexane/ethyl acetate 8:2). ^{1}H NMR (400 MHz, $CDCl_3$): δ=1.25 (t, *J*=7.1 Hz, 3H, OCH$_2$C*H$_3$*), 1.41 (qd, *J*=11.9, 3.6 Hz, 1H, NCH$_2$CHC*H$_{ax}$*H$_{eq}$), 1.47–1.58 (m, 1H, NCH$_2$C*H$_{ax}$*H$_{eq}$CH$_2$CH), 1.69 (dp, *J*=10.2, 3.6 Hz, 1H, NCH$_2$CH$_{ax}$*H$_{eq}$*CH$_2$CH), 1.89–2.00 (m, 2H, NCH$_2$CHCH$_{ax}$*H$_{eq}$*, NC*H$_{ax}$*H$_{eq}$CH$_2$CH$_2$CH), 2.11–2.20 (m, 4H, C*H$_3$*C, NC*H$_{ax}$*H$_{eq}$CH), 2.32–2.43 (m, 4H, NC*H$_2$*CH$_2$C≡C, NCH$_2$C*H$_2$*C≡C), 2.51 (tt, *J*=10.5, 3.8 Hz, 1H, NCH$_2$C*H$_{ax}$*), 2.66 (d$_{br}$, *J*=11.2 Hz, 1H, NCH$_{ax}$*H$_{eq}$*CH$_2$CH$_2$CH), 2.90 (d$_{br}$, *J*=9.9 Hz, 1H, NCH$_{ax}$*H$_{eq}$*CH), 4.12 (q, *J*=7.1 Hz, 2H, OC*H$_2$*CH$_3$), 7.10 (d, *J*=8.1 Hz, 1H, ClCCHC*H*), 7.13–7.17 (m, 1H, C≡CCCC*H*), 7.19 (dd, *J*=8.1, 1.8 Hz, 1H, ClCC*H*CH), 7.23–7.34 (m, 3H, ClCC*H*C, C≡CCCHC*H*, C≡CCCCHC*H*), 7.44–7.48 (m, 1H, C$_6$: C≡CCC*H*) ppm; ^{13}C NMR (101 MHz, $CDCl_3$): δ=14.18 (OCH$_2$*C*H$_3$), 17.58 (NCH$_2$*C*H$_2$C≡C), 19.88 (*C*H$_3$C), 24.52 (NCH$_2$*C*H$_2$CH$_2$CH), 26.79 (NCH$_2$CH*C*H$_2$), 41.81 (NCH$_2$*C*H), 53.17 (N*C*H$_2$CH$_2$CH$_2$CH), 54.95 (N*C*H$_2$CH), 57.16 (N*C*H$_2$CH$_2$C≡C), 60.28 (O*C*H$_2$CH$_3$), 80.19 (C≡*C*CH), 91.74 (*C*≡CCH), 123.33 (CH$_2$C≡C*C*), 125.31 (ClC*C*HCH), 127.15 (CH$_2$C≡CCCHCH*C*H), 127.51 (CH$_2$C≡CCCH*C*H), 129.25 (CH$_2$C≡CCC*C*H), 129.43 (ClC*C*HC), 130.90 (ClCCH*C*H), 131.91 (CH$_2$C≡CC*C*H), 132.84 (Cl*C*), 138.22 (H$_3$C*C*), 139.48 (H$_3$CC*C*), 143.13 (CH$_2$C≡CC*C*), 174.05 (*C*=O) ppm; IR (KBr): $\tilde{\nu}$=3059, 3020, 2942, 2854, 2809, 2228, 1730, 1592, 1472, 1441, 1370, 1305, 1180, 1152, 1098, 1032, 870, 820, 761 cm^{-1}; MS (EI, 70 eV) *m/z*: 409 [M]$^+$; HRMS-EI$^+$ *m/z* [M]$^+$ calcd for $C_{25}H_{28}ClNO_2$: 409.1809, found: 409.1826.

Ethyl 1-{5-[2-(4-chloro-2-methylphenyl)phenyl]pent-4-yn-1-yl}piperidine-3-carboxylate (16k):

R_f≈0.25 (hexane/ethyl acetate 8:2). ^{1}H NMR (400 MHz, $CDCl_3$): δ=1.25 (t, *J*=7.1 Hz, 3H, OCH$_2$C*H$_3$*), 1.38–1.61 (m, 4H, NCH$_2$CHC*H$_{ax}$*H$_{eq}$, NCH$_2$C*H$_2$*CH$_2$C≡C, NCH$_2$C*H$_{ax}$*H$_{eq}$CH$_2$CH), 1.71 (dp, *J*=12.4, 3.9 Hz, 1H, NCH$_2$CH$_{ax}$*H$_{eq}$*CH$_2$CH), 1.87–1.97 (m, 2H, NCH$_2$CHCH$_{ax}$*H$_{eq}$*, NC*H$_{ax}$*H$_{eq}$CH$_2$CH$_2$CH), 2.05–2.20 (m, 6H, NC*H$_{ax}$*H$_{eq}$CH, *H$_3$*CC, NC*H$_2$*CH$_2$CH$_2$C≡C), 2.25 (t, *J*=6.9 Hz, 2H, NCH$_2$CH$_2$C*H$_2$*C≡C), 2.53 (tt, *J*=10.5, 3.8 Hz, 1H, NCH$_2$C*H$_{ax}$*), 2.63 (d$_{br}$, *J*=11.6 Hz, 1H, NCH$_{ax}$*H$_{eq}$*CH$_2$CH$_2$CH), 2.87 (d$_{br}$, *J*=10.0 Hz, 1H, NCH$_{ax}$*H$_{eq}$*CH), 4.13 (q, *J*=7.1 Hz, 2H, OC*H$_2$*CH$_3$), 7.11 (d, *J*=8.2 Hz, 1H, ClCCHC*H*), 7.12–7.16 (m, 1H, C≡CCCC*H*), 7.16–7.20 (m, 1H, ClCC*H*CH), 7.24 (d, *J*=2.2 Hz, 1H, ClCC*H*C), 7.27–7.34 (m, 2H, C≡CCCHC*H*, C≡CCCCHC*H*), 7.44–7.49 (m, 1H, C≡CCC*H*) ppm; ^{13}C NMR (101 MHz, $CDCl_3$): δ=14.22 (OCH$_2$*C*H$_3$), 17.30 (NCH$_2$CH$_2$*C*H$_2$C≡C), 19.90 (H$_3$*C*C), 24.57 (NCH$_2$*C*H$_2$CH$_2$CH), 25.72 (NCH$_2$*C*H$_2$CH$_2$C≡C), 26.94 (NCH$_2$CH*C*H$_2$), 41.86 (NCH$_2$*C*H), 53.73 (N*C*H$_2$CH$_2$CH$_2$CH), 55.37 (N*C*H$_2$CH), 57.29 (N*C*H$_2$CH$_2$CH$_2$C≡C), 60.25 (O*C*H$_2$CH$_3$), 79.68 (CH$_2$C≡*C*), 93.04 (CH$_2$*C*≡C), 123.47 (CH$_2$C≡C*C*), 125.37 (ClC*C*HCH), 127.16 (CH$_2$C≡CCCHCH*C*H), 127.41 (CH$_2$C≡CCCH*C*H), 129.29 (ClC*C*HC), 129.50 (CH$_2$C≡CCC*C*H), 130.92 (ClCCH*C*H), 132.02 (CH$_2$C≡CC*C*H), 132.83 (Cl*C*), 138.22 (H$_3$C*C*), 139.59 (H$_3$CC*C*), 142.99 (CH$_2$C≡CC*C*), 174.20 (*C*=O) ppm; IR (KBr): $\tilde{\nu}$=3059, 3020, 2941, 2865, 2807, 2770, 2227, 1730, 1592, 1472, 1441, 1371, 1305, 1179, 1151, 1097, 1030, 870, 820, 761 cm^{-1}; MS (EI, 70 eV) *m/z*: 423 [M]$^+$; HRMS-EI$^+$ *m/z* [M]$^+$ calcd for $C_{26}H_{30}ClNO_2$: 423.1965, found: 423.1962.

Ethyl 1-{4-[2-(4-fluoro-2-methylphenyl)phenyl]but-3-yn-1-yl}piperidine-3-carboxylate (15l):

R_f≈0.3 (hexane/ethyl acetate 8:2). ^{1}H NMR (400 MHz, $CDCl_3$): δ=1.24 (t, *J*=7.2 Hz, 3H, OCH$_2$C*H$_3$*,), 1.41 (qd, *J*=11.8/3.7 Hz, 1H, NCH$_2$CHC*H$_{ax}$*H$_{eq}$), 1.46–1.57 (m, 1H, NCH$_2$C*H$_{ax}$*H$_{eq}$CH$_2$CH), 1.68 (dp, *J*=12.5, 3.8 Hz, 1H, NCH$_2$CH$_{ax}$*H$_{eq}$*CH$_2$CH), 1.87–2.01 (m, 2H, NCH$_2$CHCH$_{ax}$*H$_{eq}$*, NCH$_2$C*H$_{ax}$*H$_{eq}$CH$_2$CH), 2.12–2.20 (m, 4H, *H$_3$*CC, NC*H$_{ax}$*H$_{eq}$CH), 2.34–2.42 (m, 4H, NC*H$_2$*CH$_2$C≡C, NCH$_2$C*H$_2$*C≡C), 2.50 (tt, *J*=10.5, 3.8 Hz, 1H, NCH$_2$C*H$_{ax}$*), 2.65 (d$_{br}$, *J*=11.2 Hz, 1H, NCH$_{ax}$*H$_{eq}$*CH$_2$CH$_2$CH), 2.89 (d$_{br}$, *J*=11.1 Hz, 1H, NCH$_{ax}$*H$_{eq}$*CH), 4.12 (q, *J*=7.1 Hz, 2H, OC*H$_2$*CH$_3$), 6.90 (td, *J*=8.5, 2.6 Hz, 2H, FCC*H*CH), 6.95 (dd, *J*=9.8, 2.9 Hz, 1H, FCC*H*C), 7.12

(dd, *J*=8.4, 6.0 Hz, 1H, FCCHC*H*), 7.14–7.18 (m, 1H, C≡CCCC*H*), 7.24–7.33 (m, 2H, C≡CCCHC*H*, C≡CCCCHC*H*), 7.43–7.48 (m, 1H, C≡CCC*H*) ppm; ^{13}C NMR (101 MHz, $CDCl_3$): *δ*=14.16 ($OCH_2\mathit{C}H_3$), 17.51 ($NCH_2\mathit{C}H_2C{\equiv}C$), 20.11 (d, $^4J_{CF}$=1.0 Hz, $H_3\mathit{C}C$), 24.51 ($NCH_2\mathit{C}H_2CH_2CH$), 26.78 ($NCH_2CH\mathit{C}H_2$), 41.80 ($NCH_2\mathit{C}H$), 53.15 ($N\mathit{C}H_2CH_2CH_2CH$), 54.91 ($N\mathit{C}H_2CH$), 57.18 ($N\mathit{C}H_2CH_2C{\equiv}C$), 60.28 ($O\mathit{C}H_2CH_3$), 80.29 ($C{\equiv}\mathit{C}CCH$), 91.50 ($\mathit{C}{\equiv}CCCH$), 111.93 (d, $^2J_{CF}$=20.9 Hz, $FC\mathit{C}HCH$), 116.07 (d, $^2J_{CF}$=20.9 Hz, $FC\mathit{C}HC$), 123.52 ($CH_2C{\equiv}C\mathit{C}$), 127.01 ($CH_2C{\equiv}CCCH\mathit{C}H$), 127.47 ($CH_2C{\equiv}CCCHCH\mathit{C}H$), 129.50 ($CH_2C{\equiv}CCC\mathit{C}H$), 131.02 (d, $^3J_{CF}$=8.4 Hz, $FCCH\mathit{C}H$), 131.89 ($CH_2C{\equiv}CC\mathit{C}H$), 136.90 (d, $^4J_{CF}$=3.3 Hz, $H_3CC\mathit{C}$), 138.61 (d, $^3J_{CF}$=7.7 Hz, $H_3C\mathit{C}$), 143.34 ($CH_2C{\equiv}CC\mathit{C}$), 162.00 (d, $^1J_{CF}$=245.0 Hz, F*C*), 174.03 (C=O) ppm; IR (KBr): $\tilde{\nu}$=3060, 2941, 2855, 2810, 2228, 1730, 1612, 1587, 1476, 1443, 1220, 1152, 1099, 1033, 944, 816, 761 cm^{-1}; MS (EI, 70 eV) *m/z*: 393 $[M]^+$; HRMS-EI$^+$ *m/z* $[M]^+$ calcd for $C_{25}H_{28}FNO_2$: 393.2104, found: 393.2117.

Ethyl 1-{5-[2-(4-fluoro-2-methylphenyl)phenyl]pent-4-yn-1-yl}piperidine-3-carboxylate (16l):

R_f≈0.25 (hexane/ethyl acetate 8:2). ^{1}H NMR (400 MHz, $CDCl_3$): *δ*=1.25 (t, *J*=7.1 Hz, 3H, $OCH_2C\mathit{H_3}$), 1.38–1.60 (m, 4H, $NCH_2CHC\mathit{H_{ax}}H_{eq}$, $NCH_2C\mathit{H_2}CH_2CHCH$, $NCH_2C\mathit{H_{ax}}H_{eq}CH_2CH$), 1.70 (dp, *J*=12.8, 3.6 Hz, 1H, $NCH_2CH_{ax}\mathit{H_{eq}}CH_2CH$), 1.86–1.96 (m, 2H, $NCH_2CHCH_{ax}\mathit{H_{eq}}$, $NC\mathit{H_{ax}}H_{eq}CH_2CH_2CH$), 2.09 (t, *J*=10.6 Hz, 1H, $NC\mathit{H_{ax}}H_{eq}CH$), 2.14–2.20 (m, 5H, $\mathit{H_3}CC$, $NC\mathit{H_2}CH_2CH_2C{\equiv}C$), 2.24 (t, *J*=6.9 Hz, 2H, $NCH_2CH_2C\mathit{H_2}C{\equiv}C$), 2.52 (tt, *J*=10.3, 3.8 Hz, 1H, $NCH_2C\mathit{H_{ax}}$), 2.63 (d_{br}, *J*=11.3 Hz, 1H, $NCH_{ax}\mathit{H_{eq}}CH_2CH_2CH$), 2.86 ($d_{br}$, *J*=10.2 Hz, 1H, $NCH_{ax}\mathit{H_{eq}}CH$), 4.13 (q, *J*=7.1 Hz, 2H, $OC\mathit{H_2}CH_3$), 6.90 (td, *J*=8.4, 2.4 Hz, 1H, $FCC\mathit{H}CH$), 6.95 (dd, *J*=9.9, 3.0 Hz, 1H, $FCC\mathit{H}C$), 7.10–7.17 (m, 2H, C≡CCCC*H*), 7.24–7.33 (m, 2H, C≡CCCHC*H*, C≡CCCCHC*H*), 7.45–7.48 (m, 1H, C≡CCC*H*) ppm; ^{13}C NMR (101 MHz, $CDCl_3$): δ=14.20 ($OCH_2\mathit{C}H_3$), 17.28 ($NCH_2CH_2\mathit{C}H_2C{\equiv}C$), 20.13 (d, $^4J_{CF}$=1.8 Hz, $H_3\mathit{C}C$), 24.55 ($NCH_2\mathit{C}H_2CH_2CH$), 25.75 ($NCH_2CH_2\mathit{C}H_2C{\equiv}C$), 26.95 ($NCH_2CH\mathit{C}H_2$), 41.86 ($NCH_2\mathit{C}H$), 53.73 ($N\mathit{C}H_2CH_2CH_2CH$), 55.40, ($N\mathit{C}H_2CH$), 57.29 ($N\mathit{C}H_2CH_2CH_2C{\equiv}C$), 60.24 ($O\mathit{C}H_2CH_3$), 79.76 ($CH_2C{\equiv}\mathit{C}$), 92.89 ($CH_2\mathit{C}{\equiv}C$), 112.00 (d, $^2J_{CF}$=20.9 Hz, $FC\mathit{C}HCH$), 116.15 (d, $^2J_{CF}$=20.9 Hz, $FC\mathit{C}HC$), 123.68 ($CH_2C{\equiv}C\mathit{C}$), 127.02 ($CH_2C{\equiv}CCCH\mathit{C}H$), 127.37 ($CH_2C{\equiv}CCCHCH\mathit{C}H$), 129.51 ($CH_2C{\equiv}CCC\mathit{C}H$), 131.02 (d, $^3J_{CF}$=8.4 Hz, $FCCH\mathit{C}H$), 131.97 ($CH_2C{\equiv}CC\mathit{C}H$), 137.01 (d, $^4J_{CF}$=3.1 Hz, $H_3CC\mathit{C}$), 138.59 (d, $^3J_{CF}$=7.7 Hz, $H_3C\mathit{C}$), 143.23 ($CH_2C{\equiv}CC\mathit{C}$), 161.97 (d, $^1J_{CF}$=244.9 Hz, F*C*), 174.20 (*C*=O) ppm; IR (KBr): $\tilde{\nu}$=3059, 2941, 2855, 2806, 2228, 1730, 1613, 1587, 1476, 1442, 1220, 1151, 1100, 1030, 944, 860, 761 cm^{-1}; MS (EI, 70 eV) *m/z*: 407 $[M]^+$; HRMS-EI$^+$ *m/z* $[M]^+$ calcd for $C_{26}H_{30}FNO_2$: 407.2261, found 407.2274.

1-[4-(2-Phenylphenyl)but-3-yn-1-yl]piperidine-3-carboxylic acid (17a):

R_f≈0.1 (CH_2Cl_2/CH_3OH 9:1). ^{1}H NMR (400 MHz, 1N NaOD/CH_3OD 1:2, 60°C): *δ*=1.22 (qd, *J*=12.7, 3.9 Hz, 1H, $NCH_2CHC\mathit{H_{ax}}H_{eq}$), 1.38 (qt, *J*=12.5, 3.3 Hz, 1H, $NCH_2C\mathit{H_{ax}}H_{eq}CH_2CH$), 1.51 (d, *J*=13.8 Hz, 1H, $NCH_2CH_{ax}\mathit{H_{eq}}CH_2CH$), 1.66 (td, *J*=11.6, 3.0 Hz, 1H, $NC\mathit{H_{ax}}H_{eq}CH_2CH_2CH$), 1.89 ($d_{br}$, *J*=11.8 Hz, 1H, $NCH_2CHCH_{ax}\mathit{H_{eq}}$), 1.99 (t, *J*=11.3 Hz, 1H, $NC\mathit{H_{ax}}H_{eq}CH$), 2.18–2.44 (m, 5H, $NCH_2C\mathit{H_2}C{\equiv}C$, $NC\mathit{H_2}CH_2C{\equiv}C$, $NCH_2C\mathit{H_{ax}}$), 2.53 (d_{br}, *J*=10.4 Hz, 1H, $NCH_{ax}\mathit{H_{eq}}CH_2CH_2CH$), 2.88 ($d_{br}$, *J*=9.2 Hz, 1H, $NCH_{ax}\mathit{H_{eq}}CH$), 6.81–6.89 (m, 2H, C≡CCCCCHCHC*H*, C≡CCCHC*H*), 6.92 (dd, *J*=6.9, 2.1 Hz, 1H, C≡CCCC*H*), 7.09–7.16 (m, 3H, C≡CCCCHC*H*, C≡CCCCCHC*H*), 7.21–7.28 (m, 3H, C≡CCC*H*, C≡CCCCC*H*) ppm; ^{13}C NMR (101 MHz, 1N NaOD/CH_3OD 1:2, 60 °C): *δ*=17.98 ($NCH_2\mathit{C}H_2C{\equiv}C$), 25.67 ($NCH_2\mathit{C}H_2CH_2CH$), 29.06 ($NCH_2CH\mathit{C}H_2$), 46.02 ($NCH_2\mathit{C}H$), 53.81 ($NCH_2\mathit{C}H_2CH_2CH$), 57.60 ($N\mathit{C}H_2CH$), 57.93 ($N\mathit{C}H_2CH_2C{\equiv}C$), 82.50 ($C{\equiv}\mathit{C}CCH$), 93.15 ($\mathit{C}{\equiv}CCCH$), 122.98 ($CH_2C{\equiv}C\mathit{C}$), 128.18 ($CH_2C{\equiv}CCCH\mathit{C}H$), 128.63 ($C{\equiv}CCCCCHCHC\mathit{H}$), 129.11 (3C, $CH_2C{\equiv}CCCHCH\mathit{C}H$, $C{\equiv}CCCCCH\mathit{C}H$), 130.30 (2C, $C{\equiv}CCCC\mathit{C}H$), 130.42 ($CH_2C{\equiv}CCC\mathit{C}H$), 134.12 ($CH_2C{\equiv}CC\mathit{C}H$), 141.74 ($C{\equiv}CCC\mathit{C}$), 144.82 ($CH_2C{\equiv}CC\mathit{C}$), 183.61 (*C*=O) ppm; IR (KBr): $\tilde{\nu}$=3398, 3058, 2943, 2858, 2230, 1710, 1595, 1500, 1475, 1448, 1433, 1390, 1300, 1217, 1155, 1101, 1074, 1009, 879, 758, 737, 700 cm^{-1}; MS (CI, CH_5^+) *m/z*: 334 $[M+H]^+$; HRMS-EI$^+$ *m/z* $[M]^+$ calcd for $C_{22}H_{23}NO_2$: 333.1279, found: 333.1278.

1-[5-(2-Phenylphenyl)pent-4-yn-1-yl]piperidine-3-carboxylic acid (18a):

R_f≈0.1 (CH_2Cl_2/CH_3OH 9:1). ^{1}H NMR (400 MHz, 1N NaOD/CH_3OD 2:1, 60 °C): *δ*=1.24 (qd, *J*=12.6, 4.0 Hz, 1H, $NCH_2CHC\mathit{H_{ax}}H_{eq}$), 1.35–1.49 (m, 3H, $NCH_2C\mathit{H_{ax}}H_{eq}CH_2CH$, $NCH_2C\mathit{H_2}CH_2C{\equiv}C$), 1.54 ($d_{br}$, *J*=13.8 Hz, 1H, $NCH_2CH_{ax}\mathit{H_{eq}}CH_2CH$), 1.62 (td, *J*=11.8, 2.6 Hz, 1H, $NC\mathit{H_{ax}}H_{eq}CH_2CH_2CH$), 1.87–1.95 (m, 2H, $NCH_2CHCH_{ax}\mathit{H_{eq}}$, $NC\mathit{H_{ax}}H_{eq}CH$), 1.97–2.19 (m, 4H, $NCH_2CH_2C\mathit{H_2}C{\equiv}C$, $NC\mathit{H_2}CH_2CH_2C{\equiv}C$), 2.31 (tt, *J*=11.6,

3.9 Hz, 1H, NCH_2CH_{ax}), 2.51 (d_{br}, *J*=10.8 Hz, 1H, $NCH_{ax}H_{eq}CH_2CH_2CH$), 2.90 (d_{br}, *J*=11.8 Hz, 1H, $NCH_{ax}H_{eq}CH$), 6.83–6.89 (m, 2H, C≡CCCCHCH, C≡CCCHCH), 6.91–6.95 (m, 1H, C≡CCCCH), 7.09–7.17 (m, 3H, C≡CCCCCHCH, C≡CCCCCHCHCH), 7.23–7.31 (m, 3H, C≡CCCH, C≡CCCCCH) ppm; ^{13}C NMR (101 MHz, 1N NaOD/CH_3OD 2:1, 60 °C): *δ*=18.69 ($NCH_2CH_2CH_2C$≡C), 25.70 ($NCH_2CH_2CH_2CH$), 26.13 ($NCH_2CH_2CH_2C$≡C), 29.23 (NCH_2CHCH_2), 46.05 (NCH_2CH), 54.29 ($NCH_2CH_2CH_2CH$), 58.09 (NCH_2CH), 58.87 ($NCH_2CH_2CH_2C$≡C), 82.02 (CH_2C≡C), 94.31 (CH_2C≡C), 123.17 (CH_2C≡C), 128.14 (CH_2C≡CCCHCH), 128.59 (C≡CCCCCHCHCH), 129.02 (CH_2C≡CCCHCHCH), 129.12 (2 C, C≡CCCCCHCH), 130.28 (2 C, C≡CCCCCH), 130.46 (CH_2C≡CCCCH), 134.16 (CH_2C≡CCCH), 141.87 (C≡CCCC), 144.78 (CH_2C≡CCC), 183.74 (*C*=O) ppm; IR (KBr): *ṽ*=3427, 3057, 3022, 2935, 2858, 2227, 1709, 1594, 1475, 1449, 1432, 1390, 1186, 1074, 1008, 758, 737, 700 cm^{-1}; MS (CI, CH_5^+) *m/z*: 348 $[M+H]^+$; HRMS-EI$^+$ *m/z* $[M]^+$ calcd for $C_{23}H_{25}NO_2$: 347.1885, found: 347.1881.

1-{4-[2-(2-Chlorophenyl)phenyl]but-3-yn-1-yl}piperidine-3-carboxylic acid (17b):

R_f≈0.1 (CH_2Cl_2/CH_3OH 9:1). ^{1}H NMR (400 MHz, 1N NaOD/CH_3OD 1:2, NaOD = 60 °C): *δ*=1.30 (qd, *J*=12.6, 4.0 Hz, 1H, $NCH_2CHCH_{ax}H_{eq}$), 1.51 (qt, *J*=12.8, 3.8 Hz, 1H, $NCH_2CH_{ax}H_{eq}CH_2CH$), 1.68 (d, *J*=13.3 Hz, 1H, $NCH_2CH_{ax}H_{eq}CH_2CH$), 1.83 (t_{br}, *J*=11.8 Hz, 1H, $NCH_{ax}H_{eq}CH_2CH_2CH$), 1.90 (d_{br}, *J*=12.6 Hz, 1H, $NCH_2CHCH_{ax}H_{eq}$), 1.98 (t, *J*=11.4 Hz, 1H, $NCH_{ax}H_{eq}CH$), 2.23–2.44 (m, 5H, NCH_2CH_{ax}, NCH_2CH_2C≡C, NCH_2CH_2C≡C), 2.72 (d_{br}, *J*=10.8 Hz, 1H, $NCH_{ax}H_{eq}CH_2CH_2CH$), 2.91 (d_{br}, *J*=10.8 Hz, 1H, $NCH_{ax}H_{eq}CH$), 7.17–7.31 (m, 2H, C≡CCCCH, ClCCCH), 7.31–7.41 (m, 4H, C≡CCCCHCH, C≡CCCHCH, ClCCCHCH, ClCCHCH), 7.41–7.53 (m, 2H, C≡CCCH, ClCCH) ppm; ^{13}C NMR (101 MHz, 1N NaOD/CH_3OD 1:2, 60 °C): *δ*=17.31 (NCH_2CH_2C≡C), 25.32 ($NCH_2CH_2CH_2CH$), 28.83 (NCH_2CHCH_2), 45.95 (NCH_2CH), 53.72 ($NCH_2CH_2CH_2CH$), 57.27 (NCH_2CH), 57.82 (NCH_2CH_2C≡C), 81.22 (C≡CCCH), 92.94 (*C*≡CCCH), 127.61 (ClCCHCH or ClCCCHCH), 128.65 (CH_2C≡CCCHCHCH or CH_2C≡CCCHCH), 128.78 (CH_2C≡CCCHCHCH or CH_2C≡CCCHCH), 130.18 (ClCCHCH or ClCCCHCH, ClCCH), 130.35 (CH_2C≡CCCCH), 132.31 (ClCCCH), 132.57 (CH_2C≡CCCH), 133.91 (ClC), 140.90 (ClCC), 143.11 (ClCCCC), 182.92 (*C*=O) ppm; IR (KBr): *ṽ*=3428, 3057, 2941, 2859, 2807, 2231, 1710, 1590, 1466, 1441, 1428, 1389, 1217, 1192, 1156, 1127, 1100, 1071, 1034, 1005, 757 cm^{-1}; MS (CI, CH_5^+) *m/z*: 368 $[M+H]^+$; HRMS-EI$^+$ *m/z* $[M]^+$ calcd for $C_{22}H_{22}ClNO_2$: 367.1339, found: 367.1330.

1-{5-[2-(2-Chlorophenyl)phenyl]pent-4-yn-1-yl}piperidine-3-carboxylic acid (18b):

R_f≈0.1 (CH_2Cl_2/CH_3OH 9:1). ^{1}H NMR (400 MHz, 1N NaOD/CH_3OD 1:2, 60 °C): *δ*=1.32 (qd, *J*=12.6, 4.1 Hz, 1H, $NCH_2CHCH_{ax}H_{eq}$), 1.45–1.60 (m, 3H, $NCH_2CH_{ax}H_{eq}CH_2CH$, $NCH_2CH_2CH_2C$≡C), 1.67 (dp, *J*=13.4, 3.4 Hz, 1H, $NCH_2CH_{ax}H_{eq}CH_2CH$), 1.84–2.04 (m, 3H, $NCH_{ax}H_{eq}CH_2CH_2CH$, $NCH_2CHCH_{ax}H_{eq}$, $NCH_{ax}H_{eq}CH$), 2.17–2.25 (m, 4H, $NCH_2CH_2CH_2C$≡C, $NCH_2CH_2CH_2C$≡C), 2.32 (tt, *J*=11.6, 3.8 Hz, 1H, NCH_2CH_{ax}), 2.75 (d_{br}, *J*=11.3 Hz, 1H, $NCH_{ax}H_{eq}CH_2CH_2CH$), 2.96 (d_{br}, *J*=11.3 Hz, 1H, $NCH_{ax}H_{eq}CH$), 7.15–7.22 (m, 1H, C≡CCCCH), 7.23–7.29 (m, 1H, ClCCCH), 7.32–7.41 (m, 4H, C≡CCCCHCH, C≡CCCHCH, ClCCCHCH, ClCCHCH), 7.41–7.52 (m, 2H, C≡CCCH, ClCCH) ppm; ^{13}C NMR (101 MHz, 1 N NaOD/CH_3OD 1:2, 60 °C): *δ*=17.96 ($NCH_2CH_2CH_2C$≡C), 25.24 ($NCH_2CH_2CH_2CH$), 25.66 ($NCH_2CH_2CH_2C$≡C), 28.92 (NCH_2CHCH_2), 45.89 (NCH_2CH), 54.36 ($NCH_2CH_2CH_2CH$), 57.67 (NCH_2CH), 58.42 ($NCH_2CH_2CH_2C$≡C), 80.80 (CH_2C≡C), 93.96 (CH_2C≡C), 124.33 (CH_2C≡CC), 127.69 (ClCCCHCH or ClCCHCH), 128.55 (CH_2C≡CCCHCHCH or CH_2C≡CCCHCH), 128.75 (CH_2C≡CCCHCHCH or CH_2C≡CCCHCH), 130.28 (ClCCHCH or ClCCCHCH, ClCCH), 130.41 (CH_2C≡CCCCH), 132.30 (ClCCCH), 132.73 (CH_2C≡CCCH), 133.94 (ClC), 141.00 (ClCC), 143.01 (ClCCCC), 182.89 (*C*=O) ppm; IR (KBr): *ṽ*=3425, 3056, 2948, 2865, 2230, 1711, 1589, 1466, 1440, 1428, 1388, 1226, 1146, 1125, 1071, 1033, 1005, 759 cm^{-1}; MS (CI, CH_5^+) *m/z*: 382 $[M+H]^+$; HRMS-EI$^+$ *m/z* $[M]^+$ calcd for $C_{23}H_{24}ClNO_2$: 381.1496, found: 381.1493.

1-{4-[2-(2-Fluorophenyl)phenyl]but-3-yn-1-yl}piperidine-3-carboxylic acid (17c):

R_f≈0.1 (CH_2Cl_2/CH_3OH 9:1). ^{1}H NMR (400 MHz, 1N NaOD/CH_3OD 1:2, 60 °C): *δ*=1.25 (qd, *J*=12.7, 4.0 Hz, 1H, $NCH_2CHCH_{ax}H_{eq}$), 1.45 (qt, *J*=12.8, 3.8 Hz, 1H, $NCH_2CH_{ax}H_{eq}CH_2CH$), 1.62 (dp, *J*=13.4, 3.2 Hz, 1H, $NCH_2CH_{ax}H_{eq}CH_2CH$), 1.79–1.95 (m, 2H, $NCH_2CHCH_{ax}H_{eq}$, $NCH_{ax}H_{eq}CH_2CH_2CH$), 2.00 (t, *J*=11.3 Hz, 1H, $NCH_{ax}H_{eq}CH$), 2.28 (tt, *J*=11.8, 3.7 Hz, 1H, NCH_2CH_{ax}), 2.33–2.49 (m, 4H, NCH_2CH_2C≡C, NCH_2CH_2C≡C),

2.73 (d_{br}, J=11.0 Hz, 1H, NCH$_{ax}$$H_{eq}CH_2CH_2$CH), 2.93 ($d_{br}$, J=9.4 Hz, 1H, NCH$_{ax}$$H_{eq}$CH), 7.14–7.45 (m, 7H, H_{Ar}), 7.45–7.51 (m, 1H, C≡CCCH) ppm; ^{13}C NMR (101 MHz, 1N NaOD/CH$_3$OD 1:2, 60 °C): δ=17.25 (NCH$_2$$CH_2$C≡C), 25.24 (NCH$_2$$CH_2CH_2$CH), 28.76 (NCH$_2CHCH_2$), 45.89 (NCH$_2$$C$H), 53.62 (N$CH_2CH_2CH_2$CH), 57.14 (N$CH_2$CH), 57.70 (N$CH_2CH_2$C≡C), 81.28 (C≡$C$CCH), 92.64 ($C$≡CCH), 116.26 (d, $^2J_{CF}$=22.3 Hz, FCCH), 124.09 (CH$_2$C≡CC), 124.91 (FCCCHCH), 128.84 (CH$_2$C≡CCCCH or CH$_2$C≡CCCHCHCH or CH$_2$C≡CCCHCH), 129.36 (d, $^2J_{CF}$=15.5 Hz, FCC), 130.72 (CH$_2$C≡CCCCH or CH$_2$C≡CCCHCHCH or CH$_2$C≡CCCHCH), 130.78 (d, $^3J_{CF}$=6.7 Hz, FCCHCH), 132.55 (d, $^3J_{CF}$=3.1 Hz, FCCCH), 132.86 (CH$_2$C≡CCCH), 139.32 (CH$_2$C≡CCC), 160.65 (d, $^1J_{CF}$=244.8, FC), 183.02 (C=O) ppm; IR (KBr): $\tilde{\nu}$=3432, 3060, 2941, 2858, 2808, 2230, 1711, 1615, 1582, 1500, 1473, 1439, 1393, 1231, 1211, 1154, 1099, 1007, 823, 758 cm^{-1}; MS (CI, CH$_5^+$) *m/z*: 352 [M+H]$^+$; HRMS-EI$^+$ *m/z* [M]$^+$ calcd for $C_{22}H_{22}FNO_2$: 351.1635, found: 351.1624.

1-{5-[2-(2-Fluorophenyl)phenyl]pent-4-yn-1-yl}piperidine-3-carboxylic acid (18c):

R_f≈0.1 (CH$_2$Cl$_2$/CH$_3$OH 9:1). ^{1}H NMR (400 MHz, 1N NaOD/CH$_3$OD 1:2, 60 °C,): δ=1.32 (qd, J=12.5, 4.1 Hz, 1H, NCH$_2$CHCH_{ax}H$_{eq}$), 1.45–1.62 (m, 3H, NCH$_2$CH_{ax}H$_{eq}$CH$_2$CH, NCH$_2$CH_2CH$_2$C≡C), 1.67 (dp, J=13.5, 3.3 Hz, 1H, NCH$_2$CH$_{ax}$$H_{eq}CH_2$CH), 1.84–1.97 (m, 2H, NCH$_{ax}$$H_{eq}CH_2CH_2CH, NCH_2$CHCH$_{ax}$$H_{eq}$,), 2.02 (t, J=11.2 Hz, 1H, NCH_{ax}H$_{eq}$CH), 2.20–2.37 (m, 5H, NCH_2CH$_2$CH$_2$C≡C, NCH$_2$CH$_2$CH_2C≡C, NCH$_2$CH_{ax}), 2.75 (d_{br}, J=11.3 Hz, 1H, NCH$_{ax}$$H_{eq}CH_2CH_2$CH,), 2.96 ($d_{br}$, J=9.5 Hz, 1H, NCH$_{ax}$$H_{eq}$CH), 7.14–7.51 (m, 8H, H_{ar}) ppm; ^{13}C NMR (101 MHz, 1N NaOD/CH$_3$OD 1:2, 60 °C): δ = 17.91 (NCH$_2$CH$_2$$CH_2$C≡C), 25.08 (NCH$_2$$CH_2CH_2$CH), 25.52 (NCH$_2$$CH_2CH_2$C≡C), 28.76 (NCH$_2CHCH_2$), 45.71 (NCH$_2$$C$H), 54.23 (N$CH_2CH_2CH_2$CH), 57.49 (N$CH_2$CH), 58.32 (N$CH_2CH_2CH_2$C≡C), 80.90 (CH$_2$$C$≡C), 93.69 (CH$_2$C≡$C$), 116.34 (d, $^2J_{CF}$=22.2 Hz, FCCH), 124.24 (CH$_2$C≡CC), 125.01 (FCCCHCH), 128.81 (2 C, CH$_2$C≡CCCCH or/and CH$_2$C≡CCCHCHCH or/and CH$_2$C≡CCCHCH), 129.46 (d, $^2J_{CF}$=15.2 Hz, FCC), 130.78 (CH$_2$C≡CCCCH or CH$_2$C≡CCCHCHCH or CH$_2$C≡CCCHCH), 130.87 ($^3J_{CF}$=2.7 Hz, FCCHCH), 132.54 (d, $^3J_{CF}$=2.7 Hz, FCCCH), 132.98 (CH$_2$C≡CCCH), 139.24 (CH$_2$C≡CCC), 160.68 (d, $^1J_{CF}$=244.7 Hz, FC), 182.89 (C=O) ppm; IR (KBr): $\tilde{\nu}$=3431, 3058, 2946, 2864, 2230, 1710, 1613, 1583, 1500, 1473, 1438, 1388, 1230, 1209, 1107, 1007, 823, 759 cm^{-1}; MS (CI, CH$_5^+$) *m/z*: 366 [M+H]$^+$; HRMS-EI$^+$ *m/z* [M]$^+$ calcd for $C_{23}H_{24}FNO_2$: 365.1791, found: 365.1787.

1-{4-[2-(2-Methylphenyl)phenyl]but-3-yn-1-yl}piperidine-3-carboxylic acid (17d):

R_f≈0.1 (CH$_2$Cl$_2$/CH$_3$OH 9:1). ^{1}H NMR (400 MHz, 1N NaOD/CH$_3$OD 1:2, 60 °C): δ=1.23 (qd, J=12.8, 3.4 Hz, 1H, NCH$_2$CHCH_{ax}H$_{eq}$), 1.42 (q_{br}, J=12.4 Hz, 1H, NCH$_2$CH_{ax}H$_{eq}$CH$_2$CH), 1.61 (d_{br}, J=13.7 Hz, 1H, NCH$_2$CH$_{ax}$$H_{eq}CH_2$CH), 1.78 ($t_{br}$, J=11.7 Hz, 1H, NCH_{ax}H$_{eq}$CH$_2$CH$_2$CH), 1.88 (d_{br}, J=10.9 Hz, 1H, NCH$_2$CHCH$_{ax}$$H_{eq}$), 1.96 (t, J=11.0 Hz, 1H, NCH_{ax}H$_{eq}$CH), 2.06 (s, 3H, H_3CC), 2.21–2.41 (m, 5H, NCH_2CH$_2$C≡C, NCH$_2$CH_2C≡C, NCH$_2$CH_{ax}), 2.66 (d_{br}, J=9.5 Hz, 1H, NCH$_{ax}$$H_{eq}CH_2CH_2$CH), 2.87 ($d_{br}$, J=11.0 Hz, 1H, NCH$_{ax}$$H_{eq}$CH), 7.07 (d, J=6.6 Hz, 1H, H$_3$CCCCH), 7.14 (d, J=6.9 Hz, 1H, C≡CCCCH), 7.17–7.24 (m, 1H, H$_3$CCCCHCH), 7.25–7.38 (m, 4H, H$_3$CCCHCH, H$_3$CCCH, C≡CCCHCH, C≡CCCCHCH), 7.44 (d, J=7.6 Hz, 1H, C≡CCCH) ppm; ^{13}C NMR (101 MHz, 1N NaOD/CH$_3$OD 1:2, 60 °C): δ=17.11 (NCH$_2$$CH_2$C≡C), 19.87 (H$_3$$C$C), 25.06 (NCH$_2$$CH_2CH_2$CH), 28.61 (NCH$_2CHCH_2$), 45.73 (NCH$_2$$C$H), 53.36 (N$CH_2CH_2CH_2$CH), 56.90 (N$CH_2$CH), 57.43 (N$CH_2CH_2$C≡C), 81.60 (C≡$C$CCH), 92.71 ($C$≡CCH), 123.57 (CH$_2$C≡C$C$), 126.27 (H$_3$CCCCH$C$H), 128.09 (CH$_2$C≡CCCH$C$H), 128.59 (H$_3$CCCH$C$H), 128.83 (CH$_2$C≡CCCHCH$C$H), 130.22 (CH$_2$C≡CCCC$H$), 130.66 (H$_3CCC$H), 132.55 (CH$_2$C≡CC$C$H), 137.04 (H$_3CC$), 141.81 (H$_3CCC$), 145.34 (CH$_2$C≡CC$C$), 183.17 ($C$=O) ppm; IR (KBr): $\tilde{\nu}$=3421, 3057, 3018, 2933, 2860, 2228, 1714, 1593, 1474, 1442, 1381, 1217, 1193, 1156, 1122, 1102, 1006, 760 cm^{-1}; MS (CI, CH$_5^+$) *m/z*: 348 [M+H]$^+$; HRMS-EI$^+$ *m/z* [M]$^+$ calcd for $C_{23}H_{25}NO_2$: 347.1885, found: 347.1880.

1-{5-[2-(2-Methylphenyl)phenyl]pent-4-yn-1-yl}piperidine-3-carboxylic acid (18d):

R_f≈0.1 (CH$_2$Cl$_2$/CH$_3$OH 9:1). ^{1}H NMR (400 MHz, 1N NaOD/CH$_3$OD 1:2, 60 °C): δ=1.26 (qd, J=12.8, 3.8 Hz, 1H, NCH$_2$CHCH_{ax}H$_{eq}$), 1.39–1.54 (m, 3H, NCH$_2$CH_{ax}H$_{eq}$CH$_2$CH, NCH$_2$CH_2CH$_2$C≡C), 1.64 (d_{br}, J=12.9 Hz, 1H, NCH$_2$CH$_{ax}$$H_{eq}CH_2$CH), 1.77 (td, J=11.9, 2.6 Hz, 1H, NCH_{ax}H$_{eq}$CH$_2$CH$_2$CH), 1.86–1.95 (m, 2H, NCH$_2$CHCH$_{ax}$$H_{eq}$, NC$H_{ax}H_{eq}$CH), 2.04–2.21 (m, 7H, H_3CC, NCH$_2$CH$_2$CH_2C≡C, NCH_2CH$_2$CH$_2$C≡C), 2.28 (tt, J=11.9, 3.3 Hz, 1H, NCH$_2$CH_{ax}), 2.67 (d_{br}, J=9.5 Hz, 1H, NCH$_{ax}$$H_{eq}CH_2CH_2$CH), 2.91 ($d_{br}$, J=10.5 Hz, 1H,

NCH$_{ax}$*H$_{eq}$*CH), 7.03–7.16 (m, *J*=19.3, 6.8 Hz, 2H, H$_3$CCCC*H*, C≡CCCC*H*), 7.17–7.24 (m, 1H, H$_3$CCCCHC*H*), 7.25–7.36 (m, 4H, H$_3$CCCHC*H*, H$_3$CCC*H*, C≡CCCHC*H*, C≡CCCCHC*H*), 7.42 (d, *J*=7.4 Hz, 1H, C≡CCC*H*) ppm; ^{13}C NMR (101 MHz, 1N NaOD/CH$_3$OD 1:2, 60 °C): *δ*=17.88 (NCH$_2$CH$_2$*C*H$_2$C≡C), 19.91 (H$_3$*C*C), 25.06 (NCH$_2$*C*H$_2$CH$_2$CH), 25.50 (NCH$_2$CH$_2$*C*H$_2$C≡C), 28.86 (NCH$_2$CH*C*H$_2$), 45.87 (NCH$_2$*C*H), 54.06 (N*C*H$_2$CH$_2$CH$_2$CH), 57.41 (N*C*H$_2$CH), 58.18 (N*C*H$_2$CH$_2$CH$_2$C≡C), 81.14 (C≡*C*CH), 93.73 (*C*≡CCH), 123.73 (CH$_2$C≡C*C*), 126.35 (H$_3$CCCCH*C*H), 128.07 (CH$_2$C≡CCCH*C*H), 128.67 (H$_3$CCCH*C*H), 128.71 (CH$_2$C≡CCCHCH*C*H), 130.27 (CH$_2$C≡CCC*C*H), 130.75 (H$_3$CC*C*H), 132.68 (CH$_2$C≡CC*C*H), 136.99 (H$_3$C*C*), 141.95 (H$_3$CC*C*), 145.28 (CH$_2$C≡CC*C*), 183.27 (*C*=O) ppm. IR (KBr): *ṽ*=3424, 3057, 3018, 2948, 2865, 2228, 1717, 1592, 1474, 1439, 1388, 1274, 1226, 1145, 1121, 1076, 1006, 760 cm^{-1}; MS (CI, CH$_5^+$) *m/z*: 362 [M+H]$^+$; HRMS-EI$^+$ *m/z* [M]$^+$ calcd for C$_{24}$H$_{27}$NO$_2$: 361.2042, found: 361.2054.

1-{4-[2-(4-Chlorophenyl)phenyl]but-3-yn-1-yl}piperidine-3-carboxylic acid (17e):

R$_f$≈0.1 (CH$_2$Cl$_2$/CH$_3$OH 9:1). ^{1}H NMR (400 MHz, 1N NaOD/CH$_3$OD 1:2, 60 °C): *δ* = 1.24 (qd, *J*=12.5, 3.5 Hz, 1H, NCH$_2$CHC*H$_{ax}$*H$_{eq}$), 1.42 (qt, *J*=13.1, 3.5 Hz, 1H, NCH$_2$C*H$_{ax}$*H$_{eq}$CH$_2$CH), 1.56 (d$_{br}$, *J*=13.4 Hz, 1H, NCH$_2$CH$_{ax}$*H$_{eq}$*CH$_2$CH), 1.73 (td, *J*=11.5, 2.4 Hz, 1 H, NC*H$_{ax}$*H$_{eq}$CH$_2$CH$_2$CH), 1.91 (d$_{br}$, *J*=11.7 Hz, 1H, NCH$_2$CHCH$_{ax}$*H$_{eq}$*), 2.01 (t, *J*=11.3 Hz, 1H, NC*H$_{ax}$*H$_{eq}$CH), 2.25–2.50 (m, 5H, NC*H$_2$*CH$_2$C≡C, NCH$_2$C*H$_2$*C≡C, NCH$_2$C*H$_{ax}$*), 2.60 (d$_{br}$, *J*=10.8 Hz, 1H, NCH$_{ax}$*H$_{eq}$*CH$_2$CH$_2$CH), 2.92 (d$_{br}$, *J*=10.6 Hz, 1H, NCH$_{ax}$*H$_{eq}$*CH), 6.91 (d, *J*=7.2 Hz, 1H, C≡CCCC*H*), 6.97–7.08 (m, 2H, C≡CCCCHC*H*, C≡CCCHC*H*), 7.11 (d, *J*=8.3 Hz, 2H, ClCC*H*), 7.18 (d, *J*=8.5 Hz, 2H, ClCCHC*H*), 7.32 (d, *J*=7.4 Hz, 1H, C≡CCC*H*) ppm; ^{13}C NMR (101 MHz, 1N NaOD/CH$_3$OD 1:2, 60 °C): *δ*=17.40 (NCH$_2$*C*H$_2$C≡C), 25.12 (NCH$_2$*C*H$_2$CH$_2$CH), 28.53 (NCH$_2$CH*C*H$_2$), 45.52 (NCH$_2$*C*H), 53.35 (N*C*H$_2$CH$_2$CH$_2$CH), 57.02 (N*C*H$_2$CH), 57.35 (N*C*H$_2$CH$_2$C≡C), 81.62 (C≡*C*CH), 93.11 (*C*≡CCH), 122.37 (CH$_2$C≡C*C*), 128.17 (CH$_2$C≡CCCH*C*H), 128.66 (2C, ClC*C*H), 128.83 (CH$_2$C≡CCCHCH*C*H), 129.72 (CH$_2$C≡CCC*C*H), 131.25 (2 C, ClCCH*C*H), 133.78 (2C, *C*Cl, CH$_2$C≡CC*C*H), 139.74 (ClCCHCH*C*), 142.84 (CH$_2$C≡CC*C*), 183.09 (*C*=O) ppm; IR (KBr): *ṽ*=3423, 3057, 2940, 2860, 2230, 1717, 1595, 1494, 1474, 1441, 1396, 1090, 1004, 832, 760 cm^{-1}; MS (CI, CH$_5^+$) *m/z*: 368 [M+H]$^+$; HRMS-EI$^+$ *m/z* [M]$^+$ calcd for C$_{22}$H$_{22}$ClNO$_2$: 367.1339, found: 367.1339.

1-{5-[2-(4-Chlorophenyl)phenyl]pent-4-yn-1-yl}piperidine-3-carboxylic acid (18e):

R$_f$≈0.1 (CH$_2$Cl$_2$/CH$_3$OH 9:1). ^{1}H NMR (400 MHz, 1N NaOD/CH$_3$OD 1:2, 60 °C): *δ*=1.29 (qd, *J*=12.7, 3.8 Hz, 1H, NCH$_2$CHC*H$_{ax}$*H$_{eq}$), 1.43–1.61 (m, 3H, NCH$_2$C*H$_{ax}$*H$_{eq}$CH$_2$CH, NCH$_2$C*H$_2$*CH$_2$C≡C), 1.65 (d$_{br}$, *J*=12.0 Hz, 1H, NCH$_2$CH$_{ax}$*H$_{eq}$*CH$_2$CH), 1.74 (t, *J*=11.9 Hz, 1H, NC*H$_{ax}$*H$_{eq}$CH$_2$CH$_2$CH), 1.89–1.99 (m, 2H, NCH$_2$CHCH$_{ax}$*H$_{eq}$*, NC*H$_{ax}$*H$_{eq}$CH), 2.12–2.27 (m, 4H, NC*H$_2$*CH$_2$CH$_2$C≡C, NCH$_2$CH$_2$C*H$_2$*C≡C), 2.33 (tt, *J*=11.5, 3.5 Hz, 1H, NCH$_2$C*H$_{ax}$*), 2.64 (d$_{br}$, *J*=10.5 Hz, 1H, NCH$_{ax}$*H$_{eq}$*CH$_2$CH$_2$CH), 2.97 (d$_{br}$, *J*=10.4 Hz, 1H, NCH$_{ax}$*H$_{eq}$*CH), 7.03–7.10 (m, 1H, C≡CCCC*H*), 7.12–7.18 (m, 2H, C≡CCCCHC*H*, C≡CCCHC*H*), 7.23 (d, *J*=8.1 Hz, 2H, ClCC*H*), 7.28 (d, *J*=8.3 Hz, 2H, ClCCHC*H*), 7.35–7.42 (m, 1H, C≡CCC*H*) ppm; ^{13}C NMR (101 MHz, 1N NaOD/CH$_3$OD 1:2, 60 °C): *δ*=18.04 (NCH$_2$CH$_2$*C*H$_2$C≡C), 25.20 (NCH$_2$*C*H$_2$CH$_2$CH), 25.47 (NCH$_2$*C*H$_2$CH$_2$C≡C), 28.73 (NCH$_2$CH*C*H$_2$), 45.64 (NCH$_2$*C*H), 54.00 (N*C*H$_2$CH$_2$CH$_2$CH), 57.38 (N*C*H$_2$CH), 58.39 (N*C*H$_2$CH$_2$CH$_2$C≡C), 81.20 (CH$_2$C≡*C*), 94.31 (CH$_2$*C*≡C), 122.50 (CH$_2$C≡C*C*), 128.28 (CH$_2$C≡CCCH*C*H), 128.81 (2C, ClC*C*H), 128.92 (CH$_2$C≡CCCHCH*C*H), 129.87 (CH$_2$C≡CCC*C*H), 131.33 (2C, ClCCH*C*H), 133.71 (CH$_2$C≡CC*C*H), 133.82 (Cl*C*), 140.00 (ClCCHCH*C*), 143.01 (CH$_2$C≡CC*C*), 183.21 (*C*=O) ppm; IR (KBr): *ṽ*=3430, 3056, 2949, 2866, 2230, 1717, 1593, 1497, 1474, 1441, 1396, 1089, 1004, 832, 760 cm^{-1}; MS (CI, CH$_5^+$) *m/z*: 382 [M+H]$^+$; HRMS-EI$^+$ *m/z* [M]$^+$ calcd for C$_{23}$H$_{24}$ClNO$_2$: 381.1496, found: 381.1495.

1-{4-[2-(2,4-Dichlorophenyl)phenyl]but-3-yn-1-yl}piperidine-3-carboxylic acid (17f):

R$_f$≈0.1 (CH$_2$Cl$_2$/CH$_3$OH 9:1). ^{1}H NMR (500 MHz, 1N NaOD/CH$_3$OD 1:2, 60 °C): *δ*=1.27 (qd, *J*=12.8, 4.1 Hz, 1H, NCH$_2$CHC*H$_{ax}$*H$_{eq}$), 1.48 (qt, *J*=13.0, 3.9 Hz, 1H, NCH$_2$C*H$_{ax}$*H$_{eq}$CH$_2$CH), 1.64 (dp, *J*=13.6, 3.4 Hz, 1H, NCH$_2$CH$_{ax}$*H$_{eq}$*CH$_2$CH), 1.81 (td, *J*=11.8, 3.1 Hz, 1H, NC*H$_{ax}$*H$_{eq}$CH$_2$CH$_2$CH), 1.93 (d$_{br}$, *J*=13.0 Hz, 1H, NCH$_2$CHCH$_{ax}$*H$_{eq}$*), 1.98 (t, *J*=11.4 Hz, 1H, NC*H$_{ax}$*H$_{eq}$CH), 2.26–2.46 (m, 5H, NCH$_2$C*H$_{ax}$*, NC*H$_2$*CH$_2$C≡C, NCH$_2$C*H$_2$*C≡C), 2.73 (d$_{br}$, *J*=11.3 Hz, 1H, NCH$_{ax}$*H$_{eq}$*CH$_2$CH$_2$CH), 2.95 (d$_{br}$, *J*=11.3 Hz, 1H, NCH$_{ax}$*H$_{eq}$*CH), 7.14–7.18 (m, 1H, C≡CCCC*H*), 7.22 (d, *J*=8.2 Hz, 1H, ClCCC*H*), 7.32–7.38 (m, 3H, ClCC*H*CH, C≡CCCHC*H*, C≡CCCCHC*H*), 7.41–7.46 (m, 1H, C≡CCC*H*), 7.50 (d, *J*=2.1 Hz, 1H, ClCC*H*CCl) ppm; ^{13}C NMR (126 MHz,

1N NaOD/CH_3OD 1:2, 60 °C): δ=17.50 ($NCH_2CH_2C{\equiv}C$), 25.48 ($NCH_2CH_2CH_2CH$), 28.94 (NCH_2CHCH_2), 45.93 (NCH_2CH), 54.00 ($NCH_2CH_2CH_2CH$), 57.35 (NCH_2CH), 58.04 ($NCH_2CH_2C{\equiv}C$), 81.06 ($C{\equiv}CCH$), 92.92 ($C{\equiv}CCH$), 124.22 ($CH_2C{\equiv}C$), 127.89 ($ClCCHCH$, 128.86 ($CH_2C{\equiv}CCCHCH$), 129.21 ($CH_2C{\equiv}CCCHCHCH$), 129.87 ($ClCCHCCl$, 130.38 ($CH_2C{\equiv}CCCCH$), 132.78 ($CH_2C{\equiv}CCCH$), 133.54 ($ClCCCH$), 134.89 (ClC), 135.06 (ClC), 139.77 ($ClCC$), 141.83 ($CH_2C{\equiv}CCC$), 182.98 ppm (C=O) ppm; IR (KBr): $\tilde{\nu}$=3423, 3059, 2941, 2860, 2807, 2234, 1709, 1586, 1466, 1439, 1375, 1101, 1071, 1004, 866, 812, 761 cm^{-1}; MS (CI, CH_5^+) *m/z*: 402 $[M+H]^+$; HRMS-EI$^+$ *m/z* $[M]^+$ calcd for $C_{22}H_{21}Cl_2NO_2$: 401.0949, found: 401.0936.

1-{5-[2-(2,4-Dichlorophenyl)phenyl]pent-4-yn-1-yl}piperidine-3-carboxylic acid (18f):

R_f≈0.1 (CH_2Cl_2/CH_3OH 9:1). ^{1}H NMR (500 MHz, 1N NaOD/CH_3OD 1:2, 60 °C): δ=1.31 (qd, J=12.8, 4.0 Hz, 1H, $NCH_2CHCH_{ax}H_{eq}$), 1.44–1.59 (m, 3H, $NCH_2CH_{ax}H_{eq}CH_2CH$, $NCH_2CH_2CH_2C{\equiv}C$), 1.69 (dp, J=13.6, 3.0 Hz, 1H, $NCH_2CH_{ax}H_{eq}CH_2CH$), 1.80 (td, J=12.1, 2.7 Hz, 1H, $NCH_{ax}H_{eq}CH_2CH_2CH$), 1.87–1.99 (m, 2H, $NCH_2CHCH_{ax}H_{eq}$, $NCH_{ax}H_{eq}CH$), 2.11–2.27 (m, 4H, $NCH_2CH_2CH_2C{\equiv}C$, $NCH_2CH_2CH_2C{\equiv}C$), 2.31 (tt, J=11.9, 3.7 Hz, 1H, NCH_2CH_{ax},), 2.73 (d_{br}, J=11.1 Hz, 1H, $NCH_{ax}H_{eq}CH_2CH_2CH$), 2.99 (d_{br}, J=10.2 Hz, 1H, $NCH_{ax}H_{eq}CH$), 7.12–7.17 (m, 1H, $C{\equiv}CCCCH$), 7.22 (d, J=8.2 Hz, 1H, $ClCCCH$), 7.32–7.37 (m, 3H, $ClCCHCH$, $C{\equiv}CCCHCH$, $C{\equiv}CCCCHCH$), 7.40–7.45 (m, 1H, $C{\equiv}CCCH$), 7.51 (d, J=2.1 Hz, 1H, $ClCCHCCl$) ppm; ^{13}C NMR (126 MHz, 1N NaOD/CH_3OD 1:2, 60 °C): δ=18.09 ($NCH_2CH_2CH_2C{\equiv}C$), 25.56 ($NCH_2CH_2CH_2CH$), 25.82 ($NCH_2CH_2CH_2C{\equiv}C$), 29.08 (NCH_2CHCH_2), 45.97 (NCH_2CH), 54.56 ($NCH_2CH_2CH_2CH$), 57.72 (NCH_2CH), 58.73 ($NCH_2CH_2CH_2C{\equiv}C$), 80.58 ($CH_2C{\equiv}C$), 94.15 ($CH_2C{\equiv}C$), 124.38 ($CH_2C{\equiv}CC$), 127.97 ($ClCCHCH$), 128.74 ($CH_2C{\equiv}CCCHCH$), 129.19 ($CH_2C{\equiv}CCCHCHCH$), 129.98 ($ClCCHCHCCl$), 130.44 ($CH_2C{\equiv}CCCCH$), 132.93 ($CH_2C{\equiv}CCCH$), 133.52 ($ClCCCH$), 134.90 (ClC), 135.06 (ClC), 139.84 ($ClCC$), 141.66 ($CH_2C{\equiv}CCC$), 183.14 (C=O) ppm; IR (KBr): $\tilde{\nu}$=3426, 3060, 2943, 2864, 2231, 1710, 1586, 1466, 1439, 1376, 1101, 1071, 1004, 868, 813, 762 cm^{-1}; MS (CI, CH_5^+) *m/z*: 416 $[M+H]^+$; HRMS-EI$^+$ *m/z* $[M]^+$ calcd for $C_{23}H_{23}Cl_2NO_2$: 415.1106, found: 415.1097.

1-{4-[2-(2,4-Difluorophenyl)phenyl]but-3-yn-1-yl}piperidine-3-carboxylic acid (17g):

R_f≈0.1 (CH_2Cl_2/CH_3OH 9:1). ^{1}H NMR (500 MHz, 1N NaOD/CH_3OD 1:2, 60 °C): δ=1.28 (qd, J=12.6, 4.1 Hz, 1H, $NCH_2CHCH_{ax}H_{eq}$), 1.48 (qt, J=12.8, 3.8 Hz, 1H, $NCH_2CH_{ax}H_{eq}CH_2CH$), 1.64 (dp, J=13.0, 3.6 Hz, 1H, $NCH_2CH_{ax}H_{eq}CH_2CH$), 1.86–1.96 (m, 2H, $NCH_2CHCH_{ax}H_{eq}$, $NCH_{ax}H_{eq}CH_2CH_2CH$), 2.05 (t, J=11.3 Hz, 1H, $NCH_{ax}H_{eq}CH$), 2.31 (tt, J=11.6, 3.8 Hz, 1H, NCH_2CH_{ax}), 2.37–2.52 (m, 4H, $NCH_2CH_2C{\equiv}C$, $NCH_2CH_2C{\equiv}C$), 2.76 (d_{br}, J=11.1 Hz, 1H, $NCH_{ax}H_{eq}CH_2CH_2CH$), 2.92–3.01 (m, 1H, $NCH_{ax}H_{eq}CH$), 6.97–7.06 (m, 2H, $FCCHCF$, $FCCHCH$), 7.23–7.29 (m, 1H, $C{\equiv}CCCCH$), 7.30–7.42 (m, 3H, $C{\equiv}CCCCHCH$, $C{\equiv}CCCHCH$, $FCCCH$), 7.45–7.50 (m, 1H, $C{\equiv}CCCH$) ppm; ^{13}C NMR (126 MHz, 1N NaOD/CH_3OD 1:2, 60 °C): δ=17.24 ($NCH_2CH_2C{\equiv}C$), 25.18 ($NCH_2CH_2CH_2CH$), 28.69 (NCH_2CHCH_2), 45.78 (NCH_2CH), 53.75 ($NCH_2CH_2CH_2CH$), 57.13 (NCH_2CH), 57.72 ($NCH_2CH_2C{\equiv}C$), 81.17 ($C{\equiv}CCH$), 92.62 ($C{\equiv}CCH$), 104.46 (d, $^2J_{CF}$=26.2 Hz, $FCCHCF$), 111.89 (dd, $^2J_{CF}$=21.4 Hz, $^4J_{CF}$=3.7 Hz, $FCCHCH$), 124.19 ($CH_2C{\equiv}CC$), 125.76 (dd, $^2J_{CF}$=13.0 Hz, $^4J_{CF}$=3.7 Hz, FCC), 128.95 ($CH_2C{\equiv}CCCHCHCH$ or $CH_2C{\equiv}CCCHCH$), 129.02 ($CH_2C{\equiv}CCCHCHCH$ or $CH_2C{\equiv}CCCHCH$), 130.81 ($CH_2C{\equiv}CCCCH$), 132.98 ($CH_2C{\equiv}CCCH$), 133.55 (dd, $^3J_{CF}$=9.6 Hz, $^3J_{CF}$=4.7 Hz, $FCCCH$), 138.34 ($CH_2C{\equiv}CCC$), 160.76 (dd, $^1J_{CF}$=249.0 Hz, $^3J_{CF}$=12.7 Hz, FC), 163.59 (dd, $^1J_{CF}$=257.3 Hz, $^3J_{CF}$=10.3 Hz, FC), 182.83 (C=O) ppm; IR (KBr): $\tilde{\nu}$=3426, 3061, 2942, 2862, 2808, 2230, 1718, 1618, 1593, 1510, 1479, 1444, 1266, 1219, 1139, 1097, 963, 850, 762 cm^{-1}; MS (CI, CH_5^+) *m/z*: 370 $[M+H]^+$; HRMS-EI$^+$ *m/z* $[M]^+$ calcd for $C_{22}H_{21}F_2NO_2$: 369.1540 found: 369.1544.

1-{5-[2-(2,4-Difluorophenyl)phenyl]pent-4-yn-1-yl}piperidine-3-carboxylic acid (18g):

R_f≈0.1 (CH_2Cl_2/CH_3OH 9:1). ^{1}H NMR (500 MHz, 1N NaOD/CH_3OD 1:2, 60 °C): δ=1.30 (qd, J=12.4, 3.9 Hz, 1H, $NCH_2CHCH_{ax}H_{eq}$), 1.45–1.63 (m, 3H, $NCH_2CH_{ax}H_{eq}CH_2CH$, $NCH_2CH_2CH_2C{\equiv}C$), 1.67 (dp, J=13.4, 3.3 Hz, 1H, $NCH_2CH_{ax}H_{eq}CH_2CH$), 1.81–2.02 (m, 3H, $NCH_{ax}H_{eq}CH_2CH_2CH$, $NCH_2CHCH_{ax}H_{eq}$, $NCH_{ax}H_{eq}CH$), 2.22–2.37 (m, 5H, $NCH_2CH_2CH_2C{\equiv}C$, $NCH_2CH_2CH_2C{\equiv}C$), 2.74 (d_{br}, J=11.5 Hz, 1H, $NCH_{ax}H_{eq}CH_2CH_2CH$), 2.94–3.03 (m, 1H, $NCH_{ax}H_{eq}CH$), 6.98–7.06 (m, 2H, $FCCHCF$, $FCCHCH$), 7.24–7.28 (m, 1H, $C{\equiv}CCCCH$), 7.30–7.41 (m, 3H, $C{\equiv}CCCCHCH$, $C{\equiv}CCCHCH$, $FCCHCH$), 7.43–7.50 (m, 1H, $C{\equiv}CCCH$) ppm; ^{13}C NMR

(126 MHz, 1N NaOD/CH_3OD 1:2, 60 °C): δ=17.96 ($NCH_2CH_2\mathit{C}H_2C{\equiv}C$), 25.29 ($NCH_2\mathit{C}H_2CH_2CH$), 25.73 ($NCH_2\mathit{C}H_2CH_2C{\equiv}C$), 28.92 ($NCH_2CH\mathit{C}H_2$), 45.86 ($NCH_2\mathit{C}H$), 54.40 ($N\mathit{C}H_2CH_2CH_2CH$), 57.64 ($N\mathit{C}H_2CH$), 58.54 ($N\mathit{C}H_2CH_2CH_2C{\equiv}C$), 80.69 ($CH_2C{\equiv}\mathit{C}$), 93.93 ($CH_2\mathit{C}{\equiv}C$), 104.55 (d, $^2J_{CF}$=26.1 Hz, $FC\mathit{C}HCF$), 111.99 (dd, $^2J_{CF}$=21.3 Hz, $^4J_{CF}$=3.7 Hz, $FC\mathit{C}HCH$), 124.48 ($CH_2C{\equiv}C\mathit{C}$), 125.94 (dd, $^2J_{CF}$=15.9 Hz, $^4J_{CF}$=3.4 Hz, $FC\mathit{C}CH$), 128.83 ($CH_2C{\equiv}CCCHCH\mathit{C}H$ or $CH_2C{\equiv}CCCH\mathit{C}H$), 129.01 ($CH_2C{\equiv}CCCHCH\mathit{C}H$ or $CH_2C{\equiv}CCCH\mathit{C}H$), 130.85 ($CH_2C{\equiv}CCC\mathit{C}H$), 133.05 ($CH_2C{\equiv}CC\mathit{C}H$), 133.56 (dd, $^3J_{CF}$=9.7 Hz, $^3J_{CF}$=4.8 Hz, $FCC\mathit{C}H$), 138.31 ($CH_2C{\equiv}CC\mathit{C}$), 160.85 (dd, $^1J_{CF}$=248.4 Hz, $^3J_{CF}$=12.6 Hz, $F\mathit{C}$), 163.66 (dd, $^1J_{CF}$=246.4 Hz, $^3J_{CF}$=11.8 Hz, $F\mathit{C}$), 182.95 (C=O) ppm; IR (KBr): $\tilde{\nu}$=3432, 3061, 2947, 2865, 2231, 1717, 1618, 1593, 1510, 1478, 1443, 1419, 1266, 1140, 1096, 963, 850, 763 cm^{-1}; MS (CI, CH_5^+) *m/z*: 384 $[M+H]^+$; HRMS-EI$^+$ *m/z* $[M]^+$ calcd for $C_{23}H_{23}F_2NO_2$: 383.1697, found: 383.1696.

1-{4-[2-(2,4-Dimethylphenyl)phenyl]but-3-yn-1-yl}piperidine-3-carboxylic acid (17h):

R_f≈0.1 (CH_2Cl_2/CH_3OH 9:1). ^{1}H NMR (400 MHz, 1N NaOD/CH_3OD 1:2, 60 °C): δ=1.24 (qd, *J*=12.8, 4.1 Hz, 1H, $NCH_2CHC\mathit{H}_{ax}H_{eq}$), 1.45 (qt, *J*=13.3, 4.0 Hz, 1H, $NCH_2C\mathit{H}_{ax}H_{eq}CH_2CH$), 1.66 (dp, *J*=13.8, 3.4 Hz, 1H, $NCH_2CH_{ax}\mathit{H}_{eq}CH_2CH$), 1.79 (td, *J*=11.9, 2.9 Hz, 1H, $NC\mathit{H}_{ax}H_{eq}CH_2CH_2CH$), 1.86–1.93 (m, 1H, $NCH_2CHCH_{ax}\mathit{H}_{eq}$), 1.97 (t, *J*=11.4 Hz, 1H, $NC\mathit{H}_{ax}H_{eq}CH$), 2.04 (s, 3H, H_3CCC), 2.23–2.41 (m, 8H, $NC\mathit{H}_2CH_2C{\equiv}C$, $NCH_2C\mathit{H}_2C{\equiv}C$, $NCH_2C\mathit{H}_{ax}$, $\mathit{H}_3CCCHCC$), 2.70 (d_{br}, *J*=10.5 Hz, 1H, $NCH_{ax}\mathit{H}_{eq}CH_2CH_2CH$), 2.85–2.97 (m, 1H, $NC\mathit{H}_{ax}H_{eq}CH$), 6.95 (d, *J*=7.7 Hz, 1H, $H_3CCCC\mathit{H}$), 7.01 (d, *J*=8.3 Hz, 1H, $H_3CCC\mathit{H}CH$), 7.07 (s, 1H, $H_3CCC\mathit{H}CC$), 7.10–7.15 (m, 1H, $C{\equiv}CCCC\mathit{H}$), 7.28 (td, *J*=7.5, 1.6 Hz, 1H, $C{\equiv}CCCHC\mathit{H}$), 7.33 (td, *J*=7.5, 1.7 Hz, 1H, $C{\equiv}CCCCHC\mathit{H}$), 7.42 (dd, *J*=7.5, 1.4 Hz, 1H, $C{\equiv}CCC\mathit{H}$) ppm; ^{13}C NMR (101 MHz, 1N NaOD/CH_3OD 1:2, 60 °C): δ=17.38 ($NCH_2\mathit{C}H_2C{\equiv}C$), 19.87 ($H_3\mathit{C}CC$), 21.12 ($H_3\mathit{C}CCHCC$), 25.33 ($NCH_2\mathit{C}H_2CH_2CH$), 28.84 ($NCH_2CH\mathit{C}H_2$), 45.92 ($NCH_2\mathit{C}H$), 53.79 ($N\mathit{C}H_2CH_2CH_2CH$), 57.33 ($N\mathit{C}H_2CH$), 57.91 ($N\mathit{C}H_2CH_2C{\equiv}C$), 81.74 ($C{\equiv}\mathit{C}CCH$), 92.37 ($\mathit{C}{\equiv}CCCH$), 124.13 ($CH_2C{\equiv}C\mathit{C}$), 126.86 ($H_3CC\mathit{C}HCH$), 127.92 ($CH_2C{\equiv}CCCH\mathit{C}H$), 128.71 ($CH_2C{\equiv}CCCHCH\mathit{C}H$), 130.23 ($H_3CCCH\mathit{C}H$), 130.41 ($CH_2C{\equiv}CCC\mathit{C}H$), 131.27 ($H_3CC\mathit{C}HCC$), 132.54 ($CH_2C{\equiv}CC\mathit{C}H$), 136.82 ($H_3C\mathit{C}C$), 138.28 ($H_3C\mathit{C}CHCC$), 139.16 ($H_3CC\mathit{C}$), 145.60 ($CH_2C{\equiv}CC\mathit{C}$), 182.88 ($\mathit{C}$=O) ppm; IR (KBr): $\tilde{\nu}$=3442, 3054, 2942, 2923, 2859, 2808, 2228, 1712, 1614, 1476, 1441, 1376, 1303, 1214, 1190, 1155, 1103, 1038, 1005, 820, 762 cm^{-1}; MS (CI, CH_5^+) *m/z*: 362 $[M+H]^+$; HRMS-EI$^+$ *m/z* $[M]^+$ calcd for $C_{24}H_{27}NO_2$: 361.2042, found: 361.2041.

1-{5-[2-(2,4-Dimethylphenyl)phenyl]pent-4-yn-1-yl}piperidine-3-carboxylic acid (18h):

R_f≈0.1 (CH_2Cl_2/CH_3OH 9:1). ^{1}H NMR (400 MHz, 1N NaOD/CH_3OD 1:2, 60 °C): δ=1.29 (qd, *J*=12.8, 4.2 Hz, 1H, $NCH_2CHC\mathit{H}_{ax}H_{eq}$), 1.42–1.58 (m, 3H, $NCH_2C\mathit{H}_2CH_2C{\equiv}C$), 1.66 (dp, *J*=13.6, 3.2 Hz, 1H, $NCH_2CH_{ax}\mathit{H}_{eq}CH_2CH$), 1.78 (td, *J*=12.0, 2.9 Hz, 1H, $NC\mathit{H}_{ax}H_{eq}CH_2CH_2CH$), 1.86–1.98 (m, 2H, $NCH_2CHCH_{ax}\mathit{H}_{eq}$, $NC\mathit{H}_{ax}H_{eq}CH$), 2.05 (s, 3H, H_3CCC), 2.10–2.16 (m, 2H, $NCH_2CH_2C\mathit{H}_2C{\equiv}C$), 2.17–2.23 (m, 2H, $NC\mathit{H}_2CH_2CH_2C{\equiv}C$), 2.26–2.34 (m, 4H, $NCH_2C\mathit{H}_{ax}$, $\mathit{H}_3CCCHCC$), 2.70 (d_{br}, *J*=10.5 Hz, 1H, $NCH_{ax}\mathit{H}_{eq}CH_2CH_2CH$), 2.89–3.02 (m, 1H, $NC\mathit{H}_{ax}H_{eq}CH$), 6.95 (d, *J*=7.7 Hz, 1H, $H_3CCCC\mathit{H}$), 7.02 (d, *J*=7.7 Hz, 1H, $H_3CCC\mathit{H}CH$), 7.07 (s, 1H, $H_3CCC\mathit{H}CC$), 7.10 (dd, *J*=7.4, 1.5 Hz, 1H, $C{\equiv}CCCC\mathit{H}$), 7.28 (td, *J*=7.5, 1.7 Hz, 1H, $C{\equiv}CCCHC\mathit{H}$), 7.32 (td, *J*=7.5, 1.7 Hz, 1H, $C{\equiv}CCCCHC\mathit{H}$), 7.42 (dd, *J*=7.5, 1.5 Hz, 1H, $C{\equiv}CCC\mathit{H}$) ppm; ^{13}C NMR (101 MHz, 1N NaOD/CH_3OD 1:2, 60 °C): δ=17.98 ($NCH_2CH_2\mathit{C}H_2C{\equiv}C$), 19.88 ($H_3\mathit{C}CC$), 21.19 ($H_3\mathit{C}CCHCC$), 25.42 ($NCH_2\mathit{C}H_2CH_2CH$), 25.80 ($NCH_2\mathit{C}H_2CH_2C{\equiv}C$), 29.03 ($NCH_2CH\mathit{C}H_2$), 46.00 ($NCH_2\mathit{C}H$), 54.38 ($N\mathit{C}H_2CH_2CH_2CH$), 57.71 ($N\mathit{C}H_2CH$), 58.48 ($N\mathit{C}H_2CH_2CH_2C{\equiv}C$), 81.23 ($C{\equiv}\mathit{C}CCH$), 93.40 ($\mathit{C}{\equiv}CCCH$), 124.27 ($CH_2C{\equiv}C\mathit{C}$), 126.92 ($H_3CC\mathit{C}HCH$), 127.89 ($CH_2C{\equiv}CCCH\mathit{C}H$), 128.59 ($CH_2C{\equiv}CCCHCH\mathit{C}H$), 130.23 ($H_3CCCH\mathit{C}H$), 130.49 ($CH_2C{\equiv}CCC\mathit{C}H$), 131.35 ($H_3CC\mathit{C}HCC$), 132.73 ($CH_2C{\equiv}CC\mathit{C}H$), 136.76 ($H_3C\mathit{C}C$), 138.21 ($H_3C\mathit{C}CHCC$), 139.24 ($H_3CC\mathit{C}$), 145.44 ($CH_2C{\equiv}CC\mathit{C}$), 182.99 ($\mathit{C}$=O) ppm; IR (KBr): $\tilde{\nu}$=3440, 3054, 2942, 2862, 2228, 1709, 1615, 1476, 1439, 1377, 1225, 1155, 1131, 1105, 1035, 1004, 820, 762 cm^{-1}; MS (CI, CH_5^+) *m/z*: 376 $[M+H]^+$; HRMS-EI$^+$ *m/z* $[M]^+$ calcd for $C_{25}H_{29}NO_2$: 375.2198, found: 375.2192.

1-{4-[2-(2-Chloro-4-fluorophenyl)phenyl]but-3-yn-1-yl}piperidine-3-carboxylic acid (17i):

R_f≈0.1 (CH_2Cl_2/CH_3OH 9:1). ^{1}H NMR (500 MHz, 1N NaOD/CH_3OD 1:2, 60 °C): δ=1.27 (qd, *J*=12.8, 3.9 Hz, 1H, $NCH_2CHC\mathit{H}_{ax}H_{eq}$), 1.48 (qt, *J*=13.0, 3.4 Hz, 1H, $NCH_2C\mathit{H}_{ax}H_{eq}CH_2CH$), 1.65 ($d_{br}$, *J*=13.5 Hz, 1H,

$NCH_2CH_{ax}H_{eq}CH_2CH$), 1.84 (td, *J*=12.0, 2.3 Hz, 1H, $NCH_{ax}H_{eq}CH_2CH_2CH$), 1.92 (d_{br}, *J*=10.9 Hz, 1H, $NCH_2CHCH_{ax}H_{eq}$), 1.99 (t, *J*=11.3 Hz, 1H, $NCH_{ax}H_{eq}CH$), 2.26–2.47 (m, 5H, NCH_2CH_{ax}, $NCH_2CH_2C{\equiv}C$, $NCH_2CH_2C{\equiv}C$), 2.75 (d_{br}, *J*=10.6 Hz, 1H, $NCH_{ax}H_{eq}CH_2CH_2CH$), 2.96 (d_{br}, *J*=10.8 Hz, 1H, $NCH_{ax}H_{eq}CH$), 7.14 (td, *J*=8.4, 2.6 Hz, 1H, FCCHCH), 7.16–7.20 (m, 1H, C≡CCCCH), 7.25–7.31 (m, 2H, FCCHCH, FCCHCCl), 7.32–7.39 (m, 2H, C≡CCCHCH, C≡CCCCHCH), 7.42–7.46 (m, 1H, C≡CCCH) ppm; ^{13}C NMR (126 MHz, 1N NaOD/CH_3OD 1:2, 60 °C): δ=17.44 ($NCH_2CH_2C{\equiv}C$), 25.49 ($NCH_2CH_2CH_2CH$), 28.95 (NCH_2CHCH_2), 45.99 (NCH_2CH), 53.98 ($NCH_2CH_2CH_2CH$), 57.34 (NCH_2CH), 58.09 ($NCH_2CH_2C{\equiv}C$), 81.13 (C≡CCCH), 92.70 (C≡CCCH), 114.78 (d, $^2J_{CF}$=21.2 Hz, FCCHCH), 117.32 (d, $^2J_{CF}$=25.0 Hz, FCCHCCl), 124.44 ($CH_2C{\equiv}CC$), 128.83 ($CH_2C{\equiv}CCCHCH$), 129.08 ($CH_2C{\equiv}CCCHCHCH$), 130.63 ($CH_2C{\equiv}CCCCH$), 132.80 ($CH_2C{\equiv}CCCH$), 133.72 (d, $^3J_{CF}$=8.9 Hz, FCCHCH), 135.00 (d, $^3J_{CF}$=10.5 Hz, ClC), 137.38 (d, $^4J_{CF}$=3.6 Hz, ClCC), 142.04 ($CH_2C{\equiv}CCC$), 163.12 (d, $^1J_{CF}$=248.2 Hz, FC), 183.00 (C=O) ppm; IR (KBr): $\tilde{\nu}$=3434, 3061, 2941, 2858, 2231, 1710, 1604, 1503, 1473, 1442, 1388, 1256, 1201, 1062, 1041, 1006, 897, 858, 821, 762 cm^{-1}; MS (EI, 70 eV) *m/z*: 385 $[M]^+$; HRMS-EI$^+$ *m/z* $[M]^+$ calcd for $C_{22}H_{21}ClFNO_2$: 385.1249, found: 385.1219.

1-{5-[2-(2-Chloro-4-fluorophenyl)phenyl]pent-4-yn-1-yl}piperidine-3-carboxylic acid (18i):

R_f≈0.1 (CH_2Cl_2/CH_3OH 9:1). ^{1}H NMR (500 MHz, 1N NaOD/CH_3OD 1:2, 60 °C): δ=1.30 (qd, *J*=13.0, 4.1 Hz, 1H, $NCH_2CHCH_{ax}H_{eq}$), 1.46–1.58 (m, 3H, $NCH_2CHCH_{ax}H_{eq}$, $NCH_2CH_2CH_2C{\equiv}C$), 1.64–1.71 (m, 1H, $NCH_2CH_{ax}H_{eq}CH_2CH$), 1.81 (td, *J*=11.6, 2.9 Hz, 1H, $NCH_{ax}H_{eq}CH_2CH_2CH$), 1.88–1.98 (m, 2H, $NCH_{ax}H_{eq}CH$, $NCH_2CHCH_{ax}H_{eq}$), 2.14–2.27 (m, 4H, $NCH_2CH_2CH_2C{\equiv}C$, $NCH_2CH_2CH_2C{\equiv}C$), 2.32 (tt, *J*=11.9, 3.7 Hz, 1H, NCH_2CH_{ax}), 2.75 (d_{br}, *J*=11.7 Hz, 1H, $NCH_{ax}H_{eq}CH_2CH_2CH$), 2.99 (d_{br}, *J*=10.1 Hz, 1H, $NCH_{ax}H_{eq}CH$), 7.12–7.19 (m, 2H, FCCHCH, C≡CCCCH), 7.25–7.32 (m, 2H, FCCHCH, FCCHCCl), 7.32–7.39 (m, 2H, C≡CCCHCH, C≡CCCCHCH), 7.41–7.45 (m, 1H, C≡CCCH) ppm; ^{13}C NMR (126 MHz, 1N NaOD/CH_3OD 1:2, 60 °C): δ=18.06 ($NCH_2CH_2CH_2C{\equiv}C$), 25.52 ($NCH_2CH_2CH_2CH$), 25.87 ($NCH_2CH_2CH_2C{\equiv}C$), 29.12 (NCH_2CHCH_2), 46.02 (NCH_2CH), 54.58 ($NCH_2CH_2CH_2CH$), 57.76 (NCH_2CH), 58.75 ($NCH_2CH_2CH_2C{\equiv}C$), 80.66 ($CH_2C{\equiv}C$), 93.99 ($CH_2C{\equiv}C$), 114.90 (d, $^2J_{CF}$=21.3 Hz, FCCHCH), 117.45 (d, $^2J_{CF}$=25.0 Hz, FCCHCCl), 124.63 ($CH_2C{\equiv}CC$), 128.72 ($CH_2C{\equiv}CCCHCH$), 129.07 ($CH_2C{\equiv}CCCHCHCH$), 130.65 ($CH_2C{\equiv}CCCCH$), 132.89 ($CH_2C{\equiv}CCCH$), 133.67 (d, $^3J_{CF}$=8.6 Hz, FCCHCH), 135.00 (d, $^3J_{CF}$=10.5 Hz, ClC), 137.49 (d, $^4J_{CF}$=3.6 Hz, ClCC), 141.94 ($CH_2C{\equiv}CCC$), 163.08 (d, $^1J_{CF}$=248.4 Hz, FC), 183.16 (C=O) ppm; IR (KBr): $\tilde{\nu}$=3431, 3060, 2946, 2864, 2229, 1709, 1604, 1503, 1473, 1442, 1389, 1256, 1201, 1148, 1061, 1042, 1005, 896, 858, 820, 762 cm^{-1}; MS (EI, 70 eV) *m/z*: 399 $[M]^+$; HRMS-EI$^+$ *m/z* $[M]^+$ calcd for $C_{23}H_{23}ClFNO_2$: 399.1491, found: 399.1404.

1-{4-[2-(4-Chloro-2-methylphenyl)phenyl]but-3-yn-1-yl}piperidine-3-carboxylic acid (17k):

R_f≈0.1 (CH_2Cl_2/CH_3OH 9:1). ^{1}H NMR (500 MHz, 1N NaOD/CH_3OD 1:2, 60 °C): δ=1.30 (qd, *J*=12.9, 4.1 Hz, 1H, $NCH_2CHCH_{ax}H_{eq}$), 1.50 (qt, *J*=12.4, 3.7 Hz, 1H, $NCH_2CH_{ax}H_{eq}CH_2CH$), 1.67 (dp, *J*=13.4, 2.9 Hz, 1H, $NCH_2CH_{ax}H_{eq}CH_2CH$), 1.82 (t_{br}, *J*=11.1 Hz, 1H, $NCH_{ax}H_{eq}CH_2CH_2CH$), 1.91–2.03 (m, 2H, $NCH_2CHCH_{ax}H_{eq}$, $NCH_{ax}H_{eq}CH$), 2.08 (s, 3H, H_3CC), 2.26–2.50 (m, 5H, NCH_2CH_{ax}, $NCH_2CH_2C{\equiv}C$, $NCH_2CH_2C{\equiv}C$), 2.73 (d_{br}, *J*=11.2 Hz, 1H, $NCH_{ax}H_{eq}CH_2CH_2CH$), 2.97 (d_{br}, *J*=10.9 Hz, 1H, $NCH_{ax}H_{eq}CH$), 7.04 (d, *J*=8.1 Hz, 1H, ClCCHCH), 7.11–7.15 (m, 1H, C≡CCCCH), 7.20 (dd, *J*=8.2, 2.4 Hz, 1H, ClCHCH), 7.27 (d, *J*=2.4 Hz, 1H, ClCCHC), 7.31–7.40 (m, 2H, C≡CCCHCH, C≡CCCCHCH), 7.45 (dd, *J*=7.6, 1.6 Hz, 1H, C≡CCCH) ppm; ^{13}C NMR (126 MHz, 1N NaOD/CH_3OD 1:2, 60 °C): δ=17.50 ($NCH_2CH_2C{\equiv}C$), 20.06 (H_3CC), 25.49 ($NCH_2CH_2CH_2CH$), 28.95 (NCH_2CHCH_2), 45.94 (NCH_2CH), 54.01 ($NCH_2CH_2CH_2CH$), 57.33 (NCH_2CH), 58.06 ($NCH_2CH_2C{\equiv}C$), 81.39 (C≡CCCH), 92.46 (C≡CCCH), 124.05 ($CH_2C{\equiv}CC$), 126.36 (ClCCHCH), 128.54 ($CH_2C{\equiv}CCCHCH$), 129.00 ($CH_2C{\equiv}CCCHCHCH$), 130.22 ($CH_2C{\equiv}CCCCH$), 130.37 (ClCCHC), 131.94 (ClCCHCH), 132.79 ($CH_2C{\equiv}CCCH$), 133.85 (ClC), 139.48 (H_3CCC), 140.83 (H_3CCC), 144.21 ($CH_2C{\equiv}CCC$), 182.98 (C=O) ppm; IR (KBr): $\tilde{\nu}$=2425, 3059, 2926, 2857, 2228, 1711, 1592, 1472, 1442, 1391, 1195, 1097, 1006, 870, 822, 760 cm^{-1}; MS (EI, 70 eV) *m/z*: 381 $[M]^+$; HRMS-EI$^+$ *m/z* $[M]^+$ calcd for $C_{23}H_{24}ClNO_2$: 381.1496, found: 381.1493.

1-{5-[2-(4-Chloro-2-methylphenyl)phenyl]pent-4-yn-1-yl}piperidine-3-carboxylic acid (18k):

R_f≈0.1 (CH_2Cl_2/CH_3OH 9:1). ^{1}H NMR (500 MHz, 1N NaOD/CH_3OD 1:2, 60 °C): δ=1.34 (qd, J=12.7, 4.0 Hz, 1H, $NCH_2CHCH_{ax}H_{eq}$), 1.45–1.61 (m, 3H, $NCH_2CH_{ax}H_{eq}CH_2CH$, $NCH_2CH_2CH_2C{\equiv}C$), 1.71 (dp, J=13.4, 3.0 Hz, 1H, $NCH_2CH_{ax}H_{eq}CH_2CH$), 1.81 (td, J=11.7, 2.9 Hz, 1H, $NCH_{ax}H_{eq}CH_2CH_2CH$), 1.88–2.01 (m, 2H, $NCH_2CHCH_{ax}H_{eq}$, $NCH_{ax}H_{eq}CH$), 2.09 (s, 3H, H_3CC), 2.14 (t, J=8.1 Hz, 2H, $NCH_2CH_2CH_2C{\equiv}C$), 2.17–2.30 (m, 2H, $NCH_2CH_2CH_2C{\equiv}C$), 2.34 (tt, J=11.9, 3.7 Hz, 1H, NCH_2CH_{ax}), 2.73 (d_{br}, J=10.7 Hz, 1H, $NCH_{ax}H_{eq}CH_2CH_2CH$), 3.01 (d_{br}, J=10.5 Hz, 1H, $NCH_{ax}H_{eq}CH$), 7.04 (d, J=8.1 Hz, 1H, $ClCCHCH$), 7.10 (dd, J=7.5, 1.5 Hz, 1H, $C{\equiv}CCCCH$), 7.20 (d, J=7.8 Hz, 1H, $ClCCHCH$), 7.28 (s_{br}, 1H, $ClCCHC$), 7.30–7.38 (m, 2H, $C{\equiv}CCCHCH$, $C{\equiv}CCCCHCH$), 7.44 (dd, J=7.5, 1.7 Hz, 1H, $C{\equiv}CCCH$) ppm; ^{13}C NMR (126 MHz, 1N NaOD/CH_3OD 1:2, 60 °C): δ=18.07 ($NCH_2CH_2CH_2C{\equiv}C$), 20.11 (H_3CC), 25.58 ($NCH_2CH_2CH_2CH$), 25.85 ($NCH_2CH_2CH_2C{\equiv}C$), 29.09 (NCH_2CHCH_2), 45.97 (NCH_2CH), 54.57 ($NCH_2CH_2CH_2CH$), 57.68 (NCH_2CH), 58.69 ($NCH_2CH_2CH_2C{\equiv}C$), 80.93 ($CH_2C{\equiv}C$), 93.63 ($CH_2C{\equiv}C$), 124.18 ($CH_2C{\equiv}CC$), 126.45 ($ClCCHCH$), 128.51 ($CH_2C{\equiv}CCCHCH$), 128.88 ($CH_2C{\equiv}CCCHCHCH$), 130.31 ($CH_2C{\equiv}CCCCH$), 130.50 ($ClCCHC$), 131.94 ($ClCCHCH$), 132.95 ($CH_2C{\equiv}CCCH$), 133.86 (CCl), 139.46 (H_3CC), 140.89 (H_3CCC), 144.01 ($CH_2C{\equiv}CCC$), 183.14 (C=O) ppm; IR (KBr): $\tilde{\nu}$=3424, 3056, 3020, 2945, 2862, 2228, 1711, 1591, 1473, 1440, 1391, 1195, 1095, 1005, 870, 821, 763 cm^{-1}; MS (EI, 70 eV) *m/z*: 395 $[M]^+$; HRMS-EI$^+$ *m/z* $[M]^+$ calcd for $C_{24}H_{26}ClNO_2$: 395.1652, found: 395.1660.

1-{4-[2-(4-Fluoro-2-methylphenyl)phenyl]but-3-yn-1-yl}piperidine-3-carboxylic acid (17l):

R_f≈0.1 (CH_2Cl_2/CH_3OH 9:1). ^{1}H NMR (500 MHz, 1N NaOD/CH_3OD 1:2, 60 °C): δ=1.26 (qd, J=12.8, 3.9 Hz, 1H, $NCH_2CHCH_{ax}H_{eq}$), 1.47 (qt, J=13.1, 3.4 Hz, 1H, $NCH_2CH_{ax}H_{eq}CH_2CH$), 1.63 (d_{br}, J=13.5 Hz, 1H, $NCH_2CH_{ax}H_{eq}CH_2CH$), 1.80 (t_{br}, J=11.2 Hz, 1H, $NCH_{ax}H_{eq}CH_2CH_2CH$), 1.92 (d_{br}, J=13.6 Hz, 1H, $NCH_2CHCH_{ax}H_{eq}$), 1.97 (t, J=11.4 Hz, 1H, $NCH_{ax}H_{eq}CH$), 2.06 (s, 3H, H_3CC), 2.25–2.43 (m, 5H, NCH_2CH_{ax}, $NCH_2CH_2C{\equiv}C$, $NCH_2CH_2C{\equiv}C$), 2.71 (d_{br}, J=11.0 Hz, 1H, $NCH_{ax}H_{eq}CH_2CH_2CH$), 2.94 (d_{br}, J=10.8 Hz, 1H, $NCH_{ax}H_{eq}CH$), 6.91 (td, J=8.5, 2.6 Hz, 1H, $FCCHCH$), 6.98 (dd, J=10.0, 2.4 Hz, 1H, $FCCHC$), 7.04 (dd, J=8.3, 6.1 Hz, 1H, $FCCHCH$), 7.10 (dd, J=7.4, 1.1 Hz, 1H, $C{\equiv}CCCCH$), 7.30 (td, J=7.5, 1.5 Hz, 1H, $C{\equiv}CCCHCH$), 7.34 (td, J=7.5, 1.6 Hz, 1H, $C{\equiv}CCCCHCH$), 7.42 (dd, J=7.5, 1.3 Hz, 1H, $C{\equiv}CCCH$) ppm; ^{13}C NMR (126 MHz, 1N NaOD/CH_3OD 1:2, 60 °C): δ=17.41 ($NCH_2CH_2C{\equiv}C$), 20.25 (d, $^4J_{CF}$=1.8 Hz, H_3CC), 25.45 ($NCH_2CH_2CH_2CH$), 28.91 (NCH_2CHCH_2), 45.95 (NCH_2CH), 53.91 ($NCH_2CH_2CH_2CH$), 57.28 (NCH_2CH), 58.05 ($NCH_2CH_2C{\equiv}C$), 81.50 ($C{\equiv}CCH$), 92.25 ($C{\equiv}CCH$), 112.93 (d, $^2J_{CF}$=20.9 Hz, $FCCHCH$), 116.98 (d, $^2J_{CF}$=21.3 Hz, $FCCHC$), 124.22 ($CH_2C{\equiv}CC$), 128.40 ($CH_2C{\equiv}CCCHCH$), 128.97 ($CH_2C{\equiv}CCCHCHCH$), 130.49 ($CH_2C{\equiv}CCCCH$), 132.07 (d, $^3J_{CF}$=8.6 Hz, $FCCHCH$), 132.80 ($CH_2C{\equiv}CCCH$), 138.25 (d, $^4J_{CF}$=3.0 Hz, $H3CCC$), 139.86 (d, $^3J_{CF}$=7.9 Hz, H_3CC), 144.41 ($CH_2C{\equiv}CCC$), 163.21 (d, $^1J_{CF}$=243.6 Hz, FC), 183.03 (C=O) ppm; IR (KBr): $\tilde{\nu}$=3438, 3057, 3024, 2942, 2858, 2809, 2230, 1712, 1616, 1587, 1504, 1476, 1443, 1395, 1271, 1220, 1151, 1099, 1005, 944, 862, 818, 762 cm^{-1}; MS (EI, 70 eV) *m/z*: 365 $[M]^+$; HRMS-EI$^+$ *m/z* $[M]^+$ calcd for $C_{23}H_{24}FNO_2$: 365.1791, found: 365.1784.

1-{5-[2-(4-Fluoro-2-methylphenyl)phenyl]pent-4-yn-1-yl}piperidine-3-carboxylic acid (18l):

R_f≈0.1 (CH_2Cl_2/CH_3OH 9:1). ^{1}H NMR (500 MHz, 1N NaOD/CH_3OD 1:2, 60 °C): δ=1.30 (qd, J=12.8, 4.0 Hz, 1H, $NCH_2CHCH_{ax}H_{eq}$), 1.45–1.58 (m, 3H, $NCH_2CH_{ax}H_{eq}CH_2CH$, $NCH_2CH_2CH_2C{\equiv}C$), 1.67 (d_{br}, J=13.4 Hz, 1H, $NCH_2CH_{ax}H_{eq}CH_2CH$), 1.78 (td, J=12.1, 2.5 Hz, 1H, $NCH_{ax}H_{eq}CH_2CH_2CH$), 1.86–1.97 (m, 2H, $NCH_2CHCH_{ax}H_{eq}$, $NCH_{ax}H_{eq}CH$), 2.07 (s, 3H, H_3CC), 2.13 (t, J=8.0 Hz, 2H, $NCH_2CH_2CH_2C{\equiv}C$), 2.17–2.26 (m, 2H, $NCH_2CH_2CH_2C{\equiv}C$), 2.31 (tt, J=11.9, 3.6 Hz, 1H, NCH_2CH_{ax}), 2.72 (d_{br}, J=11.0 Hz, 1H, $NCH_{ax}H_{eq}CH_2CH_2CH$), 2.98 (d_{br}, J=10.6 Hz, 1H, $NCH_{ax}H_{eq}CH$), 6.92 (t_{br}, J=8.2 Hz, 1H, $FCCHCH$), 6.99 (d_{br}, J=9.6 Hz, 1H, $FCCHC$), 7.04 (dd, J=8.3, 6.1 Hz, 1H, $FCCHCH$), 7.09 (dd, J=7.5, 1.5 Hz, 1H, $C{\equiv}CCCCH$), 7.29 (td, J=7.5, 1.6 Hz, 1H, $C{\equiv}CCCHCH$), 7.33 (td, J=7.5, 1.7 Hz, 1H, $C{\equiv}CCCCHCH$), 7.41 (dd, J=7.5, 1.6 Hz, 1H, $C{\equiv}CCCH$) ppm; ^{13}C NMR (126 MHz, 1N NaOD/CH_3OD 1:2, 60 °C): δ=18.05 ($NCH_2CH_2CH_2C{\equiv}C$), 20.30 (d, $^4J_{CF}$=1.4 Hz, H_3CC), 25.50 ($NCH_2CH_2CH_2CH$), 25.86 ($NCH_2CH_2CH_2C{\equiv}C$), 29.10 (NCH_2CHCH_2), 45.98 (NCH_2CH), 54.52 ($NCH_2CH_2CH_2CH$), 57.69 (NCH_2CH), 58.67 ($NCH_2CH_2CH_2C{\equiv}C$), 81.03 ($CH_2C{\equiv}C$), 93.49 ($CH_2C{\equiv}C$), 113.06 (d, $^2J_{CF}$=21.1 Hz, $FCCHCH$), 117.15 (d, $^2J_{CF}$=20.9 Hz, $FCCHC$), 124.40 ($CH_2C{\equiv}CC$), 128.37 ($CH_2C{\equiv}CCCHCH$), 128.84 ($CH_2C{\equiv}CCCHCHCH$), 130.53 ($CH_2C{\equiv}CCCCH$), 132.06 (d, $^3J_{CF}$=8.4 Hz, $FCCHCH$), 132.91 (d, 1C, $CH_2C{\equiv}CCCH$), 138.37 (d, $^4J_{CF}$=3.0 Hz, H_3CCC), 139.85 (d, $^3J_{CF}$=7.9

Hz, H_3CC), 144.29 , (s, 1C, $CH_2C{\equiv}CCC$), 163.17 (s, ^1J=243.5 Hz, FC), 183.17 (C=O) ppm; IR (KBr): $\tilde{\nu}$=3386, 3059, 2949, 2864, 2230, 1710, 1587, 1503, 1476, 1442, 1389, 1271, 1220, 1151, 1005, 944, 863, 817, 761 cm^{-1}; MS (EI, 70 eV): *m/z*: 379 $[M]^+$; HRMS-EI$^+$ *m/z* $[M]^+$ calcd for $C_{24}H_{26}FNO_2$: 379.1948, found: 365.1948.

(*R*)-Ethyl 1-but-3-yn-1-ylpiperidine-3-carboxylate ((*R*)-7):

R_f≈0.5 (hexane/ethyl acetate 1:1). $[\alpha]^{20}_D$=-57.5 (c=1.0 in CH_2Cl_2). ^{1}H NMR (500 MHz, $CDCl_3$): δ=1.22 (t, *J*=7.1 Hz, 3H, OCH_2CH_3), 1.40 (qd, *J*=11.8, 3.9 Hz, 1H, $NCH_2CHCH_{ax}H_{eq}$), 1.48–1.60 (m, 1H, $NCH_2CH_{ax}H_{eq}CH_2CH$), 1.70 (dp, *J*=10.9, 3.8 Hz, 1H, $NCH_2CH_{ax}H_{eq}CH_2CH$), 1.87–1.94 (m, 1H, $NCH_2CHCH_{ax}H_{eq}$), 1.95 (t, *J*=2.7 Hz, 1H, C≡CH), 2.04 (td, *J*=11.0, 2.8 Hz, 1H, $NCH_{ax}H_{eq}CH_2CH_2CH$), 2.19 (t, *J*=10.6 Hz, 1H, $NCH_{ax}H_{eq}CH$), 2.32–2.38 (m, 2H, $NCH_2CH_2C{\equiv}CH$), 2.52 (tt, *J*=10.8, 3.8 Hz, 1H, NCH_2CH_{ax}), 2.58 (t, *J*=7.9 Hz, 2H, $NCH_2CH_2C{\equiv}C$), 2.75 (d, *J*=11.1 Hz, 1H, $NCH_{ax}H_{eq}CH_2CH_2CH$), 2.95 (d, *J*=11.1 Hz, 1H, $NCH_{ax}H_{eq}CH$), 4.10 (q, *J*=7.1 Hz, 2H, OCH_2CH_3) ppm; ^{13}C NMR (126 MHz, $CDCl_3$): δ=14.30 (OCH_2CH_3), 16.74 ($NCH_2CH_2C{\equiv}C$), 24.60 ($NCH_2CH_2CH_2CH$), 26.92 (NCH_2CHCH_2), 41.86 (NCH_2CH), 53.43 ($NCH_2CH_2CH_2CH_2CH$), 55.12 (NCH_2CH), 57.34 ($NCH_2CH_2C{\equiv}CH$), 60.45 (OCH_2CH_3), 69.10 (C≡CH), 82.85 (C≡CH), 174.20 (C=O) ppm; IR (KBr): $\tilde{\nu}$=3298, 2944, 2812, 2118, 1731, 1371, 1310, 1180, 1153, 1032 cm^{-1}; MS (CI, CH_5^+) *m/z*: 210 $[M+H]^+$; HRMS-EI$^+$ *m/z* $[M]^+$ calcd for $C_{12}H_{19}NO_2$: 209.1416; found: 209.1430.

(*R*)-Ethyl 1-[4-(2-bromophenyl)but-3-yn-1-yl]piperidine-3-carboxylate ((*R*)-13):

R_f≈0.3 (hexane/ethyl acetate 8:2). $[\alpha]^{20}_D$=-34.0 (c=1.0 in CH_2Cl_2). ^{1}H NMR (500 MHz, $CDCl_3$): δ=1.25 (t, *J*=7.2 Hz, 3H, OCH_2CH_3), 1.46 (qd, *J*=11.8, 4.0 Hz, 1H, $NCH_2CHCH_{ax}H_{eq}$), 1.52–1.65 (m, 1H, $NCH_2CH_{ax}H_{eq}CH_2CH$), 1.74 (dp, *J*=10.9, 3.9 Hz, 1H, $NCH_2CH_{ax}H_{eq}CH_2CH$), 1.95 (dq, *J*=12.8, 4.0 Hz, 1H, $NCH_2CHCH_{ax}H_{eq}$), 2.14 (td, *J*=11.0, 3.1 Hz, 1H, $NCH_{ax}H_{eq}CH_2CH_2CH$), 2.30 (t, *J*=10.6 Hz, 1H, $NCH_{ax}H_{eq}CH$), 2.57 (tt, *J*=10.7, 3.9 Hz, 1H, NCH_2CH_{ax}), 2.62–2.69 (m, 2H, $NCH_2CH_2C{\equiv}C$), 2.71–2.78 (m, 2H, $NCH_2CH_2C{\equiv}C$), 2.83 (d_{br}, *J*=11.1 Hz, 1H, $NCH_{ax}H_{eq}CH_2CH_2CH$), 3.06 (d_{br}, *J*=11.1 Hz, 1H, $NCH_{ax}H_{eq}CH$), 4.13 (q, *J*=7.2 Hz, 2H, OCH_2CH_3), 7.11 (td, *J*=7.7, 1.8 Hz, 1H, BrCCHCH), 7.22 (td, *J*=7.6, 1.4 Hz, 1H, BrCCCHCH), 7.42 (dd, *J*=7.7, 1.8 Hz, 1H, C≡CCCH), 7.55 (dd, *J*=8.1, 1.4 Hz, 1 H, BrCCH) ppm; ^{13}C NMR (125 MHz, $CDCl_3$): δ=14.18 (OCH_2CH_3), 17.89 ($NCH_2CH_2C{\equiv}C$), 24.59 ($NCH_2CH_2CH_2CH$), 26.80 (NCH_2CHCH_2), 41.88 (NCH_2CH), 53.35 ($NCH_2CH_2CH_2CH$), 55.09 (NCH_2CH), 57.22 ($NCH_2CH_2C{\equiv}C$), 60.28 (OCH_2CH_3), 80.01 (C≡CCCH), 93.51 (C≡CCCH), 125.38 (CBr), 125.71 (BrCC), 126.84 (BrCCCHCH), 128.75 (BrCCHCH), 132.21 (BrCCH), 133.26 (BrCCCH), 174.06 (C=O) ppm; IR (KBr): $\tilde{\nu}$=3436, 3064, 2943, 2854, 2810, 2231, 1730, 1587, 1557, 1469, 1434, 1370, 1308, 1180, 1153, 1101, 1052, 1026, 862, 754 cm^{-1}; MS (CI, CH_5^+) *m/z*: 364 $[M+H]^+$; HRMS-EI$^+$ *m/z* $[M]^+$ calcd for $C_{18}H_{22}BrNO_2$: 363.0834, found: 363.0835.

(*R*)-Ethyl 1-{4-[2-(2-methylphenyl)phenyl]but-3-yn-1-yl}piperidine-3-carboxylate ((*R*)-15d):

R_f≈0.3 (hexane/ethyl acetate 8:2). $[\alpha]^{20}_D$=-32.0 (c=1.0 in CH_2Cl_2). ^{1}H NMR (400 MHz, $CDCl_3$): δ=1.24 (t, *J*=7.1 Hz, 3H, OCH_2CH_3), 1.39 (qd, *J*=11.7, 3.6 Hz, 1H, $NCH_2CHCH_{ax}H_{eq}$), 1.45–1.56 (m, 1H, $NCH_2CH_{ax}H_{eq}CH_2CH$), 1.67 (dp, *J*=13.1/3.6 Hz, 1H, $NCH_2CH_{ax}H_{eq}CH_2CH$), 1.86–1.98 (m, 2H, $NCH_2CHCH_{ax}H_{eq}$, $NCH_{ax}H_{eq}CH_2CH_2CH$), 2.11–2.18 (m, 4H, $NCH_{ax}H_{eq}CH$, H_3CC), 2.31–2.40 (m, 4H, $NCH_2CH_2C{\equiv}C$, $NCH_2CH_2C{\equiv}C$), 2.49 (tt, *J*=10.4, 3.8 Hz, 1H, NCH_2CH_{ax}), 2.63 (dt, *J*=11.2, 3.8 Hz, 1H, $NCH_{ax}H_{eq}CH_2CH_2CH$), 2.87 (dd, *J*=11.0, 3.2 Hz, 1H, $NCH_{ax}H_{eq}CH$), 4.12 (q, *J*=7.1 Hz, 2H, OCH_2CH_3), 7.14–7.33 (m, 7H, H_{Ar}), 7.44–7.47 (m, 1H, C≡CCCH) ppm; ^{13}C NMR (101 MHz, $CDCl_3$): δ=14.17 (OCH_2CH_3), 17.46 ($NCH_2CH_2C{\equiv}C$), 19.94 (H_3CC), 24.52 ($NCH_2CH_2CH_2CH$), 26.79 (NCH_2CHCH_2), 41.80 (NCH_2CH), 53.05 ($NCH_2CH_2CH_2CH$), 54.89 (NCH_2CH), 57.13 ($NCH_2CH_2C{\equiv}C$), 60.24 (OCH_2CH_3), 80.45 (C≡CCCH), 91.28 (C≡CCCH), 123.27 ($CH_2C{\equiv}CC$), 125.15 ($CH_2C{\equiv}CCCCH$), 126.78 ($CH_2C{\equiv}CCCHCH$), 127.29 ($H_3CCCHCH$), 127.39 ($CH_2C{\equiv}CCCHCHCH$), 129.33 ($H_3CCCCHCH$), 129.54 (H_3CCCCH, H_3CCCH), 131.77 ($CH_2C{\equiv}CCCH$), 136.10 (H_3CC), 140.95 (H_3CCCC), 144.40 ($CH_2C{\equiv}CCC$), 174.06 (C=O) ppm; IR (KBr): $\tilde{\nu}$=3375, 3060, 2940, 2853, 2810, 2228, 1730, 1474, 1443, 1370, 1307, 1179, 1152, 1133, 1101, 1032, 758 cm^{-1}; MS (ESI$^+$) *m/z*: 376 $[M+H]^+$; HRMS-ESI$^+$ *m/z* $[M+H]^+$ calcd for $C_{25}H_{30}NO_2$: 376.2277, found: 376.2271.

(*R*)-Ethyl 1-{4-[2-(2,4-dichlorophenyl)phenyl]but-3-yn-1-yl}piperidine-3-carboxylate ((*R*)-15f):

R_f≈0.3 (hexane/ethyl acetate 8:2). $[\alpha]^{20}_D$=-27.7 (c=1.0 in CH_2Cl_2). ^{1}H NMR (500 MHz, $CDCl_3$): δ=1.24 (t, *J*=7.1 Hz, 3H, OCH_2CH_3), 1.42 (qd, *J*=12.0, 3.8 Hz, 1H, $NCH_2CHCH_{ax}H_{eq}$), 1.47–1.58 (m, 1H, $NCH_2CH_{ax}H_{eq}CH_2CH$), 1.69 (dp, *J*=10.8, 3.8 Hz, 1H, $NCH_2CH_{ax}H_{eq}CH_2CH$), 1.88–1.95 (m, 1H, $NCH_2CHCH_{ax}H_{eq}$), 1.99 (td, *J*=11.0, 2.8 Hz, 1H, $NCH_{ax}H_{eq}CH_2CH_2CH$), 2.18 (t, *J*=10.6 Hz, 1H, $NCH_{ax}H_{eq}CH$), 2.36–2.45 (m, 4H, $NCH_2CH_2C{\equiv}C$, $NCH_2CH_2C{\equiv}C$), 2.51 (tt, *J*=10.4, 3.7 Hz, 1H, NCH_2CH_{ax}), 2.67 (d_{br}, *J*=11.2 Hz, 1H, $NCH_{ax}H_{eq}CH_2CH_2CH$), 2.90 (d_{br}, *J*=10.0 Hz, 1H, $NCH_{ax}H_{eq}CH$), 4.12 (q, *J*=7.1 Hz, 2H, OCH_2CH_3), 7.21–7.24 (m, 1H, C≡CCCC*H*), 7.25–7.30 (m, 2H, ClCCHC*H*, ClCC*H*CH), 7.30–7.35 (m, 2H, C≡CCCHC*H*, C≡CCCCHC*H*), 7.46–7.51 (m, 2H, ClCC*H*CCCl, C≡CCC*H*) ppm; ^{13}C NMR (101 MHz, $CDCl_3$): δ = 14.19 (OCH_2CH_3), 17.60 ($NCH_2CH_2C{\equiv}C$), 24.53 ($NCH_2CH_2CH_2CH$), 26.79 (NCH_2CHCH_2), 41.81 (NCH_2CH), 53.18 ($NCH_2CH_2CH_2CH$), 54.95 (NCH_2CH), 57.13 ($NCH_2CH_2C{\equiv}C$), 60.29 (OCH_2CH_3), 79.85 (C≡CCCH), 92.25 (C≡CCCH), 123.44 ($CH_2C{\equiv}CC$), 126.50 (ClCCHCH), 127.37 (ClCCCCHCH), 127.86 ($CH_2C{\equiv}CCCHCH$), 129.08 (ClCCHCHCl), 129.48 (ClCCCCCH), 132.00 ($CH_2C{\equiv}CCCH$), 132.32 (ClCCHCH), 133.74 (CCl), 134.18 (CCl), 138.41 (ClCCHCHC), 140.62 (ClCCC), 174.03 (C=O) ppm; IR (KBr): $\tilde{\nu}$=3385, 3061, 2941, 2854, 2809, 2229, 1730, 1586, 1466, 1440, 1372, 1307, 1180, 1152, 1101, 1032, 1004, 863, 813, 760 cm^{-1}; MS (ESI$^+$) *m/z*: 430 $[M+H]^+$; HRMS-ESI$^+$ *m/z* $[M+H]^+$ calcd for $C_{24}H_{26}Cl_2NO_2$: 430.1340, found: 430.1338.

(*R*)-Ethyl 1-{4-[2-(2,4-difluorophenyl)phenyl]but-3-yn-1-yl}piperidine-3-carboxylate ((*R*)-15g):

R_f≈0.3 (hexane/ethyl acetate 8:2). $[\alpha]^{20}_D$=-31.5 (c=1.0 in CH_2Cl_2). ^{1}H NMR (400 MHz, $CDCl_3$): δ=1.24 (t, *J*=7.1 Hz, 3H, OCH_2CH_3), 1.42 (qd, *J*=12.0/3.8, 1H, $NCH_2CHCH_{ax}H_{eq}$), 1.47–1.59 (m, 1H, $NCH_2CH_{ax}H_{eq}CH_2CH$), 1.70 (dp, *J*=14.0, 3.7 Hz, 1H, $NCH_2CH_{ax}H_{eq}CH_2CH$), 1.92 (dq, *J*=12.6, 3.8, 1H, $NCH_2CHCH_{ax}H_{eq}$), 2.02 (td, *J*=11.0, 2.9 Hz, 1H, $NCH_{ax}H_{eq}CH_2CH_2CH$), 2.20 (t, *J*=10.7 Hz, 1H, $NCH_{ax}H_{eq}CH$), 2.40–2.56 (m, 5H, $NCH_2CH_2C{\equiv}C$, $NCH_2CH_2C{\equiv}C$, NCH_2CH_{ax}), 2.70 (dt, *J*=11.6, 4.2 Hz, 1H, $NCH_{ax}H_{eq}CH_2CH_2CH$), 2.93 (dd, *J*=11.1, 3.8 Hz, 1H, $NCH_{ax}H_{eq}CH$), 4.12 (q, *J*=7.1 Hz, 2H, OCH_2CH_3), 6.85–6.96 (m, 2H, FCC*H*CF, FCC*H*CH), 7.27–7.42 (m, 4H, C≡CCCC*H*, C≡CCCCHC*H*, C≡CCCHC*H*, FCCC*H*), 7.48–7.52 (m, 1H, C≡CCC*H*) ppm; ^{13}C NMR (101 MHz, $CDCl_3$): **δ**=14.17 (OCH_2CH_3), 17.58 ($NCH_2CH_2C{\equiv}C$), 24.54 ($NCH_2CH_2CH_2CH$), 26.80 (NCH_2CHCH_2), 41.83 (NCH_2CH), 53.20 ($NCH_2CH_2CH_2CH$), 54.96 (NCH_2CH), 57.18 ($NCH_2CH_2C{\equiv}C$), 60.29 (OCH_2CH_3), 80.08 (C≡CCCH), 91.67 (C≡CCCH), 103.77 (d, $^2J_{CF}$=26.3, 25.3 Hz, FCCHCF), 110.65 (dd, $^2J_{CF}$=21.2 Hz, $^4J_{CF}$=3.9 Hz, FCCHCH), 123.55 ($CH_2C{\equiv}CC$), 124.62 (dd, $^2J_{CF}$ = 15.6 Hz, $^4J_{CF}$ = 3.9 Hz, FCC), 127.53 ($CH_2C{\equiv}CCCHCH$), 127.72 ($CH_2C{\equiv}CCCHCHCH$), 129.99 ($CH_2C{\equiv}CCCCH$), 132.39 ($CH_2C{\equiv}CCCH$), 132.56 (dd, $^3J_{CF}$=9.5, $^3J_{CF}$=4.8 Hz, FCCCH), 137.15 ($CH_2C{\equiv}CCC$), 159.80 (dd, $^1J_{CF}$=250.9, $^3J_{CF}$=11.9 Hz, CF), 162.44 (dd, $^1J_{CF}$=248.6, $^3J_{CF}$=11.6 Hz, CF), 174.02 (C=O) ppm; IR (KBr): $\tilde{\nu}$=3376, 3063, 2943, 2855, 2810, 2230, 1730, 1619, 1593, 1511, 1479, 1419, 1370, 1265, 1180, 1152, 1139, 1099, 1032, 963, 849, 761 cm^{-1}; MS (ESI$^+$) *m/z*: 398 $[M+H]^+$; HRMS-ESI$^+$ *m/z* $[M+H]^+$ calcd for $C_{24}H_{26}F_2NO_2$: 397.1932, found: 398.1925.

(*R*)-Ethyl 1-{4-[2-(2-chloro-4-fluorophenyl)phenyl]but-3-yn-1-yl}piperidine-3-carboxylate ((*R*)-15i):

R_f≈0.3 (hexane/ethyl acetate 8:2). $[\alpha]^{20}_D$=-30.2 (c=1.0 in CH_2Cl_2). ^{1}H NMR (400 MHz, $CDCl_3$): δ=1.24 (t, *J*=7.1 Hz, 3H, OCH_2CH_3), 1.41 (qd, *J*=11.6, 3.5 Hz, 1H, $NCH_2CHCH_{ax}H_{eq}$), 1.47–1.58 (m, 1H, $NCH_2CH_{ax}H_{eq}CH_2CH$), 1.69 (dp, *J*=10.3, 3.7 Hz, 1H, $NCH_2CH_{ax}H_{eq}CH_2CH$), 1.91 (dq, *J*=12.8, 4.1 Hz, 1H, $NCH_2CHCH_{ax}H_{eq}$), 1.99 (td, *J*=11.0, 3.0 Hz, 1H, $NCH_{ax}H_{eq}CH_2CH_2CH$), 2.18 (t, *J*=10.7 Hz, 1H, $NCH_{ax}H_{eq}CH$), 2.35–2.46 (m, 4H, $NCH_2CH_2C{\equiv}C$, $NCH_2CH_2C{\equiv}C$), 2.50 (tt, *J*=10.5, 3.8 Hz, 1H, NCH_2CH_{ax}), 2.67 (d_{br}, *J*=11.1 Hz, 1H, $NCH_{ax}H_{eq}CH_2CH_2CH$), 2.90 (d_{br}, *J*=11.1 Hz, 1H, $NCH_{ax}H_{eq}CH$), 4.12 (q, *J*=7.2 Hz, 2H, OCH_2CH_3), 7.02 (td, *J*=8.4, 2.6 Hz, 1H, FCC*H*CH), 7.19–7.35 (m, 5H, FCC*H*CCl, C≡CCCC*H*, FCCHC*H*, C≡CCCHC*H*, C≡CCCCHC*H*), 7.46–7.51 (m, 1H, C≡CCC*H*) ppm; ^{13}C NMR (101 MHz, $CDCl_3$): *δ*=14.17 (OCH_2CH_3), 17.53 ($NCH_2CH_2C{\equiv}C$), 24.53 ($NCH_2CH_2CH_2CH$), 26.79 (NCH_2CHCH_2), 41.82 (NCH_2CH), 53.16 ($NCH_2CH_2CH_2CH$), 54.92 (NCH_2CH), 57.15 ($NCH_2CH_2C{\equiv}C$), 60.28 (OCH_2CH_3), 79.91 (C≡CCCH), 92.06 (C≡CCCH), 113.42 (d, $^2J_{CF}$=20.8 Hz, FCCHCH), 116.51 (d, $^2J_{CF}$=24.3 Hz, FCC*H*CCl), 123.62 ($CH_2C{\equiv}CC$), 127.34 ($CH_2C{\equiv}CCCHCHCH$), 127.73 ($CH_2C{\equiv}CCCHCH$), 129.70 ($CH_2C{\equiv}CCCCH$), 132.00 ($CH_2C{\equiv}CCCH$), 132.44 (d, $^3J_{CF}$=8.7 Hz, FCCHCH), 134.12 (d, $^3J_{CF}$=10.0 Hz, ClC), 135.98 (d, $^4J_{CF}$=3.1 Hz, ClCC), 140.78 ($CH_2C{\equiv}CCC$), 161.80 (d, $^1J_{CF}$=249.7 Hz, FC), 174.03 (C=O) ppm; IR (KBr): $\tilde{\nu}$=3064, 2942, 2855, 2811, 2228, 1730, 1604,

1503, 1473, 1443, 1370, 1257, 1201, 1181, 1153, 1100, 1033, 897, 858, 761 cm^{-1}; MS (ESI^+) *m/z*: 414 $[M+H]^+$; HRMS-ESI^+ *m/z* $[M+H]^+$ calcd for $C_{24}H_{26}ClFNO_2$: 414.1636, found: 414.1634.

(*R*)-1-{4-[2-(2-Methylphenyl)phenyl]but-3-yn-1-yl}piperidine-3-carboxylic acid ((*R*)-17d):

R_f≈0.1 (CH_2Cl_2/CH_3OH 9:1). $[\alpha]^{20}_D$=+36.0 (c=1.0 in CH_2Cl_2). ^1H NMR (400 MHz, 1N NaOD/CH_3OD 1:2, 60 °C): δ=1.26 (qd, *J*=12.8, 4.1 Hz, 1H, $NCH_2CHCH_{ax}H_{eq}$), 1.47 (qt, *J*=12.8, 3.5 Hz, 1H, $NCH_2CH_{ax}H_{eq}CH_2CH$), 1.63 (dp, *J*=13.2, 3.8 Hz, 1H, $NCH_2CH_{ax}H_{eq}CH_2CH$), 1.79 (t, *J*=10.8 Hz, 1H, $NCH_{ax}H_{eq}CH_2CH_2CH$), 1.88–2.01 (m, 2H, $NCH_2CHCH_{ax}H_{eq}$, $NCH_{ax}H_{eq}CH$), 2.07 (s, 3H, H_3CC), 2.22–2.43 (m, 5H, $NCH_2CH_2C{\equiv}C$, $NCH_2CH_2C{\equiv}C$, NCH_2CH_{ax}), 2.70 (d_{br}, *J*=10.5 Hz, 1H, $NCH_{ax}H_{eq}CH_2CH_2CH$), 2.92 (d_{br}, *J*=11.1 Hz, 1H, $NCH_{ax}H_{eq}CH$), 7.04 (d, *J*=7.5 Hz, 1H, H_3CCCCH), 7.11 (dd, *J*=7.2, 1.6 Hz, 1H, $C{\equiv}CCCCH$), 7.14–7.20 (m, 1H, $H_3CCCCHCH$), 7.20–7.25 (m, 2H, $H_3CCCHCH$, H_3CCCH), 7.25–7.35 (m, 2H, $C{\equiv}CCCHCH$, $C{\equiv}CCCCHCH$), 7.44 (d, *J*=7.6 Hz, 1H, $C{\equiv}CCCH$) ppm; ^{13}C NMR (101 MHz, 1N NaOD/CH_3OD 1:2, 60 °C): δ=17.49 ($NCH_2CH_2C{\equiv}C$), 20.16 (H_3CC), 25.56 ($NCH_2CH_2CH_2CH$), 29.02 (NCH_2CHCH_2), 46.04 (NCH_2CH), 53.98 ($NCH_2CH_2CH_2CH$), 57.47 (NCH_2CH), 58.18 ($NCH_2CH_2C{\equiv}C$), 81.68 ($C{\equiv}CCCH$), 91.93 ($C{\equiv}CCCH$), 124.17 ($CH_2C{\equiv}CC$), 126.36 ($H_3CCCCHCH$), 128.12 ($CH_2C{\equiv}CCCHCH$), 128.57 ($H_3CCCHCH$), 128.81 ($CH_2C{\equiv}CCCHCHCH$), 130.32 ($CH_2C{\equiv}CCCCH$), 130.42 (H_3CCCH), 132.72 ($CH_2C{\equiv}CCCH$), 137.02 (H_3CC), 142.19 (H_3CCC), 145.65 ($CH_2C{\equiv}CCC$), 182.88 (*C*=O) ppm; IR (KBr): $\tilde{\nu}$=3424, 3057, 3018, 2941, 2859, 2230, 1709, 1591, 1474, 1442, 1394, 1217, 1192, 1156, 1101, 1006, 759 cm^{-1}; MS (ESI^+) *m/z*: 348 $[M+H]^+$; HRMS-ESI^+ *m/z* $[M+H]^+$ calcd for $C_{23}H_{26}NO_2$: 348.1963, found: 348.1959.

(*R*)-1-{4-[2-(2,4-Dichlorophenyl)phenyl]but-3-yn-1-yl}piperidine-3-carboxylic acid ((*R*)-17f):

R_f≈0.1 (CH_2Cl_2/CH_3OH 9:1). $[\alpha]^{20}_D$=+26.5 (c=1.0 in CH_2Cl_2). ^1H NMR (500 MHz, 1N NaOD/CH_3OD 1:2, 60 °C): δ=1.29 (qd, *J*=12.9, 4.1 Hz, 1H, $NCH_2CHCH_{ax}H_{eq}$), 1.50 (qt, *J*=13.9, 3.7 Hz, 1H, $NCH_2CH_{ax}H_{eq}CH_2CH$), 1.66 (dp, *J*=12.8, 3.0 Hz, 1H, $NCH_2CH_{ax}H_{eq}CH_2CH$), 1.81 (td, *J*=12.3, 2.9 Hz, 1H, $NCH_{ax}H_{eq}CH_2CH_2CH$), 1.94 (d_{br}, *J*=12.7 Hz, 1H, $NCH_2CHCH_{ax}H_{eq}$), 2.00 (t, *J*=11.5 Hz, 1H, $NCH_{ax}H_{eq}CH$), 2.27–2.48 (m, 5H, NCH_2CH_{ax}, $NCH_2CH_2C{\equiv}C$, $NCH_2CH_2C{\equiv}C$), 2.76 (d_{br}, *J*=11.3 Hz, 1H, $NCH_{ax}H_{eq}CH_2CH_2CH$), 2.98 (d_{br}, *J*=11.3 Hz, 1H, $NCH_{ax}H_{eq}CH$), 7.17–7.21 (m, 1H, $C{\equiv}CCCCH$), 7.25 (d, *J*=8.2 Hz, 1H, $ClCCCH$), 7.33–7.39 (m, 3H, $ClCCHCH$, $C{\equiv}CCCHCH$, $C{\equiv}CCCCHCH$), 7.43–7.46 (m, 1H, $C{\equiv}CCCH$), 7.52 (d, *J*=2.1 Hz, 1H, $ClCCHCCl$) ppm; ^{13}C NMR (126 MHz, 1N NaOD/CH_3OD 1:2, 60 °C): δ=17.61 ($NCH_2CH_2C{\equiv}C$), 25.66 ($NCH_2CH_2CH_2CH$), 29.09 (NCH_2CHCH_2), 46.08 (NCH_2CH), 54.24 ($NCH_2CH_2CH_2CH$), 57.54 (NCH_2CH), 58.26 ($NCH_2CH_2C{\equiv}C$), 81.06 ($C{\equiv}CCCH$), 92.84 ($C{\equiv}CCCH$), 124.45 ($CH_2C{\equiv}CC$), 127.92 ($ClCCHCH$, 128.82 ($CH_2C{\equiv}CCCHCH$), 129.19 ($CH_2C{\equiv}CCCHCHCH$), 129.93 ($ClCCHCCl$, 130.45 ($CH_2C{\equiv}CCCCH$), 132.85 ($CH_2C{\equiv}CCCH$), 133.67 ($ClCCCH$), 134.97 (ClC), 135.21 (ClC), 139.96 ($ClCC$), 141.96 ($CH_2C{\equiv}CCC$), 182.80 ppm (*C*=O) ppm; IR (KBr): $\tilde{\nu}$=3435, 3060, 2935, 2856, 2808, 2231, 1711, 1586, 1466, 1440, 1375, 1102, 1071, 1004, 865, 813, 761 cm^{-1}; MS (ESI^+) *m/z*: 402 $[M+H]^+$; HRMS-ESI^+ *m/z* $[M+H]^+$ calcd for $C_{22}H_{22}Cl_2NO_2$: 402.1028, found: 402.1026.

(*R*)-1-{4-[2-(2,4-Difluorophenyl)phenyl]but-3-yn-1-yl}piperidine-3-carboxylic acid ((*R*)-17g):

R_f≈0.1 (CH_2Cl_2/CH_3OH 9:1). $[\alpha]^{20}_D$=+31.2 (c=1.0 in CH_2Cl_2). ^1H NMR (500 MHz, 1N NaOD/CH_3OD 1:2, 60 °C): δ=1.29 (qd, *J*=13.0, 4.1 Hz, 1H, $NCH_2CHCH_{ax}H_{eq}$), 1.51 (qt, *J*=13.4, 4.1 Hz, 1H, $NCH_2CH_{ax}H_{eq}CH_2CH$), 1.66 (dp, *J*=13.0, 3.3 Hz, 1H, $NCH_2CH_{ax}H_{eq}CH_2CH$), 1.86–1.97 (m, 2H, $NCH_2CHCH_{ax}H_{eq}$, $NCH_{ax}H_{eq}CH_2CH_2CH$), 2.03 (t, *J*=11.4 Hz, 1H, $NCH_{ax}H_{eq}CH$), 2.32 (tt, *J*=12.2, 3.8 Hz, 1H, NCH_2CH_{ax}), 2.39–2.52 (m, 4H, $NCH_2CH_2C{\equiv}C$, $NCH_2CH_2C{\equiv}C$), 2.79 (d_{br}, *J*=11.1 Hz, 1H, $NCH_{ax}H_{eq}CH_2CH_2CH$), 2.95–3.05 (m, 1H, $NCH_{ax}H_{eq}CH$), 6.98–7.05 (m, 2H, $FCCHCF$, $FCCHCH$), 7.26 (dd, *J*=7.2, 1.1 Hz, 1H, $C{\equiv}CCCCH$), 7.32–7.39 (m, 3H, $C{\equiv}CCCCHCH$, $C{\equiv}CCCHCH$, $FCCCH$), 7.45–7.48 (m, 1H, $C{\equiv}CCCH$) ppm; ^{13}C NMR (126 MHz, 1N NaOD/CH_3OD 1:2, 60 °C): δ=17.56 ($NCH_2CH_2C{\equiv}C$), 25.67 ($NCH_2CH_2CH_2CH$), 29.11 (NCH_2CHCH_2), 46.13 (NCH_2CH), 54.20 ($NCH_2CH_2CH_2CH$), 57.53 (NCH_2CH), 58.30 ($NCH_2CH_2C{\equiv}C$), 81.21 ($C{\equiv}CCCH$), 92.24 ($C{\equiv}CCCH$), 104.57 (d, $^2J_{CF}$=26.2 Hz, $FCCHCF$), 111.93 (dd, $^2J_{CF}$=21.3 Hz, $^4J_{CF}$=3.8 Hz, $FCCHCH$), 124.63 ($CH_2C{\equiv}CC$), 126.07 (dd, $^2J_{CF}$=16.0 Hz, $^4J_{CF}$=3.8 Hz, FCC), 129.00 (2 C, $CH_2C{\equiv}CCCHCHCH$, $CH_2C{\equiv}CCCHCH$), 130.99 ($CH_2C{\equiv}CCCCH$), 133.17 ($CH_2C{\equiv}CCCH$), 133.52 (dd, $^3J_{CF}$=9.5 Hz, $^3J_{CF}$=4.6 Hz, 1C, $FCCCH$), 138.52 (s, 1C, $CH_2C{\equiv}CCC$), 161.06 (dd, $^1J_{CF}$=249.0 Hz,

$^{3}J_{CF}$=12.7 Hz, F*C*), 163.87 (dd, $^{1}J_{CF}$=257.3 Hz, $^{3}J_{CF}$=10.3 Hz, F*C*), 182.82 (*C*=O) ppm; IR (KBr): $\tilde{\nu}$=3425, 3061, 2941, 2861, 2808, 2232, 1708, 1618, 1593, 1511, 1479, 1444, 1419, 1265, 1140, 1097, 963, 850, 762 cm^{-1}; MS (ESI^{+}) *m/z*: 370 [M+H]$^{+}$; HRMS-ESI^{+} *m/z* [M+H]$^{+}$ calcd for $C_{22}H_{22}F_2NO_2$: 370.1619 found: 370.1614.

(*R*)-1-{4-[2-(2-Chloro-4-fluoro-phenyl)phenyl]but-3-yn-1-yl}piperidine-3-carboxylic acid ((*R*)-17i):

R_f≈0.1 (CH_2Cl_2/CH_3OH 9:1). [α]$^{20}_{D}$=+28.4 (c=1.0 in CH_2Cl_2). ^{1}H NMR (500 MHz, 1N NaOD/CH_3OD 1:2, 60 °C): *δ*=1.28 (qd, *J*=12.8, 4.0 Hz, 1H, $NCH_2CHCH_{ax}H_{eq}$), 1.49 (qt, *J*=13.0., 3.4 Hz, 1H, $NCH_2CH_{ax}H_{eq}CH_2CH$), 1.65 (d_{br}, *J*=13.5 Hz, 1H, $NCH_2CH_{ax}H_{eq}CH_2CH$), 1.85 (td, *J*=12.0/2.3 Hz, 1H, $NCH_{ax}H_{eq}CH_2CH_2CH$), 1.90–2.05 (m, 2H, $NCH_2CHCH_{ax}H_{eq}$, $NCH_{ax}H_{eq}CH$), 2.24–2.48 (m, 5H, NCH_2CH_{ax}, $NCH_2CH_2C{\equiv}C$, $NCH_2CH_2C{\equiv}C$), 2.75 (d_{br}, *J*=10.8 Hz, 1H, $NCH_{ax}H_{eq}CH_2CH_2CH$), 2.97 (d_{br}, *J*=11.1 Hz, 1H, $NCH_{ax}H_{eq}CH$), 7.12 (td, *J*=8.4, 2.6 Hz, 1H, FCC*H*CH), 7.16–7.21 (m, 1H, C≡CCCC*H*), 7.24–7.31 (m, 2H, FCCHC*H*, FCC*H*CCl), 7.31–7.39 (m, 2H, C≡CCCHC*H*, C≡CCCCHC*H*), 7.41–7.47 (m, 1H, C≡CCC*H*) ppm; ^{13}C NMR (126 MHz, 1N NaOD/CH_3OD 1:2, 60 °C): *δ*=17.52 ($NCH_2CH_2C{\equiv}C$), 25.59 ($NCH_2CH_2CH_2CH$), 29.03 (NCH_2CHCH_2), 46.06 (NCH_2CH), 54.11 ($NCH_2CH_2CH_2CH$), 57.46 (NCH_2CH), 58.22 ($NCH_2CH_2C{\equiv}C$), 81.14 (C≡*C*CCH), 92.65 (*C*≡CCCH), 114.75 (d, $^{2}J_{CF}$=21.2 Hz, FC*C*HCH), 117.33 (d, $^{2}J_{CF}$=24.7 Hz, FC*C*HCCl), 124.57 ($CH_2C{\equiv}C*C*$), 128.78 ($CH_2C{\equiv}CCCHCH$), 129.05 ($CH_2C{\equiv}CCCHCHCH$), 130.67 ($CH_2C{\equiv}CCCCH$), 132.84 ($CH_2C{\equiv}CCCH$), 133.78 (d, $^{3}J_{CF}$=8.7 Hz, FCCH*C*H), 135.08 (d, $^{3}J_{CF}$=10.4 Hz, Cl*C*), 137.48 (d, $^{4}J_{CF}$=3.6 Hz, ClC*C*), 142.09 ($CH_2C{\equiv}CCC$), 163.17 (d, $^{1}J_{CF}$=248.4 Hz, F*C*), 182.87 (*C*=O) ppm; IR (KBr): $\tilde{\nu}$=3433, 3062, 2942, 2859, 2231, 1710, 1604, 1503, 1473, 1442, 1389, 1257, 1201, 1062, 1041, 1006, 897, 859, 820, 762 cm^{-1}; MS (ESI^{+}) *m/z*: 385 [M+H]$^{+}$; HRMS-ESI^{+} *m/z* [M+H]$^{+}$ calcd for $C_{22}H_{22}ClFNO_2$: 386.1323, found 386.1319.

Development of new photoswitchable azobenzene bound GABA uptake inhibitors with distinctly enhanced potency upon photoactivation

*Toni Lutz, Thomas Wein, Georg Höfner, Jörg Pabel, Matthias Eder, Julien Dine, and Klaus T. Wanner**

Department of Pharmacy – Center for Drug Research,

Butenandtstr. 5–13, D - 81377 Munich, Germany

E-Mail: Klaus.wanner@cup.uni-muenchen.de

Abstract

Inhibition of GABA transporters in the central nervous system (CNS) enhances GABA signaling and alleviates symptoms of neurological disorders such as epilepsy, assumed to correspond with low GABA levels. Recently, we reported the first photoswitchable inhibitor of GAT1, the most common GABA transporter subtype in the CNS. As an extension of this study, a series of nipecotic acid derivatives with new azo benzene bound photoswitchable N-substituents was synthesized and characterized for their functional inhibitory activity at mGAT1 both before and after photoirradiation. This led to the identification of the first photoswitchable ligands exhibiting a moderate uptake inhibition of GABA in their (*E*)-, but distinctive higher inhibitory potency in their (*Z*)-form resulting from photoirradiation. For the most efficient photoactivatable nipecotic acid derivative displaying an *N*-but-3-in-1-yl linker with a terminal diphenyldiazene unit, an inhibitory potency of 4.65±0.05 (pIC_{50}) was found for its ground state which increased by almost two log units up to 6.38±0.04 when irradiated.

Introduction

Photoswitchable ligands are compounds whose activity at a given biological target can be controlled by light and thus with high temporal and spatial precision. When irradiated with light, such ligands reversibly undergo a configurational change in their structure, which may a significantly alter their affinity to a specific target. Recently, a variety of photoswitchable ligands have been successfully developed, e.g. for the optical control of epithelial sodium channels,[1] insulin receptors,[2] the acetylcholinesterase,[3] μ-opioid receptors,[4] TRPV1-channels,[5] glutamate receptors,[6] NMDA receptors,[7] AMPA receptors,[8] local anesthetics,[9] and cell division.[10, 11] In our previous work, we have reported the first application of the concept of light controlled ligand activity to a plasma membrane bound neurotransmitter transporter, the GABA transporter GAT1, by introducing the first photoswitchable GABA uptake inhibitors.[12]

γ-Aminobutyric acid (GABA, **1**, Figure 1) is known to be the major inhibitory neurotransmitter[13] in the CNS. Upon depolarization of presynaptic GABAergic neurons, GABA is released into the synaptic cleft where it activates GABA receptors mediating further signal transduction. A reduced neurotransmission of GABA leads to an imbalance between excitatory and inhibitory neurotransmission[14] and hence plays a role in the pathogenesis of many neurological disorders such as epilepsy, neuropathic pain, depression, or anxiety.[15]

* Department für Pharmazie – Zentrum für Pharmaforschung, Ludwig-Maximilians-Universität München, Butenandtstrasse 5-13, 81377 Munich, Germany

Since the termination of GABAergic signaling is mainly caused by specific GABA transport proteins (GATs) which mediate GABA's reuptake into the presynaptic neuron or its transport into glia cells,[16] GATs represent a valuable drug target,[17] as their inhibition can contribute to restore a physiological neurotransmitter balance. The GABA transporters are membrane bound proteins belonging to the solute carrier 6 (SLC-6) family.[18] The four subtypes derived from mouse brain cells are named mGAT1, mGAT2, mGAT3, and mGAT4. By contrast, the human GATs are designated as hGAT1, hBGT1, hGAT2, and hGAT3, respectively.[17] The GABA transporter subtype 1 (hGAT1, mGAT1) is mainly located on presynaptic neurons and represents the most abundant and hence the most important subtype in the CNS for GABA uptake.[19]

The first generation of GAT inhibitors consisted of cyclic analogues of GABA like (*R*)-nipecotic acid (**2**, Figure 1)[20] exhibiting an *in vitro* functional inhibitory activity (pIC_{50}) of 5.19±0.03 at mGAT1.[21] Due to its inability to cross the blood-brain barrier,[22] the nipecotic acid was later equipped with a lipophilic side chain resulting in compounds such as tiagabine (**3**, Figure 1),[23,24] that not only enabled the amino acid to cross the BBB but even made it a highly potent and selective inhibitor for the GABA transporter subtype GAT1 (pIC_{50} = 6.88±0.12).[21] Tiagabine which is used for partial treatment of epilepsy is the only marketed drug targeting the GAT1 protein.

Recently, we introduced the highly potent and mGAT1 selective parent compounds **4** and **5** (Figure 1) that exhibit a similar inhibitory activity as tiagabine towards the aforementioned target (mGAT1: **4**: pIC_{50} = 6.79±0.12; **5**: pIC_{50} = 7.00±0.04).[25, 26] The N-substituents of these nipecotic acids are characterized by a but-3-en-1-yl and a but-3-in-1-yl linker, respectively, with a terminally attached 2-biphenyl residue. In contrast, the first photoswitchable mGAT1 inhibitors reported so far are based on an ethoxy ethyl spacer linking nipecotic acid with a diphenyldiazene or a naphthylphenyldiazene subunit as photoresponsive element.[12] Among these photosensitive compounds studied, (*R*)-**6** was found to be the most efficient photoswitchable ligand (Figure 1). This compound, (*R*)-**6**, displayed a pIC_{50} of 6.39±0.08 as its pure (*E*)-isomer whereas after irradiation with light at 375 nm inducing a (*E*)/(*Z*)-ratio of 13/87 at the photostationary state led to a reduced mGAT1 activity in a functional GABA uptake assay with a pIC_{50} value of 5.78±0.03.

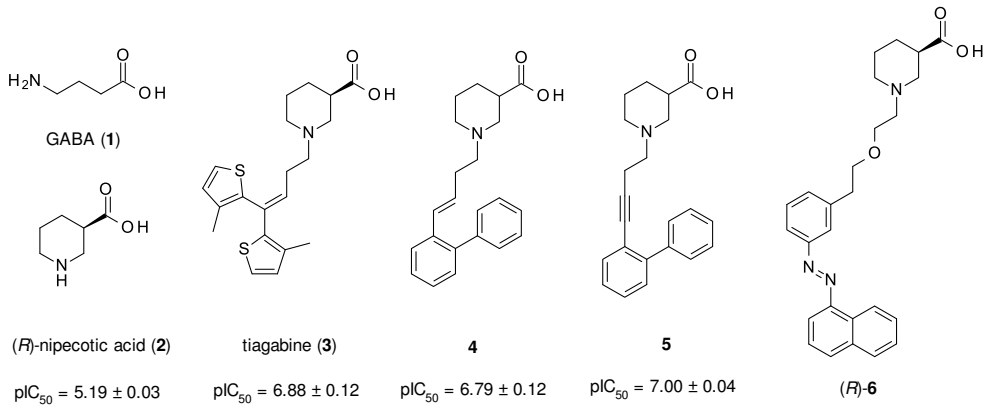

Figure 1: Structure of GABA, known potent GAT1 inhibitors, and the first photoswitchable GAT1 inhibitor (pIC_{50} values refer to mGAT1).

For the development of new nipecotic acid derivatives with photoresponsive subunits, compounds **4** and **5** were selected as templates. Herein, the biphenyl-type residue of the N-substituent was intended to be replaced by different photosensitive diaryldiazene subunits, whilst the alkenyl and alkynyl spacer originating from the amino group of the nipecotic acid unit should be preserved. Ideally, the photoswitches to be generated should exhibit a higher inhibitory potency at mGAT1 and be characterized by a difference in potency concerning their two possible conformational isomers, the (*E*)- and the (*Z*)-form, as large as possible. In this context, a further aim of this study was to identify mGAT1 inhibitors, which show a low inhibitory activity towards the target for their (*E*)-form representing the ground state and a distinctly higher potency for their (*Z*)-form that should also clearly prevail after irradiation.

Such photoswitchable mGAT1 inhibitors would nicely complement the photoresponsive compounds developed before by us with the (*E*)- as compared to the (*Z*)-form being the more potent mGAT1 ligands. Because of the limited degree, azobenzenes can be transformed from the (*E*)- to the (*Z*)-form upon irradiation with light, photoswitches with the (*Z*)-form being more active than the (*E*)-form are of great interest as they may allow to gain larger activity differences upon irradiation.

With respect to the design of the target compounds, we intended to create homology models of the hGAT1 protein, based on which docking experiments should be performed with nipecotic acid derivatives exhibiting different N-substituents. That way, the subunits of the N-substituents, the spacer, and the photoresponsive elements that would be considered well worth for the construction of the new photoswitches should be identified. Thereby, in addition to the binding affinities of different photoswitchable ligands to hGAT1, also the affinities of their ground as compared to the irradiated states to the target protein should be estimated. For the photoswitchable compounds to be synthesized, a versatile and efficient synthetic approach should be devised and all compounds should be characterized for their functional inhibitory activity towards mGAT1 before and after irradiation in GABA uptake assay.

Results and discussion

Rational design:

The structural parameters of the new photoswitchable mGAT1 inhibitors that were intended to be varied are depicted in Figure 2. The *N*-alkyl spacer interconnecting the nipecotic acid with the diaryldiazene moiety should consist of either a four or a five carbon atom chain with a terminal double or triple bond as several compounds displaying these types of spacer have previously been found to be highly active mGAT1 inhibitors.[25, 26] For the terminally attached photoresponsive element, a diphenyldiazene or a naphthyl-phenyldiazene residue should be considered with the connection of the central phenyl ring of this unit with the linker originating from all three positions, i.e. the *ortho*-, *meta*- and *para*-position.

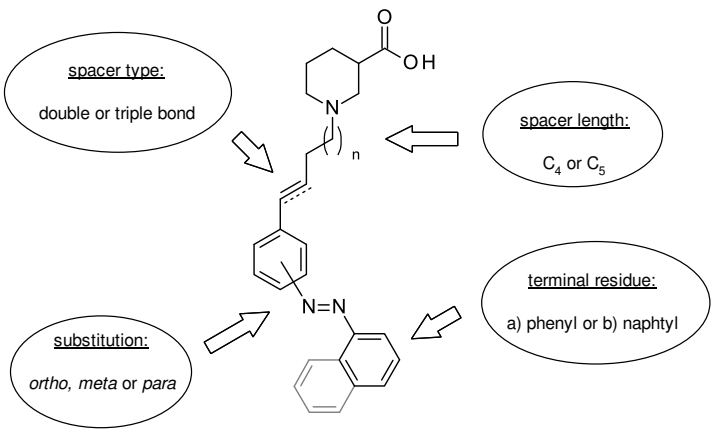

Figure 2: Parameters to be varied in the search for potent photoswitchables for nipecotic acid derivatives

Modeling:

For the identification of new and efficient photoswitchable GAT1 inhibitors, we investigated the set of compounds indicated in Figure 2 in virtual screening experiments performed with homology models of hGAT1. To this end, at first a suitable homology model of GAT1 which yields docking scores in line with the measured pIC_{50} values of the so far known photoswitchable compounds like (*R*)-**6** (Figure 1) was required. Thus, homology models of hGAT1 based on Leucine transporter (LeuT) X-Ray structures were generated.

For this purpose, the “closed” LeuT conformation pdb-id=2a65 and the “open-to-out” LeuT conformation pdb-id=3f3a were used as template structures. In the LeuT structure pdb-id = 2a65 a leucine is present in the primary binding site (S1) and four residues (Tyr108-Phe253 and Arg30-Asp404 in LeuT) shield this S1 site from the extracellular medium.[27] In contrast, in the pdb-id = 3f3a LeuT structure, two tryptophan molecules are bound, one directly in the S1 site and the second located above the first one. This keeps the gating residues far apart and the resulting LeuT conformation with the S1 site being not shielded and directly accessible from the extracellular medium is called “open-to-out”.[28] The hGAT1 homology models based on these two different LeuT conformations, which were generated with and without flexible gating residues as previously described in detail[21] were used for docking calculations. In addition, hGAT1 models were employed for this purpose that had been obtained by refining the protein structure with bound Tiagabine (**3**) by molecular simulation calculations as described in detail.[25] These models were able to predict the inhibitory activity of compounds (*R*)-**4**[25] and (*R*)-**5**[26] (Figure 1) which are highly similar to the desired photoswitchables.

The theoretical evaluations of the compounds and binding modes are based on the comparison of the AutoDock4 docking scores and the measured pIC_{50} values. Two of the aforementioned homology models of hGAT1 were able to yield docking scores for the recently published photoswitchable GAT1 inhibitors which are in line with the measured pIC_{50} values.[12] Model I had been obtained from refined MD calculations of the target protein with bound Tiagabine, model II from the “closed” LeuT conformation pdb-id-2a65 by treating the two gating residues (Tyr140-Phe294, GAT1 numbering) as flexible during docking.

When docking the ($E_{N\text{-}N}$)- and ($Z_{N\text{-}N}$)-isomers of the designed compounds depicted in Figure 2, both models predicted compounds with the *ortho*-substitution to be less active than *meta*- and *para*-substituted derivatives independent of the N-N double bond configuration. Therefore, scaffolds with *ortho*-substitution should not be further included in this study. In addition, compounds with an alkynyl spacer yielded better docking scores than those with an alkenyl linker. But no clear trend appeared regarding the influence of the length of the spacer and the nature of the terminal aryl residue, phenyl versus naphthyl. On the docking scores, the results were similar in all cases.

However, among the derivatives studied, one compound, characterized by a but-3-inyl spacer and a *meta*-substituted diphenyldiazene subunit was found that according to the docking results could be expected to be well suited for its use as a photoswitchable ligand. In both docking models, the (*E*)- and (*Z*)-isomer of this compound (*R*)-*m*-**20a** exhibited a high difference in the docking scores (model I: (*R*)-(*E*)-*m*-**20a** = -9.3 kcal/mol, (*R*)-(*Z*)-*m*-**20a** = -11.59 kcal/mol, model II: (*R*)-(*E*)-*m*-**20a** = -10.0 kcal/mol, (*R*)-(*Z*)-*m*-**20a** = -12.07 kcal/mol), clearly indicating that the photoswitched (*Z*)-isomer of (*R*)-*m*-**20a** should be more potent as compared to the (*E*)-isomer. Hence, compound (*R*)-*m*-**20a** appeared as the most promising candidate of the photoswitchable ligands that were intended to be synthesized.

Inspecting the docking poses of the (*E*)- and (*Z*)-isomer of (*R*)-*m*-**20a** in model I (Figure 3), show two significant differences which provide a rational explanation of the highly different docking scores found for the two isomers. While the interactions of the carboxyl function of both isomers is almost identical, the NH of the (*Z*)-isomer (Figure 3B) is involved in a hydrogen bond to the Phe294-CO. The H-O distance is almost perfect with 2 Å. In addition, the azo group of the (*Z*)-isomer, which is more exposed, interacts closely with the Arg69 carboxy function in a distance of 3 Å. Both interactions are not possible for the (*E*)-isomer (Figure 3A). The hydrogen bond of the NH to the Phe294-CO does not form at all, as with 3.9 Å the distance is too long. Also the distance of the distal azo nitrogen to the carboxy function of Arg69 amounting to 5.1Å is too long for a reasonable interaction of these groups. As apparent from Figure 3A, the (*E*)-configuration of the azo group straightens and hence enlarges the lipophilic N-substituent of the nipecotic acid moiety. This increased spatial demand and the decreased flexibility resulting from the alkynyl spacer appear to force the (*E*)-isomer in a docking pose which does not allow the formation of the favorable interactions that are present for the (*Z*)-isomer. Hence, the (*Z*)-isomer of (*R*)-m-**20a** can be expected to act as the more potent GAT1 inhibitor as compared to the (*E*)-form of this compound.

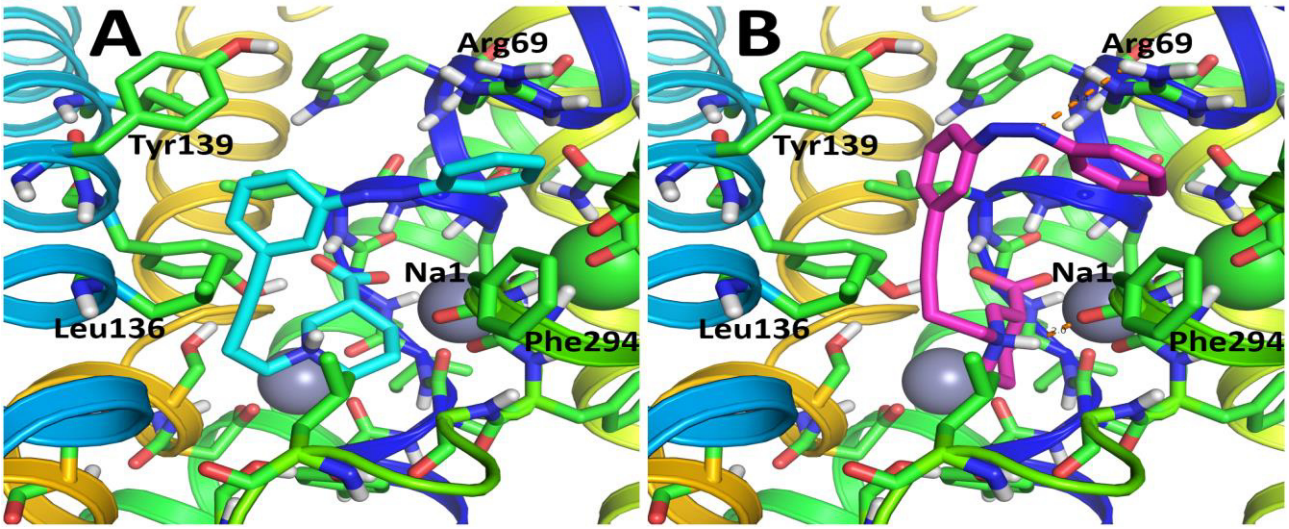

Figure 3: A) The (*E*)-isomer (cyan) and B) the (*Z*)-isomer (magenta) of (*R*)-*m*-**20a** docked into model I. The most prominent differences are the H bond between the NH of the (*Z*)-isomer to the Phe294 backbone CO (H-O distance = 2 Å) and the interaction the azo group of the *Z*-isomer and the Arg69 sidechain, both highlighted with orange dotted lines.

Chemistry:

The synthesis of photoswitchable GAT1 inhibitors containing a double bond in an all carbon spacer were intended to be performed by a Suzuki-Miyaura reaction. To this end, the nipecotic acid derivatives with an *N*-alkenyl residue provided with a terminal boronic acid ester function, i.e. **7** and **8** (Scheme 1) should be reacted with either of the two iodo substituted photoresponsive diaryldiazene subunits **9a**-**b** (Scheme 1) as shown in Scheme 1. This approach appeared most promising as it would easily allow the variation of the length of the spacer and the structure of the diaryldiazene subunit of the target compounds.

When the boronic acid esters **7** and **8** (Scheme 1) were subjected to Suzuki cross-coupling reactions with the iodo substituted diaryldiazenes **9a**-**b** (Scheme 1) under standard conditions (1 mol% Pd_2dba_3; 4 mol% SPhos, K_3PO_4 in dioxane/water, 60 °C),[29] the corresponding coupling products **10a**-**b** and **11a**-**b** (Scheme 1) were obtained in good to very good yields (78–87%). The target compounds, free nipecotic acid derivatives **12a**-**b** and **13a**-**b** were finally obtained by alkaline hydrolysis (NaOH, EtOH, rt, 6h) of the carboxylic acid esters **10a**-**b** and **11a**-**b** (Scheme 1, yield: 88–96%).

Scheme 1: General synthesis route for photoswitchable GAT1 Inhibitors containing an alkenyl spacer[a]

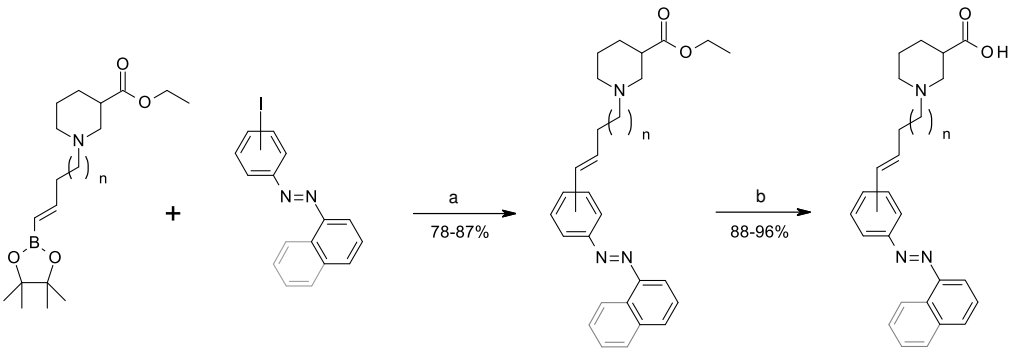

Aryl substitution: *meta* (*m*) or *para* (*p*); Terminal residue: **a** = phenyl, **b** = naphthyl

[a] Reagents and conditions: a) Pd_2dba_3 (1 mol%), SPhos (4 mol%), K_3PO_4 (2.0 eq), dioxane/water (2:1); 60 °C, 6h; b) NaOH (2 M, 3.0 eq), ethanol; r.t., 6h;

For the synthesis of photoswitchable GAT1 inhibitors with a triple bond in the spacer, a different approach as compared to the construction of the photoswitches with an alkenyl linker (Scheme 1) was followed. In preliminary experiments, the Sonogashira cross-coupling reaction of the diaryldiazenes **9a**-**b** with the linker unit already attached to the nipecotic acid moiety was found to proceed in low yields only: Therefore, first the iodo substituted diaryldiazenes **9a**-**b** (Scheme 2) were equipped with alkynyl residues that should serve as spacers in the final compounds. This was accomplished by performing a Sonogashira cross-coupling reaction of diaryldiazenes *m*-**9a**-**b** and *p*-**9a**-**b** with either but-3-yn-1-ol or pent-4-yn-1-ol [$Pd_2(dppf)_2Cl_2$ and Et_3N in THF, 1 hour, 60 °C] which led to the coupling products **14a**-**b** and **15a**-**b** in high yields (90–96%, Scheme 2). In the next step, arylalkynyl alcohols **14a**-**b** and **15a**-**b** were transformed into the corresponding tosylates **16a**-**b** and **17a**-**b** (Scheme 2) by treatment with of TsCl and Et_3N (CH_2Cl_2, 24 hours, 85–92%) which then by reaction with nipecotic acid ethyl ester (acetone, 72 h, rt) provided the esters **18a**-**b** and **19a**-**b** (84–93%, Scheme 2). Finally, upon subjection to basic hydrolysis (NaOH, EtOH, rt, 6 hours) of esters **18a**-**b** and **19a**-**b** the desired photoswitches, the nipecotic acid derivatives *m*-**20a**-**b**, *p*-**20a**-**b**, *m*-**21a**-**b,** and *p*-**21a**-**b** (yield: 87–94%) could be obtained (Scheme 2).

Scheme 2: General synthesis route for photoswitchable GAT1 Inhibitors containing an alkynyl spacer[a]

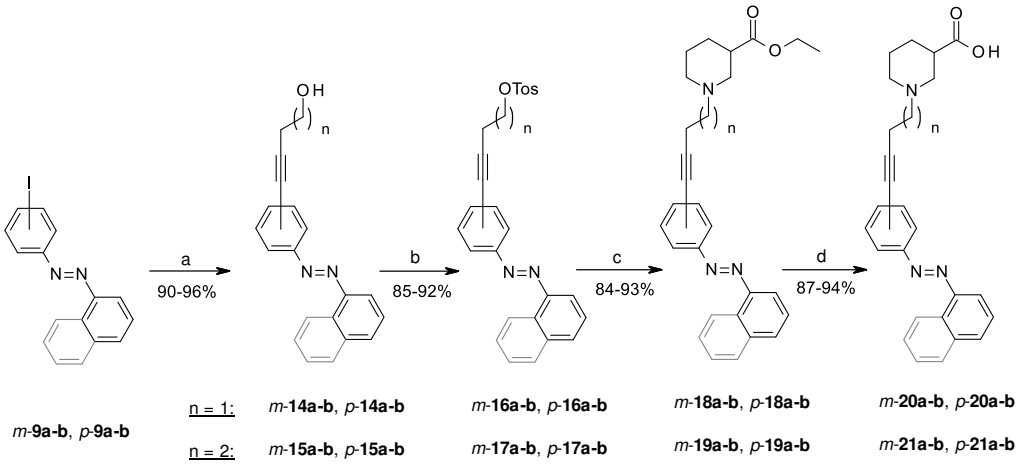

[a]Reagents and conditions: a) but-3-yn-1-ol or pent-4-yn-1-ol, $Pd_2(dppf)_2Cl_2$, Et_3N, THF; 60 °C, 1 h; b) TosCl, Et_3N, CH_2Cl_2; 0 °C → r.t., 24 h; c) nipecotic acid ethyl ester, acetone; r.t., 72 h; d) NaOH (2 M, 3.0 eq), ethanol; r.t., 6h;

Photoisomerization:

All photoswitchable compounds were characterized with regard to their potency as mGAT1 inhibitors. This characterization was performed for the pure ($E_{N\text{-}N}$)-isomers as well as the ($E_{N\text{-}N}$)/($Z_{N\text{-}N}$)-mixtures that were obtained upon irradiation until the photostationary equilibrium was reached. In preliminary experiments using UV/Vis spectroscopy and *in situ* irradiation with monochromatic light,[30] the wavelengths of 350 nm and 375 nm for the diphenyldiazene subunit and naphthylphenyldiazene subunits, respectively, were found to effect the highest percentage of ($Z_{N\text{-}N}$)-isomer at the photostationary state. For the biological testing, a 10 mM stock solution in DMSO of the individual compounds was subjected to photoisomerization by means of a Rayonet photoreactor[31] (λ_{max} = 350 nm) in case of GAT1 inhibitors containing a diphenyldiazene subunit, and with a self-built light chamber equipped with LED lamps (λ_{max} = 375 nm) for photoswitches with a naphthylphenyldiazene as photoresponsive element. In each case solutions were irradiated until the photostationary state with the maximum achievable percentage of ($Z_{N\text{-}N}$)-isomer over the ($E_{N\text{-}N}$)-isomer was reached. For compounds based on a diphenyldiazene subunit this was possible within 10–20 min, whereas it took 1–2 hours for the compounds with a naphthylphenyldiazene moiety. The percentage of the ($Z_{N\text{-}N}$)-isomer at the photostationary state was determined by ^{1}H NMR spectroscopic analysis of the respective samples.

For compounds exhibiting a diphenyldiazene subunit, i.e. *m*-**12a**, *p*-**12a**, *m*-**13a**, *p*-**13a,** *m*-**20a**, (*R*)-*m*-**20a**, *p*-**20a**, (*R*)-*p*-**20a**, *m*-**21a**, *p*-**21a**, (Table 2, entry 1-2, 5-6, 9-10 and 13-14), the ($E_{N\text{-}N}$)/($Z_{N\text{-}N}$) were in the range from 19/81 till 09/91. In case of the photoswitchable ligands with a naphthylphenyldiazene moiety, compounds *m*-**12b**, *p*-**12b**, *m*-**13b**, *p*-**13b**, *m*-**20b**, (*R*)-*m*-**20b**, *p*-**20b**, (*R*)-*p*-**20b**, *m*-**21b** and *p*-**21b**, the isomer ratios ranged from 36/64 to 16/84 (Table 2, entry 3-4, 7-8, 11-12 and 15-16). Interestingly, the half-life´s found for the thermal relaxation of the studied photoswitches in phosphate buffer (pH 7.4) followed a general trend. When as a photoresponsive element, an *m*-substituted diphenyldiazene moiety is present, the half-lives are higher (≈ 10-20 d, Table 1, entry 1 and 9). From there, it gradually decreases via compounds containing a *p*-substituted diphenyl diazene, an *m*-substituted naphthyl phenyl diazene to those with a *p*-substituted naphthyl phenyl diazene unit. For the latter, the half-lives are in the range of hours only (Table 1, entry 8 and 16) which may be attributed to the extended π-system present in these compounds. For assessment of the thermal relaxation rates in organic solvent, half-life's of all compounds with C_4 spacer were additionally reviewed in DMSO and found to be in a comparable scale (see supporting information).

For *m*-**20a**, which was found to show the highest differences in potency between the (*E*)- and (*Z*)-isomer at mGAT1 thus representing the most promising photoswitch, isomerization was additionally studied in phosphate buffer (25 µM solution, pH 7.4) as a more physiological system. For the forward isomerization with 350 nm monochromatic light,[30] found to be the best for this purpose, a (*E*)/(*Z*)-ratio of ≈ 5/95, representing the photochemical equilibrium, was reached within 10 minutes. Back isomerization by irradiation was best effected with 420 nm monochromatic light yielding an (*E*)/(*Z*)-ratio of ≈ 75/25 at the photostationary state (10 minutes). Thermal relaxation (in the dark) of the (*Z*)-isomer of *m*-**20a** was found to be very slow, the half-life of the reaction at 25 °C in phosphate buffer (pH 7.4) amounting to 22 days (Table 1, entry 9) and in DMSO at 25 °C to 15 days demonstrating the high thermal stability of (*Z*)-*m*-**20a**. Detailed kinetical data and measurements for this compound is given in the supporting information.

Biological evaluation:

Uptake inhibition at mGAT1 was determined for both the pure ($E_{N\text{-}N}$)-isomers and for the ($E_{N\text{-}N}$)/($Z_{N\text{-}N}$)-mixtures from photoequilibration (see Table 2 for isomer ratios). Compounds that were found to be highly active in one of their isomeric forms were synthesized in their enantiopure form, and additionally characterized for their subtype selectivity for mGAT1 as compared to mGAT2-mGAT4 by determining the functional inhibitory activity in [^{3}H]GABA uptake assays.[32]

Results of functional inhibitory activity at mGAT1 for compounds containing an alkenyl spacer are given in entry 1 to 8 of Table 1. The inhibitors with a *meta*-substituted diphenyldiazene subunit *m*-**12a** and *m*-**13a** (Table 1, entry 1 and 5) exhibited both a higher inhibitory potency in the photoequilibrated state than in the pure ($E_{N\text{-}N}$)-form. In case of *m*-**12a** with a C_4-spacer (pIC_{50} = 4.42±0.02; pIC_{50}* = 5.32±0.09; Table 1, entry 1) this effect is more pronounced than for the homologue *m*-**13a** (pIC_{50} = 4.42±0.01; pIC_{50}* = 4.60±0.12; Table 1, entry 5) with a C_5-linker. In contrast, the corresponding compounds with *para*-substituted diphenyldiazenes moieties *p*-**12a** and *p*-**13a** (Table 1, entry 2 and 6) show the opposite effect at mGAT1, the pure ($E_{N\text{-}N}$) isomer being about 0.6 log units more potent than the photoequilibrated mixture for both spacer length (*p*-**12a**: pIC_{50} = 5.00±0.01, pIC_{50}* = 4.43±0.03, Table 1, entry 2; *p*-**13a**: pIC_{50} = 5.24±0.01, pIC_{50}* = 4.63±0.03, Table 1, entry 6). Alike the diphenyldiazene derivatives *m*-**12a** and *m*-**13a**, also the analogous compounds *m*-**12b** and *m*-**13b** (Table 1 entry 3 and 7) with a naphthylphenyldiazene subunit, showed higher potencies after photoirradiation than the ($E_{N\text{-}N}$)-form whereby *m*-**12b** with the C_4-spacer showed a slight tendency towards higher potencies (*m*-**12b**: pIC_{50} = 4.91±0.05, pIC_{50}* = 5.23±0.01; Table 1, entry 3) than *m*-**13b** with a longer linker (*m*-**13b**: pIC_{50} = 4.71±0.07; pIC_{50}* = 5.00±0.05; Table 1, entry 7). For the analogues *para*-substituted compounds *p*-**12b** and *p*-**13b** (Table 1, entry 4 and 8) the difference in their inhibitory activity before and after irradiation (*p*-**12b**: pIC_{50} = 5.06±0.05; pIC_{50}* = 5.13±0.07; Table 1, entry 4; *p*-**13b**: pIC_{50} = 5.19±0.12; pIC_{50}* = 5.21±0.03; Table 2, entry 8) is finally so small that it appears random and not significant. Besides the data for these compounds may also have been affected by thermal back reactions during the [^{3}H]GABA uptake assay, which is the case of the compounds with a half-life of ≈ 1 h is relatively fast (Table 1 entry 4 and 8).

The test results for photoswitchable compounds exhibiting an alkynyl spacer are described in entries 9–16 of Table 2. Similar to the alkene derivatives *m*-**12a** and *m*-**13a** (Table 1, entry 1 and 5) also the *meta*-substituted diphenyldiazenes with an alkenyl linker *m*-**20a** and *m*-**21a** (Table 1, entry 9 and 13) showed higher inhibitory potencies at mGAT1 after irradiation than the non-irradiated species. Actually, *m*-**20a** (Table 1, entry 9) showed the highest increase in potency only surpassed by its enantiopure form (*R*)-*m*-20a, the pIC_{50} for mGAT1 raising from 4.49±0.10 for the pure (*E*)-isomer to of 6.05±0.05 (pIC_{50}) at the photostationary state. As it is known for mGAT1 inhibitors derived from nipecotic acid that their potency resides mainly in the (*R*)-enantiomer in addition, (*R*)-*m*-**20a** (Table 1, entry 9a) was included in this study. In case of (*R*)-m-**20a** the effects observed for *m*-**20a** (Table 1, entry 9) were even more pronounced with the initial potency (pIC_{50} = 4.65±0.05) and the increase in potency upon irradiation being somewhat higher (pIC_{50}* = 6.38±0.04). Thus, (*R*)-m-**20a** represents a highly efficient photoswitchable inhibition at mGAT1 undergoing the substantial increase in inhibitory potency upon irradiation. This is nicely visualized by the two competition curves, for the ground state and the photoequilibrated state in Figure 4. The homologues inhibitor with a C_5 instead of a C_4-spacer *m*-**21a** (Table 1, entry 13) also showed a rise in potency upon irradiation from pIC_{50} = 4.84±0.11 to pIC_{50}* = 5.39±0.07 though to a smaller extent as compared to *m*-**20a**. The *p*-substituted isomers *p*-**20a** and *p*-**21a** (Table 1, entry 10 and 14), in analogy to the compounds with an alkenyl spacer (*p*-**12a** and *p*-**13a**), showed a decrease in potency when irradiated (*p*-**20a**: pIC_{50} = 6.19±0.05; pIC_{50}* = 5.59±0.02; Table 1, entry 10; *p*-**21a**: pIC_{50} = 5.12±0.03, pIC_{50}* = 4.59±0.02; Table 1, entry 14). Thereby, for the (*E*)-form the inhibitor with the shorter spacer, *p*-**20a**, showed a distinctly higher potency at mGAT1 than its homologue *p*-**21a** (compare Table 1 entry 10 with entry 14). In case of the enantiopure (*R*)-*p*-**20a** (Table 1, entry 10a) as compared to the racemic mixture, values rose from 6.19±0.05 to 6.38±0.04 for the (*E*)-isomer and from 5.59±0.2 to 5.84±0.04 for the photochemically equilibrated mixture. Of the compounds with a naphthylphenyldiazene subunit, *m*-**20b** (Table 1, entry 11) exhibited a pIC_{50} of 5.19±0.10 for the (*E*)-form and a pIC_{50}* of 5.71±0.03 for the photochemically equilibrated mixture. In case of the enantiopure compound (*R*)-*m*-**20b** both values were slightly higher (pIC_{50} = 5.37±0.01; pIC_{50}* = 6.00±0.04; Table 1, entry 11a). For *m*-**21b** (Table 1, entry 15) with a C_5-spacer, no significant effect on potency resulted upon irradiation the pIC_{50} and the pIC_{50}* being only nominally different (pIC_{50} = 4.91±0.01; pIC_{50}* = 4.86±0.04; Table 1, entry 15). Compounds *p*-**20b** and *p*-**21b** (Table 1, entry 12 and 16) exhibited higher inhibitory potencies for the (*E*)-isomers than for the irradiated mixtures (*p*-**20b**: pIC_{50} = 6.90±0.04, pIC_{50}* = 6.64±0.03; *p*-**21b**: pIC_{50} = 5.52±0.05, pIC_{50}* = 5.31±0.13; Table 1, entry 12 and 16), but the differences were small. The same applied to the enantiopure compound (*R*)-*p*-**20b**, the (*E*)-form being more potent, but only to a small extent, as compared to the irradiated mixture ((*R*)-*p*-**20b**: pIC_{50} = 7.01±0.4; pIC_{50}* = 6.74±0.05; Table 1, entry 12a). Interestingly, (*E*)-*p*-**20b** and (*R*)-(*E*)-*p*-**20b** exhibited the highest inhibitory potencies at mGAT1 of the compounds studied, but despite that the decrease in potency upon irradiation was quite low. This might be attributed to the limited shift from the (*E*)-to the (*Z*)-form upon irradiation leading to a high content of the more active *E*-form in the photoequilibrated mixture. This rather low degree of photoisomerization is obviously associated with the *p*-substituted naphthylphenyldiazene moiety as it has been observed for all compounds containing this photoresponsive element independent of whether the linker contains a double (Table 1, entry 4 and 8) or a triple bond (Table 1, entry 12, 12a and 16).

Table 1: GABA uptake inhibition at mGAT1, (E)/(Z)-ratios, and thermal relaxation rates of all compounds

Entry	Comp.	pIC_{50} ± SEM[a]			
		mGAT1	mGAT1*[b]	(*E*)/(*Z*)-ratio[c]	$t_{1/2}$[d]
1	*m*-**12a**	4.42±0.02	5.32±0.09	14/86	13 d[e]
2	*p*-**12a**	5.00±0.01	4.43±0.03	11/89	1.1 d[f]
3	*m*-**12b**	4.91±0.05	5.23±0.01	18/82	22 h[g]
4	*p*-**12b**	5.06±0.05	5.13±0.07	36/64	1.2 h[h]
5	*m*-**13a**	4.42±0.01	4.60±0.12	15/85	12 d[g]
6	*p*-**13a**	5.24±0.01	4.63±0.03	12/88	1.9 d[f]
7	*m*-**13b**	4.71±0.07	5.00±0.05	17/83	11 h[g]
8	*p*-**13b**	5.19±0.12	5.21±0.03	36/64	1.5 h[h]
9	*m*-**20a**	4.49±0.10	6.05±0.05	19/81	22 d[f]
9a	(*R*)-*m*-**20a**	4.65±0.03	6.38±0.04	19/81	
10	*p*-**20a**	6.19±0.05	5.59±0.02	09/91	4.8 d[e]
10a	(*R*)-*p*-**20a**	6.38±0.04	5.84±0.04	09/91	
11	*m*-**20b**	5.19±0.10	5.71±0.03	17/83	18 h[g]
11a	(*R*)-*m*-**20b**	5.37±0.01	6.00±0.04	17/83	
12	*p*-**20b**	6.90±0.04	6.64±0.03	36/64	3.4 h[h]
12a	(*R*)-*p*-**20b**	7.01±0.04	6.74±0.05	36/64	
13	*m*-**21a**	4.84±0.11	5.39±0.07	19/81	15 d[g]
14	*p*-**21a**	5.12±0.03	4.59±0.02	10/90	6.8 d[e]
15	*m*-**21b**	4.91±0.07	4.86±0.10	16/84	1.8 d[g]
16	*p*-**21b**	5.52±0.05	5.31±0.13	35/65	4.3 h[h]

[a] experiments were performed three times in triplicates; [b] after photoirradiation, value of the *E/Z*-mixture; [c] at the photostationary state in DMSO; [d] determined by UV/vis-spectroscopy; [e] c = 25 µm, solvent: DMSO-d_6/phosphate-buffer (pH 7.4) = 1:400 (v/v); [f] c = 50 µm, solvent: DMSO-d_6/phosphate-buffer (pH 7.4) = 1:200 (v/v); [g] c = 20 µm, solvent: DMSO-d_6/phosphate-buffer (pH 7.4) = 1:500 (v/v); [h] c = 10 µm, solvent: DMSO-d_6/phosphate-buffer (pH 7.4) = 1:1000 (v/v).

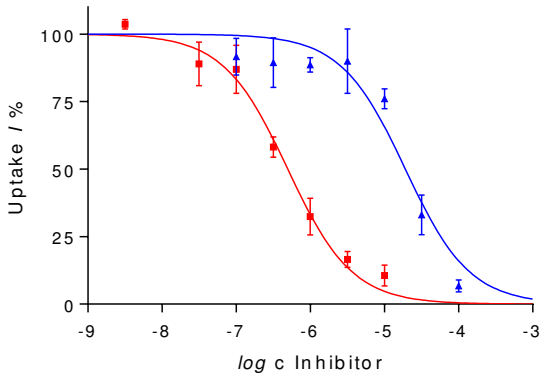

Figure 4: Inhibition of mGAT1 mediated GABA uptake by (*R*)-*m*-**20a** for its ground state (▲) and the photoequilibrated state (■) upon irradiation.

The (*E*)-forms of the enantiopure derivatives (*R*)-*m*-**20a**, (*R*)-*p*-**20a**, (*R*)-*m*-**20b**, and (*R*)-*p*-**20b** (Table 2, entry 9a, 11a, 13a, and 15a) were additionally characterized for their subtype selectivity in favor of mGAT1 as compared to mGAT2-mGAT4. In every case, the pIC_{50} values for mGAT2-4 which are in the range of 4-5 were lower than those for mGAT1 thus indicating that the (*E*)-forms of the tested compounds have a reasonable to good subtype selectivity for mGAT1. Since test compound (*R*)-*m*-**20a** (Table 1, entry 9a) had shown the most pronounced increase in inhibitory potency for the transition from the ground to the photoequilibrated state, the inhibitory potency of the photoequilibrated mixture was also studied at the other GABA transporter subtypes mGAT2-4. The here obtained values for the photoirradiated (*R*)-*m*-**20a** (remaining [^{3}H]GABA uptake in presence of 100 µM inhibitor: mGAT2: 76%, mGAT3: 60%, mGAT4: 57%, see supporting information) do not indicate a considerable activity at these GABA transporters. Hence, the increase in activity of (*R*)-*m*-**20a** by using light is specifically towards mGAT1, whereas the other subtypes remain nearly unaffected.

Overall as predicted by the modeling study described above compounds containing an alkynyl- instead of an alkenyl-spacer turned out to display higher differences in the biological activity at mGAT1 for the pure ($E_{N\text{-}N}$)-form as compared to the photoequilibrated mixture. In addition, ($E_{N\text{-}N}$)-configured alkyne derivatives with a C_4 spacer exhibit higher inhibitory potencies at mGAT1 as compared to their counterparts with a C_5 linker. Only for the two homologous compounds *m*-**20a** and *m*-**21a** with different spacer links the opposite is true.

In case of the *para*-substituted photoswitches with an alkyne linker, the potency at mGAT1 decreases upon irradiation independent of the terminal residue, whether phenyl or naphthyl is present. This decrease is, however, very small. The opposite is true for the analogues *meta*-substituted derivatives except for one compound, *m*-**21b** (table 1, entry 14) that undergoes only an insignificant change in biological activity upon irradiation, all others show a distinct increase in potency. This is most pronounced for racemic *m*-**20a** and its (*R*)-enantiomer (*R*)-*m*-**20a**, with a Δ pIC_{50} of 1.5-1.7 that also nicely highlights the structural functions required for an effective photoswitch for mGAT1, a nipecotic acid moiety, a most common motif for mGAT1 inhibitors provided with a *meta* substituted diphenyldiazene moiety at the amino nitrogen via a rather short and stiff alkyne linker.

Electrophysiology:

An electrophysiology part will be written by M. Eder as soon as respective experiments are done.

Conclusion

In summary, a series of nipecotic acid derivatives, exhibiting N-substituents with different photoresponsive elements attached to the amino nitrogen was synthesized and verified for a distinct potency increase concerning GABA uptake inhibition at mGAT1 upon photoirradiation. The N-substituents were varied regarding the length and saturation degree of the spacer as well as the types of diaryldiazenes and the kind of their substitution. Homology modeling and docking studies delivered first hints of possible appropriate N-substituents for this pupose. By means of the parallel biological test of both the ground state and the isomeric mixture of photoequilibration of each compound, (*R*)-*m*-**20a** was identified as new efficient light controllable inhibitor of this active membrane transporter which, as compared to the already existing photoswitchable mGAT1 inhibitors, contrariwise can be “switched on” through photoirradiation, in fact selectively for this targeted transporter subtype. This property, including the extent to which this effect is associated with, allowing to gain a large difference in biologic activity, is described for the first time for this target and may be a valuable feature for biological studies.

For the further extension of this application in neuroscience, future work will aim at the development of photoswitchable GABA uptake inhibitors with fast thermal relaxation kinetics by making use of specific substituents of the diaryldiazene unit in a next step.

Experimental section

Computational chemistry

For homology modelling of a "closed" GAT1 conformation the 3D structures 2A65[27] was taken from the RCSB protein databank.[33] The only available 3D structure of an "open-to-out" conformation 3F3A[27] was chosen as a template for an "open" GAT1 conformation. The human GAT1 sequence (Swiss-Prot[34] accession number P30531) was aligned to the LeuT sequence using the alignment from Skovstrup et al.[35] The Modeler software version 9v8[36] was used to generate 30 structures of each conformer. The two sodium atoms (Na1 and Na2) located close to the S1 binding site were copied into the hGAT1 structures. A chloride ion was placed into the putative chloride binding site proposed by Zomot et al.[37] and Forrest et al.[38] However, the chloride ion has no direct contact to the active site and its presence has no impact for the docking calculations. The models with the lowest Modeler objective function were checked with PROCHECK[39] for structural consistency and used for docking calculations.

The molecules for docking were exported from our in-house InstantJChem 5.4 database[40] as 2D MDL mol files. Protonation at a pH of 7.4 and the 2D to 3D conversion was done using Chemaxon Marvin 5.4.0.1[41] "cxcalc" and "molconvert". The command line tool "prepare_dpf42.py" was used for conversion into AutoDock4 pdbqt input files. Appropriate protein input files were prepared with the AutoDock tools.[42] Docking grids were calculated with "autogrid4" and docking was performed with AutoDock4 version 4.2.3.[43] The binding region was defined by a 18 Å × 18 Å × 18 Å box centered between the two gate-keeping residues Tyr139 and Phe294. The sidechains of the four gate-keeping residues (Tyr139, Phe294, Arg69, Asp451) were treated as flexible during docking. Ten poses for each molecule have been generated and scored with the AutoDock4 scoring function.[43]

Photoisomerization, Photostationary States, Half-Life.

A 1 mL aliquot of a 10 mM solution in DMSO-d_6 of all test compounds was irradiated from the outside in a quartz glass NMR tube (Wilmad) until the photostationary state was reached (within 10 min). For irradiation either a Rayonet RPR-200 (λ_{max} = 350 nm, compounds **12a**, **13a**, **20a** and **21a**)[29] or a self-built LED-lamp light chamber (λ_{max} = 375 nm, compounds **12b**, **13b**, **20b** and **21b**) was used. The latter consists of a plastic tube in which 48 single LED lamps (3.4-3.6 V, 20 mA) are fitted. After irradiation, a ^{1}H NMR spectrum was recorded immediately by a Jeol Eclipse +500 (500 MHz) spectrometer or an Avance III HD 500 MHz Bruker BioSpin spectrometer. The amount of (*Z*)- and (*E*)-isomers was in every case obtained through integration of the significant aromatic signals of the (*Z*)- and the (*E*)-isomer, giving the ratio factor α, respectively.

For determination of the reachable (*Z*)/(*E*)-ratio under physiological conditions for *m*-**20a**, an aliquot of both the irradiated and non-irradiated 10 mM stem solution in DMSO-d_6 was diluted to a concentration of 25 µM with phosphate buffer (10 mM, pH 7.4) and a UV/Vis spectrum (Cary50 spectrometer, Varian) of these samples was recorded immediately. The absorption of the pure (*Z*)-isomer ($A_{(Z)}$) at 350 nm could then be calculated from the absorption for this irradiated sample ($A_{(E/Z)}$) at 350 nm together with the absorption of the pure (*E*)-isomer ($A_{(E)}$) at 350 nm using following equation:

$$A_{(Z)} = A_{(E)} + (A_{(Z/E)} - A_{(E)}) / \alpha \quad \text{with} \quad \alpha = c_{(Z)} / (c_{(E)} + c_{(Z)})$$

The ideal wavelength for the forward and back isomerization of (*E*)- and (*Z*)-*m*-**20a** under physiological conditions was determined by UV/vis spectroscopy and in situ irradiation of the 25 µM dilution of (*E*)-*m*-**20a** using an FT-600-UMT fiber optic cable (NA 0.39), connected to a Polychrome V system monochromator (TILL photonics) with a 150 W xenon short arc lamp with an output range of 320−680 nm. (*E*)-*m*-**20a** was irradiated at different wavelengths (330, 340, 350, 360, 370 nm) until the photostationary state was reached (within 10 min). The resulting (*Z*)/(*E*)-ratio of *m*-**20a** during an irradiation could be calculated in this way:

$$\alpha = (A_{(Z/E)} - A_{(E)}) / (A_{(Z)} - A_{(E)})$$

The wavelength for back isomerization was determined in a similar way by irradiation of the photoisomerized sample of *m*-**20a** with higher wavelengths (410, 420, 430, 440 nm). The resulting (*Z*)/(*E*)-ratio of *m*-**20a** could again be calculated in the same way.

For determination of the half-life of (*Z*)-*m*-**20a** in DMSO a 1 mL aliquot of the 10 mM stem solution in DMSO-d_6 was irradiated as described initially until the photostationary state was reached (within 10 min). After irradiation, a first ^{1}H NMR spectrum was recorded immediately. The sample was stored in the dark and further ^{1}H NMR spectra were measured in defined time intervals (1, 2, 3, 5, 7, 10, 14, and 21 days). The amount of (*E*)- and (*Z*)-*m*-**20a** was obtained through integration of the affiliated aromatic signals for every spectrum, always giving the remaining proportion of (*Z*)-*m*-**20a** (α). Plotting the time versus α led to a graph which was fit to a single exponential and from which the half-life was calculated.

The half-life of (*Z*)-*m*-**20a** in phosphate buffer was determined by UV/vis spectroscopy due to a worse solubility of this compound in aqueous media. An aliquot of the irradiated 10 mM stem solution in DMSO-d_6 diluted to a concentration of 50 µM with phosphate buffer (10 mM, pH 7.4) and a UV/Vis spectrum (Cary50 spectrometer, Varian) of this sample was recorded immediately. The sample was stored in the dark and further UV spectra were recorded in defined time intervals (1, 2, 3, 5, 7, 10, 14, 21 and 28 days). The respective remaining amount of (*Z*)-*m*-**20a** was obtained for every spectra using the following equation:

$$\alpha_{(t)} = (A_{(t)} - A_{(E)}) / (A_{(Z)} - A_{(E)})$$

Plotting the time versus α again led to a graph which was fit to a single exponential for half-life calculation.

Biological testing:

A 1 mL aliquot of a 10 mM solution of all test compounds in DMSO-d_6 was irradiated as described above until the photostationary state was reached. A 20 µL aliquot was taken from this sample for the dilution series of the biological testing. From the rest, an ^{1}H NMR was measured to determine the (*Z*)/(*E*)-ratio. For the testing of the basic state a 20 µL aliquot of the not irradiated same compound was used in the same experiment.

[^{3}H]GABA uptake experiments towards mGAT1 with irradiated and not irradiated compounds were performed according to a described procedure employing HEK293 human embryonic kidney cells stably expressing the individual GABA transporters[32]. In this case test compounds were diluted under exclusion of daylight in light-protected tubes. About 200000 cells were equilibrated in 3.5 mL polystyrene tubes together with the test compound for 25 min at 25 °C in the dark in a gently shaking water bath. After addition of 25 µL of a solution containing [3H]GABA (2.2 TBq/mmol, ARC, St. Louis, MO, USA) and non-labeled GABA (final concentration 8 nM [3H]GABA and 32 nM non-labeled GABA), the cells were incubated for further 4 min under the same conditions. Incubation was stopped by filtration through Sartorius MGC filters by means of a Brandell M-24R harvester (Brandell, Gaithersburg, MD, USA). Finally, radioactivity on the filters was counted in 3 mL Rotiszint Eco Plus (Roth, Karlsruhe) using a Packard TriCarb 3200 liquid scintillation counter (PerkinElmer LAS, Boston, MA, USA).

Chemistry:

All reactions were carried out under nitrogen atmosphere in distilled solvents. Dioxane and THF were dried over sodium and distilled under nitrogen. Commercial available reagents were used without further purification. Flash column chromatography (CC) was performed using silica gel (40−60 µm). NMR spectra were measured with a Jeol Eclipse +400 (400 MHz) and a Jeol Eclipse +500 (500 MHz) spectrometer or an Avance III HD 400 MHz Bruker BioSpin and an Avance III HD 500 MHz Bruker BioSpin spectrometer. ^{1}H NMR chemical shifts were referenced to TMS or CH_3OH and ^{13}C NMR chemical shifts were referenced to $CHCl_3$ or CH_3OH. The coupling constants were stated with an accuracy of 0.4 Hz. MestreNova software was used for further analysis of the spectra. IR spectra were recorded with a FT-IR spectrometer Paragon 1000 (PerkinElmer). Samples were measured either as KBr pellets or as films on NaCl plates. Mass spectra were measured with a mass spectrometer 59827A with 59980 particle beam LC/MS interface (Hewlett-Packard). High resolution mass spectrometry was carried out with a LTQ FT (ThermoFinnigan), FAB (Xenon, 6 kV, MBA, reference PEG), or a JMS GCmate II (Jeol). Optical rotations were determined by a 241 MC Polarimeter ADP440+ at $\lambda = 589$ cm^{-1}.

Purity testing of the evaluated most active compounds (*R*)-*m*-**20a**, (*R*)-*p*-**20a**, (*R*)-*m*-**20b** and (*R*)-*p*-**20b** was done by means of analytical HPLC on a Merck-Hitachi HPLC system (L7400 intelligent pump and L7400 UV Detector) using elution from a 250 mm × 4mm LiChrospher 100RP-8 column (5 µm particle size), the UV absorbance detection set at 300, 325, 350, 375 and 400 nm, using a flow rate of 1.0 mL/min and phosphate buffer (10 mmol/L)/MeCN = 4:6 as solvent. The purity of all tested compounds was >95%.

General procedure for the Suzuki cross-coupling reactions (GP 1):

Under nitrogen atmosphere $Pd_2(dba)_3$ x $CHCl_3$ (0.01 equiv.), S-Phos (0.04 equiv.), K_3PO_4 (2.0 equiv.) and the aryl iodide (1.0 equiv.) were introduced in a Schlenk tube. The phenylboronic acid ester derivative (1.0 equiv.) was dissolved in dioxane (2 mL/mmol) and added to the reaction mixture. After the addition of H_2O (1 mL/mmol) the mixture was heated to 60 °C and stirred for 6 hours. After cooling down to rt CH_2Cl_2 (10 mL/mmol) and H_2O (10 mL/mmol) were added and the organic components were extracted with CH_2Cl_2. The combined organic layers were dried over Na_2SO_4 and the solvent was removed under reduced pressure. The crude product was purified by CC (eluting with hexane/ethyl acetate = 8:2) to give the corresponding coupling product.

General procedure for the Sonogashira cross-coupling reactions (GP 2):

Under nitrogen atmosphere $Pd(dppf)Cl_2$, (0.05 equiv.), CuI (0.2 equiv) and the corresponding aryl iodide (1.0 equiv) were introduced in a Schlenk tube. The alkyne (1.5 equiv) was dissolved in THF (1 mL/mmol) and the resulting solution was added to the reaction mixture. Triethylamine (1 mL/mmol) was added and the mixture was heated to 60 °C and stirred for 2 hours. After cooling down to rt CH_2Cl_2 (10 mL/mmol) and H_2O (10 mL/mmol) were added and the organic components were extracted with CH_2Cl_2. The combined organic layers were dried over Na_2SO_4 and the solvent was removed under reduced pressure. The crude product was purified by CC (eluting with hexane/ethyl acetate = 8:2) to give the final coupling product.

General procedure for the tosylation of alcohols (GP 3):

The alcohol (1.0 equiv) was dissolved in CH_2Cl_2 (2 mL/mmol) and Et_3N (1.5 equiv) was added. The mixture was cooled to 0 °C, *p*-toluenesulfonylchloride (1.2 equiv) was added and stirred for 24 h (0 °C to rt). Afterwards CH_2Cl_2 (10 mL/mmol) and water (10 mL/mmol) were added and the organic components were extracted with CH_2Cl_2. The combined organic layers were dried over Na_2SO_4 and the solvent was removed under reduced pressure. The crude product was purified by CC (eluting with hexane/CH_2Cl_2 = 1:1) to give the corresponsive tosylated alcohol.

General procedure for the N-alkylation of tosylates (GP 4):

The respective *p*-toluenesulfonic acid ester (1.0 equiv) was dissolved in acetone (1 mL/mmol). Then nipecotic acid ethyl ester (3.0 equiv) was added and the mixture was stirred for 48-72 hours. After the end of the reaction (control by TLC) both CH_2Cl_2 (10 mL/mmol) and of H_2O (10 mL/mmol) were added and the organic components were extracted with CH_2Cl_2. The combined organic layers were dried over Na_2SO_4 and the solvent was removed under reduced pressure. The crude product was purified by CC (eluting with hexane/ethyl acetate = 8:2) to give the corresponsive *N*-alkylated nipecotic acid ethyl ester.

General procedure for the basic hydrolysis of nipecotic acid ethyl esters (GP 5):

The corresponding ester was dissolved in EtOH (5 mL/mmol) and 2N NaOH (1.5 mL/mmol, 3.0 equiv) was added. The mixture was stirred for about 4 h at rt. After the end of the reaction (control by TLC) the solvent was completely removed under reduced pressure. The solid residue was dissolved in 25 ml/mmol of H_2O and the pH was adjusted to 6-7 (indicator paper). The organic product was extracted using CH_2Cl_2 several times. The combined organic layers were dried over Na_2SO_4 and the solvent was removed under reduced pressure. The residue was dissolved in MeOH (5 mL/mmol) followed by the addition of H_2O (50 mL/mmol) and was then freeze dried to give the corresponsive amino acid as amorphous solid.

*Ethyl 1-[(E)-4-{3-[(E)-phenylazo]phenyl}but-3-en-1-yl]piperidine-3-carboxylate (m-**10a**)*

According to GP1 starting from **7** (101 mg, 0.300 mmol), *m*-**9a** (92 mg, 0.30 mmol), $Pd_2(dba)_3$ x $CHCl_3$ (3.2 mg, 3.0 µmol), S-Phos (5.0 mg, 12 µmol) and K_3PO_4 (128 mg. 0.600 mmol) *m*-**10a** was obtained as red oil (92 mg, 78%); R_f ≈ 0.25 (pentane/ethyl acetate = 8:2). IR (NaCl): $\tilde{\nu}$ = 3060, 3024, 2940, 2853, 2804, 1729, 1468, 1446, 1370, 1306, 1179, 1151, 1104, 1032, 963, 788, 765, 691 cm^{-1}. ^1H NMR (500 MHz, $CDCl_3$, 21 °C, TMS): δ = 1.25 (t, *J* = 7.1 Hz, 3H, OCH_2CH_3), 1.46 (qd, *J* = 12.0/3.9 Hz, 1H, $NCH_2CHCH_{ax}H_{eq}$), 1.54–1.65 (m, 1H, $NCH_2CH_{ax}H_{eq}CH_2CH$), 1.74 (dp, *J* = 15.3/3.8 Hz, 1H, $NCH_2CH_{ax}H_{eq}CH_2CH$), 1.91–2.00 (m, 1H, $NCH_2CHCH_{ax}H_{eq}$), 2.05 (td, *J* = 11.0/3.0 Hz, 1H, $NCH_{ax}H_{eq}CH_2CH_2CH$), 2.22 (t, *J* = 10.6 Hz, 1H, $NCH_{ax}H_{eq}CH$), 2.41–2.49 (m, 2H, NCH_2CH_2CH=CH), 2.49–2.55 (m, 2H, NCH_2CH_2CH=CH), 2.58 (tt, *J* = 10.6/3.8 Hz, 1H, NCH_2CH_{ax}), 2.82 (d_{br}, *J* = 10.9 Hz, 1H, $NCH_{ax}H_{eq}CH_2CH_2CH$), 3.05 (d_{br}, *J* = 10.8 Hz, 1H, $NCH_{ax}H_{eq}CH$), 4.13 (q, *J* = 7.1 Hz, 2H, OCH_2CH_3), 6.33 (dt, *J* = 15.8/6.8 Hz, 1H, CH_2CH=CHC), 6.52 (d, *J* = 16.0 Hz, 1H, CH_2CH=CHC), 7.41–7.45 (m, 2H, CH=CHCCHC, CH=CHCCHCH), 7.45–7.49 (m, 1H, N=NCCHCHCH), 7.49–7.55 (m, 2H, N=NCCHCHCH), 7.73–7.79 (m, 1H, CH=CHCCHCH), 7.88–7.96 (m, 3H, CH=CHCCHCC, N=NCCHCHCH) ppm. ^{13}C NMR (126 MHz, $CDCl_3$, 21 °C, TMS): δ = 14.17 (q, 1C, OCH_2CH_3), 24.58 (t, 1C, $NCH_2CH_2CH_2CH$), 26.93 (t, 1C, NCH_2CHCH_2), 30.60 (t, 1C, NCH_2CH_2CH=CH), 41.84 (d, 1C, NCH_2CH), 53.67 (t, 1C, $NCH_2CH_2CH_2CH$), 55.30 (t, 1C, NCH_2CH), 58.37 (t, 1C, NCH_2CH_2CH=CH), 60.26 (t, 1C, OCH_2CH_3), 120.11 (d, 1C, CH=CHCCHCCH), 121.37 (d, 1C, CH=CHCCHCH), 122.77 (d, 2C, N=NCCHCHCH), 128.52 (d, 1C, CH=CHCCHCH), 129.02 (d, 2C, N=NCCHCHCH), 129.10 (d, 1C, CH=CHCCHC), 129.70 (d, 1C, CH=CHCCH), 130.16 (d, 1C, CH=CHCCH), 130.94 (d, 1C, N=NCCHCHCH), 138.65 (s, 1C, CH=CHCCHC), 152.55 (s, 1C, N=NCCHCHCH), 152.79 (s, 1C, CH=CHCCHC), 174.18 (s, 1C, C=O) ppm. MS (ESI^+) *m/z*: 392 $[M+H]^+$. HRMS (ESI^+): $[M+H]^+$ calcd for $C_{24}H_{30}O_2N_3$: 392.2338, found 392.2327.

*Ethyl 1-[(E)-4-{4-[(E)-phenylazo]phenyl}but-3-en-1-yl]piperidine-3-carboxylate (p-**10a**)*

According to GP1 starting from **7** (101 mg, 0.300 mmol), *p*-**9a** (92 mg, 0.30 mmol), $Pd_2(dba)_3$ x $CHCl_3$ (3.2 mg, 3.0 µmol), S-Phos (5.0 mg, 12 µmol) and K_3PO_4 (128 mg. 0.600 mmol) *p*-**10a** was obtained as red oil (100 mg, 85%); R_f ≈ 0.25 (pentane/ethyl acetate = 8:2). IR (NaCl): $\tilde{\nu}$ = 3433, 3060, 3030, 2977, 2940, 2853, 2805, 2770, 1729, 1648, 1597, 1466, 1441, 1370, 1302, 1226, 1179, 1152, 1100, 1032, 966, 859, 767, 688 cm^{-1}. ^1H NMR (500 MHz, $CDCl_3$, 21 °C, TMS): δ = 1.25 (t, *J* = 7.1 Hz, 3H, OCH_2CH_3), 1.46 (qd, *J* = 11.9/3.9 Hz, 1H, $NCH_2CHCH_{ax}H_{eq}$), 1.54–1.64 (m, 1H, $NCH_2CH_{ax}H_{eq}CH_2CH$), 1.74 (dp, *J* = 13.4/3.7 Hz, 1H, $NCH_2CH_{ax}H_{eq}CH_2CH$), 1.95 (dq, *J* = 13.1/3.7 Hz, 1H, $NCH_2CHCH_{ax}H_{eq}$), 2.05 (td, *J* = 10.9/2.4 Hz, 1H, $NCH_{ax}H_{eq}CH_2CH_2CH$), 2.22 (t, *J* = 10.6 Hz, 1H, $NCH_{ax}H_{eq}CH$), 2.41–2.49 (m, 2H, NCH_2CH_2CH=CH), 2.49–2.55 (m, 2H, NCH_2CH_2CH=CH), 2.58 (tt, *J* = 10.7/3.8 Hz, 1H, NCH_2CH_{ax}), 2.81 (d_{br}, *J* = 11.0 Hz, 1H, $NCH_{ax}H_{eq}CH_2CH_2CH$), 3.04 (d_{br}, *J* = 9.8 Hz, 1H, $NCH_{ax}H_{eq}CH$), 4.13 (q, *J* = 7.1 Hz, 2H, OCH_2CH_3), 6.33 (dt, *J* = 15.9/6.8 Hz, 1H, CH_2CH=CHC), 6.48 (d, *J* = 16.0 Hz, 1H, CH_2CH=CHC), 7.43–7.52 (m, 5H, N=NCCHCHCH, CH=CHCCHCHC, N=NCCHCHCH), 7.86–7.92 (m, 4H, CH=CHCCHCHC, N=NCCHCHCH) ppm. ^{13}C NMR (126 MHz, $CDCl_3$, 21 °C, TMS): δ = 14.16 (q, 1C, OCH_2CH_3), 24.56 (t, 1C, $NCH_2CH_2CH_2CH$), 26.91 (t, 1C, NCH_2CHCH_2), 30.72 (t, 1C, NCH_2CHCH_2), 41.81 (d, 1C, NCH_2CH), 53.65 (t, 1C, $NCH_2CH_2CH_2CH$), 55.28 (t, 1C, NCH_2CH), 58.27 (t, 1C, NCH_2CH_2CH=CH), 60.26 (t, 1C, OCH_2CH_3), 122.70 (d, 2C, N=NCCHCHCH), 123.19 (d, 2C, CH=CHCCHCHC), 126.54 (d, 2C, CH=CHCCHCHC), 128.99 (d, 2C, N=NCCHCHCH), 130.23 (d, 1C, CH=CHCCH), 130.56 (d, 1C, CH=CHCCH), 130.74 (d, 1C, N=NCCHCHCH), 140.34 (s, 1C, CH_2CH=CHC), 151.41 (s, 1C, CH=CHCCHCHC), 152.65 (s, 1C, N=NCCHCHCH), 174.16 (s, 1C, C=O) ppm. MS (CI^+) *m/z*: 406 $[M+H]^+$. HRMS (EI^+): M^+ calcd for $C_{24}H_{29}O_2N_3$: 391.2260, found 391.2260.

*Ethyl 1-[(E)-4-{3-[(E)-1-naphthylazo]phenyl}but-3-en-1-yl]piperidine-3-carboxylate (m-**10b**)*

According to GP1 starting from **7** (101 mg, 0.300 mmol), *m*-**9b** (107 mg, 0.30 mmol), $Pd_2(dba)_3$ x $CHCl_3$ (3.2 mg, 3.0 µmol), S-Phos (5.0 mg, 12 µmol) and K_3PO_4 (128 mg. 0.600 mmol) *m*-**10b** was obtained as red oil (106 mg, 80%); R_f ≈ 0.20 (pentane/ethyl acetate = 8:2). IR (NaCl): $\tilde{\nu}$ = 3052, 3024, 2940, 2852, 2804, 2768, 1728, 1600, 1508, 1467, 1439, 1370, 1306, 1179, 1151, 1104, 1032, 963, 802, 772 cm^{-1}. ^1H NMR (500 MHz, $CDCl_3$, 21 °C, TMS): δ = 1.25 (t, *J* = 7.1 Hz, 3H, OCH_2CH_3), 1.46 (qd, *J* = 12.0/4.0 Hz, 1H, $NCH_2CHCH_{ax}H_{eq}$), 1.54–1.66 (m, 1H, $NCH_2CH_{ax}H_{eq}CH_2CH$), 1.75 (dp, *J* = 13.2/3.6 Hz, 1H, $NCH_2CH_{ax}H_{eq}CH_2CH$), 1.96 (dq, *J* = 13.1/3.7 Hz, 1H, $NCH_2CHCH_{ax}H_{eq}$), 2.06 (td, *J* = 10.9/2.3 Hz, 1H, $NCH_{ax}H_{eq}CH_2CH_2CH$), 2.23 (t, *J* = 10.6 Hz, 1H, $NCH_{ax}H_{eq}CH$), 2.44–2.51 (m, 2H, NCH_2CH_2CH=CH), 2.53–2.63 (m, 3H, NCH_2CH_2CH=CH, NCH_2CH_{ax}), 2.83 (d, *J* = 11.0 Hz, 1H, $NCH_{ax}H_{eq}CH_2CH_2CH$), 3.06 (d, *J* = 9.8 Hz, 1H, $NCH_{ax}H_{eq}CH$), 4.14 (q, *J* = 7.1 Hz, 2H, OCH_2CH_3), 6.37 (dt, *J* = 15.9/6.8 Hz, 1H, CH_2CH=CHC), 6.56 (d, *J* = 15.9 Hz, 1H, CH_2CH=CHC), 7.46–7.50 (m, 2H, CH=CHCCHCH, CH=CHCCHCCH), 7.54–7.61 (m, 2H, N=NCCHCHCH, N=NCCCHCHCH), 7.66 (ddd, *J* = 8.4/6.8/1.3 Hz, 1H, N=NCCCHCH), 7.81 (dd, *J* = 7.5/1.1 Hz, 1H, N=NCCHCHCH), 7.86–7.91 (m, 1H, CH=CHCCHCH), 7.93 (d, *J* = 8.2 Hz, 1H, N=NCCCHCHCHCH), 7.98 (d, *J* = 8.1 Hz, 1H, N=NCCHCHCH), 8.02 (s, 1H, CH=CHCCHC), 8.93 (d, *J* = 8.4 Hz, 1H, N=NCCCH) ppm. ^{13}C NMR (126 MHz, $CDCl_3$, 21 °C, TMS): δ = 14.20 (q, 1C, OCH_2CH_3), 24.61 (t, 1C, $NCH_2CH_2CH_2CH$), 26.97 (t, 1C, NCH_2CHCH_2), 30.63 (t, 1C, NCH_2CH_2CH=CH), 41.88 (d, 1C, NCH_2CH), 53.70 (t, 1C, $NCH_2CH_2CH_2CH$), 55.34 (t, 1C, NCH_2CH), 58.40 (t, 1C, NCH_2CH_2CH=CH), 60.30 (t, 1C, OCH_2CH_3), 111.85 (d, 1C, N=NCCHCHCH), 120.82 (d, 1C, CH=CHCCHCH), 121.44 (d, 1C, CH=CHCCHCH), 123.42 (d, 1C, N=NCCCH), 125.60 (d, 1C, N=NCCHCHCH), 126.43 (d, 1C, N=NCCCHCHCH), 126.80 (d, 1C, N=NCCCHCH), 127.90 (d, 1C, N=NCCCHCHCHCH), 128.55 (d, 1C, CH=CHCCHCH), 129.18 (d, 1C, CH=CHCCHCCH), 129.80 (d, 1C, CH=CHCCH), 130.23 (d, 1C, CH=CHCCH), 131.22 (s, 1C, N=NCCCH), 131.28 (d, 1C, N=NCCHCHCH), 134.24 (s, 1C, N=NCCHCHCHC), 138.75 (s, 1C, CH=CHCCHC), 147.76 (s, 1C, N=NCCHCHCH), 153.37 (s, 1C, CH=CHCCHC), 174.21 (s, 1C, C=O) ppm. MS (ESI^+) *m/z*: 442 $[M+H]^+$. HRMS (EI^+): M^+ calcd for $C_{28}H_{31}O_2N_3$: 441.2416, found 441.2403.

*Ethyl 1-[(E)-4-{4-[(E)-1-naphthylazo]phenyl}but-3-en-1-yl]piperidine-3-carboxylate (p-**10b**)*

According to GP1 starting from **7** (101 mg, 0.300 mmol), *p*-**9b** (107 mg, 0.30 mmol), $Pd_2(dba)_3$ x $CHCl_3$ (5.4 mg, 5.0 µmol), S-Phos (5.0 mg, 12 µmol) and K_3PO_4 (128 mg. 0.600 mmol) *p*-**10b** was obtained as red oil (111 mg, 84%); R_f ≈ 0.20 (pentane/ethyl acetate = 8:2). IR (NaCl): $\tilde{\nu}$ = 3050, 3020, 2938, 2856, 2805, 2767, 1729, 1646, 1596, 1508, 1498, 1466, 1444, 1387, 1371, 1310, 1220, 1178, 1152, 1101, 1031, 966, 853, 802, 772 cm^{-1}. ^1H NMR (500 MHz, $CDCl_3$, 21 °C, TMS): δ = 1.26 (t, *J* = 7.1 Hz, 3H, OCH_2CH_3), 1.47 (qd, *J* = 12.0/3.6 Hz, 1H, $NCH_2CHCH_{ax}H_{eq}$), 1.56–1.66 (m, 1H, $NCH_2CH_{ax}H_{eq}CH_2CH$), 1.76 (dp, *J* = 15.0/3.8 Hz, 1H, $NCH_2CH_{ax}H_{eq}CH_2CH$), 1.96 (dq, *J* = 13.0/3.7 Hz, 1H, $NCH_2CHCH_{ax}H_{eq}$), 2.06 (td, *J* = 11.0/2.8 Hz, 1H, $NCH_{ax}H_{eq}CH_2CH_2CH$), 2.23 (t, *J* = 10.7 Hz, 1H, $NCH_{ax}H_{eq}CH$), 2.43–2.51 (m, 2H, NCH_2CH_2CH=CH), 2.51–2.63 (m, 3H, NCH_2CH_2CH=CH, NCH_2CH_{ax}), 2.83 (d_{br}, *J* = 11.2 Hz, 1H, $NCH_{ax}H_{eq}CH_2CH_2CH$), 3.06 (d_{br}, *J* = 10.7 Hz, 1H, $NCH_{ax}H_{eq}CH$), 4.14 (q, *J* = 7.1 Hz, 2H, OCH_2CH_3), 6.36 (dt, *J* = 15.9/6.8 Hz, 1H, CH_2CH=CHC), 6.52 (d, *J* = 16.0 Hz, 1H, CH_2CH=CHC), 7.51 (d, *J* = 8.5 Hz, 2H, CH=CHCCHCHC), 7.54–7.61 (m, 2H, N=NCCHCHCH, N=NCCCHCHCH), 7.65 (ddd, *J* = 8.3/6.8/1.3 Hz, 1H, N=NCCCHCH), 7.82 (dd, *J* = 7.5/1.0 Hz, 1H, N=NCCCHCHCHCH), 7.92 (d, *J* = 8.1 Hz, 1H, N=NCCHCHCH), 7.97 (d, *J* = 8.1 Hz, 1H, N=NCCHCHCH), 8.00 (d, *J* = 8.5 Hz, 2H, CH=CHCCHCHC), 8.93 (d, *J* = 8.5 Hz, 1H, N=NCCCH) ppm. ^{13}C NMR (126 MHz, $CDCl_3$, 21 °C, TMS): δ = 14.21 (q, 1C, OCH_2CH_3), 24.62 (t, 1C, $NCH_2CH_2CH_2CH$), 26.97

(t, 1C, NCH_2CHCH_2), 30.79 (t, 1C, NCH_2CH_2CH=CH), 41.88 (d, 1C, NCH_2CH), 53.71 (t, 1C, $NCH_2CH_2CH_2CH$), 55.34 (t, 1C, NCH_2CH), 58.33 (t, 1C, NCH_2CH_2CH=CH), 60.32 (t, 1C, OCH_2CH_3), 111.73 (d, 1C, N=NCCCHCHCHCH), 123.44 (d, 1C, N=NCCCH), 123.55 (d, 2C, CH=CHCCHCHC), 125.63 (d, 1C, N=NCCHCHCH), 126.40 (d, 1C, N=NCCCHCHCH), 126.64 (d, 2C, CH=CHCCHCHC), 126.73 (d, 1C, N=NCCCHCH), 127.89 (d, 1C, N=NCCHCHCH), 130.30 (d, 1C, CH=CHCCH), 130.72 (d, 1C, CH=CHCCH), 131.11 (d, 1C, N=NCCHCHCH), 131.27 (s, 1C, N=NCCCH), 134.25 (s, 1C, N=NCCHCHCHCH), 140.46 (s, 1C, CH_2CH=CHCH), 147.82 (s, 1C, N=NCCHCHCH), 152.07 (s, 1C, CH=CHCCHCHC), 174.22 (s, 1C, C=O) ppm. MS (ESI^+) *m/z*: 442 $[M+H]^+$. HRMS (ESI^+): $[M+H]^+$ calcd for $C_{28}H_{32}O_2N_3$: 442.2495, found 442.2486.

*Ethyl 1-[(E)-5-{3-[(E)-phenylazo]phenyl}pent-4-en-1-yl]piperidine-3-carboxylate (m-**11a**)*

According to GP1 starting from **8** (105 mg, 0.300 mmol), *m*-**9a** (92 mg, 0.30 mmol), $Pd_2(dba)_3$ x $CHCl_3$ (3.2 mg, 3.0 µmol), S-Phos (5.0 mg, 12 µmol) and K_3PO_4 (128 mg. 0.600 mmol) *m*-**11a** was obtained as red oil (98 mg, 81%); R_f ≈ 0.20 (pentane/ethyl acetate = 8:2). IR (NaCl): $\tilde{\nu}$ = 3060, 3023, 2939, 2854, 2804, 2767, 1729, 1468, 1445, 1370, 1309, 1178, 1151, 1095, 1031, 963, 787, 764, 691 cm^{-1}. ^1H NMR (500 MHz, $CDCl_3$, 21 °C, TMS): δ = 1.24 (t, *J* = 7.1 Hz, 3H, OCH_2CH_3), 1.44 (qd, *J* = 12.1/3.4 Hz, 1H, $NCH_2CHCH_{ax}H_{eq}$), 1.52–1.64 (m, 1H, $NCH_2CH_{ax}H_{eq}CH_2CH$), 1.66–1.77 (m, 3H, $NCH_2CH_2CH_2CH$=CH, $NCH_2CH_{ax}H_{eq}CH_2CH$), 1.88–2.03 (m, 2H, $NCH_2CHCH_{ax}H_{eq}$, $NCH_{ax}H_{eq}CH_2CH_2CH$), 2.15 (t, *J* = 9.6 Hz, 1H, $NCH_{ax}H_{eq}CH$), 2.26 (q, *J* = 6.9 Hz, 2H, CH_2CH=CHC), 2.36–2.42 (m, 2H, $NCH_2CH_2CH_2CH$=CH), 2.57 (tt, *J* = 10.7/3.8 Hz, 1H, NCH_2CH_{ax}), 2.78 (d_{br}, *J* = 10.7 Hz, 1H, $NCH_{ax}H_{eq}CH_2CH_2CH$), 3.01 (d_{br}, *J* = 11.2 Hz, 1H, $NCH_{ax}H_{eq}CH$), 4.12 (q, *J* = 7.1 Hz, 2H, OCH_2CH_3), 6.35 (dt, *J* = 15.8/6.8 Hz, 1H, CH_2CH=CHC), 6.47 (d, *J* = 15.8 Hz, 1H, CH_2CH=CHC), 7.40–7.44 (m, 2H, CH=CHCCHC, CH=CHCCHCH), 7.44–7.49 (m, 1H, N=NCCHCHCH), 7.49–7.53 (m, 2H, N=NCCHCHCH), 7.70–7.79 (m, 1H, CH=CHCCHCH), 7.87–7.94 (m, 3H, CH=CHCCHCCH, N=NCCHCHCH) ppm. ^{13}C NMR (126 MHz, $CDCl_3$, 21 °C, TMS): δ = 14.17 (q, 1C, OCH_2CH_3), 24.58 (t, 1C, $NCH_2CH_2CH_2CH$), 26.41 (t, 1 C, NCH_2CHCH_2), 26.97 (t, 1C, $NCH_2CH_2CH_2CH$=CH), 30.90 (t, 1C, CH_2CH=CHC), 41.86 (d, 1C, NCH_2CH), 53.80 (t, 1C, $NCH_2CH_2CH_2CH$), 55.43 (t, 1C, NCH_2CH), 58.27 (t, 1C, $NCH_2CH_2CH_2CH$=CH), 60.23 (t, 1C, OCH_2CH_3), 120.03 (d, 1C, CH=CHCCHCCH), 121.30 (d, 1C, CH=CHCCHCH), 122.77 (d, 2C, N=NCCHCHCH), 128.46 (d, 1C, CH=CHCCHCH), 129.01 (d, 2C, N=NCCHCHCH), 129.09 (d, 1C, CH=CHCCHC), 129.36 (d, 1C, CH_2CH=CHC), 130.92 (d, 1C, CH_2CH=CHC), 131.70 (d, 1C, N=NCCHCHCH), 138.77 (s, 1C, CH=CHCCHC), 152.55 (s, 1C, N=NCCHCHCH), 152.80 (s, 1C, CH=CHCCHC), 174.22 (s, 1C, C=O) ppm. MS (ESI^+) *m/z*: 406 $[M+H]^+$. HRMS (ESI^+): $[M+H]^+$ calcd for $C_{25}H_{32}O_2N_3$: 406.2494, found 406.2485.

*Ethyl 1-[(E)-5-{4-[(E)-phenylazo]phenyl}pent-4-en-1-yl]piperidine-3-carboxylate (p-**11a**)*

According to GP1 starting from **8** (105 mg, 0.300 mmol), *p*-**9a** (92 mg, 0.30 mmol), $Pd_2(dba)_3$ x $CHCl_3$ (3.2 mg, 3.0 µmol), S-Phos (5.0 mg, 12 µmol) and K_3PO_4 (128 mg. 0.600 mmol) *p*-**11a** was obtained as red oil (101 mg, 83%); R_f ≈ 0.20 (pentane/ethyl acetate = 8:2). IR (NaCl): $\tilde{\nu}$ = 3386, 3060, 3031, 2938, 2863, 2805, 2769, 1729, 1648, 1597, 1466, 1440, 1370, 1303, 1178, 1152, 1101, 1031, 966, 856, 766, 687 cm^{-1}. ^1H NMR (500 MHz, $CDCl_3$, 21 °C, TMS): δ = 1.25 (t, *J* = 7.1 Hz, 3H, OCH_2CH_3), 1.45 (qd, *J* = 12.0/3.9 Hz, 1H, $NCH_2CHCH_{ax}H_{eq}$), 1.52–1.63 (m, 1H, $NCH_2CH_{ax}H_{eq}CH_2CH$), 1.66–1.76 (m, 3H, $NCH_2CH_2CH_2CH$=CH, $NCH_2CH_{ax}H_{eq}CH_2CH$), 1.90–2.02 (m, 2H, $NCH_2CHCH_{ax}H_{eq}$, $NCH_{ax}H_{eq}CH_2CH_2CH$), 2.16 (t, *J* = 10.8 Hz, 1H, $NCH_{ax}H_{eq}CH$), 2.23–2.29 (m, 2H, CH_2CH=CHC), 2.37–2.42 (m, 2H, $NCH_2CH_2CH_2CH$=CH), 2.57 (tt, *J* = 10.6/3.8 Hz, 1H, NCH_2CH_{ax}), 2.77 (d_{br}, *J* = 11.0 Hz, 1H, $NCH_{ax}H_{eq}CH_2CH_2CH$), 3.00 (d_{br}, *J* = 9.7 Hz, 1H, $NCH_{ax}H_{eq}CH$), 4.13 (q, *J* = 7.1 Hz, 2H, OCH_2CH_3), 6.35 (dt, *J* = 15.8/6.7 Hz, 1H, CH_2CH=CHC), 6.45 (d, *J* = 15.9 Hz, 1H, CH_2CH=CHC), 7.43–7.52 (m, 5H, N=NCCHCH, CH=CHCCHCHC, N=NCCHCHCH), 7.86–7.92 (m, 4H, CH=CHCCHCHC, N=NCCHCHCH) ppm. ^{13}C NMR (126 MHz, $CDCl_3$, 21 °C, TMS): δ = 14.17 (q, 1C, OCH_2CH_3), 24.57 (t, 1C, $NCH_2CH_2CH_2CH$), 26.36 (t, 1C, $NCH_2CH_2CH_2CH$=CH), 26.96 (t, 1C, NCH_2CHCH_2), 31.03 (t, 1C, CH_2CH=CHC), 41.84 (d, 1C, NCH_2CH), 53.79 (t, 1C, $NCH_2CH_2CH_2CH$), 55.41 (t, 1C, NCH_2CH), 58.25 (t, 1C, $NCH_2CH_2CH_2CH$=CH), 60.22 (t, 1C, OCH_2CH_3), 122.69 (d, 2C, N=NCCHCHCH), 123.20 (d, 2C, CH=CHCCHCHC), 126.47 (d, 2C, CH=CHCCHCHC), 128.98 (d, 2C, N=NCCHCHCH), 129.43 (d, 1C, CH_2CH=CHC), 130.71 (d, 1C, CH_2CH=CHC), 132.59 (d, 1C, N=NCCHCHCH), 140.49 (s, 1C, CH_2CH=CHCH), 151.36 (s, 1C, CH=CHCCHCHC), 152.66 (s, 1C, N=NCCHCHCH), 174.19 (s, 1C, C=O). MS (Cl^+) *m/z*: 406 $[M+H]^+$. HRMS (EI^+): M^+ calcd for $C_{25}H_{31}O_2N_3$: 405.2416, found 405.2424.

*Ethyl 1-[(E)-5-{3-[(E)-1-naphthylazo]phenyl}pent-4-en-1-yl]piperidine-3-carboxylate (m-**11b**)*

According to GP1 starting from **8** (105 mg, 0.300 mmol), *m*-**9b** (107 mg, 0.30 mmol), $Pd_2(dba)_3$ x $CHCl_3$ (3.2 mg, 3.0 µmol), S-Phos (5.0 mg, 12 µmol) and K_3PO_4 (128 mg. 0.600 mmol) *m*-**11b** was obtained as red oil (112 mg, 82%); R_f ≈ 0.15 (pentane/ethyl acetate = 8:2). IR (NaCl): $\tilde{\nu}$ = 3332, 3052, 3024, 2938, 2861, 2805, 2768, 1729, 1600, 1508, 1467, 1442, 1371, 1310, 1178, 1151, 1031, 963, 802, 772 cm^{-1}. ^1H NMR (500 MHz, $CDCl_3$, 21 °C, TMS): δ = 1.25 (t, *J* = 7.1 Hz, 3H, OCH_2CH_3), 1.45 (qd, *J* = 12.1/3.6 Hz, 1H, $NCH_2CHCH_{ax}H_{eq}$), 1.52–1.66 (m, 1H, $NCH_2CH_{ax}H_{eq}CH_2CH$), 1.68–1.78 (m, 3H,

$NCH_2CH_{ax}H_{eq}CH_2CH$, $NCH_2CH_2CH_2CH{=}CH$), 1.90–2.05 (m, 2H, $NCH_2CHCH_{ax}H_{eq}$, $NCH_{ax}H_{eq}CH_2CH_2CH$), 2.16 (t, *J* = 10.5 Hz, 1H, $NCH_2CHCH_{ax}H_{eq}$), 2.28 (q, *J* = 6.9 Hz, 2H, $CH_2CH{=}CHC$), 2.37–2.46 (m, 2H, $NCH_2CH_2CH_2CH{=}CH$), 2.58 (tt, *J* = 10.6/3.8 Hz, 1H, NCH_2CH_{ax}), 2.80 (d_{br}, *J* = 11.3 Hz, 1H, $NCH_{ax}H_{eq}CH_2CH_2CH$), 3.03 (d_{br}, *J* = 10.5 Hz, 1H, $NCH_{ax}H_{eq}CH$), 4.13 (q, *J* = 7.1 Hz, 2H, OCH_2CH_3), 6.38 (dt, *J* = 15.8/6.8 Hz, 1H, $CH_2CH{=}CHC$), 6.52 (d, *J* = 15.9 Hz, 1H, $CH_2CH{=}CHC$), 7.45–7.50 (m, 2H, $CH{=}CHCCHCH$, $CH{=}CHCCHCCH$), 7.54–7.61 (m, 2H, $N{=}NCCHCHCH$, $N{=}NCCCHCHCH$), 7.66 (ddd, *J* = 8.4/6.8/1.3 Hz, 1H, $N{=}NCCCHCH$), 7.81 (dd, *J* = 7.5/1.1 Hz, 1H, $N{=}NCCHCHCH$), 7.86–7.91 (m, 1H, $CH{=}CHCCHCH$), 7.93 (d, *J* = 8.2 Hz, 1H, $N{=}NCCCHCHCHCH$), 7.98 (d, *J* = 8.2 Hz, 1H, $N{=}NCCHCHCH$), 8.02 (s, 1H, $CH{=}CHCCHC$), 8.93 (d, *J* = 8.4 Hz, 1H, $N{=}NCCCH$) ppm. ^{13}C NMR (126 MHz, $CDCl_3$, 21 °C, TMS): δ = 14.18 (q, 1C, OCH_2CH_3), 24.58 (t, 1C, $NCH_2CH_2CH_2CH$), 26.41 (t, 1C, $NCH_2CH_2CH_2CH{=}CH$), 26.98 (t, 1C, NCH_2CHCH_2), 30.92 (t, 1C, $CH_2CH{=}CHC$), 41.85 (d, 1C, NCH_2CH), 53.81 (t, 1C, $NCH_2CH_2CH_2CH$), 55.43 (t, 1C, NCH_2CH), 58.31 (t, 1C, $NCH_2CH_2CH_2CH{=}CH$), 60.26 (t, 1C, OCH_2CH_3), 111.81 (d, 1C, $N{=}NCCHCHCH$), 120.68 (d, 1C, $CH{=}CHCCHC$), 121.40 (d, 1C, $CH{=}CHCCHCH$), 123.41 (d, 1C, $N{=}NCCCH$), 125.58 (d, 1C, $N{=}NCCHCHCH$), 126.41 (d, 1C, $N{=}NCCCHCHCH$), 126.79 (d, 1C, $N{=}NCCCHCH$), 127.88 (d, 1C, $N{=}NCCCHCHCHCH$), 128.49 (d, 1C, $CH{=}CHCCHCH$), 129.16 (d, 1C, $CH{=}CHCCHCCH$), 129.41 (d, 1C, $CH_2CH{=}CHC$), 131.20 (s, 1C, $N{=}NCCCH$), 131.26 (d, 1C, $N{=}NCCHCHCH$), 131.75 (d, 1C, $CH_2CH{=}CHC$), 134.21 (s, 1C, $N{=}NCCHCHCHC$), 138.83 (s, 1C, $CH{=}CHCCHC$), 147.72 (s, 1C, $N{=}NCCHCHCH$), 153.34 (s, 1C, $CH{=}CHCCHC$), 174.23 (s, 1C, C=O) ppm. MS (ESI^+) *m/z*: 456 $[M+H]^+$. HRMS (EI^+): M^+ calcd for $C_{29}H_{33}O_2N_3$: 455.2572, found 455.2574.

*Ethyl 1-[(E)-5-{4-[(E)-1-naphthylazo]phenyl}pent-4-en-1-yl]piperidine-3-carboxylate (p-**11b**)*

According to GP1 starting from **8** (105 mg, 0.300 mmol), *p*-**9b** (107 mg, 0.30 mmol), $Pd_2(dba)_3$ x $CHCl_3$ (3.2 mg, 3.0 µmol), S-Phos (5.0 mg, 12 µmol) and K_3PO_4 (128 mg. 0.600 mmol) *p*-**11b** was obtained as red oil (119 mg, 87%); R_f ≈ 0.15 (pentane/ethyl acetate = 8:2). IR (NaCl): $\tilde{\nu}$ = 3050, 3028, 2940, 2852, 2804, 2769, 1729, 1646, 1597, 1508, 1498, 1466, 1446, 1387, 1371, 1310, 1221, 1179, 1153, 1100, 1032, 966, 858, 802, 772 cm^{-1}. ^{1}H NMR (500 MHz, $CDCl_3$, 21 °C, TMS): δ = 1.26 (t, *J* = 7.1 Hz, 3H, OCH_2CH_3), 1.45 (qd, *J* = 11.9/4.0 Hz, 1H, $NCH_2CHCH_{ax}H_{eq}$), 1.54–1.64 (m, 1H, $NCH_2CH_{ax}H_{eq}CH_2CH$), 1.67–1.78 (m, 3H, $NCH_{ax}H_{eq}CH_2CH_2CH$, $NCH_2CH_2CH_2CH{=}CH$), 1.92–2.04 (m, 2H, $NCH_2CHCH_{ax}H_{eq}$, $NCH_{ax}H_{eq}CH_2CH_2CH$), 2.16 (t, *J* = 10.2 Hz, 1H, $NCH_{ax}H_{eq}CH$), 2.28 (q, *J* = 6.9 Hz, 2H, $CH_2CH{=}CHC$), 2.39–2.44 (m, 2H, $NCH_2CH_2CH_2CH{=}CH$), 2.58 (tt, *J* = 10.7/3.8 Hz, 1H, NCH_2CH_{ax}), 2.79 (d_{br}, *J* = 11.5 Hz, 1H, $NCH_{ax}H_{eq}CH_2CH_2CH$), 3.02 (d_{br}, *J* = 10.7 Hz, 1H, $NCH_{ax}H_{eq}CH$), 4.14 (q, *J* = 7.1 Hz, 2H, OCH_2CH_3), 6.38 (dt, *J* = 15.8/6.7 Hz, 1H, $CH_2CH{=}CHC$), 6.48 (d, *J* = 15.9 Hz, 1H, $CH_2CH{=}CHC$), 7.51 (d, *J* = 8.5 Hz, 2H, $CH{=}CHCCHCHC$), 7.54–7.60 (m, 2H, $N{=}NCCHCHCH$, $N{=}NCCCHCHCH$), 7.65 (ddd, *J* = 8.4/6.8/1.3 Hz, 1H, $N{=}NCCCHCH$), 7.82 (dd, *J* = 7.5/1.1 Hz, 1H, $N{=}NCCCHCHCHCH$), 7.92 (d, *J* = 8.2 Hz, 1H, $N{=}NCCHCHCH$), 7.97 (d, *J* = 8.1 Hz, 1H, $N{=}NCCHCHCH$), 8.00 (d, *J* = 8.5 Hz, 2H, $CH{=}CHCCHCHC$), 8.93 (d, *J* = 8.5 Hz, 1H, $N{=}NCCCH$) ppm. ^{13}C NMR (126 MHz, $CDCl_3$, 21 °C, TMS): δ = 14.21 (q, 1C, OCH_2CH_3), 24.63 (t, 1C, $NCH_2CH_2CH_2CH$), 26.42 (t, 1C, $NCH_2CH_2CH_2CH{=}CH$), 27.01 (t, 1C, NCH_2CHCH_2), 31.10 (t, 1C, $CH_2CH{=}CHC$), 41.91 (d, 1C, NCH_2CH), 53.84 (t, 1C, $NCH_2CH_2CH_2CH$), 55.46 (t, 1C, NCH_2CH), 58.31 (t, 1C, $NCH_2CH_2CH_2CH{=}CH$), 60.28 (t, 1C, OCH_2CH_3), 111.71 (d, 1C, $N{=}NCCCHCHCHCH$), 123.45 (d, 1C, $N{=}NCCCH$), 123.56 (d, 2C, $CH{=}CHCCHCHC$), 125.63 (d, 1C, $N{=}NCCHCHCH$), 126.39 (d, 1C, $N{=}NCCCHCHCH$), 126.58 (d, 2C, $CH{=}CHCCHCHC$), 126.72 (d, 1C, $N{=}NCCCHCH$), 127.88 (d, 1C, $N{=}NCCHCHCH$), 129.50 (d, 1C, $CH_2CH{=}CHC$), 131.08 (d, 1C, $N{=}NCCHCHCH$), 131.26 (s, 1C, $N{=}NCCCH$), 132.75 (d, 1C, $CH_2CH{=}CHC$), 134.24 (s, 1C, $N{=}NCCHCHCHC$), 140.60 (s, 1C, $CH_2CH{=}CHC$), 147.82 (s, 1C, $N{=}NCCHCHCH$), 152.01 (s, 1C, $CH{=}CHCCHCHC$), 174.26 (s, 1C, C=O) ppm. MS (ESI^+) *m/z*: 456 $[M+H]^+$. HRMS (ESI^+): $[M+H]^+$ calcd for $C_{29}H_{34}O_2N_3$: 456.2651, found 456.2641.

*1-[(E)-4-{3-[(E)-Phenylazo]phenyl}but-3-en-1-yl]piperidine-3-carboxylic acid (m-**12a**)*

According to GP5 starting from *m*-**10a** (78 mg, 0.20 mmol) and 2 N NaOH (0.30 ml, 0.60 mmol) *m*-**12a** was obtained as orange amorphous solid (64 mg, 88%). IR (KBr): $\tilde{\nu}$ = 3384, 3060, 3023, 2955, 2860, 2539, 1714, 1586, 1470, 1446, 1393, 1305, 1217, 1150, 1071, 967, 924, 791, 755, 692, 665 cm^{-1}. ^{1}H NMR (500 MHz, CH_3OD + 5.0 eq 1 N NaOD, 25 °C, CH_3OH): δ = 1.29 (qd, *J* = 12.8/4.0 Hz, 1H, $NCH_2CHCH_{ax}H_{eq}$), 1.52 (qt, *J* = 13.4/3.9 Hz, 1H, $NCH_2CH_{ax}H_{eq}CH_2CH$), 1.62–1.71 (m, 1H, $NCH_2CH_{ax}H_{eq}CH_2CH$), 1.87 (td, *J* = 12.0/2.7 Hz, 1H, $NCH_{ax}H_{eq}CH_2CH_2CH$), 1.94 (d_{br}, *J* = 12.9 Hz, 1H, $NCH_2CHCH_{ax}H_{eq}$), 2.01 (t, *J* = 11.4 Hz, 1H, $NCH_{ax}H_{eq}CH$), 2.31–2.46 (m, 5H, $NCH_2CH_2CH{=}CH$, $NCH_2CH_2CH{=}CH$, NCH_2CH_{ax}), 2.84 (d_{br}, *J* = 10.9 Hz, 1H, $NCH_{ax}H_{eq}CH_2CH_2CH$), 3.08 (d, *J* = 11.0 Hz, 1H, $NCH_{ax}H_{eq}CH$), 6.20 (dt, *J* = 15.8/6.5 Hz, 1H, $CH_2CH{=}CHC$), 6.41 (d, *J* = 15.9 Hz, 1H, $CH_2CH{=}CHC$), 7.35–7.43 (m, 2H, $CH{=}CHCCHCH$, $CH{=}CHCCHCH$), 7.45–7.52 (m, 3H, $N{=}NCCHCHCH$, $N{=}NCCHCHCH$), 7.62 (dt, *J* = 7.4/1.7 Hz, 1H, $CH{=}CHCCHCCH$), 7.73 (t, *J* = 1.6 Hz, 1H, $CH{=}CHCCHC$), 7.78–7.82 (m, 2H, $N{=}NCCHCHCH$) ppm. ^{13}C NMR (126 MHz, CH_3OD + 5.0 eq 1 N NaOD, 25 °C, CH_3OH): δ = 25.50 (t, 1C, $NCH_2CH_2CH_2CH$), 29.08 (t, 1C, NCH_2CHCH_2), 30.69 (t, 1C, $NCH_2CH_2CH{=}CH$), 46.03 (d, 1C, NCH_2CH), 54.29 (t, 1C, $NCH_2CH_2CH_2CH$), 57.57 (t, 1C, NCH_2CH), 59.10 (t, 1C, $NCH_2CH_2CH{=}CH$), 120.74 (d, 1C, $CH{=}CHCCHC$), 122.26 (d, 1C, $CH{=}CHCCHCCH$), 123.59 (d, 2C, $N{=}NCCHCHCH$), 129.88 (d, 1C, $CH{=}CHCCHCH$), 130.36 (d, 2C, $N{=}NCCHCHCH$), 130.47 (d, 1C, $CH{=}CHCCHCH$), 130.59 (d, 1C, $CH{=}CHCCH$), 131.25 (d, 1C, $CH{=}CHCCH$), 132.55 (d, 1C, $N{=}NCCHCHCH$), 139.95 (s, 1C, $CH{=}CHCCHC$), 153.44 (s, 1C, $N{=}NCCHCHCH$), 153.72 (s, 1C, $CH{=}CHCCHC$), 183.28 (s, 1C, C=O) ppm. MS (ESI^+) *m/z*: 364 $[M+H]^+$. HRMS (ESI^+): $[M+H]^+$ calcd for $C_{22}H_{26}O_2N_3$: 364.2025, found 364.2016.

*1-[(E)-4-{4-[(E)-Phenylazo]phenyl}but-3-en-1-yl]piperidine-3-carboxylic acid (p-**12a**)*

According to GP5 starting from *p*-**10a** (78 mg, 0.20 mmol) and 2 N NaOH (0.30 ml, 0.60 mmol) *p*-**12a** was obtained as orange amorphous solid (65 mg, 89%). IR (KBr): $\tilde{\nu}$ = 3429, 3038, 2959, 2931, 2862, 1621, 1596, 1462, 1438, 1367, 1346, 1336, 1303, 1295, 1229, 1154, 1069, 965, 951, 860, 776, 692 cm^{-1}. ^1H NMR (500 MHz, CH_3OD + 5.0 eq 1 N NaOD, 25 °C, CH_3OH): δ = 1.32 (qd, *J* = 12.7/4.0 Hz, 1H, $NCH_2CHCH_{ax}H_{eq}$), 1.57 (qt, *J* = 13.4/3.9 Hz, 1H, $NCH_2CH_{ax}H_{eq}CH_2CH$), 1.67–1.73 (m, 1H, $NCH_2CH_{ax}H_{eq}CH_2CH$), 1.87–2.01 (m, 2H, $NCH_2CHCH_{ax}H_{eq}$, $NCH_{ax}H_{eq}CH_2CH_2CH$), 2.05 (t, *J* = 11.4 Hz, 1H, $NCH_{ax}H_{eq}CH$), 2.37 (tt, *J* = 11.5/3.5 Hz, 1H, NCH_2CH_{ax}), 2.41–2.52 (m, 4H, NCH_2CH_2CH=CH, NCH_2CH_2CH=CH), 2.90 (d_{br}, *J* = 11.0 Hz, 1H, $NCH_{ax}H_{eq}CH_2CH_2CH$), 3.13 (d_{br}, *J* = 11.1/3.2 Hz, 1H, $NCH_{ax}H_{eq}CH$), 6.34 (dt, *J* = 15.8/6.6 Hz, 1H, CH_2CH=CHC), 6.49 (d, *J* = 15.9 Hz, 1H, CH_2CH=CHC), 7.47–7.55 (m, 5H, N=NCCHCHCH, CH=CHCCHCHC, N=NCCHCHCH), 7.76–7.80 (m, 2H, CH=CHCCHCHC), 7.80–7.85 (m, 2H, N=NCCHCHCH) ppm. ^{13}C NMR (126 MHz, CH_3OD + 5.0 eq 1 N NaOD, 25 °C, CH_3OH): δ = 25.64 (t, 1C, $NCH_2CH_2CH_2CH$), 29.20 (t, 1C, NCH_2CHCH_2), 31.01 (t, 1C, NCH_2CH_2CH=CH), 46.13 (d, 1C, NCH_2CH), 54.48 (t, 1C, $NCH_2CH_2CH_2CH$), 57.71 (t, 1C, NCH_2CH), 59.21 (t, 1C, NCH_2CH_2CH=CH), 123.56 (d, 2C, N=NCCHCHCH), 124.10 (d, 2C, CH=CHCCHCHC), 127.82 (d, 2C, CH=CHCCHCHC), 130.36 (d, 2C, CH=CHCCHCHC), 131.43 (d, 1C, CH=CHCCH), 131.72 (d, 1C, CH=CHCCH), 132.33 (d, 1C, N=NCCHCHCH), 142.07 (s, 1C, CH_2CH=CHC), 152.47 (s, 1C, CH=CHCCHCHC), 153.73 (s, 1C, N=NCCHCHCH), 183.14 (s, 1C, C=O) ppm. MS (ESI^+) *m/z*: 364 $[M+H]^+$. HRMS (EI^+): M^+ calcd for $C_{22}H_{25}O_2N_3$: 363.1947, found 363.1954.

*1-[(E)-4-{3-[(E)-1-Naphthylazo]phenyl}but-3-en-1-yl]piperidine-3-carboxylic acid (m-**12b**)*

According to GP5 starting from *m*-**10b** (88 mg, 0.20 mmol) and 2 N NaOH (0.30 ml, 0.60 mmol) *m*-**12b** was obtained as orange amorphous solid (78 mg, 94%). IR (KBr): $\tilde{\nu}$ = 3428, 3049, 2937, 2857, 1708, 1589, 1508, 1439, 1387, 1345, 1201, 1153, 1079, 965803, 771, 687 cm^{-1}. ^1H NMR (400 MHz, CH_3OD + 5.0 eq 1 N NaOD, 25 °C, CH_3OH): δ = 1.29 (qd, *J* = 12.8/3.8 Hz, 1H, $NCH_2CHCH_{ax}H_{eq}$), 1.51 (qt, *J* = 13.2/3.8 Hz, 1H, $NCH_2CH_{ax}H_{eq}CH_2CH$), 1.65 (d, *J* = 14.4 Hz, 1H, $NCH_2CH_{ax}H_{eq}CH_2CH$), 1.80 (td, *J* = 12.5/3.0 Hz, 1H, $NCH_{ax}H_{eq}CH_2CH_2CH$), 1.91–2.05 (m, 2H, $NCH_2CHCH_{ax}H_{eq}$, $NCH_{ax}H_{eq}CH$), 2.20–2.42 (m, 5H, NCH_2CH_2CH=CH, NCH_2CH_2CH=CH, NCH_2CH_{ax}), 2.76 (d, *J* = 10.9 Hz, 1H, $NCH_{ax}H_{eq}CH_2CH_2CH$), 3.06 (d, *J* = 9.5 Hz, 1H, $NCH_{ax}H_{eq}CH$), 6.09 (dt, *J* = 16.0/6.4 Hz, 1H, CH_2CH=CHC), 6.30 (d, *J* = 15.8 Hz, 1H, CH_2CH=CHC), 7.25–7.35 (m, 2H, CH=CHCCHCH, CH=CHCCHCCH), 7.40 (t, *J* = 7.8 Hz, 1H, N=NCCHCHCH), 7.44–7.52 (m, 2H, N=NCCCHCHCH, N=NCCCHCH), 7.56 (dd, *J* = 7.4/0.8 Hz, 1H, N=NCCHCHCH), 7.63 (dt, *J* = 6.6/1.4 Hz, 1H, N=NCCCHCHCHCH), 7.73 (s, 1H, CH=CHCCHC), 7.79–7.85 (m, 1H, CH=CHCCHCH), 7.87 (d, *J* = 8.2 Hz, 1H, N=NCCHCHCH), 8.66 (d, *J* = 9.7 Hz, 1H, N=NCCCH) ppm. ^{13}C NMR (101 MHz, CH_3OD + 5.0 eq 1N NaOD, 25 °C, CH_3OH): δ = 25.39 (t, 1C, $NCH_2CH_2CH_2CH$), 28.97(t, 1C, NCH_2CHCH_2), 30.52 (t, 1C, NCH_2CH_2CH=CH), 45.94 (d, 1C, NCH_2CH), 54.10 (t, 1C, $NCH_2CH_2CH_2CH$), 57.44 (t, 1C, NCH_2CH), 58.92 (t, 1C, NCH_2CH_2CH=CH), 112.71 (d, 1C, N=NCCHCHCH), 121.16 (d, 1C, CH=CHCCHC), 122.33 (d, 1C, N=NCCCHCHCHCH), 123.80 (d, 1C, N=NCCCH), 126.51 (d, 1C, N=NCCHCHCH), 127.57 (d, 2C, N=NCCCHCHCH), 127.96 (d, 1C, N=NCCCHCH), 128.98 (d, 1C, CH=CHCCHCH), 129.76 (d, 1C, CH=CHCCHCH), 130.28 (d, 2C, CH=CHCCHCCH, CH=CHCCH), 131.17 (d, 1C, CH=CHCCH), 131.95 (s, 1C, N=NCCCH), 132.61 (d, 1C, N=NCCHCHCH), 135.32 (s, 1C, N=NCCHCHCHC), 139.75 (s, 1C, CH=CHCCHC), 148.25 (s, 1C, N=NCCHCHCH), 154.03 (s, 1C, CH=CHCCHC), 183.21 (s, 1C, C=O) ppm. MS (ESI^+) *m/z*: 414 $[M+H]^+$. HRMS (ESI^+): $[M+H]^+$ calcd for $C_{26}H_{28}O_2N_3$: 414.2181, found 414.2176.

*1-[(E)-5-{3-[(E)-1-Naphthylazo]phenyl}pent-4-en-1-yl]piperidine-3-carboxylic acid (p-**12b**)*

According to GP5 starting from *p*-**10b** (91 mg, 0.20 mmol) and 2 N NaOH (0.30 ml, 0.60 mmol) *p*-**12b** was obtained as orange amorphous solid (81 mg, 95%). IR (KBr): $\tilde{\nu}$ = 3426, 3048, 2940, 2860, 1707, 1588, 1507, 1449, 1386, 1345, 1220, 1143, 1079, 957, 804, 772, 686 cm^{-1}. ^1H NMR (400 MHz, CH_3OD + 5.0 eq 1 N NaOD, 25 °C, CH_3OH): δ = 1.28 (qd, *J* = 13.0/4.0 Hz, 1H, $NCH_2CHCH_{ax}H_{eq}$), 1.46–1.68 (m, 4H, $NCH_2CH_{ax}H_{eq}CH_2CH$, $NCH_2CH_{ax}H_{eq}CH_2CH$, $NCH_2CH_2CH_2CH$=CH), 1.81 (t, *J* = 10.9 Hz, 1H, $NCH_{ax}H_{eq}CH_2CH_2CH$), 1.89–2.00 (m, 2H, $NCH_2CHCH_{ax}H_{eq}$, $NCH_{ax}H_{eq}CH$), 2.06–2.20 (m, 2H, CH_2CH=CHC), 2.27–2.38 (m, 3H, $NCH_2CH_2CH_2CH$=CH, NCH_2CH_{ax}), 2.80 (d, *J* = 10.9 Hz, 1H, $NCH_{ax}H_{eq}CH_2CH_2CH$,), 3.07 (d, *J* = 10.2 Hz, 1H, $NCH_{ax}H_{eq}CH$), 6.26 (td, *J* = 16.0/6.4 Hz, 1H, CH_2CH=CHC), 6.38 (d, *J* = 15.8 Hz, 1H, CH_2CH=CHC), 7.36–7.45 (m, 2H, CH=CHCCHCCH, CH=CHCCHCH), 7.46–7.61 (m, 3H, N=NCCHCHCH, N=NCCCHCHCH, N=NCCCHCH), 7.67 (d, *J* = 7.3 Hz, 1H, N=NCCHCHCH), 7.70–7.78 (m, 1H, N=NCCCHCHCHCH), 7.83 (s, 1H, CH=CHCCHC), 7.90 (d, *J* = 7.3 Hz, 1H, CH=CHCCHCH), 7.97 (d, *J* = 8.1 Hz, 1H, N=NCCHCHCH), 8.75 (d, *J* = 7.9 Hz, 1H, N=NCCCH) ppm. ^{13}C NMR (101 MHz, CH_3OD + 5.0 eq 1 N NaOD, 25 °C, CH_3OH): δ = 25.63 (t, 1C, $NCH_2CH_2CH_2CH$), 26.68 (t, 1C, $NCH_2CH_2CH_2CH$=CH), 29.24 (t, 1C, NCH_2CHCH_2), 31.95 (t, 1C, CH_2CH=CHC), 46.12 (d, 1C, NCH_2CH), 54.60 (t, 1C, $NCH_2CH_2CH_2CH$), 57.90 (t, 1C, NCH_2CH), 59.55 (t, 1C, $NCH_2CH_2CH_2CH$=CH), 112.80 (d, 1C, N=NCCHCHCH), 121.28 (d, 1C, CH=CHCCHC), 122.32 (d, 1C, N=NCCCHCHCHCH), 123.93 (d, 1C, N=NCCCH), 126.66 (d, 1C, N=NCCHCHCH), 127.69 (d, 1C, N=NCCCHCHCH), 128.10 (d, 1C, N=NCCCHCH), 129.09 (d, 1C, CH=CHCCHCH), 129.82 (d, 1C, CH=CHCCHCH), 130.49 (d, 2C, CH=CHCCHCCH, CH_2CH=CHC), 132.22 (s, 1C, N=NCCCH), 132.67 (d, 1C, CH_2CH=CHC), 132.77 (d, 1C, N=NCCHCHCH), 135.61 (s, 1C, N=NCCHCHCHC), 140.23 (s, 1C, CH=CHCCHC), 148.59 (s, 1C, N=NCCHCHCH), 154.45 (s, 1C, CH=CHCCHC), 183.15 (s, 1C, C=O) ppm. MS (ESI^+) *m/z*: 428 $[M+H]^+$. HRMS (ESI^+): $[M+H]^+$ calcd for $C_{27}H_{30}O_2N_3$: 428.2338, found 428.2332.

*1-[(E)-5-{3-[(E)-Phenylazo]phenyl}pent-4-en-1-yl]piperidine-3-carboxylic acid (m-**13a**)*

According to GP5 starting from *m*-**11a** (81 mg, 0.20 mmol) and 2 N NaOH (0.30 ml, 0.60 mmol) *m*-**13a** was obtained as orange amorphous solid (68 mg, 90%). IR (KBr): $\tilde{\nu}$ = 3060, 3023, 2943, 2863, 2484, 1709, 1597, 1469, 1446, 1388, 1308, 1217, 1150, 1081, 1020, 965, 791, 755, 692, 662 cm^{-1}. ^1H NMR (500 MHz, CH_3OD + 5.0 eq 1 N NaOD, 25 °C, CH_3OH): δ = 1.30 (qd, *J* = 12.9/4.0 Hz, 1H, $NCH_2CHCH_{ax}H_{eq}$), 1.55 (qt, *J* = 12.9/3.4 Hz, 1H, $NCH_2CH_{ax}H_{eq}CH_2CH$), 1.62–1.73 (m, 3H, $NCH_2CH_2CH_2CH$=CH, $NCH_2CH_{ax}H_{eq}CH_2CH$), 1.88 (td, *J* = 12.0/2.8 Hz, 1H, $NCH_{ax}H_{eq}CH_2CH_2CH$), 1.92–2.02 (m, 2H, $NCH_2CHCH_{ax}H_{eq}$, $NCH_{ax}H_{eq}CH$), 2.20 (q, *J* = 7.0 Hz, 2H, CH_2CH=CHC), 2.31–2.41 (m, 3H, $NCH_2CH_2CH_2CH$=CH, NCH_2CH_{ax}), 2.87 (d_{br}, *J* = 11.1 Hz, 1H, $NCH_{ax}H_{eq}CH_2CH_2CH$), 3.09 (d_{br}, *J* = 12.1 Hz, 1H, $NCH_{ax}H_{eq}CH$), 6.34 (dt, *J* = 15.8/6.8 Hz, 1H, CH_2CH=CHC), 6.46 (d, *J* = 15.8 Hz, 1H, CH_2CH=CHC), 7.43–7.50 (m, 2H, CH=CHCCHCH, CH=CHCCHCH), 7.50–7.57 (m, 3H, N=NCCHCHCH, N=NCCHCHCH), 7.68 (dt, *J* = 7.4/1.6 Hz, 1H, CH=CHCCHCCH), 7.81 (t, *J* = 1.6 Hz, 1H, CH=CHCCHC), 7.83–7.88 (m, 2H, N=NCCHCHCH) ppm. ^{13}C NMR (126 MHz, CH_3OD + 5.0 eq 1 N NaOD, 25 °C, CH_3OH): δ = 25.60 (t, 1C, $NCH_2CH_2CH_2CH$), 26.67 (t, 1C, $NCH_2CH_2CH_2CH$=CH), 29.22 (t, 1C, NCH_2CHCH_2), 31.95 (t, 1C, CH_2CH=CHC), 46.12 (d, 1C, NCH_2CH), 54.60 (t, 1C, $NCH_2CH_2CH_2CH$), 57.83 (t, 1C, NCH_2CH), 59.51 (t, 1C, $NCH_2CH_2CH_2CH$=CH), 120.73 (d, 1C, CH=CHCCHC), 122.19 (d, 1C, CH=CHCCHCCH), 123.63 (d, 2C, N=NCCHCHCH), 129.87 (d, 1C, CH=CHCCHCH), 130.40 (d, 2C, N=NCCHCHCH), 130.47 (d, 1C, CH=CHCCHCH), 130.52 (d, 1C, CH_2CH=CHC), 132.55 (d, 1C, CH_2CH=CHC), 132.88 (d, 1C, N=NCCHCHCH), 140.24 (s, 1C, CH=CHCCHC), 153.62 (s, 1C, N=NCCHCHCH), 153.92 (s, 1C, CH=CHCCHC), 183.22 (s, 1C, C=O) ppm. MS (ESI^+) *m/z*: 378 $[M+H]^+$. HRMS (ESI^+): $[M+H]^+$ calcd for $C_{23}H_{28}O_2N_3$: 378.2182, found 378.2171.

*1-[(E)-5-{4-[(E)-Phenylazo]phenyl}pent-4-en-1-yl]piperidine-3-carboxylic acid (p-**13a**)*

According to GP5 starting from *p*-**11a** (81 mg, 0.20 mmol) and 2 N NaOH (0.30 ml, 0.60 mmol) *p*-**13a** was obtained as orange amorphous solid (70 mg, 93%). IR (KBr): $\tilde{\nu}$ = 3413, 3036, 2943, 2865, 2530, 1707, 1595, 1463, 1440, 1387, 1303, 1226, 1153, 1069, 1018, 970, 954, 853, 811, 771, 720, 691 cm^{-1}. ^1H NMR (500 MHz, CH_3OD + 5.0 eq 1 N NaOD, 25 °C, CH_3OH): δ = 1.31 (qd, *J* = 12.8/3.9 Hz, 1H, $NCH_2CHCH_{ax}H_{eq}$), 1.55 (qt, *J* = 12.9/3.8 Hz, 1H, $NCH_2CH_{ax}H_{eq}CH_2CH$), 1.65–1.71 (m, 3H, $NCH_2CH_2CH_2CH$=CH, $NCH_2CH_{ax}H_{eq}CH_2CH$), 1.87 (td, *J* = 12.0/2.4 Hz, 1H, $NCH_{ax}H_{eq}CH_2CH_2CH$), 1.97 (q, *J* = 10.7/10.0 Hz, 2H, $NCH_2CHCH_{ax}H_{eq}$, $NCH_{ax}H_{eq}CH$), 2.20 (q, *J* = 6.9 Hz, 2H, CH_2CH=CHC), 2.31–2.40 (m, 3H, NCH_2CH_{ax}, $NCH_2CH_2CH_2CH$=CH), 2.87 (d_{br}, *J* = 10.9 Hz, 1H, $NCH_{ax}H_{eq}CH_2CH_2CH$), 3.09 (d_{br}, *J* = 9.9 Hz, 1H, $NCH_{ax}H_{eq}CH$), 6.31–6.47 (m, 2H, CH_2CH=CHC, CH_2CH=CHC), 7.44–7.56 (m, 5H, N=NCCHCHCH, CH=CHCCHCHC, N=NCCHCHCH), 7.78 (d, *J* = 8.4 Hz, 2H, CH=CHCCHCHC), 7.80–7.87 (m, 2H, N=NCCHCHCH) ppm. ^{13}C NMR (126 MHz, CH_3OD + 5.0 eq 1 N NaOD, 25 °C, CH_3OH): δ = 25.62 (t, 1C, $NCH_2CH_2CH_2CH$), 26.65 (t, 1C, $NCH_2CH_2CH_2CH$=CH), 29.23 (t, 1C, NCH_2CHCH_2), 32.12 (t, 1C, CH_2CH=CHC), 46.13 (d, 1C, NCH_2CH), 54.63 (t, 1C, $NCH_2CH_2CH_2CH$), 57.85 (t, 1C, NCH_2CH), 59.53 (t, 1C, $NCH_2CH_2CH_2CH$=CH), 123.56 (d, 2C, N=NCCHCHCH), 124.13 (d, 2C, CH=CHCCHCHC), 127.75 (d, 2C, CH=CHCCHCHC), 130.36 (d, 2C, N=NCCHCHCH), 130.53 (d, 1C, CH_2CH=CHC), 132.31 (d, 1C, CH_2CH=CHC), 133.93 (d, 1C, N=NCCHCHCH), 142.20 (s, 1C, CH_2CH=CHC), 152.41 (s, 1C, CH=CHCCHCHC), 153.74 (s, 1C, N=NCCHCHCH), 183.18 (s, 1C, C=O) ppm. MS (ESI^+) *m/z*: 378 $[M+H]^+$. HRMS (EI^+): M^+ calcd for $C_{23}H_{27}O_2N_3$: 377.2103, found 377.2108.

*1-[(E)-4-{4-[(E)-1-Naphthylazo]phenyl}but-3-en-1-yl]piperidine-3-carboxylic acid (m-**13b**)*

According to GP5 starting from *m*-**11b** (88 mg, 0.20 mmol) and 2 N NaOH (0.30 ml, 0.60 mmol) *m*-**13b** was obtained as orange amorphous solid (76 mg, 92%). IR (KBr): $\tilde{\nu}$ = 3424, 3049, 2940, 2531, 1596, 1508, 1498, 1460, 1448, 1388, 1345, 1311, 1221, 1157, 1141, 968, 854, 804, 773 cm^{-1}. ^1H NMR (500 MHz, CH_3OD + 5.0 eq 1 N NaOD, 25 °C, CH_3OH): δ = 1.33 (qd, *J* = 12.3/3.6 Hz, 1H, $NCH_2CHCH_{ax}H_{eq}$), 1.58 (qt, *J* = 12.6/3.7 Hz, 1H, $NCH_2CH_{ax}H_{eq}CH_2CH$), 1.70 (dp, *J* = 13.5/3.3 Hz, 1H, $NCH_2CH_{ax}H_{eq}CH_2CH$), 1.89–2.01 (m, 2H, $NCH_2CHCH_{ax}H_{eq}$, $NCH_{ax}H_{eq}CH_2CH_2CH$), 2.05 (t, *J* = 11.5 Hz, 1H, $NCH_{ax}H_{eq}CH$), 2.33–2.51 (m, 5H, NCH_2CH_{ax}, NCH_2CH_2CH=CH, NCH_2CH_2CH=CH), 2.90 (d_{br}, *J* = 11.1 Hz, 1H, $NCH_{ax}H_{eq}CH_2CH_2CH$), 3.14 (d_{br}, *J* = 11.4 Hz, 1H, $NCH_{ax}H_{eq}CH$), 6.34 (dt, *J* = 15.9/6.6 Hz, 1H, CH_2CH=CHC), 6.49 (d, *J* = 15.6 Hz, 1H, CH_2CH=CHC), 7.51 (d, *J* = 8.5 Hz, 2H, CH=CHCCHCHC), 7.54–7.62 (m, 2H, N=NCCHCHCH, N=NCCCHCHCH), 7.65 (ddd, *J* = 8.4/6.8/1.3 Hz, 1H, N=NCCCHCH), 7.71 (dd, *J* = 7.5/1.0 Hz, 1H, N=NCCCHCHCHCH), 7.90 (d, *J* = 8.5 Hz, 2H, CH=CHCCHCHC), 7.96 (d, *J* = 8.1 Hz, 1H, N=NCCHCHCH), 8.02 (d, *J* = 8.1 Hz, 1H, N=NCCHCHCH), 8.80 (d, *J* = 8.5 Hz, 1H, N=NCCCH) ppm. ^{13}C NMR (126 MHz, CH_3OD + 5.0 eq 1 N NaOD, 25 °C, CH_3OH): δ = 25.69 (t, 1C, $NCH_2CH_2CH_2CH$), 29.25 (t, 1C, NCH_2CHCH_2), 31.06 (t, 1C, NCH_2CH_2CH=CH), 46.18 (d, 1C, NCH_2CH), 54.55 (t, 1C, $NCH_2CH_2CH_2CH$), 57.77 (t, 1C, NCH_2CH), 59.28 (t, 1C, NCH_2CH_2CH=CH), 112.67 (d, 1C, N=NCCCHCHCHCH), 123.97 (d, 1C, N=NCCCH), 124.40 (d, 2C, CH=CHCCHCHC), 126.73 (d, 1C, N=NCCHCHCH), 127.71 (d, 1C, N=NCCCHCHCH), 127.90 (d, 2C, CH=CHCCHCHC), 128.09 (d, 1C, N=NCCCHCH), 129.11 (d, 1C, N=NCCHCHCH), 131.49 (d, 1C, CH=CHCCH), 131.76 (d, 1C, CH=CHCCH), 132.28 (s, 1C, N=NCCCH), 132.51 (d, 1C, N=NCCHCHCH), 135.68 (s, 1C, N=NCCHCHCHC), 142.14 (s, 1C, CH_2CH=CHC), 148.78 (s, 1C, N=NCCHCHCH), 153.16 (s, 1C, CH=CHCCHCHC), 183.10 (s, 1C, C=O) ppm. MS (ESI^+) *m/z*: 414 $[M+H]^+$. HRMS (ESI^+): $[M+H]^+$ calcd for $C_{26}H_{28}O_2N_3$: 414.2182, found 414.2173.

*1-[(E)-5-{4-[(E)-1-Naphthylazo]phenyl}pent-4-en-1-yl]piperidine-3-carboxylic acid (p-**13b**)*

According to GP5 starting from *p*-**11b** (91 mg, 0.20 mmol) and 2 N NaOH (0.30 ml, 0.60 mmol) *p*-**13b** was obtained as orange amorphous solid (82 mg, 96%). IR (KBr): $\tilde{\nu}$ = 3425, 3050, 2935, 2857, 2530, 1718, 1596, 1508, 1498, 1448, 1387, 1345, 1310, 1221, 1142, 969, 859, 803, 773 cm^{-1}. ^{1}H NMR (500 MHz, CH_3OD + 5.0 eq 1 N NaOD, 25 °C, CH_3OH): δ = 1.29 (qd, *J* = 12.8/3.9 Hz, 1H, $NCH_2CHCH_{ax}H_{eq}$), 1.46–1.69 (m, 4H, $NCH_2CH_{ax}H_{eq}CH_2CH$, $NCH_2CH_2CH_2CH$=CH, $NCH_2CH_{ax}H_{eq}CH_2CH$), 1.81 (td, *J* = 11.6/10.8/2.4 Hz, 1H, $NCH_2CH_{ax}H_{eq}CH_2CH$), 1.90–2.00 (m, 2H, $NCH_2CHCH_{ax}H_{eq}$, $NCH_{ax}H_{eq}CH$), 2.09 (q, *J* = 7.1 Hz, 2H, CH_2CH=CHC), 2.24–2.39 (m, 3H, $NCH_2CH_2CH_2CH$=CH, NCH_2CH_{ax}), 2.80 (d_{br}, *J* = 11.4 Hz, 1H, $NCH_{ax}H_{eq}CH_2CH_2CH$), 3.07 (d_{br}, *J* = 11.4 Hz, 1H, $NCH_{ax}H_{eq}CH$), 6.24 (dt, *J* = 15.8/6.5 Hz, 1H, CH_2CH=CHC), 6.32 (d, *J* = 15.9 Hz, 1H, CH_2CH=CHC), 7.38 (d, *J* = 8.6 Hz, 2H, CH=CHCCHCHC), 7.50 (t, *J* = 7.8 Hz, 1H, N=NCCHCHCH), 7.54 (ddd, *J* = 8.0/6.9/1.3 Hz, 1H, N=NCCCHCHCH), 7.59 (ddd, *J* = 8.3/6.8/1.4 Hz, 1H, N=NCCCHCH), 7.64 (dd, *J* = 7.5/1.0 Hz, 1H, N=NCCCHCHCHCHCH), 7.81 (d, *J* = 8.5 Hz, 2H, CH=CHCCHCHC), 7.90 (d, *J* = 7.6 Hz, 1H, N=NCCHCHCH), 7.95 (d, *J* = 8.2 Hz, 1H, N=NCCHCHCH), 8.75 (d, *J* = 8.4 Hz, 1H, N=NCCCH) ppm. ^{13}C NMR (126 MHz, CH_3OD + 5.0 eq 1 N NaOD, 25 °C, CH_3OH): δ = 25.60 (t, 1C, $NCH_2CH_2CH_2CH$), 26.60 (t, 1C, $NCH_2CH_2CH_2CH$=CH), 29.21 (t, 1C, NCH_2CHCH_2), 32.11 (t, 1C, CH_2CH=CHC), 46.11 (d, 1C, NCH_2CH), 54.56 (t, 1C, $NCH_2CH_2CH_2CH$), 57.85 (t, 1C, NCH_2CH), 59.51 (t, 1C, $NCH_2CH_2CH_2CH$=CH), 112.65 (d, 1C, N=NCCCHCHCHCH), 123.98 (d, 1C, N=NCCCH), 124.38 (d, 2C, CH=CHCCHCHC), 126.70 (d, 1C, N=NCCHCHCH), 127.68 (d, 1C, N=NCCCHCHCH), 127.75 (d, 2C, CH=CHCCHCHC), 128.05 (d, 1C, N=NCCCHCH), 129.08 (d, 1C, N=NCCHCHCH), 130.50 (d, 1C, CH_2CH=CHC), 132.23 (s, 1C, N=NCCCH), 132.46 (d, 1C, N=NCCHCHCH), 133.87 (d, 1C, CH_2CH=CHC), 135.61 (s, 1C, N=NCCHCHCHC), 142.15 (s, 1C, CH_2CH=CHC), 148.67 (s, 1C, N=NCCHCHCH), 152.96 (s, 1C, CH=CHCCHCHC), 183.19 (s, 1C, C=O) ppm. MS (ESI$^+$) *m/z*: 428 $[M+H]^+$. HRMS (ESI$^+$): $[M+H]^+$ calcd for $C_{27}H_{30}O_2N_3$: 428.2338, found 428.2329.

*4-{3-[(E)-Phenylazo]phenyl}but-3-yn-1-ol (m-**14a**)*

According to GP2 starting from *m*-**9a** (308 mg, 1.00 mmol), but-3-yn-1-ol (105 mg, 1.50 mmol), $Pd(dppf)Cl_2$ (42 mg, 50 µmol), CuI (38 mg, 0.20 mmol), Et_3N (1.0 mL) and THF (1.0 mL) *m*-**14a** was obtained as orange solid (228 mg, 91%); mp 44-46 °C; R_f ≈ 0.4 (CH_2Cl_2). IR (KBr): $\tilde{\nu}$ = 3363, 3062, 2940, 2883, 2233, 1596, 1586, 1477, 1469, 1445, 1420, 1332, 1307, 1152, 1046, 1020, 898, 796, 766, 689 cm^{-1}. ^{1}H NMR (500 MHz, $CDCl_3$, 21 °C, TMS): δ = 2.12 (t, *J* = 6.0 Hz, 1 H, OH), 2.71 (t, *J* = 6.3 Hz, 2H, CH_2CH_2OH), 3.83 (q, *J* = 6.1 Hz, 2 H, CH_2OH), 7.43 (t, *J* = 7.8 Hz, 1H, C≡CCCHCH), 7.46–7.53 (m, 4H, C≡CCCHCH, N=NCCHCHCH, N=NCCHCHCH), 7.85 (dt, *J* = 7.9/1.6 Hz, 1H, C≡CCCHCCH), 7.89–7.94 (m, 2H, N=NCCHCHCH), 7.96 (t, *J* = 1.7 Hz, 1H, C≡CCCHC) ppm. ^{13}C NMR (126 MHz, $CDCl_3$, 21 °C, TMS): δ = 23.76 (t, 1C, CH_2CH_2OH), 61.05 (t, 1C, CH_2OH), 81.71 (s, 1C, CH≡CHCCH), 87.30 (s, 1C, C≡CCCH), 122.89 (d, 3C, C≡CCCHCH, N=NCCHCHCH), 124.27 (s, 1C, C≡CCCHC), 125.53 (d, 1C, C≡CCCHC), 128.99 (d, 1C, C≡CCCHCH), 129.07 (d, 2C, N=NCCHCHCH), 131.23 (d, 1C, N=NCCHCHCH), 133.82 (d, 1C, C≡CCCHCCH), 152.31 (s, 1C, N=NC), 152.40 (s, 1C, N=NC) ppm. MS (EI$^+$) *m/z*: 250 $[M]^+$. HRMS (EI$^+$): M^+ calcd for $C_{16}H_{14}ON_2$: 250.1106, found 250.1099.

*4-{4-[(E)-Phenylazo]phenyl}but-3-yn-1-ol (p-**14a**)*

According to GP2 starting from *p*-**9a** (308 mg, 1.00 mmol), but-3-yn-1-ol (105 mg, 1.50 mmol), $Pd(dppf)Cl_2$ (42 mg, 50 µmol), CuI (38 mg, 0.20 mmol), Et_3N (1.0 mL) and THF (1.0 mL) *p*-**14a** was obtained as orange solid (238 mg, 95%); mp 116-118 °C; R_f ≈ 0.4 (CH_2Cl_2). IR (KBr): $\tilde{\nu}$ = 3321, 3229, 3057, 2951, 2887, 2215, 1595, 1494, 1464, 1441, 1405, 1301, 1284, 1100, 1042, 1017, 847, 762, 686 cm^{-1}. ^{1}H NMR (500 MHz, $CDCl_3$, 21 °C, TMS): δ = 1.91 (t, *J* = 6.0 Hz, 1H, OH), 2.74 (t, *J* = 6.3 Hz, 2H, CH_2CH_2OH), 3.85 (q, *J* = 6.1 Hz, 2H, CH_2OH), 7.46–7.54 (m, 3H, N=NCCHCHCH, N=NCCHCHCH), 7.54–7.57 (m, 2H, C≡CCCHCHC), 7.84–7.89 (m, 2H, C≡CCCHCHC), 7.89–7.93 (m, 2H, N=NCCHCHCH) ppm. ^{13}C NMR (126 MHz, $CDCl_3$, 21 °C, TMS): δ = 23.95 (t, 1C, CH_2CH_2OH), 61.07 (t, 1C, CH_2OH), 82.24 (s, 1C, C≡CCCH), 89.12 (s, 1C, C≡CCCH), 122.82 (d, 2C, C≡CCCHCHC), 122.89 (d, 2C, N=NCCHCHCH), 126.06 (s, 1C, CH_2C≡CC), 129.09 (d, 2C, N=NCCHCHCH), 131.18 (d, 1C, N=NCCHCHCH), 132.46 (d, 2C, C≡CCCHCHC), 151.60 (s, 1C, C≡CCCHCHC), 152.58 (s, 1C, N=NCCHCHCH) ppm. MS (EI$^+$) *m/z*: 250 $[M]^+$. HRMS (EI$^+$): M^+ calcd for $C_{16}H_{14}ON_2$: 250.1106, found 250.1101.

*4-{3-[(E)-1-Naphthylazo]phenyl}but-3-yn-1-ol (m-**14b**)*

According to GP2 starting from *m*-**9b** (358 mg, 1.00 mmol), but-3-yn-1-ol (105 mg, 1.50 mmol), $Pd(dppf)Cl_2$ (42 mg, 50 µmol), CuI (38 mg, 0.20 mmol), Et_3N (1.0 mL) and THF (1.0 mL) *m*-**14b** was obtained as red solid (277 mg, 92%); mp 88-89 °C; R_f ≈ 0.3 (CH_2Cl_2). IR (KBr): $\tilde{\nu}$ = 3356, 3054, 2939, 2852, 2233, 1589, 1507, 1478, 1417, 1387, 1344, 1204, 1044, 896, 804, 770, 684 cm^{-1}. ^{1}H NMR (400 MHz, $CDCl_3$, 21 °C, TMS): δ = 2.12 (s, 1H, OH), 2.73 (t, *J* = 6.3 Hz, 2H, CH_2CH_2OH), 3.85 (t, *J* = 6.3 Hz, 2H, CH_2OH), 7.47 (t, *J* = 7.7 Hz, 1H, C≡CCCHCH), 7.50–7.60 (m, 3H, C≡CCCHCH, N=NCCHCHCH, N=NCCCHCHCH), 7.65 (ddd, *J* = 8.3/6.9/1.2 Hz, 1H, N=NCCCHCH), 7.81 (dd, *J* = 7.5/0.8 Hz, 1H, N=NCCHCHCH), 7.91 (d, *J* = 8.1 Hz, 1H, N=NCCCHCHCHCHCH), 7.94–8.00 (m, 2H, C≡CCCHCCH, N=NCCHCHCH), 8.07 (t, *J* = 1.5 Hz, 1H, C≡CCCHC), 8.92 (d, *J* = 8.4 Hz, 1H, N=NCCCH) ppm. ^{13}C NMR (101 MHz, $CDCl_3$, 21 °C, TMS): δ = 23.79 (t, 1C, CH_2CH_2OH), 61.05 (t, 1C,

CH_2OH), 81.76 (s, 1C, C≡*C*CCH), 87.37 (s, 1C, *C*≡CCCH), 111.87 (d, 1C, N=NCCHCH*C*H), 123.39 (d, 2C, C≡CCCHC*C*H, N=NC*C*CH), 124.31 (s, 1C, C≡C*C*CHC), 125.55 (d, 2C, C≡CC*C*HC, N=NCCH*C*HCH), 126.47 (d, 1C, N=NCCCHCH*C*H), 126.90 (d, 1C, N=NCCCH*C*H), 127.89 (d, 1C, N=NCCCHCHCH*C*H), 129.04 (d, 1C, C≡CCCH*C*H), 131.28 (s, 1C, N=NC*C*CH), 131.61 (d, 1C, N=NC*C*HCHCH), 133.93 (d, 1C, C≡CC*C*HCH), 134.21 (s, 1C, N=NCCHCHCH*C*), 147.48 (s, 1C, N=N*C*CHCHCH), 152.78 (s, 1C, C≡CCCH*C*) ppm. MS (ESI^+) *m/z*: 301 $[M+H]^+$. HRMS (ESI^+): $[M+H]^+$ calcd for $C_{20}H_{17}ON_2$: 301.1341, found 301.1334.

*4-{4-[(E)-1-Naphthylazo]phenyl}but-3-yn-1-ol (p-**14b**)*

According to GP2 starting from *p*-**9b** (358 mg, 1.00 mmol), but-3-yn-1-ol (105 mg, 1.50 mmol), Pd(dppf)Cl_2 (42 mg, 50 µmol), CuI (38 mg, 0.20 mmol), Et_3N (1.0 mL) and THF (1.0 mL) *p*-**14b** was obtained as red solid (280 mg, 93%); mp 95-97 °C; R_f ≈ 0.3 (CH_2Cl_2). IR (KBr): $\tilde{\nu}$ = 3281, 3081, 3047, 2942, 2886, 2229, 1595, 1497, 1386, 1342, 1279, 1216, 1159, 1140, 1099, 1039, 1012, 845, 801, 773 cm^{-1}. ^{1}H NMR (500 MHz, $CDCl_3$, 21 °C, TMS): δ = 2.09 (t, *J* = 5.7 Hz, 1H, OH), 2.73 (t, *J* = 6.3 Hz, 2H, C*H*$_2$CH$_2$OH), 3.84 (q, *J* = 6.0 Hz, 2H, C*H*$_2$OH), 7.51–7.60 (m, 4H, N=NCCHC*H*CH, C≡CCC*H*CHC, N=NCCCHCHC*H*), 7.63 (ddd, *J* = 8.4/6.8/1.3 Hz, 1H, N=NCCCHC*H*), 7.81 (dd, *J* = 7.5/1.1 Hz, 1H, N=NCCHCHC*H*), 7.90 (d, *J* = 8.2 Hz, 1H, N=NCCCHCHCHC*H*), 7.97 (dq, *J* = 8.1/2.0 Hz, 3H, N=NCC*H*CHCH), 8.90 (d, *J* = 8.6 Hz, 1H, N=NCCC*H*) ppm. ^{13}C NMR (126 MHz, $CDCl_3$, 21 °C, TMS): δ = 23.92 (t, 1C, *C*H$_2$CH$_2$OH), 61.02 (t, 1C, *C*H$_2$OH), 82.21 (s, 1C, C≡*C*CCH), 89.33 (s, 1C, *C*≡CCCH), 111.81 (d, 1C, N=NCCHCH*C*H), 123.09 (d, 2C, C≡CCCH*C*HC), 123.34 (d, 1C, N=NCCC*H*), 125.55 (d, 1C, N=NCCH*C*HCH), 126.09 (s, 1C, CH$_2$C≡C*C*), 126.45 (d, 1C, N=NCCCHCH*C*H), 126.87 (d, 1C, N=NCCCH*C*H), 127.90 (d, 1C, N=NCCCHCHCH*C*H), 131.31 (s, 1C, N=NC*C*CH), 131.56 (d, 1C, N=NC*C*HCHCH), 132.48 (d, 2C, C≡CCCH*C*HC), 134.23 (s, 1C, N=NCCHCHCH*C*), 147.57 (s, 1C, N=N*C*CHCHCH), 152.06 (s, 1C, C≡CCCHCH*C*) ppm. MS (ESI^+) *m/z*: 301 $[M+H]^+$. HRMS (EI^+): M^+ calcd for $C_{20}H_{16}ON_2$: 300.1263, found 300.1257.

*5-{3-[(E)-Phenylazo]phenyl}pent-4-yn-1-ol (m-**15a**)*

According to GP2 starting from *m*-**9a** (308 mg, 1.00 mmol), pent-4-yn-1-ol (126 mg, 1.50 mmol), Pd(dppf)Cl_2 (42 mg, 50 µmol), CuI (38 mg, 0.20 mmol), Et_3N (1.0 mL) and THF (1.0 mL) *m*-**15a** was obtained as orange solid (238 mg, 90%); mp 49-50 °C; R_f ≈ 0.3 (CH_2Cl_2). IR (KBr): $\tilde{\nu}$ = 3344, 3062, 2946, 2878, 2228, 1597, 1586, 1487, 1477, 1469, 1444, 1429, 1151, 1057, 1021, 923, 897, 796, 765, 689 cm^{-1}. ^{1}H NMR (500 MHz, $CDCl_3$, 21 °C, TMS): δ = 1.82–1.95 (m, 3H, C*H*$_2$CH$_2$OH, OH), 2.56 (t, *J* = 7.0 Hz, 2H, C*H*$_2$CH$_2$CH$_2$OH), 3.82 (t, *J* = 6.1 Hz, 2H, C*H*$_2$OH), 7.42 (t, *J* = 7.8 Hz, 1H, C≡CCCHC*H*), 7.45–7.53 (m, 4H, C≡CCC*H*CH, N=NCCHC*H*CH, N=NCCHCHC*H*), 7.83 (dt, *J* = 7.9/1.6 Hz, 1H, C≡CCCHCC*H*), 7.89–7.93 (m, 2H, N=NCC*H*CHCH), 7.94 (t, *J* = 1.7 Hz, 1H, C≡CCC*H*C) ppm. ^{13}C NMR (126 MHz, $CDCl_3$, 21 °C, TMS): δ = 15.91 (t, 1C, *C*H$_2$CH$_2$OH), 31.23 (t, 1C, *C*H$_2$CH$_2$CH$_2$OH), 61.58 (t, 1C, *C*H$_2$OH), 80.41 (s, 1C, C≡*C*CCH), 90.24 (s, 1C, *C*≡CCCH), 122.53 (d, 1C, C≡CC*C*HCH), 122.86 (d, 2C, N=NC*C*HCHCH), 124.67 (s, 1C, C≡C*C*CHC), 125.48 (d, 1C, C≡CC*C*HC), 128.94 (d, 1C, C≡CCCH*C*H), 129.06 (d, 2C, N=NCCH*C*HCH), 131.18 (d, 1C, N=NCCHCH*C*H), 133.74 (d, 1C, C≡CCCHC*C*H), 152.30 (s, 1C, N=N*C*), 152.40 (s, 1C, N=N*C*) ppm. MS (EI^+) *m/z*: 264 $[M]^+$. HRMS (EI^+): M^+ calcd for $C_{17}H_{16}ON_2$: 264.1263, found 264.1257.

*5-{4-[(E)-Phenylazo]phenyl}pent-4-yn-1-ol (p-**15a**)*

According to GP2 starting from *p*-**9a** (308 mg, 1.00 mmol), pent-4-yn-1-ol (126 mg, 1.50 mmol), Pd(dppf)Cl_2 (42 mg, 50 µmol), CuI (38 mg, 0.20 mmol), Et_3N (1.0 mL) and THF (1.0 mL) *p*-**15a** was obtained as orange solid (254 mg, 96%); mp 104 °C; R_f ≈ 0.3 (CH_2Cl_2). IR (KBr): $\tilde{\nu}$ = 3301, 3063, 2932, 2871, 2217, 1594, 1495, 1442, 1301, 1281, 1222, 1154, 1100, 1069, 1053, 1033, 928, 847, 766, 726, 687 cm^{-1}. ^{1}H NMR (500 MHz, $CDCl_3$, 21 °C, TMS): δ = 1.89 (p, *J* = 6.6 Hz, 2H, C*H*$_2$CH$_2$OH), 2.17 (s, 1H, OH), 2.59 (t, *J* = 7.0 Hz, 2H, C*H*$_2$CH$_2$CH$_2$OH), 3.84 (t, *J* = 6.1 Hz, 2H, C*H*$_2$OH), 7.45–7.54 (m, 5H, N=NCCHCHC*H*, N=NCCHC*H*CH, C≡CCC*H*CHC), 7.83–7.88 (m, 2H, C≡CCCHC*H*C), 7.89–7.93 (m, 2H, N=NCC*H*CHCH) ppm. ^{13}C NMR (126 MHz, $CDCl_3$, 21 °C, TMS): δ = 16.11 (t, 1C, *C*H$_2$CH$_2$OH), 31.29 (t, 1C, *C*H$_2$CH$_2$CH$_2$OH), 61.72 (t, 1C, *C*H$_2$OH), 80.98 (s, 1C, CH$_2$C≡*C*), 92.17 (s, 1C, CH$_2$*C*≡C), 122.81 (d, 2C, C≡CCCH*C*HC), 122.87 (d, 2C, N=NC*C*HCHCH), 126.53 (s, 1C, CH$_2$C≡C*C*), 129.09 (d, 2C, N=NCCH*C*HCH), 131.12 (d, 1C, N=NCCHCH*C*H), 132.32 (d, 2C, C≡CC*C*HCHC), 151.45 (s, 1C, C≡CCCHCH*C*), 152.61 (s, 1C, N=N*C*CHCHCH) ppm. MS (EI^+) *m/z*: 264 $[M]^+$. HRMS (EI^+): M^+ calcd for $C_{17}H_{16}ON_2$: 264.1263, found 264.1256.

*5-{3-[(E)-1-Naphthylazo]phenyl}pent-4-yn-1-ol (m-**15b**)*

According to GP2 starting from *m*-**9b** (358 mg, 1.00 mmol), pent-4-yn-1-ol (126 mg, 1.50 mmol), Pd(dppf)Cl_2 (42 mg, 50 µmol), CuI (38 mg, 0.20 mmol), Et_3N (1.0 mL) and THF (1.0 mL) *m*-**15b** was obtained as red solid (296 mg, 94%); mp 64-66 °C; R_f ≈ 0.2 (CH_2Cl_2). IR (KBr): $\tilde{\nu}$ = 3357, 3054, 2946, 2878, 2228, 1599, 1507, 1478, 1431, 1387, 1345, 1204, 1058, 896, 865, 804, 771, 684 cm^{-1}. ^{1}H NMR (400 MHz, $CDCl_3$, 21 °C, TMS): δ = 1.70 (s, 1H, OH), 1.90 (p, *J* = 6.7 Hz, 2H, C*H*$_2$CH$_2$OH), 2.59 (t, *J* = 7.0 Hz, 2H, C*H*$_2$CH$_2$CH$_2$OH), 3.85 (t, *J* = 6.2 Hz, 2H, C*H*$_2$OH), 7.47 (t, *J* = 7.7 Hz, 1H, C≡CCCHC*H*), 7.50–7.61 (m,

3H, C≡CCC*H*CH, N=NCCHC*H*CH, N=NCCCHCHC*H*), 7.65 (ddd, *J* = 8.3/6.8/1.3 Hz, 1H, N=NCCCHC*H*), 7.81 (dd, *J* = 7.5/1.0 Hz, 1H, N=NCCHCHC*H*), 7.92 (d, *J* = 8.2 Hz, 1H N=NCCCHCHCHC*H*), 7.94–8.01 (m, 2H, C≡CCCHCC*H*, N=NCC*H*CHCH), 8.06 (t, *J* = 1.6 Hz, 1H, C≡CCC*H*C), 8.93 (d, *J* = 8.5 Hz, 1H, N=NCCC*H*) ppm. ^{13}C NMR (101 MHz, $CDCl_3$, 21 °C, TMS): *δ* = 15.97 (t, 1C, *C*H_2CH$_2$OH), 31.27 (t, 1C, *C*H_2CH$_2$CH$_2$OH), 61.69 (t, 1C, *C*H_2OH), 80.48 (s, 1C, CH$_2$C≡*C*), 90.30 (s, 1C, CH$_2$*C*≡C), 111.88 (d, 1C, N=NCCHCH*C*H), 123.04 (d, 1C, C≡CCCHC*C*H), 123.39 (d, 1C, N=NCC*C*H), 124.73 (s, 1C, C≡C*C*CHC), 125.59 (d, 2C, C≡CC*C*HC, N=NCCH*C*HCH), 126.48 (d, 1C, N=NCCCHCH*C*H), 126.90 (d, 1C, N=NCCCH*C*H), 127.91 (d, 1C, N=NCCCHCHCH*C*H), 129.02 (d, 1C, C≡CCCH*C*H), 131.28 (s, 1C, N=NC*C*CH), 131.57 (d, 1C, N=NC*C*HCHCH), 133.87 (d, 1C, C≡CC*C*HCH), 134.22 (s, 1C, N=NCCHCHCH*C*), 147.55 (s, 1C, N=N*C*CHCHCH), 152.82 (s, 1C, C≡CCCH*C*) ppm. MS (ESI$^+$) *m/z*: 315 [M+H]$^+$. HRMS (ESI$^+$): [M+H]$^+$ calcd for $C_{21}H_{19}ON_2$: 315.1497, found 315.1492.

*5-{4-[(E)-1-Naphthylazo]phenyl}pent-4-yn-1-ol (p-**15b**)*

According to GP2 starting from *p*-**9b** (358 mg, 1.00 mmol), pent-4-yn-1-ol (126 mg, 1.50 mmol), Pd(dppf)Cl_2 (42 mg, 50 µmol), CuI (38 mg, 0.20 mmol), Et_3N (1.0 mL) and THF (1.0 mL) *p*-**15b** was obtained as red solid (301 mg, 95%); mp 98-99 °C; R_f ≈ 0.2 (CH_2Cl_2). IR (KBr): $\tilde{\nu}$ = 3411, 3047, 2952, 2927, 2895, 2835, 2215, 1595, 1497, 1437, 1343, 1215, 1067, 1047, 906, 842, 803, 773 cm^{-1}. ^{1}H NMR (500 MHz, $CDCl_3$, 21 °C, TMS): *δ* = 1.71 (s, 1H, OH), 1.89 (p, *J* = 6.6 Hz, 2H, C*H*$_2$CH$_2$OH), 2.59 (t, *J* = 7.0 Hz, 2H, C*H*$_2$CH$_2$CH$_2$OH), 3.83 (t, *J* = 6.1 Hz, 2H, C*H*$_2$OH), 7.52–7.60 (m, 4H, N=NCCHC*H*CH, C≡CCC*H*CHC, N=NCCCHCHC*H*), 7.64 (ddd, *J* = 8.4/6.8/1.3 Hz, 1H, N=NCCCHC*H*), 7.81 (dd, *J* = 7.5/1.1 Hz, 1H, N=NCCHCHC*H*), 7.91 (d, *J* = 8.2 Hz, 1H, N=NCCCHCHCHC*H*), 7.98 (dt, *J* = 8.4/1.9 Hz, 3H, N=NCC*H*CHCH, C≡CCCHC*H*C), 8.91 (d, *J* = 8.5 Hz, 1H, N=NCCC*H*) ppm. ^{13}C NMR (126 MHz, $CDCl_3$, 21 °C, TMS): *δ* = 16.11 (t, 1C, *C*H_2CH$_2$OH), 31.25 (t, 1C, *C*H_2CH$_2$CH$_2$OH), 61.66 (t, 1C, *C*H_2OH), 81.00 (s, 1C, C≡*C*CCH), 92.35 (s, 1C, *C*≡CCCH), 111.80 (d, 1C, N=NCCCHCHCH*C*H), 123.09 (d, 2C, C≡CCCHC*H*C), 123.36 (s, 1C, N=NC*C*CH), 125.73 (d, 1C, N=NCCHC*H*CHCH), 126.45 (d, 1C, N=NCCCHCH*C*H), 126.57 (s, 1C, CH$_2$C≡C*C*), 126.86 (d, 1C, N=NCCCHC*H*CH), 127.91 (d, 1C, N=NCCCHCHCH*C*H), 131.31 (s, 1C, N=NC*C*CH), 131.50 (s, 1C, N=N*C*CHCHCH), 132.36 (d, 2C, C≡CC*C*HCHC), 134.24 (s, 1C, N=NCCHCHCH*C*), 147.62 (s, 1C, N=N*C*CHCHCH), 152.08 (s, 1C, C≡CCCHCH*C*) ppm. MS (ESI$^+$) *m/z*: 315 [M+H]$^+$. HRMS (EI$^+$): M$^+$ calcd for $C_{21}H_{18}ON_2$: 314.1419, found 314.1413.

*4-{3-[(E)-Phenylazo]phenyl}but-3-yn-1-yl 4-methylbenzenesulfonate (m-**16a**)*

According to GP3 starting from *m*-**14a** (200 mg, 0.800 mmol), *p*-toluenesulfonylchloride (182 mg, 0.960 mmol), Et_3N (121 mg, 1.20 mmol) and CH_2Cl_2 (1.6 mL) *m*-**16a** was obtained as orange high viscous oil (282 mg, 87%); R_f ≈ 0.5 (pentane/CH_2Cl_2 = 1:1). IR (NaCl): $\tilde{\nu}$ = 3064, 2960, 2921, 2239, 1597, 1469, 1362, 1307, 1189, 1177, 1096, 983, 900, 799, 767, 690, 663 cm^{-1}. ^{1}H NMR (500 MHz, $CDCl_3$, 21 °C, TMS): *δ* = 2.38 (s, 3H, CH_3), 2.80 (t, *J* = 6.9 Hz, 2 H, C*H*$_2$CH$_2$O), 4.20 (t, *J* = 6.9 Hz, 2H, C*H*$_2$O), 7.30 (d, *J* = 7.9 Hz, 2H, C*H*CCH$_3$), 7.41–7.46 (m, 2H, C≡CCC*H*CH, C≡CCCHC*H*), 7.46–7.55 (m, 3H, N=NCCHC*H*CH, N=NCCHCHC*H*), 7.81–7.84 (m, 2H, O$_3$SCC*H*), 7.85–7.86 (m, 1H, C≡CCCHCC*H*), 7.87 (t, *J* = 1.5 Hz, 2H, C≡CCC*H*C), 7.89–7.94 (m, 1H, N=NCC*H*CHCH) ppm. ^{13}C NMR (126 MHz, $CDCl_3$, 21 °C, TMS): *δ* = 20.30 (t, 1C, *C*H_2CH$_2$O), 21.57 (q, 1C, CH_3), 67.64 (t, 1C, *C*H_2O), 81.90 (s, 1C, C≡*C*CCH), 84.72 (s, 1C, *C*≡CCCH), 122.88 (d, 2C, N=NC*C*HCHCH), 122.97 (d, 1C, C≡CCCHC*C*H), 123.85 (s, 1C, C≡C*C*CHC), 125.55 (d, 1C, C≡CC*C*HC), 127.91 (d, 2C, O$_3$SC*C*H), 128.97 (d, 1C, C≡CCCH*C*H), 129.08 (s, 2C, N=NCCH*C*HCH), 129.86 (d, 2C, *C*HCCH$_3$), 131.28 (d, 1C, N=NCCHCH*C*H), 132.69 (s, 1C, O$_3$SC), 133.76 (d, 1C, C≡CC*C*HCH), 144.92 (s, 1C, *C*CH$_3$), 152.25 (s, 1C, N=N*C*), 152.36 (s, 1C, N=N*C*) ppm. MS (EI$^+$) *m/z*: 404 [M]$^+$. HRMS (EI$^+$): M$^+$ calcd for $C_{23}H_{20}O_3N_2S$: 404.1195, found 404.1195.

*4-{4-[(E)-Phenylazo]phenyl}but-3-yn-1-yl 4-methylbenzenesulfonate (p-**16a**)*

According to GP3 starting from *p*-**14a** (200 mg, 0.800 mmol), *p*-toluenesulfonylchloride (182 mg, 0.960 mmol), Et_3N (121 mg, 1.20 mmol) and CH_2Cl_2 (1.6 mL) *p*-**16a** was obtained as orange high viscous oil (288 mg, 89%); R_f ≈ 0.5 (pentane/CH_2Cl_2 = 1:1). IR (NaCl): $\tilde{\nu}$ = 3070, 2970, 2914, 2225, 1597, 1495, 1431, 1364, 1292, 1185, 1174, 1154, 1097, 1064, 973, 845, 814, 794, 766, 682, 667 cm^{-1}. ^{1}H NMR (500 MHz, $CDCl_3$, 21 °C, TMS): *δ* = 2.42 (s, 3H, CH_3), 2.82 (t, *J* = 6.9 Hz, 2H, C*H*$_2$CH$_2$O), 4.21 (t, *J* = 7.0 Hz, 2H, C*H*$_2$O), 7.30–7.34 (m, 2H, C*H*CCH$_3$), 7.45–7.55 (m, 5H, C≡CCC*H*CHC, N=NCCHC*H*CH, N=NCCHCHC*H*), 7.81–7.87 (m, 4H, C≡CCCHC*H*C, O$_3$SCC*H*), 7.89–7.94 (m, 2H, N=NCC*H*CHCH) ppm. ^{13}C NMR (126 MHz, $CDCl_3$, 21 °C, TMS): *δ* = 20.48 (t, 1C, *C*H_2CH$_2$O), 21.63 (q, 1C, CH_3), 67.58 (t, 1C, *C*H_2O), 82.41 (s, 1C, C≡*C*CCH), 86.47 (s, 1C, *C*≡CCCH), 122.76 (d, 2C, C≡CCCH*C*HC), 122.90 (d, 2C, N=NC*C*HCHCH), 125.58 (s, 1C, CH$_2$C≡C*C*), 127.95 (d, 2C, O$_3$SC*C*H), 129.10 (d, 2C, N=NCCH*C*HCH), 129.89 (d, 2C, *C*HCCH$_3$), 131.25 (d, 1C, N=NCCHCH*C*H), 132.42 (d, 2C, C≡CC*C*HCHC), 132.79 (s, 1C, O$_3$SC), 144.96 (s, 1C, *C*CH$_3$), 151.69 (s, 1C, C≡CCCHCH*C*), 152.53 (s, 1C, N=N*C*CHCHCH) ppm. MS (EI$^+$) *m/z*: 404 [M]$^+$. HRMS (EI$^+$): M$^+$ calcd for $C_{23}H_{20}O_3N_2S$: 404.1195, found 404.1183.

*4-{3-[(E)-1-naphthylazo]phenyl}but-3-yn-1-yl 4-methylbenzenesulfonate (m-**16b**)*

According to GP3 starting from *m*-**14b** (240 mg, 0.800 mmol), *p*-toluenesulfonylchloride (182 mg, 0.960 mmol), Et_3N (121 mg, 1.20 mmol) and CH_2Cl_2 (1.6 mL) *m*-**16b** was obtained as red high viscous oil (313 mg, 86%); R_f ≈ 0.4 (pentane/CH_2Cl_2 = 1:1). IR (NaCl): $\tilde{\nu}$ = 3054, 2959, 2921, 2238, 1597, 1507, 1479, 1362, 1345, 1306, 1189, 1177, 1096, 983, 899, 806, 772, 685, 664 cm^{-1}. ^1H NMR (400 MHz, $CDCl_3$, 21 °C, TMS): δ = 2.34 (s, 3H, CH_3), 2.82 (t, *J* = 6.9 Hz, 2H, C$H_2$$CH_2$O), 4.22 (t, *J* = 6.9 Hz, 2H, CH_2O), 7.28 (d, *J* = 8.0 Hz, 2H, C*H*CCH_3), 7.42–7.49 (m, 2H, C≡CCC*H*CH, C≡CCCHC*H*), 7.52–7.61 (m, 2H, N=NCCHC*H*CH, N=NCCCHCHC*H*), 7.65 (ddd, *J* = 8.4/6.8/1.3 Hz, 1H, N=NCCCHC*H*), 7.79–7.85 (m, 3H, N=NCCHCHC*H*, O_3SCC*H*), 7.92 (d, *J* = 8.1 Hz, 1H, N=NCCCHCHCHC*H*), 7.95–8.02 (m, *J* = 4.9/2.5 Hz, 3H, N=NCC*H*CHCH, C≡CCCHCC*H*, C≡CCC*H*C), 8.92 (d, *J* = 8.5 Hz, 1H, N=NCCC*H*) ppm. ^{13}C NMR (101 MHz, $CDCl_3$, 21 °C, TMS): δ = 20.33 (t, 1C, *C*$H_2$$CH_2$O), 21.53 (q, 1C, CH_3), 67.63 (t, 1C, *C*H_2O), 81.95 (s, 1C, C≡*C*CCH), 84.79 (s, 1C, *C*≡CCCH), 111.84 (d, 1C, N=NCCHCH*C*H), 123.30 (d, 1C, N=NCC*C*H), 123.46 (d, 1C, C≡CCCHC*C*H), 123.90 (s, 1C, C≡*CC*CHC), 125.56 (d, 2C, C≡CC*C*HC, N=NCCH*C*HCH), 126.47 (d, 1C, N=NCCCHCHC*H*), 126.92 (d, 1C, N=NCCCH*C*H), 127.89 (d, 3C, N=NCCCHCHCH*C*H, O_3SC*C*H), 129.03 (d, 1C, C≡CCCH*C*H), 129.84 (d, 2C, *C*HCCH_3), 131.27 (s, 1C, N=NC*C*CH), 131.67 (d, 1C, N=NC*C*HCHCH), 132.67 (s, 1C, O_3SC), 133.85 (d, 1C, C≡CC*C*HCH), 134.20 (s, 1C, N=NCCHCHCHC*C*), 144.92 (s, 1C, *C*CH_3), 147.40 (s, 1C, N=N*C*CHCHCH), 152.73 (s, 1C, C≡CCCH*C*) ppm. MS (ESI^+) *m/z*: 455 $[M+H]^+$. HRMS (ESI^+): $[M+H]^+$ calcd for $C_{27}H_{23}O_3N_2S$: 455.1429, found 455.1420.

*4-{4-[(E)-1-naphthylazo]phenyl}but-3-yn-1-yl 4-methylbenzenesulfonate (p-**16b**)*

According to GP3 starting from *p*-**14b** (240 mg, 0.800 mmol), *p*-toluenesulfonylchloride (182 mg, 0.960 mmol), Et_3N (121 mg, 1.20 mmol) and CH_2Cl_2 (1.6 mL) *p*-**16b** was obtained as red high viscous oil (320 mg, 88%); R_f ≈ 0.4 (pentane/CH_2Cl_2 = 1:1). IR (NaCl): $\tilde{\nu}$ = 3048, 2967, 2920, 2228, 1595, 1507, 1495, 1351, 1339, 1306, 1215, 1188, 1176, 1096, 972, 906, 849, 815, 806, 772, 752, 658 cm^{-1}. ^1H NMR (500 MHz, $CDCl_3$, 21 °C, TMS): δ = 2.41 (s, 3H, CH_3), 2.83 (t, *J* = 6.9 Hz, 2H, C$H_2$$CH_2$O), 4.22 (t, *J* = 6.9 Hz, 2H, CH_2O), 7.28–7.34 (m, 2H, C*H*CCH_3), 7.47–7.52 (m, 2H, C≡CCC*H*CHC), 7.52–7.60 (m, 2H, N=NCCHC*H*CH, N=NCCCHCHC*H*), 7.65 (ddd, *J* = 8.4/6.8/1.3 Hz, 1H, N=NCCCHC*H*), 7.80–7.86 (m, 3H, N=NCCHCHC*H*, O_3SCC*H*), 7.92 (d, *J* = 8.2 Hz, 1H, N=NCCCHCHCHC*H*), 7.95–8.01 (m, 3H, C≡CCCHC*H*C, N=NCC*H*CHCH), 8.91 (d, *J* = 7.9 Hz, 1H, N=NCCC*H*) ppm. ^{13}C NMR (126 MHz, $CDCl_3$, 21 °C, TMS): δ = 20.50 (t, 1C, *C*$H_2$$CH_2$O), 21.60 (q, 1C, CH_3), 67.58 (t, 1C, *C*H_2O), 82.45 (s, 1C, C≡*C*CCH), 86.65 (s, 1C, *C*≡CCCH), 111.84 (d, 1C, N=NCCHCH*C*H), 123.03 (d, 2C, C≡CCCH*C*HC), 123.31 (d, 1C, N=NCC*C*H), 125.56 (d, 1C, N=NCCH*C*HCH), 125.64 (s, 1C, CH_2C≡C*C*), 126.47 (d, 1C, N=NCCCHCH*C*H), 126.91 (d, 1C, N=NCCCH*C*H), 127.92 (d, 3C, O_3SC*C*H, N=NCCCHCHCH*C*H), 129.87 (d, 2C, *C*HCCH_3), 131.34 (s, 1C, N=NC*C*CH), 131.64 (d, 1C, N=NC*C*HCHCH), 132.46 (d, 2C, C≡CC*C*HCHC), 132.81 (s, 1C, O_3SC), 134.26 (s, 1C, N=NCCHCHCHC*C*), 144.94 (s, 1C, *C*CH_3), 147.58 (s, 1C, N=N*C*CHCHCH), 152.20 (s, 1C, C≡CCCHCH*C*) ppm. MS (ESI^+) *m/z*: 455 $[M+H]^+$. HRMS (EI^+): M^+ calcd for $C_{27}H_{22}O_3N_2S$: 454.1351, found 454.1342.

*5-{3-[(E)-Phenylazo]phenyl}pent-4-yn-1-yl 4-methylbenzenesulfonate (m-**17a**)*

According to GP3 starting from *m*-**15a** (212 mg, 0.800 mmol), *p*-toluenesulfonylchloride (182 mg, 0.960 mmol), Et_3N (121 mg, 1.20 mmol) and CH_2Cl_2 (1.6 mL) *m*-**17a** was obtained as orange high viscous oil (307 mg, 92%); R_f ≈ 0.4 (pentane/CH_2Cl_2 = 1:1). IR (NaCl): $\tilde{\nu}$ = 3063, 2959, 2924, 2230, 1597, 1468, 1444, 1362, 1189, 1176, 1097, 1018, 930, 826, 812, 797, 766, 690, 664 cm^{-1}. ^1H NMR (500 MHz, $CDCl_3$, 21 °C, TMS): δ = 1.95 (p, *J* = 6.4 Hz, 2H, C$H_2$$CH_2$O), 2.32 (s, 3H, CH_3), 2.51 (t, *J* = 6.8 Hz, 2H, C$H_2$$CH_2$$CH_2$O), 4.22 (t, *J* = 6.0 Hz, 2H, CH_2O), 7.27–7.31 (m, 2H, C*H*CCH_3), 7.38 (dt, *J* = 7.6/1.5 Hz, 1H, C≡CCC*H*CH), 7.42 (td, *J* = 7.6/0.6 Hz, 1H, C≡CCCHC*H*), 7.46–7.55 (m, 3H, N=NCCHC*H*CH, N=NCCHCHC*H*), 7.79–7.86 (m, 4H, O_3SCC*H*, C≡CCC*H*C, C≡CCCHCCC*H*), 7.90–7.95 (m, 2H, N=NCC*H*CHCH) ppm. ^{13}C NMR (126 MHz, $CDCl_3$, 21 °C, TMS): δ = 15.58 (t, 1C, *C*$H_2$$CH_2$O), 21.52 (q, 1C, CH_3), 27.74 (t, 1C, *C*$H_2$$CH_2$$CH_2$O), 68.77 (t, 1C, *C*$H_2$O), 81.00 (s, 1C, C≡*C*CCH), 88.42 (s, 1C, *C*≡CCCH), 122.59 (d, 1C, C≡CCCHC*C*H), 122.88 (d, 2C, N=NC*C*HCHCH), 124.35 (s, 1C, C≡C*C*CHC), 125.50 (d, 1C, C≡CC*C*HC), 127.88 (d, 2C, O_3SC*C*H), 128.92 (d, 1C, C≡CCCH*C*H), 129.10 (d, 2C, N=NCCH*C*HCH), 129.83 (d, 2C, *C*HCCH_3), 131.26 (d, 1C, N=NCCHCH*C*H), 132.69 (s, 1C, O_3SC), 133.71 (d, 1C, C≡CC*C*HCH), 144.78 (s, 1C, *C*CH_3), 152.27 (s, 1C, N=N*C*), 152.40 (s, 1C, N=N*C*) ppm. MS (EI^+) *m/z*: 418 $[M]^+$. HRMS (EI^+): M^+ calcd for $C_{24}H_{22}O_3N_2S$: 418.1351, found 418.1349.

*5-{4-[(E)-Phenylazo]phenyl}pent-4-yn-1-yl 4-methylbenzenesulfonate (p-**17a**)*

According to GP3 starting from *p*-**15a** (212 mg, 0.800 mmol), *p*-toluenesulfonylchloride (182 mg, 0.960 mmol), Et_3N (121 mg, 1.20 mmol) and CH_2Cl_2 (1.6 mL) *p*-**17a** was obtained as orange high viscous oil (308 mg, 92%); R_f ≈ 0.4 (pentane/CH_2Cl_2 = 1:1). IR (NaCl): $\tilde{\nu}$ = 3068, 3049, 2976, 2942, 2921, 2228, 1597, 1494, 1461, 1438, 1352, 1291, 1191, 1178, 1155, 1098, 1018, 977, 933, 844, 814, 765, 683, 664 cm^{-1}. ^1H NMR (500 MHz, $CDCl_3$, 21 °C, TMS): δ = 1.96 (p, *J* = 6.5 Hz, 2H, C$H_2$$CH_2$O), 2.38 (s, 3H, CH_3), 2.53 (t, *J* = 6.8 Hz, 2H, C$H_2$$CH_2$$CH_2$O), 4.22 (t, *J* = 6.0 Hz, 2H, CH_2O), 7.29–7.33 (m, 2H, C*H*CCH_3), 7.40–7.45 (m, 2H, C≡CCC*H*CHC), 7.46–7.55 (m, 3H, N=NCCHC*H*CH, N=NCCHCHC*H*), 7.80–7.86 (m, 4H,

C≡CCCHC*H*C, O_3SCC*H*), 7.89–7.94 (m, 2H, N=NCC*H*CHCH) ppm. ^{13}C NMR (126 MHz, $CDCl_3$, 21 °C, TMS): δ = 15.78 (t, 1C, *C*H_2CH$_2$O), 21.61 (q, 1C, CH_3), 27.77 (t, 1C, *C*H_2CH$_2$CH$_2$O), 68.77 (t, 1C, *C*H_2O), 81.53 (s, 1C, C≡*C*CCH), 90.35 (s, 1C, *C*≡CCCH), 122.75 (d, 2C, C≡CCCH*C*HC), 122.88 (d, 2C, N=NC*C*HCHCH), 126.14 (s, 1C, CH$_2$C≡C*C*), 127.93 (d, 2C, O_3SC*C*H), 129.10 (d, 2C, N=NCCH*C*HCH), 129.85 (d, 2C, *C*HCCH$_3$), 131.19 (d, 1C, N=NCCHCH*C*H), 132.30 (d, 2C, C≡CC*C*HCHC), 132.80 (s, 1C, O_3SC), 144.81 (s, 1C, *C*CH$_3$), 151.49 (s, 1C, C≡CCCHCH*C*), 152.56 (s, 1C, N=N*C*CHCHCH) ppm. MS (EI$^+$) *m/z*: 418 [M]$^+$. HRMS (EI$^+$): M$^+$ calcd for $C_{24}H_{22}O_3N_2S$: 418.1351, found 418.1339.

*5-{3-[(E)-1-naphthylazo]phenyl}pent-4-yn-1-yl 4-methylbenzenesulfonate (m-**17b**)*

According to GP3 starting from *m*-**15b** (304 mg, 0.800 mmol), *p*-toluenesulfonylchloride (182 mg, 0.960 mmol), Et_3N (121 mg, 1.20 mmol) and CH_2Cl_2 (1.6 mL) *m*-**17b** was obtained as red high viscous oil (337 mg, 90%); R_f ≈ 0.3 (pentane/CH_2Cl_2 = 1:1). IR (NaCl): $\tilde{\nu}$ = 3055, 2958, 2924, 2850, 2231, 1598, 1507, 1479, 1434, 1362, 1189, 1176, 1097, 1017, 975, 933, 832, 806, 773, 686, 663 cm^{-1}. ^{1}H NMR (400 MHz, $CDCl_3$, 21 °C, TMS): δ = 1.96 (p, *J* = 6.5 Hz, 2H, C*H*$_2$CH$_2$O), 2.29 (s, 3H, CH_3), 2.52 (t, *J* = 6.8 Hz, 2H, C*H*$_2$CH$_2$CH$_2$O), 4.22 (t, *J* = 6.0 Hz, 2H, C*H*$_2$O), 7.26 (d, *J* = 8.5 Hz, 2H, C*H*CCH$_3$), 7.38–7.49 (m, 2H, C≡CCC*H*CH, C≡CCCHC*H*), 7.52–7.60 (m, 2H, N=NCCHC*H*CH, N=NCCCHCHC*H*), 7.65 (ddd, *J* = 8.4/6.8/1.3 Hz, 1H, N=NCCCHC*H*), 7.78–7.85 (m, 3H, O_3SCC*H*, N=NCCHCHC*H*), 7.89–8.01 (m, 4H, N=NCCCHCHCHC*H*, N=NCC*H*CHCH, C≡CCCHCC*H*, C≡CCC*H*C), 8.93 (d, *J* = 8.5 Hz, 1H, N=NCCC*H*) ppm. ^{13}C NMR (101 MHz, $CDCl_3$, 21 °C, TMS): δ = 15.59 (t, 1C, *C*H_2CH$_2$O), 21.47 (q, 1C, CH_3), 27.68 (t, 1C, *C*H_2CH$_2$CH$_2$O), 66.76 (t, 1C, *C*H_2O), 81.02 (s, 1C, C≡*C*CCH), 88.50 (s, 1C, *C*≡CCCH), 111.81 (d, 1C, N=NCCHCH*C*H), 123.00 (d, 1C, N=NCC*C*H), 123.29 (d, 1C, C≡CCCHC*C*H), 124.47 (s, 1C, C≡C*C*CHC), 125.55 (d, 2C, C≡CC*C*HC, N=NCCH*C*HCH), 126.46 (d, 1C, N=NCCCHCH*C*H), 126.91 (d, 1C, N=NCCCH*C*H), 127.86 (d, 3C, N=NCCCHCHCH*C*H, O_3SC*C*H), 128.96 (d, 1C, C≡CCCH*C*H), 129.79 (d, 2C, *C*HCCH$_3$), 131.26 (s, 1C, N=NC*C*CH), 131.63 (d, 1C, N=NC*C*HCHCH), 132.62 (s, 1C, O_3SC), 133.77 (d, 1C, C≡CC*C*HCH), 134.19 (s, 1C, N=NCCHCHCH*C*), 144.75 (s, 1C, *C*CH$_3$), 147.41 (s, 1C, N=N*C*CHCHCH), 152.72 (s, 1C, C≡CCCH*C*) ppm. MS (ESI$^+$) *m/z*: 469 [M+H]$^+$. HRMS (ESI$^+$): [M+H]$^+$ calcd for $C_{28}H_{25}O_3N_2S$: 469.1586, found 469.1577.

*5-{4-[(E)-1-naphthylazo]phenyl}pent-4-yn-1-yl 4-methylbenzenesulfonate (p-**17b**)*

According to GP3 starting from *p*-**15b** (304 mg, 0.800 mmol), *p*-toluenesulfonylchloride (182 mg, 0.960 mmol), Et_3N (121 mg, 1.20 mmol) and CH_2Cl_2 (1.6 mL) *p*-**17b** was obtained as red high viscous oil (345 mg, 92%); R_f ≈ 0.3 (pentane/CH_2Cl_2 = 1:1). IR (NaCl): $\tilde{\nu}$ = 3056, 2985, 2961, 2940, 2921, 2235, 1596, 1497, 1356, 1349, 1217, 1191, 1176, 1097, 1013, 930, 847, 837, 815, 804, 778, 660 cm^{-1}. ^{1}H NMR (500 MHz, $CDCl_3$, 21 °C, TMS): δ = 1.97 (p, *J* = 6.5 Hz, 2H, C*H*$_2$CH$_2$O), 2.38 (s, 3H, CH_3), 2.54 (t, *J* = 6.8 Hz, 2H, C*H*$_2$CH$_2$CH$_2$O), 4.23 (t, *J* = 6.0 Hz, 2 H, C*H*$_2$O), 7.29–7.33 (m, 2H, C*H*CCH$_3$), 7.44–7.49 (m, 2H, C≡CCC*H*CHC), 7.54–7.61 (m, 2H, N=NCCHCHC*H*, N=NCCCHCHC*H*), 7.65 (ddd, *J* = 8.4/6.8/1.3 Hz, 1H, N=NCCCHC*H*), 7.80–7.85 (m, 3H, N=NCCHCHC*H*, O_3SCC*H*), 7.92 (d, *J* = 8.2 Hz, 1H, N=NCCCHCHCHC*H*), 7.95–8.01 (m, 3H, N=NCC*H*CHCH, C≡CCCHC*H*C), 8.92 (d, *J* = 7.9 Hz, 1H, N=NCCC*H*) ppm. ^{13}C NMR (126 MHz, $CDCl_3$, 21 °C, TMS): δ = 15.81 (t, 1C, *C*H_2CH$_2$O), 21.59 (q, 1C, CH_3), 27.78 (t, 1C, *C*H_2CH$_2$CH$_2$O), 68.78 (t, 1C, *C*H_2O), 81.58 (s, 1C, CH$_2$C≡*C*), 90.53 (s, 1C, CH$_2$*C*≡C), 111.84 (d, 1C, N=NCCHCH*C*H), 123.03 (d, 2C, C≡CCCH*C*HC), 123.33 (d, 1C, N=NCC*C*H), 125.58 (d, 1C, N=NCCH*C*HCH), 126.21 (s, 1C, CH$_2$C≡C*C*), 126.48 (d, 1C, N=NCCCHCH*C*H), 126.90 (d, 1C, N=NCCCH*C*H), 127.93 (d, 3C, N=NCCCHCHCH*C*H, *C*HCCH$_3$), 129.84 (d, 2C, *C*HCCH$_3$), 131.34 (s, 1C, N=NC*C*CH), 131.59 (d, 1C, N=NC*C*HCHCH), 132.35 (d, 2C, C≡CC*C*HCHC), 132.82 (s, 1C, O_3SC), 134.27 (s, 1C, N=NCCHCHCH*C*), 144.79 (s, 1C, N=NCCHCHCH*C*), 147.62 (s, 1C, N=N*C*CHCHCH), 152.03 (s, 1C, C≡CCCHCH*C*) ppm. MS (ESI$^+$) *m/z*: 469 [M+H]$^+$. HRMS (EI$^+$): M$^+$ calcd for $C_{28}H_{24}O_3N_2S$: 468.1508, found 468.1495.

*Ethyl 1-{4-[3-[(E)-phenylazo]phenyl}but-3-yn-1-yl]piperidine-3-carboxylate (m-**18a**)*

According to GP4 starting from *m*-**16a** (121 mg, 0.300 mmol), nipecotic acid ethyl ester (142 mg, 0.900 mmol), acetone (0.3 mL) and a reaction time of 72 h *m*-**18a** was obtained as orange oil (102 mg, 87%); R_f ≈ 0.25 (pentane/EtOAc = 8:2). IR (NaCl): $\tilde{\nu}$ = 3062, 2927, 2853, 2810, 2229, 1729, 1596, 1467, 1446, 1369, 1306, 1179, 1152, 1133, 1101, 1033, 797, 766, 690 cm^{-1}. ^{1}H NMR (500 MHz, $CDCl_3$, 21 °C, TMS): δ = 1.24 (t, *J* = 7.1 Hz, 3H, OCH$_2$C*H*$_3$), 1.46 (qd, *J* = 12.3/4.4 Hz, 1H, NCH$_2$CHC*H*$_{ax}$H$_{eq}$), 1.54–1.64 (m, 1H, NCH$_2$C*H*$_{ax}$H$_{eq}$CH$_2$CH), 1.75 (dp, *J* = 11.0/3.9 Hz, 1H, NCH$_2$CH$_{ax}$*H*$_{eq}$CH$_2$CH), 1.95 (dq, *J* = 13.5/4.2 Hz, 1H, NCH$_2$CHCH$_{ax}$*H*$_{eq}$), 2.13 (td, *J* = 11.0/2.8 Hz, 1H, NC*H*$_{ax}$H$_{eq}$CH$_2$CH$_2$CH), 2.30 (t, *J* = 10.6 Hz, 1H, NC*H*$_{ax}$H$_{eq}$CH), 2.55–2.65 (m, 3H, NCH$_2$C*H*$_{ax}$, NCH$_2$C*H*$_2$C≡C), 2.70–2.76 (m, 2H, NC*H*$_2$CH$_2$C≡C), 2.82 (d$_{br}$, *J* = 11.2 Hz, 1H, NCH$_{ax}$*H*$_{eq}$CH$_2$CH$_2$CH), 3.06 (d$_{br}$, *J* = 10.4 Hz, 1H, NCH$_{ax}$*H*$_{eq}$CH), 4.13 (q, *J* = 7.1 Hz, 2H, OC*H*$_2$CH$_3$), 7.43 (t, *J* = 7.8 Hz, 1H, C≡CCCHC*H*), 7.45–7.53 (m, 4H, N=NCCHCHC*H*, N=NCCHC*H*CH, C≡CCC*H*CH), 7.83 (ddd, *J* = 7.9/1.9/1.3 Hz, 1H, C≡CCCHCC*H*), 7.89–7.93 (m, 2H, N=NCC*H*CHCH), 7.95 (t, *J* = 1.7 Hz, 1H, C≡CCC*H*C) ppm. ^{13}C NMR (126 MHz, $CDCl_3$, 21 °C, TMS): δ = 14.17 (q, 1C, OCH$_2$*C*H$_3$), 17.64 (t, 1C, NCH$_2$*C*H$_2$C≡C), 24.54 (t, 1C, NCH$_2$*C*H$_2$CH$_2$CH), 26.78 (t, 1C, NCH$_2$CH*C*H$_2$), 41.81 (d, 1C, NCH$_2$*C*H), 53.34 (t, 1C, N*C*H$_2$CH$_2$CH$_2$CH), 55.06 (t, 1C, N*C*H$_2$CH), 57.37 (t, 1C, N*C*H$_2$CH$_2$C≡C), 60.28 (t, 1C, O*C*H$_2$CH$_3$), 80.64 (s, 1C, C≡*C*CCH), 89.26 (s, 1C, *C*≡CCCH), 122.42 (d, 1C, C≡CCCHC*C*H), 122.86 (d, 2C, N=NC*C*HCHCH), 124.72 (s, 1C, C≡C*C*CHC), 125.57 (d, 1C, C≡CC*C*HC), 128.90 (d, 1C, C≡CCCH*C*H), 129.04 (d, 2C, N=NCCH*C*HCH), 131.14 (d,

1C, N=NCCHCH*C*H), 133.74 (d, 1C, C≡CC*C*HCH), 152.46 (d, 2C, N=N*C*), 174.05 (s, 1C, C=O) ppm. MS (ESI$^+$) *m/z*: 390 [M+H]$^+$. HRMS (ESI$^+$): [M+H]$^+$ calcd for $C_{24}H_{28}O_2N_3$: 390.2182, found 390.2173.

*(R)-Ethyl 1-(4-{3-[(E)-phenylazo]phenyl}but-3-yn-1-yl)piperidine-3-carboxylate ((R)-m-**18a**)*

According to GP4 starting from *m*-**16a** (121 mg, 0.300 mmol), nipecotic acid ethyl ester (142 mg, 0.900 mmol), acetone (0.3 mL) and a reaction time of 72 h (*R*)-*m*-**18a** was obtained as orange oil (102 mg, 87%); $[\alpha]^{20}_D$ = -12.1 (c = 0.1 in CH_2Cl_2); R_f ≈ 0.25 (pentane/EtOAc = 8:2). IR (NaCl): $\tilde{\nu}$ = 3062, 2927, 2853, 2810, 2229, 1729, 1596, 1467, 1446, 1369, 1306, 1179, 1152, 1133, 1101, 1033, 797, 766, 690 cm^{-1}. ^{1}H NMR (500 MHz, $CDCl_3$, 21 °C, TMS): δ = 1.23 (t, *J* = 7.1 Hz, 3H, OCH$_2$C*H$_3$*), 1.45 (qd, *J* = 12.0/4.4 Hz, 1H, NCH$_2$CHC*H$_{ax}$*H$_{eq}$), 1.52–1.64 (m, 1H, NCH$_2$C*H$_{ax}$*H$_{eq}$CH$_2$CH), 1.73 (dp, *J* = 10.7/3.8 Hz, 1H, NCH$_2$CH$_{ax}$*H$_{eq}$*CH$_2$CH), 1.93 (dq, *J* = 13.1/4.1 Hz, 1H, NCH$_2$CHCH$_{ax}$*H$_{eq}$*), 2.12 (td, *J* = 10.9/3.1 Hz, 1H, NC*H$_{ax}$*H$_{eq}$CH$_2$CH$_2$CH), 2.29 (t, *J* = 10.6 Hz, 1H, NC*H$_{ax}$*H$_{eq}$CH), 2.53–2.65 (m, 3H, NCH$_2$C*H$_{ax}$*, NCH$_2$C*H$_2$*C≡C), 2.67–2.74 (m, 2H, NC*H$_2$*CH$_2$C≡C), 2.80 (d$_{br}$, *J* = 11.3 Hz, 1H, NCH$_{ax}$*H$_{eq}$*CH$_2$CH$_2$CH), 3.04 (d$_{br}$, *J* = 10.9 Hz, 1H, NCH$_{ax}$*H$_{eq}$*CH), 4.12 (q, *J* = 7.2 Hz, 2H, OC*H$_2$*CH$_3$), 7.42 (t, *J* = 7.7 Hz, 1H, C≡CCCHC*H*), 7.44–7.53 (m, 4H, N=NCCHCH*C*H, N=NCCHC*H*CH, C≡CCC*H*CH), 7.82 (ddd, *J* = 7.9/2.0/1.3 Hz, 1H, C≡CCCHCC*H*), 7.88–7.93 (m, 2H, N=NCC*H*CHCH), 7.94 (t, *J* = 1.7 Hz, 1H, C≡CCC*H*C) ppm. ^{13}C NMR (126 MHz, $CDCl_3$, 21 °C, TMS): δ = 14.13 (q, 1C, OCH$_2$*C*H$_3$), 17.60 (t, 1C, NCH$_2$*C*H$_2$C≡C), 24.50 (t, 1C, NCH$_2$*C*H$_2$CH$_2$CH), 26.73 (t, 1C, NCH$_2$CH*C*H$_2$), 41.76 (d, 1C, NCH$_2$*C*H), 53.29 (t, 1C, N*C*H$_2$CH$_2$CH$_2$CH), 55.02 (t, 1C, N*C*H$_2$CH), 57.33 (t, 1C, N*C*H$_2$CH$_2$C≡C), 60.22 (t, 1C, O*C*H$_2$CH$_3$), 80.61 (s, 1C, C≡*C*CCH), 89.23 (s, 1C, *C*≡CCCH), 122.39 (d, 1C, C≡CCCHC*C*H), 122.82 (d, 2C, N=NC*C*HCHCH), 124.69 (s, 1C, C≡C*C*CHC), 125.53 (d, 1C, C≡CC*C*HC), 128.85 (d, 1C, C≡CCCH*C*H), 128.99 (d, 2C, N=NCCH*C*HCH), 131.11 (d, 1C, N=NCCHCH*C*H), 133.69 (d, 1C, C≡CC*C*HCH), 152.33 (d, 2C, N=N*C*), 173.98 (s, 1C, C=O) ppm. MS (ESI$^+$) *m/z*: 390 [M+H]$^+$. HRMS (ESI$^+$): [M+H]$^+$ calcd for $C_{24}H_{28}O_2N_3$: 390.2182, found 390.2173.

*Ethyl 1-(4-{4-[(E)-phenylazo]phenyl}but-3-yn-1-yl)piperidine-3-carboxylate (p-**18a**)*

According to GP4 starting from *p*-**16a** (125 mg, 0.300 mmol), nipecotic acid ethyl ester (142 mg, 0.900 mmol), acetone (0.3 mL) and a reaction time of 48 h *p*-**18a** was obtained as orange oil (103 mg, 88%); R_f ≈ 0.25 (pentane/EtOAc = 8:2). IR (NaCl): $\tilde{\nu}$ = 3069, 2945, 2862, 2805, 2211, 1725, 1595, 1585, 1495, 1465, 1442, 1368, 1297, 1271, 1222, 1189, 1153, 1096, 1032, 1018, 841, 769, 687 cm^{-1}. ^{1}H NMR (400 MHz, $CDCl_3$, 21 °C, TMS): δ = 1.25 (t, *J* = 7.1 Hz, 3H, OCH$_2$C*H$_3$*), 1.46 (qd, *J* = 11.8/3.7 Hz, 1H, NCH$_2$CHC*H$_{ax}$*H$_{eq}$), 1.53–1.65 (m, 1H, NCH$_2$C*H$_{ax}$*H$_{eq}$CH$_2$CH), 1.75 (dp, *J* = 12.9/3.5 Hz, 1H, NCH$_2$CH$_{ax}$*H$_{eq}$*CH$_2$CH), 1.96 (dq, *J* = 13.0/4.0 Hz, 1H, NCH$_2$CHCH$_{ax}$*H$_{eq}$*), 2.14 (td, *J* = 10.8/2.2 Hz, 1H, NC*H$_{ax}$*H$_{eq}$CH$_2$CH$_2$CH), 2.30 (t, *J* = 10.7 Hz, 1H, NC*H$_{ax}$*H$_{eq}$CH), 2.53–2.68 (m, 3H, NCH$_2$C*H$_{ax}$*, NCH$_2$C*H$_2$*C≡C), 2.69–2.76 (m, 2H, NC*H$_2$*CH$_2$C≡C), 2.82 (d$_{br}$, *J* = 11.2 Hz, 1H, NCH$_{ax}$*H$_{eq}$*CH$_2$CH$_2$CH), 3.06 (d$_{br}$, *J* = 10.4 Hz, 1H, NCH$_{ax}$*H$_{eq}$*CH), 4.14 (q, *J* = 7.1 Hz, 2H, OC*H$_2$*CH$_3$), 7.44–7.55 (m, 5H, N=NCCHCH*C*H, N=NCCHC*H*CH, C≡CCC*H*CHC), 7.82–7.88 (m, 2H, C≡CCCHC*H*C), 7.89–7.94 (m, 2H, N=NCC*H*CHCH) ppm. ^{13}C NMR (101 MHz, $CDCl_3$, 21 °C, TMS): δ = 14.18 (q, 1C, OCH$_2$*C*H$_3$), 17.77 (t, 1C, NCH$_2$*C*H$_2$C≡C), 24.55 (t, 1C, NCH$_2$*C*H$_2$CH$_2$CH), 26.78 (t, 1C, NCH$_2$CH*C*H$_2$), 41.80 (d, 1C, NCH$_2$*C*H), 53.34 (t, 1C, N*C*H$_2$CH$_2$CH$_2$CH), 55.05 (t, 1C, N*C*H$_2$CH), 57.32 (t, 1C, N*C*H$_2$CH$_2$C≡C), 60.31 (t, 1C, O*C*H$_2$CH$_3$), 81.17 (s, 1C, C≡*C*CCH), 91.21 (s, 1C, *C*≡CCCH), 122.80 (d, 4C, C≡CCCH*C*HC, N=NC*C*HCHCH), 126.53 (s, 1C, CH$_2$C≡C*C*), 129.05 (d, 2C, N=NCCH*C*HCH), 131.09 (d, 1C, N=NCCHCH*C*H), 132.29 (d, 2C, C≡CC*C*HCHC), 151.37 (s, 1C, C≡CCCHCH*C*), 152.54 (s, 1C, N=N*C*CHCHCH), 174.07 (s, 1C, C=O) ppm. MS (ESI$^+$) *m/z*: 390 [M+H]$^+$. HRMS (EI$^+$): M$^+$ calcd for $C_{24}H_{27}O_2N_2$: 389.2103, found 389.2095.

*(R)-Ethyl 1-(4-{4-[(E)-phenylazo]phenyl}but-3-yn-1-yl)piperidine-3-carboxylate ((R)-p-**18a**)*

According to GP4 starting from *p*-**16a** (125 mg, 0.300 mmol), nipecotic acid ethyl ester (142 mg, 0.900 mmol), acetone (0.3 mL) and a reaction time of 48 h (*R*)-*p*-**18a** was obtained as orange oil (103 mg, 88%); $[\alpha]^{20}_D$ = -13.2 (c = 0.1 in CH_2Cl_2); R_f ≈ 0.25 (pentane/EtOAc = 8:2). IR (NaCl): $\tilde{\nu}$ = 3064, 2942, 2859, 2805, 2213, 1729, 1595, 1584, 1495, 1464, 1440, 1370, 1310, 1269, 1220, 1183, 1153, 1099, 1033, 1018, 849, 764, 686 cm^{-1}. ^{1}H NMR (400 MHz, $CDCl_3$, 21 °C, TMS): δ = 1.25 (t, *J* = 7.1 Hz, 3H, OCH$_2$C*H$_3$*), 1.46 (qd, *J* = 12.1/4.0 Hz, 1H, NCH$_2$CHC*H$_{ax}$*H$_{eq}$), 1.53–1.65 (m, 1H, NCH$_2$C*H$_{ax}$*H$_{eq}$CH$_2$CH), 1.75 (dp, *J* = 11.6/3.7 Hz, 1H, NCH$_2$CH$_{ax}$*H$_{eq}$*CH$_2$CH), 1.95 (dq, *J* = 12.5/4.1 Hz, 1H, NCH$_2$CHCH$_{ax}$*H$_{eq}$*), 2.14 (td, *J* = 11.1/3.2 Hz, 1H, NC*H$_{ax}$*H$_{eq}$CH$_2$CH$_2$CH), 2.30 (t, *J* = 10.7 Hz, 1H, NC*H$_{ax}$*H$_{eq}$CH), 2.53–2.67 (m, 3H, NCH$_2$C*H$_{ax}$*, NCH$_2$C*H$_2$*C≡C), 2.69–2.76 (m, 2H, NC*H$_2$*CH$_2$C≡C), 2.82 (d$_{br}$, *J* = 11.2 Hz, 1H, NCH$_{ax}$*H$_{eq}$*CH$_2$CH$_2$CH), 3.06 (d$_{br}$, *J* = 10.8 Hz, 1H, NCH$_{ax}$*H$_{eq}$*CH), 4.14 (q, *J* = 7.1 Hz, 2H, OC*H$_2$*CH$_3$), 7.44–7.56 (m, 5H, N=NCCHCH*C*H, N=NCCHC*H*CH, C≡CCC*H*CHC), 7.83–7.88 (m, 2H, C≡CCCHC*H*C), 7.89–7.94 (m, 2H, N=NCC*H*CHCH) ppm. ^{13}C NMR (101 MHz, $CDCl_3$, 21 °C, TMS): δ = 14.18 (q, 1C, OCH$_2$*C*H$_3$), 17.76 (t, 1C, NCH$_2$*C*H$_2$C≡C), 24.54 (t, 1C, NCH$_2$*C*H$_2$CH$_2$CH), 26.78 (t, 1C, NCH$_2$CH*C*H$_2$), 41.79 (d, 1C, NCH$_2$*C*H), 53.34 (t, 1C, N*C*H$_2$CH$_2$CH$_2$CH), 55.05 (t, 1C, N*C*H$_2$CH), 57.31 (t, 1C, N*C*H$_2$CH$_2$C≡C), 60.31 (t, 1C, O*C*H$_2$CH$_3$), 81.16 (s, 1C, C≡*C*CCH), 91.21 (s, 1C, *C*≡CCCH), 122.80 (d, 4C, C≡CCCH*C*HC, N=NC*C*HCHCH), 126.52 (s, 1C, CH$_2$C≡C*C*), 129.05 (d, 2C, N=NCCH*C*HCH), 131.09 (d, 1C, N=NCCHCH*C*H), 132.29 (d, 2C, C≡CC*C*HCHC), 151.37 (s, 1C, C≡CCCHCH*C*), 152.53 (s, 1C, N=N*C*CHCHCH), 174.06 (s, 1C, C=O) ppm. MS (ESI$^+$) *m/z*: 390 [M+H]$^+$. HRMS (EI$^+$): M$^+$ calcd for $C_{24}H_{27}O_2N_3$: 389.2103, found 389.2095.

*Ethyl 1-(4-{3-[(E)-1-naphthylazo]phenyl}but-3-yn-1-yl)piperidine-3-carboxylate (m-**18b**)*

According to GP4 starting from *m*-**16b** (136 mg, 0.300 mmol), nipecotic acid ethyl ester (142 mg, 0.900 mmol), acetone (0.3 mL) and a reaction time of 48 h *m*-**18b** was obtained as orange oil (113 mg, 86%); R_f ≈ 0.20 (pentane/EtOAc = 8:2). IR (NaCl): $\tilde{\nu}$ = 3054, 2942, 2854, 2809, 2230, 1729, 1598, 1508, 1467, 1445, 1370, 1305, 1206, 1180, 1153, 1133, 1101, 1033, 896, 804, 771 cm^{-1}. ^{1}H NMR (400 MHz, $CDCl_3$, 21 °C, TMS): δ = 1.24 (t, *J* = 7.1 Hz, 3H, OCH_2CH_3), 1.46 (qd, *J* = 11.8/3.7 Hz, 1H, $NCH_2CHCH_{ax}H_{eq}$), 1.53–1.66 (m, 1H, $NCH_2CH_{ax}H_{eq}CH_2CH$), 1.75 (dp, *J* = 13.5/3.7 Hz, 1H, $NCH_2CH_{ax}H_{eq}CH_2CH$), 1.96 (dq, *J* = 13.2/3.8 Hz, 1H, $NCH_2CHCH_{ax}H_{eq}$), 2.14 (td, *J* = 10.9/2.6 Hz, 1H, $NCH_{ax}H_{eq}CH_2CH_2CH$), 2.31 (t, *J* = 10.6 Hz, 1H, $NCH_{ax}H_{eq}CH$), 2.54–2.70 (m, 3H, NCH_2CH_{ax}, $NCH_2CH_2C{\equiv}C$), 2.71–2.79 (m, 2H, $NCH_2CH_2C{\equiv}C$), 2.83 (d_{br}, *J* = 11.0 Hz, 1H, $NCH_{ax}H_{eq}CH_2CH_2CH$), 3.07 (d_{br}, *J* = 9.1 Hz, 1H, $NCH_{ax}H_{eq}CH$), 4.13 (q, *J* = 7.1 Hz, 2H, OCH_2CH_3), 7.47 (t, *J* = 7.7 Hz, 1H, C≡CCCHCH), 7.50–7.61 (m, 3 H, C≡CCCHCH, N=NCCHCHCH, N=NCCCHCHCH), 7.65 (ddd, *J* = 8.4/6.8/1.3 Hz, 1H, N=NCCCHCH), 7.81 (dd, *J* = 7.5/1.0 Hz, 1H, N=NCCHCHCH), 7.92 (d, *J* = 8.1 Hz, 1H, N=NCCCHCHCHCH), 7.95–8.01 (m, 2H, N=NCCHCHCH, C≡CCCHCCH), 8.06 (t, *J* = 1.6 Hz, 1H, C≡CCCHC), 8.93 (d, *J* = 8.5 Hz, 1H, N=NCCCH) ppm. ^{13}C NMR (101 MHz, $CDCl_3$, 21 °C, TMS): δ = 14.15 (q, 1C, OCH_2CH_3), 17.62 (t, 1C, $NCH_2CH_2C{\equiv}C$), 24.51 (t, 1C, $NCH_2CH_2CH_2CH$), 26.75 (t, 1C, $NCH_2CH_2CH_2$), 41.75 (d, 1C, NCH_2CH), 53.31 (t, 1C, $NCH_2CH_2CH_2CH$), 55.02 (t, 1C, NCH_2CH), 57.33 (t, 1C, $NCH_2CH_2C{\equiv}C$), 60.29 (t, 1C, OCH_2CH_3), 80.69 (s, 1C, C≡CCH), 89.28 (s, 1C, C≡CCH), 111.80 (d, 1C, N=NCCHCHCH), 123.01 (d, 1C, C≡CCCHCCH), 123.35 (d, 1C, N=NCCCH), 124.72 (s, 1C, C≡CCCHC), 125.54 (d, 2C, C≡CCCHC, N=NCCHCHCH), 126.43 (d, 1C, N=NCCCHCHCH), 126.84 (d, 1C, N=NCCCHCH), 127.86 (d, 1C, N=NCCCHCHCHCH), 128.96 (d, 1C, C≡CCCHCH), 131.26 (s, 1C, N=NCCCH), 131.53 (d, 1C, N=NCCHCHCH), 133.83 (d, 1C, C≡CCCHCH), 134.17 (s, 1C, N=NCCHCHCHC), 147.46 (s, 1C, N=NCCHCHCH), 152.76 (s, 1C, C≡CCCHC), 174.04 (s, 1C, C=O) ppm. MS (ESI$^+$) *m/z*: 440 [M+H]$^+$. HRMS (ESI$^+$): [M+H]$^+$ calcd for $C_{28}H_{30}O_2N_3$: 440.2338, found 440.2330.

*(R)-Ethyl 1-(4-{3-[(E)-1-naphthylazo]phenyl}but-3-yn-1-yl)piperidine-3-carboxylate ((R)-m-**18b**)*

According to GP4 starting from *m*-**16b** (136 mg, 0.300 mmol), nipecotic acid ethyl ester (142 mg, 0.900 mmol), acetone (0.3 mL) and a reaction time of 48 h (*R*)-*m*-**18b** was obtained as orange oil (113 mg, 86%); $[\alpha]^{20}_D$ = -8.6 (c = 0.1 in CH_2Cl_2); R_f ≈ 0.20 (pentane/EtOAc = 8:2). IR (NaCl): $\tilde{\nu}$ = 3054, 2941, 2853, 2809, 2230, 1728, 1598, 1507, 1467, 1444, 1370, 1305, 1206, 1180, 1152, 1133, 1101, 1033, 896, 804, 772 cm^{-1}. ^{1}H NMR (400 MHz, $CDCl_3$, 21 °C, TMS): δ = 1.25 (t, *J* = 7.1 Hz, 3H, OCH_2CH_3), 1.46 (qd, *J* = 11.8/3.7 Hz, 1H, $NCH_2CHCH_{ax}H_{eq}$), 1.54–1.67 (m, 1H, $NCH_2CH_{ax}H_{eq}CH_2CH$), 1.76 (dp, *J* = 14.5/3.9 Hz, 1H, $NCH_2CH_{ax}H_{eq}CH_2CH$), 1.96 (dq, *J* = 13.0/4.0 Hz, 1H, $NCH_2CHCH_{ax}H_{eq}$), 2.15 (td, *J* = 11.0/2.8 Hz, 1H, $NCH_{ax}H_{eq}CH_2CH_2CH$), 2.31 (t, *J* = 10.6 Hz, 1H, $NCH_{ax}H_{eq}CH$), 2.55–2.69 (m, 3H, NCH_2CH_{ax}, $NCH_2CH_2C{\equiv}C$), 2.72–2.78 (m, 2H, $NCH_2CH_2C{\equiv}C$), 2.84 (d_{br}, *J* = 11.0 Hz, 1H, $NCH_{ax}H_{eq}CH_2CH_2CH$), 3.07 (d_{br}, *J* = 10.1 Hz, 1H, $NCH_{ax}H_{eq}CH$), 4.13 (q, *J* = 7.1 Hz, 2H, OCH_2CH_3), 7.47 (t, *J* = 7.7 Hz, 1H, C≡CCCHCH), 7.50–7.61 (m, 3H, C≡CCCHCH, N=NCCHCHCH, N=NCCCHCHCH), 7.66 (ddd, *J* = 8.4/6.8/1.3 Hz, 1H, N=NCCCHCH), 7.81 (dd, *J* = 7.5/1.0 Hz, 1H, N=NCCHCHCH), 7.92 (d, *J* = 8.1 Hz, 1H, N=NCCCHCHCHCH), 7.95–8.01 (m, 2H, N=NCCHCHCH, C≡CCCHCCH), 8.06 (t, *J* = 1.6 Hz, 1H, C≡CCCHC), 8.93 (d, *J* = 8.6 Hz, 1H, N=NCCCH) ppm. ^{13}C NMR (101 MHz, $CDCl_3$, 21 °C, TMS): δ = 14.18 (q, 1C, OCH_2CH_3), 17.66 (t, 1C, $NCH_2CH_2C{\equiv}C$), 24.55 (t, 1C, $NCH_2CH_2CH_2CH$), 26.79 (t, 1C, $NCH_2CH_2CH_2$), 41.80 (d, 1C, NCH_2CH), 53.36 (t, 1C, $NCH_2CH_2CH_2CH$), 55.07 (t, 1C, NCH_2CH), 57.37 (t, 1C, $NCH_2CH_2C{\equiv}C$), 60.31 (t, 1C, OCH_2CH_3), 80.72 (s, 1C, C≡CCH), 89.32 (s, 1C, C≡CCH), 111.85 (d, 1C, N=NCCHCHCH), 123.02 (d, 1C, C≡CCCHCCH), 123.39 (d, 1C, N=NCCCH), 124.76 (s, 1C, C≡CCCHC), 125.58 (d, 2C, C≡CCCHC, N=NCCHCHCH), 126.45 (d, 1C, N=NCCCHCHCH), 126.87 (d, 1C, N=NCCCHCH), 127.89 (d, 1C, N=NCCCHCHCHCH), 128.98 (d, 1C, C≡CCCHCH), 131.29 (s, 1C, N=NCCCH), 131.54 (d, 1C, N=NCCHCHCH), 133.85 (d, 1C, C≡CCCHCH), 134.22 (s, 1C, N=NCCHCHCHC), 147.52 (s, 1C, N=NCCHCHCH), 152.82 (s, 1C, C≡CCCHC), 174.07 (s, 1C, C=O) ppm. MS (ESI$^+$) *m/z*: 440 [M+H]$^+$. HRMS (ESI$^+$): [M+H]$^+$ calcd for $C_{28}H_{30}O_2N_3$: 440.2338, found 440.2329.

*Ethyl 1-(4-{4-[(E)-1-naphthylazo]phenyl}but-3-yn-1-yl)piperidine-3-carboxylate (p-**18b**)*

According to GP4 starting from *p*-**16b** (136 mg, 0.300 mmol), nipecotic acid ethyl ester (142 mg, 0.900 mmol), acetone (0.3 mL) and a reaction time of 72 h *p*-**18b** was obtained as orange oil (114 mg, 87%); R_f ≈ 0.20 (pentane/EtOAc = 8:2). IR (NaCl): $\tilde{\nu}$ = 3050, 2940, 2854, 2808, 2219, 1729, 1595, 1497, 1467, 1444, 1370, 1303, 1217, 1180, 1153, 1099, 1032, 844, 802, 772 cm^{-1}. ^{1}H NMR (500 MHz, $CDCl_3$, 21 °C, TMS): δ = 1.25 (t, *J* = 7.1 Hz, 3H, OCH_2CH_3), 1.47 (qd, *J* = 11.6/4.0 Hz, 1H, $NCH_2CHCH_{ax}H_{eq}$), 1.54–1.65 (m, 1H, $NCH_2CH_{ax}H_{eq}CH_2CH$), 1.75 (dp, *J* = 11.0/3.9 Hz, 1H, $NCH_2CH_{ax}H_{eq}CH_2CH$), 1.95 (dq, *J* = 13.0/4.0 Hz, 1H, $NCH_2CHCH_{ax}H_{eq}$), 2.14 (td, *J* = 10.9/2.8 Hz, 1H, $NCH_{ax}H_{eq}CH_2CH_2CH$), 2.32 (t, *J* = 10.6 Hz, 1H, $NCH_{ax}H_{eq}CH$), 2.58 (tt, *J* = 10.6/3.8 Hz, 1H, NCH_2CH_{ax}), 2.63–2.69 (m, 2H $NCH_2CH_2C{\equiv}C$), 2.70–2.76 (m, 2H, $NCH_2CH_2C{\equiv}C$), 2.82 (d_{br}, *J* = 11.1 Hz, 1H, $NCH_{ax}H_{eq}CH_2CH_2CH$), 3.06 (d_{br}, *J* = 8.5 Hz, 1H $NCH_{ax}H_{eq}CH$), 4.14 (q, *J* = 7.1 Hz, 2H, OCH_2CH_3), 7.52–7.60 (m, 4H, C≡CCCHCH, N=NCCHCHCH, N=NCCCHCHCH), 7.64 (ddd, *J* = 8.4/6.8/1.3 Hz, 1H, N=NCCCHCH), 7.82 (dd, *J* = 7.5/1.0 Hz, 1H, N=NCCHCHCH), 7.91 (d, *J* = 8.2 Hz, 1H, N=NCCCHCHCHCH), 7.94–8.01 (m, 3H, C≡CCCHCHC, N=NCCHCHCH), 8.92 (d, *J* = 7.9 Hz, 1H, N=NCCCH) ppm. ^{13}C NMR (126 MHz, $CDCl_3$, 21 °C, TMS): δ = 14.19 (q, 1C, OCH_2CH_3), 17.84 (t, 1C, $NCH_2CH_2C{\equiv}C$), 24.56 (t, 1C, $NCH_2CH_2CH_2CH$), 26.80 (t, 1C, $NCH_2CH_2CH_2$), 41.83 (d, 1C, NCH_2CH), 53.36 (t, 1C, $NCH_2CH_2CH_2CH$), 55.09 (t, 1C, NCH_2CH), 57.33 (t, 1C, $NCH_2CH_2C{\equiv}C$), 60.30 (t, 1C, OCH_2CH_3), 81.25 (s, 1C,

C≡*C*CCH), 91.41 (s, 1C, *C*≡CCCH), 111.80 (d, 1C, N=NCCHCH*C*H), 123.06 (d, 2C, C≡CCCH*C*HC), 123.37 (d, 1C, N=NCC*C*H), 125.56 (d, 1C, N=NCCH*C*HCH), 126.43 (d, 1C, N=NCCCHCH*C*H), 126.63 (s, 1C, $CH_2C{\equiv}C{\equiv}C$), 126.84 (d, 1C, N=NCCCH*C*H), 127.89 (d, 1C, N=NCCCHCHCH*C*H), 131.32 (s, 1C, N=NC*C*CH), 131.47 (d, 1C, N=NC*C*HCHCH), 132.35 (d, 2C, C≡CC*C*HCHC), 134.25 (s, 1C, N=NCCHCHCH*C*), 147.64 (s, 1C, N=N*C*CHCHCH), 151.95 (s, 1C, C≡CCCHCH*C*), 174.04 (s, 1C, C=O) ppm. MS (ESI^+) *m/z*: 440 $[M+H]^+$. HRMS (EI^+): M^+ calcd for $C_{28}H_{29}O_2N_3$: 439.2260, found 439.2269.

*(R)-Ethyl 1-(4-{4-[(E)-1-naphthylazo]phenyl}but-3-yn-1-yl)piperidine-3-carboxylate ((R)-p-**18b**)*

According to GP4 starting from *p*-**16b** (136 mg, 0.300 mmol), nipecotic acid ethyl ester (142 mg, 0.900 mmol), acetone (0.3 mL) and a reaction time of 72 h (*R*)-*p*-**18b** was obtained as orange oil (114 mg, 87%); $[\alpha]^{20}_D$ = -9.3 (c = 0.1 in CH_2Cl_2); R_f ≈ 0.20 (pentane/EtOAc = 8:2). IR (NaCl): $\tilde{\nu}$ = 3049, 2940, 2854, 2806, 2212, 1725, 1595, 1495, 1465, 1439, 1367, 1302, 1216, 1185, 1157, 1100, 1033, 844, 801, 774 cm^{-1}. ^1H NMR (500 MHz, $CDCl_3$, 21 °C, TMS): δ = 1.26 (t, *J* = 7.1 Hz, 3H, OCH_2CH_3), 1.47 (qd, *J* = 11.8/4.0 Hz, 1H, $NCH_2CHCH_{ax}H_{eq}$), 1.55–1.65 (m, 1H, $NCH_2CH_{ax}H_{eq}CH_2CH$), 1.75 (dp, *J* = 10.9/3.9 Hz, 1H, $NCH_2CH_{ax}H_{eq}CH_2CH$), 1.96 (dq, *J* = 13.0/3.8 Hz, 1H, $NCH_2CHCH_{ax}H_{eq}$), 2.15 (td, *J* = 10.9/2.7 Hz, 1H, $NCH_{ax}H_{eq}CH_2CH_2CH$), 2.32 (t, *J* = 10.6 Hz, 1H, $NCH_{ax}H_{eq}CH$), 2.59 (tt, *J* = 10.6/3.8 Hz, 1H, NCH_2CH_{ax}), 2.63–2.68 (m, 2H $NCH_2CH_2C{\equiv}C$), 2.71–2.77 (m, 2H, $NCH_2CH_2C{\equiv}C$), 2.82 (d_{br}, *J* = 11.2 Hz, 1H, $NCH_{ax}H_{eq}CH_2CH_2CH$), 3.07 (d_{br}, *J* = 9.5 Hz, 1H $NCH_{ax}H_{eq}CH$), 4.14 (q, *J* = 7.1 Hz, 2H, OCH_2CH_3), 7.52–7.60 (m, 4H, C≡CCC*H*CHC, N=NCCHC*H*CH, N=NCCCHCHC*H*), 7.64 (ddd, *J* = 8.3/6.8/1.3 Hz, 1H, N=NCCCHC*H*), 7.82 (dd, *J* = 7.5/1.0 Hz, 1H, N=NCCHCHC*H*), 7.92 (d, *J* = 8.1 Hz, 1H, N=NCCCHCHCHC*H*), 7.96–8.00 (m, 3H, C≡CCCHC*H*C, N=NCC*H*CHCH), 8.92 (d, *J* = 8.1 Hz, 1H, N=NCCC*H*) ppm. ^{13}C NMR (126 MHz, $CDCl_3$, 21 °C, TMS): δ = 14.18 (q, 1C, OCH_2CH_3), 17.83 (t, 1C, $NCH_2CH_2C{\equiv}C$), 24.56 (t, 1C, $NCH_2CH_2CH_2CH$), 26.79 (t, 1C, NCH_2CHCH_2), 41.83 (d, 1C, NCH_2CH), 53.35 (t, 1C, $NCH_2CH_2CH_2CH$), 55.09 (t, 1C, NCH_2CH), 57.32 (t, 1C, $NCH_2CH_2C{\equiv}C$), 60.29 (t, 1C, OCH_2CH_3), 81.25 (s, 1C, C≡*C*CCH), 91.41 (s, 1C, *C*≡CCCH), 111.80 (d, 1C, N=NCCHCH*C*H), 123.06 (d, 2C, C≡CCCH*C*HC), 123.37 (d, 1C, N=NCC*C*H), 125.56 (d, 1C, N=NCCH*C*HCH), 126.43 (d, 1C, N=NCCCHCH*C*H), 126.63 (s, 1C, $CH_2C{\equiv}C{\equiv}C$), 126.83 (d, 1C, N=NCCCH*C*H), 127.89 (d, 1C, N=NCCCHCHCH*C*H), 131.32 (s, 1C, N=NC*C*CH), 131.46 (d, 1C, N=NC*C*HCHCH), 132.35 (d, 2C, C≡CC*C*HCHC), 134.25 (s, 1C, N=NCCHCHCH*C*), 147.64 (s, 1C, N=N*C*CHCHCH), 151.94 (s, 1C, C≡CCCHCH*C*), 174.04 (s, 1C, C=O) ppm. MS (ESI^+) *m/z*: 440 $[M+H]^+$. HRMS (EI^+): M^+ calcd for $C_{28}H_{29}O_2N_3$: 439.2260, found 439.2247.

*Ethyl 1-(5-{3-[(E)-phenylazo]phenyl}pent-4-yn-1-yl)piperidine-3-carboxylate (m-**19a**)*

According to GP4 starting from *m*-**17a** (125 mg, 0.300 mmol), nipecotic acid ethyl ester (142 mg, 0.900 mmol), acetone (0.3 mL) and a reaction time of 72 h *m*-**19a** was obtained as orange oil (111 mg, 92%); R_f ≈ 0.2 (pentane/EtOAc = 8:2). IR (NaCl): $\tilde{\nu}$ = 3061, 2925, 2852, 2807, 2228, 1729, 1596, 1468, 1446, 1371, 1305, 1177, 1151, 1132, 1104, 1029, 896, 795, 766, 690 vor cm^{-1}. ^1H NMR (500 MHz, $CDCl_3$, 21 °C, TMS): δ = 1.25 (t, *J* = 7.1 Hz, 3H, OCH_2CH_3), 1.42–1.52 (m, 1H, $NCH_2CHCH_{ax}H_{eq}$), 1.53–1.63 (m, 1H, $NCH_2CH_{ax}H_{eq}CH_2CH$), 1.73 (dp, *J* = 11.1/4.0 Hz, 1H, $NCH_2CH_{ax}H_{eq}CH_2CH$), 1.81 (p, *J* = 7.1 Hz, 2H, $NCH_2CH_2CH_2C{\equiv}C$), 1.93 (dq, *J* = 13.0/4.0 Hz, 1H, $NCH_2CHCH_{ax}H_{eq}$), 2.03 (t, *J* = 9.7 Hz, 1H, $NCH_{ax}H_{eq}CH_2CH_2CH$), 2.21 (t, *J* = 10.2 Hz, 1H, $NCH_{ax}H_{eq}CH$), 2.45–2.53 (m, 4H, $NCH_2CH_2CH_2C{\equiv}C$, $NCH_2CH_2CH_2C{\equiv}C$), 2.57 (tt, *J* = 10.4/3.8 Hz, 1H, NCH_2CH_{ax}), 2.77 (d_{br}, *J* = 10.9 Hz, 1H, $NCH_{ax}H_{eq}CH_2CH_2CH$), 2.99 (d_{br}, *J* = 10.1 Hz, 1H, $NCH_{ax}H_{eq}CH$), 4.13 (q, *J* = 7.1 Hz, 2H, OCH_2CH_3), 7.43 (t, *J* = 7.7 Hz, 1H, C≡CCCHC*H*), 7.45–7.54 (m, 4H, N=NCCHCHC*H*, N=NCCHC*H*CH, C≡CCC*H*CH), 7.83 (ddd, *J* = 7.9/1.9/1.3 Hz, 1H, C≡CCCHCC*H*), 7.90–7.93 (m, 2H, N=NCC*H*CHCH), 7.95 (t, *J* = 1.7 Hz, 1H, C≡CCC*H*C) ppm. ^{13}C NMR (126 MHz, $CDCl_3$, 21 °C, TMS): δ = 14.17 (q, 1C, OCH_2CH_3), 17.34 (t, 1C, $NCH_2CH_2CH_2C{\equiv}C$), 24.55 (t, 1C, $NCH_2CH_2CH_2CH$), 25.98 (t, 1C, $NCH_2CH_2CH_2C{\equiv}C$), 26.91 (t, 1C, NCH_2CHCH_2), 41.84 (d, 1C, NCH_2CH), 53.83 (t, 1C, $NCH_2CH_2CH_2CH$), 55.45 (t, 1C, NCH_2CH), 57.64 (t, 1C, $NCH_2CH_2CH_2C{\equiv}C$), 60.22 (t, 1C, OCH_2CH_3), 80.08 (s, 1C, $CH_2C{\equiv}C$), 90.80 (s, 1C, $CH_2C{\equiv}C$), 122.27 (d, 1C, C≡CCCHCC*H*), 122.85 (d, 2C, N=NCC*H*CHCH), 124.90 (s, 1C, C≡C*C*CHC), 125.57 (d, 1C, C≡CCCHC), 128.87 (d, 1C, C≡CCCH*C*H), 129.02 (d, 2C, N=NCCH*C*HCH), 131.11 (d, 1C, N=NCCHCH*C*H), 133.72 (d, 1C, C≡CC*C*HCH), 152.36 (d, 2C, N=N*C*), 174.17 (s, 1C, C=O) ppm. MS (ESI^+) *m/z*: 404 $[M+H]^+$. HRMS (ESI^+): $[M+H]^+$ calcd for $C_{25}H_{30}O_2N_3$: 404.2338, found 404.2331.

*Ethyl 1-(5-{4-[(E)-phenylazo]phenyl}pent-4-yn-1-yl)piperidine-3-carboxylate (p-**19a**)*

According to GP4 starting from *p*-**17a** (125 mg, 0.300 mmol), nipecotic acid ethyl ester (142 mg, 0.900 mmol), acetone (0.3 mL) and a reaction time of 48 h *p*-**19a** was obtained as orange oil (113 mg, 93%); R_f ≈ 0.2 (pentane/EtOAc = 8:2). IR (NaCl): $\tilde{\nu}$ = 3062, 2942, 2866, 2807, 2770, 2224, 1730, 1597, 1496, 1467, 1443, 1371, 1301, 1220, 1178, 1152, 1101, 1029, 846, 767, 678 cm^{-1}. ^1H NMR (400 MHz, $CDCl_3$, 21 °C, TMS): δ = 1.26 (t, *J* = 7.1 Hz, 3H, OCH_2CH_3), 1.47 (qd, *J* = 12.2/3.4 Hz, 1H, $NCH_2CHCH_{ax}H_{eq}$), 1.52–1.65 (m, 1H, $NCH_2CH_{ax}H_{eq}CH_2CH$), 1.74 (dp, *J* = 10.9/4.1/3.6 Hz, 2H, $NCH_2CH_{ax}H_{eq}CH_2CH$), 1.82 (p, *J* = 7.2 Hz, 2H, $NCH_2CH_2CH_2C{\equiv}C$), 1.93 (dq, *J* = 12.5/3.5 Hz, 1H, $NCH_2CHCH_{ax}H_{eq}$), 2.03 (td, *J* = 11.0/1.9 Hz, 1H, $NCH_{ax}H_{eq}CH_2CH_2CH$), 2.20 (t, *J* = 11.0 Hz, 1H, $NCH_{ax}H_{eq}CH$), 2.46–2.53 (m, 4H, $NCH_2CH_2CH_2C{\equiv}C$, $NCH_2CH_2CH_2C{\equiv}C$), 2.57 (tt, *J* = 10.4/3.8 Hz, 1H, NCH_2CH_{ax}), 2.78 (d_{br}, *J* = 11.2 Hz, 1H, $NCH_{ax}H_{eq}CH_2CH_2CH$), 2.99 (d_{br}, *J* =

10.7 Hz, 1H, NCH$_{ax}$*H$_{eq}$*CH), 4.13 (q, *J* = 7.1 Hz, 2H, OC*H*$_2$CH$_3$), 7.44–7.54 (m, 5H, N=NCCHCHC*H*, N=NCCHC*H*CH, C≡CCC*H*CHC), 7.86 (d, *J* = 8.5 Hz, 2H, C≡CCCHC*H*C), 7.89–7.93 (m, 2H, N=NCC*H*CHCH) ppm. ^{13}C NMR (101 MHz, CDCl$_3$, 21 °C, TMS): *δ* = 14.19 (q, 1C, OCH$_2$*C*H$_3$), 17.51 (t, 1C, NCH$_2$CH$_2$*C*H$_2$C≡C), 24.57 (t, 1C, NCH$_2$*C*H$_2$CH$_2$CH), 25.96 (t, 1C, NCH$_2$*C*H$_2$CH$_2$C≡C), 26.94 (t, 1C, NCH$_2$CH*C*H$_2$), 41.85 (d, 1C, NCH$_2$*C*H), 53.85 (t, 1C, N*C*H$_2$CH$_2$CH$_2$CH), 55.45 (t, 1C, N*C*H$_2$CH), 57.67 (t, 1C, N*C*H$_2$CH$_2$CH$_2$C≡C), 60.27 (t, 1C, O*C*H$_2$CH$_3$), 80.64 (s, 1C, CH$_2$C≡*C*), 92.83 (s, 1C, CH$_2$*C*≡C), 122.80 (d, 4C, C≡CCCH*C*HC, N=NC*C*HCHCH), 126.75 (s, 1C, CH$_2$C≡C*C*), 129.05 (d, 2C, N=NCCH*C*HCH), 131.06 (d, 1C, N=NCCHCH*C*H), 132.26 (d, 2C, C≡CC*C*HCHC), 151.31 (s, 1C, C≡CCCHCH*C*), 152.55 (s, 1C, N=N*C*CHCHCH), 174.22 (s, 1C, C=O) ppm. MS (ESI$^+$) *m/z*: 404 [M+H]$^+$. HRMS (EI$^+$): M$^+$ calcd for C$_{25}$H$_{29}$O$_2$N$_3$: 403.2260, found 403.2257.

*Ethyl 1-(5-{3-[(E)-1-naphthylazo]phenyl}pent-4-yn-1-yl)piperidine-3-carboxylate (m-**19b**)*

According to GP4 starting from *m*-**17b** (140 mg, 0.300 mmol), nipecotic acid ethyl ester (142 mg, 0.900 mmol), acetone (0.3 mL) and a reaction time of 48 h *m*-**19b** was obtained as orange oil (124 mg, 91%); R_f ≈ 0.15 (pentane/EtOAc = 8:2). IR (NaCl): $\tilde{\nu}$ = 3054, 2941, 2807, 2770, 2229, 1729, 1596, 1507, 1467, 1444, 1371, 1344, 1306, 1204, 1178, 1151, 1105, 1030, 896, 805, 772 cm^{-1}. ^{1}H NMR (400 MHz, CDCl$_3$, 21 °C, TMS): *δ* = 1.25 (t, *J* = 7.1 Hz, 3H, OCH$_2$C*H*$_3$), 1.47 (qd, *J* = 12.3/4.1 Hz, 1H, NCH$_2$CHC*H*$_{ax}$H$_{eq}$), 1.53–1.66 (m, 1H, NCH$_2$C*H*$_{ax}$H$_{eq}$CH$_2$CH), 1.74 (dp, *J* = 13.1/3.7 Hz, 1H, NCH$_2$CH$_{ax}$*H*$_{eq}$CH$_2$CH), 1.84 (p, *J* = 7.2 Hz, 2H, NCH$_2$C*H*$_2$CH$_2$C≡C), 1.93 (dq, *J* = 12.8/3.8 Hz, 1H, NCH$_2$CHCH$_{ax}$*H*$_{eq}$), 2.04 (td, *J* = 11.3/2.4 Hz, 1H, NC*H*$_{ax}$H$_{eq}$CH$_2$CH$_2$CH), 2.21 (t, *J* = 10.4 Hz, 1H, NC*H*$_{ax}$H$_{eq}$CH), 2.47–2.54 (m, 4H, NCH$_2$CH$_2$C*H*$_2$C≡C, NC*H*$_2$CH$_2$CH$_2$C≡C), 2.58 (tt, *J* = 10.5/3.9 Hz, 1H, NCH$_2$C*H*$_{ax}$), 2.79 (d$_{br}$, *J* = 11.1 Hz, 1H, NCH$_{ax}$*H*$_{eq}$CH$_2$CH$_2$CH), 3.01 (d$_{br}$, *J* = 10.5 Hz, 1H, NCH$_{ax}$*H*$_{eq}$CH), 4.13 (q, *J* = 7.1 Hz, 2H, OC*H*$_2$CH$_3$), 7.47 (t, *J* = 7.7 Hz, 1H, C≡CCCHC*H*), 7.50–7.60 (m, 3H, C≡CCC*H*CH, N=NCCHC*H*CH, N=NCCCHCHC*H*), 7.65 (ddd, *J* = 8.4/6.8/1.3 Hz, 1H, N=NCCCHC*H*), 7.82 (dd, *J* = 7.5/1.1 Hz, 1H, N=NCCHCHC*H*), 7.92 (d, *J* = 8.1 Hz, 1H, N=NCCCHCHCHC*H*), 7.94–8.00 (m, 2H, N=NCC*H*CHCH, C≡CCCHCC*H*), 8.06 (t, *J* = 1.6 Hz, 1H, C≡CCC*H*C), 8.93 (d, *J* = 8.5 Hz, 1H, N=NCCC*H*) ppm. ^{13}C NMR (101 MHz, CDCl$_3$, 21 °C, TMS): *δ* = 14.17 (q, 1C, OCH$_2$*C*H$_3$), 17.38 (t, 1C, NCH$_2$*C*H$_2$CH$_2$C≡C), 24.54 (t, 1C, NCH$_2$*C*H$_2$CH$_2$CH), 25.96 (t, 1C, NCH$_2$CH$_2$*C*H$_2$C≡C), 26.91 (t, 1C, NCH$_2$CH*C*H$_2$), 41.81 (d, 1C, NCH$_2$*C*H), 53.84 (t, 1C, N*C*H$_2$CH$_2$CH$_2$CH), 55.42 (t, 1C, N*C*H$_2$CH), 57.68 (t, 1C, N*C*H$_2$CH$_2$CH$_2$C≡C), 60.25 (t, 1C, O*C*H$_2$CH$_3$), 80.15 (s, 1C, C≡*C*CCH), 90.85 (s, 1C, *C*≡CCCH), 111.82 (d, 1C, N=NCCHCH*C*H), 122.86 (d, 1C, C≡CCCHC*C*H), 123.38 (d, 1C, N=NCC*C*H), 124.93 (s, 1C, C≡C*C*CHC), 125.56 (d, 2C, C≡CC*C*HC, N=NCCH*C*HCH), 126.43 (d, 1C, N=NCCCHCH*C*H), 126.85 (d, 1C, N=NCCCH*C*H), 127.87 (d, 1C, N=NCCCHCHCH*C*H), 128.96 (d, 1C, C≡CCCH*C*H), 131.27 (s, 1C, N=NC*C*CH), 131.51 (d, 1C, N=NC*C*HCHCH), 133.84 (d, 1C, C≡CC*C*HCH), 134.19 (s, 1C, N=NCCHCHCH*C*), 147.51 (s, 1C, N=N*C*CHCHCH), 152.80 (s, 1C, C≡CCCH*C*), 174.19 (s, 1C, C=O) ppm. MS (ESI$^+$) *m/z*: 454 [M+H]$^+$. HRMS (ESI$^+$): [M+H]$^+$ calcd for C$_{29}$H$_{32}$O$_2$N$_3$: 454.2495, found 454.2485.

*Ethyl 1-(5-{4-[(E)-1-naphthylazo]phenyl}pent-4-yn-1-yl)piperidine-3-carboxylate (p-**19b**)*

According to GP4 starting from *p*-**17b** (140 mg, 0.300 mmol), nipecotic acid ethyl ester (142 mg, 0.900 mmol), acetone (0.3 mL) and a reaction time of 72 h *p*-**19b** was obtained as orange oil (122 mg, 90%); R_f ≈ 0.15 (pentane/EtOAc = 8:2). IR (NaCl): $\tilde{\nu}$ = 3051, 2942, 2807, 2770, 2223, 1730, 1596, 1497, 1467, 1445, 1371, 1303, 1217, 1178, 1152, 1101, 1030, 1012, 845, 802, 772 cm^{-1}. ^{1}H NMR (500 MHz, CDCl$_3$, 21 °C, TMS): *δ* = 1.26 (t, *J* = 7.1 Hz, 3H, OCH$_2$C*H*$_3$), 1.48 (qd, *J* = 11.9/3.9 Hz, 1H, NCH$_2$CHC*H*$_{ax}$H$_{eq}$), 1.53–1.65 (m, 1H, NCH$_2$C*H*$_{ax}$H$_{eq}$CH$_2$CH), 1.74 (dp, *J* = 11.2/4.0 Hz, 1H, NCH$_2$CH$_{ax}$*H*$_{eq}$CH$_2$CH), 1.83 (p, *J* = 7.1 Hz, 2H, NCH$_2$C*H*$_2$CH$_2$C≡C), 1.94 (dq, *J* = 13.0/3.8 Hz, 1H, NCH$_2$CHCH$_{ax}$*H*$_{eq}$), 2.05 (td, *J* = 10.8/2.1 Hz, 1H, NC*H*$_{ax}$H$_{eq}$CH$_2$CH$_2$CH), 2.22 (t, *J* = 10.7 Hz, 1H, NC*H*$_{ax}$H$_{eq}$CH), 2.47–2.55 (m, 4H, NCH$_2$CH$_2$C*H*$_2$C≡C, NC*H*$_2$CH$_2$CH$_2$C≡C), 2.58 (tt, *J* = 10.4/3.8 Hz, 1H, NCH$_2$C*H*$_{ax}$), 2.78 (d$_{br}$, *J* = 11.2 Hz, 1H, NCH$_{ax}$*H*$_{eq}$CH$_2$CH$_2$CH), 3.00 (d$_{br}$, *J* = 10.1 Hz, 1H, NCH$_{ax}$*H*$_{eq}$CH), 4.14 (q, *J* = 7.1 Hz, 2H, OC*H*$_2$CH$_3$), 7.52–7.61 (m, 4H, C≡CCC*H*CHC, N=NCCHC*H*CH, N=NCCCHCHC*H*), 7.65 (ddd, *J* = 8.3/6.8/1.3 Hz, 1H, N=NCCCHC*H*), 7.82 (dd, *J* = 7.5/1.0 Hz, 1H, N=NCCHCHC*H*), 7.92 (d, *J* = 8.1 Hz, 1H, N=NCCCHCHCHC*H*), 7.95–8.01 (m, 3H, C≡CCCHC*H*C, N=NCC*H*CHCH), 8.92 (d, *J* = 8.4 Hz, 1H, N=NCCC*H*) ppm. ^{13}C NMR (126 MHz, CDCl$_3$, 21 °C, TMS): *δ* = 14.21 (q, 1C, OCH$_2$*C*H$_3$), 17.56 (t, 1C, NCH$_2$*C*H$_2$CH$_2$C≡C), 24.60 (t, 1C, NCH$_2$*C*H$_2$CH$_2$CH), 26.01 (t, 1C, NCH$_2$CH$_2$*C*H$_2$C≡C), 26.97 (t, 1C, NCH$_2$CH*C*H$_2$), 41.90 (d, 1C, NCH$_2$*C*H), 53.88 (t, 1C, N*C*H$_2$CH$_2$CH$_2$CH), 55.50 (t, 1C, N*C*H$_2$CH), 57.70 (t, 1C, N*C*H$_2$CH$_2$CH$_2$C≡C), 60.29 (t, 1C, O*C*H$_2$CH$_3$), 80.73 (s, 1C, C≡*C*CH), 93.02 (s, 1C, *C*≡CCCH), 111.81 (d, 1C, N=NCCHCH*C*H), 123.09 (d, 3C, C≡CCCH*C*HC, CH$_2$C≡C*C*), 123.40 (d, 1C, N=NCC*C*H), 125.59 (d, 1C, N=NCCH*C*HCH), 126.45 (d, 1C, N=NCCCHCH*C*H), 126.83 (d, 1C, N=NCCCH*C*H), 127.91 (d, 1C, N=NCCCHCHCH*C*H), 131.34 (s, 1C, N=NC*C*CH), 131.46 (d, 1C, N=NC*C*HCHCH), 132.35 (d, 2C, C≡CC*C*HCHC), 134.28 (s, 1C, N=NCCHCHCH*C*), 147.69 (s, 1C, N=N*C*CHCHCH), 151.91 (s, 1C, C≡CCCHCH*C*), 174.22 (s, 1C, C=O) ppm. MS (ESI$^+$) *m/z*: 454 [M+H]$^+$. HRMS (EI$^+$): M$^+$ calcd for C$_{29}$H$_{31}$O$_2$N$_3$: 453.2416, found 453.2403.

*1-(4-{3-[(E)-Phenylazo]phenyl}but-3-yn-1-yl)piperidine-3-carboxylic acid (m-**20a**)*

According to GP5 starting from *m*-**18a** (78 mg, 0.20 mmol) and 2 N NaOH (0.30 ml, 0.60 mmol) *m*-**20a** was obtained as orange amorphous solid (68 mg, 94%). IR (KBr): $\tilde{\nu}$ = 3433, 3060, 2942, 2861, 2522, 2233, 1713, 1595, 1469, 1447, 1392,

1306, 1200, 1152, 1071, 1019, 999, 924, 898, 797, 767, 690 cm^{-1}. ^1H NMR (500 MHz, CD_3OD + 5 eq 1N NaOD, 21 °C, CH_3OH): δ = 1.32 (qd, *J* = 12.7/3.9 Hz, 1H, $NCH_2CHCH_{ax}H_{eq}$), 1.57 (qt, *J* = 13.3/4.0 Hz, 1H, $NCH_2CH_{ax}H_{eq}CH_2CH$), 1.71 (d_{br}, *J* = 13.7 Hz, 1H, $NCH_2CH_{ax}H_{eq}CH_2CH$), 1.91–2.06 (m, 2H, $NCH_2CHCH_{ax}H_{eq}$, $NCH_{ax}H_{eq}CH_2CH_2CH$), 2.11 (t, *J* = 11.4 Hz, 1H, $NCH_{ax}H_{eq}CH$), 2.37 (tt, *J* = 11.9/3.7 Hz, 1H, NCH_2CH_{ax}), 2.58–2.73 (m, 4H, $NCH_2CH_2C{\equiv}C$, $NCH_2CH_2C{\equiv}C$), 2.92 (d_{br}, *J* = 10.7 Hz, 1H, $NCH_{ax}H_{eq}CH_2CH_2CH$), 3.10 (d_{br}, *J* = 10.2 Hz, 1H, $NCH_{ax}H_{eq}CH$), 7.42–7.49 (m, 2H, $C{\equiv}CCCHCH$, $C{\equiv}CCCHCH$), 7.49–7.56 (m, 3H, $N{=}NCCHCHCH$, $N{=}NCCHCHCH$), 7.73–7.80 (m, 2H, $C{\equiv}CCCHC$, $C{\equiv}CCCHCCH$), 7.80–7.87 (m, 2H, $N{=}NCCHCHCH$) ppm. ^{13}C NMR (126 MHz, CD_3OD + 5 eq 1N NaOD, 21 °C, CH_3OH): δ = 17.50 (t, 1C, $NCH_2CH_2C{\equiv}C$), 25.57 (t, 1C, $NCH_2CH_2CH_2CH$), 29.04 (t, 1C, NCH_2CHCH_2), 46.07 (d, 1C, NCH_2CH), 54.16 (t, 1C, $NCH_2CH_2CH_2CH$), 57.41 (t, 1C, NCH_2CH), 58.23 (t, 1C, $NCH_2CH_2C{\equiv}C$), 81.49 (s, 1C, $C{\equiv}CCCH$), 90.16 (s, 1C, $C{\equiv}CCCH$), 123.37 (d, 1C, $C{\equiv}CCCHC$), 123.73 (d, 2C, $N{=}NCCHCHCH$), 125.85 (s, 1C, $C{\equiv}CCCHC$), 126.09 (d, 1C, $C{\equiv}CCCHCH$), 130.39 (d, 2C, $N{=}NCCHCHCH$), 130.48 (d, 1C, $C{\equiv}CCCHCH$), 132.79 (s, 1C, $C{\equiv}CCCHCHC$), 135.00 (d, 1C, $C{\equiv}CCCHCCH$), 153.42 (d, 2C, $N{=}NC$), 183.06 (s, 1C, C=O) ppm. MS (ESI^+) *m/z*: 362 $[M+H]^+$. HRMS (ESI^+): $[M+H]^+$ calcd for $C_{22}H_{24}O_2N_3$: 362.1869, found 362.1860.

*(R)-1-(4-{3-[(E)-Phenylazo]phenyl}but-3-yn-1-yl)piperidine-3-carboxylic acid ((R)-m-**20a**)*

According to GP5 starting from (*R*)-*m*-**18a** (78 mg, 0.20 mmol) and 2 N NaOH (0.30 ml, 0.60 mmol) (*R*)-*m*-**20a** was obtained as orange amorphous solid (68 mg, 94%); $[\alpha]^{20}_D$ = +20.4 (c = 0.1 in CH_2Cl_2). IR (KBr): $\tilde{\nu}$ = 3425, 3060, 2939, 2864, 2526, 2235, 1714, 1594, 1469, 1447, 1392, 1306, 1202, 1151, 1071, 1017, 1000, 924, 898, 798, 767, 691 cm^{-1}. ^1H NMR (400 MHz, CD_3OD + 5 eq 1N NaOD, 21 °C, CH_3OH): δ = 1.35 (qd, *J* = 13.1/4.2 Hz, 1H, $NCH_2CHCH_{ax}H_{eq}$), 1.60 (qt, *J* = 12.5/4.0 Hz, 1H, $NCH_2CH_{ax}H_{eq}CH_2CH$), 1.73 (d_{br}, *J* = 13.7 Hz, 1H, $NCH_2CH_{ax}H_{eq}CH_2CH$), 1.94–2.09 (m, 2H, $NCH_2CHCH_{ax}H_{eq}$, $NCH_{ax}H_{eq}CH_2CH_2CH$), 2.13 (t, *J* = 11.3 Hz, 1H, $NCH_{ax}H_{eq}CH$), 2.39 (tt, *J* = 11.8/3.7 Hz, 1H, NCH_2CH_{ax}), 2.64–2.74 (m, 4H, $NCH_2CH_2C{\equiv}C$, $NCH_2CH_2C{\equiv}C$), 2.95 (d_{br}, *J* = 10.7 Hz, 1H, $NCH_{ax}H_{eq}CH_2CH_2CH$), 3.10 (d_{br}, *J* = 11.1 Hz, 1H, $NCH_{ax}H_{eq}CH$), 7.46–7.52 (m, 2H, $C{\equiv}CCCHCH$, $C{\equiv}CCCHCH$), 7.52–7.59 (m, 3H, $N{=}NCCHCHCH$, $N{=}NCCHCHCH$), 7.78–7.85 (m, 2H, $C{\equiv}CCCHC$, $C{\equiv}CCCHCCH$), 7.85–7.91 (m, 2H, $N{=}NCCHCHCH$) ppm. ^{13}C NMR (101 MHz, CD_3OD + 5 eq 1N NaOD, 25 °C, CH_3OH): δ = 17.69 (t, 1C, $NCH_2CH_2C{\equiv}C$), 25.79 (t, 1C, $NCH_2CH_2CH_2CH$), 29.24 (t, 1C, NCH_2CHCH_2), 46.24 (d, 1C, NCH_2CH), 54.46 (t, 1C, $NCH_2CH_2CH_2CH$), 57.67 (t, 1C, NCH_2CH), 58.49 (t, 1C, $NCH_2CH_2C{\equiv}C$), 81.51 (s, 1C, $C{\equiv}CCCH$), 90.09 (s, 1C, $C{\equiv}CCCH$), 123.34 (d, 1C, $C{\equiv}CCCHC$), 123.82 (d, 2C, $N{=}NCCHCHCH$), 126.11 (s, 1C, $C{\equiv}CCCHC$), 126.25 (d, 1C, $C{\equiv}CCCHCH$), 130.38 (d, 2C, $N{=}NCCHCHCH$), 130.46 (d, 1C, $C{\equiv}CCCHCH$), 132.70 (s, 1C, $C{\equiv}CCCHCHC$), 135.01 (d, 1C, $C{\equiv}CCCHCCH$), 153.66 (d, 2C, $N{=}NC$), 182.82 (s, 1C, C=O) ppm. MS (ESI^+) *m/z*: 362 $[M+H]^+$. HRMS (ESI^+): $[M+H]^+$ calcd for $C_{22}H_{24}O_2N_3$: 362.1869, found 362.1858.

*1-(4-{4-[(E)-Phenylazo]phenyl}but-3-yn-1-yl)piperidine-3-carboxylic acid (p-**20a**)*

According to GP5 starting from *p*-**18a** (78 mg, 0.20 mmol) and 2 N NaOH (0.30 ml, 0.60 mmol) *p*-**20a** was obtained as orange amorphous solid (65 mg, 91%). IR (KBr): $\tilde{\nu}$ = 3478, 3395, 3060, 2930, 2533, 1711, 1601, 1461, 1430, 1397, 1301, 1290, 1219, 1153, 1123, 1108, 1054, 972, 921, 870, 847, 798, 768, 688 cm^{-1}. ^1H NMR (500 MHz, CD_3OD + 5 eq 1N NaOD, 21 °C, CH_3OH): δ = 1.34 (qd, *J* = 13.0/4.1 Hz, 1H, $NCH_2CHCH_{ax}H_{eq}$), 1.58 (qt, *J* = 12.5/4.0 Hz, 1H, $NCH_2CH_{ax}H_{eq}CH_2CH$), 1.72 (d_{br}, *J* = 13.3 Hz, 1H, $NCH_2CH_{ax}H_{eq}CH_2CH$), 1.97 (d_{br}, *J* = 12.7 Hz, 1H, $NCH_2CHCH_{ax}H_{eq}$), 2.04 (td, *J* = 11.8/2.4 Hz, 1H, $NCH_{ax}H_{eq}CH_2CH_2CH$), 2.13 (t, *J* = 11.4 Hz, 1H, $NCH_{ax}H_{eq}CH$), 2.38 (tt, *J* = 12.3/3.6 Hz, 1H, NCH_2CH_{ax}), 2.62–2.77 (m, 4H, $NCH_2CH_2C{\equiv}C$, $NCH_2CH_2C{\equiv}C$), 2.94 (d_{br}, *J* = 11.2 Hz, 1H, $NCH_{ax}H_{eq}CH_2CH_2CH$), 3.13 (d_{br}, *J* = 10.8 Hz, 1H, $NCH_{ax}H_{eq}CH$), 7.46–7.59 (m, 5H, $C{\equiv}CCCHCHC$, $N{=}NCCHCHCH$, $N{=}NCCHCHCH$), 7.77–7.82 (m, 2H, $C{\equiv}CCCHCHC$), 7.83–7.88 (m, 2H, $N{=}NCCHCHCH$) ppm. ^{13}C NMR (126 MHz, CD_3OD + 5 eq 1N NaOD, 21 °C, CH_3OH): δ = 17.73 (t, 1C, $NCH_2CH_2C{\equiv}C$), 25.67 (t, 1C, $NCH_2CH_2CH_2CH$), 29.12 (t, 1C, NCH_2CHCH_2), 46.16 (d, 1C, NCH_2CH), 54.31 (t, 1C, $NCH_2CH_2CH_2CH$), 57.54 (t, 1C, NCH_2CH), 58.29 (t, 1C, $NCH_2CH_2C{\equiv}C$), 82.02 (s, 1C, $C{\equiv}CCCH$), 92.15 (s, 1C, $C{\equiv}CCCH$), 123.71 (d, 4C, $C{\equiv}CCCHCHC$, $N{=}NCCHCHCH$), 127.94 (s, 1C, $CH_2C{\equiv}CC$), 130.38 (d, 2C, $N{=}NCCHCHCH$), 132.66 (d, 1C, $N{=}NCCHCHCH$), 133.43 (d, 2C, $C{\equiv}CCCHCHC$), 152.61 (s, 1C, $C{\equiv}CCCHCHC$), 153.71 (s, 1C, $N{=}NCCHCHCH$), 182.96 (s, 1C, C=O) ppm. MS (ESI^+) *m/z*: 362 $[M+H]^+$. HRMS (EI^+): M^+ calcd for $C_{22}H_{23}O_2N_3$: 361.1790, found 361.1786.

*(R)-1-(4-{4-[(E)-Phenylazo]phenyl}but-3-yn-1-yl)piperidine-3-carboxylic acid ((R)-p-**20a**)*

According to GP5 starting from (*R*)-*p*-**18a** (78 mg, 0.20 mmol) and 2 N NaOH (0.30 ml, 0.60 mmol) (*R*)-*p*-**20a** was obtained as orange amorphous solid (65 mg, 91%); $[\alpha]^{20}_D$ = +21.5 (c = 0.1 in CH_2Cl_2). IR (KBr): $\tilde{\nu}$ = 3422, 3061, 2927, 2852, 2230, 1702, 1596, 1467, 1440, 1374, 1333, 1299, 1220, 1153, 1099, 1071, 928, 843, 770, 726, 688 cm^{-1}. ^1H NMR (500 MHz, CD_3OD + 5 eq 1N NaOD, 21 °C, CH_3OH): δ = 1.30 (qd, *J* = 13.0/4.1 Hz, 1H, $NCH_2CHCH_{ax}H_{eq}$), 1.54 (qt, *J* = 12.1/3.8 Hz, 1H, $NCH_2CH_{ax}H_{eq}CH_2CH$), 1.70 (d_{br}, *J* = 13.3 Hz, 1H, $NCH_2CH_{ax}H_{eq}CH_2CH$), 1.95 (d_{br}, *J* = 12.7 Hz, 1H, $NCH_2CHCH_{ax}H_{eq}$), 2.00 (td, *J* = 12.1/2.8 Hz, 1H, $NCH_{ax}H_{eq}CH_2CH_2CH$), 2.13 (t, *J* = 11.4 Hz, 1H, $NCH_{ax}H_{eq}CH$), 2.35 (tt, *J* = 12.0/3.7 Hz, 1H, NCH_2CH_{ax}), 2.57–2.68 (m, 4H, $NCH_2CH_2C{\equiv}C$, $NCH_2CH_2C{\equiv}C$), 2.89 (d_{br}, *J* = 11.2 Hz, 1H, $NCH_{ax}H_{eq}CH_2CH_2CH$), 3.08 (d_{br}, *J* = 11.5 Hz, 1H, $NCH_{ax}H_{eq}CH$), 7.41–7.45 (m, 2H, $C{\equiv}CCCHCHC$), 7.49–7.53 (m, 3H, $N{=}NCCHCHCH$, $N{=}NCCHCHCH$), 7.69–7.72 (m, 2H,

C≡CCCHC*H*C), 7.77–7.81 (m, 2H, N=NCC*H*CHCH) ppm. ^{13}C NMR (126 MHz, CD_3OD + 5 eq 1N NaOD, 21 °C, CH_3OH): δ = 17.46 (t, 1C, $NCH_2CH_2CH_2C{\equiv}C$), 25.38 (t, 1C, $NCH_2CH_2CH_2CH$), 28.88 (t, 1C, NCH_2CHCH_2), 46.16 (d, 1C, NCH_2CH), 53.91 (t, 1C, $NCH_2CH_2CH_2CH$), 57.14 (t, 1C, NCH_2CH), 57.89 (t, 1C, $NCH_2CH_2C{\equiv}C$), 81.96 (s, 1C, C≡*C*CCH), 92.25 (s, 1C, *C*≡CCCH), 123.60 (d, 4C, C≡CCCH*C*HC, N=NC*C*HCHCH), 127.66 (s, 1C, $CH_2C{\equiv}CC$), 130.38 (d, 2C, N=NC*C*HCHCH), 132.73 (d, 1C, N=NCCHCH*C*H), 133.35 (d, 2C, C≡CC*C*HCHC), 152.26 (s, 1C, C≡CCCHCH*C*), 153.36 (s, 1C, N=N*C*CHCHCH), 183.17 (s, 1C, C=O) ppm. MS (ESI$^+$) *m/z*: 362 $[M+H]^+$. HRMS (EI$^+$): M^+ calcd for $C_{22}H_{23}O_2N_3$: 361.1790, found 361.1792.

*1-(4-{3-[(E)-1-naphthylazo]phenyl}but-3-yn-1-yl)piperidine-3-carboxylic acid (m-**20b**)*

According to GP5 starting from *m*-**18b** (88 mg, 0.20 mmol) and 2 N NaOH (0.30 ml, 0.60 mmol) *m*-**20b** was obtained as orange amorphous solid (75 mg, 91%). IR (KBr): $\tilde{\nu}$ = 3427, 3053, 2939, 2857, 2807, 2231, 1709, 1596, 1507, 1478, 1467, 1448, 1387, 1344, 1307, 1204, 1155, 1101, 1013, 896, 804, 771, 685 cm^{-1}. ^{1}H NMR (500 MHz, CD_3OD + 5 eq 1N NaOD, 21 °C, CH_3OH): δ = 1.38 (qd, *J* = 12.8/4.1 Hz, 1H, $NCH_2CHCH_{ax}H_{eq}$), 1.63 (qt, *J* = 13.2/3.8 Hz, 1H, $NCH_2CH_{ax}H_{eq}CH_2CH$), 1.76 (dp, *J* = 13.3/3.3 Hz, 1H, $NCH_2CH_{ax}H_{eq}CH_2CH$), 1.98–2.10 (m, 2H, $NCH_2CHCH_{ax}H_{eq}$, $NCH_{ax}H_{eq}CH_2CH_2CH$), 2.17 (t, *J* = 11.4 Hz, 1H, $NCH_{ax}H_{eq}CH$), 2.43 (tt, *J* = 12.0/3.8 Hz, 1H, NCH_2CH_{ax}), 2.64–2.78 (m, 4H, $NCH_2CH_2C{\equiv}C$, $NCH_2CH_2C{\equiv}C$), 2.97 (d$_{br}$, *J* = 10.7 Hz, 1H, $NCH_{ax}H_{eq}CH_2CH_2CH$), 3.17 (d$_{br}$, *J* = 10.8 Hz, 1H, $NCH_{ax}H_{eq}CH$), 7.51–7.56 (m, 2H, C≡CCC*H*CH, C≡CCCHC*H*), 7.59 (t, *J* = 7.8 Hz, 1H, N=NCCHC*H*CH), 7.62 (ddd, *J* = 8.4/6.8/1.4 Hz, 1H, N=NCCCHCHC*H*), 7.66 (ddd, *J* = 8.4/6.8/1.4 Hz, 1H, N=NCCCHC*H*), 7.75 (dd, *J* = 7.5/1.0 Hz, 1H, N=NCCHCHC*H*), 7.89–7.95 (m, 2H, C≡CCC*H*C, C≡CCCHCC*H*), 7.98 (d, *J* = 7.9 Hz, 1H, N=NCCCHCHCHC*H*), 8.06 (d, *J* = 8.2 Hz, 1H, N=NCC*H*CHCH), 8.80 (dd, *J* = 8.3/0.7 Hz, 1H, N=NCCC*H*) ppm. ^{13}C NMR (126 MHz, CD_3OD + 5 eq 1N NaOD, 21 °C, CH_3OH): δ = 17.61 (t, 1C, $NCH_2CH_2CH_2C{\equiv}C$), 25.67 (t, 1C, $NCH_2CH_2CH_2CH$), 29.13 (t, 1C, NCH_2CHCH_2), 46.15 (d, 1C, NCH_2CH), 54.29 (t, 1C, $NCH_2CH_2CH_2CH$), 57.56 (t, 1C, NCH_2CH), 58.34 (t, 1C, $NCH_2CH_2C{\equiv}C$), 81.57 (s, 1C, C≡*C*CCH), 90.19 (s, 1C, *C*≡CCCH), 112.85 (d, 1C, N=NCCHCH*C*H), 123.86 (d, 1C, C≡CCCHC*C*H), 125.97 (s, 1C, C≡C*C*CHC), 126.15 (d, 1C, N=NCC*C*H), 126.63 (d, 2C, N=NCCH*C*HCH, N=NCC*C*H), 127.73 (d, 1C, N=NCCCHCH*C*H), 128.21 (d, 1C, N=NCCCH*C*H), 129.10 (d, 1C, N=NCCCHCHCH*C*H), 130.52 (d, 1C, C≡CCCH*C*H), 132.33 (s, 1C, N=NC*C*CH), 132.99 (d, 1C, N=NC*C*HCHCH), 135.05 (d, 1C, C≡CC*C*HCH), 135.65 (s, 1C, N=NCCHCHCH*C*), 148.45 (s, 1C, N=N*C*CHCHCH), 154.02 (s, 1C, C≡CCCH*C*), 182.96 (s, 1C, C=O) ppm. MS (ESI$^+$) *m/z*: 412 $[M+H]^+$. HRMS (EI$^+$): M^+ calcd for $C_{26}H_{25}O_2N_3$: 411.1947, found 411.1952.

*(R)-1-(4-{3-[(E)-1-naphthylazo]phenyl}but-3-yn-1-yl)piperidine-3-carboxylic acid ((R)-m-**20b**)*

According to GP5 starting from (*R*)-*m*-**18b** (88 mg, 0.20 mmol) and 2 N NaOH (0.30 ml, 0.60 mmol) (*R*)-*m*-**20b** was obtained as orange amorphous solid (75 mg, 91%) ; $[\alpha]^{20}_D$ = +18.6 (c = 0.1 in CH_2Cl_2). IR (KBr): $\tilde{\nu}$ = 3427, 3051, 2937, 2855, 2807, 2230, 1709, 1589, 1507, 1478, 1467, 1447, 1387, 1344, 1305, 1203, 1154, 1102, 1012, 896, 804, 771, 685 cm^{-1}. ^{1}H NMR (500 MHz, CD_3OD + 5 eq 1N NaOD, 21 °C, CH_3OH): δ = 1.38 (qd, *J* = 12.8/3.9 Hz, 1H, $NCH_2CHCH_{ax}H_{eq}$), 1.62 (qt, *J* = 12.9/3.7 Hz, 1H, $NCH_2CH_{ax}H_{eq}CH_2CH$), 1.75 (dp, *J* = 13.3/3.3 Hz, 1H, $NCH_2CH_{ax}H_{eq}CH_2CH$), 1.97–2.09 (m, 2H, $NCH_2CHCH_{ax}H_{eq}$, $NCH_{ax}H_{eq}CH_2CH_2CH$), 2.16 (t, *J* = 11.4 Hz, 1H, $NCH_{ax}H_{eq}CH$), 2.43 (tt, *J* = 11.9/3.7 Hz, 1H, NCH_2CH_{ax}), 2.65–2.75 (m, 4H, $NCH_2CH_2C{\equiv}C$, $NCH_2CH_2C{\equiv}C$), 2.96 (d$_{br}$, *J* = 10.9 Hz, 1H, $NCH_{ax}H_{eq}CH_2CH_2CH$), 3.17 (d$_{br}$, *J* = 11.0 Hz, 1H, $NCH_{ax}H_{eq}CH$), 7.48–7.54 (m, 2H, C≡CCC*H*CH, C≡CCCHC*H*), 7.59 (t, *J* = 7.8 Hz, 1H, N=NCCHC*H*CH), 7.62 (ddd, *J* = 8.4/6.8/1.4 Hz, 1H, N=NCCCHCHC*H*), 7.66 (ddd, *J* = 8.4/6.8/1.4 Hz, 1H, N=NCCCHC*H*), 7.72 (dd, *J* = 7.5/0.9 Hz, 1H, N=NCCHCHC*H*), 7.87–7.93 (m, 2H, C≡CCC*H*C, C≡CCCHCC*H*), 7.96 (d, *J* = 7.8 Hz, 1H, N=NCCCHCHCHC*H*), 8.04 (d, *J* = 8.1 Hz, 1H, N=NCC*H*CHCH), 8.78 (dd, *J* = 8.2/0.7 Hz, 1H, N=NCCC*H*) ppm. ^{13}C NMR (126 MHz, CD_3OD + 5 eq 1N NaOD, 21 °C, CH_3OH): δ = 17.59 (t, 1C, $NCH_2CH_2CH_2C{\equiv}C$), 25.65 (t, 1C, $NCH_2CH_2CH_2CH$), 29.11 (t, 1C, NCH_2CHCH_2), 46.13 (d, 1C, NCH_2CH), 54.25 (t, 1C, $NCH_2CH_2CH_2CH$), 57.53 (t, 1C, NCH_2CH), 58.31 (t, 1C, $NCH_2CH_2C{\equiv}C$), 81.57 (s, 1C, C≡*C*CCH), 90.18 (s, 1C, *C*≡CCCH), 112.86 (d, 1C, N=NCCHCH*C*H), 123.86 (d, 1C, C≡CCCHC*C*H), 125.97 (s, 1C, C≡C*C*CHC), 126.15 (d, 1C, N=NCC*C*H), 126.61 (d, 2C, N=NCCH*C*HCH, N=NCC*C*H), 127.71 (d, 1C, N=NCCCHCH*C*H), 128.18 (d, 1C, N=NCCCH*C*H), 129.09 (d, 1C, N=NCCCHCHCH*C*H), 130.49 (d, 1C, C≡CCCH*C*H), 132.30 (s, 1C, N=NC*C*CH), 132.98 (d, 1C, N=NC*C*HCHCH), 135.02 (d, 1C, C≡CC*C*HCH), 135.61 (s, 1C, N=NCCHCHCH*C*), 148.40 (s, 1C, N=N*C*CHCHCH), 153.97 (s, 1C, C≡CCCH*C*), 182.97 (s, 1C, C=O) ppm. MS (ESI$^+$) *m/z*: 412 $[M+H]^+$. HRMS (EI$^+$): M^+ calcd for $C_{26}H_{25}O_2N_3$: 411.1947, found 411.1949.

*1-(4-{4-[(E)-1-naphthylazo]phenyl}but-3-yn-1-yl)piperidine-3-carboxylic acid (p-**20b**)*

According to GP5 starting from *p*-**18b** (88 mg, 0.20 mmol) and 2 N NaOH (0.30 ml, 0.60 mmol) *p*-**20b** was obtained as orange amorphous solid (74 mg, 90%). IR (KBr): $\tilde{\nu}$ = 3431, 3050, 2941, 2859, 2224, 1708, 1596, 1507, 1497, 1450, 1388, 1345, 1303, 1218, 1191, 1156, 1143, 1099, 1011, 843, 803, 773 cm^{-1}. ^{1}H NMR (400 MHz, DMSO-d_6, 60 °C, DMSO): δ = 1.38 (q$_{br}$, *J* = 12.0 Hz, 1H, $NCH_2CHCH_{ax}H_{eq}$), 1.49 (q$_{br}$, *J* = 11.5 Hz, 1H, $NCH_2CH_{ax}H_{eq}CH_2CH$), 1.67 (d$_{br}$, *J* = 12.4 Hz, 1H, $NCH_2CH_{ax}H_{eq}CH_2CH$), 1.82 (d$_{br}$, *J* = 11.2 Hz, 1H, $NCH_2CHCH_{ax}H_{eq}$), 2.14 (t$_{br}$, *J* = 11.0 Hz, 1H, $NCH_{ax}H_{eq}CH_2CH_2CH$), 2.27 (t$_{br}$, *J* = 10.8 Hz, 1H, $NCH_{ax}H_{eq}CH$), 2.45 (t$_{br}$, *J* = 10.6 Hz, 1H, NCH_2CH_{ax}), 2.60–2.70 (m, 4H, $NCH_2CH_2C{\equiv}C$, $NCH_2CH_2C{\equiv}C$), 2.74 (d$_{br}$, *J* = 10.8 Hz, 1H, $NCH_{ax}H_{eq}CH_2CH_2CH$), 2.96 (d$_{br}$, *J* = 11.1 Hz, 1H, $NCH_{ax}H_{eq}CH$), 7.65 (d, *J* = 8.3 Hz, 2H, C≡CCC*H*CHC),

7.67–7.71 (m, 2H, N=NCCHC*H*CH, N=NCCCHCHC*H*), 7.75 (t, *J* = 7.5 Hz, 1H, N=NCCCHC*H*), 7.83 (d, *J* = 7.5 Hz, 1H, N=NCCHCHC*H*), 8.04 (d, *J* = 8.3 Hz, 2H, C≡CCCHC*H*C), 8.10 (d, *J* = 8.2 Hz, 1H, N=NCCCHCHCHC*H*), 8.19 (d, *J* = 8.0 Hz, 1H, N=NCC*H*CHCH), 8.89 (d, *J* = 8.4 Hz, 1H, N=NCCC*H*) ppm. ^{13}C NMR (101 MHz, DMSO-*d*$_6$, 60 °C, DMSO): *δ* = 17.65 (t, 1C, NCH$_2$*C*H$_2$C≡C), 24.50 (t, 1C, NCH$_2$*C*H$_2$CH$_2$CH), 27.03 (t, 1C, NCH$_2$CH*C*H$_2$), 41.61 (d, 1C, NCH$_2$*C*H), 53.14 (t, 1C, N*C*H$_2$CH$_2$CH$_2$CH), 55.45 (t, 1C, N*C*H$_2$CH), 57.09 (t, 1C, N*C*H$_2$CH$_2$C≡C), 81.34 (s, 1C, C≡*C*CCH), 93.32 (s, 1C, *C*≡CCCH), 112.34 (d, 1C, N=NCCHCH*C*H), 123.27 (d, 1C, N=NCC*C*H), 123.65 (d, 2C, C≡CCCH*C*HC), 126.34 (d, 1C, N=NCCH*C*HCH), 126.87 (s, 1C, CH$_2$C≡C*C*), 127.31 (d, 1C, N=NCCCHCH*C*H), 127.93 (d, 1C, N=NCCCH*C*H), 128.65 (d, 1C, N=NCCCHCHCH*C*H), 131.07 (s, 1C, N=NC*C*CH), 132.50 (d, 1C, N=NC*C*HCHCH), 132.96 (d, 2C, C≡CC*C*HCHC), 134.46 (s, 1C, N=NCCHCHCH*C*), 147.20 (s, 1C, N=N*C*CHCHCH), 151.88 (s, 1C, C≡CCCHCH*C*), 175.57 (s, 1C, C=O) ppm. MS (ESI$^+$) *m/z*: 411 [M]$^+$. HRMS (EI$^+$): M$^+$ calcd for $C_{26}H_{25}O_2N_3$: 411.1947, found 411.1925.

*(R)-1-(4-{4-[(E)-1-naphthylazo]phenyl}but-3-yn-1-yl)piperidine-3-carboxylic acid ((R)-p-**20b**)*

According to GP5 starting from (*R*)-*p*-**18b** (88 mg, 0.20 mmol) and 2 N NaOH (0.30 ml, 0.60 mmol) (*R*)-*p*-**20b** was obtained as orange amorphous solid (74 mg, 90%); $[\alpha]^{20}_D$ = +17.8 (c = 0.1 in CH_2Cl_2). IR (KBr): $\tilde{\nu}$ = 3426, 3051, 2943, 2863, 2226, 1708, 1596, 1507, 1498, 1450, 1388, 1345, 1303, 1218, 1191, 1156, 1143, 1099, 1011, 843, 803, 775 cm^{-1}. ^{1}H NMR (500 MHz, DMSO-*d*$_6$, 60 °C, DMSO): *δ* = 1.36 (qd, *J* = 11.8/3.5 Hz, 1H, NCH$_2$CHC*H*$_{ax}$H$_{eq}$), 1.47 (qt, *J* = 12.0/3.6 Hz, 1H, NCH$_2$C*H*$_{ax}$H$_{eq}$CH$_2$CH), 1.65 (dp, *J* = 12.2/3.6 Hz, 1H, NCH$_2$CH$_{ax}$*H*$_{eq}$CH$_2$CH), 1.80 (dq, *J* = 12.7/3.8 Hz, 1H, NCH$_2$CHCH$_{ax}$*H*$_{eq}$), 2.13 (t$_{br}$, *J* = 9.7 Hz, 1H, NC*H*$_{ax}$H$_{eq}$CH$_2$CH$_2$CH), 2.26 (t$_{br}$, *J* = 10.1 Hz, 1H, NC*H*$_{ax}$H$_{eq}$CH), 2.43 (tt, *J* = 10.8/3.7 Hz, 1H, NCH$_2$C*H*$_{ax}$), 2.63–2.67 (m, 4H, NCH$_2$C*H*$_2$C≡C, NC*H*$_2$CH$_2$C≡C), 2.73 (d$_{br}$, *J* = 11.0 Hz, 1H, NCH$_{ax}$*H*$_{eq}$CH$_2$CH$_2$CH), 2.95 (d$_{br}$, *J* = 9.5 Hz, 1H, NCH$_{ax}$*H*$_{eq}$CH), 7.63 (d, *J* = 8.5 Hz, 2H, C≡CCC*H*CHC), 7.65–7.70 (m, 2H, N=NCCHC*H*CH, N=NCCCHCHC*H*), 7.73 (ddd, *J* = 8.3/6.8/1.2 Hz, 1H, N=NCCCHC*H*), 7.82 (dd, *J* = 7.6/0.8 Hz, 1H, N=NCCHCHC*H*), 8.02 (d, *J* = 8.5 Hz, 2H, C≡CCCHC*H*C), 8.08 (d, *J* = 8.1 Hz, 1H, N=NCCCHCHCHC*H*), 8.17 (d, *J* = 8.1 Hz, 1H, N=NCC*H*CHCH), 8.87 (d, *J* = 8.4 Hz, 1H, N=NCCC*H*) ppm. ^{13}C NMR (126 MHz, DMSO-*d*$_6$, 60 °C, DMSO): *δ* = 17.62 (t, 1C, NCH$_2$*C*H$_2$C≡C), 24.47 (t, 1C, NCH$_2$*C*H$_2$CH$_2$CH), 26.99 (t, 1C, NCH$_2$CH*C*H$_2$), 41.56 (d, 1C, NCH$_2$*C*H), 53.12 (t, 1C, N*C*H$_2$CH$_2$CH$_2$CH), 55.39 (t, 1C, N*C*H$_2$CH), 57.05 (t, 1C, N*C*H$_2$CH$_2$C≡C), 81.36 (s, 1C, C≡*C*CCH), 93.28 (s, 1C, *C*≡CCCH), 112.34 (d, 1C, N=NCCHCH*C*H), 123.28 (d, 1C, N=NCC*C*H), 123.66 (d, 2C, C≡CCCH*C*HC), 126.35 (d, 1C, N=NCCH*C*HCH), 126.87 (s, 1C, CH$_2$C≡C*C*), 127.32 (d, 1C, N=NCCCHCH*C*H), 127.94 (d, 1C, N=NCCCH*C*H), 128.67 (d, 1C, N=NCCCHCHCH*C*H), 131.08 (s, 1C, N=NC*C*CH), 132.52 (d, 1C, N=NC*C*HCHCH), 132.97 (d, 2C, C≡CC*C*HCHC), 134.47 (s, 1C, N=NCCHCHCH*C*), 147.20 (s, 1C, N=N*C*CHCHCH), 151.89 (s, 1C, C≡CCCHCH*C*), 175.56 (s, 1C, C=O) ppm. MS (ESI$^+$) *m/z*: 411 [M]$^+$. HRMS (EI$^+$): M$^+$ calcd for $C_{26}H_{25}O_2N_3$: 411.1947, found 411.1934.

*1-(5-{3-[(E)-phenylazo]phenyl}pent-4-yn-1-yl)piperidine-3-carboxylic acid (m-**21a**)*

According to GP5 starting from *m*-**19a** (81 mg, 0.20 mmol) and 2 N NaOH (0.30 ml, 0.60 mmol) *m*-**21a** was obtained as orange amorphous solid (67 mg, 89%). IR (KBr): $\tilde{\nu}$ = 3428, 3061, 2941, 2862, 2804, 2481 2230, 1711, 1595, 1469, 1446, 1389, 1339, 1307, 1202, 1152, 1071, 1019, 999, 926, 897, 797, 767, 691 cm^{-1}. ^{1}H NMR (500 MHz, CD$_3$OD + 5 eq 1N NaOD, 21 °C, CH$_3$OH): *δ* = 1.32 (qd, *J* = 12.7/4.0 Hz, 1H, NCH$_2$CHC*H*$_{ax}$H$_{eq}$), 1.56 (qt, *J* = 13.3/4.0 Hz, 1H, NCH$_2$C*H*$_{ax}$H$_{eq}$CH$_2$CH), 1.71 (d$_{br}$, *J* = 13.7 Hz, 1H, NCH$_2$CH$_{ax}$*H*$_{eq}$CH$_2$CH), 1.74–1.86 (m, 2H, NCH$_2$C*H*$_2$CH$_2$C≡C), 1.89–1.99 (m, 2H, NCH$_2$CHCH$_{ax}$*H*$_{eq}$, NC*H*$_{ax}$H$_{eq}$CH$_2$CH$_2$CH), 2.02 (t, *J* = 11.4 Hz, 1H, NC*H*$_{ax}$H$_{eq}$CH), 2.36 (tt, *J* = 11.9/3.6 Hz, 1H, NCH$_2$C*H*$_{ax}$), 2.44 (t, *J* = 7.1 Hz, 2H, NCH$_2$CH$_2$C*H*$_2$C≡C), 2.47–2.54 (m, 2H, NC*H*$_2$CH$_2$CH$_2$C≡C), 2.90 (d$_{br}$, *J* = 11.0 Hz, 1H, NCH$_{ax}$*H*$_{eq}$CH$_2$CH$_2$CH), 3.11 (d$_{br}$, *J* = 11.2 Hz, 1H, NCH$_{ax}$*H*$_{eq}$CH), 7.45–7.50 (m, 2H, C≡CCC*H*CH, C≡CCCHC*H*), 7.50–7.57 (m, 3H, N=NCCHC*H*CH, N=NCCHCHC*H*), 7.75–7.80 (m, 2H, C≡CCC*H*C, C≡CCCHCC*H*), 7.82–7.87 (m, 2H, N=NCC*H*CHCH) ppm. ^{13}C NMR (101 MHz, CD$_3$OD + 5 eq 1N NaOD, 25 °C, CH$_3$OH): *δ* = 18.15 (t, 1C, NCH$_2$CH$_2$C*H*$_2$C≡C), 25.60 (t, 1C, NCH$_2$*C*H$_2$CH$_2$CH), 26,24 (t, 1C, NCH$_2$*C*H$_2$CH$_2$C≡C), 29.19 (t, 1C, NCH$_2$CH*C*H$_2$), 46.10 (d, 1C, NCH$_2$*C*H), 54.66 (t, 1C, N*C*H$_2$CH$_2$CH$_2$CH), 57.88 (t, 1C, N*C*H$_2$CH), 59.09 (t, 1C, N*C*H$_2$CH$_2$CH$_2$C≡C), 81.05 (s, 1C, C≡*C*CCH), 91.73 (s, 1C, *C*≡CCCH), 123.33 (d, 1C, C≡CC*C*HC), 123.75 (d, 2C, N=NC*C*HCHCH), 126.03 (s, 1C, C≡C*C*CHC), 126.25 (d, 1C, C≡CC*C*HCH), 130.39 (d, 2C, N=NCCH*C*HCH), 130.49 (d, 1C, C≡CCCH*C*H), 132.78 (s, 1C, C≡CCCHCH*C*), 134.96 (d, 1C, C≡CCCHC*C*H), 153.46 (d, 2C, N=N*C*), 183.16 (s, 1C, C=O) ppm. MS (ESI$^+$) *m/z*: 376 [M+H]$^+$. HRMS (ESI$^+$): [M+H]$^+$ calcd for $C_{23}H_{26}O_2N_3$: 376.2025, found 376.2017.

*1-(5-{4-[(E)-phenylazo]phenyl}pent-4-yn-1-yl)piperidine-3-carboxylic acid (p-**21a**)*

According to GP5 starting from *p*-**19a** (81 mg, 0.20 mmol) and 2 N NaOH (0.30 ml, 0.60 mmol) *p*-**21a** was obtained as orange amorphous solid (66 mg, 87%). IR (KBr): $\tilde{\nu}$ = 3423, 3041, 2938, 2224, 1702, 1596, 1495, 1481, 1463, 1441, 1381, 1300, 1220, 1152, 1099, 1069, 1010, 956, 925, 846, 767, 725, 686 cm^{-1}. ^{1}H NMR (400 MHz, DMSO-*d*$_6$, 60 °C, DMSO): *δ* = 1.48 (qd, *J* = 12.0/4.5 Hz, 1H, NCH$_2$CHC*H*$_{ax}$H$_{eq}$), 1.64–1.81 (m, 2H, NCH$_2$C*H*$_{ax}$H$_{eq}$CH$_2$CH, NCH$_2$CH$_{ax}$*H*$_{eq}$CH$_2$CH), 1.85–1.96 (m, 3H, NCH$_2$CHCH$_{ax}$*H*$_{eq}$, NCH$_2$C*H*$_2$CH$_2$C≡C), 2.48–2.52 (m, 1H, NCH$_2$C*H*$_{ax}$), 2.56 (t, *J* = 7.1 Hz, 2H, NCH$_2$CH$_2$C*H*$_2$C≡C), 2.60–2.69 (m, 1H, NC*H*$_{ax}$H$_{eq}$CH$_2$CH$_2$CH), 2.68–2.77 (m, 1H, NC*H*$_{ax}$H$_{eq}$CH), 2.78–2.90 (m, 2H, NC*H*$_2$CH$_2$CH$_2$C≡C), 3.04 (d$_{br}$, *J* = 10.4

Hz, 1H, NCH$_{ax}$*H$_{eq}$*CH$_2$CH$_2$CH), 3.20 (d$_{br}$, *J* = 10.4 Hz, 1H, NCH$_{ax}$*H$_{eq}$*CH), 7.56–7.64 (m, 5H, C≡CCC*H*CHC, N=NCCHC*H*CH, N=NCCHCHC*H*), 7.84–7.91 (m, 4H, C≡CCCHC*H*C, N=NCC*H*CHCH) ppm. ^{13}C NMR (101 MHz, DMSO-*d$_6$*, 60 °C, DMSO): *δ* = 18.90 (t, 1C, NCH$_2$CH$_2$*C*H$_2$C≡C), 24.89 (t, 1C, NCH$_2$*C*H$_2$CH$_2$CH), 26.23 (t, 1C, NCH$_2$*C*H$_2$CH$_2$C≡C), 27.91 (t, 1C, NCH$_2$CH*C*H$_2$), 42.00 (d, 1C, NCH$_2$*C*H), 54.61 (t, 1C, N*C*H$_2$CH$_2$CH$_2$CH), 55.97 (t, 1C, N*C*H$_2$CH), 58.30 (t, 1C, N*C*H$_2$CH$_2$CH$_2$C≡C), 82.96 (s, 1C, C≡*C*CCH), 95.13 (s, 1C, *C*≡CCCH), 124.86 (d, 4C, C≡CCCH*C*HC, N=NC*C*HCHCH), 128.46 (s, 1C, CH$_2$C≡C*C*), 131.68 (d, 2C, N=NC*C*HCHCH), 133.86 (d, 1C, N=NCCHCH*C*H), 134.65 (d, 2C, C≡CC*C*HCHC), 153.25 (s, 1C, C≡CCCHCH*C*), 154.36 (s, 1C, N=N*C*CHCHCH), 176.08 (s, 1C, C=O) ppm. MS (ESI$^+$) *m/z*: 376 [M+H]$^+$. HRMS (EI$^+$): M$^+$ calcd for $C_{23}H_{25}O_2N_3$: 375.1947, found 375.1939.

*1-(5-{3-[(E)-1-naphthylazo]phenyl}pent-4-yn-1-yl)piperidine-3-carboxylic acid (m-**21b**)*

According to GP5 starting from *m*-**19b** (91 mg, 0.20 mmol) and 2 N NaOH (0.30 ml, 0.60 mmol) *m*-**21b** was obtained as orange amorphous solid (74 mg, 87%). IR (KBr): $\tilde{\nu}$ = 3426, 3050, 2933, 2801, 2764, 2227, 1571, 1507, 1478, 1466, 1407, 1344, 1203, 1154, 1103, 1012, 895, 804, 770, 685 cm^{-1}. ^{1}H NMR (500 MHz, CD$_3$OD + 5 eq 1N NaOD, 21 °C, CH$_3$OH): *δ* = 1.31 (qd, *J* = 12.7/4.0 Hz, 1H, NCH$_2$CHC*H$_{ax}$*H$_{eq}$), 1.55 (qt, *J* = 13.0/3.5 Hz, 1H, NCH$_2$C*H$_{ax}$*H$_{eq}$CH$_2$CH), 1.67 (d$_{br}$, *J* = 13.4 Hz, 1H, NCH$_2$CH$_{ax}$*H$_{eq}$*CH$_2$CH), 1.79 (p, *J* = 7.1 Hz, 2H, NCH$_2$C*H*$_2$CH$_2$C≡C), 1.86–1.96 (m, 2H, NCH$_2$CHCH$_{ax}$*H$_{eq}$*, NC*H$_{ax}$*H$_{eq}$CH$_2$CH$_2$CH), 2.01 (t, *J* = 11.5 Hz, 1H, NC*H$_{ax}$*H$_{eq}$CH), 2.36 (tt, *J* = 11.8/3.5 Hz, 1H, NCH$_2$C*H$_{ax}$*), 2.43 (t, *J* = 6.9 Hz, 2H, NCH$_2$CH$_2$C*H*$_2$C≡C), 2.46–2.53 (m, 2H, NC*H*$_2$CH$_2$CH$_2$C≡C), 2.87 (d, *J* = 11.0 Hz, 1H, NCH$_{ax}$*H$_{eq}$*CH$_2$CH$_2$CH), 3.10 (d, *J* = 10.7 Hz, 1H, NCH$_{ax}$*H$_{eq}$*CH), 7.41–7.49 (m, 2H, C≡CCC*H*CH, C≡CCCHC*H*), 7.49–7.62 (m, 3H, N=NCCHC*H*CH, N=NCCCHCHC*H*, N=NCCCHC*H*), 7.68 (d, *J* = 6.8 Hz, 1H, N=NCCHCHC*H*), 7.81–7.89 (m, 2H, C≡CCC*H*C, C≡CCCHCC*H*), 7.92 (d, *J* = 7.3 Hz, 1H, N=NCCCHCHCHC*H*), 8.00 (d, *J* = 8.1 Hz, 1H, N=NCC*H*CHCH), 8.73 (d, *J* = 8.1 Hz, 1H, N=NCCC*H*) ppm. ^{13}C NMR (126 MHz, CD$_3$OD + 5 eq 1N NaOD, 21 °C, CH$_3$OH): *δ* = 18.19 (t, 1C, NCH$_2$CH$_2$*C*H$_2$C≡C), 25.65 (t, 1C, NCH$_2$*C*H$_2$CH$_2$CH), 26.31 (t, 1C, NCH$_2$*C*H$_2$CH$_2$C≡C), 29.23 (t, 1C, NCH$_2$CH*C*H$_2$), 46.12 (d, 1C, NCH$_2$*C*H), 54.73 (t, 1C, N*C*H$_2$CH$_2$CH$_2$CH), 57.95 (t, 1C, N*C*H$_2$CH), 59.14 (t, 1C, N*C*H$_2$CH$_2$CH$_2$C≡C), 81.14 (s, 1C, C≡*C*CCH), 91.74 (s, 1C, *C*≡CCCH), 112.83 (d, 1C, N=NCCHCH*C*H), 123.83 (d, 1C, C≡CCCHC*C*H), 125.97 (s, 1C, C≡C*C*CHC), 126.12 (d, 1C, N=NCC*C*H), 126.63 (d, 2C, N=NCCH*C*HCH, N=NCC*C*H), 127.73 (d, 1C, N=NCCCHCH*C*H), 128.21 (d, 1C, N=NCCCH*C*H), 129.10 (d, 1C, N=NCCCHCHCH*C*H), 130.52 (d, 1C, C≡CCCH*C*H), 132.31 (s, 1C, N=NC*C*CH), 132.99 (d, 1C, N=NC*C*HCHCH), 134.99 (d, 1C, C≡CC*C*HCH), 135.63 (s, 1C, N=NCCHCHCH*C*), 148.40 (s, 1C, N=N*C*CHCHCH), 153.99 (s, 1C, C≡CCCH*C*), 183.11 (s, 1C, C=O) ppm. MS (ESI$^+$) *m/z*: 426 [M+H]$^+$. HRMS (EI$^+$): M$^+$ calcd for $C_{27}H_{27}O_2N_3$: 425.2103, found 425.2085.

*1-(5-{4-[(E)-1-naphthylazo]phenyl}pent-4-yn-1-yl)piperidine-3-carboxylic acid (p-**21b**)*

According to GP5 starting from *p*-**19b** (91 mg, 0.20 mmol) and 2 N NaOH (0.30 ml, 0.60 mmol) *p*-**21b** was obtained as orange amorphous solid (75 mg, 88%). IR (KBr): $\tilde{\nu}$ = 3427, 3051, 2949, 2860, 2227, 1708, 1625, 1596, 1497, 1383, 1344, 1300, 1216, 1187, 1157, 1142, 1098, 1080, 1012, 843, 803, 775 cm^{-1}. ^{1}H NMR (500 MHz, DMSO-*d$_6$*, 60 °C, DMSO): *δ* = 1.35–1.54 (m, 2H, NCH$_2$CHC*H$_{ax}$*H$_{eq}$, NCH$_2$C*H$_{ax}$*H$_{eq}$CH$_2$CH), 1.61–1.71 (m, 1H, NCH$_2$CH$_{ax}$*H$_{eq}$*CH$_2$CH), 1.71–1.84 (m, 3H, NCH$_2$C*H*$_2$CH$_2$C≡C, NCH$_2$CH$_{ax}$*H$_{eq}$*CH$_2$CH), 2.08 (t$_{br}$, *J* = 9.5 Hz, 1H, NC*H$_{ax}$*H$_{eq}$CH$_2$CH$_2$CH), 2.22 (t$_{br}$, *J* = 10.1 Hz, 1H, NC*H$_{ax}$*H$_{eq}$CH), 2.37–2.49 (m, 3H, NCH$_2$C*H$_{ax}$*, NCH$_2$CH$_2$C*H*$_2$C≡C), 2.51–2.57 (m, 2H, NC*H*$_2$CH$_2$CH$_2$C≡C), 2.66 (d$_{br}$, *J* = 9.7 Hz, 1H, NCH$_{ax}$*H$_{eq}$*CH$_2$CH$_2$CH), 2.85 (d$_{br}$, *J* = 10.3 Hz, 1H, NCH$_{ax}$*H$_{eq}$*CH), 7.60–7.70 (m, 4H, C≡CCC*H*CHC, N=NCCHC*H*CH, N=NCCCHCHC*H*), 7.73 (t, *J* = 7.5 Hz, 1H, N=NCCCHC*H*), 7.81 (d, *J* = 7.4 Hz, 1H, N=NCCHCHC*H*), 8.01 (d, *J* = 8.1 Hz, 2H, C≡CCCHC*H*C), 8.07 (d, *J* = 7.8 Hz, 1H, N=NCCCHCHCHC*H*), 8.16 (d, *J* = 8.2 Hz, 1H, N=NCC*H*CHCH), 8.86 (d, *J* = 8.5 Hz, 1H, N=NCCC*H*) ppm. ^{13}C NMR (101 MHz, DMSO-*d$_6$*, 60 °C, DMSO): *δ* = 17.06 (t, 1C, NCH$_2$CH$_2$*C*H$_2$C≡C), 24.29 (t, 1C, NCH$_2$*C*H$_2$CH$_2$C≡C), 25.87 (t, 1C, NCH$_2$*C*H$_2$CH$_2$CH), 26.90 (t, 1C, NCH$_2$CH*C*H$_2$), 41.48 (d, 1C, NCH$_2$*C*H), 53.60 (t, 1C, N*C*H$_2$CH$_2$CH$_2$CH), 55.68 (t, 1C, N*C*H$_2$CH), 57.10 (t, 1C, N*C*H$_2$CH$_2$CH$_2$C≡C)), 80.67 (s, 1C, C≡*C*CCH), 94.25 (s, 1C, *C*≡CCCH), 112.27 (d, 1C, N=NCCHCH*C*H), 123.03 (d, 1C, N=NCC*C*H), 123.28 (d, 2C, C≡CCCH*C*HC), 126.01 (d, 1C, N=NCCH*C*HCH), 126.80 (s, 1C, CH$_2$C≡C*C*), 126.97 (d, 1C, N=NCCCHCH*C*H), 127.58 (d, 1C, N=NCCCH*C*H), 128.34 (d, 1C, N=NCCCHCHCH*C*H), 130.76 (s, 1C, N=NC*C*CH), 132.06 (d, 1C, N=NC*C*HCHCH), 132.65 (d, 2C, C≡CC*C*HCHC), 134.26 (s, 1C, N=NCCHCHCH*C*), 147.21 (s, 1C, N=N*C*CHCHCH), 151.77 (s, 1C, C≡CCCHCH*C*), 175.23 (s, 1C, C=O) ppm. MS (ESI$^+$) *m/z*: 426 [M+H]$^+$. HRMS (ESI$^+$): [M+H]$^+$ calcd for $C_{27}H_{28}O_2N_3$: 426.2182, found 426.2172.

Literature

1. Schönberger, M.; Althaus, M.; Fronius, M.; Clauss, W.; Trauner, D. Controlling epithelial sodium channels with light using photoswitchable amilorides. *Nat Chem* **2014,** 6, 712-719.
2. Broichhagen, J.; Podewin, T.; Meyer-Berg, H.; von Ohlen, Y.; Johnston, N. R.; Jones, B. J.; Bloom, S. R.; Rutter, G. A.; Hoffmann-Röder, A.; Hodson, D. J.; Trauner, D. Optical Control of Insulin Secretion Using an Incretin Switch. *Angewandte Chemie International Edition* **2015**, 54, 1-6.
3. Broichhagen, J.; Jurastow, I.; Iwan, K.; Kummer, W.; Trauner, D. Optical Control of Acetylcholinesterase with a Tacrine Switch. *Angewandte Chemie International Edition* **2014,** 53, 7657-7660.
4. Schönberger, M.; Trauner, D. A Photochromic Agonist for μ-Opioid Receptors. *Angewandte Chemie International Edition* **2014,** 53, 3264-3267.
5. Frank, J. A.; Moroni, M.; Moshourab, R.; Sumser, M.; Lewin, G. R.; Trauner, D. Photoswitchable fatty acids enable optical control of TRPV1. *Nat Commun* **2015,** 6.
6. Rullo, A.; Reiner, A.; Reiter, A.; Trauner, D.; Isacoff, E. Y.; Woolley, G. A. Long wavelength optical control of glutamate receptor ion channels using a tetra-ortho-substituted azobenzene derivative. *Chemical Communications* **2014**, 50, 14613–14615.
7. Laprell, L.; Repak, E.; Franckevicius, V.; Hartrampf, F.; Terhag, J.; Hollmann, M.; Sumser, M.; Rebola, N.; DiGregorio, D. A.; Trauner, D. Optical control of NMDA receptors with a diffusible photoswitch. *Nat Commun* **2015,** 6, 8076.
8. Laprell, L.; Hüll, K.; Stawski, P.; Schön, C.; Michalakis, S.; Biel, M.; Sumser, M. P.; Trauner, D. Restoring Light Sensitivity in Blind Retinae Using a Photochromic AMPA Receptor Agonist. *ACS Chemical Neuroscience* **2015**, 7, 15–20.
9. Schoenberger, M.; Damijonaitis, A.; Zhang, Z.; Nagel, D.; Trauner, D. Development of a New Photochromic Ion Channel Blocker via Azologization of Fomocaine. *ACS Chemical Neuroscience* **2014,** 5, 514-518.
10. Castle, Brian T.; Odde, David J. Optical Control of Microtubule Dynamics in Time and Space. *Cell* **2015,** 162, 243-245.
11. Borowiak, M.; Nahaboo, W.; Reynders, M.; Nekolla, K.; Jalinot, Pierre; Hasserodt, J.; Rehberg, M.; Delattre, M.; Zahler, S.; Vollmar, A.; Trauner, D.; Thorn-Seshold, O. Photoswitchable Inhibitors of Microtubule Dynamics Optically Control Mitosis and Cell Death. *Cell* **2015,** 162, 403-411.
12. Quandt, G.; Höfner, G.; Pabel, J.; Dine, J.; Eder, M.; Wanner, K. T. First Photoswitchable Neurotransmitter Transporter Inhibitor: Light-Induced Control of γ-Aminobutyric Acid Transporter 1 (GAT1) Activity in Mouse Brain. *Journal of Medicinal Chemistry* **2014,** 57, 6809-6821.
13. Bowery, N. G.; Smart, T. G. GABA and glycine as neurotransmitters: a brief history. *British Journal of Pharmacology* **2006,** 147, S109-S119.
14. Foster, A. C.; Kemp, J. A. Glutamate- and GABA-based CNS therapeutics. *Current Opinion in Pharmacology* **2006,** 6, 7-17.
15. Europe, W. H. O. Neurological disorders, public health challenges. http://www.who.int/mental_health/neurology/neurodiso/en/index.html
16. Borden, L. A. GABA TRANSPORTER HETEROGENEITY: PHARMACOLOGY AND CELLULAR LOCALIZATION. *Neurochemistry International* **1996,** 29, 335-356.
17. Madsen, K. K.; Clausen, R. P.; Larsson, O. M.; Krogsgaard-Larsen, P.; Schousboe, A.; Steve White, H. Synaptic and extrasynaptic GABA transporters as targets for anti-epileptic drugs. *Journal of Neurochemistry* **2009,** 109, 139-144.
18. Bröer, S.; Gether, U. The solute carrier 6 family of transporters. *British Journal of Pharmacology* **2012,** 167, 256-278.
19. Lehre, A. C.; Rowley, N. M.; Zhou, Y.; Holmseth, S.; Guo, C.; Holen, T.; Hua, R.; Laake, P.; Olofsson, A. M.; Poblete-Naredo, I.; Rusakov, D. A.; Madsen, K. K.; Clausen, R. P.; Schousboe, A.; White, H. S.; Danbolt, N. C. Deletion of the betaine–GABA transporter (BGT1; slc6a12) gene does not affect seizure thresholds of adult mice. *Epilepsy research* **2011,** 95, 70-81.
20. Krogsgaard-Larsen, P.; Falch, E.; Larsson, O. M.; Schousboe, A. GABA uptake inhibitors: relevance to antiepileptic drug research. *Epilepsy Research* **1987,** 1, 77-93.
21. Wein, T.; Petrera, M.; Allmendinger, L.; Höfner, G.; Pabel, J.; Wanner, K. T. Different Binding Modes of Small and Large Binders of GAT1. *ChemMedChem* **2016,** 11, 509-518.
22. Andersen, K. E.; Sørensen, J. L.; Huusfeldt, P. O.; Knutsen, L. J. S.; Lau, J.; Lundt, B. F.; Petersen, H.; Suzdak, P. D.; Swedberg, M. D. B. Synthesis of Novel GABA Uptake Inhibitors. 4. Bioisosteric Transformation and Successive Optimization of Known GABA Uptake Inhibitors Leading to a Series of Potent Anticonvulsant Drug Candidates. *Journal of Medicinal Chemistry* **1999,** 42, 4281-4291.
23. Ali, F. E.; Bondinell, W. E.; Dandridge, P. A.; Frazee, J. S.; Garvey, E.; Girard, G. R.; Kaiser, C.; Ku, T. W.; Lafferty, J. J.; Moonsammy, G. I.; Oh, H.-J.; Rush, J. A.; Setler, P. E.; Stringer, O. D.; Venslavsky, J. W.; Volpe, B. W.; Yunger,

L. M.; Zirkle, C. L. Orally Active and Potent Inhibitors of γ-Aminobutyric Acid Uptake. *Journal of Medicinal Chemistry* **1985,** 28, 653-660.
24. Dalby, N. O. GABA-level increasing and anticonvulsant effects of three different GABA uptake inhibitors. *Neuropharmacology* **2000,** 39, 2399-2407.
25. Petrera, M.; Wein, T.; Allmendinger, L.; Sindelar, M.; Pabel, J.; Höfner, G.; Wanner, K. T. Development of Highly Potent GAT1 Inhibitors: Synthesis of Nipecotic Acid Derivatives by Suzuki–Miyaura Cross-Coupling Reactions. *ChemMedChem* **2016,** 11, 519-538.
26. Lutz, T.; Wein, T.; Höfner, G.; Wanner, K. T. Development of Highly Potent GAT1 Inhibitors: Synthesis of Nipecotic Acid Derivatives with aryl alkinyl ligand. *ChemMedChem* **2017**, 12, 1-11.
27. Yamashita, A., Singh, S. K., Kawate, T., Jin, Y. & Gouaux, E. Crystal structure of a bacterial homologue of Na^+/Cl^--dependent neurotransmitter transporters. *Nature* **2005,** 437, 1–9.
28. Singh, S. K., Piscitelli, C. L., Yamashita, A. & Gouaux, E. A competitive inhibitor traps LeuT in an open-to-out conformation. *Science* **2008,** 322, 1655–1661.
29. Martin, R.; Buchwald, S. L. Palladium-Catalyzed Suzuki−Miyaura Cross-Coupling Reactions Employing Dialkylbiaryl Phosphine Ligands. American Chemical Society **2008,** 41, 1461–1473.
30. Polychrome V system monochromator; TILL photonics.
31. Rayonet Reactor (Model RPR-200); Southern New England Ultraviolet Company: Branford, CT.
32. Kragler, A.; Höfner, G.; Wanner, K. T. Synthesis and biological evaluation of aminomethylphenol derivatives as inhibitors of the murine GABA transporters mGAT1–mGAT4. *European Journal of Medicinal Chemistry* **2008,** 43, 2404-2411.
33. H. M. Berman, J. Westbrook, Z. Feng, G. Gilliland, T. N. Bhat, H. Weissig, I. N. Shindyalov, P. E. Bourne, *Nucleic Acids Research* **2000**, *28*, 235-242.
34. B. Boeckmann, A. Bairoch, R. Apweiler, M.-C. Blatter, A. Estreicher, E. Gasteiger, M. J. Martin, K. Michoud, C. O'Donovan, I. Phan, S. Pilbout, M. Schneider, *Nucleic Acids Research* **2003**, *31*, 365-370.
35. S. Skovstrup, O. Taboureau, H. Bräuner-Osborne, F. S. Jørgensen, *ChemMedChem* **2010**, *5*, 986-1000.
36. M.-y. Shen, A. Sali, *Protein Science : A Publication of the Protein Society* **2006**, *15*, 2507-2524.
37. E. Zomot, A. Bendahan, M. Quick, Y. Zhao, J. A. Javitch, B. I. Kanner, *Nature* **2007**, *449*, 726-730.
38. L. R. Forrest, S. Tavoulari, Y.-W. Zhang, G. Rudnick, B. Honig, *Proceedings of the National Academy of Sciences* **2007**, *104*, 12761-12766.
39. R. A. Laskowski, M. W. MacArthur, D. S. Moss, J. M. Thornton, *Journal of Applied Crystallography* **1993**, *26*, 283-291.
40. v. Instant JChem, ChemAxon, **2010**.
41. v. Marvin, ChemAxon, **2010**.
42. M. F. Sanner, *Journal of Molecular Graphics and Modelling* **1999**, *17*, 55-84.
43. R. Huey, G. M. Morris, A. J. Olson, D. S. Goodsell, *Journal of Computational Chemistry* **2007**, *28*, 1145-1152.

Development of new photoswitchable azobenzene bound GABA uptake inhibitors with distinctly enhanced potency upon photoactivation

Toni Lutz, Thomas Wein, Georg Höfner, Jörg Pabel, Matthias Eder, Julien Dine, and Klaus T. Wanner

Department of Pharmacy – Center for Drug Research,

Butenandtstr. 5–13, D - 81377 Munich, Germany

E-Mail: Klaus.wanner@cup.uni-muenchen.de

- Supporting Information -

Content:

1 Photochemical Isomerization of (*E*)- and (*Z*)-*m*-**20a**:

1.1 Calculation of the absorption of pure (*Z*)-*m*-**20a**:

A 1 mL aliquot of a 10 mM solution in DMSO-d_6 of (*E*)-*m*-**20a** was irradiated in a NMR tube (Wilmad) until the photostationary state was reached (within 10 min). For irradiation a Rayonet RPR-200 (λ_{max} = 350 nm) was used. Afterwards, a ^{1}H NMR spectrum was recorded. The amount of both isomers of *m*-**20a** was obtained through integration of the significant aromatic signals of the (*Z*)- and the (*E*)-isomer, giving the ratio factor α. By ^{1}H NMR spectroscopy a (*Z*)/(*E*)-ratio of ≈ 80/20 was found within this experiment ($\alpha_{(Z)}$ = 0.802).

For determination of the reachable (*Z*)/(*E*)-ratio of *m*-**20a** under physiological conditions an aliquot of both the irradiated and non-irradiated 10 mM stem solution in DMSO-d_6 was taken and diluted to a concentration of 25 µM with phosphate buffer (10 mM, pH 7.4) and a UV/Vis spectrum (Cary50 spectrometer, Varian) of these samples was recorded at the same time. The absorption (A) at 350 nm for this irradiated sample ($A_{(E/Z)}$) was found to be 0.101. Together with the UV/Vis spectrum of the pure (*E*)-isomer (A_E = 0.295) the absorption of the pure (*Z*)-isomer could then be calculated using following equation:

$$A_{(Z)} = A_{(E)} + (A_{(Z/E)} - A_{(E)}) / \alpha_{(Z)} \quad \text{with} \quad \alpha_{(Z)} = c_{(Z)} / (c_{(E)} + c_{(Z)})$$

In this manner the absorption of the pure (*Z*)-isomer was calculated to be 0.053.

1.2 Determination of a suitable wavelength for forward-isomerization of (*E*)-*m*-**20a**:

The ideal wavelength for the photoisomerization of the (*E*)- and (*Z*)-isomer of *m*-**20a** was determined by UV/vis spectroscopy and in situ irradiation of the 25 µM dilution of (*E*)-*m*-**20a** using an FT-600-UMT fiber optic cable (NA 0.39), connected to a Polychrome V system monochromator (TILL photonics) with a 150 W xenon short arc lamp with an output range of 320−680 nm. (*E*)-*m*-**20a** was irradiated at different wavelengths (330, 340, 350, 360, 370 nm) until the photostationary state was reached (within 10 min). The resulting (*Z*)/(*E*)-ratio of *m*-**20a** during an irradiation could be calculated in this way:

$$\alpha_{(Z)} = (A_{(Z/E)} - A_{(E)}) / (A_{(Z)} - A_{(E)})$$

Using 350 nm for the forward-isomerization (photostationary state: $A_{(Z/E)}$ = 0.066) the final value for $\alpha_{(Z)}$ was calculated to be 0.946.

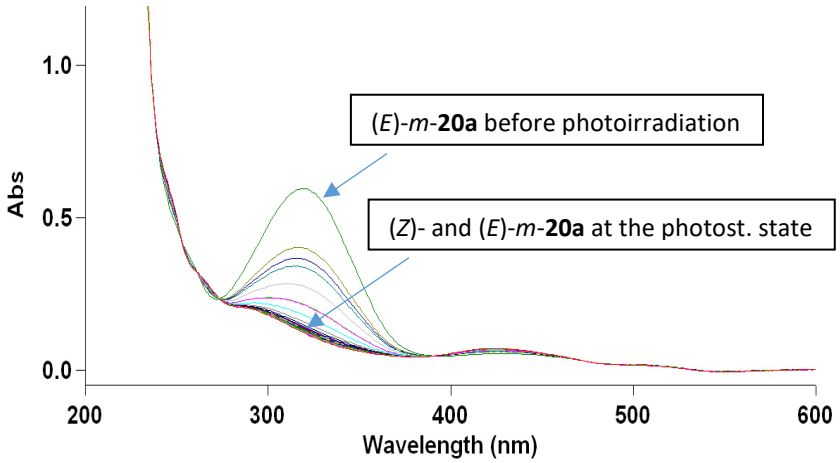

t (min)	$A_{(t)}$ 350 nm	$\alpha_{(Z)}$
0	0.295	0
0.5	0.205	0.372
1	0.185	0.455
2	0.140	0.640
3	0.108	0.773
4	0.079	0.893
5	0.072	0.921
6	0.069	0.933
7	0.067	0.942
8	0.066	0.946
9	0.066	0.946
10	0.066	0.946

Results for other wavelengths:

340 nm: $A_{(10)}$ = 0.071; $\alpha_{(Z)}$ = 0.925 360 nm: $A_{(10)}$ = 0.089; $\alpha_{(Z)}$ = 0.851 370 nm: $A_{(10)}$ = 0.141; $\alpha_{(Z)}$ = 0.636

1.3 Determination of a suitable wavelength for back-isomerization of (*Z*)-*m*-**20a**:

The wavelength for back isomerization was determined in a similar way by irradiation of the photoisomerized sample of *m*-**20a** with higher wavelengths (410, 420, 430, 440 nm).

Using 420 nm for the back-isomerization (photostationary state: $A_{(Z/E)}$ = 0.235) the final value for $\alpha_{(Z)}$ was calculated to be 0.248.

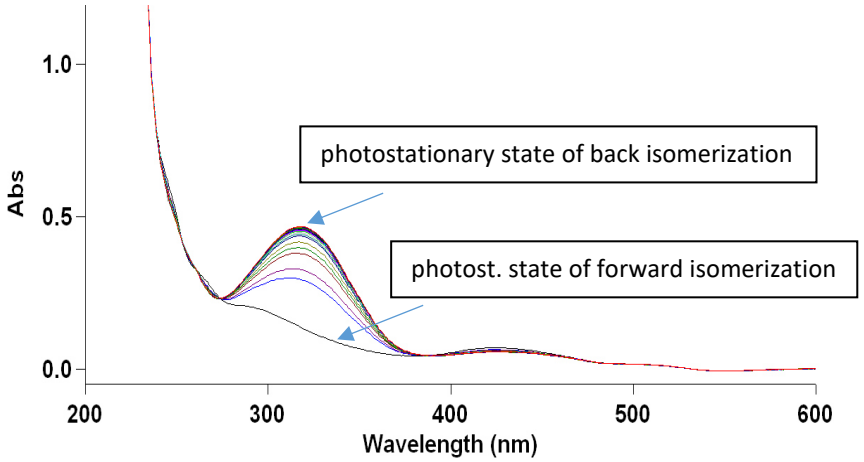

t (min)	$A_{(t)}$ 350 nm	$\alpha_{(Z)}$
0	0.066	0.946
0.5	0.146	0.615
1	0.163	0.545
2	0.200	0.393
3	0.219	0.337
4	0.225	0.314
5	0.228	0.277
6	0.231	0.264
7	0.232	0.260
8	0.234	0.252
9	0.235	0.248
10	0.235	0.248

Results for other wavelengths:

410 nm: $A_{(10)}$ = 0.214; $\alpha_{(Z)}$ = 0.335 430 nm: $A_{(10)}$ = 0.208; $\alpha_{(Z)}$ = 0.360 440 nm: $A_{(10)}$ = 0.177; $\alpha_{(Z)}$ = 0.487

2 Half-life´s of thermal relaxation

2.1 Determination of the half-life of (*Z*)-*m*-**20a** in phosphate buffer

For the half-life under physiological conditions an aliquot of the photoirradiated 10 mM stem solution of *m*-**20a** in DMSO-d_6 (with α = 0.802) was diluted to a concentration of 50 µM with phosphate buffer (pH 7.4) and a UV/Vis spectrum (Cary50 spectrometer, Varian) of this sample was recorded immediately ($A_{(0)}$ = 0.202). The sample was stored in the dark and further UV spectra were recorded in defined time intervals. The amount of (*Z*)- and (*E*)-*m*-**20a** was obtained for every spectra using the following equation:

$\alpha_{(t)} = (A_{(t)} - A_{(E)}) / (A_{(Z)} - A_{(E)})$

with $A_{(E)}$ = 0.575 (measured) and $A_{(Z)}$ = 0.110 (calculated by $A_{(Z)} = A_{(E)} + (A_{(0)} - A_{(E)}) / \alpha_{(Z)}$).

$A_{(t)}$ 350 nm	time (d)	$\alpha_{(Z)}$	$t_{(1/2)}$
0.202	0	80.2	
0.212	1	78.1	26.2
0.223	2	75.7	24.0
0.234	3	73.3	23.1
0.256	5	68.6	22.2
0.285	7	62.8	19.8
0.307	10	57.6	20.9
0.339	14	50.8	21.3
0.378	21	42.4	22.8
0.411	28	35.3	23.6

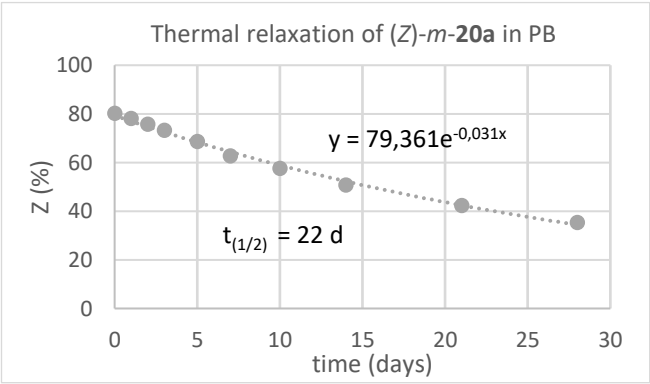

Calculations based on equations for 1st order kinetics: $N_{(Z)} = N_{(0)} \cdot e^{-k_{-1} \cdot t}$ and $t_{1/2} = \ln 2 / k_{-1}$.

2.1 Determination of the half-life of (*Z*)-*m*-**20a** in DMSO

A 10 mM solution in DMSO-d_6 of (*E*)-*m*-**20a** was irradiated by means of a Rayonet RPR-200 (λ_{max} = 350 nm) in a NMR tube until the photostationary state was reached. At the beginning of the experiment, a first ^{1}H NMR spectrum was recorded. The sample was stored in the dark and further ^{1}H NMR spectra were measured in defined time intervals. The amount of (*E*)- and (*Z*)-*m*-**20a** was obtained through integration of the affiliated aromatic signals for every spectrum, giving the remaining proportion of (*Z*)-*m*-**20a** (α_Z) respectively:

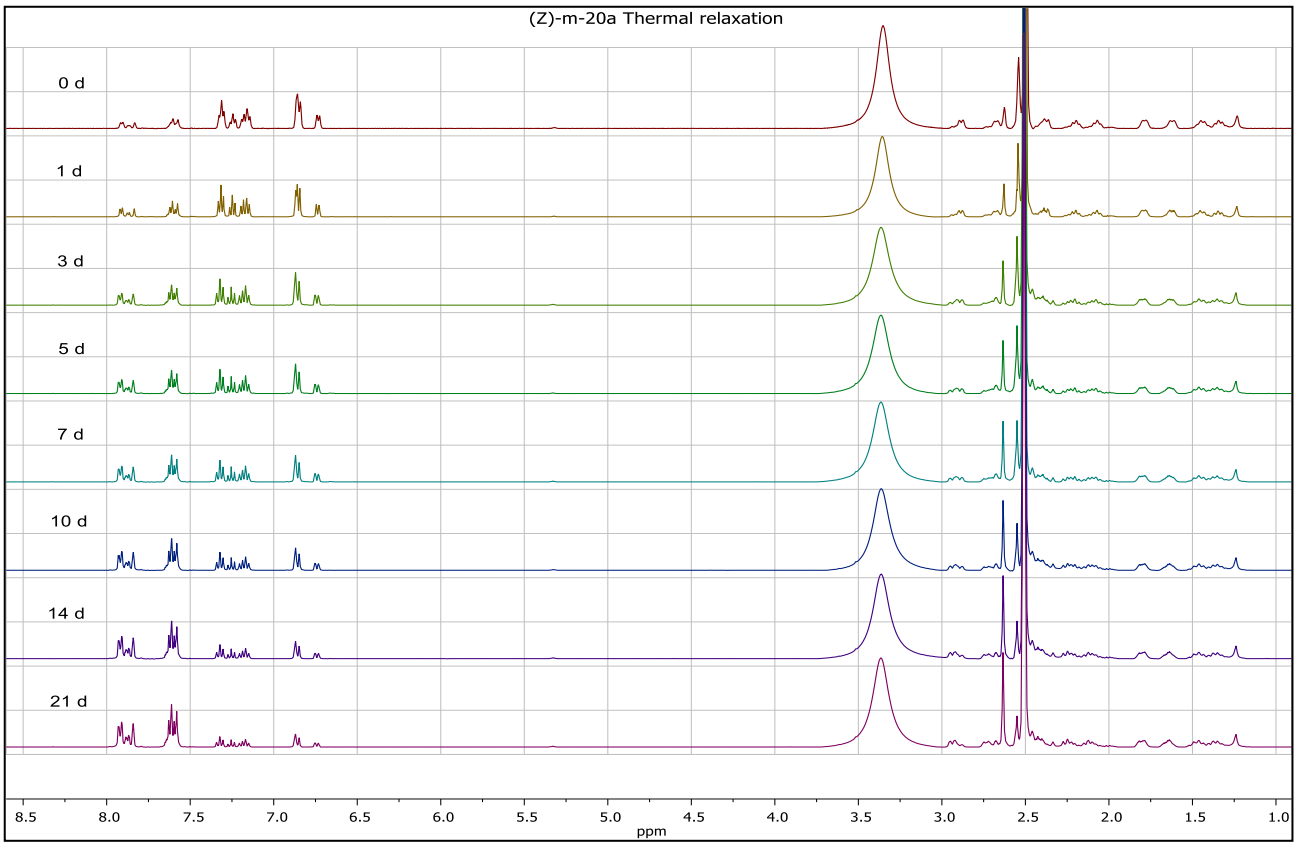

time (d)	1H (E)*	1H (Z)*	total*	Z (%)
0	1.01	4.23	5.24	80.7
1	1.03	3.07	4.10	74.9
3	1.01	2.04	3.05	66.8
5	1.01	1.46	2.47	59.1
7	1.02	1.15	2.17	53.0
10	1.00	0.80	1.80	44.4
14	1.00	0.53	1.53	34.6
21	1.02	0.35	1.37	25.6

*average integration for 1H (E) and 1H (Z) of aromatic signals

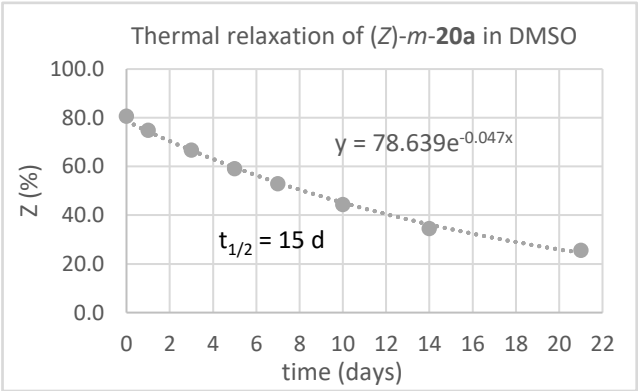

Thermal relaxation rates in DMSO of further compounds are given in the following table:

Comp.	$t_{(1/2)}$	Comp.	$t_{(1/2)}$
m-**12a**	14 d	*m*-**20a**	15 d
p-**12a**	32 h	*p*-**20a**	38 h
m-**12b**	8.5	*m*-**20b**	19 h
p-**12b**	40 min	*p*-**20b**	3.0 h

3 Biological test data for GABA transporter subtypes mGAT2-4

Results for functional inhibitory activity of the enantiopure photoswitchable GAT inhibitors towards the GABA transporter subtypes mGAT2-4 are given in the following table:

Comp.	pIC_{50} ± SEM[a]		
	mGAT2	mGAT3	mGAT4
(*R*)-*m*-**20a**	61% (76%[b])	4.17 (60%[b])	68% (57%[b])
(*R*)-*p*-**20a**	51%	4.42	4.36
(*R*)-*m*-**20b**	4.61	4.72	4.56
(*R*)-*p*-**20b**	58%	5.07	4.65

[a] due to low inhibitory activities only one experiment was performed in triplicate; percentages represent remaining [^{3}H]GABA uptake in presence of 100 µM inhibitor. [b] after irradiation at the photostationary state.

Tetrahedron 72 (2016) 1579–1589

Contents lists available at ScienceDirect

Tetrahedron

journal homepage: www.elsevier.com/locate/tet

A general approach to substituted diphenyldiazenes

Toni A. Lutz, Patrick Spanner, Klaus T. Wanner *

Ludwig-Maximilians-Universität München, Department of Pharmacy – Center for Drug Research, Butenandtstr. 5–13, D – 81377 Munich, Germany

ARTICLE INFO

Article history:
Received 15 December 2015
Received in revised form 1 February 2016
Accepted 3 February 2016
Available online 5 February 2016

Dedicated to Professor Dr. Eberhard Reimann with warmest wishes on the occasion of his 80th birthday

Keywords:
Substituted diphenyldiazenes
Azo coupling
N,N-Diallyl protection group
Cleavage of *N,N*-diallyl groups (deallylation)
Photoswitchable ligands

ABSTRACT

A general and practical synthetic method for the construction of unsymmetrically substituted diphenyldiazenes based on classical azo coupling reaction has been developed. A key feature of this method is the use of *N,N*-diallyl protected aniline derivatives as coupling components. The *N,N*-diallyl moiety of the coupling component warrants sufficient reactivity and allows to avoid formation of constitutional isomers resulting from intermediate triazene formation. Furthermore, subsequent to the coupling reaction, the *N,N*-diallyl aminofunction, can be replaced by other substituents including hydrogen via diazonium ion intermediates. In general, following this approach target compounds can be obtained in reasonable to good yields.

1. Introduction

Aromatic azo compounds have found widespread application in chemical and pharmaceutical industry. They are classically used for instance as dyes and pigments,[1] food additives, indicators for pH-measurements,[2] initiators for radical reactions,[3] as therapeutic agents[4,5] or as part of drug delivery systems.[6] Meanwhile a major focus of azobenzenes is on their use as light sensitive molecular switches,[7–9] as for example, for photoresponsive liquid crystals.[10–12] But in recent time, many papers appeared in particular on the use of photoswitchable ligands for photopharmacology, e.g., for the optical control of epithelial sodium channels,[13] insulin receptors,[14] the acetylcholinesterase,[15] μ-opioid receptors,[16] TRPV1-channels,[17] glutamate receptors,[18] NMDA receptors,[19] AMPA receptors,[20] local anesthetics[21] and cell division.[22] We recently described the use of this method to control the activity of a neurotransmitter transporter, the GABA transporter GAT1, employing a photoswitchable ligand.[23]

Because of the broad interest in azo compounds, several methods have been developed for their synthesis in the past.[24] Classical approaches comprise azo coupling reaction,[25] the Mills reaction,[26] and the Wallach reaction.[27] Recently, additional preparative methods have been reported such as the reductive coupling of aromatic nitro derivatives[28] or the oxidative coupling of aniline derivatives.[29] However, the substitution pattern of the aromatic azo compounds accessible by these methods is in general quite limited. Thus, when dimerization reactions such as the reductive coupling of nitro compounds are applied to establish the respective phenyl azo derivatives, homo and hetero coupling will inevitably lead to symmetrically and unsymmetrically substituted azo compounds and as a consequence thereof to poor yields. Clearly, the well known azo coupling reactions in which diazonium salts are reacted with aromatic systems give access to a broad array of differently substituted target compounds. But this approach suffers from distinct limitations as well. In this case the coupling component to be reacted with the diazonium salt must display a sufficiently high electron density, typically achieved by the presence of a hydroxy- or an amino group to undergo the desired conversion.

In the context with the development of new photoswitchable ligands for GABA transporters, we sought for a very specific substitution pattern of the diphenyldiazene unit, that is, exhibiting two main features (Scheme 1): There should be a halogen function at one of the two phenyl moieties allowing the assembly of the final photosensitive target compounds or precursors by cross coupling reactions like Suzuki, Sonogashira or Heck reactions. The second phenyl moiety should exhibit substituents such as halogens or alkyl groups preferentially in the *ortho* or the *para* position or in both

* Corresponding author. Tel.: +49 0 89 2180 77249; fax: +49 0 89 2180 77247; e-mail address: klaus.wanner@cup.uni-muenchen.de (K.T. Wanner).

http://dx.doi.org/10.1016/j.tet.2016.02.011
0040-4020/

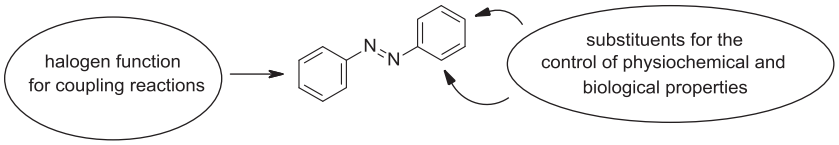

Scheme 1. Design of the desired target compounds.

since due to former results substituents in these positions were expected to improve binding affinities to GABA transporters.[30] Moreover, particularly substituents in the *ortho* or *para* position might also allow to tune the kinetics of the *E*/*Z*-isomerization of the photosensitive compounds as well as the wavelength of the necessary light used for isomerization which is often a decisive factor for the use of photoswitchable compounds in organic tissues.

We considered azo coupling reactions as the most efficient and versatile synthetic approach to the desired azo compounds **3** (Scheme 2). For such coupling reactions, the diazonium salt **1** should be used exhibiting an iodine substituent that should allow to use the target compound for Palladium catalyzed coupling reactions. The main problem, however, to solve was the question which reactant might be employed as nucleophile in the azo coupling reaction. Benzene derivatives with halogen function but devoid of any activating groups such as an OH or an NH_2 group increasing electron density of the aromatic system like **2** do not come into consideration as they are known to fail in azo coupling reactions. Given the fact that primary aromatic amino groups can be efficiently exchanged by e.g., halogene substituents by Sandmeyer or Schiemann reactions, the use of aniline derivatives **4**, the electron density of which should be high enough to undergo the desired coupling reaction, appears quite tempting. But in that case, an exchange of the azo and the amino group may occur between the coupling reagents via triazenes as intermediates which would ultimately result in a variety of structurally isomeric azo compounds.

It appeared to us that this problem could be easily solved, if the aniline derivatives **4** displaying a primary amino function were replaced by benzene derivatives **6** exhibiting a tertiary amino function carrying suitable protecting groups. Due to the protecting groups, triazene formation and side reactions resulting therefrom could be ruled out whereas compounds **6** should be still amenable to azo coupling reactions owing to the positive mesomeric effect of the amino group. Given its easy introduction and efficient removal without a significant effect on the electron donor ability of amino groups, we considered allyl residues as the most appropriate protecting groups for the purpose of this study. In the present paper, we wish to report on the results of our study utilizing *N,N*-diallyl protected aniline derivatives **6** for azo coupling reactions and the subsequent transformation of the primary coupling products **7** into azo benzene derivatives **5** exhibiting a primary amino group by N-deprotection and further on the replacement of the primary amino group by various substituents (→**3**). To the best of our knowledge, the above outlined synthetic concept has not been reported before.

2. Results and discussions

The primary step of our synthetic sequence that should give access to a broad variety of differently substituted azo benzenes **3** and **5,** the coupling reaction between a diazonium salt and *N,N*-diallyl substituted aniline derivative was in general performed as follows. The diazonium salts of anilines **1**, i.e., **1a** and **1b**, were generated right before their use by treating the respective iodo

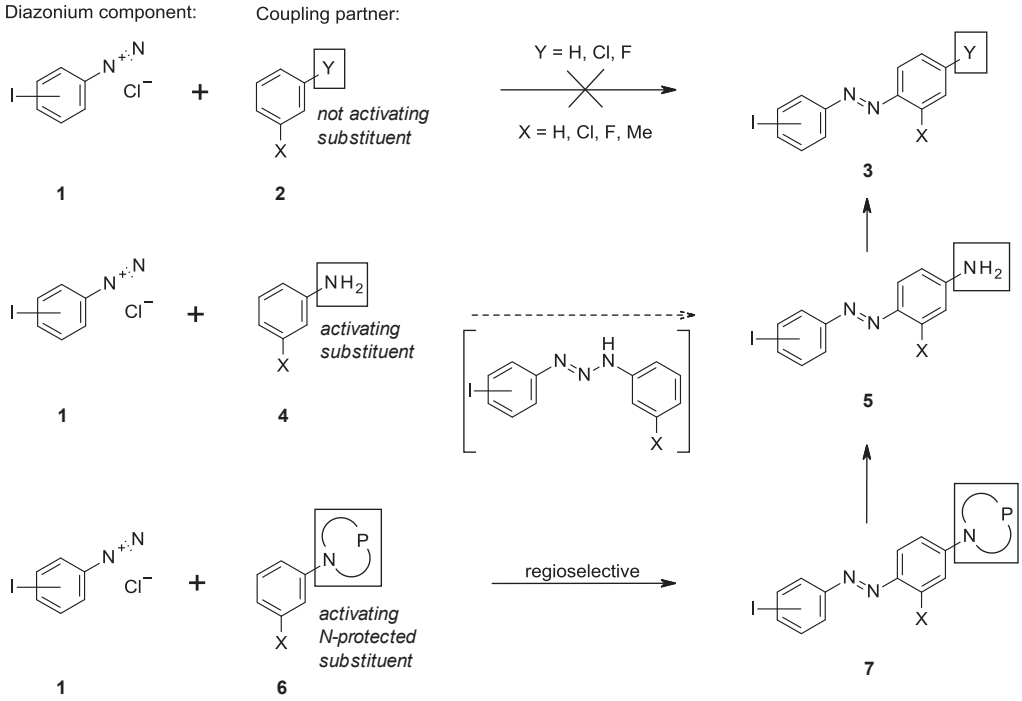

Scheme 2. Synthesis of substituted diphenyldiazenes by azo coupling.

aniline in a mixture of EtOH and 2 M HCl (3 equiv) with $NaNO_2$ (1.1 equiv in H_2O; excess $NaNO_2$ destroyed by addition of H_2NSO_3H). For the azo coupling reactions, the resulting solution was then added to a solution of the respective *N,N*-diallylaniline (in $EtOH/H_2O$) at 0 °C, in which, where indicated, also NaOAc or a further amount of 2 M HCl was present. The reaction mixture, the pH of which was estimated by means of indication paper, was finally stirred at 0 °C for the time given, before the product was isolated by extraction and purified by flash chromatography.

When diazonium salt **1** was reacted with *N,N*-diallylaniline (**8a**) under weak acidic pH conditions (pH ≈ 4), the reaction was complete within 4 h providing **9a** in 94% yield (Table 1, entry 1). For the coupling reaction of **1a** with the *m*-chloro substituted aniline derivative **8b**, longer reaction times were required. After 4 h as in the aforementioned reaction with **8a**, only 53% of **9b** were obtained which could be raised to 61% and 64% upon extension of the reaction time to 16 and 36 h, respectively (Table 1, entries 2–4).

When the compounds were allowed to react for 36 h but at a higher pH (≈5–6, adjusted by extra NaOAc), the yield lowered to 32% whereas 71% of **9b** could be isolated by running the reaction at a lower pH (Table 1, entry 6, pH ≈ 2–3, adjusted by omission of NaOAc). But when the pH was further reduced (to ≈1–2 by addition of 2 equiv of 2 M HCl) instead of an additional increase in yield a slight reduction occurred (Table 1, entry 7) indicating the pH optimum for the reaction to be ≈2–3. In case of the coupling reaction of **1a** with the *m*-fluoro substituted aniline derivative **8c** yields amounted to 55% (Table 1, entry 8) and 56% (Table 1, entry 9) only performed at the pH values of ≈4 and ≈2–3 that had so far appeared to be the most rewarding. For the more electron-rich 3-methyl substituted aniline derivative **8d**, the coupling reaction proceeded again quite smoothly. At both pH values, ≈4 and ≈2–3, the reaction was complete within 4 h yielding the coupling product in 92% and 85%, respectively (Table 1, entries 10–11).

The reaction conditions that had turned out best for the preparation of the diazobenzenes **9a**–**d** were finally also applied to the synthesis of regioisomers **10a**–**d** exhibiting the iodo substituent in *meta* position. That way, by coupling **8a**–**d** with *meta* iodo substituted diazonium salt **1b**, the corresponding diazobenzenes **10a**–**d** could be obtained in reasonable to good yields (51–84%, Table 2, entries 1–4).

The next step aimed at the deprotection of the tertiary amino function in **9a**–**d** and **10a**–**d** which should be accomplished by isomerization of the two allyl residues and subsequent hydrolysis of the thus formed aminovinyl units.

First attempts were performed with **9a** employing Pd/C, $Rh(PPh_3)_3Cl_2$ or $Ru(PPh_3)_3Cl_2$ in EtOH or THF also in presence of additives such as ethanolamine or trimethylamine, or the use of potassium *tert*-butoxide in DMSO or toluene remained unsuccessfully as either no reaction occurred or a complex mixture of products was formed. Finally, the transition metal catalyst $RuClH(CO)(PPh_3)_3$ reported by Krompiec et al.[31] to effect C–C double bond isomerization in *N*-allylamines was found to be well suited for our purposes, i.e., the isomerization of **9a** to **11a**. Thus when **9a** was heated with 1 Mol % of $RuClH(CO)(PPh_3)_3$ in CH_2Cl_2 to 60 °C in a microwave reactor, a clean reaction to the divinylamine **11a** occurred, which was complete within 2 h. Product **11a** was found to be labile. Therefore, neither **11a** nor the related products **11b**–**d** and **12a**–**d** were isolated, instead the solutions from the isomerization containing these compounds directly used for the next step.

The conditions required for the hydrolysis of the divinylamine function to liberate the primary amino group were exemplarily examined for **11a** to which end the solution of this compound resulting from the isomerization reaction was used without any purification. Treatment of **11a** with HCl, HOAc, NH_4Cl or water did not provide the desired amine or only as part of a complex reaction mixture. However, upon treatment of the CH_2Cl_2 solution of **11a**, obtained from the isomerization reaction, with $NH_3^+OHCl^-$ (10 equiv) and NEt_3 (5 equiv) at 60 °C for 3 h, a procedure developed for the cleavage of pyrrols,[32] a clear conversion to the free amino derivative occurred delivering **13a** in 96% yield.

The same procedure for the removal of the allyl protecting groups comprising isomerization and hydrolysis worked also well for **9b**–**9d** and the regioisomers regarding the iodo substituted **10a**–**d**, for the latter of which the reaction times for both steps had, however, to be extended to 4 h and 6 h, respectively, providing the target compounds **13b**–**d** and **14a**–**d** in yields from 87 to 95%.

The respective results that could be achieved for the cleavage of the *N,N*-diallylaniline protection group in these cases are shown in Table 3.

Table 1
Formation of diphenyldiazenes **9a**–**d** from diazotized 4-iodoaniline **1a** and *N,N*-diallylanilines **8a**–**d**[a]

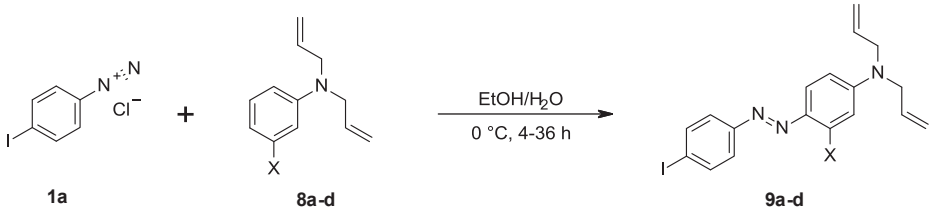

1a **8a-d** **9a-d**

Entry	Educt	X	Additives[b]	pH range[c]	Reaction time [h]	Product	Yield:
1	**8a**	H	NaOAc, 2 equiv	≈4	4	**9a**	94%
2	**8b**	Cl	NaOAc, 2 equiv	≈4	4	**9b**	53%
3	**8b**	Cl	NaOAc, 2 equiv	≈4	16	**9b**	61%
4	**8b**	Cl	NaOAc, 2 equiv	≈4	36	**9b**	64%
5	**8b**	Cl	NaOAc, 4 equiv	≈5–6	36	**9b**	32%
6	**8b**	Cl	—	≈2–3	36	**9b**	71%
7	**8b**	Cl	2M HCl, 2 equiv	≈1–2	36	**9b**	68%
8	**8c**	F	NaOAc, 2 equiv	≈4	36	**9c**	55%
9	**8c**	F	—	≈2–3	36	**9c**	56%
10	**8d**	Me	NaOAc, 2 equiv	≈4	4	**9d**	92%
11	**8d**	Me	—	≈2–3	4	**9d**	85%

[a] A solution of **1a** was freshly generated from 4-iodoaniline by addition of $NaNO_2$ (1.1 equiv) and 2M HCl (3.0 equiv) in $EtOH/H_2O$ (2:1). This solution was then added to a separate solution of **8a**–**d** in $EtOH/H_2O$ (2:1).
[b] Further additives added to the solution of the coupling component **8a**–**d** where indicated.
[c] Determined from the reaction mixture directly after the addition of the solution of **1a** to the solution of **8a**–**d**.

Table 2
Formation of diphenyldiazenes **10a**–**d** from diazotated 3-iodoaniline **1b** and *N,N*-diallylanilines **8a**–**d**[a]

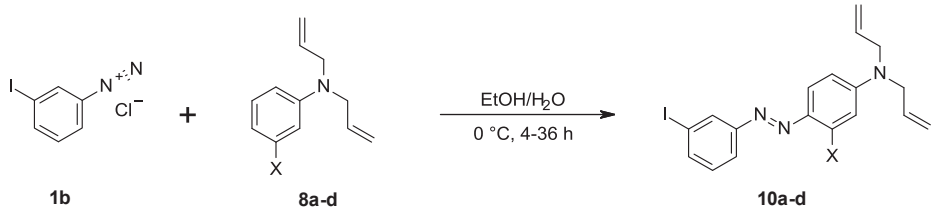

1b **8a-d** **10a-d**

Entry	Educt	X	Additives[b]	pH range[c]	Reaction time [h]	Product	Yield:
1	**8a**	H	NaOAc, 2 equiv	≈4	4	**10a**	80%
2	**8b**	Cl	—	≈2–3	36	**10b**	63%
3	**8c**	F	—	≈2–3	36	**10c**	51%
4	**8d**	Me	NaOAc, 2 equiv	≈4	4	**10d**	84%

[a] A solution of **1b** was freshly generated from 4-iodoaniline by addition of $NaNO_2$ (1.1 equiv) and 2M HCl (3.0 equiv) in EtOH/H_2O (2:1). This solution was then added to a separate solution of **8a**–**d** in EtOH/H_2O (2:1).
[b] Further additives added to the solution of the coupling component **8a**–**d** where indicated.
[c] Determined from the reaction mixture directly after the addition of the solution of **1b** to the solution of **8a**–**d**.

To demonstrate the synthetic utility of the thus obtained diphenyldiazenes, prototypic reactions for the replacement of the amino group in **13a**–**d** by hydrogen, chlorine, and fluorine have been performed.

Reductive removal of the amino group in **13a**–**d** could be accomplished following a standard procedure. Treatment with $NaNO_2$ (3 equiv) and H_3PO_2 (20 equiv) of **13a**–**d** in THF provided the desired desamino derivatives **15a**–**d** in reasonable to good yields (Table 4, 66–75%).

Substitution of the amino group in the aniline derivatives obtained in this study by chlorine or fluorine in a Sandmeyer and Schiemann reaction is feasible as well, as shown for **13a**. Treatment of **13a** with *tert*-BuONO and 4-dodecylbenzenesulfonic acid in tetrachloromethane and subsequent heating with triethylamine following a literature procedure[33] provided the chloroderivative **16** in 52%. For this transformation, it occurred crucial that CCl_4 was employed as solvent as with other organic solvent which were required because of the poor solubility of **13a** in water, partial

Table 3
Deallylation of diphenyldiazenes **9** and **10** via isomerization and subsequent hydrolysis

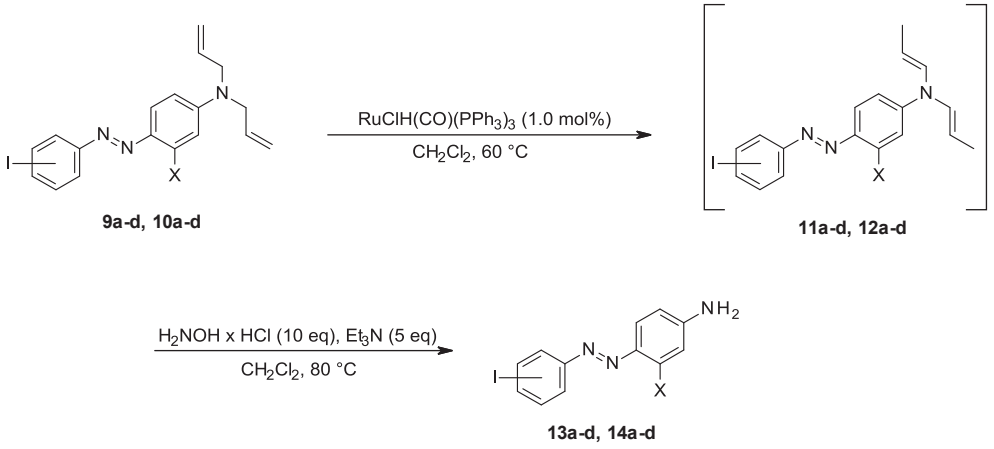

9a-d, 10a-d **11a-d, 12a-d** **13a-d, 14a-d**

Entry		Educt	X	Isomerization time [h]	Hydrolysis time [h]	Product	Yield:
1		**9a**	H	2	3	**13a**	96%
2		**9b**	Cl	2	3	**13b**	93%
3		**9c**	F	2	3	**13c**	91%
4		**9d**	Me	2	3	**13d**	95%
5		**10a**	H	4	6	**14a**	92%
6		**10b**	Cl	4	6	**14b**	88%
7		**10c**	F	4	6	**14c**	87%
8		**10d**	Me	4	6	**14d**	90%

Table 4
Reductive removal of the amino group in aniline derivatives **13a–d**

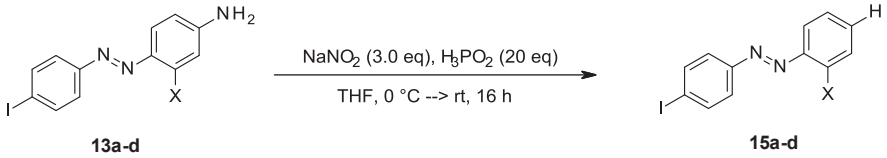

13a-d **15a-d**

Entry	Educt	X	Product	Yield:
1	**13a**	H	**15a**	75%
2	**13b**	Cl	**15b**	66%
3	**13c**	F	**15c**	68%
4	**13d**	Me	**15d**	71%

replacement of the amino substituent by hydrogen occurred leading to diminished yields.

Similarly, the fluorine derivative **17** could be prepared in a Schiemann reaction treating **13a** with *tert*-BuONO and $BF_3 \cdot Et_2O$ (followed by heating to 120 °C) the yield amounting to 63% (Scheme 3). According to these results, the synthetic sequence of azo coupling with *N,N*-diallyl protected aniline derivatives, subsequent deprotection and substitution of the amino group represents a highly efficient and versatile access to differently substituted diphenyldiazene derivatives (see Scheme 4).

Having successfully accomplished the formation of amino substituted diphenyldiazenes by azo coupling reactions with N-protected aniline derivatives, we wondered whether an analogous reaction could possibly also be performed with 1-aminonaphthalene in either N-protected or even unprotected form.

Interestingly, in this case a protection of the primary amino group was not required. When the diazonium salts **1a** and **1b** derived from 4-iodoaniline and 3-iodoaniline were reacted with 1-aminonaphtalene (**18**) the corresponding azo coupling products **19a** and **19b** were formed without any sign of isomeric products that could have resulted from intermediate triazene formation. Also the yields for the products amounting to 91% and 93% for **19a** and **19b**, respectively, were very high. As in the case of the amino substituted diphenyldiazenes the reductive elimination of the amino group in **19a–b** employing $NaNO_2$ and H_3PO_2 worked here well, too, providing the desaminated phenylnaphtyl diazenes **20a–b** in good yields (**20a**: 72%; **20b**: 68%).

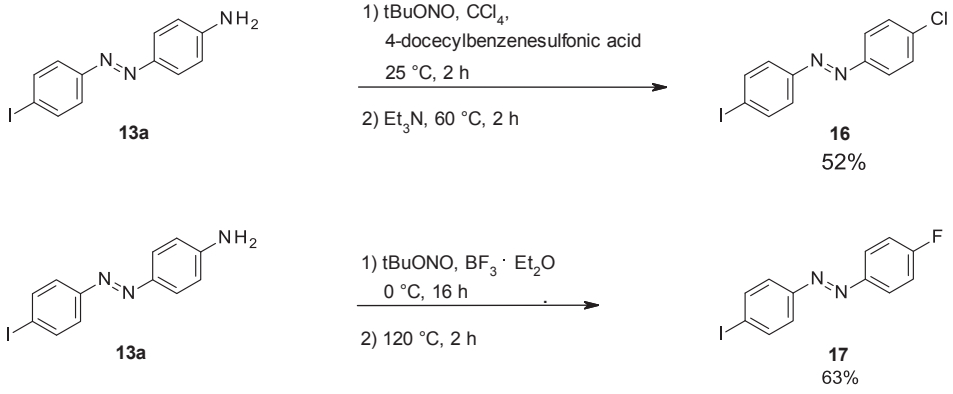

Scheme 3. Replacement of the amino group in **13a** by a chlorine and fluorine substituent.

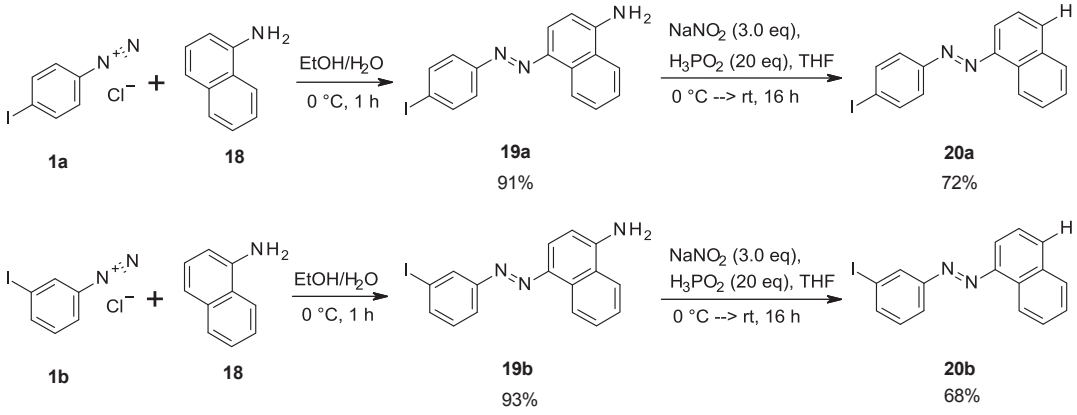

Scheme 4. Azo coupling of diazotated iodoaniline **1a–b** with 1-aminonaphthaline (**18**).

Of these compounds, the naphtylphenyl diazene derivative **20b** has already successfully been used as a building block for the construction of a valuable photoswitchable ligand of the GABA transporter GAT1.[23]

3. Conclusion

Based on diazonium chemistry, a highly versatile synthetic route to substituted diphenyldiazenes exhibiting an iodo substituent on one of the two aromatic rings and additional substituents on the other has been established.

The method comprises the coupling of diazonium salts derived from iodo substituted aniline derivatives on the one with *N,N*-diallyl protected anilines on the other side. The key feature of this approach is to be seen in the use of the temporary protection of the amino group of the aniline derivative with two *N*-allyl residues. The *N,N*-diallyl residue warrants sufficient reactivity of the benzene derivatives for azo coupling reactions whereas the N-protection of the amino group rules out side reaction that would otherwise arise from intermediate triazene formation. Further, the primary amino group accessible by deprotection of the *N,N*-diallyl moiety after the azo coupling reaction has the advantage to provide the opportunity for a broad array of transformation reactions as exemplified by its replacement by hydrogen, chlorine or fluorine substituents employing common methods. Overall the synthetic method outlined in this paper provides a broadly applicable and flexible approach to differently substituted diphenyl diazenens derivatives which equipped with a suitable functional group, such as an iodine substituent for metal catalyzed coupling reactions, can be rewarding building blocks for the construction of photoswitchable bioactive compounds.

4. Experimental section

4.1. General methods

For all reactions only distilled solvents were used. THF and NEt_3 were dried over sodium and distilled under nitrogen. CH_2Cl_2 was distilled from CaH_2 under nitrogen. Commercial available reagents were used without further purification. Flash column chromatography was performed using silica gel (40–60 μm). NMR spectra were measured with a Jeol Eclipse +400 (400 MHz) and a Jeol Eclipse +500 (500 MHz) spectrometer or an Avance III HD 400 MHz Bruker BioSpin and an Avance III HD 500 MHz Bruker BioSpin spectrometer. ^1H NMR chemical shifts were referenced to TMS and ^{13}C NMR chemical shifts were referenced to $CHCl_3$. The coupling constants were stated with an accuracy of 0.5 Hz. MestreNova software was used for further analysis of the spectra. IR spectra were recorded with an FT-IR spectrometer Paragon 1000 (PerkinElmer). Samples were measured either as KBr pellets or as films on NaCl plates. Spectrum v2.00 software (PerkinElmer) was used for analysis. Mass spectra were measured with a mass spectrometer 59827A with 59980 particle beam LC/MS interface (Hewlett–Packard). High resolution mass spectrometry was carried out with an LTQ FT (ThermoFinnigan), FAB (Xenon, 6 kV, MBA, reference PEG), or a JMS GCmate II (Jeol).

4.2. General procedure for the allylation of aniline derivatives (GP1)

The corresponding aniline was dissolved in EtOH (2 mL/mmol) and H_2O (0.5 mL/mmol) was added. Ally bromide (2.4 equiv) and Na_2CO_3 (1.2 equiv) were added and the mixture was heated to reflux for the indicated time. After the end of the reaction, the main part of the alcohol was removed by distillation. CH_2Cl_2 (5 mL/mmol) and H_2O (5 mL/mmol) were added and the product was extracted with CH_2Cl_2 (3×). The combined organic layers were dried over Na_2SO_4 and the solvent was removed under reduced pressure. The crude product was purified by flash chromatography (eluting with pentane) to give the diallylated derivatives.

4.3. General procedure for the azo coupling (GP2)

The corresponding iodo aniline (1.0 equiv) was dissolved in of EtOH (3 mL/mmol) und 2N HCl (1.5 mL/mmol, 3.0 equiv) was added. The mixture was cooled to 0 °C and a pre-cooled solution of $NaNO_2$ (1.1 equiv) in H_2O (1.5 mL/mmol) was added dropwise over a period of 10 min. After the end of the addition, the solution was stirred for further 10 min at 0 °C. Then the excess of $NaNO_2$ was removed by the addition of amidosulfuric acid (0.2 equiv) once again followed by stirring for 10 min at 0 °C (suspension A).

The corresponding *N,N*-diallyl aniline derivative (1.0 equiv) was dissolved in EtOH (20 mL/mmol) and 10 mL/mmol water was added (solution B). If indicated, to this solution is also added either NaOAc (2.0 equiv) or a further amount of 2N HCl (1 mL/mmol, 2.0 equiv) additionally.

Suspension A was then added to solution B at 0 °C, the pH was determined of the resulting mixture (indicator paper) and it was stirred for the indicated time at 0 °C. Afterwards it was allowed to warm up to rt slowly followed by the addition of both CH_2Cl_2 (20 mL/mmol) and H_2O (20 mL/mmol). The aqueous phase was made alkaline (pH 10–12) by the addition of NaOH and the product was extracted with CH_2Cl_2 (3×). The combined organic layers were dried over Na_2SO_4 and the solvent was removed under reduced pressure. The crude product was purified by flash chromatography (eluting with pentane/CH_2Cl_2=8/2) to give the clean azo compound.

4.4. General procedure for the deallylation of the diallylamines (GP3)

Under nitrogen the corresponding *N,N*-diallyl amine (1.0 equiv) and $RuClH(CO)(PPh_3)_3$ (0.01 equiv) were introduced in a pressure tube and dissolved in of CH_2Cl_2 (5 mL/mmol). The tube was sealed air tightly and the solution was heated to 60 °C for the indicated time. After cooling to rt both $H_2NOH{\times}HCl$ (10 equiv) and Et_3N (5 equiv) were added and the mixture was heated to 80 °C for the indicated time. After cooling to rt, once again H_2O (5 mL/mmol) was added and the product was extracted with CH_2Cl_2 (3×). The combined organic layers were dried over Na_2SO_4 and the solvent was removed under reduced pressure. The crude product was purified by flash chromatography (eluting with pentane/dichloromethane=1/1) to give the corresponding primary aromatic amine.

4.5. General procedure for the reductive dediazoniation of the aromatic amines (GP4)

The corresponding primary aromatic amine derivative (1.0 equiv) was dissolved in THF (20 mL/mmol), cooled to 0 °C and hypophosphorous acid (50% solution in water, 20 equiv) was added. Sodium nitrite (3.0 equiv) was added and the mixture was stirred for 4 h at 0 °C and then at rt for further 12 h. Afterwards there were added CH_2CL_2 (20 mL/mmol) and water (20 mL/mmol) and the aqueous phase was made alkaline (pH 10–12) with 2N NaOH. The product was extracted with CH_2Cl_2 (3×). The combined organic layers were dried over Na_2SO_4 and the solvent was removed under reduced pressure. The crude product was purified by flash chromatography (eluting with pentane) to give the corresponding reduced species.

4.6. Characterization data of new products

*4.6.1. N,N-Diallylaniline (**8a**).* According to GP1 from aniline (4.7 g, 50 mmol), allylbromide (14.8 g, 120 mmol) and K_2CO_3 (6.4 g, 60 mmol). The reaction time was 3 h **8a** was obtained as colorless oil (8.20 g, 95%). TLC: $R_f \approx 0.3$ (pentane). IR (NaCl): $\tilde{\nu}$=3084, 3062, 2979, 2912, 2858, 1642, 1599, 1574, 1505, 1388, 1357, 1233, 1181, 988, 918, 746, 691 cm^{-1}. ^1H NMR (500 MHz, $CDCl_3$, 21 °C, TMS): δ=3.90 (dt, J=4.6/1.6 Hz, 4H), 5.10–5.21 (m, 4H), 5.84 (ddt, J=17.2/10.1/4.9 Hz, 2H), 6.63–6.72 (m, 3H), 7.14–7.23 (m, 2H) ppm ^{13}C NMR (126 MHz, $CDCl_3$, 21 °C, TMS): δ=52.81 (2C), 112.41 (2C), 116.06 (2C), 116.38, 129.16 (2C), 134.12 (2C), 148.78 ppm. M ($C_{12}H_{15}N$)=173.25. MS (EI+): *m/z*: 173.1 (M^+). HRMS (EI+): M^+ calcd for $C_{12}H_{15}N$: 173.1204; found 173.1205.

*4.6.2. N,N-Diallyl-3-chloroaniline (**8b**).* According to GP1 from 3-chloro-aniline (6.4 g, 50 mmol), allylbromide (14.8 g, 120 mmol) and K_2CO_3 (6.4 g, 60 mmol). The reaction time was 4 h **8b** was obtained as colorless oil (9.60 g, 92%). TLC: $R_f \approx 0.3$ (pentane). IR (NaCl): $\tilde{\nu}$=3083, 3008, 2981, 2910, 2865, 1642, 1594, 1560, 1493, 1417, 1385, 1357, 1235, 1180, 1101, 985, 920, 830, 759, 681 cm^{-1}. ^1H NMR (500 MHz, $CDCl_3$, 21 °C, TMS): δ=3.89 (dt, J=4.0/1.7 Hz, 4H), 5.14 (dq, J=8.8/1.7 Hz, 2H), 5.17 (m, 2H), 5.82 (ddt, J=16.8/10.7/4.8 Hz, 2H), 6.54 (ddd, J=8.4/2.4/0.9 Hz, 1H), 6.63 (m, 2H), 7.07 (t, J=8.0 Hz, 1H) ppm ^{13}C NMR (126 MHz, $CDCl_3$, 21 °C, TMS): δ=52.81 (2C), 110.48, 112.19, 116.20, 116.36 (2C), 130.08, 133.36 (2C), 135.07, 149.85 ppm. M ($C_{12}H_{14}ClN$)=207.7. MS (EI+): *m/z*: 207.1 (M^+). HRMS (EI+): M^+ calcd for $C_{12}H_{14}ClN$ 207.0815; found 207.0808.

*4.6.3. N,N-Diallyl-3-fluoroaniline (**8c**).* According to GP1 from 3-fluoro-aniline (5.6 g, 50 mmol), allylbromide (14.8 g, 120 mmol) and K_2CO_3 (6.4 g, 60 mmol). The reaction time was 4 h **8c** was obtained as colorless oil (9.01 g, 94%). TLC: $R_f \approx 0.3$ (pentane). IR (NaCl): $\tilde{\nu}$=3083, 3008, 2981, 2912, 2866, 1642, 1619, 1578, 1500, 1418, 1389, 1357, 1333, 1257, 1184, 1158, 991, 960, 922, 822, 753, 681 cm^{-1}. ^1H NMR (500 MHz, $CDCl_3$, 21 °C, TMS): δ=3.89 (dt, J=3.8/1.7 Hz, 4H), 5.14 (dq, J=5.1/1.7 Hz, 2H), 5.16–5.18 (m, 2H), 5.82 (ddt, J=17.7/9.8/4.8 Hz, 2H), 6.32–6.38 (m, 2H), 6.43 (ddd, J=8.4/2.3/0.9 Hz, 1H), 7.04–7.14 (m, 1H) ppm ^{13}C NMR (126 MHz, $CDCl_3$, 21 °C, TMS): δ=52.93 (2C), 99.34 (d, $^2J_{CF}$=26.1 Hz), 102.77 (d, $^2J_{CF}$=21.6 Hz), 107.91 (d, $^4J_{CF}$=2.0 Hz), 116.32 (2C), 130.13 (d, $^3J_{CF}$=10.4 Hz), 133.49 (2C), 150.54 (d, $^3J_{CF}$=10.7 Hz), 164.24 (d, $^1J_{CF}$=241.5 Hz) ppm. M ($C_{12}H_{14}FN$)=191.2. MS (EI+): *m/z*: 191.1 (M^+). HRMS (EI+): M^+ calcd for $C_{12}H_{14}FN$ 191.1110; found 191.1108.

*4.6.4. N,N-Diallyl-3-methylaniline (**8d**).* According to GP1 from 3-methyl-aniline (5.4 g, 50 mmol), allylbromide (14.8 g, 120 mmol) and K_2CO_3 (6.4 g, 60 mmol). The reaction time was 4 h **8d** was obtained as colorless oil (8.12 g, 87%). TLC: $R_f \approx 0.3$ (pentane). IR (NaCl): $\tilde{\nu}$=3079, 3042, 3006, 2978, 2916, 2861, 1641, 1601, 1581, 1497, 1417, 1385, 1357, 1333, 1249, 1179, 990, 954, 917, 837, 764, 691 cm^{-1}. ^1H NMR (500 MHz, $CDCl_3$, 21 °C, TMS): δ=2.28 (s, 3H), 3.89 (dt, J=4.5/1.6 Hz, 4H), 5.12–5.19 (m, 4H), 5.84 (ddt, J=17.2/10.0/4.9 Hz, 2H), 6.46–6.55 (m, 3H), 7.03–7.12 (m, 1H) ppm ^{13}C NMR (126 MHz, $CDCl_3$, 21 °C, TMS): δ=22.05, 52.75 (2C), 109.66, 113.11, 116.00 (2C), 117.36, 129.05, 134.21 (2C), 138.82, 148.89 ppm. M ($C_{13}H_{17}N$)=187.28. MS (EI+): *m/z*: 187.1 (M^+). HRMS (EI+): M^+ calcd for $C_{13}H_{17}N$ 187.1361; found 187.1355.

*4.6.5. N,N-Diallyl-4-[(E)-(4-iodophenyl)azo]aniline (**9a**).* According to GP2 solution A was made of 4-iodoaniline (2.24 g, 10.0 mmol) in EtOH (30 mL) and 2 N HCl (15 ml, 30 mmol), sodium nitrite (0.76 g, 11.0 mmol) in H_2O (10 mL) and amidosulfuric acid (0.20 g, 2.0 mmol). Solution B was obtained from **8a** (1.77 g, 10.0 mmol) in EtOH (200 mL) and H_2O (100 mL) and an addition of sodium acetate (1.70 g, 20.0 mmol). The resulting pH was about 4. The reaction time was 4 h at 0 °C. **9a** was obtained as red solid (3.80 g, 94%). TLC: $R_f \approx 0.4$ (pentane/CH_2Cl_2=8/2). Mp: 41 °C. IR (KBr): $\tilde{\nu}$=3075, 3006, 2974, 2864, 1596, 1512, 1401, 1383, 1350, 1310, 1234, 1158, 1137, 1001, 938, 919, 829 cm^{-1}. ^1H NMR (500 MHz, $CDCl_3$, 21 °C, TMS): δ=3.98 (dt, J=4.0/1.6 Hz, 4H), 5.13–5.22 (m, 4H), 5.84 (ddt, J=17.1/10.1/4.7 Hz, 2H), 6.70–6.74 (m, 2H), 7.53–7.58 (m, 2H), 7.75–7.79 (m, 2H), 7.79–7.84 (m, 2H) ppm ^{13}C NMR (126 MHz, $CDCl_3$, 21 °C, TMS): δ=52.89 (2C), 95.36, 111.87 (2C), 116.65 (2C), 124.05 (2C), 125.30 (2C), 132.83 (2C), 138.15 (2C), 143.76, 151.41, 152.64 ppm. M ($C_{18}H_{18}IN_3$)=403.26. MS (ESI+): *m/z*: 404.1 ($[M+H]^+$). HRMS (ESI+): M^+ calcd for $C_{18}H_{19}IN_3$ 404.0545; found 404.0617.

*4.6.6. N,N-Diallyl-3-chloro-4-[(E)-(4-iodophenyl)azo]aniline (**9b**).* According to GP2 solution A was made of 4-iodoaniline (2.24 g, 10.0 mmol) in EtOH (30 mL) and 2 N HCl (15 mL, 30 mmol), sodium nitrite (0.76 g, 11.0 mmol) in H_2O (10 mL) and amidosulfuric acid (0.20 g, 2.0 mmol). Solution B was obtained from **8b** (2.12 g, 10.0 mmol) in EtOH (200 mL) and H_2O (100 mL) without any further additions. The resulting pH was between 2 and 3. The reaction time was 36 h at 0 °C. **9b** was obtained as red solid (3.12 g, 71%). TLC: $R_f \approx 0.4$ (pentane/CH_2Cl_2=8/2). Mp: 81 °C. IR (KBr): $\tilde{\nu}$=3429, 3078, 3004, 2975, 2885, 1590, 1503, 1381, 1344, 1322, 1300, 1229, 1191, 1176, 1126, 1043, 1002, 925, 835, 802 cm^{-1}. ^1H NMR (500 MHz, $CDCl_3$, 21 °C, TMS): δ=3.97 (dt, J=4.7/1.8 Hz, 4H), 5.16 (dq, J=17.1/1.6 Hz, 2H), 5.21 (dq, J=10.3/1.4 Hz, 2H), 5.83 (ddt, J=17.1/10.2/4.7 Hz, 2H), 6.58 (dd, J=9.3/2.8 Hz, 1H), 6.77 (d, J=2.8 Hz, 1H), 7.59–7.62 (m, 2H), 7.74 (d, J=9.2 Hz, 1H), 7.77–7.81 (m, 2H) ppm ^{13}C NMR (126 MHz, $CDCl_3$, 21 °C, TMS): δ=52.92 (2C), 96.09, 111.01, 112.30, 116.95 (2C), 118.59, 124.45 (2C), 132.28 (2C), 138.25 (2C), 138.87, 139.21, 151.82, 152.70 ppm. M ($C_{18}H_{17}ICIN_3$)=437.70. MS (EI+): *m/z*: 437.0 (M^+). HRMS (EI+): M^+ calcd for $C_{18}H_{17}ICIN_3$ 437.0156; found 437.0146.

*4.6.7. N,N-Diallyl-3-fluoro-4-[(E)-(4-iodophenyl)azo]aniline (**9c**).* According to GP2 solution A was made of 4-iodoaniline (2.24 g, 10.0 mmol) in EtOH (30 mL) and 2 N HCl (15 mL, 30 mmol), sodium nitrite (0.76 g, 11.0 mmol) in H_2O (10 mL) and amidosulfuric acid (0.20 g, 2.0 mmol). Solution B was obtained from **8c** (1.95 g, 10.0 mmol) in EtOH (200 mL) and H_2O (100 mL) without any further additions. The resulting pH was between 2 and 3. The reaction time was 36 h at 0 °C. **9c** was obtained as red solid (2.36 g, 56%). TLC: $R_f \approx 0.4$ (pentane/CH_2Cl_2=8/2). Mp: 72 °C. IR (KBr): $\tilde{\nu}$=3078, 3003, 2976, 2923, 1610, 1560, 1511, 1395, 1381, 1350, 1330, 1232, 1184, 1108, 1001, 919, 828 cm^{-1}. ^1H NMR (500 MHz, $CDCl_3$, 21 °C, TMS): δ=3.94–3.98 (m, 4H), 5.16 (dq, J=17.2/1.6 Hz, 2H), 5.21 (dq, J=10.4/1.6 Hz, 2H), 5.82 (ddt, J=17.0/10.0/4.7 Hz, 2H), 6.41–6.48 (m, 2H), 7.55–7.60 (m, 2H), 7.70–7.75 (m, 1H), 7.75–7.80 (m, 2H) ppm ^{13}C NMR (126 MHz, $CDCl_3$, 21 °C, TMS): δ=53.00 (2C), 95.83, 98.85 (d, J=24.9 Hz), 108.22 (d, J=1.5 Hz), 116.94 (2C), 118.71 (d, J=2.2 Hz), 124.23 (2C), 131.64 (d, J=7.1 Hz), 132.27 (2C), 138.18 (2C), 152.72, 153.00 (d, J=11.6 Hz), 162.49 (d, J=255.5 Hz) ppm. M ($C_{18}H_{17}IFN_3$)=421.25. MS (EI+): *m/z*: 421.0 (M^+). HRMS (EI+): M^+ calcd for $C_{18}H_{17}IFN_3$ 421.0451; found 421.0450.

*4.6.8. N,N-Diallyl-3-methyl-4-[(E)-(4-iodophenyl)azo]aniline (**9d**).* According to GP2 solution A was made of 4-iodoaniline (2.24 g, 10.0 mmol) in EtOH (30 mL) and 2 N HCl (15 ml, 30 mmol), sodium nitrite (0.76 g, 11.0 mmol) in H_2O (10 mL) and amidosulfuric acid (0.20 g, 2.0 mmol). Solution B was obtained from **8d** (1.91 g, 10.0 mmol) in EtOH (200 mL) and H_2O (100 mL) and an addition of sodium acetate (1.70 g, 20.0 mmol). The resulting pH was about 4. The reaction time was 4 h at 0 °C. **9d** was obtained as red solid (3.84 g, 92%). TLC: $R_f \approx 0.4$ (pentane/CH_2Cl_2=8/2). Mp: 68 °C. IR (KBr): $\tilde{\nu}$=3075, 3002, 2974, 2920, 2886, 1596, 1565, 1503, 1378, 1347, 1324, 1298, 1232, 1190, 1102, 1001, 957, 920, 835, 821, 802 cm^{-1}. ^1H NMR (500 MHz, $CDCl_3$, 21 °C, TMS): δ=2.66 (s, 3H),

3.94–3.99 (m, 4H), 5.13–5.20 (m, 4H), 5.84 (ddt, *J*=17.0/9.9/4.7 Hz, 2H), 6.51–6.56 (m, 2H), 7.53–7.57 (m, 2H), 7.68–7.73 (m, 1H), 7.74–7.78 (m, 2H) ppm ^{13}C NMR (126 MHz, $CDCl_3$, 21 °C, TMS): δ=18.36, 52.70 (2C), 94.99, 110.39, 112.84, 116.54 (2C), 117.11, 124.14 (2C), 132.96 (2C), 138.09 (2C), 141.58, 141.94, 151.39, 153.03 ppm. M ($C_{19}H_{20}IN_3$)=417.29. MS (EI+): *m/z*: 417.1 (M^+). HRMS (EI+): M^+ calcd for $C_{19}H_{20}IN_3$ 417.0702; found 417.0694.

*4.6.9. N,N-Diallyl-4-[(E)-(3-iodophenyl)azo]aniline (**10a**).* According to GP2 solution A was made of 3-iodoaniline (2.24 g, 10.0 mmol) in EtOH (30 mL) and 2 N HCl (15 ml, 30 mmol), sodium nitrite (0.76 g, 11.0 mmol) in H_2O (10 mL) and amidosulfuric acid (0.20 g, 2.0 mmol). Solution B was obtained from **8a** (1.77 g, 10.0 mmol) in EtOH (200 mL) and H_2O (100 mL) and an addition of sodium acetate (1.70 g, 20.0 mmol). The resulting pH was about 4. The reaction time was 4 h at 0 °C. **10a** was obtained as red high vicious oil (3.22 g, 80%). TLC: R_f≈0.4 (pentane/CH_2Cl_2=8/2). IR (KBr): $\tilde{\nu}$=3070, 3060, 3006, 2980, 2920, 1642, 1599, 1565, 1512, 1420, 1387, 1354, 1334, 1312, 1233, 1177, 1156, 1138, 1052, 991, 921, 820, 783, 701 cm^{-1}. ^{1}H NMR (500 MHz, $CDCl_3$, 21 °C, TMS): δ=3.97–4.04 (m, 4H), 5.13–5.24 (m, 4H), 5.86 (ddt, *J*=16.9/9.8/4.7 Hz, 2H), 6.74 (d, *J*=9.1 Hz, 2H), 7.19 (t, *J*=7.9 Hz, 1H), 7.67 (d, *J*=7.8 Hz, 1H), 7.78–7.81 (m, 1H), 7.82 (d, *J*=9.1 Hz, 2H), 8.16 (t, *J*=1.6 Hz, 1H) ppm ^{13}C NMR (126 MHz, $CDCl_3$, 21 °C, TMS): δ=52.78 (2C), 94.60, 111.73 (2C), 116.55 (2C), 122.85, 125.27 (2C), 129.95, 130.43, 132.68 (2C), 137.78, 143.59, 151.41, 154.08 ppm. M ($C_{18}H_{18}IN_3$)=403.3. MS (EI+): *m/z*: 403.1 (M^+). HRMS (EI+): M^+ calcd for $C_{18}H_{18}IN_3$ 403.0545; found 403.0546.

*4.6.10. N,N-Diallyl-3-chloro-4-[(E)-(3-iodophenyl)azo]aniline (**10b**).* According to GP2 solution A was made of 3-iodoaniline (2.24 g, 10.0 mmol) in EtOH (30 mL) and 2 N HCl (15 ml, 30 mmol), sodium nitrite (0.76 g, 11.0 mmol) in H_2O (10 mL) and amidosulfuric acid (0.20 g, 2.0 mmol). Solution B was obtained from **8b** (2.12 g, 10.0 mmol) in EtOH (200 mL) and H_2O (100 mL) without any further additions. The resulting pH was between 2 and 3. The reaction time was 36 h at 0 °C. **10b** was obtained as red solid (2.75 g, 63%). TLC: R_f≈0.4 (pentane/CH_2Cl_2=8/2). Mp: 74 °C. IR (KBr): $\tilde{\nu}$=3070, 3062, 3006, 2980, 2922, 1591, 1501, 1438, 1382, 1353, 1225, 1173, 1133, 1040, 991, 923, 782 cm^{-1}. ^{1}H NMR (500 MHz, $CDCl_3$, 22 °C, TMS): δ=3.93–4.00 (m, 4H), 5.16 (d, *J*=17.2 Hz, 2H), 5.21 (d, *J*=10.3 Hz, 2H), 5.82 (ddt, *J*=18.7/9.4/4.4 Hz, 2H), 6.57 (dd, *J*=9.2/2.1 Hz, 1H), 6.77 (d, *J*=2.6 Hz, 1H), 7.18 (t, *J*=7.9 Hz, 1H), 7.68 (d, *J*=7.8 Hz, 1H), 7.72 (d, *J*=9.2 Hz, 1H), 7.84 (d, *J*=8.0 Hz, 1H), 8.19 (t, *J*=1.7 Hz, 1H). ppm ^{13}C NMR (126 MHz, $CDCl_3$, 22 °C, TMS): δ=52.75 (2C), 94.58, 110.80, 112.10, 116.80 (2C), 118.45, 122.86, 130.45, 130.71, 132.08 (2C), 138.23, 138.88, 138.97, 151.74, 154.02 ppm. M ($C_{18}H_{17}IN_3Cl$)=437.7. MS (EI+): *m/z*: 437.0 (M^+). HRMS (EI+): M^+ calcd for $C_{18}H_{17}IN_3Cl$ 437.0156; found 437.0150.

*4.6.11. N,N-Diallyl-3-fluoro-4-[(E)-(3-iodophenyl)azo]aniline (**10c**).* According to GP2 solution A was made of 3-iodoaniline (2.24 g, 10.0 mmol) in EtOH (30 mL) and 2 N HCl (15 ml, 30 mmol), sodium nitrite (0.76 g, 11.0 mmol) in H_2O (10 mL) and amidosulfuric acid (0.20 g, 2.0 mmol). Solution B was obtained from **8c** (1.95 g, 10.0 mmol) in EtOH (200 mL) and H_2O (100 mL) without any further additions. The resulting pH was between 2 and 3. The reaction time was 36 h at 0 °C. **10c** was obtained as red solid (2.16 g, 51%). TLC: R_f≈0.4 (pentane/CH_2Cl_2=8/2). Mp: 65 °C. IR (KBr): $\tilde{\nu}$=3082, 3062, 3007, 2981, 2922, 1613, 1566, 1510, 1387, 1355, 1331, 1235, 1182, 1112, 991, 921, 821, 783 cm^{-1}. ^{1}H NMR (500 MHz, $CDCl_3$, 22 °C, TMS): δ=3.95–4.00 (m, 4H), 5.17 (dd, *J*=17.2/1.4 Hz, 2H), 5.22 (dd, *J*=10.4/1.3 Hz, 2H), 5.83 (ddt, *J*=17.1/9.9/4.7 Hz, 2H), 6.41–6.50 (m, 2H), 7.18 (t, *J*=7.9 Hz, 1H), 7.68 (dt, *J*=7.7/1.1 Hz, 1H), 7.72 (m, 1H), 7.81 (dt, *J*=8.0/1.3 Hz, 1H), 8.17 (t, *J*=1.7 Hz, 1H) ppm ^{13}C NMR (126 MHz, $CDCl_3$, 22 °C, TMS): δ=52.87 (2C), 94.56, 98.69 (d, $^2J_{CF}$=24.9 Hz), 108.07 (d, $^4J_{CF}$=1.5 Hz), 116.82 (2C), 117.07, 118.63 (d, $^3J_{CF}$=2.2 Hz), 122.82, 130.28, 130.43, 131.45 (d, $^3J_{CF}$=7.2 Hz), 132.09 (2C), 138.10, 152.98 (d, $^2J_{CF}$=11.6 Hz), 154.10, 162.42 (d, $^1J_{CF}$=255.9 Hz) ppm. M ($C_{18}H_{17}IN_3F$)=421.3. MS (EI+): *m/z*: 421.0 (M^+). HRMS (EI+): M^+ calcd for $C_{18}H_{17}IN_3F$ 421.0451; found 421.0450.

*4.6.12. N,N-Diallyl-3-methyl-4-[(E)-(3-iodophenyl)azo]aniline (**10d**).* According to GP2 solution A was made of 3-iodoaniline (2.24 g, 10.0 mmol) in EtOH (30 mL) and 2 N HCl (15 ml, 30 mmol), sodium nitrite (0.76 g, 11.0 mmol) in H_2O (10 mL) and amidosulfuric acid (0.20 g, 2.0 mmol). Solution B was obtained from **8d** (1.91 g, 10.0 mmol) in EtOH (200 mL) and H_2O (100 mL) and an addition of sodium acetate (1.70 g, 20.0 mmol). The resulting pH was about 4. The reaction time was 4 h at 0 °C. **10d** was obtained as red solid (3.52 g, 84%). TLC: R_f≈0.4 (pentane/CH_2Cl_2=8/2). Mp: 65 °C. IR (KBr): $\tilde{\nu}$=3070, 3061, 3006, 2979, 2920, 1598, 1503, 1381, 1354, 1228, 1177, 1107, 991, 915, 804, 782 cm^{-1}. ^{1}H NMR (500 MHz, $CDCl_3$, 22 °C, TMS): δ=2.68 (s, 3H), 3.97–4.01 (m, 4H), 5.14–5.22 (m, 4H), 5.86 (ddt, *J*=17.0/9.8/4.7 Hz, 2H), 6.52–6.57 (m, 2H), 7.18 (t, *J*=7.9 Hz, 1H), 7.66 (d, *J*=7.8 Hz, 1H), 7.68–7.71 (m, 1H), 7.79 (d, *J*=8.0 Hz, 1H), 8.14 (t, *J*=1.7 Hz, 1H). ^{13}C NMR (126 MHz, $CDCl_3$, 22 °C, TMS): δ=18.27, 52.60 (2C), 110.25, 112.72, 116.45 (2C) 117.07, 122.79, 130.23, 130.41, 132.82 (2C), 137.51, 141.66 ppm. M ($C_{19}H_{20}IN_3$)=417.3. MS (EI+): *m/z*: 417.1 (M^+). HRMS (EI+): M^+ calcd for $C_{19}H_{20}IN_3$ 417.0702; found 417.0704.

*4.6.13. 4-[(E)-(4-Iodophenyl)azo]aniline (**13a**).* According to GP3 with *N,N*-diallyl-4-[(*E*)-(4-iodophenyl)azo]aniline (**9a**, 2.02 g, 5.00 mmol) in CH_2Cl_2 (25 mL) the double bond isomerization was caused by RuClH(CO) (PPh_3)$_3$ (48 mg, 50 μmol) and heating for 2 h. The subsequent hydrolysis was induced by adding of hydroxylamine hydrochloride (3.47 g, 50.0 mmol) and triethylamine (2.53 g, 25.0 mmol) and heating for 3 h **13a** was obtained as orange solid (1.55 g, 96%). TLC: R_f≈0.3 (pentane/CH_2Cl_2=1/1). Mp: 164 °C. IR (KBr): $\tilde{\nu}$=3440, 3359, 1612, 1593, 1561, 1501, 1422, 1387, 1279, 1142, 1131, 1051, 997, 842 cm^{-1}. ^{1}H NMR (500 MHz, $CDCl_3$, 21 °C, TMS): δ=4.08 (s, 2H), 6.68–6.77 (m, 2H), 7.53–7.62 (m, 2H), 7.75–7.85 (m, 4H) ppm ^{13}C NMR (126 MHz, $CDCl_3$, 21 °C, TMS): δ=96.02, 114.74 (2C), 124.18 (2C), 125.46 (2C), 138.27 (2C), 145.45, 150.03, 152.41 ppm. M ($C_{12}H_{10}IN_3$)=323.1. MS (EI+): *m/z*: 323.1 (M^+). HRMS (EI+): M^+ calcd for $C_{12}H_{10}IN_3$ 322.9919; found 322.9919.

*4.6.14. 3-Chloro-4-[(E)-(4-iodophenyl)azo]aniline (**13b**).* According to GP3 with *N,N*-diallyl-3-chloro-4-[(*E*)-(4-iodophenyl)azo]aniline (**9b**, 2.19 g, 5.00 mmol) in CH_2Cl_2 (25 mL) the double bond isomerization was caused by RuClH(CO) (PPh_3)$_3$ (48 mg, 50 μmol) and heating for 2 h. The subsequent hydrolysis was induced by adding of hydroxylamine hydrochloride (3.47 g, 50.0 mmol) and triethylamine (2.53 g, 25.0 mmol) and heating for 3 h **13b** was obtained as orange solid (1.66 g, 93%). TLC: R_f≈0.3 (pentane/CH_2Cl_2=1/1). Mp: 175 °C. IR (KBr): $\tilde{\nu}$=3415, 3328, 3212, 1627, 1595, 1489, 1413, 1301, 1242, 1187, 1043, 1001, 899, 859, 837 cm^{-1}. ^{1}H NMR (500 MHz, $CDCl_3$, 25 °C, TMS): δ=4.13 (s, 2H), 6.57 (dd, *J*=8.9/2.4 Hz, 1H), 6.81 (d, *J*=2.6 Hz, 1H), 7.60–7.65 (m, 2H), 7.71 (d, *J*=8.9 Hz, 1H), 7.79–7.84 (m, 2H) ppm ^{13}C NMR (126 MHz, $CDCl_3$, 25 °C, TMS): δ=96.57, 113.57, 114.97, 118.87, 124.44 (2C), 138.23 (2C), 138.49, 140.81, 150.37, 152.39 ppm. M ($C_{12}H_9ClIN_3$)=357.6. MS (EI+): *m/z*: 357.0 (M^+). HRMS (EI+): M^+ calcd for $C_{12}H_9ClIN_3$ 356.9530; found 356.9523.

*4.6.15. 3-Fluoro-4-[(E)-(4-iodophenyl)azo]aniline (**13c**).* According to GP3 with *N,N*-diallyl-3-fluoro-4-[(*E*)-(4-iodophenyl)azo]aniline (**9c**, 2.11 g, 5.00 mmol) in CH_2Cl_2 (25 mL) the double bond isomerization was caused by RuClH(CO) (PPh_3)$_3$ (48 mg, 50 μmol) and heating for 2 h. The subsequent hydrolysis was induced by adding

of hydroxylamine hydrochloride (3.47 g, 50.0 mmol) and triethylamine (2.53 g, 25.0 mmol) and heating for 3 h **13c** was obtained as orange solid (1.55 g, 91%). TLC: $R_f \approx 0.3$ (pentane/CH_2Cl_2=1/1). Mp: 167 °C. IR (KBr): $\tilde{\nu}$=3438, 1635, 1615, 1587, 1498, 1429, 1245, 1119, 1004, 828 cm^{-1}. ^1H NMR (500 MHz, $CDCl_3$, 25 °C, TMS): δ=4.19 (s, 2H), 6.42–6.51 (m, 2H), 7.56–7.62 (m, 2H), 7.71 (t, J=8.8 Hz, 1H), 7.77–7.83 (m, 2H) ppm ^{13}C NMR (126 MHz, $CDCl_3$, 25 °C, TMS): δ=96.34, 101.49 (d, $^2J_{CF}$=23.2 Hz), 110.76, 119.05, 124.23 (2C), 133.12 (d, $^3J_{CF}$=6.8 Hz), 138.18 (2C), 151.57 (d, $^2J_{CF}$=11.8 Hz), 152.42, 162.21 (d, $^1J_{CF}$=257.0 Hz) ppm. M ($C_{12}H_9FIN_3$)=341.1. MS (EI+): *m/z*: 341.0 (M^+). HRMS (EI+): M^+ calcd for $C_{12}H_9FIN_3$ 340.9825; found 340.9820.

*4.6.16. 3-Methyl-4-[(E)-(4-iodophenyl)azo]aniline (**13d**).* According to GP3 with *N,N*-diallyl-3-methyl-4-[(*E*)-(4-iodophenyl)azo]aniline (**9d**, 2.09 g, 5.00 mmol) in CH_2Cl_2 (25 mL) the double bond isomerization was caused by RuClH(CO) (PPh_3)$_3$ (48 mg, 50 μmol) and heating for 2 h. The subsequent hydrolysis was induced by adding of hydroxylamine hydrochloride (3.47 g, 50.0 mmol) and triethylamine (2.53 g, 25.0 mmol) and heating for 3 h **13d** was obtained as orange solid (1.60 g, 95%). TLC: $R_f \approx 0.3$ (pentane/CH_2Cl_2=1/1). Mp: 118 °C. IR (KBr): $\tilde{\nu}$=3457, 3424, 3388, 3331, 3210, 2923, 1616, 1593, 1491, 1417, 1385, 1322, 1255, 1227, 1185, 1111, 1001, 826 cm^{-1}. ^1H NMR (500 MHz, $CDCl_3$, 25 °C, TMS): δ=2.63 (s, 3H), 3.99 (s, 2H), 6.51 (dd, J=8.7/2.9 Hz, 1H), 6.56 (d, J=3.1 Hz, 1H), 7.54–7.58 (m, 2H), 7.65 (d, J=8.7 Hz, 1H), 7.76–7.81 (m, 2H) ppm ^{13}C NMR (126 MHz, $CDCl_3$, 25 °C, TMS): δ=17.68, 95.48, 112.92, 115.78, 117.24, 124.12 (2C), 138.06 (2C), 141.67, 143.38, 149.85, 152.67 ppm. M ($C_{13}H_{12}IN_3$)= 337.2. MS (EI+): *m/z*: 337.0 (M^+). HRMS (EI+): M^+ calcd for $C_{13}H_{12}IN_3$ 337.0076; found 337.0081.

*4.6.17. 4-[(E)-(3-Iodophenyl)azo]aniline (**14a**).* According to GP3 with *N,N*-diallyl-4-[(*E*)-(3-iodophenyl)azo]aniline (**10a**, 2.02 g, 5.00 mmol) in CH_2Cl_2 (25 mL) the double bond isomerization was caused by RuClH(CO) (PPh_3)$_3$ (48 mg, 50 μmol) and heating for 4 h. The subsequent hydrolysis was induced by adding of hydroxylamine hydrochloride (3.47 g, 50.0 mmol) and triethylamine (2.53 g, 25.0 mmol) and heating for 6 h **14a** was obtained as orange solid (1.48 g, 92%). TLC: $R_f \approx 0.3$ (pentane/CH_2Cl_2=1/1). Mp: 88 °C. IR (KBr): $\tilde{\nu}$=3447, 3365, 1618, 1597, 1503, 1459, 1427, 1397, 1287, 1218, 1138, 832 cm^{-1}. ^1H NMR (500 MHz, $CDCl_3$, 25 °C, TMS): δ=4.08 (s, 2H), 6.70–6.74 (m, 2H), 7.21 (t, J=7.9 Hz, 1H), 7.69–7.72 (m, 1H), 7.77–7.83 (m, 3H), 8.17 (t, J=1.8 Hz, 1H) ppm ^{13}C NMR (126 MHz, $CDCl_3$, 25 °C, TMS): δ=94.62, 114.60 (2C), 123.06, 125.46 (2C), 130.14, 130.54, 138.29, 145.28, 150.05, 153.84 ppm. M ($C_{12}H_{10}IN_3$)=323.1. MS (EI+): *m/z*: 323.0 (M^+). HRMS (EI+): M^+ calcd for $C_{12}H_{10}IN_3$ 322.9920; found 322.9920.

*4.6.18. 3-Chloro-4-[(E)-(3-iodophenyl)azo]aniline (**14b**).* According to GP3 with *N,N*-diallyl-3-chloro-4-[(*E*)-(4-iodophenyl)azo]aniline (**10b**, 2.19 g, 5.00 mmol) in CH_2Cl_2 (25 mL) the double bond isomerization was caused by RuClH(CO) (PPh_3)$_3$ (48 mg, 50 μmol) and heating for 4 h. The subsequent hydrolysis was induced by adding of hydroxylamine hydrochloride (3.47 g, 50.0 mmol) and triethylamine (2.53 g, 25.0 mmol) and heating for 6 h **14b** was obtained as orange solid (1.58 g, 88%). TLC: $R_f \approx 0.3$ (pentane/CH_2Cl_2=1/1). Mp: 112 °C. IR (KBr): $\tilde{\nu}$=3448, 3434, 3343, 1615, 1593, 1488, 1419, 1407, 1301, 1289, 1238, 1131, 1044, 899, 864, 818, 782, 672 cm^{-1}. ^1H NMR (500 MHz, $CDCl_3$, 25 °C, TMS): δ=4.14 (s, 2H), 6.56 (dd, J=8.9/3.1 Hz, 1H), 6.80 (d, J=2.9 Hz, 1H), 7.21 (t, J=7.9 Hz, 1H), 7.69 (d, J=8.7 Hz, 1H), 7.73 (d, J=7.9 Hz, 1H), 7.86 (d, J=7.9 Hz, 1H), 8.21 (t, J=1.6 Hz, 1H) ppm ^{13}C NMR (126 MHz, $CDCl_3$, 25 °C, TMS): δ=94.55, 113.51, 114.91, 118.88, 123.00, 130.53, 130.94, 138.65, 138.74, 140.70, 150.49, 153.84 ppm. M ($C_{12}H_9ClIN_3$)=357.6. MS (EI+): *m/z*: 357.0 (M^+). HRMS (EI+): M^+ calcd for $C_{12}H_9ClIN_3$ 356.9530; found 356.9521.

*4.6.19. 3-Fluoro-4-[(E)-(3-iodophenyl)azo]aniline (**14c**).* According to GP3 with *N,N*-diallyl-3-fluoro-4-[(*E*)-(4-iodophenyl)azo]aniline (**10c**, 2.11 g, 5.00 mmol) in CH_2Cl_2 (25 mL) the double bond isomerization was caused by RuClH(CO) (PPh_3)$_3$ (48 mg, 50 μmol) and heating for 4 h. The subsequent hydrolysis was induced by adding of hydroxylamine hydrochloride (3.47 g, 50.0 mmol) and triethylamine (2.53 g, 25.0 mmol) and heating for 6 h **14c** was obtained as orange solid (1.49 g, 87%). TLC: $R_f \approx 0.3$ (pentane/CH_2Cl_2=1/1). Mp: 107 °C. IR (KBr): $\tilde{\nu}$=3471, 3379, 1621, 1575, 1497, 1427, 1318, 1245, 1161, 1118, 957, 836, 782 cm^{-1}. ^1H NMR (500 MHz, $CDCl_3$, 25 °C, TMS): δ=4.21 (s, 2H), 6.39–6.51 (m, 2H), 7.21 (t, J=7.9 Hz, 1H), 7.63–7.76 (m, 2H), 7.79–7.87 (m, 1H), 8.18 (t, J=1.7 Hz, 1H) ppm ^{13}C NMR (126 MHz, $CDCl_3$, 25 °C, TMS): δ=94.58, 101.46 (d, $^2J_{CF}$=23.4 Hz), 110.77 (d, $^4J_{CF}$=2.2 Hz), 119.13 (d, $^3J_{CF}$=1.9 Hz), 123.00, 130.55, 133.05 (d, $^3J_{CF}$=6.9 Hz), 138.63, 151.77 (d, $^2J_{CF}$=11.9 Hz), 153.94, 162.31 (d, $^1J_{CF}$=257.5 Hz) ppm. M ($C_{12}H_9FIN_3$)=341.1. MS (EI+): *m/z*: 341.0 (M^+). HRMS (EI+): M^+ calcd for $C_{12}H_9FIN_3$ 340.9825; found 340.9828.

*4.6.20. 3-Methyl-4-[(E)-(4-iodophenyl)azo]aniline (**14d**).* According to GP3 with *N,N*-diallyl-3-methyl-4-[(*E*)-(3-iodophenyl)azo]aniline (**10d**, 2.09 g, 5.00 mmol) in CH_2Cl_2 (25 mL) the double bond isomerization was caused by RuClH(CO) (PPh_3)$_3$ (48 mg, 50 μmol) and heating for 4 h. The subsequent hydrolysis was induced by adding of hydroxylamine hydrochloride (3.47 g, 50.0 mmol) and triethylamine (2.53 g, 25.0 mmol) and heating for 6 h **14d** was obtained as orange solid (1.52 g, 90%). TLC: $R_f \approx 0.3$ (pentane/CH_2Cl_2=1/1). Mp: 106 °C. IR (KBr): $\tilde{\nu}$=3454, 3369, 3051, 1616, 1598, 1591, 1461, 1402, 1308, 1255, 1218, 1104, 885, 858, 758 cm^{-1}. ^1H NMR (500 MHz, $CDCl_3$, 25 °C, TMS): δ=2.65 (s, 3H), 4.01 (s, 2H), 6.51 (dd, J=8.6/2.7 Hz, 1H), 6.57 (d, J=2.8 Hz, 1H), 7.20 (t, J=7.9 Hz, 1H), 7.64 (d, J=8.8 Hz, 1H), 7.67–7.72 (m, 1H), 7.77–7.85 (m, 1H), 8.15 (t, J=1.8 Hz, 1H) ppm ^{13}C NMR (126 MHz, $CDCl_3$, 25 °C, TMS): δ=17.73, 94.55, 112.89, 115.75, 117.34, 122.92, 130.40, 130.47, 137.99, 141.86, 143.34, 149.97, 154.19 ppm. M ($C_{13}H_{12}IN_3$)=337.2. MS (EI+): *m/z*: 337.0 (M^+). HRMS (EI+): M^+ calcd for $C_{13}H_{12}IN_3$ 337.0076; found 337.0072.

*4.6.21. (E)-(4-Iodophenyl)phenyldiazene (**15a**).* According to GP4 starting from 4-[(*E*)-(4-iodophenyl)azo]aniline (**13a**, 162 mg, 0.50 mmol) in THF (10 mL), 50% wt solution of hypophosphorous acid (1.32 g, 10.0 mmol) and sodium nitrite (105 mg, 1.00 mmol) **15a** was obtained as orange solid (115 mg, 75%). TLC: $R_f \approx 0.3$ (pentane). Mp: 105 °C. IR (KBr): $\tilde{\nu}$=3055, 1636, 1561, 1459, 1441, 1403, 1204, 1148, 1051, 992, 914, 880, 793, 768, 761, 685 cm^{-1}. ^1H NMR (400 MHz, $CDCl_3$, 25 °C, TMS): δ=7.46–7.55 (m, 3H), 7.65 (d, J=8.5 Hz, 2H), 7.86 (d, J=8.5 Hz, 2H), 7.89–7.94 (m, 2H). ^{13}C NMR (101 MHz, $CDCl_3$, 25 °C, TMS): δ=97.69, 122.99 (2C), 124.49 (2C), 129.16 (2C), 131.36, 138.36 (2C), 151.94, 152.46 ppm. M ($C_{12}H_9IN_2$)= 308.1. MS (EI+) *m/z* (%): 308.0 (57, M^+), 230.0 (11), 203.0 (40), 152.1 (15), 105.0 (52), 77.0 (100), 76.0 (36). HRMS (EI+): M^+ calcd for $C_{12}H_9IN_2$ 307.9810; found 307.9798.

*4.6.22. (E)-(2-Chlorophenyl)-(4-iodophenyl)diazene (**15b**).* According to GP4 starting from 3-chloro-4-[(*E*)-(4-iodophenyl)azo]aniline (**13b**, 180 mg, 0.50 mmol) in THF (10 mL), 50% wt solution of hypophosphorous acid (1.32 g, 10.0 mmol) and sodium nitrite (105 mg, 1.00 mmol) **15b** was obtained as orange solid (112 mg, 66%). TLC: $R_f \approx 0.25$ (pentane). Mp: 101 °C. IR (KBr): $\tilde{\nu}$=3063, 1636, 1577, 1568, 1480, 1469, 1390, 1149, 1050, 1004, 830, 760, 717 cm^{-1}. ^1H NMR (500 MHz, $CDCl_3$, 25 °C, TMS): δ=7.32 (t, J=7.6 Hz, 1H), 7.39 (t, J=7.6 Hz, 1H), 7.55 (d, J=7.9 Hz, 1H), 7.65–7.71

(m, 3H), 7.86 (d, *J*=8.2 Hz, 2H) ppm ^{13}C NMR (126 MHz, $CDCl_3$, 25 °C, TMS): δ=98.48, 117.46, 124.83 (2C), 127.25, 130.74, 131.98, 135.59, 138.39 (2C), 148.42, 151.96 ppm. M ($C_{12}H_8ClIN_2$)=342.6. MS (EI+) *m/z* (%): 344.0 (22, M^+), 343.0 (10, M^+), 342.0 (66, M^+), 231.0 (69), 203.0 (100), 152.1 (13), 139.0 (24) 111.0 (56), 76.0 (50), 75.0 (21). HRMS (EI+): M^+ calcd for $C_{12}H_8ClIN_2$ 341.9421; found 341.9413.

*4.6.23. (E)-(2-Fluorophenyl)-(4-iodophenyl)diazene (**15c**).* According to GP4 starting from 3-fluoro-4-[(*E*)-(4-iodophenyl)azo]aniline (**13c**, 171 mg, 0.50 mmol) in THF (10 mL), 50% wt solution of hypophosphorous acid (1.32 g, 10.0 mmol) and sodium nitrite (105 mg, 1.00 mmol) **15c** was obtained as orange solid (111 mg, 68%). TLC: R_f≈0.25 (pentane). Mp: 115 °C. IR (KBr): $\tilde{\nu}$=3063, 1628, 1605, 1586, 1576, 1567, 1480, 1389, 1264, 1213, 1151, 1103, 1049, 1005, 827, 756 cm^{-1}. ^{1}H NMR (500 MHz, $CDCl_3$, 25 °C, TMS): δ=7.20 (t, *J*=7.7 Hz, 1H), 7.23–7.29 (m, 1H), 7.42–7.48 (m, 1H), 7.66 (d, *J*=8.5 Hz, 2H), 7.74 (td, *J*=7.9/1.6 Hz, 1H), 7.85 (d, *J*=8.4 Hz, 2H) ppm ^{13}C NMR (126 MHz, $CDCl_3$, 25 °C, TMS): δ=98.30, 117.12 (d, $^2J_{CF}$=19.5 Hz), 117.64, 124.29 (d, $^3J_{CF}$=3.1 Hz), 124.66 (2C), 132.85 (d, $^3J_{CF}$=8.6 Hz), 138.36 (2C), 140.42 (d, $^2J_{CF}$=7.3 Hz), 152.01, 160.19 (d, $^1J_{CF}$=258.4 Hz) ppm. M ($C_{12}H_8FIN_2$)=326.1. MS (EI+) *m/z* (%): 326.0 (65, M^+), 231.0 (73), 203.0 (100), 123.0 (14), 95.1 (30), 76.1 (53), 75.0 (17). HRMS (EI+): M^+ calcd for $C_{12}H_8FIN_2$ 325.9716; found 325.9716.

*4.6.24. (E)-(2-Methylphenyl)-(4-iodophenyl)diazene (**15d**).* According to GP4 starting from 3-methyl-4-[(*E*)-(4-iodophenyl)azo]aniline (**13d**, 168 mg, 0.50 mmol) in THF (10 mL), 50% wt solution of hypophosphorous acid (1.32 g, 10.0 mmol) and sodium nitrite (105 mg, 1.00 mmol) **15d** was obtained as orange solid (116 mg, 72%). TLC: R_f≈0.25 (pentane). Mp: 105 °C. IR (KBr): $\tilde{\nu}$=3063, 2923, 1576, 1564, 1477, 1459, 1427, 1390, 1058, 1052, 1003, 832, 764, 721 cm^{-1}. ^{1}H NMR (400 MHz, $CDCl_3$, 25 °C, TMS): δ=2.70 (s, 3H), 7.22–7.28 (m, 1H), 7.29–7.39 (m, 2H), 7.59–7.66 (m, 3H), 7.79–7.87 (m, 2H) ppm ^{13}C NMR (101 MHz, $CDCl_3$, 25 °C, TMS): δ=17.52, 97.34, 115.36, 124.51 (2C), 126.42, 131.30 (2C), 138.27 (2C), 138.41, 150.46, 152.24 ppm. M ($C_{13}H_{11}IN_2$)=322.1. MS (EI+) *m/z* (%): 322.0 (59, M^+), 231.0 (11), 203.0 (42), 195.1 (15), 119.1 (19), 91.1 (100), 76.0 (21), 65.0 (16). HRMS (EI+): M^+ calcd for $C_{13}H_{11}IN_2$ 321.9967; found 321.9957.

*4.6.25. (E)-(4-Chlorophenyl)-(4-iodophenyl)diazene (**16**).* 4-[(*E*)-(4-Iodophenyl)azo]aniline (**13a**, 162 mg, 0.50 mmol, 1.00 equiv) was dissolved in CCl_4 (10 mL). 4-dodecylbenzenesulfonic acid (163 mg, 0.50 mmol, 1.00 equiv) was added and the mixture was stirred for 5 min at room temperature. Then *tert*-butyl nitrite (310 mg, 3.00 mmol, 6.00 equiv) was added and the reaction mixture was stirred at room temperature until the initial aromatic amine disappeared (TLC, pentane/ethyl acetate=8/2; the reaction was complete after about 2 h). Triethylamine (51 mg, 0.50 mmol, 1.00 equiv) was added and the reaction mixture was heated to 80 °C for 2 h resulting in an instant nitrogen evolving. After cooling to room temperature again, H_2O (10 mL) was added and the product was extracted with CH_2Cl_2 (3×). The combined organic layers were dried over Na_2SO_4 and the solvent was removed under reduced pressure. The crude product was purified by flash chromatography (pentane) to give 14 as orange solid (90 mg, 52%). TLC: R_f≈0.2 (pentane). Mp: 178 °C. IR (KBr): $\tilde{\nu}$=3064, 1575, 1565, 1472, 1389, 1088, 1050, 1003, 835 cm^{-1}. ^{1}H NMR (400 MHz, $CDCl_3$, 21 °C, TMS): δ=7.46–7.51 (m, 2H), 7.61–7.67 (m, 2H), 7.82–7.90 (m, 4H) ppm ^{13}C NMR (126 MHz, $CDCl_3$, 21 °C, TMS): δ=98.20, 124.36 (2C), 124.63 (2C), 129.55 (2C), 137.43, 138.54 (2C), 150.87, 151.83 ppm. M ($C_{12}H_8ClIN_2$)=342.6. MS (EI+) *m/z* (%): 344 (33), 342.0 (100, M^+), 231.0 (42), 203.0 (90), 139.1 (32), 113 (20), 111.1 (65), 76.1 (45). HRMS (EI+): M^+ calcd for $C_{12}H_8ClIN_2$ 341.9421; found 341.9421.

*4.6.26. (E)-(4-Fluorophenyl)-(4-iodophenyl)diazene (**17**).* 4-[(*E*)-(4-Iodophenyl)azo]aniline (**13a**, 162 mg, 0.50 mmol, 1.00 equiv) was dissolved in CH_2Cl_2 (5 mL) and the mixture was cooled to 0 °C. Boron trifluoride etherate (106 mg, 0.75 mmol, 1.50 equiv) was added and the mixture was stirred for 5 min at 0 °C. Then *tert*-butyl nitrite (103 mg, 1.00 mmol, 2.00 equiv) was added dropwise and the mixture was stirred for 16 h (0 °C to rt). Afterwards pentane (10 mL) was added and the precipitated diazonium salt was filtered off and washed with pentane. The residue was heated to 120 °C for 2 h and the obtained product was directly purified by flash chromatography (eluting with pentane) to give **15** as orange solid (102 mg, 63%). TLC: R_f≈0.2 (pentane). Mp: 128 °C. IR (KBr): $\tilde{\nu}$=3059, 1595, 1569, 1498, 1473, 1389, 1229, 1127, 1005, 840 cm^{-1}. ^{1}H NMR (400 MHz, $CDCl_3$, 21 °C, TMS): δ=7.15–7.22 (m, 2H), 7.59–7.65 (m, 2H), 7.82–7.87 (m, 2H), 7.92 (dd, *J*=8.2/5.5 Hz, 2H) ppm ^{13}C NMR (126 MHz, $CDCl_3$, 21 °C, TMS): δ=97.85, 116.25 (d, $^2J_{CF}$=22.9 Hz, 2C), 124.54 (2C), 125.14 (d, $^3J_{CF}$=9.0 Hz, 2C), 138.47 (2C), 149.03 (d, $^4J_{CF}$=3.0 Hz), 151.81, 164.66 (d, $^1J_{CF}$=252.6 Hz) ppm. M ($C_{12}H_8FIN_2$)=326.1. MS (EI+) *m/z* (%): 326.1 (100, M^+), 231.0 (24), 203.0 (63), 123.1 (34), 95 (75), 76.1 (44). HRMS (EI+): M^+ calcd for $C_{12}H_8FIN_2$ 325.9716; found 325.9716.

*4.6.27. 4-[(E)-(4-Iodophenyl)azo]naphthalen-1-amine (**19a**).* According to GP2 solution A was made of 4-iodoaniline (1.12 g, 5.00 mmol) in EtOH (15 mL) and 2 N HCl (7.5 mL, 15.0 mmol), sodium nitrite (0.38 g, 5.50 mmol) in water (5 mL) and amidosulfuric acid (0.10 g, 1.0 mmol). Solution B was obtained from 1-naphthylamine (0.73 g, 5.0 mmol) in EtOH (100 mL) and H_2O (50 mL) and an addition of 2 N HCl (5.0 ml, 10 mmol). The resulting pH was between 1 and 2. The reaction time was 1 h at 0 °C. **19a** was obtained as dark red solid (1.78 g, 95%). TLC: R_f≈0.4 (pentane/CH_2Cl_2=1/1). Mp: 204 °C. IR (KBr): $\tilde{\nu}$=3416, 3298, 3186, 3012, 1638, 1571, 1514, 1464, 1385, 1336, 1191, 1142, 1052, 999, 826, 755 cm^{-1}. ^{1}H NMR (400 MHz, $CDCl_3$, 21 °C, TMS): δ=4.66 (s, 2H), 6.82 (d, *J*=8.3 Hz, 1H), 7.56 (ddd, *J*=8.3/6.8/1.3 Hz, 1H), 7.66 (ddd, *J*=8.4/6.8/1.2 Hz, 1H), 7.70–7.73 (m, 2H), 7.82 (d, *J*=8.5 Hz, 1H), 7.84–7.87 (m, 2H), 7.94 (d, *J*=8.3 Hz, 1H), 9.02 (d, *J*=8.5 Hz, 1H) ppm ^{13}C NMR (101 MHz, $CDCl_3$, 21 °C, TMS): δ=95.90, 109.26, 114.31, 120.73, 122.53, 124.17, 124.44 (2C), 125.59, 127.41, 133.38, 138.35 (2C), 140.37, 146.81, 153.04 ppm. M ($C_{16}H_{12}IN_3$)=373.2. MS (ESI$^+$) *m/z*: 374.1 ([M+H]$^+$). HRMS (EI+): calcd for $C_{16}H_{12}IN_3$, 373.0076; found 373.0069.

*4.6.28. 4-[(E)-(3-Iodophenyl)azo]naphthalen-1-amine (**19b**).* According to GP2 solution A was made of 3-iodoaniline (1.12 g, 5.00 mmol) in EtOH (15 mL) and 2 N HCl (7.5 mL, 15.0 mmol), sodium nitrite (0.38 g, 5.50 mmol) in water (5 mL) and amidosulfuric acid (0.10 g, 1.0 mmol). Solution B was obtained from 1-naphthylamine (0.73 g, 5.0 mmol) in EtOH (100 mL) and H_2O (50 mL) and an addition of 2 N HCl (5.0 mL, 10 mmol). The resulting pH was between 1 and 2. The reaction time was 1 h at 0 °C. **19b** was obtained as dark red solid (1.76 g, 94%). TLC: R_f≈0.4 (pentane/CH_2Cl_2=1/1). Mp: 123 °C. IR (KBr): $\tilde{\nu}$=3396, 3328, 3235, 3054, 1647, 1619, 1574, 1515, 1466, 1400, 1339, 1213, 1159, 992, 880, 845, 832, 790, 756 cm^{-1}. ^{1}H NMR (400 MHz, $CDCl_3$, 21 °C, TMS): δ=4.66 (s, 2H), 6.79 (d, *J*=8.4 Hz, 1H), 7.25 (t, *J*=7.9 Hz, 1H), 7.52–7.58 (m, 1H), 7.63–7.69 (m, 1H), 7.73 (dt, *J*=8.0/1.3 Hz, 1H), 7.80 (d, *J*=8.5 Hz, 1H), 7.90–7.97 (m, 2H), 8.30 (t, *J*=1.7 Hz, 1H), 9.03 (d, *J*=8.4 Hz, 1H) ppm ^{13}C NMR (101 MHz, $CDCl_3$, 21 °C, TMS): δ=94.67 (s, 1C), 109.02 (d, 1C), 114.29 (d, 1C), 120.56 (d, 1C), 122.27 (s, 1C), 123.28 (d, 1C), 124.01 (d, 1C), 125.44 (d, 1C), 127.35 (d, 1C), 130.35 (d, 1C), 130.56 (d, 1C), 133.24 (s, 1C), 138.16 (d, 1C), 140.06 (s, 1C), 146.82 (s, 1C), 154.32 (s, 1C) ppm. M ($C_{16}H_{12}IN_3$)=373.19. MS (ESI$^+$) *m/z*: 374.1 ([M+H]$^+$). HRMS (EI+): calcd for $C_{16}H_{12}IN_3$, 373.0076; found 373.0069.

*4.6.29. (E)-(4-Iodophenyl)-(1-naphthyl)diazene (**20a**).* According to GP4 starting from **16a** (1.50 g, 4.00 mmol) in THF (80 mL), 50% wt solution of hypophosphorous acid (10.6 g, 80.0 mmol) and sodium

nitrite (0.56 g, 8.00 mmol) **20a** was obtained as red solid (1.03 g, 72%). TLC: $R_f \approx 0.2$ (pentane). Mp: 116 °C. IR (KBr): $\tilde{\nu}$=3045, 2999, 1577, 1564, 1508, 1473, 1391, 1343, 1297, 1213, 1094, 1054, 1002, 862, 823, 797, 768 cm^{-1}. ^1H NMR (400 MHz, $CDCl_3$, 21 °C, TMS): δ=7.52–7.60 (m, 2H), 7.64 (ddd, J=8.4/6.8/1.3 Hz, 1H), 7.72–7.77 (m, 2H), 7.81 (dd, J=7.5/1.0 Hz, 1H), 7.85–7.89 (m, 2H), 7.91 (d, J=8.2 Hz, 1H), 7.98 (d, J=8.1 Hz, 1H), 8.89 (d, J=8.4 Hz, 1H) ppm ^{13}C NMR (101 MHz, $CDCl_3$, 21 °C, TMS): δ=97.89, 112.09, 123.46, 124.84 (2C), 125.72, 126.66, 127.10, 128.10, 131.47, 131.89, 134.43, 138.52 (2C), 147.60, 152.55 ppm. M ($C_{16}H_{11}IN_2$)=358.18. MS (ESI^+) m/z: 359.0 ($[M+H]^+$). HRMS (EI+): calcd for $C_{16}H_{11}IN_2$, 357.9967; found 357.9963.

*4.6.30. (E)-(3-Iodophenyl)-(1-naphthyl)diazene (**20b**).* According to GP4 starting from **16b** (1.50 g, 4.00 mmol) in THF (80 mL), 50% wt solution of hypophosphorous acid (10.6 g, 80.0 mmol) and sodium nitrite (0.56 g, 8.00 mmol) **20b** was obtained as red solid (0.98 g, 68%). TLC: $R_f \approx 0.2$ (pentane). Mp: 95 °C. IR (KBr): $\tilde{\nu}$=3048, 1562, 1508, 1454, 1403, 1386, 1344, 1206, 990, 909, 888, 800, 789, 768, 682 cm^{-1}. ^1H NMR (400 MHz, $CDCl_3$, 21 °C, TMS): δ=7.29 (t, J=7.9 Hz, 1H), 7.53–7.61 (m, 2H), 7.64–7.69 (m, 1H), 7.79–7.83 (m, 2H), 7.93 (d, J=8.2 Hz, 1H), 7.98–8.03 (m, J=10.8/5.4/4.5 Hz, 2H), 8.36 (t, J=1.8 Hz, 1H), 8.91 (d, J=8.4 Hz, 1H) ppm ^{13}C NMR (101 MHz, $CDCl_3$, 21 °C, TMS): δ=97.89, 112.09, 123.46, 124.84, 125.72, 126.66, 127.10, 128.10, 131.47, 131.89, 134.43, 138.52, 147.60, 152.55 ppm. M ($C_{16}H_{11}IN_2$)=358.18. MS (ESI^+) m/z: 359.0 ($[M+H]^+$). HRMS (EI+): calcd for $C_{16}H_{11}IN_2$, 357.9967; found 357.9963.

References and notes

1. Hunger, K. *Industrial Dyes: Chemistry, Properties, Applications*; Wiley-VCH GmbH & KGaA: Weinheim, 2003.
2. Pandey, A. N. D.; Mehrotra, J. K. *Colourage* **1979**, *26*, 25.
3. Athey, R. D. *Eur. Coat. J.* **1998**, *3*, 146.
4. Sandborn, W. J. *Am. J. Gastroenterol.* **2002**, *97*, 2939.
5. Cisnetti, F.; Ballardini, R.; Credi, A.; Gandolfi, M. T.; Masiero, S.; Negri, F.; Pieraccini, S.; Spada, G. P. *Chem.—Eur. J.* **2004**, *10*, 2011.
6. Jain, A.; Gupta, Y.; Jain, S. K. *Crit. Rev. Ther. Drug Carr. Syst.* **2006**, *23*, 349.
7. Feringa, B. L.; van Delden, R. A.; Koumura, N.; Geertsema, E. M. *Chem. Rev.* **2000**, *100*, 1789.
8. Beharry, A. A.; Woolley, G. A. *Chem. Soc. Rev.* **2011**, *40*, 4422.
9. Woolley, G. A. *Nat. Chem.* **2012**, *4*, 75.
10. Tazuke, S.; Kurihara, S.; Ikeda, T. *Chem. Lett.* **1987**, *16*, 911.
11. Kurihara, S.; Ikeda, T.; Tazuke, S. *Mol. Cryst. Liq. Cryst.* **1990**, *178*, 117.
12. Wuckert, E.; Harjung, M. D.; Kapernaum, N.; Mueller, C.; Frey, W.; Baro, A.; Giesselmann, F.; Laschat, S. *Phys. Chem. Chem. Phys.* **2015**, *17*, 8382.
13. Schönberger, M.; Althaus, M.; Fronius, M.; Clauss, W.; Trauner, D. *Nat. Chem.* **2014**, *6*, 712.
14. Broichhagen, J.; Podewin, T.; Meyer-Berg, H.; von Ohlen, Y.; Johnston, N. R.; Jones, B. J.; Bloom, S. R.; Rutter, G. A.; Hoffmann-Röder, A.; Hodson, D. J.; Trauner, D. *Angew. Chem., Int. Ed.* **2015**, http://dx.doi.org/10.1002/anie.201506384
15. Broichhagen, J.; Jurastow, I.; Iwan, K.; Kummer, W.; Trauner, D. *Angew. Chem., Int. Ed.* **2014**, *53*, 7657.
16. Schönberger, M.; Trauner, D. *Angew. Chem., Int. Ed.* **2014**, *53*, 3264.
17. Frank, J. A.; Moroni, M.; Moshourab, R.; Sumser, M.; Lewin, G. R.; Trauner, D. *Nat. Commun.* **2015**, *6*, 7118.
18. Rullo, A.; Reiner, A.; Reiter, A.; Trauner, D.; Isacoff, E. Y.; Woolley, G. A. *Chem. Commun.* **2014**, 14613.
19. Laprell, L.; Repak, E.; Franckevicius, V.; Hartrampf, F.; Terhag, J.; Hollmann, M.; Sumser, M.; Rebola, N.; DiGregorio, D. A.; Trauner, D. *Nat. Commun.* **2015**, *6*, 8076.
20. Laprell, L.; Hüll, K.; Stawski, P.; Schön, C.; Michalakis, S.; Biel, M.; Sumser, M. P.; Trauner, D. *ACS Chem. Neurosci.* **2015**, http://dx.doi.org/10.1021/acschemneuro.5b00234
21. Schoenberger, M.; Damijonaitis, A.; Zhang, Z.; Nagel, D.; Trauner, D. *ACS Chem. Neurosci.* **2014**, *5*, 514.
22. Castle, B. T.; Odde, D. J. *Cell* **2015**, *162*, 243.
23. Quandt, G.; Höfner, G.; Pabel, J.; Dine, J.; Eder, M.; Wanner, K. T. *J. Med. Chem.* **2014**, *57*, 6809.
24. Merino, E. *Chem. Soc. Rev.* **2011**, *40*, 3835.
25. Haghbeen, K.; Tan, E. W. *J. Org. Chem.* **1998**, *63*, 4503.
26. Davey, M. H.; Lee, V. Y.; Miller, R. D.; Marks, T. J. *J. Org. Chem.* **1999**, *64*, 4976.
27. Shimao, I.; Oae, S. *Bull. Chem. Soc. Jpn.* **1983**, *56*, 643.
28. Gund, S. H.; Shelkar, R. S.; Nagarkar, J. M. *RSC Adv.* **2014**, *4*, 42947.
29. Takeda, Y.; Okumura, S.; Minakata, S. *Angew. Chem., Int. Ed.* **2012**, *51*, 7804.
30. Sindelar, M.; Lutz, T. A.; Petrera, M.; Wanner, K. T. *J. Med. Chem.* **2013**, *56*, 1323.
31. Krompiec, S.; Krompiec, M.; Penczek, R.; Ignasiak, H. *Coord. Chem. Rev.* **2008**, *252*, 1819.
32. Mathieu, S.; Gradl, S. N.; Ren, L.; Wen, Z.; Aliagas, I.; Gunzner-Toste, J.; Lee, W.; Pulk, R.; Zhao, G.; Alicke, B.; Boggs, J. W.; Buckmelter, A. J.; Choo, E. F.; Dinkel, V.; Gloor, S. L.; Gould, S. E.; Hansen, J. D.; Hastings, G.; Hatzivassiliou, G.; Laird, E. R.; Moreno, D.; Ran, Y.; Voegtli, W. C.; Wenglowsky, S.; Grina, J.; Rudolph, J. *J. Med. Chem.* **2012**, *55*, 2869.
33. Kutonova, K. V.; Trusova, M. E.; Postnikov, P. S.; Filimonov, V. D. *Russ. Chem. Bull.* **2012**, *61*, 206.